Analysis of β-catenin activation in mouse skin carcinogenesis.

Abdullah Alyamani

PhD Thesis submitted to the University of Glasgow
In fulfilment of the requirements for the
Degree of Doctor of Philosophy

School of Medicine
College of Medical, Veterinary and Life Sciences
University of Glasgow

March 2021

Summary

β-catenin overexpression was investigated in transgenic mouse skin carcinogenesis to determine at which stage β-catenin deregulation became causal in co-operation with *ras* and *fos* oncogene activation and/or loss of tumour suppresser genes *p53, p21* and *PTEN*. β-catenin has two major functions in being a major node for canonical Wnt signalling, nuclear relocation regulates transcriptional targets LEF/TCF and increased nuclear β-catenin expression associates with tumour progression; whilst membranous β-catenin binds to E-cadherin to form cell-cell adhesion complexes and their failure is associated with invasion. Thus, in cutaneous squamous cell carcinoma [SCC], β-catenin mutations result in constitutive overexpression via mutations in exon 3, the site for removal via ubiquination, or failures in genes that regulate β-catenin, such as APC and GSK3β. However, despite the clear relevance of β-catenin in SCC, few studies have directly explored constitutive β-catenin overexpression employing classic multi-stage mouse skin carcinogenesis to help unravel the mechanism of β-catenin deregulation. Therefore, to investigate stage-specific roles in skin carcinogenesis, β-catenin overexpression was targeted to transgenic mouse epidermis employing RU486-inducible *cre/lox* and expression of an exon 3-ablated *β-catenin* transgene [*K14creP.Δ3β-cat*]. The effect of β-catenin overexpression was assessed in co-operation with activated Ras [*HK1.ras*] and Fos [*HK1.fos*] and loss of PTEN-regulated AKT activation [*Δ5PTEN*], together with p53 and p21 ablation.

Initial experiments targeted β-catenin overexpression to *K14creP.Δ3β-cat*$^{flx/wt}$ mouse epidermis and showed HF anomalies, and alterations to keratinocyte differentiation observed in previous studies; and discovered that *K14creP.Δ3β-cat*$^{flx/wt}$ mice displayed compensatory p53/p21 expression in response to β-catenin that may inhibit spontaneous papillomatogenesis. Indeed, creation of the *HK1.ras.K14creP.Δ3β-catenin* genotype was expected to give typical *HK1.ras* papillomas and as *Δ3β-catenin* expression was now independent of PTEN/AKT/GSK3β signalling this may have given malignancy. However, *HK1.ras-K14creP.Δ3β-cat*$^{flx/wt}$ mice lacked papillomas, yet possessed *Δ3β-catenin*-associated HF abnormalities, skin keratosis and altered epidermal differentiation observed previously; typified by patchy keratin K1 but a unique lack of hyperproliferation marker K6 expression. *HK1.ras-K14creP.Δ3β-cat*$^{flx/wt}$ hyperplasia also expressed membranous β-catenin in basal layers, unlike supra-basal expression typical of control

hyperplasia; and this triggered compensatory p53/p21 responses that may underlie this paradoxical lack of tumours.

These novel findings challenged current dogma that β-catenin overexpression facilitates carcinogenesis and were further compounded by a lack of tumours in *HK1.ras/Δ3β-catenin* co-operation experiments with conditional *p53* loss. Importantly, in *K14creP.Δ3β-cat*$^{flx/wt}$ *.p53*$^{flx/flx}$ mice, p53 loss inhibited *Δ3β-catenin* phenotypes indicating that p53-mediated responses played major roles in development of these skin phenotypes. In addition, *HK1.ras-K14creP.Δ3β-cat*$^{flx/wt}$*.p53*$^{flx/flx}$ mice also lacked these early phenotypes and exhibited differentiation abnormalities typified by an absence of K1/K6 expression; with elevated p21 and novel expression of p53 family members p63/p73. In particular, strong p73 expression in *HK1.ras-K14creP.Δ3β-cat*$^{flx/wt}$*.p53*$^{flx/flx}$ epidermis and HFs, suggests that at these early stages of papillomatogenesis, oncogenic *Δ3β-catenin* could be blocked/circumvented by p63/p73expression. That these epidermal responses to β-catenin deregulation depended upon p53 was further confirmed by p21 knockout, which failed to block responses to *Δ3β-catenin*.

Although the majority of *HK1.ras-K14creP.Δ3β-cat*$^{flx/wt}$ and *HK1.ras-K14creP.Δ3β-cat*$^{flx/wt}$*.p53*$^{flx/flx}$ mice lacked tumours, four individuals did develop tumours and shared a specific characteristic whilst most individuals expressed *K14creP.Δ3β-cat*$^{flx/wt}$ due to leakage of *K14.creP* activity in these rare individuals, the epidermis developed normally into adulthood as *K14.cre* had not leaked. This absence of *Δ3β-catenin* responses in juvenile epidermis requiring RU486-mediated β-catenin overexpression in adults apparently allowed these individuals to establish an epidermal context permissive for papilloma formation; as originally theorised. Moreover, whilst *HK1.ras-K14creP.Δ3β-cat*$^{flx/wt}$ mice developed papillomas, *HK1.ras-K14creP.Δ3β-cat*$^{flx/wt}$*.p53*$^{flx/flx}$ tumours rapidly progressed to aggressive SCC due loss of p53, despite the presence of p21. Such *HK1.ras-K14creP.Δ3β-cat*$^{flx/wt}$*.p53*$^{flx/flx}$ conversion to SCC involved reduced membranous β-catenin expression and increased nuclear β-catenin, together with E-cadherin loss at the invasive front. This reinforces the idea that β-catenin deregulation in juvenile development can be overcome by p63 or p73 [but not p21]; however, in papillomas, p53 loss in conjunction with nuclear β-catenin induces conversion and additional E-cadherin loss facilitates collective invasion.

This paradoxical tumour block also manifests in Δ3β-catenin co-operation with *HK1.fos* and *K14creP-Δ5PTEN* genotypes [*HK1.fos-K14creP.Δ5PTEN*$^{flx/flx}$*.Δ3β-cat*$^{flx/wt}$]. In this context, a

novel skin phenotype was also observed; typified by a keratotic, folded, scale-like skin exhibiting numerous cysts, increased HF abnormalities, and a disturbed premature/accelerated epidermal differentiation. This [dubbed pangolin-like] skin maybe the first to demonstrate direct co-operation between fos and β-catenin deregulation, resulting in anomalous differentiation consistent with roles such as keratinocytes commitment to differentiation, and possibly the decision-making of stem cells in their various niches. These data suggest that the block to tumourigenesis following β-catenin activation maybe relatively generic, appearing in both fos and fos/PTEN genotypes. Furthermore, p53 loss failed to elicit papillomas, however *HK1.fos-K14creP.Δ3β-cat*$^{flx/wt}$*.p53*$^{flx/flx}$ mice again displayed a striking lack of the pangolin skin phenotype which clearly indicates responses to β-catenin overexpression were dependent on p53 function or responses to p53 loss.

In vitro analysis of primary transgenic keratinocytes and cell lines produced results more consistent with expectations for β-catenin overexpression in terms of inducing resistance to calcium-induced differentiation indicative of a transformed phenotype; and the ability to grow from clonal density, which suggests a malignant phenotype in *HK1.ras-K14creP.Δ3β-cat*$^{flx/wt}$ and *HK1.fos-K14creP.Δ5PTEN*$^{flx/flx}$*.Δ3β-cat*$^{flx/wt}$ cell lines. Indeed, migration and cell seeding experiments highlighted that β-catenin overexpression may return *K14creP.Δ3β-cat*$^{flx/wt}$ cells to a more juvenile/neonatal state, as they exhibited a seeding potential similar to neonatal primary keratinocytes; consistent with previous observations that demonstrated β-catenin regulates keratinocyte signalling to alter the dermal extra cellular matrix in neonatal skin.

Overall, this study shows β-catenin roles in developing papillomas and progression to SCC was more complex and context dependent than originally anticipated. Logically, in being exposed to environmental carcinogens, an epidermis has evolved options to prevent benign tumour formation, which becomes lost as papillomas progress to SCC. The findings of this study were intriguing and identified potent responses to β-catenin deregulation in juvenile epidermis that maybe quite general given they appeared in ras/β-catenin/p53; fos/β-catenin/p53; ras/p53 and fos/p53 models and maybe applicable to internal epithelia. These models highlight several aspects to be pursued in future to gain understanding and fill the void concerning causal roles for β-catenin overexpression in cutaneous carcinogenesis. In the final analysis the discovery of the mechanism underlying this tumour inhibition may identify targets for new treatments.

Table of contents

Contents

List of Tables

List of Figures

Chapter 1

Chapter 3

Chapter 4

Acknowledgements

First and foremost, I would like to express my appreciation and my sincere gratitude to my primary supervisor Dr. David A Greenhalgh for his excellent support, invaluable insights, enthusiasm, and constructive criticism during the entire period of this research. I would like also to express my sincere appreciation to the invaluable advice and guidance provided by my second supervisor Dr. Jean Quinn throughout this PhD. I consider myself lucky for having the chance to learn from and work with such excellent scientists.

Significantly, I would like to immensely acknowledge and thank Saudi Arabia Ministry of Education for accepting me in their scholarship programme and for the generous financial support for this research. This research also would not have been possible without the support of the Scott Endowment for Dermatology Research.

I would like also to extend my thanks to the staff at the CRF especially Stuart Lannigan, and Dennis Duggan for their efforts in providing the best animal care and husbandry throughout this study, which was critical for the completion of this research. Also, I would like to thank my colleague Dr. Carol McMenemy for discussing and sharing her valuable scientific ideas and insights on my work throughout this research.

Finally, I would like to thank my mother Hanan Khuqeer and my father Mohammad Alyamani for their support in every aspect of my life. Also, a special thanks to my sister Dr. Hanin Alyamani, for her continued support, and help during my PhD journey.

Author declaration

I declare that, except where explicit reference is made to the contribution of others, that this PhD thesis is the result of my own work and has not been submitted for any other degree at the University of Glasgow or any other institution.

Abdullah Mohammad Alyamani

March 2021

Abbreviations list

β-cat	β-catenin
BSA	Bovine serum albumin
BrdU	5-Bromo-2-deoxyuridine
Cre	Cyclisation recombination gene of bacteriophage P1
DAB	3,3'-Diaminobenzidine
DMBA	Dimethylbenzanthracene
DMEM	Dulbecco's modified eagle medium
DNA	Deoxyribonucleic acid
dNTPs	Deoxynucleotide Triphosphates
g	Gram
EDTA	Ethylenediaminetetra-acetate
FCS	Foetal calf serum
GAP	GTPase Activating
GDP	Guanine diphosphate
GSK3β	Glycogen synthase kinase beta
GTP	Guanine triphosphate

H&E	Hematoxylin and eosin
HCL	Hydrochloric acid
HF	Hair follicle
HK1.ras	Transgenic mice expressing v-ras^{Ha} from a modified human keratin K1 vector
HK1.fos	Transgenic mice expressing v-fos from a modified human keratin K1 vector
IFC	Immunofluorescent
IHC	Immunohistochemistry
IFE	Interfollicular epidermis
KPC	Keratinocyte Precursor Cells
MAPK	Mitogen activated protein kinase
µg	microgram
mg	milligram
µl	microlitre
ml	millilitre
PBS	Phosphate buffered saline
PCR	Polymerase chain reaction

pdSCC	Poorly differentiated squamous cell carcinoma
p21	Tumour Suppressor Protein 21
p53	Tumour Suppressor Protein 53
p63	Tumour Suppressor Protein 63
p73	Tumour Suppressor Protein 73
PI3K	Phosphatidylinositol 3-kinase
PIP3	Phosphatidylinositol 3,4,5-triphosphate
PTEN	Protein phosphatase and tensin homologue
SCC	Squamous cell carcinoma
SDS	Sodium dodecyl sulphate
SDS-PAGE	SDS polyacrylamide gel electrophoresis
TBST	Tris-buffered saline and Tween20
TPA	12-O-tetradecanoylphorbol-13-acetate
TSG	Tumour suppressor gene
wdSCC	Well differentiated squamous cell carcinoma

Chapter 1: Introduction

General Introduction: The development of transgenic mice that accurately mimic the multistage nature of carcinogenesis provides an ideal opportunity to study the molecular mechanism underlying tumour progression (*Ogilvie et al., 2017; Lampreht Tratar et al., 2018; Tuveson, 2021*). These models offer a tractable approach to verify causal roles for mutations commonly associated with skin carcinogenesis; explore how progression mechanisms unfold *in vivo;* and also have the potential to identify systems that have evolved to inhibit carcinogenesis at each specific stage (*Ogilvie et al., 2017; Lampreht Tratar et al., 2018; Tuveson, 2021*). In clinical terms, the most significant events from the patient viewpoint are those that drive the malignant conversion of benign tumours to carcinomas and subsequent progression to tumours with increasing metastatic potential (*Hanahan and Weinberg, 2011*); and this aspect of tumour progression is a particular strength of this model (*Greenhalgh and Roop, 1994*).

The project builds upon an established, well-characterised carcinogenesis model, with a flexibility to explore a variety of pathways; whilst gaining valuable insights on mechanisms inhibiting/driving tumour progression. Hence, analysis of how the progression mechanism unfolds *in vivo* helps validate suspected driver mutations and identify changes to additional key oncogenes and/or TSGs. This will advance the understanding of how normal molecular processes fail and provide insight for the potential to inhibit this process in proof-of–principal genotypes. By default, this approach also provides novel information regarding normal epithelial differentiation, e.g., effects of β-catenin on keratinocyte differentiation and roles in epidermal barrier maintenance.

Many human carcinomas exhibit mutations in β-catenin, a component of the adhesion complex, which moves to the nucleus to help integrate membrane signals and alter critical gene expression during cell growth (*Morin, 1999; Doglioni et al., 2003; Grigoryan et al., 2008; Krishnamurthy and Kurzrock, 2018*). Thus stage-specific loss or overexpression may drive or inhibit both malignant conversion and the early stages of malignant progression (*Malanchi, et al., 2008; Grigoryan et al., 2008*). Therefore, in this study inducible expression of a stabilised [exon 3-ablated] β-catenin was used to investigate whether canonical β-catenin/Wnt signalling is key to driving skin carcinogenesis (*Doglioni et al., 2003*) and further investigate whether temporal failures in cell-cell adhesion facilitate invasion during the early stages of malignant progression (*Morin, 1999; Doglioni et al., 2003; Grigoryan et al., 2008;*

Krishnamurthy and Kurzrock, 2018). This study may therefore provide valuable insights into the complex molecular interplay involved in skin carcinogenesis, and a platform to evaluate potential therapeutic value of β-catenin/Wnt signalling interdiction.

1.1 Carcinogenesis

Carcinogenesis can be defined as the time taken for normal cells to acquire cancer cell abilities that allow survival, uncontrolled proliferation and invasion thorough the affected organ to become metastatic and ultimately fatal (*Hanahan and Weinberg, 2011*). Often, these abilities are driven by DNA mutation that effects gene expression or gene function that eliminate or alter their roles to induces excess proliferation, facilitate invasion and impair cell-cell adhesion. The most fundamental capability that cancerous cells first acquire is a sustained proliferation state due to inherited [i.e. Cowden's disease (*Liaw et al., 1997*)] or acquired genetic mutation [i.e. from sun exposure (*Zeigler et al., 1994*)] that disturb the normal homeostasis of cell signalling and deregulate subsequent cell growth via maintained cell cycle vitality (*Hanahan and Weinberg, 2011*). These functions and capabilities can be acquired in various types of tumours through different mechanisms and act as drivers or failed inhibitors at different times in the different contexts of multistep tumorigenesis. Thus, once generated, a specific tumour can remain benign, regress or eventually convert to malignancy depending upon the stage-specific responses deployed to inhibit this process.

Several pathways are common to many tumour types. For instance, a common example is a mutation that affects the *ras* family of oncogenes (*Hanahan and Weinberg, 2011; Fernández-Medarde and Santos, 2011; Hobbs et al., 2016*). Here mutations in the GTPase activity that govern the negative feedback loop to inhibit ras activity results in a sustained active state of ras signalling [see below], which affect a plethora of downstream cell signalling pathways that promote proliferation, cell migration, and cell cycle vitality (*Hanahan and Weinberg, 2011; Fernández-Medarde and Santos, 2011; Hobbs et al., 2016*). In addition, once an overt tumour is formed in clinical terms for the patient the most important stage is the progression to malignancy and increasing invasive potential. In this aspect the failure of cell-cell adhesion signalling is a vital component; thus, another common pathway involves somatic mutations in the *β-catenin* gene, that affect its degradation or the molecules that regulate its removal via ubiquination which leads to overexpression and amplification of canonical Wnt signalling.

This results in deregulation of several crucial transcriptional targets and additional failures in direct cell-cell adhesion via β-catenin interactions with E-cadherin (*Morin, 1999; Grigoryan et al., 2008; Krishnamurthy and Kurzrock, 2018*).

The failure in appropriate responses is often in the domain of tumour suppressor genes. Whilst both of these exemplary pathways are common in many types of cancer as highlighted below, cancerous cells acquiring a sustained proliferation state is not enough for tumorigenesis as they need to acquire another vital ability to evade or overcome the tumour suppresser genes responses such as *p53* which is part of the p53 protein superfamily that includes *p53, p63* and *p73* (*Mollereau and Ma, 2014*). The guardian of the genome p53 was found to be defective in more than half of human cancers cases, as it acts as DNA repair mechanism via either apoptosis or cell-cycle arrest in response to cellular stress signals such as excess proliferation (*Mollereau and Ma, 2014; Kastenhuber and Lowe, 2017*). In the absence of these protective responses or if the DNA repair mechanism is not sufficient to halt cancerous cell growth due to irreversible DNA damage, this would result in facilitating tumourigenesis as cancerous cells acquire several other capabilities including resisting apoptosis, immortal replication, angiogenesis and finally invasion and possibly metastasis (*Hanahan and Weinberg, 2011).* The ability of cancerous cells to maintain sustained proliferation and overcome tumour suppresser responses are both essential steps in the process of a multistage carcinogenesis, which will be explored in this study in the context of cutaneous squamous cell carcinoma.

This intricate process of carcinogenesis requires a multi-staged step for tumourigenesis and one of the most valuable tools to study this complicated mechanism is the use of transgenic mice models. This study utilizes the classic skin model of carcinogenesis that involves 3 stages: the initiation and promotion stages to form a benign tumour [papilloma] which may or may not undergo malignant conversion to squamous cell carcinoma [SCC] (*Huang and Balmain, 2014; Balmain and Yuspa, 2014*).

In this study one logical candidate that fits this profile for a multi-stage carcinogenesis study is β-catenin. The deregulation of membrane adhesion and proliferation mediated by failure to regulate β-catenin has been implicated in skin and many alternate tumour types (*Morin, 1999; Grigoryan et al., 2008*). However, although β-catenin′s roles were implicated in SCC due to Wnt/β-catenin activation being central for activation of several proto-oncogenes and also being a integral protein in maintaining cell-cell adhesion, to date no study directly investigated

constitutive activation of β-catenin involvement in developing SCC and this study aims to fill that void in literature.

1.2 Skin layers

The skin is the largest organ of the body and its main function is to act as a barrier from physical harm, as well as preventing loss of body fluids. Skin is comprised of different layers all geared to maintain a protective barrier that helps regulate body temperature and is one of the largest bio reactors e.g. Vitamin D production. Skin can be divided into three layers; the epidermis separated by the basement membrane from the dermis with all the appendages such as sebaceous and sweat glands and hair follicles and finally beneath it is the subcutaneous layer comprised mainly of fat, blood and muscle cells (*Alonso and Fuchs, 2003; Blanpain and Fuchs, 2006*).

The epidermis can be further subdivided into four layers compartments [Fig. 1.1]; *stratum basale [Basal layer],* spinous layer [suprabasal layer], granular layer and cornified layer/envelope (*Alonso and Fuchs, 2003; Blanpain and Fuchs, 2006*). Each layer is formed by keratinocytes that differentiate outwards from the previous layers and express specific keratins, as they commit to terminal differentiation and collectively form a mature stratified epithelium (*Alonso and Fuchs, 2003; Blanpain and Fuchs, 2006*).

The *stratum basale,* also known as the basal layer is the innermost layer of the epidermis which is attached to the basement membrane that separate epidermis from the dermis. This layer is the proliferative layer composed of proliferative transit amplifying keratinocytes and occasional interfollicular epidermal stem cells, whereas most pluripotent stem cells residue in the bulge region of the hair follicle (*Watt and Collins, 2008*). Together these sets of cells feed the proliferation required to maintain the epidermis as a stem cell divides into a stem and daughter cell; in turn the transit amplifying keratinocytes divide into a TA and a daughter cell that commits to the terminal differentiation programme (*Rangel-Huerta and Maldonado, 2017*). Hence the epidermis is continually renewed and mutation containing postmitotic or virally infected cells are eventually sequestered into the environment. This the process of maintaining correct epidermal homeostasis, hair follicle self-renewal and response to skin wounding is under complex control of Wnt signalling as it contributes to the maintenance of hair follicles, sebaceous gland and transit amplifying keratinocytes needed for epidermal differentiation. (*Alonso and Fuchs,2003; Blanpain and Fuchs, 2006; Watt and Collins, 2008*)

[Fig. 1.2]. As outlined in detail below, this brings in one of the main reasons for investigating the roles of β-catenin in skin cancer as β-catenin helps govern the homeostasis of hair follicle morphogenesis and differentiation via their integral role in Wnt signalling (*Morin, 1999; Grigoryan et al., 2008*).

The proliferative basal layer expresses keratin14 [K14] and keratin 5[K5] (*Yuspa et al., 1989; Yuspa, 1994*), whilst the hair follicle express other keratins such as K15 (*Blanpain and Fuchs, 2006*), in addition to keratin K6 which is also a marker for wounding or hyperproliferation in the epidermis (*Rothnagel et al., 1999*) [Fig. 1.1]. Moving upward as proliferative cells in the basal layer commit to differentiate to the spinous layer or supra-basal layer, which express early differentiation markers K1 and K10 (*Blanpain and Fuchs, 2006)*. These keratins are connected through a framework of intermediate filaments that anchor the basal cells to the basement membrane via hemidesmosomes and connect the keratins to intracellular junctions via desmosomes (*Blanpain and Fuchs, 2006*). These desmosomes are made up mainly of cadherin proteins and found to be highly abundant in the supra-basal layer which gives this layer the ability to withstood mechanical stress, whilst the basal layer possess a more dynamic frame- work of cell-cell adherent junctions with microtubules and actin filaments mediated via β-catenin and E-cadherin proteins (*Young et al., 2003; Blanpain and Fuchs, 2006*). This involvement of β-catenin in maintaining cellular adhesion or focal adhesion between the cells in the epidermis is the major reason for investigating β-catenin deregulation in the processes of skin cancer invasion.

Further, to maintain correct adhesion and signalling between epidermal cells the anchorage of both desmosomes and hemidesmosomes requires attachment of cytoplasmic intermediate filaments formed from the correct expression of keratins (*Green and Jones, 1996; Jones et al., 2017*). These intermediate filaments span from the nucleus and extend to the protein structure of desmosomes and hemidesmosome. Thus, providing epidermal cells with tissue integrity and elasticity to withstand mechanical stress whilst maintaining cellular adhesion and signalling via binding to cadherin meditated desmosomal arrangements at the cell membrane (*Green and Jones, 1996; Jones et al., 2017*) [Fig. 1.1].

Following on subsequently in keratinocyte differentiation, the cells of the supra-basal layer migrate into the granular layer which contains keratohyalin granules that help to produce one

of the late-stage differentiation markers, filaggrin and other markers in this layer include structural proteins such as loricrin and keratinocyte transglutaminase (*Candi et al., 2005*). The outmost layer known as the cornified envelope is formed via filaggrin collapsing and flatting the shape of cells giving it the cornified characteristic and reinforcing this layer by process of cross linking several proteins including loricrin regulated by transglutaminase (*Candi et al., 2005; Blanpain and Fuchs, 2006*).

Another major component of the process of epidermal terminal differentiation is the signalling controlled by Calcium ions (Ca^{2+}), also known as calcium dependent terminal differentiation (*Hennings et al., 1980; Lee and Lee, 2018*). The influx of Ca^{2+} ions into keratinocytes drives terminal differentiation as the concentration of Ca^{2+} ions gradually increases from low levels in basal layers that increases in supra-basal to higher concentrations up until cornification (*Hennings et al., 1980; Lee and Lee, 2018*). This process also serves as valuable tool allowing the culture of primary keratinocytes *in vitro* under low calcium conditions as well as controlling the induction of terminal differentiation by increasing the concentration of Ca^{2+}; which is strategy used in this study to investigate oncogenic transformation as this induces resistance to normal terminal differentiation (*Hennings et al., 1980; Greenhalgh et al., 1989*).

Finally, its needs to be noted that since this study is conducted on mouse model, the epidermis of animals with fur are normally very thin [1-2~layers thick] compared to humans (*Sundberg and King, 1996)*. However, at neonatal stage[3-4~days] mice epidermis is thicker as it is hyperplastic until hair follicle is formed, then it will start to thin out and remain constant in adult mice unless hyperplasia is triggered via genetic mutation or wounding (*Sundberg and King, 1996)*. This neonatal hyperplasia makes new-born mice ideal to produce primary keratinocytes for *in vitro* studies (*Hennings et al., 1980; Strickland et al., 1988; Greenhalgh et al., 1989)*.

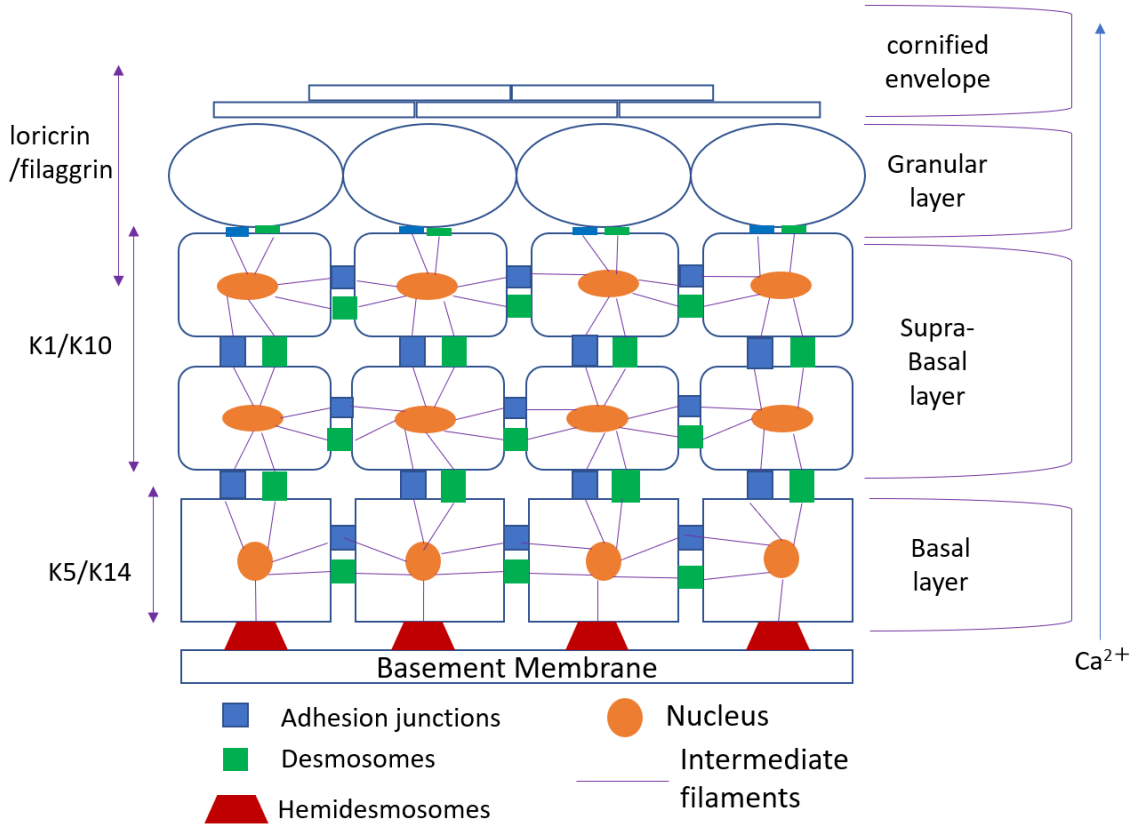

Figure 1. 1: Schematic diagram of normal stratified epidermis with different markers expressed in each layer.

Basal layer cells express K5-K14 and they are anchored to the basement membrane via hemi-desmosomes [red junctions] and cells are connected to each other via desmosomes [green junction] as well as adherent junctions [blue junctions]. Desmosomes and adhesions junctions also connect and surround the supra-basal layer cells which expresses early differentiation markers K1-K10 as basal layer commit to differentiation, whilst late-stage differentiation markers such as loricrin and filaggrin are expressed in granular layer and cornified envelope. The cytoplasmic intermediate filaments [purple lines] emerge from the nucleated cells [orange circle] and links to hemi-desmosomes and desmosomes at cells membrane. The epidermis terminal differentiation program is influenced by concentration of Ca^{2+}as the concentration gradually increases from low levels in basal layer to highest concentration in upper differentiated layers.

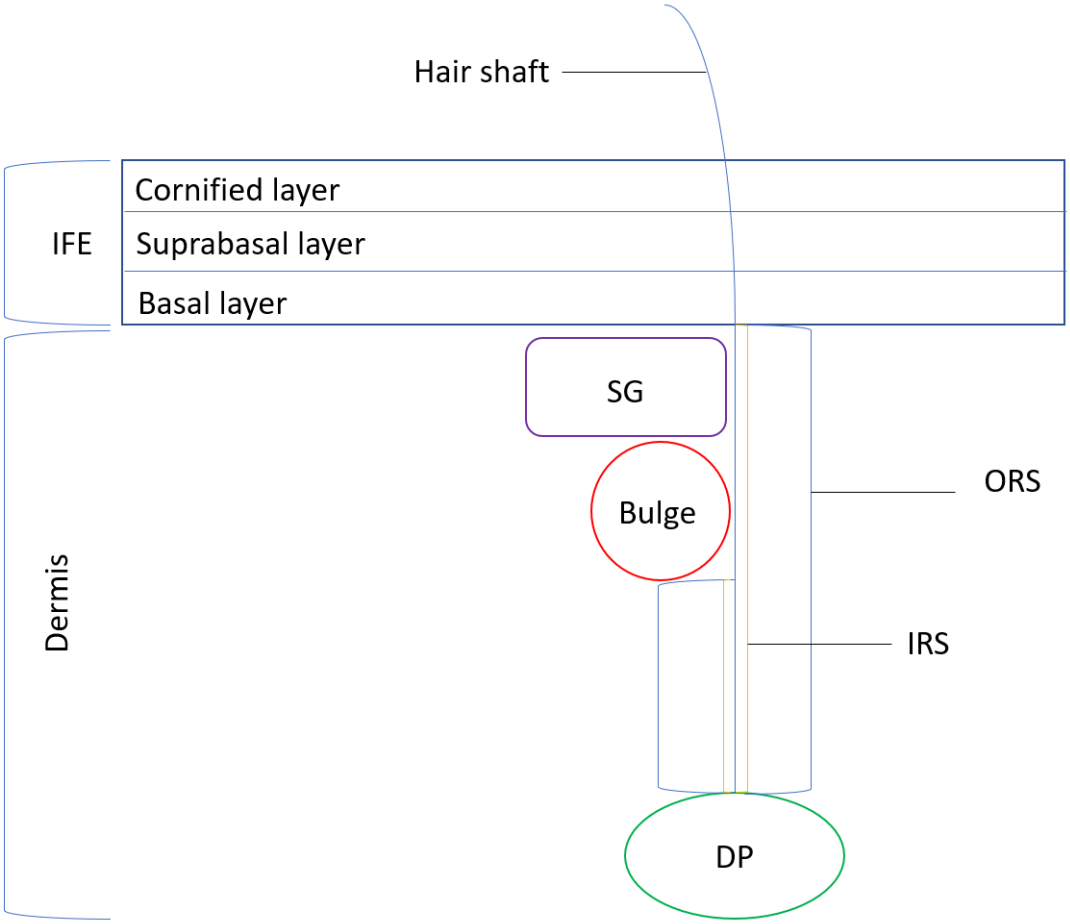

Figure 1. 2: Schematic diagram of normal hair follicle compartments.

Hair follicles are formed in the dermis and at the base of the HF is the dermal papilla [DP], that attached to outer root sheath [ORS], the inner root sheath [IRS] and the developing HF in between IRS. Within The ORS, the bulge region of the HF is located just underneath the sebaceous gland [SG]. As the HF develop to form the hair shaft at the surface of the skin it gradually releases itself from the surrounding sheath to form the hair shaft, thus completing the hair cycle. The bulge region contains the pluripotent stem cells regulated via Wnt/β-catenin signalling and contribute to the maintenance of HFs, SGs and transit amplifying keratinocytes needed for epidermal differentiation.

1.3 Skin cancer and squamous cell carcinoma

Skin cancer is the most prevalent type of malignancy in humans worldwide and more is predominant in the Caucasian population with growing estimation of over a million cases reported each year *(Simões et al., 2015).* Skin cancers can be divided into two types: melanomas and non-melanoma skin cancers [NMSC], which represent the vast majority of cases. Although NMSC considered to be relatively less fatal than melanomas, the increasing number of cases which represent nearly 90% of skin cancer cases burden the health care providers to give patients the best prognosis and treatment. *(Simões et al., 2015; Jones et al., 2020).*

Non-melanomas can be also subcategorised into two major types known as basal cell carcinoma [BCC] representing majority of cases and squamous cell carcinoma [SCC], where SCC is the aggressive type out of the two with higher chance of metastasis and associated with a higher mortality rate (*Huang and Balmain, 2014*; *Barton et al., 2017*). Although BCC cases are higher, the mechanism of developing BCC is well documented to be mostly associated with deregulation of Wnt/sonic hedgehog pathway, whilst SCC could arise from a wide range of signalling irregularities (*Clifford and DiGiovanni, 2010; Huang and Balmain, 2014*).

Squamous cell carcinomas cases are generally associated with skin exposure to UV light, however recent studies have found that developing SCC could be a consequence of hereditary diseases such as multiple self-healing squamous epithelioma, and dyskeratosis *congenita* or sporadic mutation in several key genes (*Huang and Balmain, 2014*), which found to be frequently associated with SCC cases including *Ha-RAS, K-RAS, p53, NOTCH1* and *NOTCH2* (*Huang and Balmain, 2014*). Mutations in these genes were implicated in many types of cancers, but in the context of SCC they highlighted the recurrence of these mutations in different types of Squamous tumours found in skin, neck, head and lung (*Huang and Balmain, 2014*). This finding also suggests that individual developing SCC might be susceptible to other types of diseases or it might be a feature of an underlying illness due to carrying these mutations (*Barton et al., 2017*).

The treatment of SCCs usually requires surgical treatment with or without chemotherapy depending on the seriousness of the condition, however metastasised SCCs are associated with poor long-term prognosis, adding to that the number of new cases each year which burden the health care providers worldwide *(Clifford and DiGiovanni, 2010; Huang and Balmain, 2014;*

Barton et al., 2017). This highlights the importance of providing a better understanding of the mechanism of developing SCCs to help design a better countermeasure to this disease. To achieve that goal, the use of animal models has proven to be a valuable tool in studying the multistep process of carcinogenesis as expanded on in the next section.

1.4 Genetic engineering of animals to study carcinogenesis.

The use of animal models, specifically mice, are one of the most useful tools employed in studying and understanding human cancer for the past century (*Tuveson, 2021*). In terms of cellular and molecular characteristics that govern carcinogenesis the tumour biology between humans and mice shares an estimate of 80% similarity in mutated genes (*Waterston et al., 2002*). This has led to the current great advancement in developing mouse models that offer tractable systems to understand cancer molecular biology via inducing mutations into the transgenic mouse genome in a spatially or/and temporal expressed manner (*Ogilvie et al., 2017; Lampreht Tratar et al., 2018; Tuveson, 2021*).

The creation of transgenic mice can generally be accomplished via three methods involving insertion of new DNA into the mouse genome (*Lampreht Tratar et al., 2018*). The methods are retroviral infection of mouse embryos at different developmental stages, the standard method of microinjection of DNA constructs directly into the pronucleus of fertilized mouse oocytes or lastly via a gene-targeted transgene approach that involves mouse embryonic stem [ES] cell manipulation at specific loci (*Lampreht Tratar et al., 2018*). These different approaches have been used over the years to mimic human cancer biology by creating transgenic mice carrying a gain of function [GOF] mutation or a loss of function [LOF] mutation at specific genes related to the development of a specific type of cancer.

1.4.1 Loss of function mutations in transgenic mice

Inducing a LOF mutation in a transgenic mouse that causes silencing or depletion of specific gene function is a useful tool to investigate possible therapeutic targets and understanding the cause and effect of the gene function in cancer development (*Lampreht Tratar et al., 2018*). This approach has been applied to study different types of genes including oncogenes [e.g. ras, fos], tumour suppresser genes [e.g. p53, p21, PTEN] and even housekeeping genes [e.g actin] (*Walrath et al, 2010*). The knockout of specific gene function or expression was typically accomplished via two methods: either by constitutive knockout, where gene expression is inactivated in every cell or via conditional knockout where the gene expression is inactivated in specific tissues and/or is inducibly modified at specific stages of mouse development or in adults (*Kersten et al., 2017*).

The constitutive knockout also known as generic or conventional knockout uses a gene-targeted transgene approach to create the transgenic mouse (*Jiang, 2013*). Briefly, in this approach genetically modified embryonic stem cells with the targeted transgene are microinjected into mouse embryos and then transferred to pesudopregrant mice. The mice give birth to chimeric offspring carrying both genetically modified cells and normal cells. These chimeric offspring would then be mated with wild type or ICR mice and PCR testing would reveal successful inheritance of the targeted transgene (*Agarwal et al., 2009*). The TSGs p21 and p53 are excellent examples of the constitutive knockout approach [See Chapter 6] as this knock out method tested their general effect on body homeostasis as well as carcinogenesis due to the loss of gene expression with other activated oncogenes such as ras and fos (*Donehower et al., 1992; Greenhalgh et al., 1996*). However, this approach suffers from two major disadvantages, as it does not mimic the sporadic mutations that frequently appear in human carcinogenesis (*Maddison et al., 2005*) and this method is also not applicable to genes that induce embryonic lethality (*Eisener-Dorman et al., 2009*) such as β-catenin and E-cadherin (*Grigoryan et al., 2008; Tian et al., 2011).*

On the other hand, employing an inducible element to the conditional knockout method offers a gateway to overcome the limitations of the constitutive knockout approach e.g., animal viability. Thus, inducible knockout can mimic the sporadic mutations in human carcinogenesis more accurately by inducing the mutation both spatially and temporally at the chosen time and avoiding embryonic lethality or reduced viability in adults (*Walrath et al, 2010*).

The application of the conditional knockout method requires use of bacterial Cre [Cre-loxP] or yeast FLP enzyme [FLP-FRT] technologies, where both function as a tissue specific recombinase to catalyze recombination of a targeted DNA segments encoding specific gene function flanked by loxP sites or FRT sites (*Branda and Dymecki, 2004; Saunders, 2015; Lampreht Tratar et al., 2018*). This technology can be used to either inactivate or activate a gene function depending on the placement and the orientation of the targeted flanked sequence by loxP or FRT (*Saunders, 2015; Kim et al., 2018*). For instance, to create a cre-loxP mouse targeting a specific gene expression in specific tissue [e.g., skin], separate Cre and loxP mice would be created. For example for keratinocytes Cre recombinase can be expressed by promotors such as keratin 14 [K14] or Keratin 5 [K5] (*Brown et al., 1998; Berton et al., 2000; Zhou et al., 2002; Huang and Balmain, 2014 Kim et al., 2018*) to create [K14.creP] or K5 driven cre [K5.creP].

Creating this transgene requires a standard transgene insertion method via microinjection of DNA constructs directly into the pronucleus of fertilized mouse oocytes, where offspring are screened for successful inheritance of the incorporated transgene (*Gordon and Ruddle, 1981; Lampreht-Tratar et al., 2018*). On the other hand, the mouse carrying the flanked sequence by loxP is frequently generated using the gene-targeted transgene approach discussed in the constitutive knockout method. However, here the embryonic stem cells are manipulated to incorporate loxP sites between targeted sequences via selective recombination, where ES resistant clones are inserted into zygotes to create chimeric offspring these are screened for carriers of the loxP transgene known as the Floxed allele (*Lampreht Tratar et al., 2018*). Once the transgene of promotor driven Cre [i.e. K14.creP] and the loxP flanked sequence transgene [i.e PTEN exon 5 or p53 exon 2-10; see chapter 6/7] are generated, they are crossed to create the conditional knockout mouse under the control of cre activation, where this activation could be either non-inducible or inducible (*Saunders, 2015*; *Lampreht Tratar et al., 2018*).

Employing the inducible Cre.loxP technology utilizes the full potential of this approach by having a tissue specific spatial and temporal control over cre activation that consequently activates the targeted mutation flanked by loxP at intended times by the investigator (*Kellendonk et al., 1996; 1999; Whitfield et al., 2015; Saunders, 2015; Kim et al., 2018; Lampreht Tratar et al., 2018*). The inducible system of cre recombinase requires the use of a hormonal binding domain of steroids receptors which include progesterone, estrogen, glucocorticoid, mineralocorticoid and androgen receptors (*Kellendonk et al., 1996; 1999;*

Whitfield et al., 2015; Saunders, 2015; Kim et al., 2018; Lampreht Tratar et al., 2018). The cre recombinase DNA sequence is fused to a mutated form of a hormonal binding domain of choice depending on the type and requirement of the experiment (*Kellendonk et al., 1996; 1999; Whitfield et al., 2015*). For instance, progesterone and estrogen based receptors are both frequently used to provide temporal control yet differ in application.

Thus, cre activity is regulated by fusion to a mutated form of human progesterone ligand binding domain [PLBD] known as Cre.PR1 and can only be activated once a synthetic anti progesterone treatment RU486 is applied to the transgenic animal (*Kellendonk et al., 1996; 1999*) otherwise Cre is sequestered in the cytoplasm. This treatment results in dimerization of the PLBD element and translocation into the nucleus, where the cre component binds to DNA at loxP sites, which result in an irreversible ablation of loxP -flanked [floxed] DNA sequences (*Kellendonk et al., 1996; 1999*). Thus, providing a useful tool to study LOF or GOF mutations at different stages of development and avoids the possible embryonic lethality or genetic defect that may arise from embryonic stage activation. In addition to studying compensatory elements and phenotypes development in response to the induced mutation (*Kellendonk et al., 1996; 1999; Saunders, 2015; Lampreht Tratar et al., 2018*).

This briefly summarises the evolution of inducing germline mutations in transgenic mice and below the differences between the constitutive and conditional LOF approach are outlined together with some similarity in inducing GOF mutations.

1.4.2 Gain of function

The GOF approach in transgenic mice is widely used to study the roles of oncogenes overexpression in driving cancer development (*Lampreht Tratar et al., 2018*). Thus, to achieve this purpose several methods of inducing GOF mutation in transgenic mouse have been developed.

One of which is the classical constitutive random insertion model, where the transgene gene is incorporated randomly into the genome causing GOF of a specific gene expression (*Iwakuma and Lozano, 2007; Konishi et al., 2007*). This can be achieved by viral vector-based transfection of mouse early embryos and implantation of these embryos into female mice where offspring are crossed with ICR mice and can be screened for carriers of the transgene

(*Lampreht Tratar et al., 2018*). More commonly This is achieved via microinjection of DNA constructs directly into the pronucleus of fertilized mouse oocytes where offspring of the mated mice are screened for carriers of the incorporated transgene (*Greenhalgh et al., 1993a; Greenhalgh et al., 1993b; Lampreht Tratar et al., 2018*) [e.g. HK1.ras or HK1.fos see section 1.5]. Here the main drawback is random incorporation of the transgene which may yield unwanted results or birth defects due to uncontrollable expression levels and random integration (*Lampreht Tratar et al., 2018*).

To overcome this limitation, a Knock-in Permissive Locus Model can be employed where a more stable GOF is induced using a known genetic loci called ROSA26 (*Hohenstein et al 2008*; *Casola, 2010*). This loci lacks the expression of any essential genes for body hemostasis and is devised to integrate the GOF transgene under a more controlled expression in conjunction with Cre recombinase to utilize spital and temporal control as well (*Hohenstein et al 2008*; *Casola, 2010*).

Alternatively, the cre.loxP system can incorporate a STOP sequence [strong transcription and translation termination sequence], where the STOP cassette is flanked by loxP site and placed in between the promoter and coding sequence of the target gene (*Jackson et al., 2001*). Thus, the gene of interest cannot be transcribed without cre activation that excises the STOP sequence flanked by loxP resulting in expression of the gene of interest in the targeted tissue in spital and temporal manner (*Jackson et al., 2001; Masre et al., 2017; 2020*).

This briefly summarises some common technologies used in recent years and this study utilized a variety of the discussed approaches as illustrated in sections 1.6-1.8 and Chapters 3-7 below. However, before the evolution of genetic engineering of transgenic mice, a steppingstone in the use of animal models to study carcinogenesis was the use of the classic mouse model of two-stage chemical carcinogenesis.

1.5 The classic mouse model of two-stage chemical carcinogenesis

The animal model of two-stage chemical carcinogenesis is one of the most valuable tools used over the last 100 years that led to a better understanding of cancer development overall (*Balmain and Yuspa, 2014*). This model helped in defining the classical stages of cancer development known as the initiation stage, promotion stage given it the name the two-stage chemical carcinogenesis which result in tumour formation that may or may not progress to malignancy (*Yuspa et al., 1991; Yuspa, 1994; Balmain and Yuspa, 2014*).

The model works via applying doses of chemical mutagen that induces mutations resulting in establishing a pool of cancerous cells and applying another dose of a mutagen at separate time that induces mutations resulting in prompting cancerous cells which could be used together in this fashion or independently from each other in this model (*Yuspa, 1994*). One of the most common initiator mutagens is 7,12-dimethyl-benzanthracene [DMBA], which at low doses leads to inducing several mutations resulting in irreversible DNA damage such as *HRAS* mutation at codon 61 (*Balmain, et al 1985; Roop et al., 1986*). This specific mutation of *HRAS* has been identified to be the main initiating mutation in this model and recent studies have reported this mutation as well to be the most common RAS mutation found in human SCCs (*Huang and Balmain, 2014*). The targeted regions of the epidermis in the initiating step are the proliferative basal layer and bulge region of the hair follicle where most of the stem cells residue (*Huang and Balmain, 2014*).

However, a low-level dose of DMBA is usually not sufficient to produce a tumour therefore promotion is needed via applying another mutagen such as 12-O-Tetradecanoylphorbol-13-acetate [TPA], that induces several other mutations resulting in activation of other pathways including *c-fos* which is highly involved in epidermal proliferation and differentiation *(Greenhalgh and Yuspa., 1988; Greenhalgh et al., 1990).*

Two stage chemical carcinogenesis involving DMBA initiation and TPA promotion leads to formation of squamous cell papilloma with the earliest appearing at 10-12 weeks and are usually TPA independent (*Hennings et al., 1993*) with the majority appearing over the next 20 -60 weeks and are usually dependent on continued TPA promotion. Thus, the first sets usually persist and 10% to 20% progress to squamous cell carcinoma; whist the later cohort typically regress on cessation of TPA promotion *(Hennings et al., 1993).* However, the rate of progression and conversion is highly dependent on the type of mutagens used as initiator and

to some extent on the promoter employed, as well as the level of dose applied to the animal (*Hennings et al., 1993; Yuspa, 1994 Balmain et al., 1994*).

Briefly, in the DMBA/TPA two-stage chemical carcinogenesis model, the sub-carcinogenic dose employed in initiation induced multiple mutations mainly *HaRAS* at codon 61 which led to sustained proliferation due to activation of the ras pathway [see below]. Subsequent promotion with TPA amplified the proliferation rate by activating the fos oncogene which is downstream of the ras pathway. This led to formation of squamous papillomas that may or may not progress to carcinoma.

Although the two-stage chemical carcinogenesis model has provided a valid system to study carcinogenesis (*Hennings et al., 1993; Yuspa, 1994 Balmain et al., 1994*), it suffers from a major flaw, as the use of such mutagens induces numerus mutations that may be irrelevant to the carcinogenic process. Therefore, as outlined below in this study an animal model was employed that mimics the classic two-stage chemical carcinogenesis resulting in papillomas and carcinomas but without the need to use mutagens.

1.6 The HK1 transgenic mouse model of multistage carcinogenesis

Transgenic mouse models of carcinogenesis have evolved greatly over the last 30 years, and one of the great advances in this field is the ability to mimic the two-stage chemical carcinogenesis model via the use of keratin promotors [modified keratin targeting vectors] to achieve exclusive epidermal expression of an oncogene [i.e. *HaRAS, C-FOS*] to initiate carcinogenesis instead of using mutagens (i.e. DMBA). Thus, in cancer studies, the ability to stably introduce genes into the germline of mice has greatly enhanced prospects for the generation of relevant animal models to explore the molecular mechanism of neoplastic disease *in vivo* (*Stewart et al., 1984; Rothnagel et al., 1993; Greenhalgh and Roop, 1994).*

Aside from investigating a known genetic insult, transgenic mice offer the possibility to determine the influence of factors critical for tumour progression, such as blood supply, an intact immune system, hormonal and cell-mediated growth controls, and physical barriers to cell growth. These parameters are absent in cell culture systems, however once developed, cells derived from transgenic models are easily exploited for further *in vitro* experimentation. A useful transgenic model system must be able to assess relevant multiple, stage-specific

genetic or epigenetic insults. In this respect, mouse skin is an ideal target tissue, being the classical laboratory animal model for multi-stage carcinogenesis for the last 50 years, with an inherent discrete series of well-defined tumour pathologies and well characterised molecular biology (*Balmain and Yuspa, 2014).* This fact, coupled to the well characterised molecular biology of skin makes, it an ideal tissue to couple to the latest in inducible gene switch technology to explore oncogene and TSG synergism in vivo with typically a minimal threat to the viability of the animal.

In the design of these studies, a strength in terms of animal research is that by employment of epidermal-specific expression vectors coupled to an inducible cre/lox system (*Berton et al., 2000*), disease is prevented in internal organs or during embryogenesis and development- but as this project evolved, this was not the case. Moreover, in addition to being able to localise disease to a specific skin site, use of inducible systems gives breeder animals that are non-phenotypic until application of the inducer hormone, a significant feature of the refinement category of the 3Rs during breeding. As found in this β-catenin model, such internal expression can compromise animal viability particularly when assessing multiple insults.

Another major advantage of skin is the accessibility which facilitates application of the inducer hormone to localize the disease and allows macroscopic observation of neoplastic events without invasive procedures. Once established each parental genotype becomes a comparison control in the exploration of transgene synergism in bi-genic and tri-genic genotypes to help minimize numbers.

In this study the model uses a modified human keratin 1 (HK1) as targeting vector to achieve exclusive epidermal expression of HaRAS and C-FOS oncogenes (*Greenhalgh et al., 1993 a-c*). The HK1 vector is a truncated form of the human K1 gene that is missing several regulatory elements in comparison to the mouse K1 (MK1) gene, which results in the HK1 being expressed in 30-40% of the basal layer keratinocytes with proliferative potential, whilst the indigenous MK1 is only expressed in rare basal cells as they commit to differentiation (*Rothnagel et al., 1991; 1993*) [Fig. 1.3]. Further this HK1 vector 1 targets exclusively to the interfollicular epidermis [IFE] [Fig. 1.3], which for ras and/or fos activation resulted in formation of benign papillomas that do not spontaneous convert to carcinoma (*Greenhalgh et al., 1993a-c; 1995; Greenhalgh and Roop, 1994*). On the other hand, using basal layer keratin

as promoter such as Keratin5 that also targeted HaRAS expression to the outer sheath of the hair follicle and bulge region where most of the epidermal stem cells reside; which resulted in the formation of malignant SCCs and spindle carcinomas (*Brown et al., 1998*).

This expression in the basal layer, made this truncated HK1 clone an ideal vector to achieve expression exclusive to the epidermis and target the proliferating basal layer keratinocytes with activated oncogenes (*Rosenthal et al., 1991*). Thus, mimicking the two-stage chemical carcinogenesis, the initiating and promotion stages to form papilloma in this model can be done by expressing activated ras and fos oncogenes with HK1 as vector *[HK1.ras]* and [*HK1.fos*] to achieve the expression in the keratinocyte basal layer of the intra-follicular epidermis without the use of mutagens (*Greenhalgh et al., 1993 a-c; 1995; Greenhalgh and Roop, 1994*). Given that these papillomas do not convert to malignancy without additional oncogene or TPA promotion (*Greenhalgh et al., 1995*) it makes them ideal to study causal roles of other oncogenes involved in tumour progression and conversion to carcinoma (*Greenhalgh et al., 1995; Wang et al., 1995; 1998; Yao 2006; 2008; Macdonald et al., 2014; Masre 2017; 2020*)

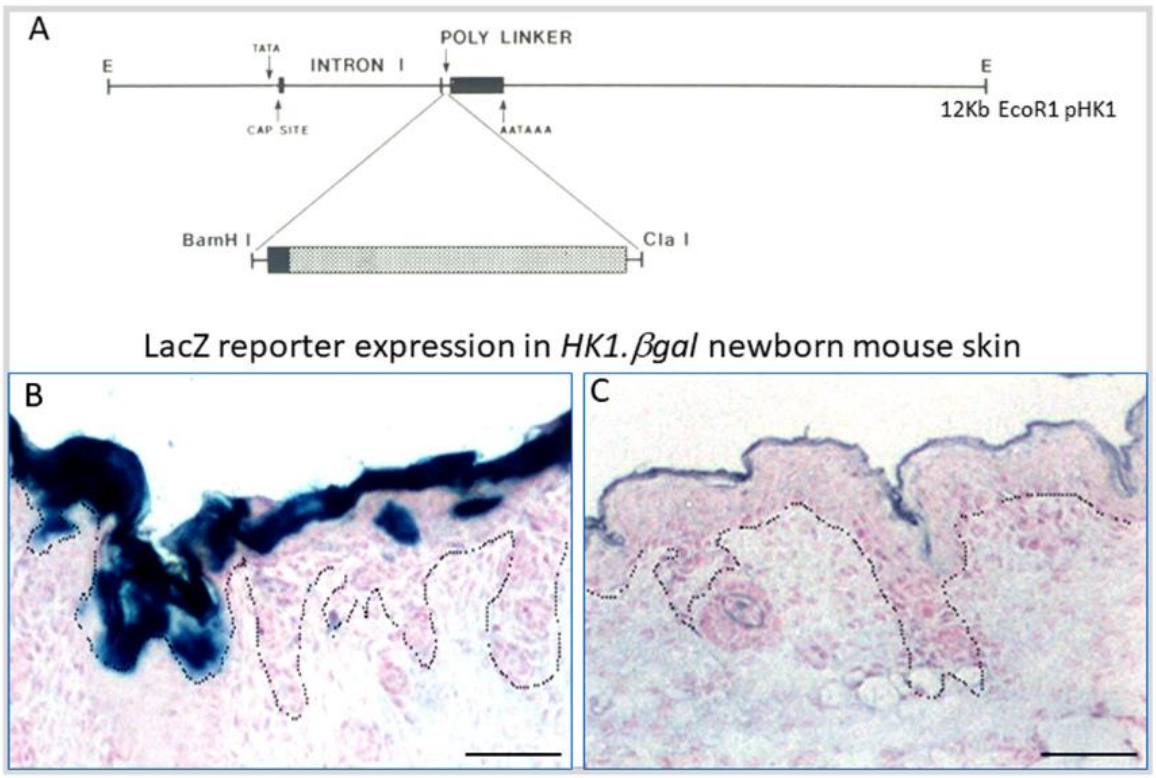

Figure 1. 3: Confirmation of the expression profile of the HK1 vector:

[A] Diagram of human keratin 1 [HK1] targeting vector. This is based on the 12-kb EcoRl clone of the human keratin 1 gene which proved to be truncated; missing the 3' flanking sequences that contain the Ca^{2+}-responsive regulatory elements for correct supra-basal expression and is expressed in proliferative basal cells. This enabled the targeting of transgene expression exclusively to basal layer keratinocytes [but not follicles] and also following conversion to malignancy *HK1 vector* expression is detectable in SCC (*Greenhalgh et al., 1995)*. In this model activated v-ras^{Ha} or FBR/J v-fos genes were inserted at the Bam Hl and Cla l sites (*Greenhalgh et al, 1993a; 1993b*). [B] Introduction of the LacZ reporter gene in *HK1.β-gal* mice and staining newborn frozen sections with X-gal, confirms HK1 vector expression in the basal layers of interfollicular epidermis but not hair follicles. [C] Wild type neonatal sibling control epidermis (*Greenhalgh et al., 1995*). Scale bars. 75µm

1.6.1 Phenotypes produced in *HK1.ras* transgenic mice

The ras family of oncogenes including *Ha-ras, K-ras* and *N-ras* are one of the first oncogenes to be discovered over the last 30 years. This family play a crucial role in cellular proliferation, cell cycle vitality, cells migration, apoptosis and senescence. This can be attributed to ras being the gate keeper of a plethora of downstream effectors that a play major role in cellular proliferation and differentiation *(Fernández-Medarde and Santos, 2011; Hobbs et al., 2016).*

The ras gene activation is governed by GTPases activation cycle between ras-GDP binding inactive state and ras-GTP binding active state, which is the process that is conveniently found to be defective in mutated ras leading constitutive activation of ras pathway [Ras-GTP binding active state on ras *(Huang and Balmain, 2014; Hobbs et al., 2016).* In skin ras can be activated via epidermal growth factor receptor [EGFR] signalling, which plays a vital role in skin homeostasis *(Kern et al., 2011; Doma et al., 2013).* EGFR signalling leads to downstream switching of ras-GDP [inactive] binding to ras-GTP [active] starting the ras pathway cascade known as Ras/MAPK pathway, where ras activates RAF which phosphorylates MEK and activates ERK leading to activation of several transcriptional targets such as AP-1 complex via activating *fos/jun* component [Fig. 1.4] *(Deng and Karin, 1994; Roberts and Der, 2007; Doma et al., 2013).* Ras also activates other pathways such as the phosphoinositide-3 kinases (PI3K)/AKT pathway (*Martini et al., 2014; Hopkins and Parsons, 2014*) that induces cellular proliferation and resistance to apoptosis [Fig. 1.4] (*Martini et al., 2014; Hopkins and Parsons, 2014*). This pathway is of interest in this study as the PI3K/AKT pathway is negatively regulated by tumour suppresser gene PTEN (*Hopkins and Parsons, 2014*) and deregulation of this pathway could induce β-catenin overexpression through AKT associated phosphorylation of GSK3-β that is responsible for down regulating β-catenin [Fig. 1.4] [see β-catenin section], which is a mechanism hypothesized to be highly associated with the result seen in co-operation between *ras, fos* and *PTEN* loss *(Yao et al., 2006;2008; Macdonald et al., 2014*) [see chapter 3].

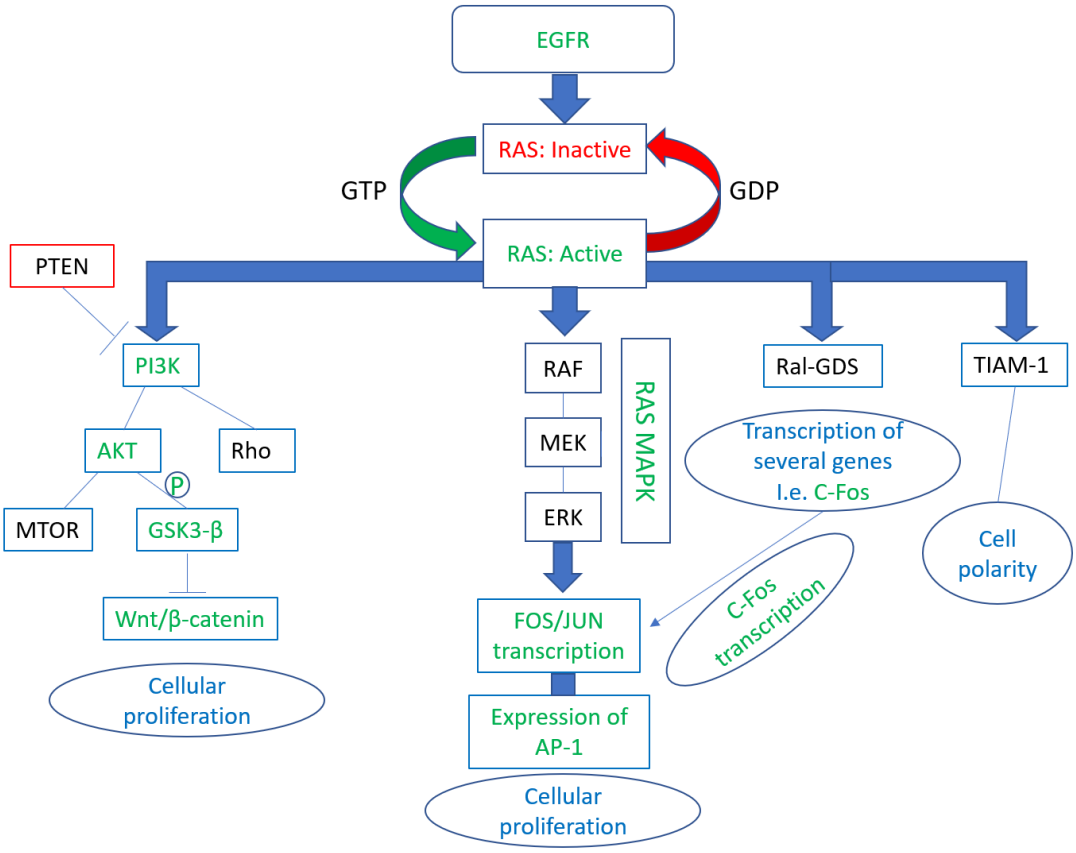

Figure 1. 4: Schematic diagram of RAS activation and downstream signalling [green highlighted pathways are of interest in this study].

EGFR Signalling triggers GTPase activity of ras from the resting GDP-bound state to the active GTP-bound state resulting in activating several pathways downstream of the MAPK pathway cascade including activation of transcription of Fos/Jun family members [i.e., C-fos] leading to active expression of AP-1 which induces cellular proliferation and differentiation. Ras activation also interacts with PI3K/AKT pathway which is also inhibited by PTEN regulation. This failure of PTEN [as in the HK1 model] leads to oncogenic activation of AKT that phosphorylates GSK3-β to inactivate roles in β-catenin degradation and thus activating Wnt/β-catenin pathway resulting in increased cellular proliferation.

The implications of *ras* in all of these pathways has increased the research attempting to find an anti-ras therapy, since ras mutations are found in approximately 30% of all types of human tumours. Most of ras mutations are missense found in three hotspot codons 12,13 and 61 *(Fernández-Medarde and Santos, 2011; Hobbs et al., 2016)*. In human SCCs cases including skin, head, neck and lung, Ha-Ras mutations are the most prevalent, where according to most recent studies the specific mutation at codon 61 is the most common *(Huang and Balmain, 2014)*.

This specific mutation is known as the initiating mutation in the DMBA treated mouse model of two-stage chemical carcinogenesis and the codon 61 mutation is also the mutation that activates v-ras^{HA} [Harvey murine sarcoma virus (Ha-MSV)]. When this *v-ras^{HA}* gene was infected into mouse primary keratinocytes the results showed a transforming phenomena in terms of resistance to calcium induced terminal differentiation (*Hennings et al., 1980*) and increased proliferation in response to *v-ras^{HA}* activation (*Roop et al., 1986*). Furthermore, when these infected cells were grafted onto nude mouse skin this resulted in formation of benign papillomas (*Roop et al., 1986*). Thus, this study established the ability of *v-ras^{HA}* to mimic the initiation step of DMBA-mediated two-stage chemical carcinogenesis but, it still required a promotion agent in the form of wounding to form the papilloma *(Roop et al.,1986*).

This study has facilitated the ability of driving ras activation in skin using a keratin promoter. The model uses the HK1 promoter (*Rosenthal et al., 1991*) to drive exclusive epidermal expression of v-ras, creating *HK1.ras* transgene (*Greenhalgh et al., 1993a)*. There are two transgenic mouse strains of *HK1.ras* in this study, known as *HK1.ras^{1205}* and *HK1.ras^{1276} (Greenhalgh et al., 1993a).* Mice carrying *HK1.ras^{1205}* are capable of developing a stable benign papilloma, within 6-7 weeks in response to wounding promotion, whilst the *HK1.ras^{1276} line* is insensitive to wound promotion and needs the promotion stimulus from *HK1.fos* to produce papillomas (*Greenhalgh et al., 1993c*). This project employs *HK1.ras* line 1205 not 1276, and is thus referred to as *HK1.ras* throughout the text.

Mice carrying the *HK1.ras* transgene can be identified grossly at neonatal stage [~3-5day] by having a wrinkly skin phenotype, that disappears during neonatal development via a massive hyperkeratosis beginning by d10 such that by d21 these mice start to maintain a normal looking skin indistinguishable from wildtype mice at adulthood. Of importance, these papillomas formed by *HK1.ras* expression did not convert to malignancy unless treated repeatedly with TPA, which make this model ideal to study the genetic mutations that drive malignant conversion and tumour progression *(Greenhalgh et al., 1993c; 1995).*

1.6.2 Phenotypes produced in *HK1.fos* transgenic mice

Fos is a family of genes [c-fos, fosB, Fra-1, Fra-2] that form a heterodimer with jun family of genes [c-jun, junB, and junD] and bind to DNA to regulate transcription of the activator protein 1 [AP-1]. This plays a crucial role in skin homeostasis, cellular proliferation, differentiation and apoptosis. In skin homeostasis AP-1 transcriptional factors are highly implicated in regulating terminal differentiation (*Fisher et al., 1991; Greenhalgh et al., 1993b; Basset-Seguin et al., 1994; Angel et al., 2001; Eckert et al., 2013*). AP-1 is one of the transcriptional targets of the ras-MAPK pathway as mentioned earlier, and it was reported that increased expression of AP-1 associated transcriptional factors promote tumorigenesis (*Young et al., 1999*) which was associated with a significant increase in AP-1 transcription genes specially C-FOS (*Greenhalgh and Yuspa., 1988; Greenhalgh et al., 1990; Schlingemann et al., 2003*). The roles of fos in skin was also investigated in transgenic mouse skin using LacZ/fos fusion which illustrated that fos is expressed in all layers of the intrafollicular epidermis [IFE] including hair follicle (*Smeyne et al., 1992*).

Similarly, in adult humans the expression of fos was also normally found in basal layer and upper differentiated layers of the epidermis *(Fisher et al., 1991; Greenhalgh et al., 1993b; Basset-Seguin et al., 1994; Angel et al., 2001)*. This indicate that fos is an essential component in maintaining epidermal differentiation and deregulation of its function could result in facilitating tumorigenesis. To test fos roles in tumourigenesis, an in-vitro study tested inducing transfection of the FBJ murine osteosarcoma virus *v-fos* gene into a papilloma LINE SP1 (*Strickland et al., 1997*) derived from DMBA/TPA promotion and thus expressing an activated ras^{HA} (*Greenhalgh and Yuspa, 1988*). This experiment resulted in formation of malignant SCC when grafted into nude mice skin (*Greenhalgh and Yuspa, 1988*) Further experimentation confirmed the co-operation of *v-fos* and $v\text{-}ras^{HA}$ via infection into primary mouse keratinocytes and grafting into nude mice skin which again resulted in highly aggressive SCCs (*Greenhalgh et al., 1990*). In this study primary keratinocytes carrying *v-fos* alone resulted in a hyperplastic skin in grafts, whilst cell lines carrying $v\text{-}ras^{HA}$ produced benign papilloma (*Greenhalgh et al., 1990*). Both of these studies highlighted that overexpression of fos alone was insufficient to produce skin tumours, however co-operation with ras activation enable tumorigenesis and malignant conversion which highlight the promotion potential of fos as an oncogene.

The roles of c-fos in SCCs using HK1 promoter tested the effect of driving c-fos expression exclusively in the epidermis. This was conducted in a similar manner to HK1.ras, where the viral form of aggressive v-fos driven from Finkel-Biskis-Jenkins (FBJ) osteosarcoma virus (*Greenhalgh et al., 1990*) was used to construct HK1.fos transgene*; (Greenhalgh et al., 1993b).* In the absence of other events, tumour development in *HK1.fos* mice took 8-12 months post ear-tag wounding for *HK1.fos* mice to develop benign, highly keratotic papillomas *(Greenhalgh et al., 1993b*) and as outlined below required the initiating elements of ras^{Ha} activation (*Greenhalgh et al., 1990; 1993c*) as a prior event to papilloma formation. Of note in the *in vitro* grafting experiments (*Greenhalgh et al., 1988; 1990)* this led to metastatic SCC, whereas in vivo the more relevant HK1 transgenic mouse model led to stable autonomous papillomas without spontaneous malignant conversion (see below*; Greenhalgh et al., 1993c).*

Indeed, in the HK1 model TPA promotion was often required to induce malignancy and *HK1.fos* mice required applying TPA treatment for over 12 months which eventually resulted in papillomas that converted to SCC *(Greenhalgh et al., 1995*) and here endogenous *c-*ras^{Ha} was found to be activated (*Sutter et al., 1994; Greenhalgh et al., 1995)*. Thus, again ras and fos with extended TPA promotion was required for conversion to malignancy. These data indicate that unlike *in vitro* models and graft assays, even *HK1.fos* combined with amplified expression of c-fos alone was insufficient for tumour progression (*Greenhalgh et al., 1993b*) and other multiple oncogenic events are needed such as *HK1.ras* (*Greenhalgh et al., 1995*) or long-term promotion from wounding or TPA to elicit even a benign papilloma- hence these mice are ideal to study the requirements for papilloma formation and malignant conversion.

Additionally, in other transgenic mouse studies conducted on constitutive expression of fos resulted in osteosarcomas and chondrosarcomas due to fos roles in promoting bone growth, whilst fos null studies showed several defects including osteoporosis, lymphopenia and delayed gametogenesis (*Saez et al., 1995*). However, on an epidermal level c-fos null mice showed a fairly normal epidermal differentiation pattern indistinguishable from normal mouse (*Saez et al., 1995*). This suggests that c-fos absence in the early stages of tumour promotion could be taken over by other oncogenes in response to TPA treatment [v-ras/c-fos null], but later stage malignant conversion is highly dependent on c-fos expression [v-ras/c-fos wildtype].

1.6.3 Phenotypes of *HK1.ras/fos* mice and tumour development

To develop squamous cell benign papilloma in the *HK1.ras* genotypes, wound promotion was required, which was activated via tagging the mice ear. Hence *HK1.ras[1205]* develop a benign a papilloma within 8-10 weeks post ear tag wounding in 100% of animals; whilst *HK1.fos* genotypes develop a delayed papilloma 8 -12 moths post tagging (*Greenhalgh et al., 1993a; 1993b*). One aspect of the *HK1.ras* 1205 strain was their acute sensitivity to wound or TPA promotion. Given this observation and experiments performed in the USA, this indicated that use of this line crossed with *HK1.fos* mice could exceed the limits of animal experimentation in the UK ; thus as outlined above the alternate *HK1.ras* ^{1276} strain was employed in these co-operation experiments (*Greenhalgh et al., 1993c*). *HK1.ras* ^{1276} mice never develop papillomas however when crossed with HK1.fos mice in the UK, the bi-genic *HK1.ras*^{1276}*/fos* progeny now develop papillomas over a slower 4-6 month period (*Greenhalgh et al., 1993c)*[Fig. 1.5] and these were subsequently employed in *HK1.ras*, *HK1.fos* and PTEN loss experiments (*Yao et al., 2006; 2008; Macdonald et al., 2014*).

The HK1 promoter enabled *HK1.ras/fos* to be expressed at a late stage of embryonic development [day ~19] thus avoiding any lethality *in utero* and the exclusive epidermal expression driving constitutive expression of *ras* and *fos* oncogenes which elicits a notable increase in changes to the overt appearance of these mice. Again, mice carrying the *HK1.ras* transgene can be identified grossly at the neonatal stage [~3-5day] by having a wrinkly skin phenotype, that shortly disappears via a massive hyperkeratosis by d10 and by d21 *HK1.ras* mice of either strain maintain a normal looking skin indistinguishable from adult wild type mice. The overt appearance of these mice is shown in Fig. 1.5, and here the *HK1.ras*^{1276}*/fos* mice initially exhibit a greater degree of wrinkled skin resulting in a greater hyperkeratosis which can persist into early adulthood but then returns to normal. With respect to papillomatogenesis the wound sensitive *HK1.ras* line produces larger papillomas compared to age matched *HK1.ras*^{1276}*/fos*, but if the tag is lost in *HK1.ras* 1205 line papillomas typically regress whereas 1276/fos papillomas persist- however these papillomas did not spontaneously convert to malignancy even when maintained for over 12 -16 months, unlike in many other models (*Brown et al., 1998*).

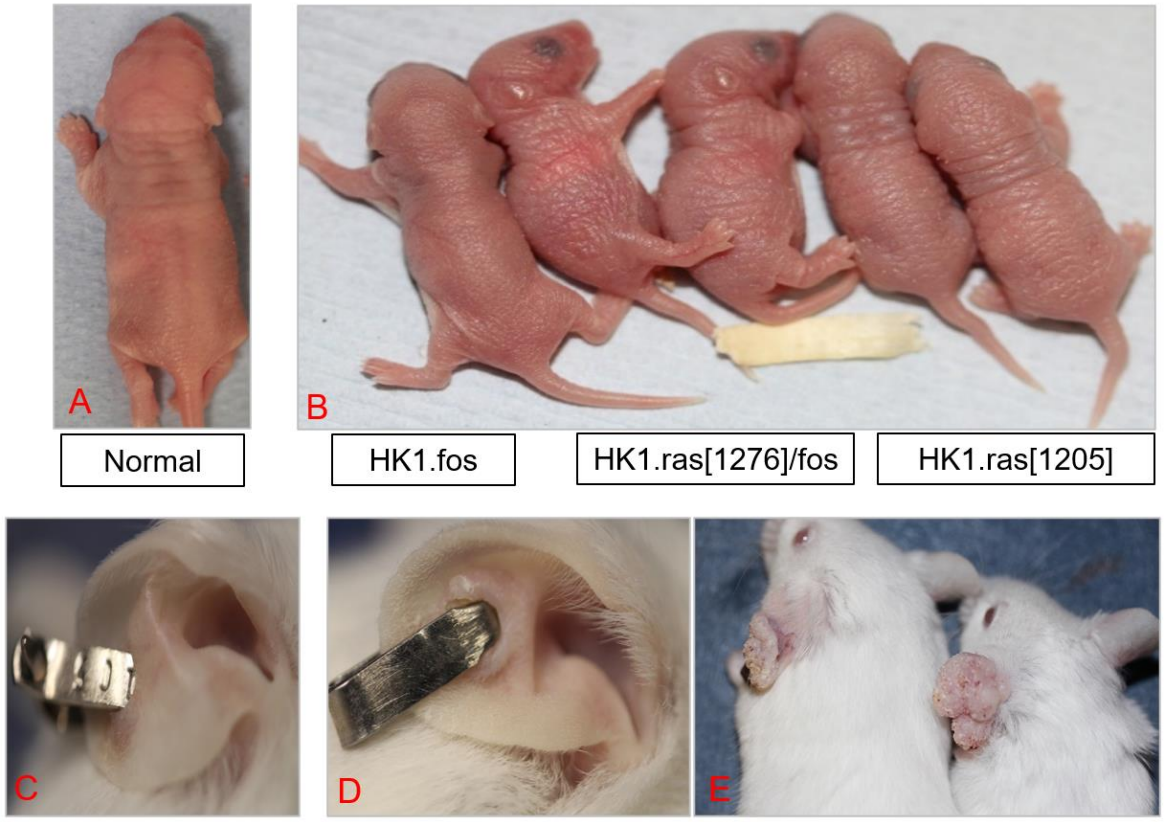

Figure 1. 5: Overt appearance of HK1.ras and or fos mice from neonatal stage to formation of benign ear papillomas at tagged ear sites.

[A] Normal mouse neonatal skin. [B] *HK1.ras[1276]/fos* neonatal skin shows a wrinkly skin phenotype with slightly increased severity of phenotype in the 2 middle neonates compared to fos [left] and the two 1205 alone [right]. [C] shows Normal tagged ear, whilst [D] *HK1.fos* mouse eventually exhibits bi-lateral keratotic ears beginning in the tagged ear but no overt papillomas until 10 -12 months and not in all mice. [E] *HK1.ras*[1205] developed benign papillomas typically within 6-10 weeks in 100% of animals that are prone to regress if the tag is lost; and similarly *HK1.ras[1276]/fos* mice developed smaller papillomas initially at wounding site that occasionally became bi-lateral.

Histologically, in *HK1.fos* mice the epidermis showed no significant abnormalities compared to normal [Fig. 1.6] except for a mild hyperplasia that arises around at 3-4 month after birth in tagged ears (*Greenhalgh et al., 1993b*) similar to the hyperplasia produced in neonatal 1205 neonatal mice consistent with wrinkled skin appearance; whilst co-operation of *HK1.ras*^{1276} and *HK1.fos* showed histologically similar phenotypes but with increased severity such as degree of hyperplasia and hyperkeratosis [Fig. 1.6] (*Greenhalgh et al.,1993c*). With time

HK1.ras and *HK1.ras/fos* mice exhibited papilloma histotypes with little evidence of malignant conversion [Fig. 1.6].

In order to confirm this histotype and assess effects on differentiation, *HK1.ras/fos* mice were assessed by double-labelled immunofluorescence staining to investigate the epidermal changes in differentiation via keratin expression and this also served as a valuable tool to assess the degree of tumour invasiveness in these genotypes. For instance, assessing the expression of K14 provide a good mapping of the epidermis, as it is a basal layer keratin expressed in hair follicles and throughout the epidermis due to its high stability as a protein. This made K14 the standard counterstain[red] in analysing different genotypes in this model to highlight the epidermis, hair follicles and tumour *(Greenhalgh et al., 1993a; 1993b).* In addition analysing the expression of the early differentiation marker K1 that is normally expressed in supra-basal layers becomes reduced as papillomas convert to malignancy and is lost during progression to aggressive SCC and thus served as one of the main tools to assess the differentiation pattern and the benign nature of the papillomas formed. As shown in Fig. 1.6 analysis of UK biopsies also confirms these original data, in normal epidermis, keratin mK1[green] against K14[red] is expressed in the supra basal epidermis; whilst mK6α is confined to the HFs together with K14 [Fig. 1.6B&C.]

In epidermal hyperplasia *HK1.ras/fos* [*HK1.ras*^{1205} identical] [not shown] IF analysis showed that K1[green] maintains this normal expression again confined to the now expanded supra-basal layers, with a delay in its onset due to expansion of the proliferative layer as highlighted by the thicker K14 positive basal layers throughout the epidermis [Fig. 1.6E]. This K1 expression is maintained in the supra-basal layer in typical benign papillomas formed in this model, again confirming their benign nature and indicting that differentiation remains relatively ordered despite ras and fos expression in this model *(Greenhalgh et al., 1993a; 1993b; 1995).* Similarly, in the HK1 model the hyperproliferation marker K6α [green]/K14[red], normally only expressed in hair follicles or in response to epidermal stress such as wounding or psoriasis, was expressed strongly in the hyperplasia in addition to the normal hair follicle expression [Fig. 1.6 C]. Hyperplastic genotypes displayed strong and uniform mK6α expression in the interfollicular basal and supra-basal layers [Fig. 1.6] which was also the case in benign papillomas regardless of genotype (*Greenhalgh et al., 1993a-b; 1995*) [Fig. 1.6 I].

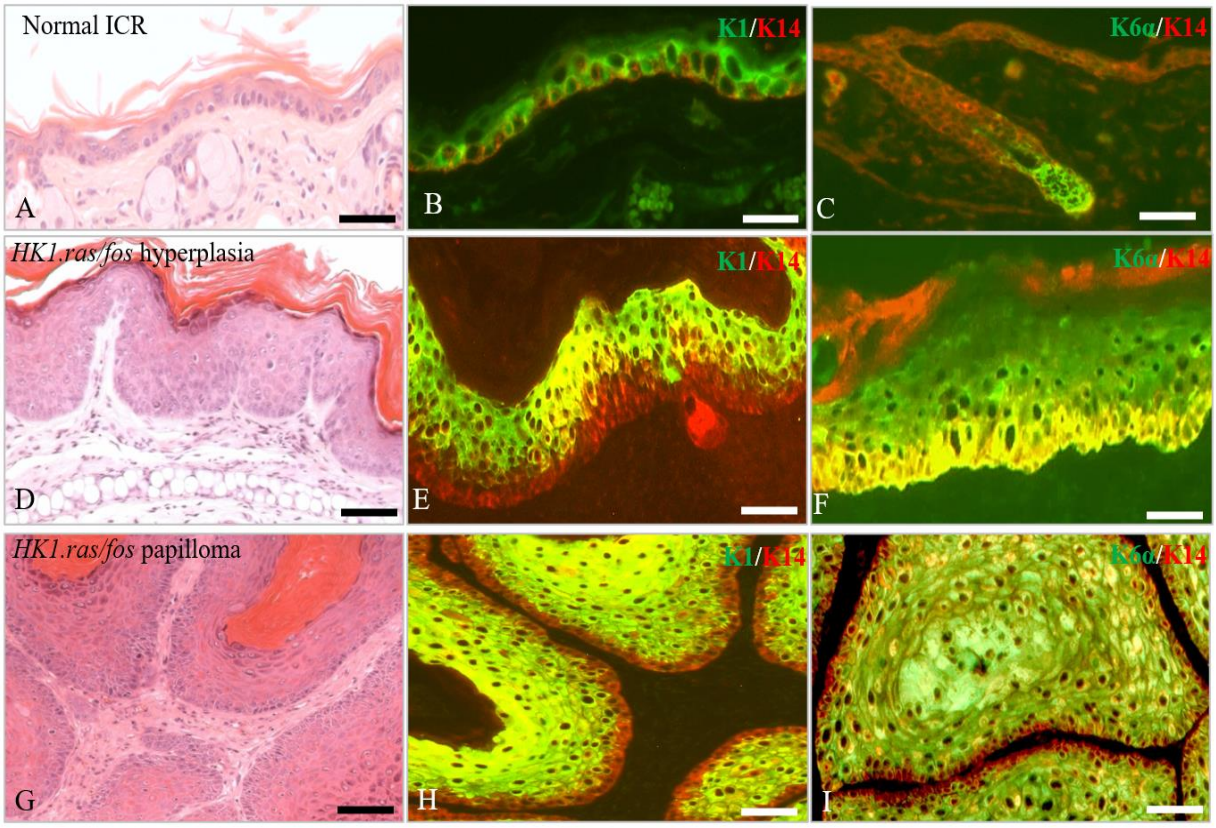

Figure 1. 6: Histotype and expression of keratin K1 and K6α expression in HK1.ras/fos hyperplasia and papilloma

[A] H&E staining of normal mouse skin shows the thin nature of the epidermis being only one or two cells in depth; also visible are typical telogen [resting] follicles with associated sebaceous glands. [B] Double-labelled IF analysis of early differentiation marker keratin K1 (green) expression against keratin K14 (red) shows normal K1 expression is confined to the supra-basal layers, whereas [C] shows K6α expression normally expressed in hair follicles only. [D] Typical pre-neoplastic epidermal hyperplasia in *HK1.ras/fos* mice is typified by expansion of supra-basal layer [acanthosis] due to increased proliferation in the expanded basal layers that give rise to a papillomatous [folded] epidermis consistent with the appearance of wrinkled skin. [E] Analysis of K1 in hyperplasia maintains a normal expression in the expanded supra-basal layer, whist K14 expression is more prominent in the expanded basal layer. [F] In response to the stress signals of epidermal hyperplasia, mK6α is expressed strongly in both basal and supra-basal layers. [G] Histology of typical *HK1.ras/fos* papillomas again show an ordered nature to differentiation where K1 expression remains strongly supra-basal confirming the benign nature of the tumour, whilst [H] mK6α also remains strongly expressed in both basal and supra basal layers. Scale bars: A,D,E&F: 50µm; B: 25µm; D,G,H&I: 100µm **[confirmatory experiment to illustrate the *HK1.ras/fos* model]**

To help investigate the mechanism driving stage-specific tumour progression in this model, the phenotypes produced by the combination of genotypes also involved assessing tumour suppresser gene expression at different stages from the early hyperplasia through the benign papilloma intermediates and eventual malignant carcinomas *(Yao et al., 2006;2008;*

Macdonald et al., 2014). In particular, given their frequency of inactivation in human carcinogenesis, the tumour suppresser genes [TSG] p53 and P21 were of great importance in assessing changes to the epidermal differentiation and the causality of their overexpression in response to ras and fos activation and potential consequences of their inactivation at each specific stage of tumour progression.

In humans, p53 is the most mutated tumour suppresser gene in cancer, as it is responsible for inducing protective cellular mechanism such as DNA repair, cell cycle arrest and apoptosis, in response to cellular stress signals including genetic instability and excess proliferation (*Kastenhuber and Lowe., 2017*). In human spontaneous SCC, p53 was found to be frequently mutated and in DMBA/TPA mice model, p53 was found to be commonly mutated or lost in SCCs (*Huang and Balmain, 2014*). This enforces the roles of p53 in epidermal homeostasis and tumour prevention in SCCs; however, the story is far more complex as in this model loss of p53 induced an intriguing paradox of blocking papilloma formation the *HK1.ras* mice (*Greenhalgh et al., 1996*) that is explored further in this study. The p21 is one of the major downstream effectors of p53 and plays a crucial role in DNA repair, cell cycle arrest, apoptosis and epidermal differentiation as a counter mechanism to tumorigenesis and genetic instability (*Topley et al., 1999*). This is clearly exemplified below in *HK1.fos-Δ5PTEN* mice and the aetiology of keratoacanthoma (*Yao et al., 2008*); and also in *HK1.ras/fos-Δ5PTEN* mice as it appeared to antagonise both AKT and β-catenin to delay malignant progression [below] (*Macdonald et al., 2014*).

In the *HK1.ras/fos* mouse model, the expression of p53 was sporadic and very weak in early stages of hyperplasia and as the epidermis expanded to form the papilloma, p53 expression becomes very strong and nuclear halting any further progression. Similarly, for p21 in early stages of hyperplasia it was almost absent from the epidermis and as the papillomas form it became strong and nuclear *(Yao et al., 2006; 2008; Macdonald et al., 2014)* [Fig. 1.7].

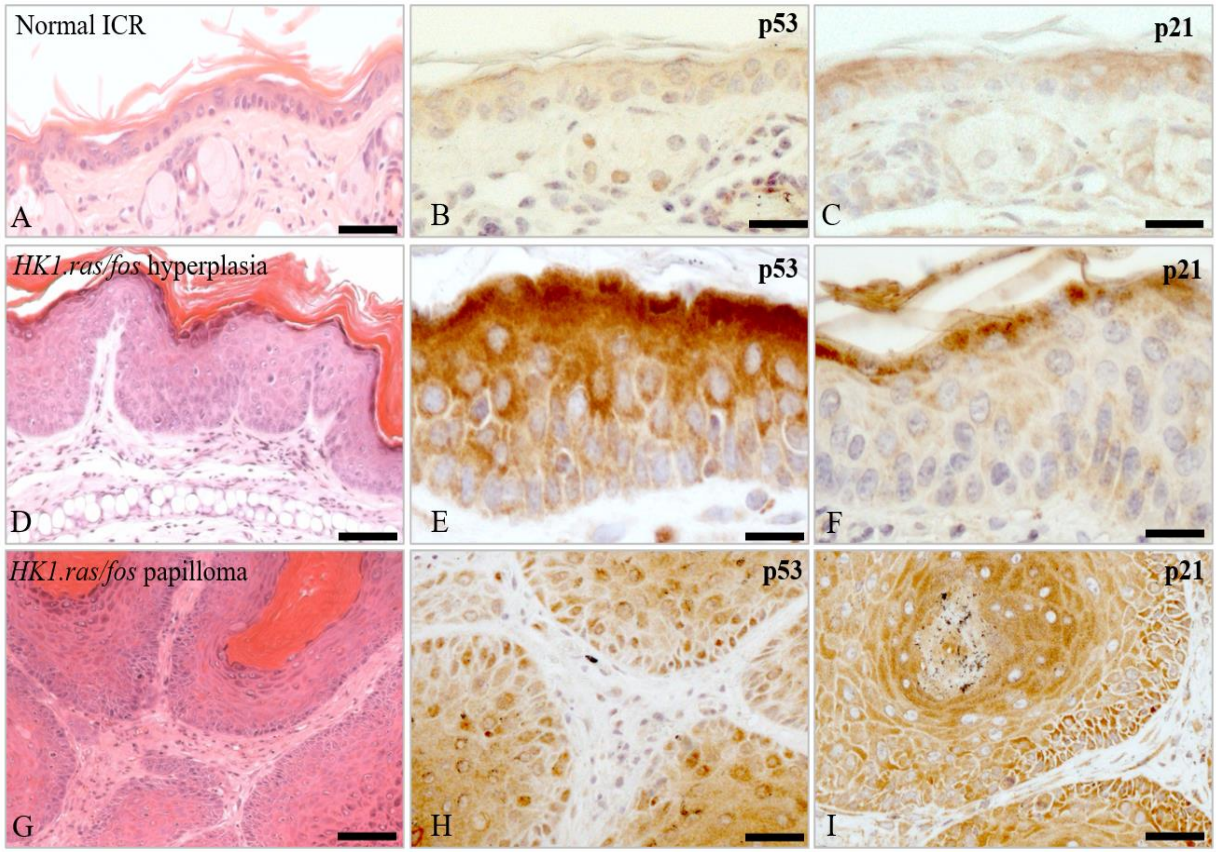

Figure 1. 7: p53 and p21 expression in HK1.ras/fos hyperplasia and papilloma.

[A-C] Histology of normal epidermis and IHC analysis shows only sporadic low level expression of p53 and p21. [D-F] pre-neoplastic *HK1.ras/fos* epidermal hyperplasia also shows only cytoplasmic expression of p53 expression on IHC analysis and [E] only weak p21expression. [F]. In contrast [G] shows HK1.ras/fos papillomas and display [H] strong nuclear expression of p53 in all basal layer keratinocytes with [I] increasing expression of basal layer p21. Scale bars: 50µm **[confirmatory experiment to illustrate the *HK1.ras/fos* model]**

The expression of p53/p21 and different keratin analysed in this model provide a compelling case for the stability of the benign papillomas formed in *HK1.ras*^{1205} or *HK1.ras*^{1276}*/fos* genotypes as they do not regress or progress without an additional oncogene effecter or a mutagen [i.e. TPA] to elicit conversion to carcinoma. This observation made this model ideal to study the roles of different oncogenes in the context of SCC, which was first used via assessing the effect of inducing AKT activation via loss of PTEN associated regulation of PI3K pathway.

1.7 Investigation of the roles for *PTEN/PI3K/AKT* pathway deregulation in *HK1.ras fos* carcinogenesis and implication of β-catenin deregulation

As outlined above exclusive epidermal expression of activated ras^{Ha} and/or *fos* [*HK1.ras; HK1.fos*] provided stable autonomous pre-malignant papillomas ideal to study mechanisms driving malignant conversion and progression. Thus, subsequently this approach has successfully tested several oncogene combinations and loss of common tumour suppressor genes such as p53, p21 and importantly PTEN. Indeed, as detailed below [1.6.1], it is the data from earlier PTEN studies involving co-operation between *HK1.fos* and inactivation of PTEN regulation of AKT activities that identified specific roles for GSK3β inactivation in the formation of highly differentiated benign tumour known as keratoacanthomas [KA], which in turn provide the foundations to this project by identifying the importance of this *AKT/GSK3β/β-catenin* axis and of β-catenin in particular in this project.

As detailed in chapter 3, whilst PTEN loss promoted papillomatogenesis with ras and fos oncogene promotion in carcinogenesis studies (*Yao et al., 2006;2008; Macdonald et al., 2014*) new data now confirm that increased membranous β-catenin activation in basal layers, downstream of the PTEN/AKT deregulation was associated with the induction of p53 and p21 leading to a KA aetiology (*Yao et al., 2008*). Moreover, following p53 loss in *HK1.fos/ras/Δ5PTEN* mice, decreased membranous and increased cytoplasmic/nuclear β-catenin expression appears to drive early-stage malignant progression to more aggressive SCC (*Alyamani et al.,* Manuscript in Preparation). Thus, the canonical β-catenin/Wnt signalling pathway [see section 1.8] may be a key component to induced compensatory p53-mediated responses that inhibit malignant conversion but drive a KA aetiology; but once p53 is lost nuclear β-catenin is associated with malignant progression [Chapter 3: sections 3.2 & 3.3].

Therefore, inducible β-catenin overexpression would directly investigate/validate mutations driving/inhibiting PTEN mediated carcinogenesis, given that PTEN functions as a tumour suppresser working through Phosphatidylinositol-4,5-bisphosphate 3-kinase (PI3K) dependent and independent mechanisms, in which in the dependent mechanism the PTEN facilitates the removal of the phosphate from phosphatidylinositol 3,4,5 trisphosphate (PIP3) in position 3 of the inositol ring preferably *(Hopkins and Parsons, 2014)*. This action results in negatively

regulating AKT, which is also a negative regulator of GSK3-β via phosphorylation that down regulates β-catenin *(Morin, 1999; Hopkins and Parsons, 2014)* and directly links PTEN and β-catenin signalling.

This may have several implications, one involving the canonical Wnt signalling and a second dependent on adhesion signalling deregulations as another important function of PTEN, independent of PI3K mechanism, includes regulating [inhibiting] cell migration (*Hopkins and Parsons, 2014*) and a role as a scaffolding protein aiding cell-cell connectivity (*Subauste et al., 2005*) [See Chapter 8:Scatter/migration assays]. Hence the appealing co-operation potential with β-catenin also regulating genomic stability [hence the compensatory p53 responses] as well as regulation of mitogen-activated protein kinase (MAPK) signalling pathway (*Hopkins and Parsons, 2014*) which links to the MAPK kinase pathway consistent with the co-operation between PTEN and ras fos outlined [below].

Initially PTEN was an attractive TSG to investigate in this HK1 mouse model as mutations in the PTEN gene cause PTEN hereditary tumour syndromes (PHTS) such as Cowden disease (*Liaw et al., 1997; Fistarol et al., 2002; Suzuki et al., 2003; Song et al., 2012*). This familial cancer susceptibility syndrome commences with the appearance of cutaneous hyperkeratosis and harmatomas prior to development of internal tumours at multiple sites (*Tan et al., 2012*). This syndrome not only highlights the ability of the epidermis to resist carcinogenesis compared to alternate tissues [as clearly exemplified in this transgenic mouse study] but also demonstrates additional important roles for PTEN in keratinocyte differentiation *(Tan et al., 2012)* and maintenance of the epidermal barrier (*Subauste et al., 2005*). Furthermore, the loss of PTEN through mutations in human cancers was seen almost as frequently as the loss of the most well-known tumour suppresser gene p53 (*Parsons et al., 2004; Stiles et al., 2004; Downward, 2004*). However, to model PTEN loss in transgenic mice was complicated by the fact that PTEN knockout was found to be lethal and use of the cre loxP system to induce expression loss throughout embryogenesis leads to a very rapid progression to SCCs in chemical carcinogenesis (*Suzuki et al., 1998; 2003*).

Therefore, in this approach an RU486-inducible *cre/loxP* system was employed to mutate PTEN and assess the consequences in the HK1 model (*Berton et al., 2000; Yao et al., 2006;2008; Macdonald et al., 2014*). Here two strains of mice are employed one contains a keratin K14 driven cre recombinase protein fused to the progesterone ligand binging domain (PLBD) the other is a target strain comprised of *loxP*-flanked exons or stop codons. Thus, the cre recombinase is expressed in all keratinocytes but cre activity remains in the cytoplasm. After topical treatment of RU486, the cre is then translocated into the nucleus where it can ablate or delete the sequences flanked by lox P sites. (see Fig. 1.8). Here epidermal specificity is achieved via topical administration of RU486 and the K14 promoter is used to achieve cre expression in the basal layer of the epidermis and hair follicles- including stem cells *(Berton et al., 2000).* Thus, the expression of K14 and the requirement for topical RU486 results in the ablation of exon 5 of PTEN in highly localised areas of the skin or at specific time points.

For instance, pre-papilloma formation or post papilloma formation by RU486 treatment usually on the ear and back *(Yao et al., 2006).* In this instance the target mouse contains a PTEN allele modified to have loxP sites engineered to flank exons 5 (*Wu et al., 2003*), which are ablated to give the mutated form of PTEN (Δ5PTEN) that fails to inhibit AKT signalling in this model (*Yao et al., 2006; 2008*). Typically, this is sufficient to ensure that RU486 treatment is required to elicit a phenotype but as found in this study there can be a degree of cre leakage into the nucleus, independent of RU486 that until this project was not observed to give a phenotype–thus showing the potency of deregulated β-catenin signalling.

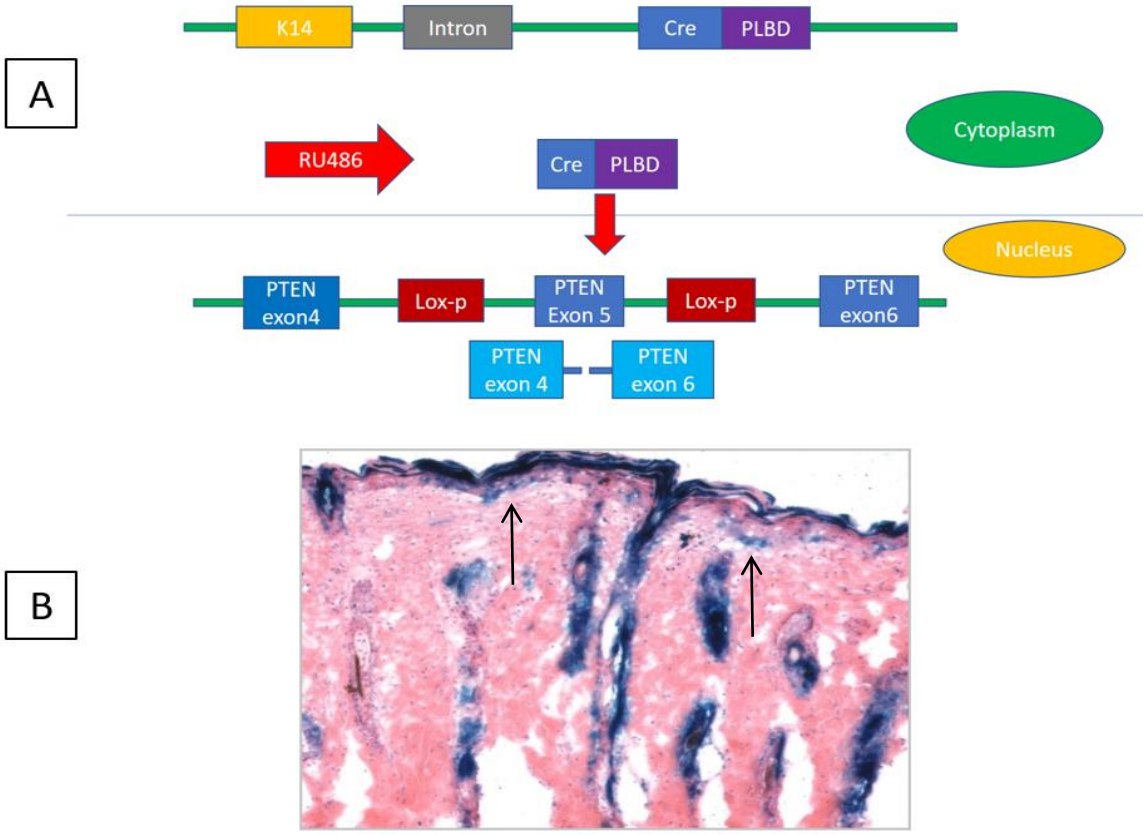

Figure 1. 8: Schematic diagram illustrates the mechanism of the inducible cre/loxP system with RU468 treatment in bi-genic *K14.creP/PTEN*$^{flx/flx}$ mice.

[A] Inactivation of *PTEN*-mediated AKT regulation is achieved by ablation of exon 5, the phosphatase site. The keratin K14 driven cre is used to achieve exclusive expression to the epidermis and hair follicles. The cre is bound to the progesterone ligand binging domain (PLBD) in the cytoplasm. Treatment with RU486 induced PLBD dimerization and translocation into the nucleus where cre acts to delete sequences flanked by lox P sites; in this case PTEN exon 5 [Δ5*PTEN*$^{flx/flx}$]. [B] K14.creP/flx-stop-flx-β-gal staining 5 weeks post single RU486 treatment confirms expression in proliferative keratinocytes and stem cells constant with *K14.creP* targeting. Note also the strands of blue cells in the epidermis [arrows], indicating the population of IFE stem cells.

1.7.1 Co-operation between *HK1.ras/fos* and *PTEN* loss of *AKT* inhibition

In the initial model, Δ*5PTEN* [$PTEN^{flx/flx}$] mice were mated to HK1.ras mice creating the Δ5PTEN/$K14^{creP}$/HK1.ras transgenic mice [*HK1.ras.Δ5PTEN*] and resulted in a rapid onset of papillomatogenesis, but without malignant conversion unless the mice were also treated with TPA promotion (*Yao et al., 2006*). Additionally, another study on mice was also done in corporation with fos activation *(Yao et al., 2008)*. This study used a similar method with Δ*5PTEN* [$PTEN^{flx/flx}$] and *HK1.fos*. The *HK1.fos.*Δ*5PTEN* mice treated with RU486 exhibiting features of hyperplasia, hyperkeratosis and the development of tumours that became highly differentiated and progressed to keratoacanthomas [KA] and not to carcinomas *(Yao et al., 2008)*.

This observation was later attributed to the increased activity of phosphorylated AKT [p-AKT] which resulted in elevated levels of GSK3β inactivation that triggered tumour suppressive action from p53 and p21. This p53 and p21 response thus diverted proliferating papilloma keratinocytes into a differentiation programme resulting in progression to KA not SCC *(Yao et al., 2008)*. The p-AKT inactivated GSK3β through phosphorylation at serine 9 and overexpression of this process resulted in the high levels of phosphorylated GSK3β (p-GSK3β). This triggered high level responses of p53 and p21 which resulted in a reduction in AKT activity that resulted in accelerating the keratinocyte differentiation and KA formation *(Yao et al., 2008)*. It is theorised that, this AKT inactivation of GSKβ involved increasing nuclear βcatenin and this triggered the p53 and p21 responses [see below].

Furthermore, a more recent study investigated the co-operation of Δ*5PTEN* with both ras [*HK1.ras*] and fos [*HK1.fos*] oncogenes finding that RU468 treatment of *HK1.ras/fos-K14creP.Δ5PTEN*$^{flx/flx}$ skin resulted in increased hyperplasia and formation of proliferating cysts. Moreover, papillomatogenesis was accelerated but malignant conversion was now delayed, and tumours seemed to stall at a well-differentiated squamous cell carcinoma (wdSCC) histotype *(Macdonald et al., 2014)*. Moreover, despite several oncogenic effectors, malignant conversion required additional loss of p53, which made papillomas prone to convert; but the appearance of p53-independent, persistent p21 expression limited early-stage malignant progression. This p21 expression inhibited cyclin D1 and cyclin E2 activity (*Macdonald et al., 2014)* and persistent p21 expression appeared to antagonise AKT1 to limit

the progression to a wdSCC state for a period of time. This status was maintained until the p21 was lost and now increased activity of p-AKT led to more aggressive SCC *(Macdonald et al., 2014)*.

This increasing AKT observation again brings into question the involvement of β-catenin, as high levels of p-AKT activity will lead to inactivated GSK3-β that result in stabilizing β-catenin which may be involved in this malignant progression. Indeed, the p53 /p21 responses in KA formation may be due to anomalous nuclear β-catenin expression. The tumour supportive activity of p53 and p21 was elevated during hyperplasia, cyst and papilloma formation. Of relevance to this model the cyst formation was actually attributed to the expression of p53 and p21 that caused the alteration in the excess proliferation into increased differentiation which resulted in cyst formation *(Macdonald et al., 2014)* but the data in this current study suggests that β-catenin was involved also.

Similarly, follicular cyst formation was seen before in a β-catenin related study where K14 was used as a promoter to target the hair follicles and aimed to see the consequences of preventing the binding of Lef1 (ΔNLef1) to β-catenin in hair follicles (HF) and epidermis (*Niemann et al., 2002*). Here in this study, the mice lost hair within 6 weeks of age and began to develop dermal cysts derived from the base of the hair follicles. This study conclude that the levels of β-catenin signalling helped determine the differentiation of keratinocytes into hair or interfollicular epidermis as well as irregularities within the pathway and aberrant levels of β-catenin signalling can lead to formation of cyst and HF tumours (*Niemann et al., 2002*). This study in addition to the previously illustrated study associated with the loss of PTEN in KA formation, suggest the involvement of deregulated β-catenin signalling and formation of skin tumours (*Niemann et al., 2002; Yao et al., 2008; Macdonald et al., 2014*).

This idea was quite attractive since β-catenin signalling is strongly implicated from the observation of increasing AKT activity which led to the high levels of inactivated GSK3-β that suggest an accumulation of cytoplasmic β-catenin which probably caused the compensatory responses of p53 and p21 in KA; but in the triple model β-catenin accumulation in the cytoplasm and nucleus may have contributed to malignant conversion to wdSCC or early progression to aggressive SCC *(Yao et al., 2008; Macdonald et al., 2014)*. The investigation of β-catenin expression in these tumours was an immediate goal in this study.

1.8 β-catenin and its role in skin cancer

In this study one logical candidate that fits this profile for a multi-stage carcinogenesis study is β-catenin, which is a protein that has a dual role. It interacts with E-cadherin in cell-cell adhesion and is known to be a key regulator in the canonical Wnt signalling pathway (*Morin, 1999; Grigoryan et al., 2008*). The deregulation of membrane adhesion and proliferation mediated by failure to regulate β-catenin has been implicated in many tumours including skin, colon, breast and prostate cancers (*Morin, 1999; Grigoryan et al., 2008*). However, its exact role in skin carcinogenesis remains poorly defined, in terms of when it becomes activated and its roles in membranous versus nuclear signalling. Therefore, in this study the main aim was to assess β-catenin overexpression in stage–specific skin carcinogenesis (*Gat et al., 1998**;*** *Niemann et al., 2002; Kretzschmar et al., 2015*).

The β-catenin gene also known as CTNNB-1 consists of 16 exons and can be divided into three binding domains. The largest domain consists of ~550 amino acids known as central repeats or armadillo repeats and this domain is associated with binding to E-cadherin to form the complex needed for β-catenin to assume cell-cell adhesion function (*Gao et al., 2018*) [Fig. 1.9]. The C-terminal domain of the β-catenin gene consists of ~100 amino acids and possesses the binding site for canonical Wnt signalling transcriptional targets T cell factor[TCF] and lymphoid enhancer binding factor [LEF] [Fig. 1.9]. The N-terminal domain consists of ~150 amino acid and contains the phosphorylation site for binding of β-catenin with its down-regulator GSK3β at serine and threonine residues in exon3 [Fig. 1.9]. This is the key feature of maintaining normal levels of cytoplasmic β-catenin that regulate canonical Wnt signalling pathway and the interactions with E cadherin (*Morin, 1999; Grigoryan et al., 2008*). Thus, exon 3 has been reported to be the mutation hotspot in β-catenin and is mostly associated with missense mutations which have been reported in human carcinomas and in two-stage DMBA/TPA carcinogenesis (*Grigoryan et al., 2008*). This site is also exploited in many studies to give constitutive β-catenin overexpression *(Harada et al., 1999).*

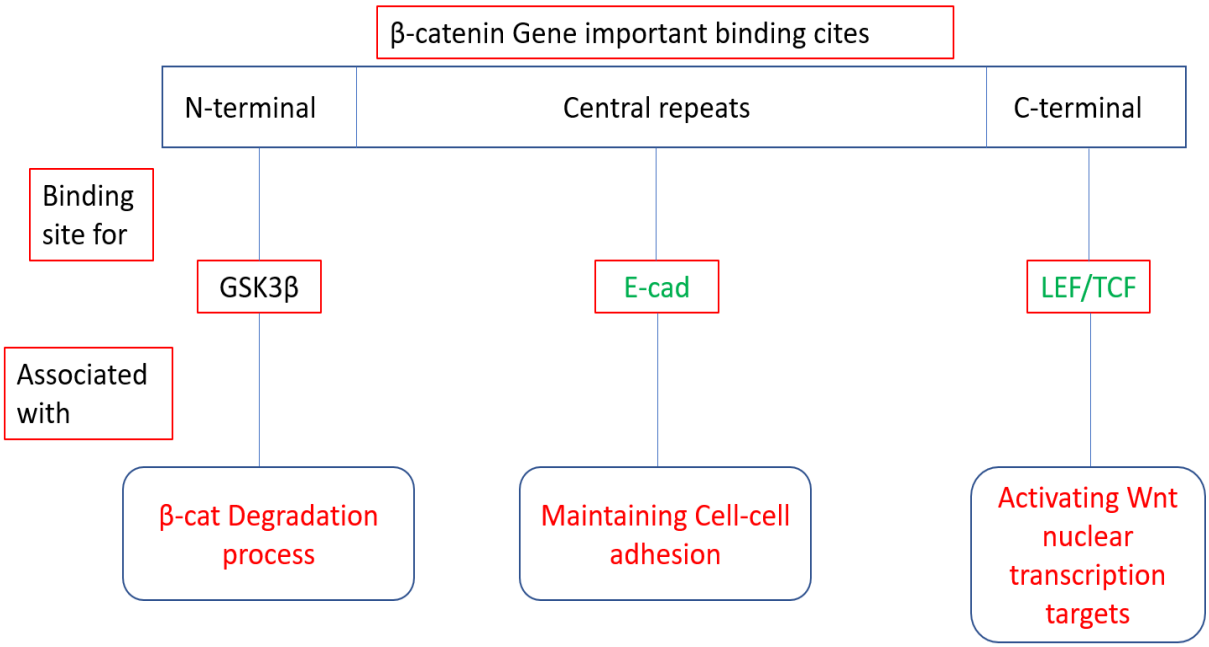

Figure 1. 9: Important binding sites in the normal functions of the β-catenin gene [CTNNB-1].

In the N-terminal domain of the gene, β-catenin binds to GSK3β to start the down regulation process of β-catenin to prevent cytoplasmic accumulation, whilst the biggest region of the gene binds to E-cadherin to form the cell-cell adhesion complex and the C-terminal of the gene binds to LEF/TCF in the nucleus to activate transcriptional targets of Wnt signalling.

Moreover, one of the central roles of β-catenin is to act as a cell-cell adhesion protein in conjunction with E cadherin (*Morin, 1999; Grigoryan et al., 2008*). E-cadherin is a major player in the family of Cadherin molecules, which function as cell-cell adhesion molecules that are essential in regulating calcium dependent adhesion between the cells as well as playing roles in morphogenesis and tissue homeostasis (*Takeichi, 1991; Young et al., 2003*). E-cadherin is highly expressed in the epithelial cells and the intracellular link between E-cadherin and the actin cytoskeleton is formed by the catenin family component (*Takeichi, 1991; Young et al., 2003*). In this process, cytoplasmic β-catenin gets recruited by cytoplasmic E-cadherin and binds to α-catenin to form a complex that links to the actin filaments network creating adherent junctions between the cells [cell-cell adhesion] (*Aberle et al., 1994; Jou et al., 1995; Pai et al., 1996*). These adhesion junctions formed via β-catenin/E-cadherin interactions are one of the important junctions to maintain the homeostasis of epidermal terminal differentiation and hair follicle morphology as well (*Young et al., 2003*). It has been

shown also that knocking out either β-catenin or E-cadherin in transgenic mice resulted in embryonic lethality as the adhesive capacity of cells are crucial at the embryonic development stage (*Grigoryan et al., 2008*). The loss or reduction of adherent junction expression via loss of E-cadherin or gain of function mutation β-catenin has been associated with facilitating carcinogenesis which is simultaneously accompanied by β-catenin nuclear localization (*Jeanes et al., 2008*) as also shown in this study [Chapters 3 and 6].

This increased nuclear localization of β-catenin in carcinomas highlights another major signalling role in the regulation of the canonical Wnt signalling pathway. The canonical pathway is activated by Wnt ligands binding to Frizzled and LRP receptors, and this results in inhibition of glycogen synthase kinase 3-β via phosphorylation on serine 9 (p-GSK3β) activity, causing β-catenin to become stabilized in the cytoplasm. Then free β-catenin travels into the nucleus where it binds to the transcription target genes of Wnt signalling, which are T cell factor (TCF) and lymphoid enhancer binding factor (LEF) (*Behrens et al., 1996; 1998; Grigoryan et al., 2008*). Given that β-catenin is known to have an essential role in hair follicle development, morphogenesis and differentiation via transactivation of Wnt signalling transcriptional targets complex of LEF/TCF (*Lim and Nusse, 2013*) has been associated with each of the stages of hair development, such as placode formation, HF renewal cycle and differentiation of the hair shaft. Additionally, Wnt/β-catenin activation consequently activates other signalling pathways associated with hair follicle maintenance such as Notch and Sonic hedgehog (*Watt and Collins, 2008*).

Wnt/β-catenin signalling also regulates the epidermal pluripotent stem cells that reside in the bulge region of HFs, that are needed for maintaining normal epidermal terminal differentiation and hair follicle differentiation, which also links Wnt/β-catenin to the roles it plays in embryonic and juvenile stages of development. Embryonically Wnt/β-catenin signalling is highly involved in the formation of the body anterior and posterior axis, hence why null mutation of β-catenin induced embryonic lethality as it resulted in a failure in forming body axis in mouse studies (*Grigoryan et al., 2008*). This was also supported by influence of Wnt/ β-catenin on up regulating bone morphogenic protein BMP signalling (*Närhi et al.,2008)* which is essential to embryonic formation of bones. This sums up the second significant role of β-catenin as signal transduction molecules and a co-transcriptional activator in the Wnt signalling system.

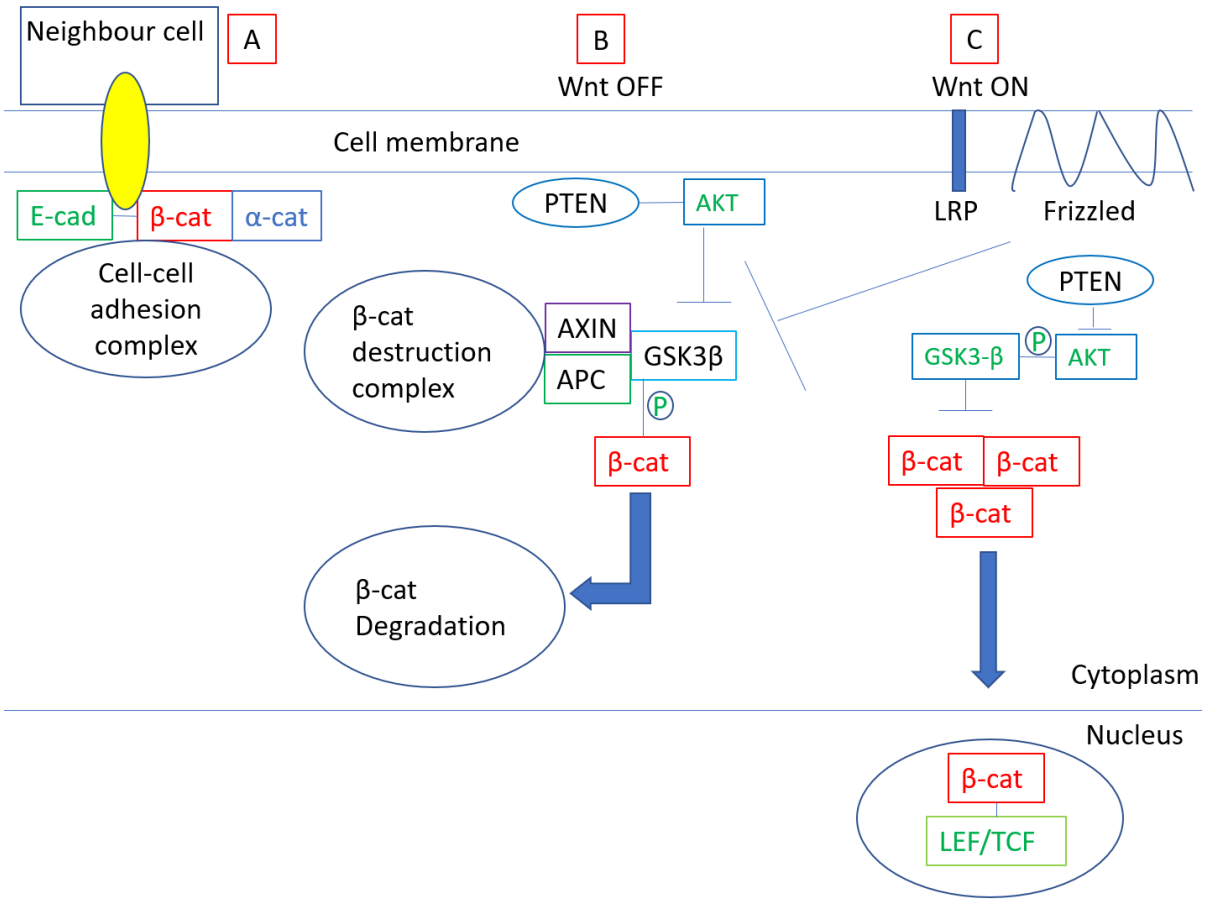

Figure 1. 10: Schematic diagram of the β-catenin pathway.

[A] β-catenin binds to α-catenin and E-cadherin in the cytoplasm to form the cell-cell adhesion complex at the cell membrane to maintain cellular adhesion with neighbouring cells. [B] In the absence of Wnt signalling receptors and suppression of AKT mediated GSK3β inactivation via PTEN, GSK3β forms a complex with APC and Axin that binds to and down regulates β-catenin via phosphorylation leading to cytoplasmic degradation of the protein via the ubiquitin pathway and preventing cytoplasmic accumulation. [C] In presence of Wnt receptors Frizzeld and LRP and activation of AKT, the β-catenin destruction complex is de-activated due to GSK3β phosphorylation via AKT which leads to cytoplasmic accumulation of β-catenin and translocation into the nucleus to activate Wnt signalling target genes Lef/TCF.

These studies highlight the importance of β-catenin being correctly regulated, which happen via a complex of several molecules. One of its important regulators is adenomatous polyposis coli (APC) via its interaction with GSK3β to form a complex that down regulates β-catenin

(*Behrens et al., 1996; 1998; Ikeda et al., 1998*) via targeting it for ubiquination. GSK3β seems to be the first step in the subsequent degradation by phosphorylating β-catenin within a multi protein complex that involves APC and Axin proteins (*Behrens et al., 1996; 1998; Ikeda et al., 1998*). This observation is highly significant as GSK3β inactivation via phosphorylation by AKT is thought to be an important feature in the failure to regulate β-catenin degradation (*Grigoryan et al., 2008*). AKT negatively regulates GSK3β, which results in stabilization of β-catenin and preventing its degradation by GSK3β activity (*Morin, 1999; Grigoryan et al., 2008*).

AKT as mentioned above is regulated by PTEN which functions as a tumour suppresser working through Phosphatidylinositol-4,5-bisphosphate 3-kinase (PI3K) dependent and independent mechanisms, where the dependent mechanism facilitates the removal of the phosphate from phosphatidylinositol 3,4,5 trisphosphate (PIP3) in position 3 of the inositol ring preferably (*Hopkins and Parsons, 2014*). This action results in negative regulation of AKT activities, which down regulates β-catenin as outlined above (*Morin, 1999; Grigoryan et al., 2008*; *Hopkins and Parsons, 2014*) and provides a direct link between PTEN and β catenin and thus are important in the regulation to prevent carcinogenesis.

The deregulation of β-catenin levels that result in stabilizing the protein such as gain of function mutation i.e. exon3 missense mutations have been associated with multiple human carcinomas and also frequently reported in two-stage DMBA/TPA carcinogenesis (*Grigoryan et al., 2008*). The influence of β-catenin stabilization has been associated in several types of cancers (*Morin, 1999; Grigoryan et al., 2008*). One of most common examples is colon cancer due to APC/β-catenin regulation as APC is found to be mutated in around 80% of colon cancer cases and a loss of APC expression has been associated with elevated β-catenin expression and facilitating tumorigenesis due to failure in forming the GSK3β/APC β catenin destruction complex (*Morin, 1999*). This APC/β-catenin interaction has proven to be also important in developing melanoma skin cancer, which highlights the importance of preventing β-catenin cytoplasmic accumulation even if the gene itself is not mutated, a failure of β-catenin regulator to assume it function such as GSK3β or APC could consequently lead to overexpression of β-catenin (*Morin, 1999*). The importance of this is due to Wnt/β-catenin being a gateway to several proto-oncogenes down stream of its nuclear transcription targets LEF1/TCF including MYC-1, cyclinD1, Notch, Sonic hedgehog[SHH] and c-fos (*Gerdes and Yuspa, 2005; Ambler and Watt, 2007; Grigoryan et al., 2008; Saadeddin et al., 2009; McCubrey et al., 2016*). This

is why Wnt/β-catenin is associated with many carcinomas such as colon, prostate, ovarian, melanoma and non-melanoma skin cancers *(Morin, 1999; Gerdes and Yuspa, 2005; Grigoryan et al., 2008).*

The association of non-melanoma skin cancers [SCC/BCC] derived from Wnt/β-catenin signalling ability to overexpress sonic hedgehog[SHH] which associated with most cases of BCC (*Gerdes and Yuspa, 2005*) and also Notch which associated with both BCC and SCC (*Gerdes and Yuspa, 2005; Rodilla et al, 2009; Wang et al., 2011; South et al., 2014; Sherwood and Leigh et al., 2016*).

The other direct implication of β-catenin involvement in SCC was demonstrated in mouse studies. Thus, as β-catenin being a regulator of HF bulge stem cells niche, a correlation has been established between SCC cells driven by Ha-ras mutation to be carrying similar cellular characteristics of bulge stem cells which directly implicate β-catenin as contributor to SCC development (*Malanchi, et al., 2008*). Additionally, conditionally knocking out β-catenin resulted in either blockage or regression of DMBA/TPA tumours, which again indicate that β-catenin expression was a necessity for the development of SCCs (*Grigoryan et al., 2008*). The majority of transgenic mice study showed that overexpression of β-catenin was associated with development of HF abnormalities and HF tumours. The constitutive β-catenin activation in mice studies was mainly associated with multiple hair follicle abnormalities. These abnormalities include de novo HF, formation of epidermal cyst and HF tumours such as pilomatricomas and trichofolliculoma (*Gat et al., 1998; Huelsken et al., 2001; Grigoryan et al., 2008*), which were also reported in humans carrying gain of function mutations of β-catenin (*Grigoryan et al., 2008*). Grossly most transgenic mice with constitutive β-catenin activation were scruffy and had alopecia despite the increased placode formation due a failure to develop normal complete HF because of incorrect control of Wnt/β-catenin signalling(*Gat et al., 1998; Närhi et al.,2008)*. The early constitutive activation of β-catenin in juvenile stage was also associated with developing enlarged extremities [feet/tail] due to Wnt/β-catenin activation having a central role in forming body axis (*Grigoryan et al., 2008*) and also β-catenin activation resulting in up regulating bone morphogenetic protein [BMP] signalling (*Närhi et al., 2008*) hence the big feet.

However, despite many studies conducted on gain of function β-catenin, to date none have directly explored constitutive activation of β-catenin in a multi-stage carcinogenesis model.

This is possibly because the effect of overexpression β-catenin on facilitating carcinogenesis and that knocking out the gene resulted in tumour regression in a multi-stage carcinogenesis model (*Malanchi, et al., 2008*). Thus, it may be that the result of constitutive activation of β-catenin was taken for granted as it would be expected to likely lead to producing aggressive carcinomas. Studies in HK1 model of multi-stage carcinogenesis would support this idea yet indicated that possibly the effect of β-catenin on carcinogenesis was more complex and context dependent was observed.

For instance, *HK1.fos-K14creP.Δ5PTEN*$^{flx/flx}$ co-operation resulted in KA formation instead of SCC and this result was associated with compensatory high levels of p53/p21 (*Yao et al., 2008*). This result was attributed to elevated levels of inactivated GSK3-β [p-GSK3β] due to Δ5PTEN activating p-AKT. Thus, β-catenin involvement was implied, as GSK3-β/APC/AXIN destruction complex of β-catenin could not be formed due to continuous inactivation of GSK3-β via AKT. Whilst this proved to be correct, in this context β-catenin overexpression resulted in epidermal differentiation response that inhibited malignant conversion. However, in *HK1.ras/fos-K14creP.Δ5PTEN*$^{flx/flx}$ mice this led to malignant conversion to SCC, likely facilitated by increased nuclear β-catenin following the loss of p53/p21 expression. In both contexts an increase in β-catenin expression resulted in different results in conjunction with p53/p21 expression.

Therefore, to investigate inducible constitutive activation of β-catenin in the HK1 model an inducible K14.creP/loxP gene switch was employed to target Δ3β-catenin expression to the epidermis [Fig. 1.11]. As outlined above, epidermal specificity is achieved via topical administration of RU486 and the K14 promoter is used to achieve cre expression in the basal layer of the epidermis and hair follicles - including stem cells (*Berton et al., 2000*). Thus, this results in the ablation of exon 3 of β-catenin that contains the phosphorylation binding site for GSK3-β which eliminates the GSK3β/APC/Axin down regulating complex. This approach appears to be the first of its kind that directly investigates β-catenin roles in skin carcinogenesis and attempts to fill the void in literature by directly assessing β-catenin causality in co-operation with *HK1.ras/fos/Δ5PTEN* in SCC development.

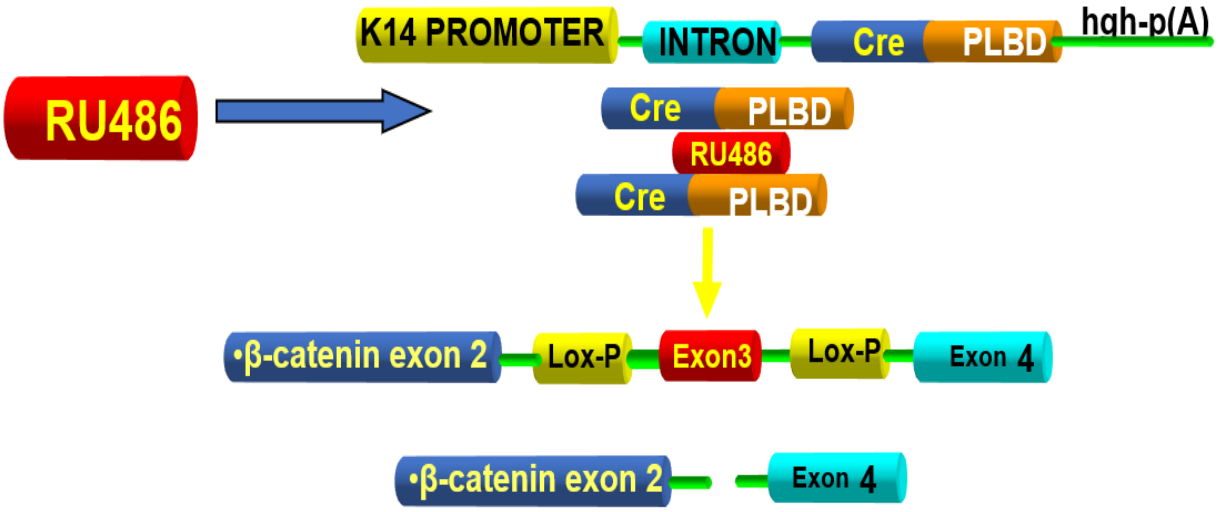

Figure 1. 11: The schematic diagram illustrates the mechanism of the inducible cre/loxP system with RU468 treatment in the ablation of exon 3 in β-catenin and the PCR analysis confirming Δ3β-catenin activation.

The keratin K14.creP driven cre is used to achieve exclusive cre expression in all keratinocytes. To activate cre in the epidermis and hair follicles transgenic mouse skin is treated with RU486 and the PLBD translocates into the nucleus where cre activity deletes the sequence flanked by lox P sites. In this model exon 3 the binding site for β-catenin ubiquination is removed resulting in constitutive activation.

1.9 Aim and objectives

Aim of the study: Can inducible β-catenin overexpression induce malignant conversion of benign papillomas and progression to aggressive malignant SCC in co-operation with oncogenic ras [*HK1.ras*] or fos [*HK1.fos*] activation and/or PTEN loss [*Δ5PTEN*] and what is the underlying molecular mechanism; or alternately can the epidermis mount a protective (tumour suppressive) role that inhibits carcinogenesis at each stage.

Objectives:

- To investigate endogenous β-catenin status at each specific stage in *HK1.ras/fos-K14creP.Δ5PTEN*$^{flx/flx}$ multistage carcinogenesis and investigate the interactions with additional relevant gene expression as the mechanism unfolds [Chapter 3].
- To confirm whether inducible overexpression of a constitutively active β-catenin mutant [Δ3β-catenin] in the interfollicular epidermis of transgenic mice will induce stage specific progression of papillomas in co-operation with exclusive epidermal ras activation and achieve malignant SCC; or assess whether additional events are required such as inducible loss of p53/p21 TSG expression [Chapters 4/5/6].
- To assess whether inducible Δ3β-catenin can cooperate with fos and PTEN mutation via loss of AKT regulation and alter a keratoacanthoma aetiology and overcome a compensatory p53/p21 expression response that leads to carcinoma [Chapter 7].
- To mimic in vivo analysis of inducible Δ3β-catenin in vitro in co-operation with ras, fos and PTEN [Chapter 8]

Chapter 2: Materials and Methods

2.1 MATERIALS

2.1.1 PCR and DNA isolation materials

- Taq DNA polymerase, 10X PCR buffer and 50mM Magnesium Chloride, DNTPs [Invitrogen] and specific oligos described in Table 2.2
- 6x DNA loading buffer (0.25% bromophenol blue, 0.25% xylene and 30% glycerol)
- DNA lysis buffer (50mM Tris.HCl,100mM EDTA,100mM NaCl,1% SDS, pH 8.0)
- Proteinase K (Sigma)

2.1.2 Immunohistochemistry [IHC] and immunofluorescence [IF] materials

- Ethanol [VWR chemicals]
- Xylene [Sigma]
- Bovine serum albumin [Thermo Fisher Scientific]
- Normal goat serum [Thermo Fisher Scientific]
- Permafluor solution [Thermo Fisher Scientific]
- DAB (3,3'-diaminobenzidine) staining [Dako]
- 125 mg/kg 5-bromo-4-deoxyuridine [BrdU, Sigma]
- acid alcohol [99ml 70% ethanol and 1ml 1M Hydrochloric acid]
- Haematoxylin [Sigma]
- 10mM sodium citrate buffer (Lab Vision, Fremont, CA)
- 3% hydrogen peroxide solution
- PBS [Thermo Fisher Scientific]
- Antibodies and concentration used detailed in Table 2.4

2.1.3 Cell culture materials

- 500mL DMEM(1X) [gibco] 4.5g/L D-Glucose.
- 10% foetal calf serum [treated with chelex to remove Ca^{+2}]
- 15% keratinocyte growth media [PromoCell]
- T75 flasks, T25 flasks, haemocytometer, 60 mm dishes
- L-Glutamine, sodium pyruvate, penicillin/streptomycin [Sigma Aldrich]
- .25% $^{w}/_{v}$ trypsin (Gibco/Invitrogen)

2.2 METHODS

2.2.1 Breeding of transgenic animals and 3Rs strategy

To investigate the effects of inducible, constitutive β-catenin activation in skin carcinogenesis, several epidermal-specific genotypes have been created [Table 2.1]. These transgenic genotypes possess a combination of activated ras [strains *HK1.ras1205 & 1276*] and fos [*HK1.fos*] oncogenes in addition to a mutant PTEN tumour suppresser gene. *HK1.ras* and *HK1.fos* mice were maintained as heterozygotes in an outbred ICR background as one copy of the transgene was sufficient to produce initial epidermal hyperplasia and/or benign papillomas (*Greenhalgh et al., 1993a-c; 1995 Greenhalgh and Roop, 1994*).

In this model, to study the requirements for malignant conversion, deregulated PTEN/AKT signalling was achieved using an RU-486 inducible *cre/loxP* system employed to induce specific mutation at specific times (*Yao et al., 2006; 2008; Macdonald et al., 2014*). This approach was also employed to activate β-catenin and conditionally knockout p53 via deleting exons 2 to exon10 (*Jonkers et al., 2001*). The tumour suppresser transgenes p53 [$p53^{flx/flx}$] and PTEN [$\Delta 5PTEN^{flx/flx}$] were kept as homozygotes to elicit their phenotype, while β-catenin [$\Delta 3\beta\text{-}cat^{flx/wt}$] strains were kept mostly as heterozygotes as this was sufficient to produce the *Δ3β-catenin* phenotype. This study also used embryonic knockout of tumour suppresser gene p21 [*p21KO*] (*Martín-Caballero et al., 2001*), but only in preliminary experiments.

All mice were crossed with the *K14.creP* regulator strain to activate cre recombinase and bi-genic mice were topically treated with RU-468. Each cohort included at least 15-20 mice in repeat experiments; with 10 control mice [without *K14.creP* or without RU486 treatment]. All mice were ear tagged within 3-4 weeks of birth and were treated with RU486 [5mg/ml] [15ul ears/back] weekly for 4 weeks post ear tagging. All transgenic lines were bred under project licence project P82170325 according to the rules and regulations of the UK Home Office in the CRF facility of University of Glasgow.

The breeding strategy utilized the principles of 3RS [Replacement, Reduction, and Refinement]. In terms of Replacement, the primary goal of the project is to establish transgenic mice to identify/verify causal roles for multiple, relevant mutations that drive stage-specific tumour progression, explore the subsequent mechanism and identify putative

compensatory sentinel systems that have evolved to inhibit carcinogenesis. Thus, unlike cell culture systems, transgenic mice offer the possibility to determine the influence of factors critical to malignant progression such as blood supply, an intact immune system, hormonal and cell-mediated growth controls, together with the physical barriers that inhibit tumour cell growth and invasion. However, the experiments also utilised skin keratinocytes cultured from neonatal transgenic mice to assess transformation states in carcinogenicity and clonal growth; to investigate tumour invasion. These *in vitro* results will be compared to *in vivo* data to aid in assessment of tumour progression in parallel to monitoring malignant progression in adults.

In terms of Reduction, the constant monitoring of the transgenic mice permits the experiments to be terminated as soon as significant data has been obtained, thus minimising suffering, whilst obtaining meaningful data. As generation of these cohorts requires breeding of multiple transgenic mice lines, breeding strategies are carefully structured and rigorously monitored to ensure that only the minimum numbers are generated. Thus, given the requirement for a regulator transgene and topical treatments, an individual transgenic mouse breeder can carry multiple target transgenes which again reduces the overall numbers of animals needed for the experiments. Additionally, breeders also act as untreated controls for non-specific events e.g. insertional mutation; whilst bi-genic progeny become the comparison controls for tri-genics, and since several genotypes have already been fully characterised, repeating these as comparison controls is unnecessary, further reducing numbers required.

In terms of Refinement, the advantages of epidermal models in the design of these studies, was a distinct strength where employment of keratinocyte-specific expression vectors coupled to an inducible cre/lox system prevents disease during embryogenesis/development or in adult internal organs. Also, in most cases animals are non-phenotypic until application of RU486, thus compound transgenic genotypes can be maintained that lack a phenotype until treated and disease can be highly localised e.g., ear tip or small dorsal areas. This is a significant facet of the refinement category during the breeding to create the necessary genotypes, which can often compromise animal viability, particularly when assessing multiple genetic insults. Another major advantage of skin is the accessibility, which not only facilitates application to localise disease but also allows macroscopic observation of early neoplastic events without invasive procedures.

Moreover, in the case of increased severity of phenotypes in compound genotypes associated with Δ3β-catenin co-operation, a scoring system was devised and applied to such genotypes at the time of tail biopsy to ensure that these animals remained within the moderate category of the regulations for animal experimentation in the UK. Thus, the severity of phenotypes was divided into three degrees: Score 0, mild with only little obvious phenotype and a full size at tail biopsy and these individuals often required RU486 treatment to elicit β-catenin phenotypes; Score 1, the most typical outcome and the much rarer Score 2, where significant hyperplasia appeared by d16 and mice were also a smaller size indicative of digestive problems following weaning possibly due to β-catenin activation in the colon (*Grigoryan et al., 2008; Huels et al., 2015*). Table 2.1 below shows the genotypes established and the number generated for this study.

Table 2. 1: Compound Genotypes created in this study.

Genotypes	*Total number*	Serve as	*Chapters*
HK1.ras^{1205}	**90**	**Control**	**3/4/5/6**
HK1.fos	**23**	**Control**	**7**
HK1.ras^{1276}/fos	**15**	**Control**	**3**
HK1.fos-K14creP.Δ5PTEN$^{flx/flx}$	**18**	**Target genotype**	**3**
HK1.ras/fos-K14creP.Δ5PTEN$^{flx/flx}$	**18**	**Target genotype**	**3**
K14creP.Δ3β-cat$^{flx/wt}$	**74**	**Target genotype**	**4**
HK1.ras^{1205}-K14creP.Δ3β-cat$^{flx/wt}$	**58**	**Target genotype**	**5**
K14creP.Δ3β-cat$^{wt/flx}$.p53$^{flx/flx}$	**26**	**Target genotype**	**6**
HK1.ras-K14creP.p53$^{flx/flx}$	**22**	**Control**	**6**
HK1.ras- K14creP.Δ3β-cat$^{wt/flx}$.p53$^{flx/flx}$	**15**	**Target genotype**	**6**
K14creP.Δ3β-cat$^{wt/flx}$.p21KO	**15**	**Preliminary target**	**6**
HK1.ras- K14creP.Δ3β-cat$^{wt/flx}$.p21KO	**15**	**Preliminary target**	**6**
HK1.fos-K14creP.Δ5PTEN$^{flx/flx}$.Δ3β-cat$^{wt/flx}$	**18**	**Target genotype**	**7**
HK1.ras/fos-K14creP.Δ3β-cat$^{wt/flx}$	**18**	**Target genotype**	**7**
HK1.fos-K14creP.Δ3β-cat$^{wt/flx}$	**15**	**Target genotype**	**7**
HK1.fos-K14creP.Δ3β-cat$^{wt/flx}$.p53$^{flx/flx}$	**16**	**Preliminary target**	**7**

2.2.2 Analysis of mouse and tumour genotype by PCR.

Single genotype, bi-genic and tri-genic combinations were identified using Polymerase chain reaction [PCR] employing DNA isolated from tail and tumour tissues. Adult/juvenile mice [~4 weeks] were anaesthetised and tail tips [~3mm] placed in labelled tubes, frozen immediately and stored at -20^{o}C. In addition, PCR genotype was re-confirmed at biopsy from frozen tumour or back skin samples [~2mm].

DNA lysis buffer [50mM Tris.HCl,100mM EDTA,100mM NaCl,1% SDS, pH 8.0] containing 20mg/ml proteinase K [Sigma] was then added [500ul] to each Eppendorf tube and the tails digested overnight at 55°C with a brief vortex after ~2-3 hours incubation to aid digestion. Samples were centrifuged to remove debris [13,000 rpm for 15min, RT] and an equal volume of ice-cold ethanol added to precipitate the DNA at the interface, which was wound onto a pipette tip and transferred to a new tube containing 300ul of water to be dissolved for PCR use or stored for sequencing.

All PCRs were performed as 25ul reactions, consisting of PCR buffer 10x [2.5ul][Invitrogen], $MgCl_{2+}$ [2.5ul/2.5mM] [Invitrogen] , specific forward and reverse primers for targeted transgene [0.5ul/0.5mM], dNTPs[0.25ul/0.25mM], Taq polymerase[0.25ul/0.25mM][Invitrogen], finally DNA sample[2.5ul] and distilled water to make up the required volume [25ul].

The specific oligos as well as programmes required for each transgene are illustrated below [Tables 2.2 and 2.3]. To visualize the PCR product results, electrophoresis was conducted [~30 min 90 v] using agarose gels [1% for single bands ~400-~700 e.g. *HK1.ras* and *K14.creP*, up to 1.5% for better separation of smaller doublet bands e.g. *β-catenin*, 2% for small bands ~150-~250 e.g. p21KO] with 5ul of 20 mg/mL ethidium bromide added to 150ml of TAE [Tris-acetate-EDTA] buffer cooled-down [60^{0}C] to visualize the results under UV light and the gel was photographed.

Table 2. 2: Gene primers and band sizes.

Gene	primers	Expected band size
β-catenin	Forward:5'-CTG CGT GGA CAA TGG CTA CT-3'	Floxed allele at ~500bp and wild type allele at ~324bp
	Reverse: 5'-TCC ATC AGG TCA GCT GTA AAA A-3'	
HK1.ras	Forward: 5`-GGATCCGATGACAGAATACAAGC-3`	550bp
	Reverse: 5`-ATCGATCAGGACAGCACACTTGCA-3`	
HK1.fos	Forward: 5`-GGATCCATGATGTTCTCGGGTTTC-3`	750bp
	Reverse: :5`-CGATTATTGCCACCCTGCCATG-3`.	
PTEN	Forward: 5`-ACTCAAGGCAGGGATGAGC-3`	Floxed allele at ~1300bp wild type allele at ~1200bp Δ5 band at ~500bp
	Reverse: 5`-GTCATCTTCACTTAGCCATTGG-3`	
K14.creP	Forward: 5`-TCATTTGGAACGCCCACT-3	410bp
	Reverse: 5'- CCACCGTCAGTACGTGAGAT	
*XJK5creP**	Forward: 5`-TACAGCTCCTGGGCAACGTG -3`	400bp
	Reverse: 5`-CACAGCATTGGAGTCAGAAG-3`	
21	Forward: 5`- TCT TGT GTT TCA GCC ACA GGC Reverse: 5`- TGT CAG GCT GGT CTG CCT CC	wild type allele at ~430bp
	P21-5- ATT TTC CAG GGA TCT GAC TC R1N-1A- CCA GAC TGC CTT GGG AAA AGC	Null allele at ~150bp
p53	Forward: 5`- CAC AAA AAC AGG TTA AAC CCA G	Floxed allele at ~584bp wild type allele at ~431bp Δ p53 band at 612bp
	Reverse: 5`- AGC ACA TAG GAG GCA GAG AC	

Table 2. 3:PCR conditions

Genes	denaturation		denaturation		Annealing		extension		extension		cycles
β-catenin	95^0	2min	95^0	30sec	60^0	30sec	72^0	1min	72^0	10min	36
HK1.ras	95^0	5min	95^0	30sec	56^0	1min	72^0	1min	72^0	10min	35
HK1.fos	95^0	2min	95^0	30sec	62^0	30sec	72^0	1min	72^0	10min	35
PTEN	95^0	2min	95^0	30sec	63^0	1min	72^0	1.30 min	72^0	10min	36
K14.creP	95^0	5min	95^0	30sec	58^0	45sec	72^0	1min	72^0	5min	35
XJK5creP*	95^0	5min	95^0	30sec	58^0	45sec	72^0	1min	72^0	5min	35
p21	95^0	2min	95^0	30sec	59^0	30sec	72^0	1min	72^0	3min	36
p53	94^0	3min	94^0	30sec	58^0	20sec	72^0	1min	72^0	5min	32

2.2.3 BrdU labelling and biopsy procedure.

All biopsied mice were injected with 125 mg/kg 5-bromo-4-deoxyuridine (BrdU, Sigma) 2 hours before culling to determine cellular proliferation and mitotic index. Collected tissue [skin and tumour] biopsies were routinely fixed in [10% v/v] buffered formalin pH 7.4 for 24hrs at 4^{o}C before being sent for histological processing provided by University of Glasgow Vet Pathology Dept to be embedded in paraffin and stained with haematoxylin and eosin for microscopic analysis. At biopsy tissues were also snap frozen in liquid nitrogen and stored at -70^{o}C for western blot analysis, cryosectioning or DNA isolation.

2.2.4 Section preparation for Haematoxylin and Eosin staining [H&E], Immunofluorescence [IF], and Immunohistochemistry [IHC].

For immunofluorescence and immunohistochemistry [IF/IHC] 5-7um paraffin sections were incubated with several different antibodies [Table 2.4]. The paraffin sections were first deparaffinised [oven heating at 60°C for 30mins followed by 30mins incubation in 100% Xylene]. Xylene [Sigma] was removed by 5min rinse in absolute ethanol and sections rehydrated by rocking in phosphate buffered saline [PBS] pH 7.4 [10 mins]. Hydrated sections were then subjected to antigen retrieval in 10mM sodium citrate buffer [Lab Vision, Fremont, CA] boiled for 3 mins and allowed to cool-down for at least 30min.

For double- labelled immunofluorescence after the antigen retrieval step, sections were washed in PBS [5min] then directly blocked in e.g.10% bovine serum albumin [BSA] made in PBS to minimize unspecific binding. Sections were stained overnight in a humidified atmosphere at 4^{0}C, with 100-150ul of primary antibodies at the appropriate concentration [Table 2.4] made in 10% blocking serum e.g. employing rabbit anti-K1[diluted at 1/100] and guinea-pig anti-K14 [diluted at 1/400] made in 10%BSA in PBS. In each case sections were counterstained for keratin K14 with a guinea pig anti-K14 antibody employed to delineate the epidermis or tumour. Next day, sections were washed in PBS [10 min] then incubated with a secondary biotinylated goat anti-guinea pig [60min] antibody made in 10% BSA in PBS [60 min] to amplify labelling affinity for Texas red. Sections were then subjected to final incubation [60min/dark box/RT] with FITC-labelled anti-rabbit IgG [Jackson Labs] to highlight primary antibody targeted protein [green] and Streptavidin-Texas Red [Vector Labs]

to highlight the K14 counterstain in follicles and intra follicular epidermis [red]. After final incubation slides were mounted with Permafluor solution [Thermo Fisher Scientific], coverslipped and stored at 4^0C until photographed using a Zeiss microscope and Axio vision 3.0 imaging. For BrdU labelling, following antigen retrieval, BrdU-labelled cells were identified by overnight incubation [4^0C] with FITC-conjugated anti-BrdU. Positive cells [green] were counted from 3 separate areas of five different mice per cohort and the mitotic index expressed as BrdU-labelled cells per mm of basement membrane.

For immunohistochemistry [IHC] analysis, a similar protocol was followed, however after the antigen retrieval step slides were incubated in 3% [v/v] hydrogen peroxide for 10 min to block endogenous peroxidase activity. Sections were then washed in PBS, dried and blocked in 10% serum of the secondary antibody species [10min] e.g 10% normal goat serum [NGS] made in PBS. Sections were stained overnight at 4^0C with 100-150ul of primary antibodies with appropriate concentration [Table 2.4] made in 10% blocking serum in a humidified atmosphere e.g. rabbit anti-p53 [diluted at 1/100] in NGS made in PBS. Next day, sections were washed in PBS [10 min] and incubated with HRP-conjugated anti-rabbit antibody [Vector labs] [diluted at 1/100] made in 10% bovine serum albumin [BSA] in PBS for 60 min at room temperature. Sections were then washed in PBS [10 mins] and followed by DAB [3,3'-diaminobenzidine] staining [Dako] which was prepared shortly before applying it to the sections. Each section was stained for 3-5min depending on the type of antibody used and sections were washed immediately with tap water to stop the reaction. Sections were then counterstained with Haematoxylin for 15-20 seconds, then washed with tap water several times before gently dipping [X3] in acid alcohol [99ml 70% ethanol and 1ml 1M Hydrochloric acid] to de-stain Haematoxylin, then briefly washed with tap water and immersed in Scott's tap water for 1min to stain the nuclei blue. Sections were dehydrated by immersion in absolute ethanol [5 min] then, xylene [5 min] and sections were then left to dry at room temperature prior to mounting. Dried sections were mounted [PERTEX mounting medium] and cover-slipped for photography using a Zeiss microscope and Axio Vision 3.1 imaging.

Table 2. 4: IF and IHC Antibodies.

Antibody	Dilution	Provider/catalogue number
Rabbit anti-K1	1:100	Biolegend cat no:905601
Guinea pig anti-K14	1:400	Fitzgerald cat no:20R-cp002
Rabbit anti-K6a	1:100	Biolegend cat: 905701
Rabbit Anti-K15	1:100	Abcam: ab52816
Rabbit anti-β-catenin	1:50	SIGMA HPA029159/ Abcam: ab32572
Rabbit anti-E-cadherin	1:100	Proteintech cat no: 20874
Rabbit anti-p53	1:150	SIGMA SAB4503000/ SIGMA SAB4503015/ abcam:ab31333/abcam:ab131442
Rabbit anti-P21	1:150	Proteintech cat no: 10355-1-AP
Rabbit anti-p63	1:100	Proteintech cat no: 12143-1-AP
Rappit anti-p73	1:100	Abcam: ab40658
Rat anti-BrdU	1:100	Abcam: ab6326
Donkey Anti-Rat Alexa Fluor	1:100	Abcam: ab150153
biotinylated goat anti-guinea pig/Streptavidin-Texas Red	1:100	Vector Labs
FITC-labelled anti-rabbit IgG	1:100	Jackson Labs
HRP conjugated anti-rabbit	1:100	Vector Labs

2.2.4 Method for cell culture

Primary keratinocytes derived from new-born transgenic mouse epidermis were cultured as described (*Hennings et al., 1980; Greenhalgh et al., 1989*) and after primary keratinocyte genotype PCR analysis, 17 cell lines were derived from specific genotypes [see chapter8]. All cell lines were maintained in appropriate media as shown below [Table 2.5] supplemented with 10% foetal calf serum, which was previously treated with Chelex resin [mesh 100] to reduce Ca^{+2} levels from ~3.6mM to ~0.01 mM as described previously (*Brennan et al., 1975*). Briefly, 200g of chelex 100 resin was added to 500ml distilled water, and the pH adjusted to pH7.2-4 with HCl. The resin was filtered through a Buchner funnel and added to 500ml of foetal calf serum, allowed to be mixed for 1 hour and then filter-sterilised through a 22micron filter resulting in very low Ca^{+2} foetal calf serum ~ 0.01mM.

New-born mice (24 hrs old) were injected with pentobarbital and stored in 70% ethanol as a sterilization step while being transferred to the lab where each mouse was placed in a 60mm dish. Tail tips were taken from each neonate to confirm their genotype via PCR. Their skins were then removed, stretched on plastic lid and then and floated on 0.25% $^{w}/_{v}$ trypsin (Gibco/Invitrogen) in sterile serum free media overnight at 4^0C. The following day, after confirming their genotypes, each epidermis was separated from the dermis and 3-4 skins of the same genotype mixed together for 30min in 15ml tube in 10ml of DMEM media (Gibco) without Ca^{2+} containing 10% chelexed foetal calf serum to inhibit trypsin activity, and the calcium concentration adjusted to 0.05mM Ca^{+2} with sterile 0.3M $CaCl_2$ [Low Ca^{+2}] [Table 2.5]. Following gentle rocking [30mins] each cell solution was filtered through sterile gauze into 50ml tubes to remove the cornified layer and other cell debris, centrifuged [at 800 rpm] and the keratinocyte pellet resuspended in Low Ca^{+2} media.

The cells were counted using a haemocytometer and 5 $x10^6$ cells were plated into 60 mm dishes containing 3 - 5ml of medium to establish primary cell lines; or 2 x 10^7 cells in 20ml of medium per T75 flasks and 5 $x10^6$ cells per T25 flasks to minimise contamination and cultured in Low Ca^{+2} media supplemented with 15% [v/v] Keratinocyte Growth Media (PromoCell) [clonal growth media] with medium changes every 3-4 days. By four weeks colonies formed in 60 mm dishes and these were carefully trypsinised and plated into T25 flasks and cultured for another 3-8 weeks; with ad hoc sub-culture dependent upon their genotype and growth criteria, including levels of confluence and cellular sensitivity to

trypsinisation. For example, a rapidly growing primary cell line at passage 2 or 3 with 80% confluency and high sensitivity to trypsinisation would be split 1/5 into T75 flasks for different assays; while slower growing more normal cell lines with resistance to trypsinisation take longer time to cultivate and smaller split e.g., 1/2.

Each cell line was sub-cultured into four T75 flasks per different assays to be conducted on the cell lines. Morphology assays to assess their ability to commit to terminal differentiation and/or resistance to calcium induced terminal differentiation indicative of malignancy, were conducted by culturing three T25 flasks to confluence until normal proliferative cobblestone keratinocytes in Low Ca^{2+} media were formed indicative of a basal-layer morphology; then increasing the calcium concentration in the other two T25 flasks to 0.075mM Ca^{2+} to photograph a flatter morphology and instigate a supra-basal morphology at 24hrs; and then increasing high calcium concentration by 0.125mM Ca^{2+}in the last T25 flask to photograph their final differentiated morphology at 24hrs. All T25s were fixed in 10% buffered formalin for 15min and rinsed in water for photography.

Clonal growth assays were also performed to test transformation and resistance to calcium induced terminal differentiation (*Hennings et al.,1980; Greenhalgh et al.,1989*). Keratinocytes from low passage [Sc 3-5] cell lines were plated out into 16 dishes seeded at 250 cells/60mm dish and incubated for 24h. Then 8 of them were maintained in low Cal 0.05mM Ca^{2+} whilst the other 8 were moved to Hi Cal 0.125mM Ca^{2+}. These dishes were maintained for 27 days in the appropriate media [High or low calcium] before being fixed in formalin and stained with Rhodamine B to show keratinocyte growth. This assay identified which cell lines had malignant capabilities based on their growth profile from clonal density.

To further assess growth, migration and transformation, a “Scatter Assay” was performed. Cells were plated out in T25s flasks initially placed at 30^0 angle and grown to confluency. For each cell line, six T25s were prepared and after reaching confluence three flasks were kept at a low calcium concentration and three challenged with high calcium concentration, where transformed cell lines seeded beyond the determined growth line as typically cell lines do not seed, unlike primary keratinocytes or highly invasive cell lines.

For all of these tissue culture experiments two established immortalized and well characterised cell lines were used as comparison control. SP1 benign papilloma cell line derived from DMBA/TPA papillomas with activated ras^{Ha} which are transformed but not malignant in nude

mouse graft assays and T52 malignant keratinocytes, where SP1 cells were transfected with FBJ v-fos to become malignant (*Strickland et al., 1988; Greenhalgh et al., 1989*).

All primary cell lines were cultured on slides for immunocytochemistry [ICC] in low and high calcium concentration to test the expression of different proteins in the cells. This was conducted by culturing six slides for each cell line, once they reach 80% confluency 2 slides were fixed in methanol whilst the other 4 were switched to 0.075mM Ca^{2+} for 2 slides to be fixed at 24h and last 2 at 72h in methanol in -20^{o}C.

The genotypes of all cultured cell lines were re-confirmed via DNA Isolation. This was carried out by culturing one T75 to confluency, trypsinising and transferring the cells into an Eppendorf tube and DNA isolated as described above. For western blot analysis, each cell line was analysed for the expression of different proteins and this will be discussed in the next section. All cell lines were frozen-down in liquid nitrogen for cryo-storage. Cell lines produced are shown in results chapter 8.

Table 2. 5: Media formulations used for tissue culture analysis

Media content					**Used for**
Low ca^{+2} media	500mL DMEM(1X)(Gibco) 4.5g/L D-Glucose.	50mL 10% foetal calf serum (treated with chelex 100 to remove Ca^{+2})	0.05mM Ca^{+2}	50mL 15% keratinocyte growth media (PromoCell)	Maintaining Cell lines
High Ca^{+2} media	500mL DMEM(1X)(Gibco) 4.5g/L D-Glucose.	50 mL 10% foetal calf serum (treated with chelex to remove Ca^{+2})	0.125mM Ca^{+2}	50mL 15% keratinocyte growth media (PromoCell)	Inducing calcium terminal differentiation
Clonal low Ca^{+2} media	500mL DMEM(1X)(Gibco) 4.5g/L D-Glucose.	50mL 10%fotal calf serum (treated with chelex to remove Ca^{+2})	0.05mM Ca^{+2}	50mL 15% keratinocyte growth media (PromoCell)	maintaining primary normal keratinocytes

Chapter 3: Analysis of endogenous β-catenin expression in multistage *HK1.ras/fos-K14creP.Δ5PTEN*$^{flx/flx}$ carcinogenesis

Chapter 3 Results: To begin to investigate activation of β-catenin in a multi-stage carcinogenesis model, the tumours were recreated in *HK1.fos-K14creP.Δ5PTEN*$^{flx/flx}$ KA formation and *HK1.ras/fos-K14creP.Δ5PTEN*$^{flx/flx}$ SCC and the data compared to analysis of βcatenin in archival tumours. As outlined above, epidermal specificity is achieved via topical administration of RU486 and the K14 promoter is used to achieve cre expression in the basal layer of the epidermis and hair follicles- including stem cells *(Berton et al., 2000).* Previously, this resulted in elevated levels of inactivated GSK3-β [p-GSK3β] due to Δ5PTEN activation of p-AKT that triggered compensatory p53/p21 expression in *HK1.fos-K14creP.Δ5PTEN*$^{flx/flx}$ KA and formation of SCC following p53 loss in *HK1.ras/fos-K14creP.Δ5PTEN*$^{flx/flx}$ *mice* (*Yao et al., 2008; Macdonald et al., 2014*). Thus, β-catenin involvement was implied, but was not actually assessed in these earlier studies. This has been resolved in this chapter and also includes an investigation of E-cadherin expression. In both contexts an increase in β-catenin expression resulted in quite different results in conjunction with p53/p21 expression; whilst nuclear β-catenin and reduced E-cadherin expression were consistent with roles in driving malignant progression.

3.1 Analysis of biopsy DNA to determine mouse genotype and confirm *cre* activity.

Transgenic mouse genotypes were routinely identified via PCR analysis using DNA samples isolated from progeny tail tips and again confirmed in adult biopsy tissues. Typically, *K14.creP, HK1.ras, HK1.fos and Δβ-catenin* strains were maintained as heterozygotes in an outbred ICR background. This use of an outbred ICR background provides a more robust viability and the larger litters guarantee the chance of getting the required compound genotype in a minimum number of litters. For example, C57 or Balb c mice typically give 6/7 pups per mating, and thus do not guarantee a complete genotype when the targeted genotype is up to six alleles. Therefore, mating these mice with ICR compensates for their potential phenotype

variability; however, it must be noted that phenotype variability was found to be an advantage as it gave survivors in mice with severe phenotypes or a phenotypic example in mice with weak or subtle phenotypes.

Furthermore, breeding was not taken beyond the F5 generation to avoid any possible phenotypes from in-breeding. This was confirmed by Benavides and colleagues, who extensively studied this phenomenon (*Benavides et al., 2020*); concluding that as long as the outbred colony maintained was refreshed via regular mating with new ICR mice [routinely around or before F5]. This approach gave mice with a satisfactory background and avoided phenotypes due to in-breeding [F. Benavides; personal communication, IECC meeting October, 2018].

For instance, F3 *HK1.ras.K14.creP-Δ3β-catenin*$^{flx/wt}$ mice were full or medium sized; however, to generate the more complex genotypes e.g. *HK1.fos-K14creP.Δ5PTEN*$^{flx/flx}$ *.Δ3β-cat*$^{flx/wt}$ two more rounds of breeding were required to F5. This resulted in more severe phenotypes, where some mice exhibited abnormally small sizes, giving rise to this concern regarding inbreeding. However, as these studies unfolded, despite the inducible nature of the gene switch, this was associated with an unavoidable β-catenin mediated malnutrition in weaned juveniles due to internal leaky expression; yet in alternate keratin-cre driven models this internal expression was fatal in earlier models employing Δ3β-catenin mice (*Järvinen et al., 2006*); as confirmed in this study as no litters of *K5.cre.Δ3β-catenin* were obtained [not shown].

As shown in Fig 3.1 PCR analysis confirmed genotypes containing the *HK1.ras* and *HK1.fos* transgenes Fig 3.1 A & B, employing oligo primers specific to activated *v-ras*^{Ha} and FBJ/R *v-fos* oncogenes [See chapter 2 Table 2.2] (*Greenhalgh et al.,1993a; 1993b*). Oligos specific for the *creP* component of *K14creP* (*Berton et al., 2000*) identified *K14creP* positivity by a band at 410bp [Fig. 3.1 C].

In addition, recent attempts have been initiated to minimise a spontaneous β-catenin phenotype via use of a mutated cre regulator gene employing the [alleged leak-proof] *XJ5-creP** regulator transgene (*Zhou et al., 2002*). This XJK5creP* is similar to the K14-creP regulator in terms of targeted expression in basal-layer keratinocytes, follicles and stem cells (*Zhou et al., 2002*), and was designed to minimise leakage due to a mutation in the PLBD. Separate oligomers were designed to identify this new genotype now maintained as

homozygotes [Fig. 3.1D] and preliminary experiments do indeed block this spontaneous β-catenin phenotype but in this background XJK5creP*/β-catenin are currently devoid of any phenotype, thus in future experiments these mice appear to require extensive, prolonged RU486 treatments.

Identification of genotypes heterozygous and homozygous for the loxP-flanked exon5 *PTEN* allele employed oligos sets 1 & 2 [Fig.3.1E] and typically homozygous *Δ5PTEN*$^{flx/flx}$ lines were maintained for mating with *K14creP.Δ5PTEN*$^{wt/flx}$ mice to generate *K14creP.Δ5PTEN*$^{flx/flx}$. To confirm functional ablation of loxP-flanked exon 5 DNA isolated from topical RU486 treated biopsies employed *PTEN* oligo sets 1 & 3 to identify the truncated 500bp Δ5PTEN band in RU486 treated K14creP groups [Fig. 3.1 F].

However, it should be noted that this 500bp Δ5PTEN band was absent in untreated *K14creP.Δ5PTEN*$^{flx/flx}$ genotypes and genotypes lacking *K14creP* [Fig. 3.1C&E-F] were also devoid of this band, thus there was no spontaneous loss of exon 5 either. This result [also appearing in *p53* analysis below] was consistent with the observations that typically phenotypes are seldom derived from leakage of the regulator and appeared confined to β-catenin in this model *(Yao 2006;2008 Macdonald et al., 2014; Masre et al 2017, 2020*). Thus given this new β-catenin observation, *K14.creP.Δ5PTEN*$^{flx/flx}$ mice were reassessed for spontaneous RU486 independent cre leakage into the nucleus and this was observed randomly when older mice were maintained for > 6-9 months which exhibited occasional mild ear keratosis and no obvious internal problems.

Conditional knockout of *p53* [*K14creP.Δp53*$^{flx/flx}$] mice were also employed where exons 2 to exon 10 become deleted after RU486 treatment to inactivate function (*Berton et al., 2000; Jonkers et al., 2001*). Using oligo sets 1 and 2 specific for *p53* intron 1 [shown Fig. 3.1G; or 3 and 4 specific for intron 10] breeding colonies were maintained as *Δp53*$^{flx/flx}$ homozygotes and the *K14creP.Δp53*$^{flx/flx}$ genotypes were created by mating *K14creP.Δp53*$^{wt/flx}$ with *Δp53*$^{flx/flx}$ to generate *K14creP.Δp53*$^{flx/flx}$. *The K14.cre* activity to create the *Δp53* allele was confirmed by the use of oligo pairs: intron 1 forward 1 & intron 10 4 reverse, giving a *Δp53* band at 612 bp [Fig. 3.1 H]. Here the typical lack of detectable cre leakage is highlighted in lane 3 where untreated *K14creP.p53*$^{flx/flx}$ skin biopsy DNA does not possess the Δp53 band. However, if such leakage did occur the loss of p53 in the epidermis would go undetected, as p53 null mice

did not develop a phenotype in the absence of additional mutations such as *HK1.ras* (*Greenhalgh et al., 1996*).

To identify *p21* gene knockout, specific primers 1 & 2 were employed that detect the wild type p21 allele [$p21^{wt}$] at 430bp, and this band is absent in KO mice [Fig. 3.1I-J]. In addition to avoid false negatives and identify heterozygous mice, the $p21^{ko}$or $p21^{het}$ genotype was confirmed by employing oligos to the 5' and 3' non-coding sequences which gave a band at 180 bp indicating the KO allele (*Martín-Caballero et al., 2001*), whilst heterozygous p21 mice were identified by virtue of possessing both wt bands at 430 and the KO-specific allele at 180 bp bands [Fig. 3.1I-J].

β-catenin transgenic mice were identified by oligo primers specific to introns 2 and 4 of the loxP flanked exon 3 allele, giving a wt band at 324bp and the floxed allele at 500bp (*Harada et al., 1999*). Successful *Δ3β-catenin* activation was confirmed using another specific set of oligoes giving a 200bp band in mice carrying both *K14creP and Δ3β-catenin* [$K14creP.\Delta3\beta\text{-}cat^{flx/wt}$] transgenes. However, given the apparent potency of β-catenin in this model, typically RU486-treated *K14creP.Δ3β-cat* mice were maintained as heterozygotes [$K14creP.\Delta3\beta\text{-}cat^{flx/wt}$] as a novel, level of spontaneous phenotypes appeared in this model due to cre activity apparently independent of RU486 treatment. As cited above, this leakage was a phenomenon previously only observed in occasional older [> 6 month], untreated tri-genic $HK1.ras/fos\text{-}\Delta5PTEN^{flx/flx}$ or older bi-genic $HK1.ras\text{-}\Delta5PTEN^{flx/flx}$ mice, which had each displayed a significant degree of neonatal ras/fos-associated hyperplasia (*Greenhalgh et al 1993c*) during development that continued into adults (*Yao et al., 2006;2008; Macdonald et al., 2014*). As described in detail below, this gene switch leakage in bi-genic $K14creP.\Delta3\beta\text{-}cat^{flx/wt}$ mice resulted in a juvenile phenotype from approx. 10 days post birth [following the first anagen] unless intriguingly being inhibited by loss of p53 in the $p53^{flx/flx}$ progeny as well. However, unlike similar approaches employing constitutive keratin-driven cre (*Järvinen et al., 2006*), the $K14creP.\Delta3\beta\text{-}cat^{flx/wt}$ heterozygotes and homozygotes were viable, and this may explain the current lack of classic skin chemical/transgenic carcinogenesis studies using these mice.

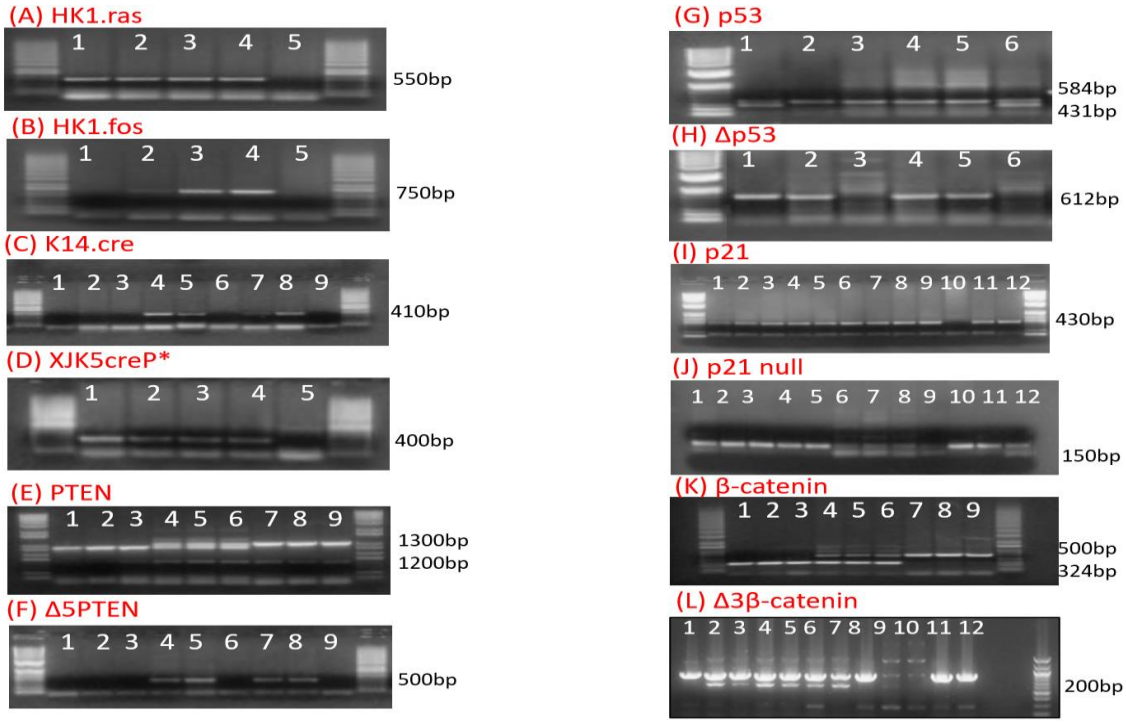

Figure 3. 1: Confirmation of genotype by PCR analysis.

[A] *HK1.ras* positive mice exhibit a 550bp band [lanes 1-4]; absent in negative control DNA [lane 5]. [B] *HK1.fos* positive mice exhibit a 750bp band [lanes 2-4; lanes 1 & 5: negative control]. [C] *K14.creP* positive mice exhibit 410bp band [lanes 4-5 & 7-8]. [F] Positive XJK5creP* mice give a 400bp band [lanes 1-4; lane 5: negative control]. [E] A gel corresponding to [C], shows the *PTEN*^{wt} allele band at 1200bp [lanes 1-3], with *K14creP.Δ5PTEN*$^{flx/wt}$ heterozygotes [lane 4-6] and *K14creP.Δ5PTEN*$^{flx/flx}$ homozygotes [lanes 7-9] show the additional loxP-flanked *Δ5PTEN* allele at 1300bp. [F] Also corresponding to D/C, only RU486 treated *K14creP.Δ5PTEN*$^{flx/wt}$ mice [lanes 4-5] and *K14creP.Δ5PTEN*$^{flx/flx}$ [lanes 7-8] show successful ablation of exon 5 [*Δ5PTEN*] with positive band at 500bp [G] Analysis of p53 mice employing intron1 oligos 1 & 2 gives a p53^{wt} band at 431bp [lane 1], p53$^{flx/flx}$ band at 584bp [lanes 2-5] and a doublet in p53$^{flx/wt}$ heterozygosity [lane 6]. [H] To confirm cre activity a 612bp Δp53^{flx} band appears in RU486-treated *K14creP*.p53$^{flx/flx}$ mice [lanes 1-2; 4-5], which is absent in untreated RU486 *K14creP*.p53$^{flx/flx}$ skin [lane 3] or RU486-treated but *K14creP* negative p53$^{flx/flx}$ skin [lane 6]. [I] Confirmation of p21 knockout involved a lack of a 430bp band using oligos specific for the wt allele [lane 10] and data combined with [J] where oligos specific to the 5' and 3' non-coding sequences give DNA positive for the null allele at 150bp [lane 10]; whilst heterozygosity [lanes 1-5 & 11-12] is indicated by presence of both bands. (K) *Δ3β-catenin* allele analysis shows wild-type *β-catenin* allele at 324bp [lanes 1-3], with mice heterozygous for the loxP-flanked exon 3 possess both wt and floxed allele bands at 500bp [lanes 4-6]; with homozygotes possessing the loxP-flanked exon 3 allele at 500bp [lane 7-9]. [L] Successful ablation of exon 3 [Δ3β-catenin] in RU486-treated *K14creP.Δ3β-cat*$^{flx/wt}$ mice is indicated in lanes 2-7 by the appearance of a lower less intense 200bp band indicative of the heterozygous nature of Δ3β-catenin expression and the greater amount of non-epidermal tissue in these skin biopsy samples. Lanes 9 & 10 wt DNA; lanes 11 & 12 non cre Δ3β-catenin alone; thus showing the leakage is K14.creP specific.

3.2 Analysis of endogenous β-catenin status in multistage *HK1.ras/fos-K14creP.Δ5PTEN$^{flx/flx}$* carcinogenesis

β-catenin expression status was analysed in tri-genic *HK1.ras/fos-K14creP.Δ5PTEN$^{flx/flx}$* carcinogenesis model together with the bi-genic combinations and *HK1.ras/fos* and *K14cre.Δ5PTEN* alone strains. As outline in the introduction these mice were ideal to assess possible β-catenin roles at each stage of tumour formation (*Greenhalgh et al., 1993a-c*; *Yao et al., 2006; 2008; Macdonald et al., 2014*) and for this study these genotypes were re-established to provide fresh material for β-catenin analysis in addition to initial use of archival samples; and for use as comparison controls following RU486-mediated β-catenin activation.

As shown in Fig. 3.2, the new combinations of *HK1.ras/fos-K14creP.Δ5PTEN$^{flx/flx}$* mice gave identical results to those produced in previous studies (*Greenhalgh et al., 1993 a-c;* Yao *et al., 2006; 2008; Macdonald et al., 2014*). *HK1.ras* activation (*Greenhalgh et al., 1993a; 1993c*) provided the initiation step [Fig. 3.2A] that initially results in a thickened scaly skin in neonates that resolves in adults [Fig. 3.2A see chapter 1 Fig. 1.5]. Histologically *HK1.ras* activation induced epidermal hyperplasia, and this persists in adult ears and is the precursor to an overt papilloma in the *HK1.ras^{1205}* strain [Fig. 3.2E]. (*Greenhalgh et al., 1993a*). Of note, two strains of *HK1*.ras mice exist, line 1205 which is highly sensitive to promotion thus the ear tag wounding results in papillomas in 100% of animals within 6-8 weeks, whereas line 1276 maintains a simple hyperplasia due to induction of p53 [see below] (*Masre et al., 2020*). *HK1.ras^{1205}* papillomas are similar to *HK1.ras/fos*, [Fig. 3.2B see chapter 4]; and histologically these tumours show no sign of malignant conversion. However if the tag is lost, *HK1.ras^{1205}* papillomas regress whereas in *HK1.ras/fos* papillomas are autonomous, as the promotion stimulus is provided by *HK1.fos*, yet together *HK1.ras^{1276}/HK1.fos* results in a benign papilloma that does not spontaneously convert to malignancy [Fig. 3.2F] (*Greenhalgh et al., 1993c*). *HK1.fos* mice eventually exhibit a hyperkeratotic ear skin consistent with roles in keratinocytes differentiation (*Greenhalgh et al., 1993b*; see chapter 7) [NB: Crosses of 1205 and *HK1.fos* produce a phenotype too severe for UK experimentation].

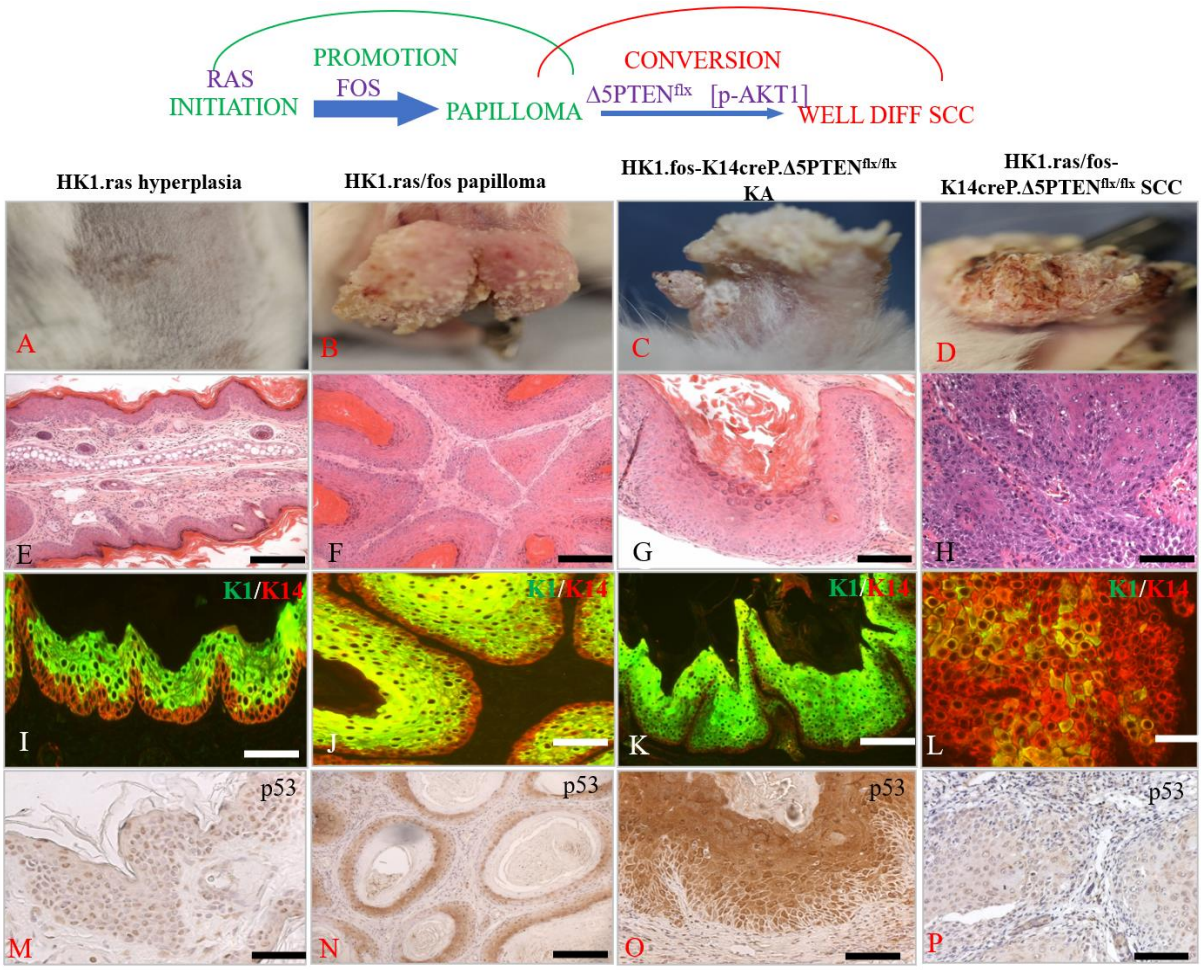

Figure 3. 2: HK1.ras/fos-K14creP.Δ5PTEN$^{flx/flx}$ carcinogenesis phenotypes; histopathology, mK1 differentiation marker analysis and p53 expression

Upper: Schematic diagram shows ras initiates; fos promotes; but malignant conversion requires PTEN [and/or p53] loss.[A-D]: Overt *HK1.ras/fos-K14creP.Δ5PTEN$^{flx/flx}$* phenotypes: (A) *HK1.ras^{1205}* residual hyperplasia; (B) *HK1.ras/fos* benign papilloma; (C) Highly keratotic *HK1.fos-K14creP.Δ5PTEN$^{flx/flx}$* keratoacanthoma [KA] and [D] malignant *HK1.ras/fos-K14creP.Δ5PTEN$^{flx/flx}$* SCC. [E-H] Histopathology of (E) *HK1.ras^{1205}* neonatal ear skin hyperplasia (F) *HK1.ras/fos* squamous papilloma; (G) *HK1.fos-K14creP.Δ5PTEN$^{flx/flx}$* keratoacanthoma: typified by extensive keratin layers and a disorganised epidermal differentiation; (H) Aggressive, invading *HK1.ras/fos-K14creP.Δ5PTEN$^{flx/flx}$* SCC exhibit multiple mitotic figures. [I-L] IF analysis of keratin K1 vs keratin K14 expression. (I/J) Hyperplasia and papillomas show strong K1 expression confined to supra-basal layers with K14 showing expanded proliferative basal layers. (K) KAs show K1 expression in basal keratinocytes indicating an accelerated differentiation. (L) *HK1.ras/fos-K14creP.Δ5PTEN$^{flx/flx}$* SCC exhibits K1 loss indicating aggressive SCC. [M-P] IHC analysis of p53 shows expression increases but is lost on conversion. (M) Sporadic p53 expression in *HK1.ras^{1205}* hyperplasia becomes strong in (N) papillomas and stronger still in (O) KAs with clear nuclear expression in basal keratinocytes; however (P) p53 expression is lost in *HK1.ras/fos-K14creP.Δ5PTEN$^{flx/flx}$* SCC. Scale bars: 50µm

This phenotypic stability of benign papillomas indicated that these mice were ideal to study malignant conversion, and given its role in the familial cancer syndrome of Cowden's disease (*Hopkins et al., 2014*), the failure of PTEN-mediated AKT inhibition via ablation of exon 5 [*Δ5PTEN*] was the first addition to this model to study roles in papilloma formation and conversion to malignancy (*Yao et al., 2006;2008; Macdonald et al., 2014*). Initial experiments first introduced PTEN mutation into the *HK1.ras* model [*HK1.ras.Δ5PTEN*$^{flx/flx}$] which resulted in accelerated papillomatogenesis, as seen with earlier models (*Greenhalgh et al., 1995*). Benign papillomas required TPA promotion treatment to convert to malignancy and this resulted in very aggressive poorly differentiated SCCs (*Yao et al., 2006*). Later studies showed that such TPA promotion was necessary to overcome a protection invoked via elevated levels of p53 and p21 in response to PTEN loss of AKT regulation (*Macdonald et al., 2014*) and earlier studies involving HK1.fos co-operation with PTEN loss[*Δ5PTEN*] demonstrated that the KA aetiology had been dependent upon this compensatory expression of p53 and p21 that first inhibited proliferation as determined by BrdU labelling analysis and subsequent induction of keratinocyte differentiation via p21 (*Toply et al., 1999*) indicated by premature keratin K1 expression (*Yao et al., 2008*).

Indeed, it was the co-operation between *HK1.fos* and *Δ5PTEN* that first highlighted the important roles for β-catenin in this model in terms of the compensatory responses deployed by the epidermis in order to maintain its homeostasis and inhibit tumour progression at each individual stage. In the co-operation of *HK1.fos.K14.Δ5PTEN*, novel benign keratoacanthomas [KA] developed [Fig. 3.2C]. This benign, regression prone tumour is typified in humans by the histological changes from papilloma in terms of a massive degree of hyperkeratosis resulting in the overt keratotic appearance of classic KA [Fig. 3.2C&G]. Here significant compensatory p53 and p21 expression [below] was triggered by high levels of p-AKT due to the lack of PTEN exon5, that in turn inactivated GSK3β (Yao et al., 2008); leading to [then assumed] deregulation of β-catenin [confirmed below Fig. 3.3 (*Alyamani et al.,* manuscript in preparation)] This appearance of β-catenin in the basal layers of the earlier papilloma-like stage induced a corresponding burst of p53 (Fig. 3.2O) which caused the massive keratosis of KA [Fig. 3.2C&G] (*Yao et al., 2008*). This was also observed in ROCK2-mediated studies in this model that again led to β-catenin mediated induction of p53 and inhibition of papillomas (*Masre et al., 2020*)- a noteworthy finding given the results in Chapter 5. In the tri-genic

HK1.ras^{1276}*/fos.Δ5PTEN* genotypes, with the addition of activated ras^{Ha}, mice now showed a novel malignant progression, following p53 loss in late stage papillomas initially to wdSCC, that progressed to poorly differentiated SCC [pdSCC] following additional p21 loss and uniform p-AKT1 activation (*Macdonald et al., 2014*) which showed increasingly aggressive tumour phenotypes with clear sign of invasion and a highly disorganized epidermis [Fig. 3.2D&H].

To help confirm the histotype analysis, double-labelled IF analysis was conducted for expression of keratin1 [mK1; green], an early stage differentiation marker expressed in supra-basal layers and also used as a marker to indicate late-stage benign papilloma from an early wdSCC carcinogenesis, as it is progressively lost during conversion to SCC (*Macdonald et al., 2014*). In these experiments, expression of Keratin14 [mK14; red] was routinely employed to delineate either the epidermis and follicles, or tumour from surrounding stroma. As shown in Fig 3.2 I & J, both typical hyperplasia and papillomas show a relatively normal supra-basal expression of K1, in a context where the basal layer expands as indicated by a wider K14^{+ve} [red] basal layer due to a proliferative response to *ras* and/or *fos* activation.

Of note, in the KAs produced by *HK1.fos-K14creP.Δ5PTEN*$^{flx/flx}$ co-operation, an accelerated and premature differentiation pattern was indicated by strong and novel K1 expression in the basal layers, with mK1 expression levels often masking K14 co-expression [Fig 3.2 K]. This result was consistent with a premature commitment to differentiation giving the massive levels of keratosis associated with this tumour type (*Yao et al., 2008*) and the new findings on the responses to anomalous expression of basal-layer β-catenin [below]. However, in tri genic *HK1.ras/fos-K14creP.Δ5PTEN*$^{flx/flx}$ SCCs, K1 expression was greatly reduced indicative of malignant conversion [Fig. 3.2L].

This differentiation analysis was followed by investigation of p53 expression given its roles in human carcinogenesis (*Mollereau and Ma, 2014*). Surprisingly typically early *HK1.ras* and *HK1.fos* hyperplasia showed an initial weak and only sporadic expression [Fig. 3.2M] which was similar to normal epidermis [chapter 1 Fig 1.7] possibly indicative of epidermal tolerance to excess proliferation such as in normal wound healing and the possibly danger to barrier maintenance from deregulated, p53-mediated, apoptosis (*Calautti et al., 2005*) and therefore giving only sporadic expression in those basal keratinocytes completing the cell cycle.

However, with time and degree of hyperplasia i.e. the greater hyperplasia in RU486-treated *HK1.ras/fos-K14creP.Δ5PTEN$^{flx/flx}$* , p53 expression became stronger such that on progression to papilloma p53 was expressed in the nuclei of most basal layer keratinocytes [Fig. 3.2 N&O], which helped in halting any further malignant progression. This was observed in e.g. *HK1.ras.K14.Δ5PTEN* bi-genic papillomas that required TPA promotion to achieve malignancy, where early p53 loss was observed in aggressive papillomas making them susceptible to conversion via accumulation of new mutants (*Yao et al., 2006*). Indeed all KAs showed very strong p53 expression in the basal layers [Fig. 3.2 O]correlating with the massive increase in differentiation [Fig. 3.2K] due to GSK3-β induction of both p53 [and p21] in basal layers (*Yao et al., 2008*), while, tri-genic SCCs with additional ras activation had lost expression of p53 again at the papillomas stage leading to conversion to wdSCC; although expression of p21 [not shown] inhibited early progression which was then lost and tumours progressed to pdSCC [Fig. 3.2P].

3.3 Analysis of β-catenin and E-cadherin expression in *HK1.ras/fos-K14creP.Δ5PTEN$^{flx/flx}$* carcinogenesis

Previously, and mainly based on the levels of inactivated p-GSK3β observed in *HK1.fos-K14creP.Δ5PTEN$^{flx/flx}$* mice (*Yao et al., 2008*), it was assumed that loss of GSK3β-mediated β-catenin ubiquination resulted in the potential persistence of nuclear β-catenin and thus deregulation of Wnt signalling. Thus, at a specific stage in the aetiology of KA, a level of GSK3β inactivation may have achieved a threshold of elevated β-catenin that triggered the compensatory p53 expression responses that led to cessation of proliferation, and the excess p21 that induced the irregular differentiation and hyperkeratosis. In addition, this PTEN-AKT/β-catenin axis was possibly involved in the malignant conversion observed in *HK1.ras/fos-K14creP.Δ5PTEN$^{flx/flx}$* mice following p53 loss and to some extent alongside that of deregulated E-cadherin signalling, β-catenin co-operated with AKT to drive malignant progression following p21 loss *(Macdonald et al.*, 2014). Therefor to finally confirm these ideas and provide data for endogenous β-catenin status in each of the HK1 models, endogenous β-catenin and E-cadherin expression were assessed at different stages of progression using archival and new *HK1.ras/fos-K14creP.Δ5PTEN$^{flx/flx}$* biopsies [Fig. 3.3; (*Alyamani et al.,* Manuscript in Preparation)].

In early *HK1.ras*^{1205} or *HK1.ras*^{1276}*/fos* hyperplasia β-catenin expression appeared to be increased over normal yet appeared confined to the supra-basal layers and remained strongly membranous [Fig 3.3A&E], in a similar fashion to that of normal epidermis. [below chapter 4 Fig. 4.4C]. In *HK1.ras* papillomas this profile persisted [chapter 5 Fig. 5.14E&F] but in autonomous *HK1.ras/fos* papillomas occasional strands of basal layer β-catenin were detected [Fig. 3.3B&F]. Here β-catenin expression exhibited a strong membranous expression in both basal and supra-basal layers but now with sporadic detectable nuclear expression [Fig. 3.3F] that paralleled the increasing expression of nuclear p53 [Fig 3.3N]. Furthermore, *HK1.fos-K14creP.Δ5PTEN*$^{flx/flx}$ KAs showed even greater β-catenin expression levels in both basal and supra-basal layers again with both membranous expression as well as clear detectable nuclear expression [Fig. 3.3C&G]. This combination of membranous and now easily detectable β-catenin expression correlated with strong [Δ5PTEN/AKT-mediated] p-GSK3β inactivation observed previously (*Yao et al., 2008*) associated with an increase in nuclear p53 expression [Fig. 3.3O] and a massive differentiation response resulting in a novel KA aetiology [Fig. 3.2C&G]; an observation repeated in ROCK2 mice where such β-catenin -mediated p53 expression inhibits papilloma formation (*Masre et al., 2020*). Moreover, whilst hyperplasia and papillomas gave a β-catenin profile of both membranous nuclear profile similar to KA, in *HK1.ras/fos.K14.Δ5PTEN* mice on conversion to SCC, membranous β-catenin expression was greatly reduced, especially in the invasive basal layers that now possessed a very strong cytoplasmic/nuclear β-catenin expression, particularly prominent in the more sensitive IHC analysis [Fig. 3.3D&H]. This may be indicative of driving malignant progression via increased transcription and membrane loss a compromise of focal adhesion signalling, which led to E-cadherin analysis [below].

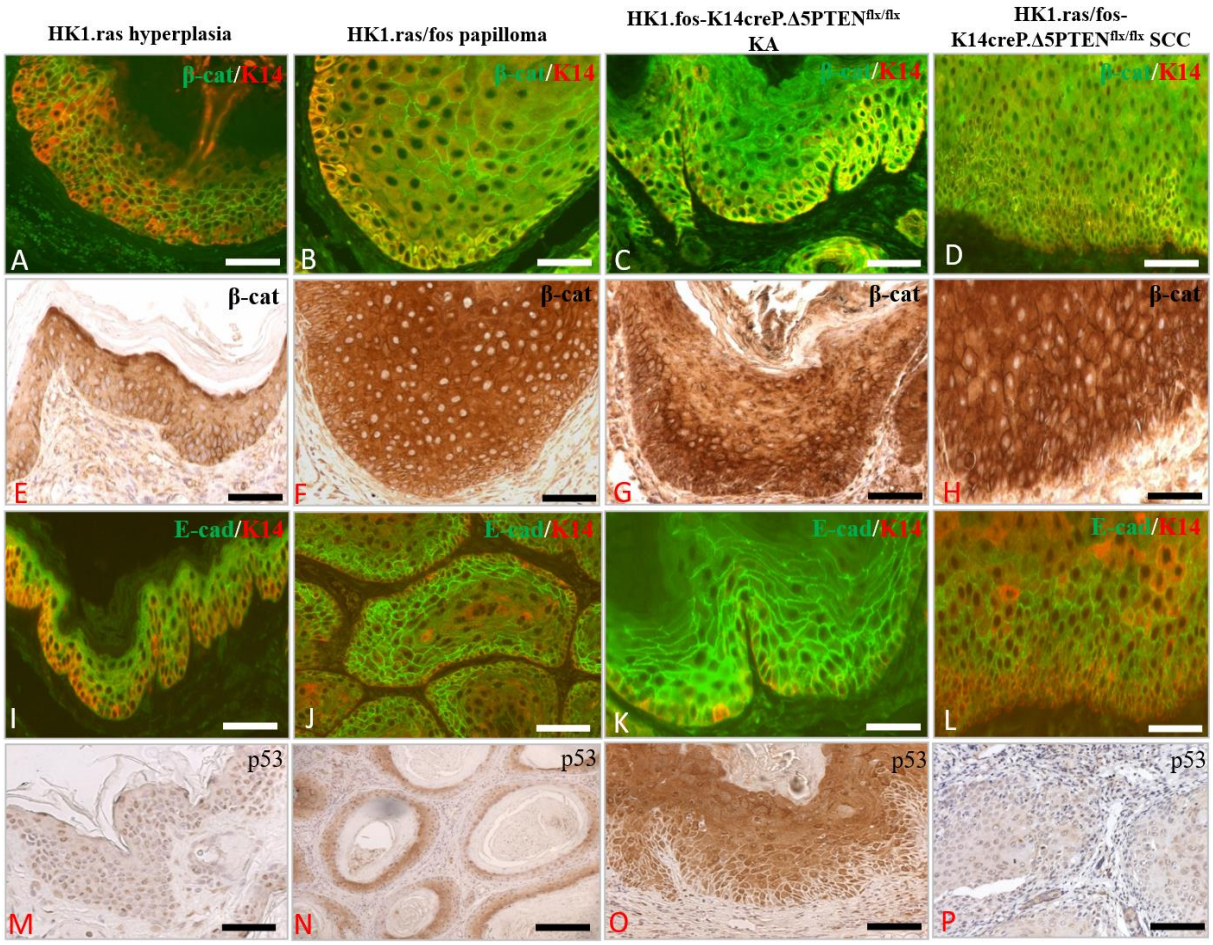

Figure 3. 3: β-catenin and E-cadherin vs. p53 expression in *HK1.ras/fos-K14creP.Δ5PTEN*$^{flx/flx}$ carcinogenesis.

[A] Early and [E] later *HK1.ras* hyperplasia shows membranous β-catenin expression in supra-basal layers with occasional strands of basal layer expression. [B & F] *HK1.ras/fos* papillomas show increasing membranous expression in basal layers but sporadic nuclear expression. [C & G] *HK1.fos-K14creP.Δ5PTEN*$^{flx/flx}$ KA exhibit strong membranous expression in all layers and nuclear expression in basal keratinocytes correlating with high p53 responses. [D & H] *HK1.ras/fos-K14creP.Δ5PTEN*$^{flx/flx}$ SCCs show strong nuclear expression following p53 loss, with reduced membranous expression consistent with failures in adhesion helping invasion. [I] Hyperplastic E-cadherin expression is membranous and supra-basal mimicking β-catenin. [J] E-cadherin expression in papillomas is supra-basal again similar to β-catenin. [K] *HK1.fos-K14creP.Δ5PTEN*$^{flx/flx}$ KAs exhibit E-cadherin in basal layers, similar to β-catenin, associated with anomalous, accelerated differentiation. [L] *HK1.ras/fos-K14creP.Δ5PTEN*$^{flx/flx}$ SCCs show reduced E-cadherin expression at the invasive front, suggesting a loss of cell-cell adhesion but retain some supra-basal expression consistent with a model of collective invasion. [M] p53 analysis shows sporadic hyperplasia expression becomes elevated in [N] papillomas and stronger in [O] KAs correlating with increased β-catenin expression; however, [P] p53 expression is weak/lost in SCC correlating with reduced membranous/increased nuclear β-catenin and loss of E-cadherin expression in the invading cells. Scale bars: 50μm

E-cadherin is an essential part of the cell-cell adhesion complex needed for normal epidermal barrier functions and with β-catenin roles in the signalling functions from the plasma membrane to nucleus (*Jeanes et al., 2008*). Given these intimate interactions and the β-catenin results which showed alterations in membranous expression depending on the stage of tumour progression; E-cadherin levels were assessed in stage specific *HK1.ras/fos-K14creP.Δ5PTEN*$^{flx/flx}$ phenotypes [Fig. 3.3I-L]. In *HK1.ras* mice, E-cadherin expression in hyperplasia remained essentially similar to normal with supra-basal layer membranous expression [Fig. 3.3 I] consistent with focal adhesions that aid in epidermal barrier functions. In *HK1.ras/fos* papillomas, E-cadherin expression was increased but again appeared in supra-basal basal layers with occasional strands of positive basal-layer keratinocytes possibly to aid the inhibition of conversion in this model via appropriate cell-cell adhesion signalling to increase adhesion and possible signal to induce p53 expression via β-catenin [Fig. 3.3J]. In *HK1.fos-K14creP.Δ5PTEN*$^{flx/flx}$ KAs strong supra-basal E-cadherin expression became strongly expressed in the basal layers, constant with its protective roles from tumour invasion due to elevated, increased differentiation (*Chiles et al., 2003; Jeanes et al., 2008*) and thus increasing cell-cell adhesion [Fig 3.3 K] and preventing invasion. This expression profile correlated with both membranous and nuclear β-catenin expression that induced the strong compensatory expression of p53 [Fig 3.3C,G,K,O]. However, in aggressive *HK1.ras/fos-K14creP.Δ5PTEN*$^{flx/flx}$ SCCs membranous E-cadherin expression disappeared in the invasive basal layers that co expressed nuclear β-catenin [Fig. 3.3D,H,L,P].

These results reinforce β-catenin involvement in aiding malignant progression as it suggests that the loss of p53 and nuclear localization of β-catenin in SCCs greatly reduce the ability of E-cadherin to form focal adhesion junctions in the invasive front; an observation consistent with the collective invasion profiles observed in human SCC (*Hesse et al., 2016*). It also appears that the anomalous expression of β-catenin in the basal layers correlates with the resulting expression of p53 and p21, a significant observation that has relevance for the results in chapter 6 in facilitation of tumour invasion via failures in cell-cell signalling once the unique and paradoxical block of tumour formation induced in response to β-catenin overexpression was overcome.

Table 3. 1: Summary of β-catenin and E-cadherin expression in *HK1.ras/fos-K14creP.Δ5PTEN$^{flx/flx}$* carcinogenesis

Genotype analysed	[N]	Analysed for expression of	Data summary
HK1.ras hyperplasia	90	β-catenin, E-cadherin and p53 expression	Control hyperplasia showing membranous, supra basal layer β-catenin and E-cadherin expression correlates with a lack of basal layer p53 [similar to normal ICR expression]
HK1.ras/fos papillomas	15	β-catenin, E-cadherin and p53 expression	Control papilloma showing both membranous supra and basal layer β-catenin and E-cadherin expression correlates with basal layer p53 expression
HK1.ras/fos-K14creP.Δ5PTEN$^{flx/flx}$ SCC	18	β-catenin, E-cadherin and p53 expression	SCC showing membranous β-catenin/E-cadherin expression becomes reduced in basal layers but cytoplasmic/nuclear β-catenin expression becomes detectable and correlates with a loss of p53 expression
HK1.fos-K14creP.Δ5PTEN$^{flx/flx}$ KA	18	β-catenin, E-cadherin and p53 expression	KA showed increased membranous β-catenin/ E-cadherin expression levels in both basal and supra-basal layers with detectable nuclear/cytoplasmic β-catenin, correlating with basal layer p53
Conclusion: Increased cytoplasmic/nuclear β-catenin expression via loss of GSK3β-mediated β-catenin ubiquination, aids in driving malignant conversion in *HK1.ras/fos-K14creP.Δ5PTEN$^{flx/flx}$* SCCs following loss of p53. This was constant with reduced membranous β-catenin/E-cadherin basal layer expression indicative of reduced cell-cell adhesion. However, in benign *HK1.fos-K14creP.Δ5PTEN$^{flx/flx}$* KA with the absence of ras activation, increased membranous basal layer expression of β-catenin/E-cadherin and detectable nuclear β-catenin activation triggered increased basal layer p53 expression thus halting malignant conversion via strengthened cell-cell adhesion unlike SCCs aetiology. These data indicate that β-catenin roles in carcinogenesis are context dependent and the outcome will depend other oncogene activation and TSGs responses.			

Chapter 4: Analysis of β-catenin overexpression in transgenic mouse skin

4.1 Introduction

β-catenin is a dual function protein, it acts to maintain the epithelial cellular barrier via forming a cell-cell adhesion complex with E-cadherin, Thus, failure of this function has been associated with facilitating tumorigenesis (*Grigoryan et al., 2008*; *Jeanes et al., 2008*). β-catenin also acts as a nuclear transcriptional activator of canonical Wnt/β-catenin signalling targets LEF/TCF, which are associated with hair follicle differentiation and morphogenesis (*Grigoryan et al., 2008*). An over expression of this pathway via β-catenin gain of function mutation has been associated with several types of cancer such as colon, prostate, ovarian, melanoma and non-melanoma skin cancers (*Morin, 1999; Gerdes and Yuspa, 2005; Grigoryan et al., 2008*).

Previous studies conducted on constitutive activation of β-catenin in skin resulted in HF abnormalities, hence Wnt/β-catenin roles in regulating hair follicles differentiation and morphogenesis. These studies reported HF abnormalities such as increased formation of HF placode, de novo HF, formation of epidermal cyst and HF tumours such as pilomatricoma and trichofolliculoma (*Gat et al., 1998; Huelsken et al., 2001; Grigoryan et al., 2008*). However, IFE tumours such as cutaneous squamous cell carcinoma were not reported in response to constitutive activation of β-catenin alone in skin.

Therefore, in this analysis the aim was to investigate the phenotype similarities of inducible constitutive activation of β-catenin in *K14creP.Δ3β-cat*$^{flx/wt}$ to previous studies and investigate the effect on epidermal terminal differentiation and TSGs expression in response to β-catenin activation. Thus, before analysing *K14creP.Δ3β-cat*$^{flx/wt}$ co-operation with *HK1.ras* to assess its roles in SCC development and whether it would result in a similar or contrary effect on tumorigenesis in comparison to the endogenous β-catenin analysis in multistage *HK1.ras/fos-K14creP.Δ5PTEN*$^{flx/flx}$ carcinogenesis [see chapter 3]

4.2 K14creP.Δ3β-cat$^{flx/wt}$ over expression in mouse skin induced hair follicle abnormalities and hair follicle tumours.

The first step taken to directly analyse the effects of constitutive β-catenin activation in the *HK1.ras/fos-K14creP.Δ5PTEN$^{flx/flx}$* model was to create expression of *Δ3β-catenin* in mouse epidermis by mating *K14.creP* with *Δ3β-catenin* [*K14.creP.Δ3β-cat$^{flx/wt}$*]. As outlined in Fig. 4.1 A, exon 3 of *β-catenin* is flanked by lox-P sites thus in principle following topical application of RU486, constitutive β-catenin activation was induced via removal of the APC/GSK3β binding complex to eliminate its negative regulation by cytoplasmic ubiquination (*Harada et al., 1999; Berton et al., 2000*). Routine PCR analysis confirmed *K14creP.Δ3β-cat$^{flx/wt}$* genotypes [Fig. 4.1B] and β-catenin transgenic mice [*Δ3β-catenin*] were identified by oligo primers [Table. 2.2] specific to intron 2 and 4 of the loxP flanked exon 3 allele giving a wt band at 324bp and the floxed allele at 500bp (*Harada et al., 1999; Berton et al., 2000*). In addition, successful *Δ3β-catenin* activation was confirmed using another specific set of oligos giving a band at 200bp band in mice carrying both *K14creP and Δ3β-catenin* [*K14creP.Δ3β-cat$^{flx/wt}$*] transgenes [Fig. 4.1C], ideally in response to RU486 treatment but as discovered this was not necessarily the case for all *K14.creP.Δ3β-cat$^{flx/wt}$* mice on this outbred ICR background RU486 treatment due to the potency of β-catenin deregulation.

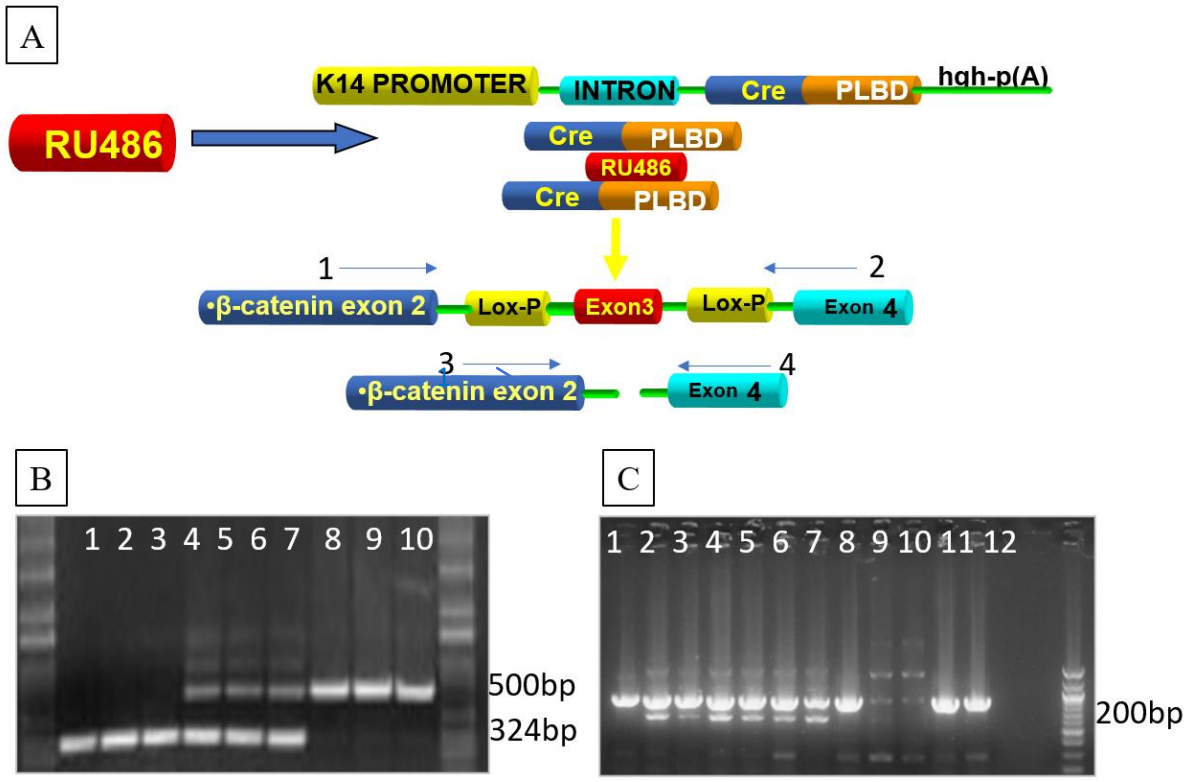

Figure 4. 1: A schematic diagram to illustrate the mechanism of RU486-inducible cre/loxP system in the ablation of exon 3 in β-catenin and PCR analysis confirming Δ3β-catenin expression.

[A] The keratin *K14creP* driven cre is used to achieve exclusive cre expression in all keratinocytes. To activate cre in the epidermis and hair follicles transgenic mouse skin is treated with RU486 and the PLBD translocates into the nucleus where cre activity deletes the sequence flanked by lox P sites. In this model exon 3 the binding site for β-catenin ubiquination is removed resulting in constitutive activation. Oligo primers 1 & 2 are employed to identify the loxP alleles and 3 & 4 to confirm cre activity.

[B] PCR analysis of Δ3β-catenin allele genotypes shows the wild-type β-catenin allele at 324bp [lanes 1-3], whilst mice heterozygous for the loxP-flanked exon 3 possessed both the wt band and the additional floxed allele band at 500bp [lanes 4-6]; this band also appeaerd in mice homozygous for the loxP-flanked exon 3 allele [lane 7-9].

[C] Successful ablation of exon 3 [Δ3β-catenin] in RU486-treated *K14.creP-Δ3β-catenin*$^{flx/wt}$ mice is indicated in lanes 2-7 by the appearance of a lower less intense 200bp band indicative of the heterozygous nature of *Δ3β-catenin* expression and the greater amount of non epidermal tissue in these skin biopsy samples. Lanes 9 & 10 wt DNA; lanes 11 & 12 non-cre *Δ3β-catenin* alone; thus showing the leakage is K14creP specific.

Typically, *K14creP.Δ3β-cat* mice were maintained as heterozygotes [*K14creP.Δ3β-cat*$^{flx/wt}$] due to a low level of spontaneous cre activity appearing in increasing numbers of juveniles as progressive additional transgenes were introduced. This resulted in skin phenotypes apparently independent of overexpression in this model. As cited above, this novel phenomenon was previously observed only in sub-sets of older, untreated tri-genic *HK1.ras/fos-K14creP.Δ5PTEN*$^{flx/flx}$ or bi-genic *HK1.ras-Δ5PTEN*$^{flx/flx}$ mice that had undergone a more severe hyperplastic phase in neonatal development (*Yao et al., 2006; 2008; Macdonald et al., 2014*).

Thus, whilst most *K14creP.Δ3β-cat*$^{flx/wt}$ mice still required RU486 treatment to fully elicit a Δ3β-catenin phenotype, frequently by 16-24d [i.e. post the initial anagen phase] juvenile mice often exhibited mild alopecia and a general disheveled scruffiness to the coat, and enlarged extremities that comprise of abnormal oversized feet, with a thickened hyperkeratotic tail and large ears [Fig. 4.2A-G]. In addition, and particularly following RU486 treatment, the shaven dorsal sites exhibited a mild keratosis within a week of initial treatment [Fig. 4.2I] and at these sites typically the fur remained sparse.

It was also noted that juvenile *K14creP.Δ3β-cat*$^{flx/wt}$ mice varied in body size some being similar to normal ICR or smaller when compared to *K14creP* and *Δ3β-catenin* alone siblings. This varied appearance and the severity of these overt juvenile phenotypes were attributed to the randomness of early RU486-independent cre leakage as well as the differing genetic backgrounds of individual family trees on this outbred ICR background. Nonetheless, once introduced to the RU486 treatment regime, all *K14.creP.Δ3β-cat*$^{flx/wt}$ produced similar levels of phenotype regardless of their genetic background.

These findings were very similar to many previous transgenic mouse studies that reported identical gross abnormalities involving mice where constitutive β-catenin activation was achieved in the epidermis (*Gat et a.,1998; Van Mater et al., 2003; Celso et al.,2004; Närhi et al 2008*). However, in all these models, effects of β-catenin overexpression focussed on hair follicle development and anomalies and later to effects on stem cells and useful paracrine effects on fibroblasts but to date none have exploit such mice in the development of classic skin carcinogenesis models.

Figure 4. 2: *K14creP.Δ3β-cat*$^{flx/wt}$ mouse phenotypes.

[A] RU486-treated *K14creP.Δ3β-cat*$^{flx/wt}$ mice shows a general lack of correct hair growth resulting in a dishevelled appearance. Also note the peri-orbital hyperkeratosis and abnormal fibrisse; and the fact these mice are full sized in this litter. [B] Higher magnification of *K14creP.Δ3β-cat*$^{flx/wt}$ shows a larger and thickened keratotic ear compared to [C] a normal ear. [D] *K14creP.Δ3β-cat*$^{flx/wt}$ mice show phenotypically abnormal tails-independent of RU486-treatment with a thickened appearance, and a greasy appearance. Also the feet of *K14creP.Δ3β-cat*$^{flx/wt}$ mice exhibited increased hyperkeratosis on the palmoplantar surface [E] At higher magnification *K14creP.Δ3β-cat*$^{flx/wt}$ possess phenotypically larger feet compared to normal, with a swollen, oedematous nature suggesting effects on dermal physiology alongside that of greasy fur. [F & G] Higher magnification shows increased alopecia resulting in dishevelled fur in *K14creP.Δ3β-cat*$^{flx/wt}$ again with larger feet against [H] normal ICR. [I] a typical RU486-treated *K14creP.Δ3β-cat*$^{flx/wt}$ dorsal skin displays a lack of regrown fur and a mild hyperkeratosis compared to [J] RU486-treated normal skin.

Histologically the epidermis of RU486-treated K14creP.Δ3β-cat$^{flx/wt}$ mice was dominated by the appearance of multiple hair follicle abnormalities such as the increased formation of *de novo* hair follicle placodes; especially obvious in the ear histotype [Fig. 4.3A] but with little in the way of fully formed hair shafts at higher magnification [Fig. 4.3B vs. E] hence the general mild alopecia and dishevelled appearance of the fur.

These hair follicle abnormalities were more apparent on back skin histotypes and were accompanied by formation of cysts [Fig. 4.3C], since this area normally possess more hair follicles than the ears and consistent with previous reports (*Närhi et al., 2008*) despite the increased numbers of placodes the actual hair regrowth following RU486 treatment was poor [Fig. 4.3C]. Here the treated skin shows a wrinkled nature yet on comparison to a typical *HK1.ras* or *HK1.fos* epidermis [above chapter 3: Fig.1.5] RU486-treated *K14creP.Δ3β-cat*$^{flx/wt}$ exhibits only a minimal interfollicular epidermis [IFE] hyperplasia [Fig. 4.3B,C,F] often only slightly more hyperplastic than normal epidermis [Fig. 4.3F vs. G]. Also, despite excess basal layer expression of β-catenin [see below Fig. 4.4] the histotype shows a relatively ordered keratinocyte differentiation pattern, although at the molecular level, keratin expression was clearly disrupted [below Fig. 4.5].

The lack of proper fur was explained by the apparent failure of hair follicle differentiation and possibly due to the formation of cysts from failed HF development and the beginnings of hair follicle tumours. Indeed, the diversion of failed HFs to form large cysts may be a protective measure to inhibit progression, as observed in *HK1.ras/fos-Δ5PTEN*$^{flx/flx}$ mice (*Macdonald et al., 2014*) and where this proliferative diversion failed to happen, benign trichofolliculomas formed [Fig. 4.3D] (*Gat et a., l998*). Furthermore, this effect of β-catenin overexpression would account for the observation that prior to the first synchronised anagen, neonatal pups appeared relatively normal despite the potential for leakage of *cre* activity whilst the embryonic epidermis developed.

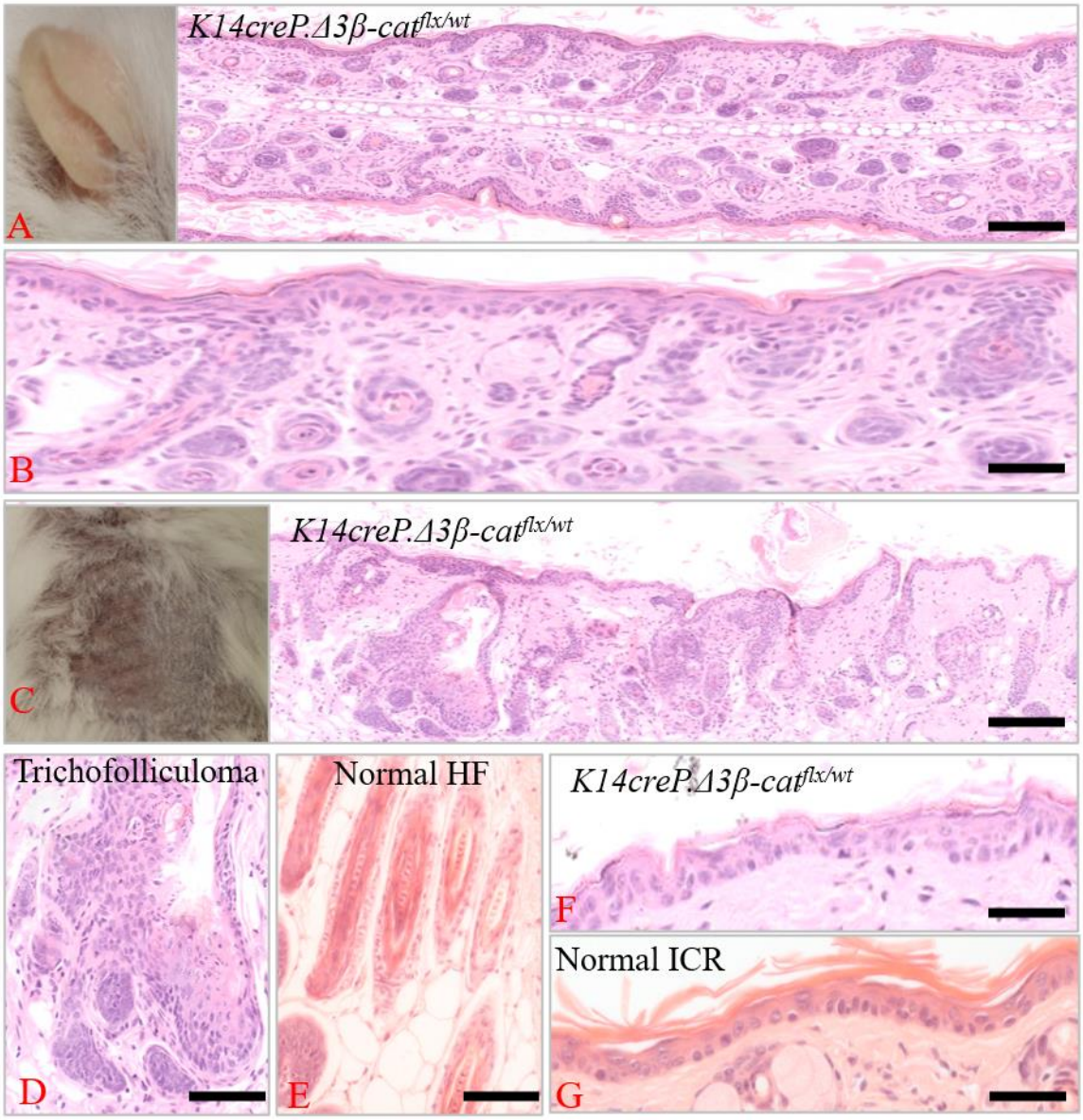

Figure 4. 3: Histological analysis of *K14creP.Δ3β-cat*$^{flx/wt}$ mice.

[A] RU486-treated *K14creP.Δ3β-cat*$^{flx/wt}$ ear histology exhibits multiple hair follicle abnormalities, with numerous placodes; whilst [B] higher magnification also highlights the minimal interfollicular epidermal [IFE] hyperplasia. [C] RU486-treated *K14creP.Δ3β-cat*$^{flx/wt}$ back skin histology also exhibits *de novo* hair follicles, now with overt hair follicle tumors [Trichofolliculoma] and formation of cysts. [D] Higher magnification of a typical early trichofolliculoma compared to [E] normal hair follicle morphology in ICR skin. [F] Higher magnification of treated *K14creP.Δ3β-cat*$^{flx/wt}$ back skin again exhibits minimal IFE hyperplasia compared to [G] normal ICR. Scale bars: A&C: 150μm; B: 75μm; D-G: 50μm.

To confirm the increase in β-catenin expression from a combination of exogenous transgene and endogenous gene expression, the overall levels were assessed in *K14creP.Δ3β-cat*$^{flx/wt}$ genotypes using both IF and IHC staining [Fig. 4.4]. In both experiments strong β-catenin

expression was observed in supra-basal and basal layers, as well as hair follicles [Fig. 4.4A]. In RU486-treated *K14creP.Δ3β-cat*$^{flx/wt}$ genotypes, a notable increase in nuclear expression was observed in basal layer and follicular keratinocytes as expected due to increased activated *Δ3β-catenin* expression from a lack of the ubiquination site following K14creP regulator activity [Fig. 4.4B&E]. This contrasted to the predominantly membranous and suprabasal expression of endogenous β-catenin in normal mice [Fig. 4.4C&F]. Constitutive high levels of β-catenin were also observed in both quiescent and anagen hair follicles and particularity in those degenerating into cysts or trichofolliculomas [Fig. 4.4A&B].

This level of overall β-catenin expression in *K14creP.Δ3β-cat*$^{flx/wt}$ mice reconfirmed the PCR result of Δ3β-catenin activation [Fig. 4.4A-C] and illustrated the consequences of deregulated β-catenin expression in terms of this spatial pattern together with increased nuclear expression, which highlights the importance of β-catenin/Wnt signalling in maintaining skin homeostasis and the epithelium of multiple organs throughout the body (*Lim and Nusse, 2013*).

The increased β-catenin expression in *K14creP.Δ3β-cat*$^{flx/wt}$ mice [Fig. 4.5A-C] was assessed using *ImageJ* software to quantify β-catenin levels [Fig. 4.6]. The assessment evaluated β-catenin nuclear localization and overall increase in strands of 10 basal layer cells of *K14creP.Δ3β-cat*$^{flx/wt}$ *in* 3 different skins [n1-3] and these analysed areas were identified as regions of interest [ROI] [Fig. 4.6A-I]. Using the colour threshold function of *ImageJ* software that identifies the localization of labelled fluorescence staining, β-catenin nuclear localization was detected in all ROI cells giving 100% [10cells/mm2] nuclear localization of β-catenin in *K14creP.Δ3β-cat*$^{flx/wt}$ [n1-3] [Fig. 4.6A-J]. Additionally, the overall expression of β-catenin, which includes cytoplasmic and nuclear expression, was estimated to be 55% of the ROI areas[n1-3] [Fig. 4.6K]. These results were consistent with the lack of the ubiquination site in the Δ3β-catenin protein (*Harada et al., 1999; Berton et al., 2000*) and also consistent with cell adhesion roles of β-catenin/E-cadherin (*Takeichi, 1991; Young et al., 2003*). Therefore, this analysis confirmed that in *K14creP.Δ3β-cat*$^{flx/wt}$ Δ3β-catenin, levels of β-catenin nuclear expression increased without affecting the cytoplasmic pool of β-catenin/E-cadherin, which seems rather strengthened [see below Fig. 4.7]. Similar quantification analysis of β-catenin expression in control *HK1.ras*[n1-3] hyperplasia [Fig. 4.6L-T] showed that β-catenin nuclear localization was detected only in 3% [1cell/mm2] of all ROI cells [Fig. 4.6U] and the overall expression of β-catenin [cytoplasmic/nuclear] estimated to occupy only 14% of ROI areas[n1-3] [Fig. 4.6X] constant with the lack of β-catenin activation. Thus, the nuclear localization

assessment of β-catenin showed a 10 fold increase in the *K14creP.Δ3β-cat*$^{flx/wt}$ cohort 100% [10cells/mm2] compared to the *HK1.ras* control 3% [1cell/mm2] [Fig. 4.6V], however the statical analysis between the two cohorts showed P>0.05[No significance] [Fig. 4.6X] which could be due the small number of cohorts.

In addition to complement this analysis the β-catenin cytoplasmic partner E-cadherin was analysed and showed an almost identical expression profile to that of β-catenin in terms of both supra-basal and basal layer expression in addition to hair follicles [Fig. 4.6]. This suggests that cell-cell adhesion is maintained via E-cadherin/β-catenin interactions (*Takeichi, 1991; Young et al., 2003*) and the potential cytoplasmic function of E-cadherin to act as a sponge (*Huels et al., 2015*) and provide further regulation of β-catenin levels was still intact and indeed seemed to be strengthened by Δ3β-catenin activation as observed in colon carcinogeesis (*Huels et al., 2015*).

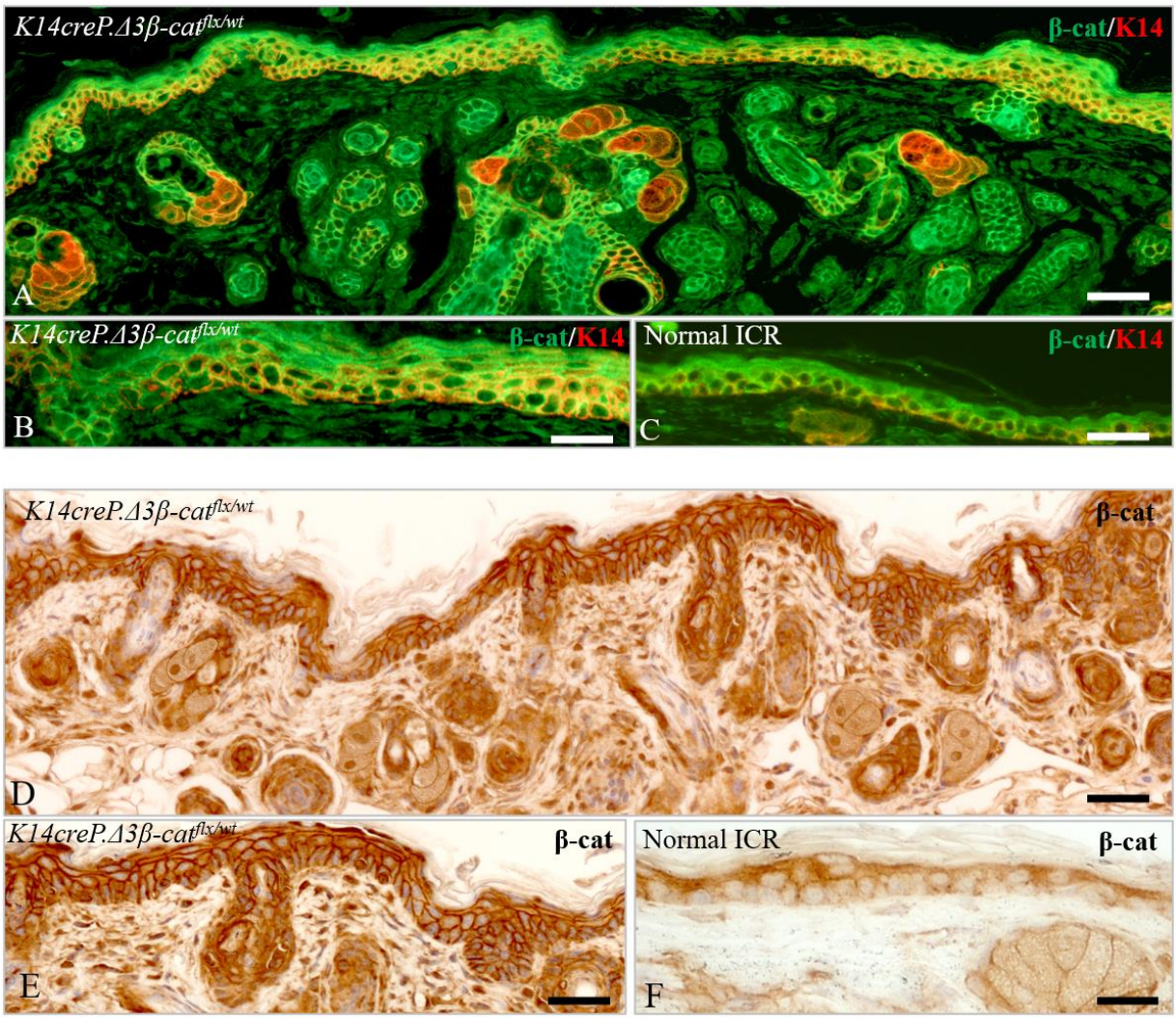

Figure 4. 4: Analysis of β-catenin expression in *K14creP.Δ3β-cat*$^{flx/wt}$ mice.

Upper panels*:* [A] Double-labelled fluorescence analysis of RU486-treated *K14creP.Δ3β-cat*$^{flx/wt}$ skin shows both membranous and nuclear expression of β-catenin [green] against K14 [red] in basal and supra-basal layers of the IFE and in hair follicles due to *Δ3β-catenin* activation. [B] At higher magnification RU486-treated *K14creP.Δ3β-cat*$^{flx/wt}$ keratinocytes show nuclear and membranous expression in basal layers compared to [C] the mainly supra-basal expression of endogenous βcatenin in normal ICR. ***Lower Panels****:* [D] IHC analysis shows membranous and nuclear expression of β-catenin in basal and supra-basal layers of RU486-treated *K14creP.Δ3β-cat*$^{flx/wt}$ skin as well as hair follicles. [E] Higher magnification confirms nuclear and membranous expression in basal layer compared to [F] supra-basal layer expression in normal ICR epidermis. Scale bars: A&D: 100μm; B,C,E&F: 50μm

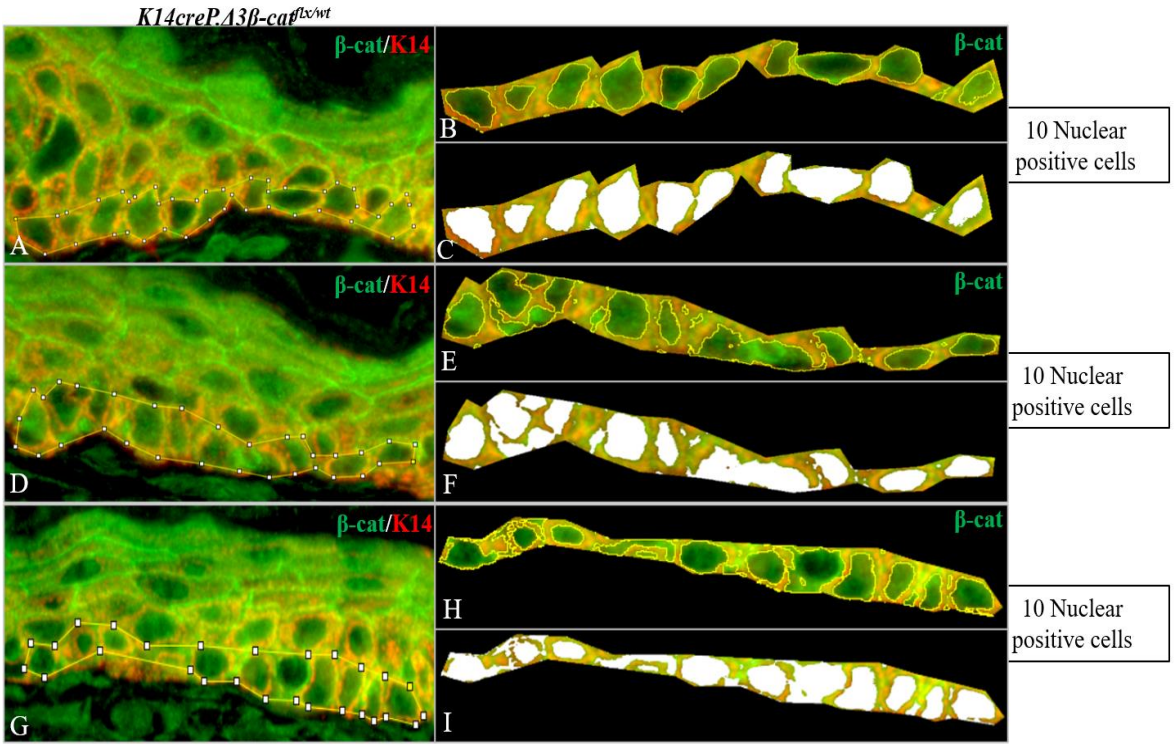
K14crePΔ3ß-catflx/wt
β-cat/K14
β-cat
A
B
C
D
E
F
G
H
I
10 Nuclear positive cells
10 Nuclear positive cells
10 Nuclear positive cells

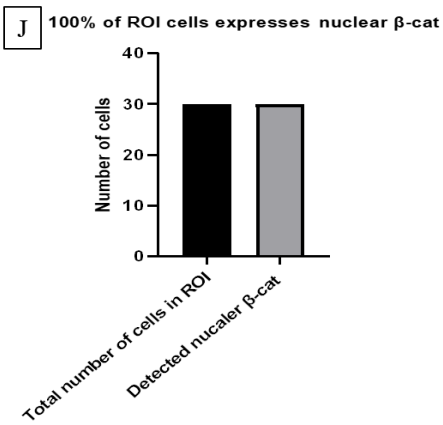
J
100% of ROI cells expresses nuclear β-cat
Number of cells
40
30
20
10
0
Total number of cells in ROI
Detected nucaler β-cat

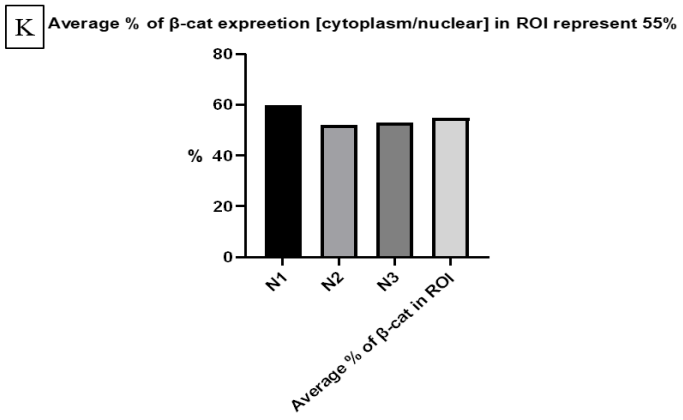
K
Average % of β-cat expreetion [cytoplasm/nuclear] in ROI represent 55%
%
80
60
40
20
0
N1
N2
N3
Average % of β-cat in ROI

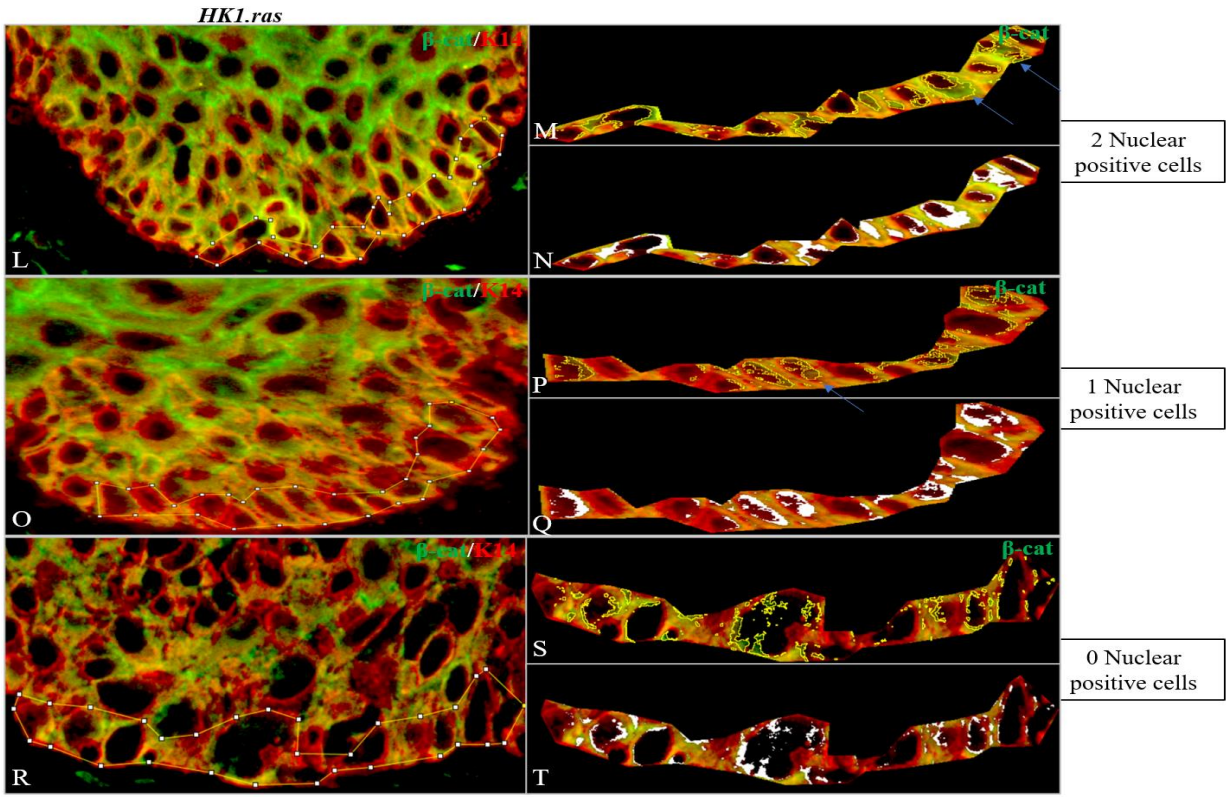

U 3% of ROI cells expresses nuclear β-cat

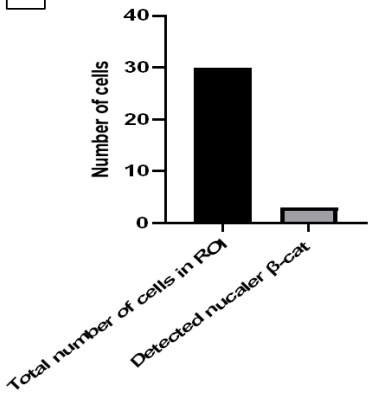

V Average % of β-cat expreetion [cytoplasm/nuclear] in ROI represent 14%

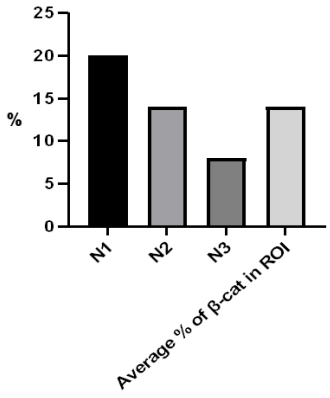

W Comparison of detected nuclear β-cat expression in ROI cells between the two genotypes

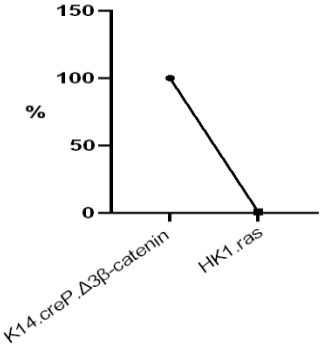

X Mann-Whitney test ranks plot

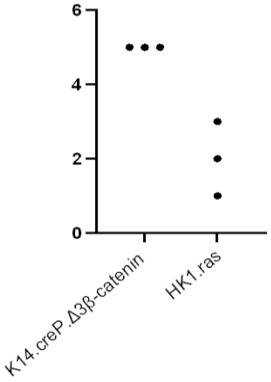

-K14creP.Δ3β-cat
Median=10

-HK1.ras
Median=1

P value=0.1000
[No significance= P>0.05]

Figure 4. 5: Quantification of increased nuclear β-catenin expression in *K14creP.Δ3β-cat$^{flx/wt}$* hyperplasia compared to *HK1.ras* control hyperplasia.

Upper panel: [A-I] Shows 3 areas (n3) of double-labelled fluorescence analysis of RU486-treated *K14creP.Δ3β-cat$^{flx/wt}$* skin that exhibits both membranous and nuclear expression of β-catenin [green] against K14 [red]. [A-C] shows highlighted ROI of 10 basal layer cells [A] in *K14creP.Δ3β-cat$^{flx/wt}$* (n1) and [B&C] Using the colour threshold function of *ImageJ* software that identifies the localization of labelled fluorescence staining, shows β-catenin (green threshold) to be detected in the cell nucleus of all 10 basal layer cells of ROI (10/10). Similarly, [D-I] shows β-catenin to be detected in the cell nucleus of all 10 basal layer cells of ROI (10/10) in both [D-F] *K14creP.Δ3β-cat$^{flx/wt}$* (n2) and [G-I] *K14creP.Δ3β-cat$^{flx/wt}$* (n3). [J] shows the quantification of nuclear β-catenin expression in all 3 analysed ROI cells in *K14creP.Δ3β-cat$^{flx/wt}$* (n1-3) gives 100% nuclear localization of β-catenin (10cells/mm2). [K] shows quantification of total β-catenin expression [cytoplasmic/nuclear] in each of ROI areas [n1-3] in *K14creP.Δ3β-cat$^{flx/wt}$* to represent an average of 55%.

Lower panel: [L-T] Shows 3 areas (n3) of double-labelled fluorescence analysis of *HK1.ras* skin shows less membranous and nuclear expression of β-catenin [green] against K14 [red]. [L-N] shows highlighted ROI of 10 basal layer cells [L] in *HK1.ras* (n1) and [M&N] Using the colour threshold function of *ImageJ* software, shows β-catenin (green threshold) to be detected in the cell nucleus of 2 cells (arrows) out of 10 basal layer cells of ROI (2/10). Similarly, [O-T] shows β-catenin to be detected in the cell nucleus of 1 (arrow) out of 10 basal layer cells of ROI (1/10) in *HK1.ras* (n2), whilst [R-T] shows no detected nuclear β-catenin in any of the cell nucleus of 10 basal layer cells of ROI (0/10) in *HK1.ras* (n3). [U] shows the quantification of nuclear β-catenin expression in all 3 analysed ROI cells in *HK1.ras* (n1-3) gives 3% nuclear localization of β-catenin (1cell/mm2). [V] shows quantification of total β-catenin expression [cytoplasmic/nuclear] in each of ROI areas [n1-3] in *HK1.ras*(n1-3*)* to represent an average of 14%. [W] Schematic diagram compares the output percentage of nuclear β-catenin expression in analysed *K14creP.Δ3β-cat$^{flx/wt}$* (n1-3) 100%(10cells/mm2) and *HK1.ras* (n1-3) 3%(1cell/mm2). [X] Schematic diagram shows the result of Mann-Whitney test ranks of the analysed values from *K14creP.Δ3β-cat$^{flx/wt}$* (n1-3) and *HK1.ras* (n1-3*)* with a median of 10 and 1 respectively and P value of 0.1000 (No significance= P>0.05).

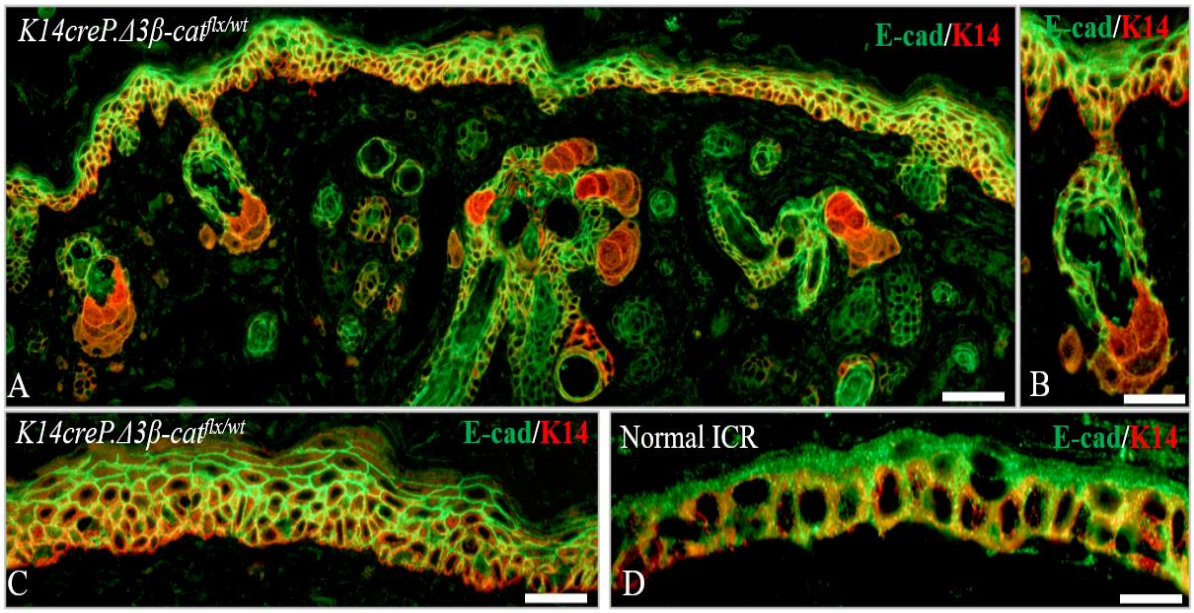

Figure 4. 6: Analysis of E-cadherin expression in *K14creP.Δ3β-cat*$^{flx/wt}$ mice.

[A] RU486-treated *K14creP.Δ3β-cat*$^{flx/wt}$ skin shows strong membranous expression of E-cadherin in both supra-basal and basal layer that parallels the increased β-catenin expression. [B] Higher magnification shows expression of E-cadherin in hair follicles prior to major deformation, whilst [C] shows that the mild hyperplasia exhibits basal layer E-cadherin expression but with fewer cells expressing nuclear E-cadherin. [D] RU486-treated normal control ICR epidermis mainly exhibits supra basal and non-basement membrane expression of E-cadherin consistent with the epidermal location of adherence and tight junctions. Scale bars: A: 100μm; B,C,E&F: 50μm

These phenotypes were constant with previous studies employing constitutive activation of β-catenin, (*Gat et a.,1998; Van Mater et al., 2003; Celso et al.,2004; Närhi et al 2008; Grigoryan et al., 2008*) and these highlight the important β-catenin roles in hair morphogenesis and differentiation. However, whilst later studies have studied effects on IFE and the stem cell niche (*Watt and Collins, 2008*) few investigate further the effects on IFE differentiation [below] and here in *K14creP.Δ3β-cat*$^{flx/wt}$ mice only a mild hyperplasia is observed with relatively little hyperkeratosis, which is a finding possibly consistent with β-catenin roles in adherence and latter stages of differentiation given its supra-basal location.

Therefore, to assess the effect of elevated β-catenin in terms of levels and incorrect spatial expression, the status of the early keratinocyte differentiation marker keratin K1 (*Rosenthal et al., 1991*) and the proliferation associated HF keratin K6α *(Rothnagel et al., 1999)* were analysed [Fig. 4.7: A-D; E-H]. Keratin K1 is typically expressed as keratinocytes commit to

differentiate and exit the basal layer [shown in Fig. 4.7D] and is thus expressed throughout the spinus and granular layers [Fig. 4.7C&D]. However, in the mild hyperplasia induced by deregulated *K14crePΔ3β-cat*$^{flx/wt}$ keratin K1 expression was completely disorganised, despite the apparent ordered profile observed in histological analysis [above]. At low magnification, K1 expression is clearly patchy and sporadic [Fig. 4.7A] whilst at high magnification, K1 expression appears either delayed or often disappears [Fig. 4.7B].

This suggests a lack of correct differentiation into supra-basal keratinocytes as indicated by the predominance of the proliferative basal layer K14 counterstain. It may be that the appearance of excess basal layer β-catenin may increase the numbers of anomalous adherence junctions as suggested by the E-cadherin staining [above] which affect epidermal rigidity and manifest as altered differentiation maker expression, as observed in the increased rigidity induced by ROCK in this model (*Masre et al., 2020*) In addition with respect to the increased p53 and p21 expression [below], whist in some contexts excess p21 appears to drive the commitment to the early stages of differentiation (*Topley et al., 1999*) other reports suggest an inhibitory role in the latter stages of differentiation consistent with this patchy K1 finding (*Di Cunto et al., 1998*) [Fig. 4.7B]

Similarly, the hyperproliferation marker K6α showed expression confined to the abnormal hair follicles [Fig. 4.7 E & F] yet expression was completely absent in the mildly hyperplastic IFE. The lack of a significant hyperplastic epidermis would be consistent with this lack of K6α expression when compared to that of *HK1.ras* and to-date is a novel observation in this HK1 model [Fig. 4.7 E & F vs H]. Again, it may be that the excess increase in adherence alters the hyperproliferation signals that accompany the response to wounding that typically induces K6α expression *(Rothnagel et al., 1999*). This also replicates the result of previous studies that investigated K6α expression with gain of function β-catenin (*Van Mater et al., 2003*). Otherwise, normal K6 expression is confined to the hair follicle in adults [Fig. 4.7 G] but interestingly neonatal skin also does not express K6α yet is naturally hyperplastic *(Rothnagel et al., 1999*).

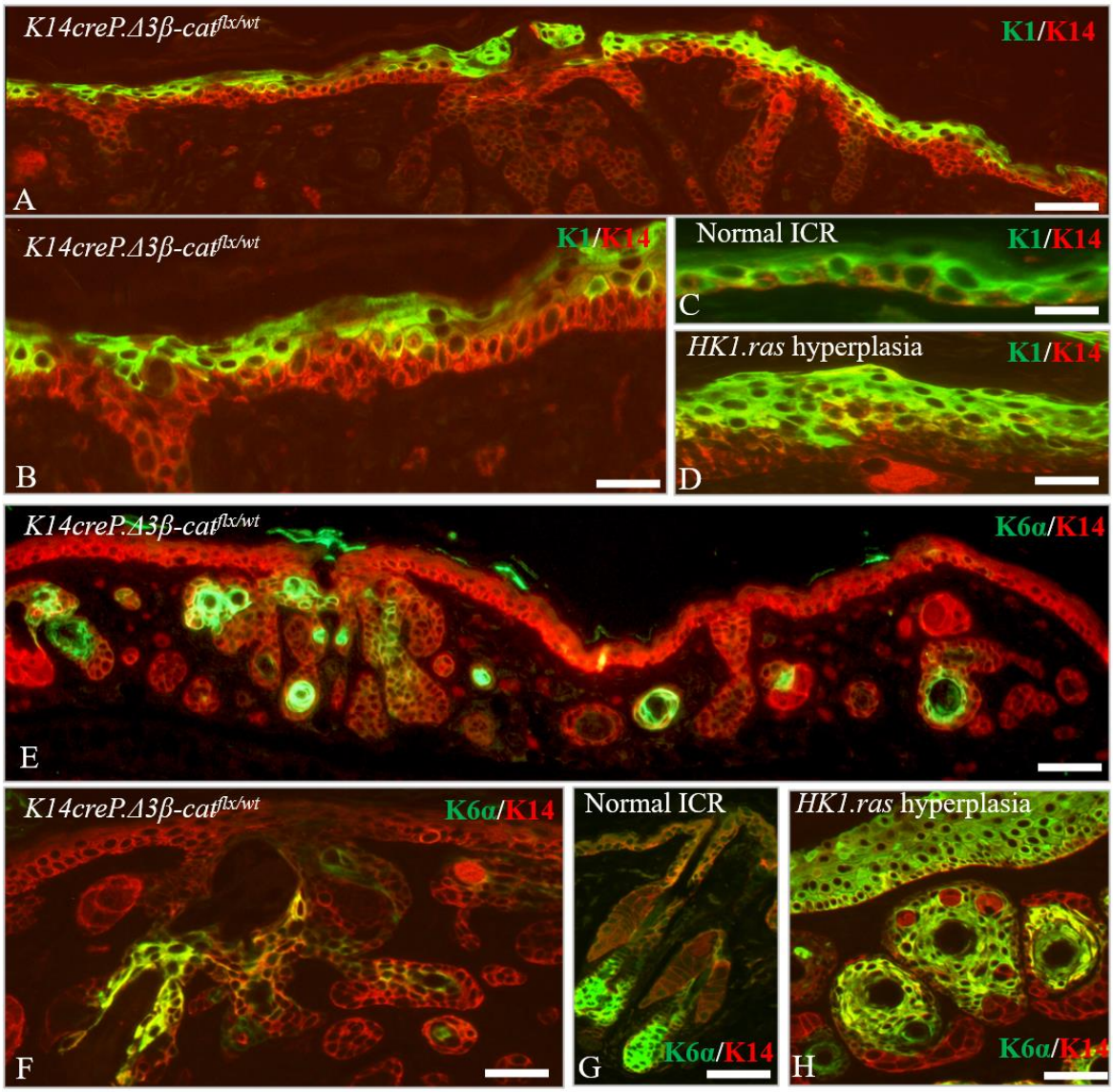

Figure 4. 7: Early differentiation marker K1 and hyperproliferation marker K6 expression in *K14creP.Δ3β-cat*$^{flx/wt}$.

[A-D] Analysis of keratin 1(green) expression: [A] Composite images at low magnification show that the mild hyperplasia in RU486-treated *K14creP.Δ3β-cat*$^{flx/wt}$ epidermis exhibits an altered, focal expression profile with weaker patchy expression in supra-basal layers, that at [B] higher magnification is sometimes absent indicating a significant change to differentiation in the upper supra-basal layers.[C] Supra-basal K1 expression in normal ICR is not clear due to the thinness of normal mouse epidermis but can be clearly seen in [D] hyperplastic epidermis from HK1.ras mice where K1 is smoothly expressed in supra-basal layers.

[E-H] Analysis of keratin 6 (green) expression: [E] Composite keratin K6 images in RU486-treated *K14creP.Δ3β-cat*$^{flx/wt}$ epidermis at low and [F] higher magnification show K6 expression remains confined to the anomalous hair follicles and K6 expression is absent from the hyperplastic IFE; a novel finding to date in the HK1 model. [G] Normal ICR show K6 expression expressed in hair follicles. [H] *HK1.ras* hyperplasia shows strong, uniform K6 expression in both IFE and hair follicles. Scale bars: A&E: 100µm; B,F&H: 50µm: C,D&G: 30µm

Collectively these data show that constitutive activation of β-catenin disturbed the normal epidermal differentiation programme marked by abnormal K1 expression, yet the epidermis still managed to cope with this altered differentiation programme giving a fairly ordered histology as observed for K1. Also given the potency of β-catenin activation, it was a surprise that typically the IFE exhibited only a mild degree of hyperplasia [above]. Therefore, the status of tumour suppresser genes p53 and p21 were also assessed in this genotype to investigate their response to Δ3β-catenin activation [Fig. 4.8].

Analysis of p53 expression found an increase in nuclear p53 expression in the basal layers of *K14creP.Δ3β-cat*$^{flx/wt}$ IFE and this was observed to be particularly strong in the abnormal follicles- possibly in attempts to inhibit further progression of the trichofolliculomas [Fig. 4.8A-C]. Whereas normal ICR epidermis exhibits little p53 unless the keratinocyte is completing the cell cycle [Fig. 4.8 D; far right keratinocyte] or is progressing from hyperplasia to papilloma [above Chapter 3 *HK1.ras/fos* papilloma], given the threat to barrier function from apoptosis due to excess p53 expression (*Calautti et al., 2005; Yao et al., 2008*).

Moreover, analysis of p21 found a significant increase in nuclear expression in both basal and supra-basal layers and also in the abnormal follicles [Fig. 4.8E-G]. Of note normal cells typically expressed little basal p21 as observed for p53, unless the cell was committing to differentiate [Fig. 4.8H]. However, this example exhibits weak p21 expression in the upper layers previously speculated to aid in cessation of differentiation and the commencement of cornification (*Di Cunto et al., 1998*). Thus, as suggested above, excess p21 in the upper layers of *K14creP.Δ3β-cat*$^{flx/wt}$ IFE may result in the lack of K1 expression- yet give rise to increased cornification and mild keratosis [Fig. 4.2I]; whilst in *HK1.fos-K14creP.Δ5PTEN*$^{flx/flx}$ KAs, this excess of p21 in response to AKT-mediated increases of β-catenin expression also gives a massive keratosis coupled to and driven by the increased differentiation in co-operation with *HK1.fos*. [above chapter 3]. Furthermore, increased differentiation was also observed in *K14.creP/ROCK*^{er} mice in response to anomalous β-catenin-mediated AKT expression *(Masre et al., 2020*) thus again linking β-catenin to PTEN/AKT regulation (*Yao et al., 2008*).

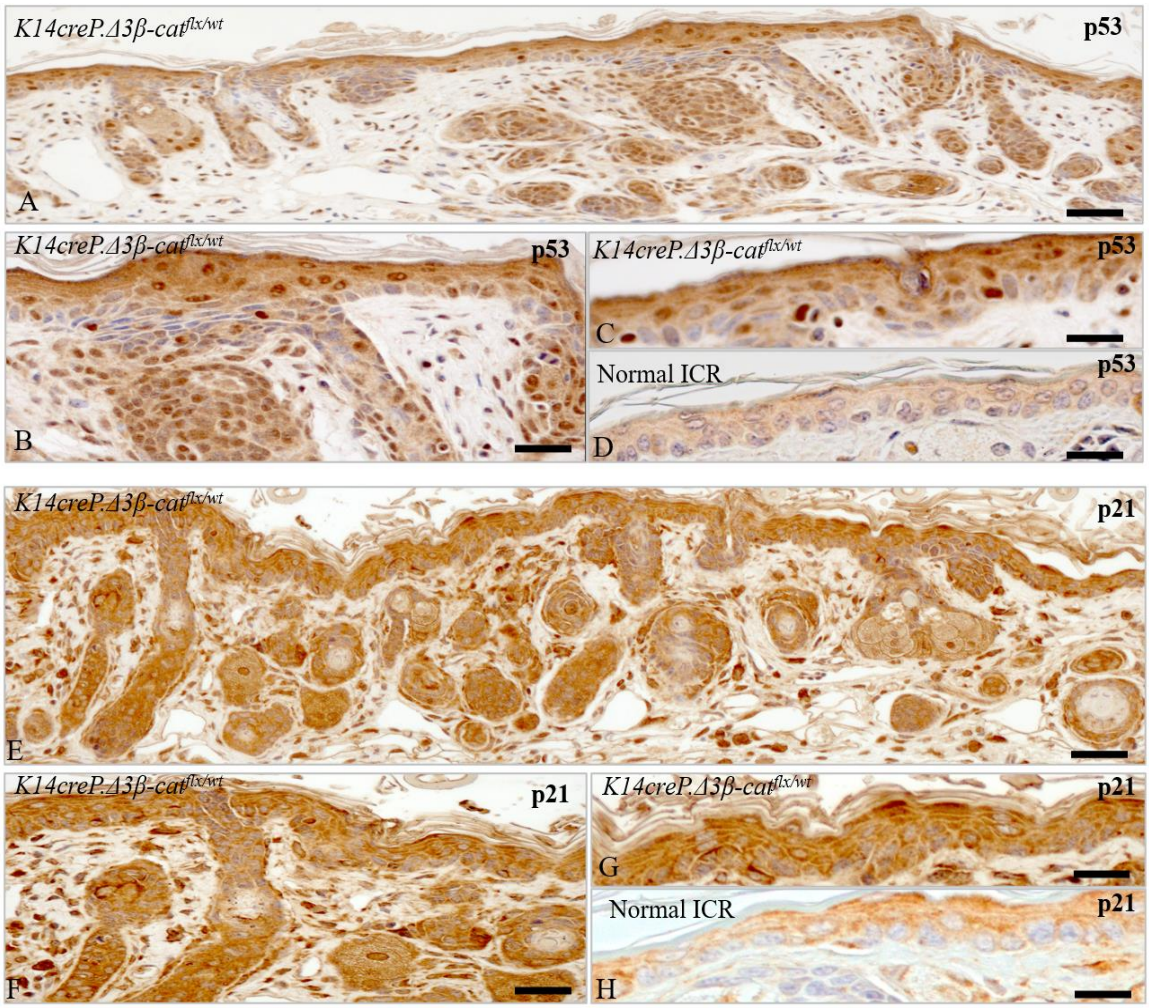

Figure 4. 8: Analysis of p53/p21 expression in *K14creP.Δ3β-cat*$^{flx/wt}$ skin.

[A] Analysis of p53 at low and [B] higher magnification shows strong nuclear expression in both basal-layer and hair follicle keratinocytes. [C] High magnification compares strong nuclear p53 expression in mild *K14creP.Δ3β-cat*$^{flx/wt}$ IFE to [D] a typical lack of p53 expression in normal ICR with a single positive cell [far right]. [E & F] Analysis of p21 shows stronger nuclear expression in basal-layer and hair follicles, whilst [G] higher magnification of *K14creP.Δ3β-cat*$^{flx/wt}$ IFE shows strong expression in all layers compared to [H] weak expression in the supra basal granular layers of normal ICR IFE. Scale bars: A&E: approx. 100µm; B&F: 50µm: C,D,G&H: 30µm

Overall expression of p53 and p21 together with the disturbance to the ordered differentiation and anomalous keratin expression indicate that the epidermis is highly sensitive to the consequence of β-catenin activation and via its roles in canonical Wnt signalling that effect increased proliferation and hair follicle development together with its roles in adhesion signalling with E-cadherin that effects the pluripotent stem cells fate that is needed for epidermal homeostasis (*Grigoryan et al., 2008*).

Table 4. 1: Summary of mouse skin phenotypes following *K14creP.Δ3β-cat$^{flx/wt}$* over expression

Genotype analysed	[N]	Analysed for expression of	Data summary
Normal ICR	10	β-catenin, E-cadherin, K1, K6α, p53 and p21 expressions	-Normal supra basal layer expression of β-catenin and E-cadherin - Ordered normal differentiation indicative by suprabasal layer K1 and normal K6α expression confined to the HF -little or sporadic expression of p53/p21
HK1.ras hyperplasia	90	K1, K6α, expressions	-Control hyperplasia showing ordered differentiation despite hyperplastic epidermis. -Ordered suprabasal layer expression of K1 but K6α expression in both suprabasal and basal layer due to *HK1.ras* activation and stress signals.
K14creP.Δ3β-cat$^{flx/wt}$	74	β-catenin, E-cadherin, K1, K6α, p53 and p21 expressions	-No IFE tumours -HF tumours -minimal IFE hyperplasia -Increased cytoplasmic/nuclear basal layer β-catenin with increased membranous basal layer β-catenin/E-cadherin due to Δ3β-catenin -Altered terminal differentiation indicated by patchy K1 expression but with oddly normal K6α expression - nuclear basal layer expression of p53/p21 halting Δ3β-catenin induced proliferation
Conclusion: constitutive β-catenin activation [*Δ3β-catenin*] induces HF tumors and HF abnormalities constant with previous studies yet lack IFE tumours presumably due to strengthen cell-cell adhesion [β-catenin/E-cadherin] correlating with basal layer expression of TSGs [p53/p21] which consequently alters terminal differentiation.			

4.3 Summary

The constitutive activation of β-catenin expression was achieved in this study using an inducible K14.creP/loxP gene switch [*K14creP.Δ3β-cat*$^{flx/wt}$], where RU486 treatment [applied to ears and back skin] would result in deletion of the exon 3 sequence flanked by loxP sites. Exon3 is located in the N-terminus of the gene where serine and threonine residue were identified as the phosphorylation binding site for GSK3-β to initiate β-catenin ubiquitination (*Behrens et al., 1996; 1998; Ikeda et al., 1998*). The deletion of this exon 3 sequence [*K14. Δ3β-catenin*] mediated via cre recombinase resulted in an in-frame shortened sequence between exon 2 and 4 of the β-catenin gene [*Δ3β-catenin*] (*Harada et al., 1999; Berton et al., 2000; Grigoryan et al., 2008*). Thus, preventing formation of the β-catenin destruction complex [GSK3-β/APC/Axin] and resulted in sustained activation of β-catenin, also known as gain of function mutation, in *K14creP.Δ3β-cat*$^{flx/wt}$ mouse skin.

This gave the ability to induce constitutive activation of β-catenin functions associated with nuclear transcription roles in Wnt signalling and cytoplasmic roles in cell-cell adhesion with E-cadherin. This mimics the mutation hotspots in exon3 observed in human carcinomas, and those also frequently reported in two-stage DMBA/TPA carcinogenesis model (*Grigoryan et al., 2008*) giving rise to the β-catenin overexpression and nuclear localization similar to the expression pattern observed in earlier in *HK1.ras/fos-K14creP.Δ5PTEN*$^{flx/flx}$ co-operation, that facilitated carcinogenesis (*Macdonald et al., 2014*). [See chapter 3].

Activated *Δ3β-catenin* expression was routinely confirmed via PCR analysis, additionally gross *Δ3β-catenin* phenotype was very apparent and easily distinguishable from a normal ICR mouse. Due to the potency of *Δ3β-catenin* phenotype, as cre leaked early and independent of RU486 treatment this resulted in gross appearance of Δ3β-catenin phenotypes around 16 to 24 days of age [ear tag time], which is similar to a previous study that induced constitutive activation of *Δ3β-catenin* using a K14cre gene switch (*Gat et al., 1998; Harada et al., 1999; Berton et al., 2000*).

These results were very similar to all previous transgenic mouse studies that reported identical gross abnormalities involving mice where constitutive β-catenin activation was achieved in the epidermis by a variety of genetic approaches, such as direct fusion of mutant stabilised β-catenin with a keratin K14 promoter (*Närhi et al 2008*), some involving inducible expression via a tamoxifen 4HT activated switch (*Van Mater et al., 2003; Celso et al.,2004*). In cases

being driven by an earlier weaker promoter such as that involving sporadic K14.cre regulator gene that is expressed in approx. 10-15% of keratinocytes (*Gat et al., 1998*) or those requiring daily 4HT treatments, mice appeared full sized with little effects on development or overt internal problems. However, if driven by a potent keratin promoter such as K5cre, β-catenin overexpression proved to be lethal (*Järvinen et al., 2006*), and thus it appears that none were subsequently reported to have been used in the development of transgenic skin carcinogenesis models; rather each focussed on effects on hair follicle development and later on the effects on stem cells but oddly, none exploit these mice in the development of classic skin carcinogenesis models only constitutive knockouts have been investigated (*Grigoryan et al., 2008*) .

The answer to this may lie in the observation in this model that the outbred nature of the ICR mice juvenile *K14.creP-Δ3β-catenin*$^{flx/wt}$ mice varied in body sizes being similar or smaller compared to normal ICR mice or *K14.creP* and *Δ3β-catenin* alone siblings. This varied appearance and severity was due to the randomness of RU486-independent cre leakage as well as the differing genetic backgrounds of individual family trees on this outbred ICR background. However, this would clearly affect viability if expressed in the internal organs – hence resulting in a smaller size and **w**hilst the gross phenotype of *Δ3β-catenin* varied slightly in severity and appearance due to the randomness of early cre leakage, once mice were treated with RU486 all exhibited a similar degree of phenotype.

These phenotypes of *K14creP.Δ3β-cat*$^{flx/wt}$ mice were identical with alternate studies that targeted β-catenin gain of function to the skin or follicles and showed alopecia, scruffiness, bigger ears, abnormal feet and tail as well as a variation in body sizes compared to a normal ICR mice (*Gat et al., 1998*). Although the gene switch in this study was targeting the skin via *K14.creP,* the effect of Δ3β-catenin was not exclusive to the epidermis which affected the size of the body and limbs as well. This can be attributed to the major roles that canonical Wnt/β-catenin signalling plays in embryonic and juvenile stages of development. Embryonically Wnt/β-catenin signalling is highly involved in the formation of the body anterior and posterior axis, hence why null mutation of β-catenin induced embryonic lethality as it resulted in a failure in forming body axis in mouse studies (*Grigoryan et al., 2008*). Also, it should be noted here that presumably the cre leakage had the potential for *Δ3β-catenin* activation early, yet the effect on body extremities such as tail and feet as well as the IFE phenotypes required a follicular effect observed post 16 but within 24 days of age.

The histology showed an increase in the number of hair follicles [ear and back] with the expected hair follicle anomalies such as formation of de novo hair follicles and benign hair follicle tumours (*Gat et al., 1998; Huelsken et al., 2001; Grigoryan et al., 2008*), consistent with β-catenin mediated over expression of Wnt signalling transcriptional targets LEF1 and TCF which are associated with hair follicle formation, differentiation and hair follicle tumours (*Niemann et al., 2002; Grigoryan et al., 2008*).

This finding reaffirmed β-catenin roles in not only hair follicle formation and differentiation but also in affecting the dermis signals to form more hair follicles which is observed in a study that overexpressed Lef-1 using a K14 gene switch. However, this study lacked the effect on the size of the limbs observed here with Δ3β-catenin, suggesting that β-catenin has roles that affect a plethora of other signalling mechanism and not exclusively to hair follicle morphogenesis. The effect of Δ3β-catenin activation on the size of the limbs could be attributed to findings that Wnt/β-catenin activation up regulates Bone Morphogenic Protein (BMP) that is required for bone, cartilage and muscle formation (*Närhi, et al., 2008),* hence the enlarged extremities. Further, the alopecia that *K14creP.Δ3β-cat*$^{flx/wt}$ mice usually exhibit can be explained by the finding that, despite the increased formation of hair placode due to Δ3β-catenin activation, most of the initiated HFs fail to produce normal hair due to incorrect control of Wnt/β-catenin signalling (*Närhi, et al., 2008*)

Although beyond the scope of this project in terms of developing a multistage β-catenin model for SCC, the follicle tumours observed in these Δ3β-catenin mice are variously describe as folliculoma, trichofolliculoma or pilomatricoma [Fig. 4.2D], which were reported in previous mouse studies that overexpressed β-catenin (*Gat et al., 1998; Chan et al., 1999 Grigoryan et al., 2008*), and have also been reported in humans as a result of gain of function mutations in the β-catenin gene (*Grigoryan et al., 2008; Chan et al., 1999*). Indeed, in parallel studies to this approach, β-catenin deregulation co-operated with PTEN loss [*K14.Δ5PTEN.Δ3β-catenin]* to give HF tumours that mimicked trichochilemomas observed in Cowdens disease [see chapter 7].

Furthermore, *K14creP.Δ3β-cat*$^{flx/wt}$ mice exhibited minimal interfollicular hyperplasia [IFE] compared to normal epidermis, and expression of differentiation markers was altered. This clearly indicates that *Δ3β-catenin* activation altered IFE homeostasis as well as hair morphology, which is probably due to β-catenin roles in regulating epidermal pluripotent stem

cells that are needed for epidermal terminal differentiation and hair follicle differentiation (*Grigoryan et al., 2008*). The early differentiation marker K1 showed an abnormal expression profile suggesting the commitment to differentiate was disrupted and expression of the hyperproliferation marker K6α was only confined to the hair follicle consistent with reduced IFE hyperplasia and previous studies that investigated K6 expression with gain of function β-catenin (*Van Mater et al., 2003*). Additionally, the normal expression of K6 in adult mice is confined to the hair follicle and interestingly even in naturally hyperplastic neonatal skin epidermis K6α is not expressed *(Rothnagel et al., 1999*). Thus, it is interesting to speculate that here deregulated β-catenin expression may return the adult *K14creP.Δ3β-cat*$^{flx/wt}$ skin to a more juvenile/neonatal state, consistent with increased numbers of HFs with altered terminal differentiation indicated by K1 and the lack of K6α expression. This speculation was supported by the finding of a previous study that concluded that gain of function β-catenin alters the dermal extra cellular matrix into a neonatal state (*Collins et al., 2011*), which could possibly explain the K1/K6α expressions and altered differentiation in *K14creP.Δ3β-cat*$^{flx/wt}$ skin.

This clearly indicated that Δ3β-catenin activation affected the normal epidermal differentiation homeostasis but still was not enough to elicit IFE tumours such as SCCs, which is evident by the lack of both IFE hyperplasia and K6 expression. This brings in the roles of p53/p21 that may be partly responsible for these findings as *K14creP.Δ3β-cat*$^{flx/wt}$ epidermis showed strong expression in response to Δ3β-catenin and here p53 may act to counter Wnt signalling induced proliferation, hence a reduced K6, and anomalous basal layer p21 acts to induce differentiation (*Topley et al., 1999*). Although this too may be context dependent and p21 may also have inhibitory roles in the upper layers of *K14creP.Δ3β-cat*$^{flx/wt}$ IFE resulting in increased cornification and mild keratosis constant with the scruffiness, scaly appearance to the skin phenotype of these mice.

These data indicate that the epidermis is highly sensitive to overexpression of β-catenin, unlike other oncogenes such as *HK1.ras* or the loss of *PTEN* which alone do not invoke the same p53/p21 responses in hyperplasia and again compensatory p53/p21 appears later in KA formation following a threshold of GSK3β inactivation and accumulation of β-catenin (*Yao et al., 2008*). This induction of β-catenin was also seen in ROCK mediated models and here the induced p53/p21 expression also inhibited papillomatogenesis (*Masre et al., 2020*), a result supporting the investigation of p53 and p21 in *K14creP.Δ3β-cat*$^{flx/wt}$ and also *HK1.ras*-

K14creP.Δ3β-cat$^{flx/wt}$ phenomenon as illustrated below [Chapter 5]. Finally, this analysis of *K14creP.Δ3β-cat*$^{flx/wt}$ reinforces the importance of assessing β-catenin roles in a multistage skin carcinogenesis model to reveal hidden responses as found in the following chapters.

Chapter 5: β-catenin overexpression in *HK1.ras* transgenic mouse skin

5.1 Introduction

In chapter 3, analysis of carcinogenesis in *HK1.ras/fos-K14creP.Δ5PTEN$^{flx/flx}$* mice found that β-catenin expression in *HK1.ras* or *HK1.ras/fos* papillomas was mainly membranous in the supra-basal layer and thus similar to normal β-catenin expression. In *HK1.fos-K14creP.Δ5PTEN$^{flx/flx}$* KA formation, β-catenin became strongly basal and also strongly nuclear to induce compensatory p53/p21 expression in response to AKT-mediated GSK3β inactivation and this basal layer β-catenin expression led to a KA outcome rather than SCC [above Fig 3.3; (*Yao et al., 2008*)]. In *HK1.ras/fos–-K14creP.Δ5PTEN$^{flx/flx}$* mice, again elevated levels of basal layer β-catenin were already detectable in hyperplasia and papillomas that also now exhibited early p53 and p21 expression. However, with the addition of activated *HK1.ras* in *HK1.fos-K14creP.Δ5PTEN$^{flx/flx}$* tumours or loss of PTEN function in *HK1.fos/ras* papillomas, as they converted to malignancy following p53 loss (*Macdonald et al., 2014*), nuclear β-catenin expression increased in the basal layers and was less membranous as wdSCC progressed further to become pdSCCs [above chapter 3: Fig 3.3].

Furthermore, β-catenin expression was paralleled by initial increases in E-cadherin and p53/p21 expression in benign tumours including tri-genic -*K14creP.Δ5PTEN$^{flx/flx}$*, but again following p53 loss, in parallel with excess nuclear/reduced membranous β-catenin E-cadherin and thus cell-cell adhesion was progressively lost at the invasive front, which alongside p21 loss [above] helped drive malignant progression and tumour invasion [Chapter 3: Figs. 3.2 and 3.3].

Therefore, as hypothesised in the aims of *Chapter 1*, it was anticipated that crossing *K14creP.Δ3β-cat$^{flx/wt}$* mice with *HK1.ras* mice would lead to a more rapid papilloma formation, resulting in aggressive papillomas followed by earlier malignant conversion. It was also thought that as Δ3β-catenin expression was independent of the deregulated PTEN/AKT/GSK3β signalling in *HK1.ras/fos-K14creP.Δ5PTEN$^{flx/flx}$* mice and may also have circumvented the protective p53 responses observed in *HK1.ras* or *HK1.ras/fos* papillomas that prevent conversion [Chapter 3]. However, a contrary completely unexpected result was observed.

5.2 Analysis of *HK1.ras-K14creP.Δ3β-cat$^{flx/wt}$* mice show a paradoxical lack of papillomas

Following the clear implication of endogenous β-catenin involvement in the various tumours involved in *HK1.ras/fos-K14creP.Δ5PTEN$^{flx/flx}$* carcinogenesis [above], to investigate when β-catenin played a causal role in papilloma formation or their malignant conversion, *K14creP.Δ3β-cat$^{flx/wt}$* mice were bred with *HK1.ras.* Over many years, this *HK1.ras ^{1205}* mouse line has been a main feature of modelling papilloma formation (*Greenhalgh et al., 1993a;1993c; 1996*) and their conversion (*Wang et al., 1997; 1998; Masre et al., 2017*). In these experiments mice develop papillomas in the wounded [tag] ear in 100 % of cases. Given the outbred background these can appear by 6-7 weeks and become large [7-10 mm diameter]; or it may take up to 8-10 weeks for papillomas to appear and these will typically remain fairly small [3-6 mm diameter] up 12/14 weeks. If not tagged *HK1.ras^{1205}* do not exhibit tumours [typically for breeding, pups can be identified by a wrinkly skin, thus normal are culled and adult breeders do not have to be tagged; this achieves the refinement clause in the 3Rs].

However, on rare occasions a subset of *HK1.ras* mice [< 0.1%] exhibit papillomas that developed on other areas of the body. These arise in specific litters and their appearance has been random over the past 30 years. These are designated type 2 papillomas and characterised by a rapid growth but are easily identified by their smooth, less keratotic appearance. Such type 2 papillomas maybe the equivalent of papillomas that arise early in DMBA/TPA promotion (*Hennings et al.,1985; 1993*) and these typically become malignant given the additional mutations elicited by DMBA treatment. In the *HK1.ras* model they remain benign but exhibit a more aggressive histological phenotype than the common [type 1] ear tag papillomas. As outlined above these type 1 papillomas do not progress to SCC again due to strong nuclear basal layer p53 expression and as β-catenin expression remains membranous and mainly supra-basal [chapter 3].

These tumour growth profiles of papillomas by 8-10 weeks without conversion were maintained in all *K14.creP/HK1.ras* and all [non-cre] *HK1.ras -Δ3β-catenin* control progeny [with or with out RU486-treatment] and subsequent breeders, together with all *HK1.ras* alone littermates and ear-tagged breeders.

Figure 5. 1: Phenotypes of *HK1.ras-K14creP.Δ3β-cat*$^{flx/wt}$ mice.

[A & B] At 8 weeks post ear-tag wounding, RU486-treated *HK1.ras-K14creP.Δ3β-cat*$^{flx/wt}$ mice show no sign of papilloma developing yet still exhibit the typical Δ3β-catenin phenotype of a scruffy hyperkeratotic skin and thickened hyperplastic ears; compared to an age-matched *HK1.ras* littermate that develop papillomas by 8-10 weeks and lack any other overt phenotype. [C] Shows four littermates where the two middle animals are *HK1.ras-K14creP.Δ3β-cat*$^{flx/wt}$ and have not develop papillomas, flanked by two *HK1.ras* mice that here show the range of papillomas developing either small or very large papillomas at the tagged ear. [D] Repeat experiments show 8 week old *HK1.ras-K14creP.Δ3β-cat*$^{flx/wt}$ mice with no ear tumours against [E] *HK1.ras* littermates again showing papilloma with different sizes 8 weeks post ear-tag wounding. To date, only two *HK1.ras-K14creP.Δ3β-cat*$^{flx/wt}$ mice developed papillomas. Both [F & G] have smaller papillomas at 12 weeks compared to their *HK1.ras* littermate controls, which had rapidly developed large papillomas.

In contrast *HK1.ras-K14creP.Δ3β-cat*$^{flx/wt}$ mice showed an intriguing, almost paradoxical result, as almost all mice lacked papillomas or any type of tumour at 8-10 weeks [n = 58] produced in triple repeat experiments or as controls for p53 and p21 analysis over 3 years. In almost all cases *HK1.ras-K14creP.Δ3β-cat*$^{flx/wt}$ mice remained tumour free for the typically 12-14 weeks before biopsy, and where the spontaneous β-catenin phenotype was less severe, a cohort of RU486-treated *HK1.ras-K14creP.Δ3β-cat*$^{flx/wt}$ individuals were maintained for 22 weeks without producing papillomas [n=5].

This is shown in Fig. 5.1, RU486-treated *HK1.ras-K14creP.Δ3β-cat*$^{flx/wt}$ mice showed no sign of papilloma formation [Fig 5.1: A-D], compared to their age-matched *HK1.ras* littermates which also show the variation in size typical of papillomas in this model [Fig 5.1C, E-G]. Again the *HK1.ras-K14creP.Δ3β-cat*$^{flx/wt}$ mice exhibited the mild alopecia with dishevelled fur and possibly increased hyperkeratotic skin [Fig 5.2 below]. To date, only two *HK1.ras-K14creP.Δ3β-cat*$^{flx/wt}$ mice have developed papillomas. Both animals initially exhibited a much weaker spontaneous Δ3β-catenin phenotype and following RU486 treatment at 12 weeks have smaller papillomas compared to their *HK1.ras* littermate controls [Fig. 5.1F&G]. Of note in both cases these *HK1.ras* siblings had rapidly developed large papillomas at the ear tag suggesting that these mice had developed from a background possibly prone to development of the more aggressive Type 2 papillomas outlined above.

A direct comparison of *HK1.ras-K14creP.Δ3β-cat*$^{flx/wt}$ and *K14creP.Δ3β-cat*$^{flx/wt}$ is shown in Fig 5.2 and demonstrates that the phenotypes typical of Δ3β-catenin overexpression were slightly increased particular in terms of the hyperkeratosis observed and again these mice varied in body size associated with the time and extent of RU486-independent cre activity commenced during the development of these mice. *HK1.ras-K14creP.Δ3β-cat*$^{flx/wt}$ phenotypes show increased thickened ear skin and also peri-orbital skin thickening which was also apparent on the thicker foot skin giving larger feet [Fig. 5.2A-C]. The most obvious change was the increased nature of the dishevelled fur giving a more scruffy appearance to adult skin [Fig.5.2C&D] with an increased back skin hyperkeratosis and alopecia in response to RU486 treatment. This varied depending upon the time of cre leakage but typically gave a more folded nature to the *HK1.ras-K14creP.Δ3β-cat*$^{flx/wt}$ skin [Fig. 5.2E&G] compared to similar RU486-treated *K14creP.Δ3β-cat*$^{flx/wt}$ control skin that show a less severe overall phenotype [Fig.5.2E&G]. However, this folded skin phenotype was far less than that induced by *HK1.fos* co-operation with *K14creP.Δ3β-cat*$^{flx/wt}$ mice [see chapter 7].

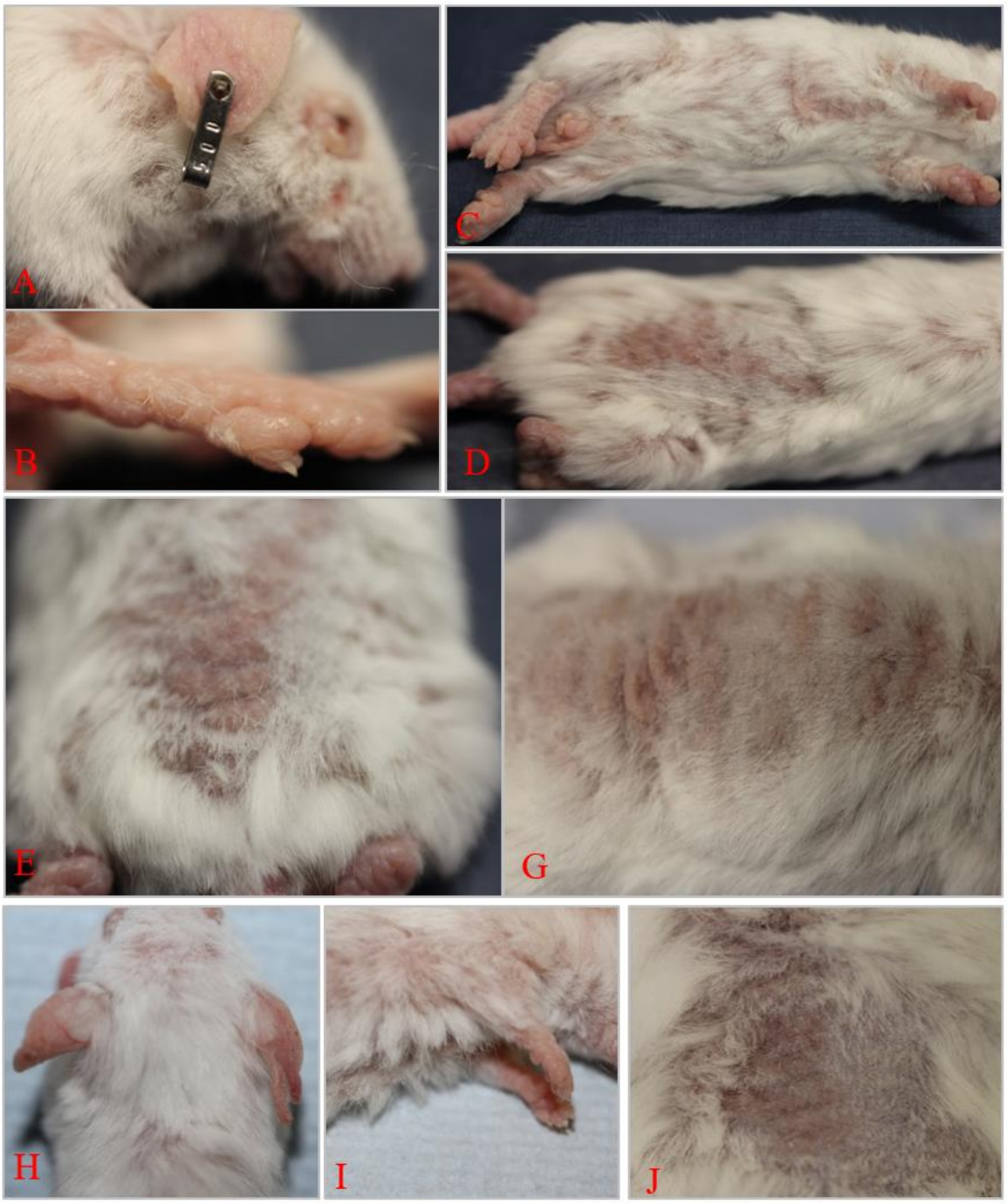

Figure 5. 2:Comparison of *HK1.ras-K14creP.Δ3β-cat*$^{flx/wt}$ and *K14creP.Δ3β-cat*$^{flx/wt}$ phenotypes.

[A-G] *HK1.ras-K14creP.Δ3β-cat*$^{flx/wt}$ phenotypes show an increased [A] ear hyperplasia and hyperkeratosis and peri-orbital skin thickening. [B & C] Again large feet were observed with an increased thickening to the hyperkeratotic foot skin. [D] An increase back skin hyperkeratosis and alopecia appeared at the RU486 treated site together with an increased in the overall scruffy nature of the skin, whilst [E & G] shows a variation on the intensity of the hyperkeratosis in *HK1.ras-K14creP.Δ3β-cat*$^{flx/wt}$ mice. [H-J] RU486-treated *K14creP.Δ3β-cat*$^{flx/wt}$ mice typically show a less severe phenotype.

These findings suggest that *Δ3β-catenin* activation in *HK1.ras-K14creP.Δ3β-cat*$^{flx/wt}$ induces early protective epidermal responses that prevent the formation of wound-associated [Type1] papillomas which are observed in 100% of *HK1.ras [1205]* mice. This increase in phenotype observed in *HK1.ras-K14creP.Δ3β-cat*$^{flx/wt}$ mice over time increased further in subsets of mice following the increased number of crosses required to generate these complex genotypes. Eventually this became of concern with regard to their long-term viability. Thus a scoring system was devised and applied to these genotypes at the time of tail biopsy to ensure that these animals remained within the moderate category of the regulations for animal experimentation in the UK. The severity of phenotypes in *HK1.ras-K14creP.Δ3β-cat*$^{flx/wt}$ mice was divided into three degrees: Score 0[N=10/phenotypic post RU486 treatment], mild with only little obvious phenotype and a full size at tail biopsy and these individuals often required RU486 treatment to elicit β-catenin phenotypes; Score 1[N=42/phenotypic by d16-24], the most typical outcome, as shown in Fig 5.1 and 5.2; and the much rarer Score 2 [N=6/phenotypic by d16], where significant hyperplasia appeared by d16 and mice were also a smaller size indicative of digestive problems following weaning possibly due to β-catenin activation in the colon (*Grigoryan et al., 2008; Huels et al., 2015*).

The initial appearance of such score 2 mice followed the in-breeding to create the more complex genotypes e.g., see β-catenin co-operation with fos and PTEN in chapter 7 [but intriguingly not p53 loss; chapter 6] and this development necessitated significant changes to the Licence to perform these experiments. Thus, to comply with the revised animal licence limits and end points following the first appearance of such score 2 mice [late 2018]; only those score 2 individuals deemed of scientific importance were maintained and typically not more than 6-7 weeks to assess for signs of papilloma formation. Each was closely monitored daily and diet supplemented with baby food from d16-20, prior to weaning and to date in the *HK1.ras-K14creP.Δ3β-cat*$^{flx/wt}$ genotype all score 2 mice produced also exhibited a blockage of tumour formation.

This difference in phenotype severity was reflected in the histological analysis but in general typical *HK1.ras-K14creP.Δ3β-cat*$^{flx/wt}$ histotypes [both ear and back] showed a common histotypes of the expected Δ3β-catenin-associated hair follicle abnormalities but now with an overlay of increased epidermal hyperplasia due *HK1.ras* activation [Figs 5.3-5.5; score 1 phenotypes shown unless otherwise indicated].

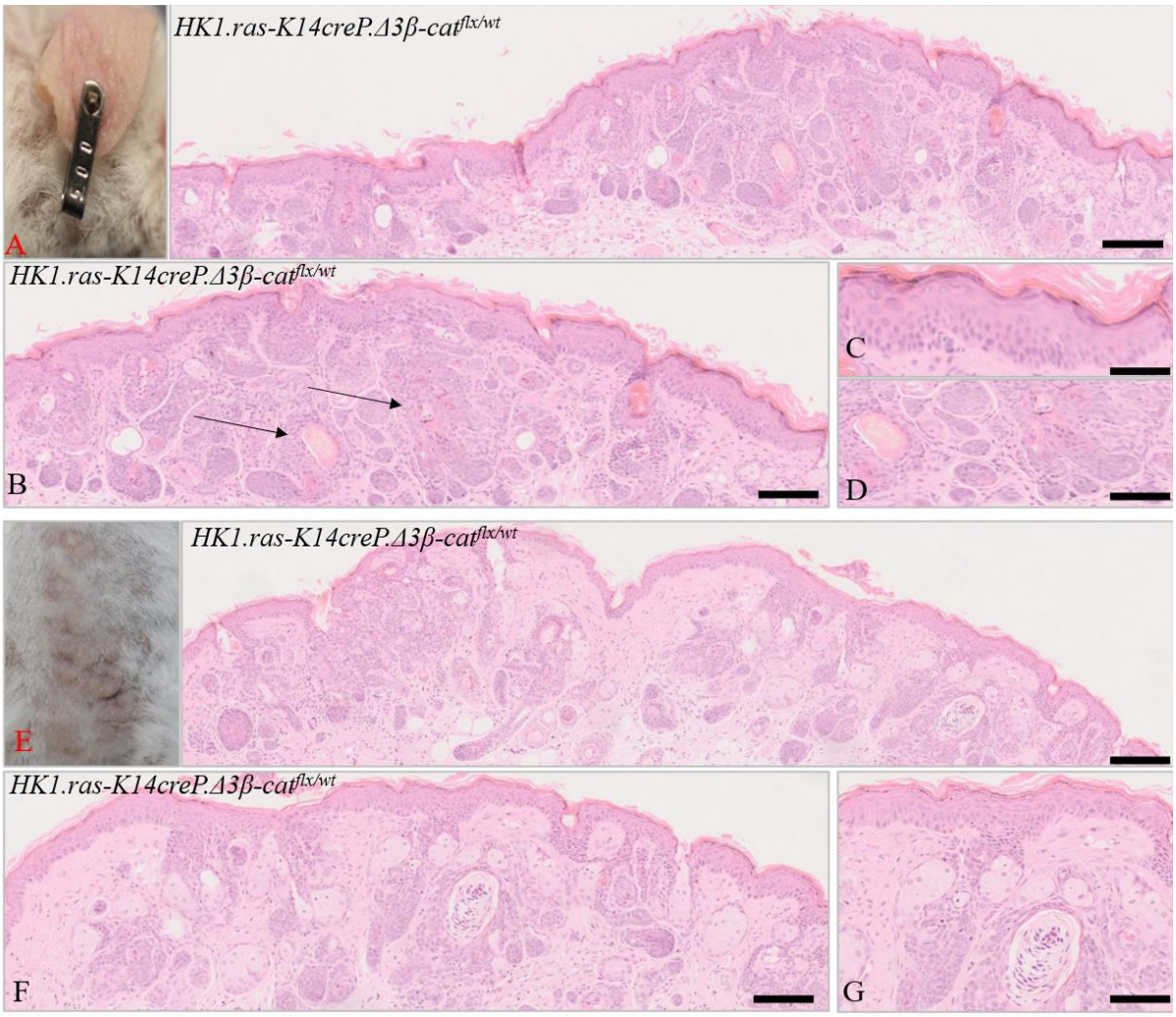

Figure 5. 3: Histotypes of RU486-treated *HK1.ras-K14creP.Δ3β-cat*$^{flx/wt}$ skin.

[A-D] *HK1.ras-K14creP.Δ3β-cat*$^{flx/wt}$ ear skin at 8 weeks post ear tag. [A] Low magnification and [B] higher magnification composite images of ear [insert] histotype shows typical Δ3β-catenin-associated hair follicle abnormalities with formation of cysts and the onset of trichofolliculomas [arrows] now with increased levels of IFE hyperplasia compared to *K14creP.Δ3β-cat*$^{flx/wt}$ alone [see fig 5.4D] [C] At higher magnification increased *HK1.ras-K14creP.Δ3β-cat*$^{flx/wt}$ hyperplasia also displays a disordered differentiation with changes to the ordered nature of basal layer keratinocytes and a marked acanthosis; whilst [D] little effect of *HK1.ras* activation is observed on cyst formation or HF abnormalities. [E-G] Back skin [insert] of same RU486-treated *HK1.ras-K14creP.Δ3β-cat*$^{flx/wt}$ mouse shows overall increased in de novo hair follicles with typical HF abnormalities, trichofolliculomas and cysts with again an increased IFE hyperplasia. [F & G] Higher magnification again shows a disturbed differentiation pattern of the basal layer keratinocytes. Scale bars: A&E: 150µm; B&F: 100µm; C&D: 30µm; G: 50µm

The increased hyperplasia in these *HK1.ras-K14creP.Δ3β-cat*$^{flx/wt}$ mice [Fig. 5.3A-C; Fig 5.4A&B] thus accounted for the overall increased degree of thickened ear and foot skin and also the increased keratosis appearing at RU486-treated sites; although compared to a typical *HK1.ras* control skin, the degree of hyperplasia was less and this resulted in less of a papillomatous [folded] *HK1.ras-K14creP.Δ3β-cat*$^{flx/wt}$ epidermis [FIG. 5.5C]. This observation is likely to centre on the expression of both p53 and p21 in the *HK1.ras-K14creP.Δ3β-cat*$^{flx/wt}$ hyperplasia compared to a *HK1.ras* alone skin [below Fig. 5.9]. Further one feature of note in the increased *HK1.ras-K14creP.Δ3β-cat*$^{flx/wt}$ hyperplasia was the appearance of an odd basal layer which exhibited a disordered differentiation in terms of many more basal layer keratinocytes as well as an increased acanthosis [Fig. 5.3C&G; Fig. 5.4B; Fig. 5,5D] compared to that of *HK1.ras* [Fig. 5.5F]. The increased numbers of disorganised basal layer cells thus reflects the confusion of proliferative signals elicited by basal layer expression of *Δ3β-catenin* and ras^{Ha} activation and this leads to an acanthosis.

A direct comparison of the histotypes displayed by these various overt phenotypes is shown in Fig 5.4 and this confirmed that these variations were associated with the degree and timing of phenotypes associated with Δ3β-catenin expression. For instance, the typical score 0 or score 1 phenotypes exhibited mild increases in hyperplasia associated with *HK1.ras* expression and possessed the follicular phenotypes typical of the histotypes seen in *K14creP.Δ3β-cat*$^{flx/wt}$ [Fig. 5.4A&B vs. D]. In contrast *HK1.ras-K14creP.Δ3β-cat*$^{flx/wt}$ with a score 2 designation exhibited a severe set of *Δ3β-catenin* follicular phenotypes with clear folliculomas and cysts, consistent with an early expression of *Δ3β-catenin* during development possibly before juvenile mice began their first phase of anagen [Fig. 5.4C]. Moreover, in these score 2 histotypes, whilst the IFE was disorganized it lacked the increased hyperplasia associated with *HK1.ras* but instead possessed an increased keratosis [Fig. 5.4C] suggestive of an increased differentiation rate as typically seen in combinations of *HK1.fos-K14creP.Δ3β-cat*$^{wt/flx}$ and *K14.Δ5PTEN.Δ3β-catenin* mice [See Chapter 7]. Such increased differentiation responses were also suggested by KA aetiology where anomalous endogenous β-catenin expression in basal layer keratinocytes [Chapter 1] induced p53 to inhibit proliferation and p21 to induce differentiation. Therefore, in these specific score 2 mice the phenotype appears to be dependent upon β-catenin leakage and development of HF phenotypes and not *HK1.ras* – as observed for p53 loss [Chapter 6 below].

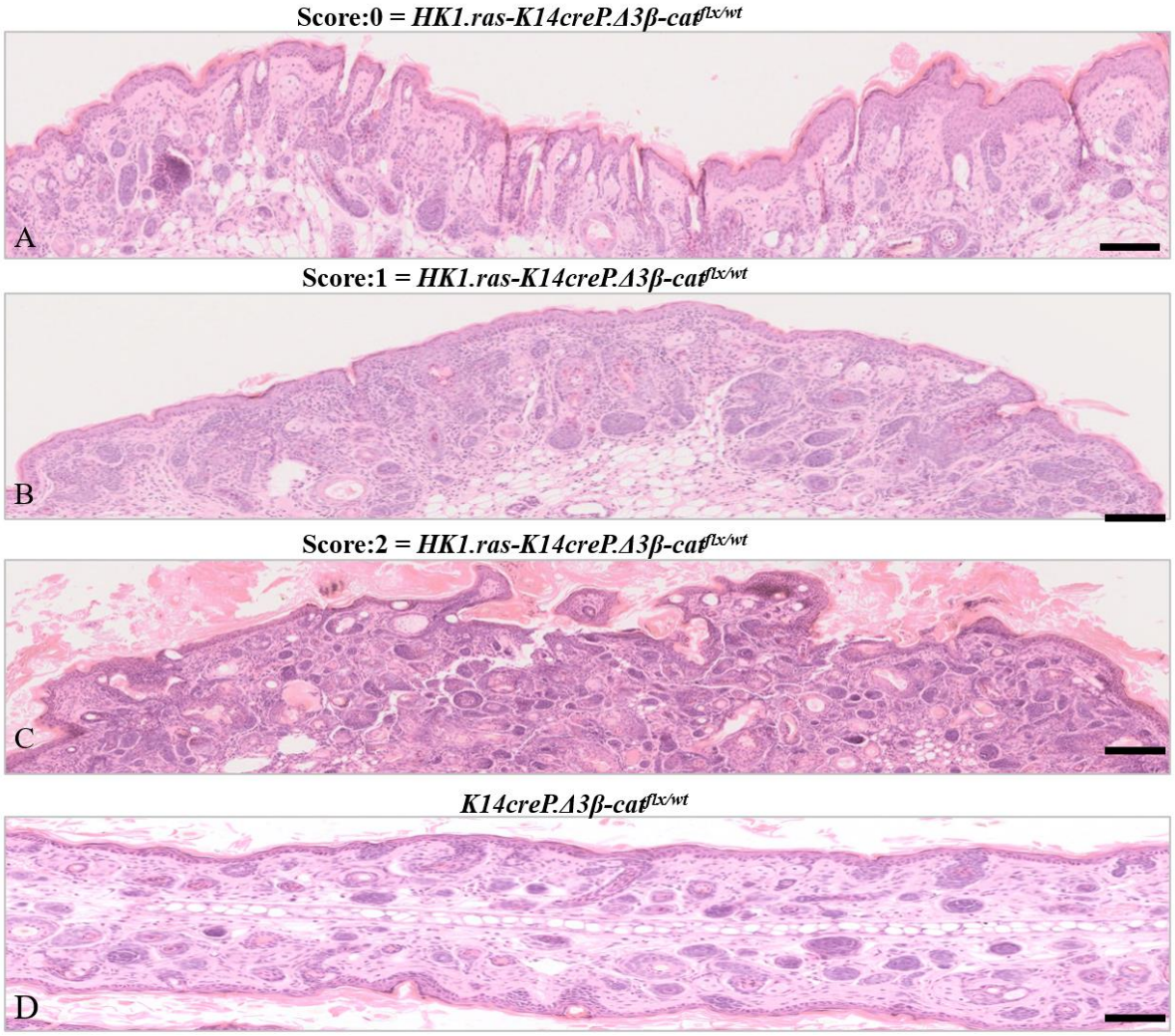

Figure 5. 4: Histological variation in *HK1.ras-K14creP.Δ3β-cat*$^{flx/wt}$ phenotype severity.

[A] Typical representative of *HK1.ras-K14creP.Δ3β-cat*$^{flx/wt}$ skin associated with score 0 [N=10] exhibits mild increased *HK1.ras* -associated hyperplasia but only mild *Δ3β-catenin*-associated follicular phenotypes. [B] Representative skin from a typical *HK1.ras-K14creP.Δ3β-cat*$^{flx/wt}$ score 1 [N=42] mouse is associated with increased hyperplasia and disturbed basal layer differentiation and a greater degree of typical Δ3β-catenin follicular phenotypes. [C] In the most sever *HK1.ras-K14creP.Δ3β-cat*$^{flx/wt}$ score 2 [N=6] skin the histotype is associated with severe Δ3β-catenin follicular phenotypes and whilst the IFE is disorganised and is dominated by excessive keratosis yet exhibits a relative lack of a significant increase in hyperplasia. [D] Typical degree of phenotype severity [now designated score 1] in RU486-treated *K14creP.Δ3β-cat*$^{flx/wt}$ without *HK1.ras* associated increase in hyperplasia. Scale bars: A-D: 150µm

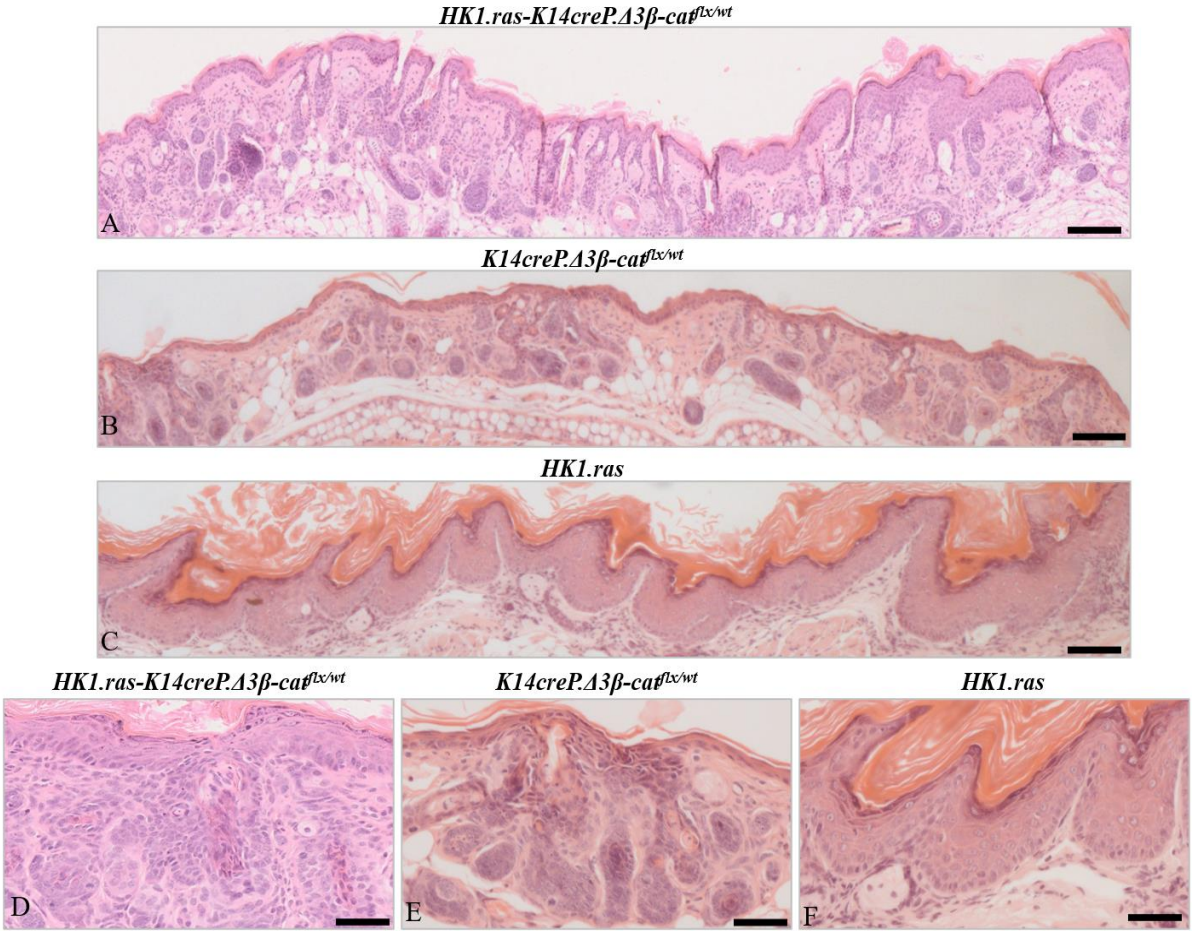

Figure 5. 5: Histotypes of *HK1.ras-K14creP.Δ3β-cat*$^{flx/wt}$ compared to *K14creP.Δ3β-cat*$^{flx/wt}$ and *HK1.ras* littermates.

[A] shows [score 0 above] *HK1.ras-K14creP.Δ3β-cat*$^{flx/wt}$ exhibiting hyperplastic epidermis and multiple hair follicle abnormalities, whilst [B] shows *K14creP.Δ3β-cat*$^{flx/wt}$ to be lacking hyperplastic IFE with less hair follicle abnormalities and [C] shows *HK1.ras* IFE with papillomatous [foldy] hyperplasia and an ordered keratinocyte differentiation not seen in *HK1.ras-K14creP.Δ3β-cat*$^{flx/wt}$ IFE. [D] At higher magnification *HK1.ras-K14creP.Δ3β-cat*$^{flx/wt}$ hyperplasia shows a disorganised IFE basal layer differentiation and multiple follicular abnormalities, compared to [E] minimal IFE hyperplasia with less follicular abnormalities and [F] *HK1.ras* papillomatous hyperplasia with ordered differentiation. Scale bars: A-C: 150 µm; D-F: 50µm

Given these data, the next series of experiments investigated whether this lack of papilloma formation derived from p53 and p21 expression or an increased differentiation response. For instance, did *HK1.ras* expression affect the status of Δ3β-catenin expression in terms of levels and epidermal location, as in chapter 3 *HK1.ras* expression was associated with supra-basal β-catenin expression [Fig. 3.8] minimal p53 and p21 and resultant papilloma development. In addition, given the increased keratosis observed in score 2 mice there was the idea that the general increase in keratosis observed in *HK1.ras-K14creP.Δ3β-cat*$^{flx/wt}$ mouse skin was a differentiation response to *ras*^{Ha} and β-catenin co-operation, possibly indicated by a return to increased differentiation marker keratin K1 expression as seen in *HK1.ras* epidermis but which was sporadic at best in *K14creP.Δ3β-cat*$^{flx/wt}$ mouse skin. This too may have inhibited papilloma formation with either p53 or p21 responses as seen in ROCK mice which also induced AKT/β-catenin in basal layer keratinocytes and an inhibition of papillomas (*Masre et al., 2020*).

As shown in Figs 5.6 and 5.7 an increase in β-catenin expression was detected in *HK1.ras-K14creP.Δ3β-cat*$^{flx/wt}$ hyperplasia in both IF and IHC staining. As with *K14creP.Δ3β-cat*$^{flx/wt}$ mice [above], again β-catenin showed increased expression in the proliferative basal layers with both membranous and nuclear β-catenin expression clearly visible [Fig. 5.6:A-E; Fig. 5.7A]; with membranous expression particularly prominent in the expanded acanthotic layers [Fig. 5.6E; Fig. 5.7A] compared to the less hyperplastic *K14creP.Δ3β-cat*$^{flx/wt}$ hyperplasias[Fig 5.6F; Fig 5.7B], while the *HK1.ras* littermates exhibited supra-basal β-catenin expression as observed previously [Fig. 5.6G; Fig. 5.7C]. Thus *HK1.ras* expression did not alter the β-catenin expression profile.

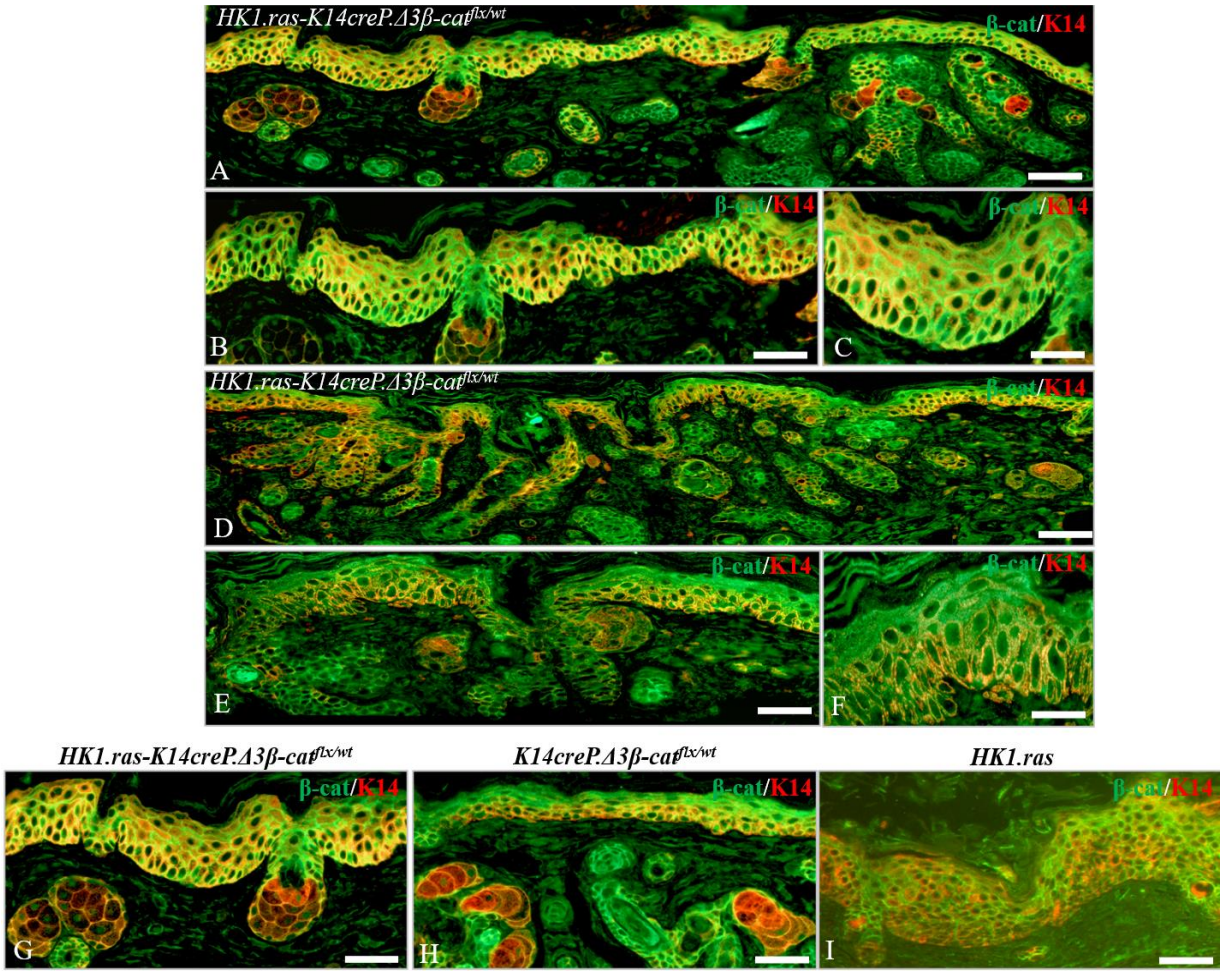

Figure 5. 6: Analysis of β-catenin expression in *HK1.ras-K14creP.Δ3β-cat*$^{flx/wt}$ compared to *K14creP.Δ3β-cat*$^{flx/wt}$ and *HK1.ras* littermates.

[A] *HK1.ras-K14creP.Δ3β-cat*$^{flx/wt}$ mice [score 0] show overall strong expression of β-catenin in IFE and HFs. [B&C] Higher magnification shows nuclear localization of β-catenin in basal layer keratinocytes also with strong membranous expression in both the basal-layer and expanded [acanthotic] supra-basal layers. Similarly, [D] shows the increased phenotypes in score 1 animals with a greater degree of HF abnormalities that again exhibit strong β-catenin expression in IFE and hair follicles; whilst [E&F] higher magnification shows nuclear localization of β-catenin with strong membranous basal-layer expression.[G-I] Higher magnification comparison of β-catenin expression in [G] hyperplastic *HK1.ras-K14creP.Δ3β-cat*$^{flx/wt}$ IFE with nuclear and membranous basal-layer expression to [H] minimal *K14creP.Δ3β-cat*$^{flx/wt}$ IFE hyperplasia that also exhibits nuclear and membranous basal-layer expression; and [I] greater *HK1.ras* hyperplasia exhibiting only supra-basal β-catenin expression. Scale bars: A & C: 150 µm; B&D: 100µm; E-G: 50µm

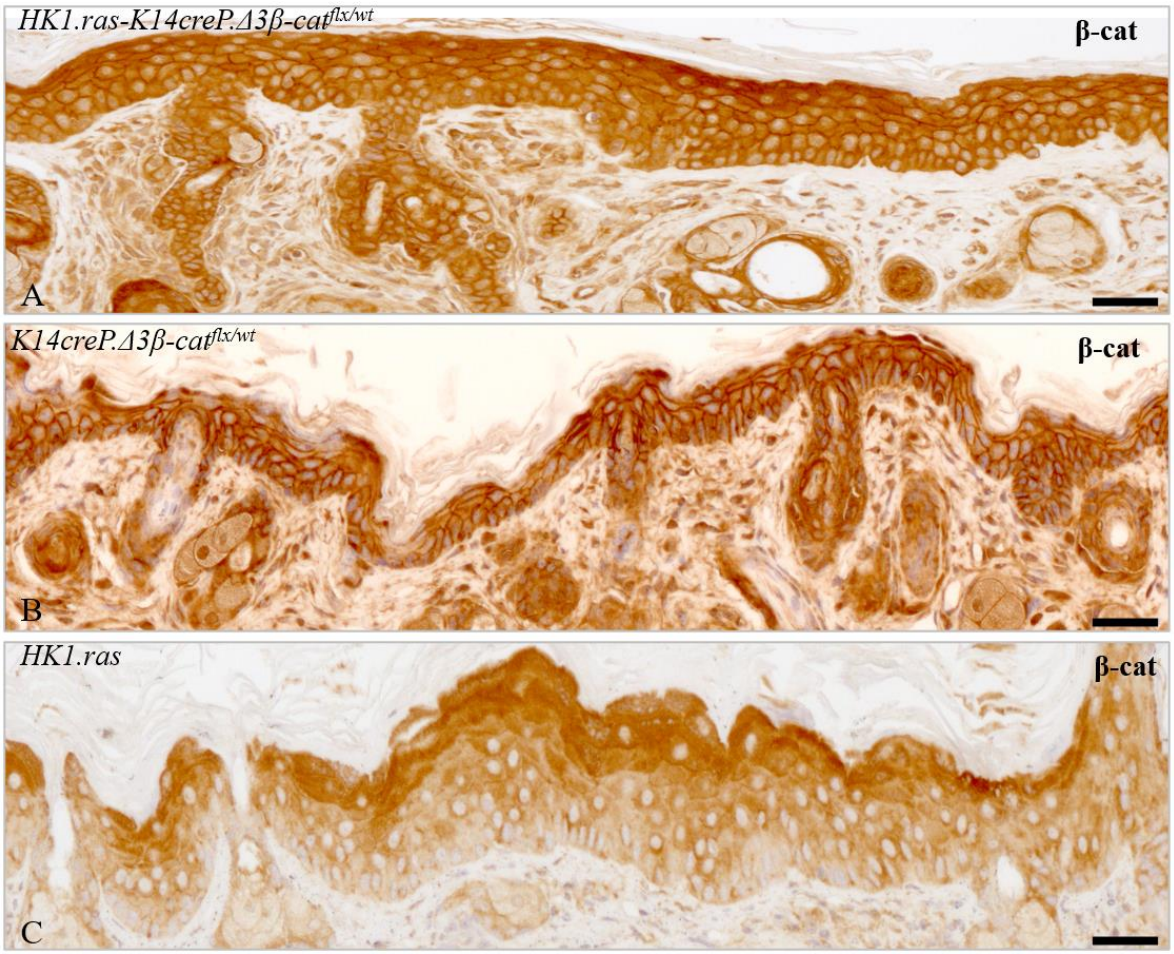

Figure 5. 7: IHC analysis confirms similar nuclear β-catenin expression in *HK1.ras-K14creP.Δ3β-cat*$^{flx/wt}$ and *K14creP.Δ3β-cat*$^{flx/wt}$ basal layers compered to *HK1.ras* skin.

[A] RU-486 treated *HK1.ras-K14creP.Δ3β-cat*$^{flx/wt}$ exhibits an IFE hyperplasia with strong β-catenin expression in both supra-basal and basal layers with clear nuclear expression in epidermal and abnormal follicular keratinocytes. Similarly [B] *K14creP.Δ3β-cat*$^{flx/wt}$ shows same expression in all layers but with a minimal IFE hyperplasia compared to [C] *HK1.ras* showing only suprabasal layer expression with no detectable nuclear expression of β-catenin. Scale bars: A-C: 100 µm

Analysis of E-cadherin showed an identical expression profile to that of β-catenin in terms of both supra-basal and basal layer expression in the IFE in addition to hair follicles [Fig 5.8]. Here E-cadherin levels displayed prominent membranous expression in the suprabasal acanthosis again mimicking that of β-catenin [Fig. 5.8 B vs. C]. Compared to *HK1.ras controls* which again showed mainly membranous supra-basal layer expression [Fig 5.8D], these β-catenin/E-cadherin expression similarities suggest an increase in cell-cell adhesion signalling in *HK1.ras-K14creP.Δ3β-cat*$^{flx/wt}$ mice, which could be aiding in the prevention of tumours forming (*Chiles et al., 2003; Jeanes et al., 2008*). Further, in both *HK1.ras-*

K14creP.Δ3β-cat$^{flx/wt}$ and *K14creP.Δ3β-cat*$^{flx/wt}$ epidermis, E-cadherin expression appeared mainly membranous and cytoplasmic but not nuclear [Fig. 5.8B&C]. Thus, the proposed function to act as a cytoplasmic sponge (*Huels et al., 2015*) and provide further regulation of β-catenin levels prior to nuclear relocation was still intact and indeed seemed to be strengthened by Δ3β-catenin activation particularly in the more affected hair follicles. This result may also highlight attempts to limit cell transformation and tumour formation mediated by excess Δ3β-catenin expression as observed in colon carcinogenesis (*Huels et al., 2015*).

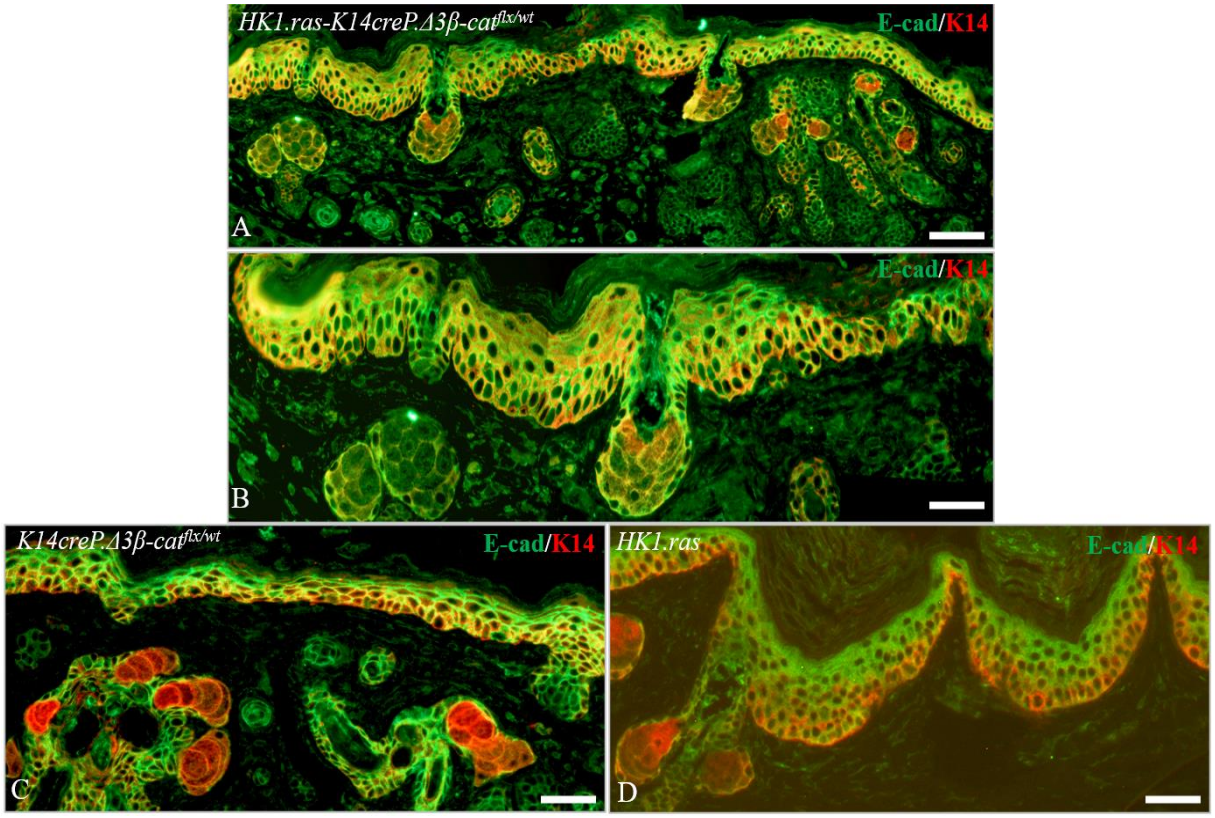

Figure 5. 8: Analysis of E-cadherin expression in *HK1.ras-K14creP.Δ3β-cat*$^{flx/wt}$ compered to *K14creP.Δ3β-cat*$^{flx/wt}$ and *HK1.ras* controls.

[A] *HK1.ras-K14creP.Δ3β-cat*$^{flx/wt}$ exhibits strong E-cadherin expression in supra-basal and basal layer epidermis together with hair follicles. [B] Higher magnification shows strong membranous expression similar to β-catenin expression but without obvious nuclear expression. [C] *K14creP.Δ3β-cat*$^{flx/wt}$ is similar but with less hyperplasia whilst [D] *HK1.ras* hyperplasia exhibits supra-basal E-cadherin expression. Scale bars: A: 100 µm; B-D: 75µm

One new feature of *HK1.ras-K14creP.Δ3β-cat*$^{flx/wt}$ mice was the appearance of increased skin keratosis compared to the typical *K14creP.Δ3β-cat*$^{flx/wt}$ littermates [Fig. 5.1 & Fig. 5.2]. This was likely due to the increased levels of proliferation and the sequential differentiation of the resultant keratinocytes. However, the histology of this increased hyperplasia showed a novel disturbed basal layer differentiation [Figs 5.3C & G; 5.5D] and a greater degree of typical *Δ3β-catenin* follicular phenotypes- particularly in the rarer score 3 histotype [Fig 5.4C] that appeared to have a lesser degree of hyperplasia yet far more keratosis suggesting here that increased differentiation may be a feature of tumour inhibition too in these more severe mice.

Therefore, to assess this novel disordered IFE differentiation seen histologically in *HK1.ras-K14creP.Δ3β-cat*$^{flx/wt}$, again the early differentiation marker keratin K1 and the hyperproliferation/disease-associated keratin K6α were investigated. In Fig 5.9A-C the increased *HK1.ras-K14creP.Δ3β-cat*$^{flx/wt}$ hyperplasia again displayed a quite patchy, confused profile indicating that several sets of transit amplifying keratinocytes failed to differentiate correctly. Here typical of K1 expression in both *HK1.ras-K14creP.Δ3β-cat*$^{flx/wt}$ hyperplasia and to a less degree *K14creP.Δ3β-cat*$^{flx/wt}$ siblings, was the lack of expression in the upper epidermal layers, again suggesting a delay in K1 expression was mediated by responses Δ3-βcatenin expression [Fig. 5.9B-D vs. E]. In contrast *HK1.ras* littermate epidermal hyperplasia shows a smooth and ordered supra-basal layer expression of K1 with a thicker basal layer [red] due to lack of inhibitory p53 expression but with an ordered differentiation profile Fig 5.9E due to the normal low expression of p21.

Thus unlike *HK1.ras* skin, *HK1.ras-K14creP.Δ3β-cat*$^{flx/wt}$ keratinocytes appear to be receiving very confused conflicting signals regarding proliferation and differentiation. In some patches of epidermis, K1 was expressed relatively normally possibly due to the co-expression of *HK1.ras* [Fig. 5.9A&C vs. E] given its expression profile in approx. 30-50% basal layer keratinocytes [(*Greenhalgh et al., 1993*) chapter 1 HK1.βcal expression Fig. 1.3], and this may account in part for the patches of keratosis observed *HK1.ras-K14creP.Δ3β-cat*$^{flx/wt}$ skin [Fig. 5.1A].

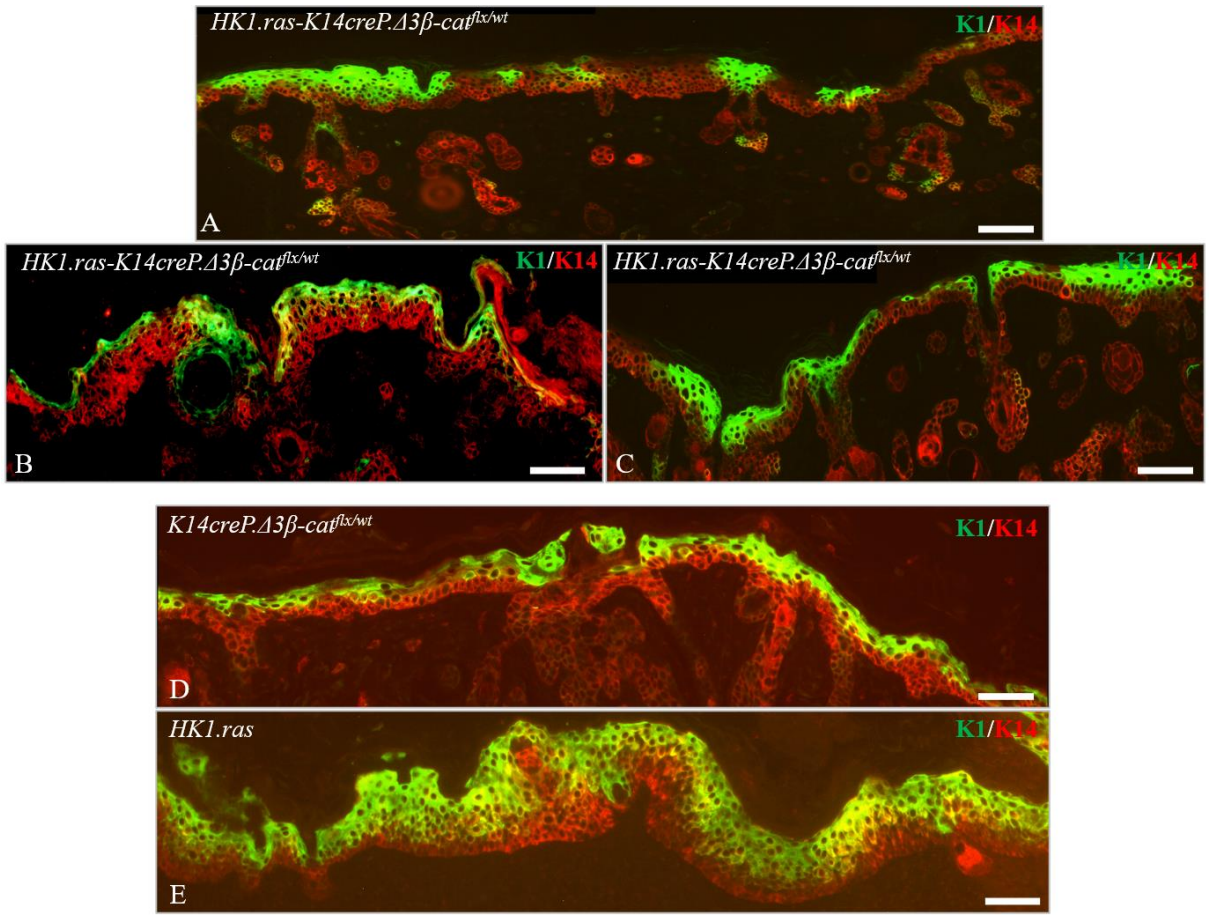

Figure 5. 9: Analysis of early differentiation marker K1 in HK1.ras-K14creP.Δ3β-cat$^{flx/wt}$ compered to K14creP.Δ3β-cat$^{flx/wt}$ and HK1.ras genotypes.

[A-C] *HK1.ras-K14creP.Δ3β-cat$^{flx/wt}$* epidermis shows distinct variations of confused, patchy and in some areas loss of K1 expression in the areas of increased hyperplasia. [B] also shows K1 positive cysts demonstrating that IFE can also form cysts together with [C] HF responses to βcatenin overexpression. [D] This example of K1 expression in a *K14creP.Δ3β-cat$^{flx/wt}$ score 0* epidermis shows a less patchy but disordered K1 expression in the final differentiating layers; whilst [E] *HK1.ras* littermate hyperplasia shows s smooth and ordered suprabasal layer expression of K1 with a thicker basal layer [red] due to lack of inhibitory p53 and p21 expression. Scale bars: A: 100 µm; B-E: 75µm

However, what was quite striking is shown in Fig 5.9A&C, where there appears to be a distinct lateral cut off to the patchy K1 expression (*Porter et al., 2000*) compared to the *K14creP.Δ3β-cat$^{flx/wt}$* control [Fig 5.9D] which exhibits less hyperplasia and thus less expansion of the K14 staining [red]. This maybe possibly consistent with β-catenin effects on an individual stem cell niche (*Watt and Collins, 2008*) where β-catenin alters the correct differentiation programme decisions throughout the transit amplifying daughter keratinocytes

from a given individual epidermal stem cell unit [See also mK15 section below; *Porter et al., 2000*). Indeed, this odd proliferation/differentiation decision appears to produce the proliferation dead end of K1 positive interfollicular cysts [Fig 5.9B] which would also divert keratinocytes away from papilloma formation.

The relatively little hyperkeratosis observed histologically may be a finding consistent with β-catenin roles in latter stages of differentiation given its supra-basal location involving increased cell-cell adherence. As suggested above in Chapter 4 incorrect differentiation in both *K14creP.Δ3β-cat*$^{flx/wt}$ *and HK1.ras-K14creP.Δ3β-cat*$^{flx/wt}$ a lack of supra-basal keratinocytes indicated by the expanded K14 positive basal layer may be due to excess basal layer β-catenin/E-cadherin and an increased number of anomalous adherence junctions which affect epidermal rigidity. Thus, from a barrier viewpoint the keratins associated with maintaining a supra-basal layer are reduced consistent with the observed acanthosis. Possibly altered differentiation maker expression is due to the context of p21 expression [below] as in some contexts excess p21 displays an inhibitory role in differentiation and affects a commitment to differentiate (*Di Cunto et al., 1998; Topley et al., 1999*) consistent with this delayed and patchy K1 finding.

Investigation of the hyperproliferation marker K6α in *HK1.ras-K14creP.Δ3β-cat*$^{flx/wt}$ hyperplasia also showed a similar disruption of the ordered keratinocyte differentiation and expression was almost absent from *HK1.ras-K14creP.Δ3β-cat*$^{flx/wt}$ epidermis [Fig 5.10], a result observed for *K14creP.Δ3β-cat*$^{flx/wt}$ [Fig 5.10D above Fig 4.6] but was strongly expressed in *HK1.ras* control hyperplasia [Fig 5.10E]. Again, K6α expression appeared to be confined to the abnormal hair follicles yet expression was completely absent in the mildly hyperplastic IFE and to-date in the HK1 model this novel observation is unique to Δ3βcatenin expression. As speculated for K1 above, this change in K6α expression may reflect the excess increase in adherence junctions which in turn alters the hyperproliferation signals derived from cell-cell interactions that are typically disrupted in wounding. These are normally essential for the cell division and keratinocyte migration and thus disruption of the filament network [intermediate and actinomycin] would affect movement that is carried out by the underlying cytoskeletal network that regulate mechanical tension through adherence junctions and hemidesmosomes (*Masre et al., 2020 Samuel et al., 2011*). Hence these and other responses to *HK1.ras* activation that typically induce K6 expression *(Rothnagel et al., 1999*) are overcome by those

elicited in *HK1.ras-K14creP.Δ3β-cat*$^{flx/wt}$ skin i.e. p53 and p21 [see Fig. 5.11 & Fig. 5.12] amongst others [e.g. p63 and p73; below chapter 6].

These data suggest that in *HK1.ras-K14creP.Δ3β-cat*$^{flx/wt}$ *epidermis* Δ3β-catenin combined with ras^{Ha} activation resulting amplification of the mild *Δ3β*-catenin ILE hyperplasia seen in *K14creP.Δ3β-cat*$^{flx/wt}$ mice and a more disrupted keratinocyte differentiation. However, this did not aid in the generation of tumourigenesis typically induced via *HK1.ras* transgene and data below supported the idea that this may be due to compensatory p53 and p21 expression, as observed in *HK1.ras/fos-K14creP.Δ5PTEN*$^{flx/flx}$ mice [Chapter 3; (*Yao et al., 2006; 2008; Macdonald et al., 2014*)].

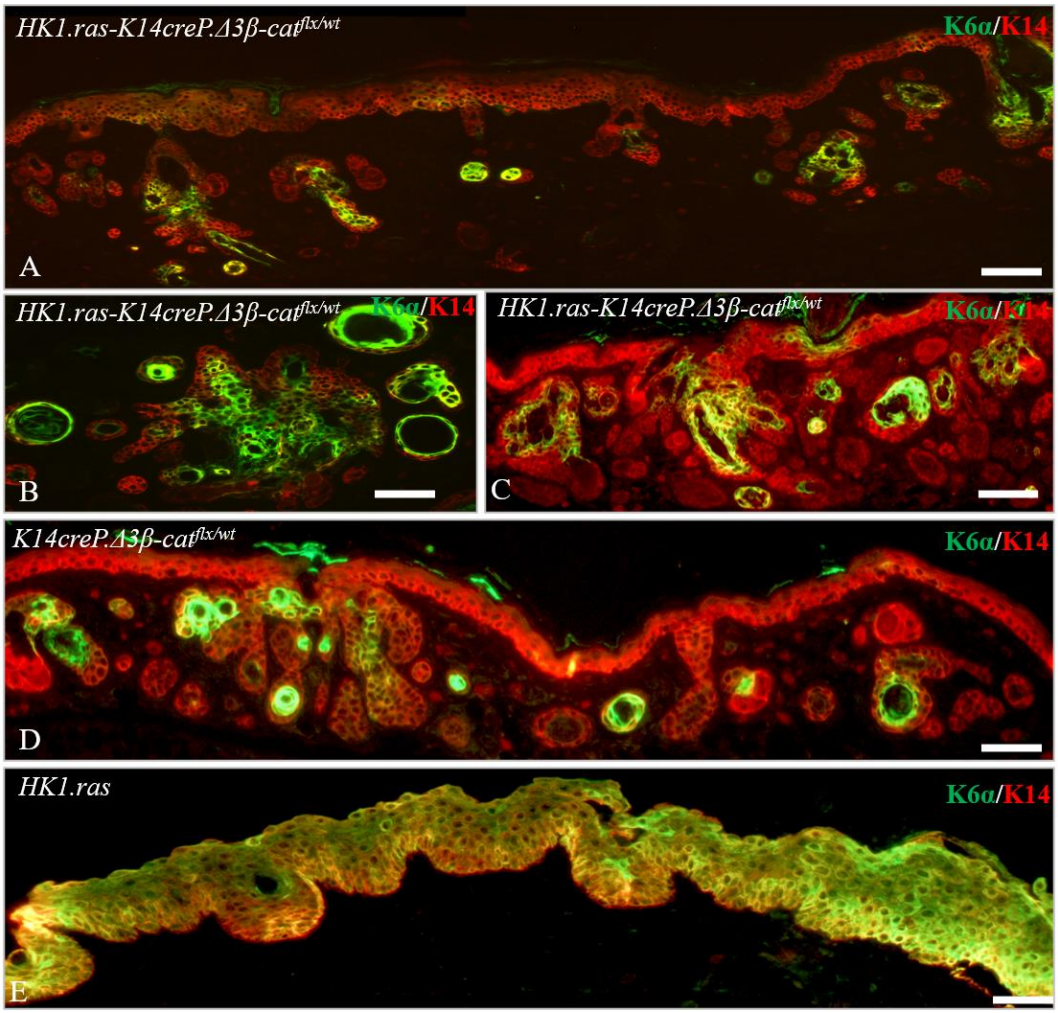

Figure 5. 10: Analysis of hyperproliferation marker keratin K6 in *HK1.ras-K14creP.Δ3β-cat*$^{flx/wt}$, *K14creP.Δ3β-cat*$^{flx/wt}$ and *HK1.ras* epidermis.

[A-C] Typical RU486-treaated *HK1.ras-K14creP.Δ3β-cat*$^{flx/wt}$ hyperplasia lack K6α expression in the IFE and expression is confined to hair follicles. [B & C] Most cysts express K6 being derived from a HF origin, but not all HFs had K6 expression depending upon the degree of HF anomalies. [D] *K14creP.Δ3β-cat*$^{flx/wt}$ skin shows K6α expression confined to many but not all hair follicles. [E] *HK1.ras* shows strong expression in the hyperplastic IFE constant with K6 hyperproliferation and a lack of inhibitory p53 /P21 expression. Scale bars: A, D & E: approx. 100 µm; B: approx. 30µm; C: 75µm

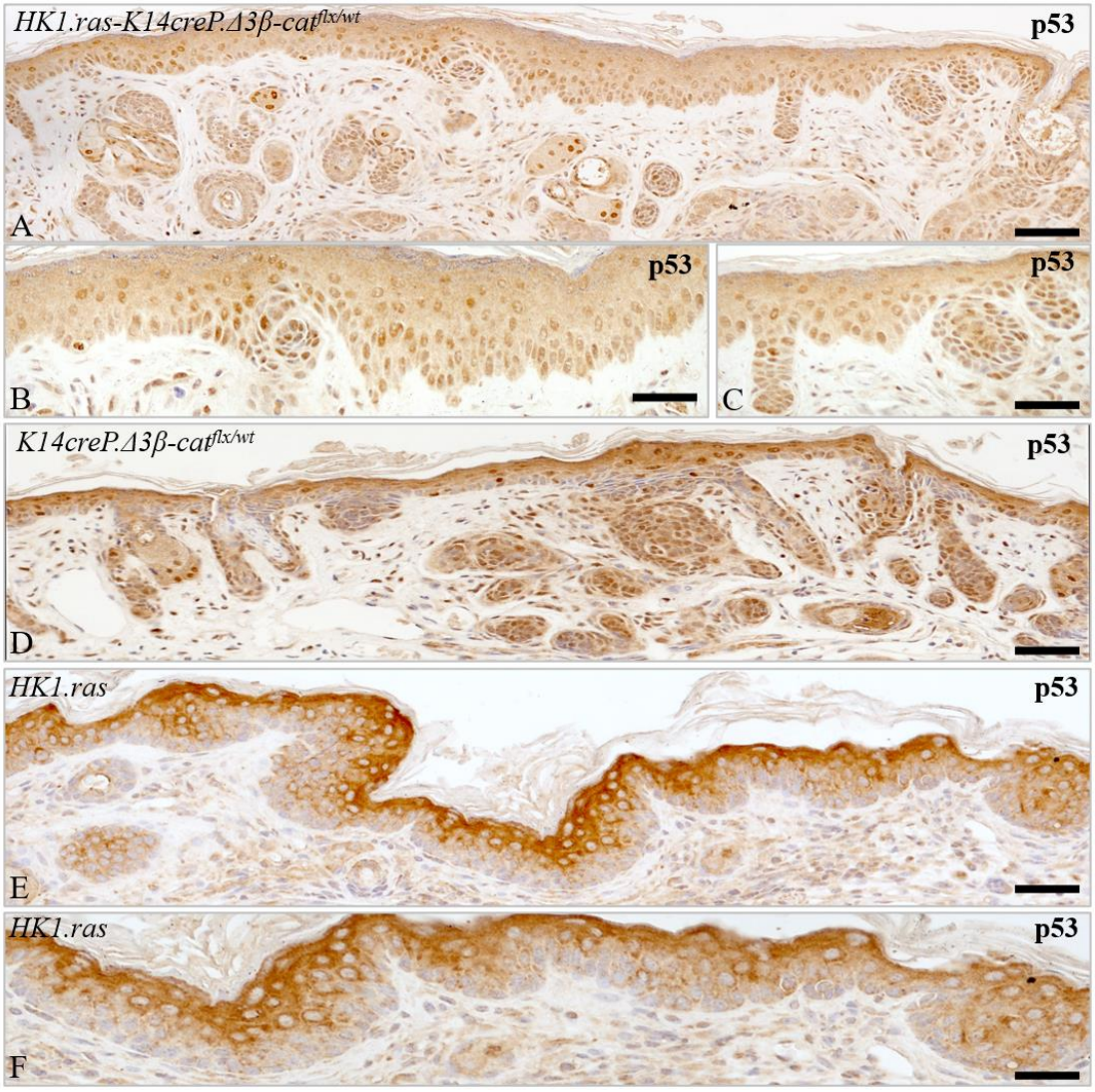

Figure 5. 11: Analysis of p53 expression in HK1.ras-K14creP.Δ3β-cat$^{flx/wt}$.

[A-C] RU486-treated *HK1.ras-K14creP.Δ3β-cat$^{flx/wt}$* hyperplasia shows strong p53 expression in basal and supra-basal layers and HFs. [B & C] Higher magnification shows elevated nuclear p53 expression; as does [D] *K14creP.Δ3β-cat$^{flx/wt}$* littermate skin. [E & F] *HK1.ras* hyperplasia typically lacks basal layer p53 expression until just prior to overt papilloma formation and with this p53 antibody appears only cytoplasmic in the supra-basal layers. Scale bars: A, D & E: 100 µm; B & F: 50µm; C: 30µm

Therefore, prompted by the paradoxical lack of tumours in the *HK1.ras-K14creP.Δ3β-cat*$^{flx/wt}$ mice the p53 and p21 status was assessed. Analysis of p53 expression [Fig 5.11] in treated [and non treated score 1 skins] found an increase in nuclear p53 expression in the basal layers similar to that observed in *K14creP.Δ3β-cat*$^{flx/wt}$ IFE [Fig. 5.11A-C vs. D]. Typically, p53 expression appeared more intense with more uniform nuclear expression in the *HK1.ras - Δ3βcatenin* IFE consistent with the response to co-expression of both activated ras and β-catenin [Fig 5.11 A-C] compared to *K14creP.Δ3β-cat*$^{flx/wt}$ IFE alone [Fig. 5.11D], whilst follicular expression appeared particularly intense in the more transformed HFs and in both cases [Fig. 5.11A-D]. This HF result was consistent with a relative lack of progression to more aggressive HF tumours (*Misago et al., 2012*) compared to other studies where β-catenin was overexpressed throughout embryonic development (*Gat et a.,1998*). NB Consistent with this idea all attempts to create non-inducible K5-βcat/p53 genotypes in studies geared to assess effects of p53 knockout failed to produce pups or pups died shortly after birth [see below; *Järvinen et al., 2006]*

In contrast, *HK1.ras* epidermis exhibited little basal layer p53 [Fig. 5.11E&F] unless a keratinocyte was completing the cell cycle or over time began progressing from late stage hyperplasia to the beginnings of papilloma, where p53 expression increased and became basal]. Thus, the epidermis appears relatively tolerant of ras activation as judged by the fairly normal differentiation responses [above; Chapter 3] and thus p53 is not invoked and this avoids the possibility of apoptosis and a failure of the barrier function. Indeed, it is speculated that the normal supra-basal expression of AKT maybe geared to block p53-mediated apoptosis giving time for terminal differentiation (*Calautti et al., 2005; Macdonald et al., 2014*).

Thus, these *HK1.ras-K14creP.Δ3β-cat*$^{flx/wt}$ *vs HK1.ras* data suggest that Δ3β-catenin maybe integral to induction of p53 [and p21] which disrupts this process giving an altered confused expression of differentiation markers. Further with respect to papillomas formation in *HK1.ras-K14creP.Δ3β-cat*$^{flx/wt}$ mice this strong p53 expression in all layers would inhibit tumours that appear in *HK1.ras* alone mice, and this response is sufficiently potent to block both the regression prone, wound-associated type 1 and the aggressive type 2 papillomas. An idea supported by similar p53 responses also observed in ROCK-mediated β-catenin activation that also blocked papilloma formation (*Masre et al., 2020*).

A similar story appears for analysis of p21 which also found a significant increase in nuclear expression in both *HK1.ras-K14creP.Δ3β-cat*$^{flx/wt}$ basal and supra-basal layers and also in the abnormal follicles [Fig. 5.12A-C] as observed in *K14creP.Δ3β-cat*$^{flx/wt}$ IFE but again absent in *HK1.ras* epidermis [Fig. 5.12D vs. E&F]. Of note p21 expression in *HK1.ras* mice again appeared less than that of p53 and typically expressed little basal p21 unless the cell was committing to differentiate.

Thus, as previously speculated for *K14creP.Δ3β-cat*$^{flx/wt}$ epidermis [Chapter 4] again in *HK1.ras-K14creP.Δ3β-cat*$^{flx/wt}$ mice excess p21 in the basal layers may increase the commitment to differentiate and, with ras-induced hyperplasia, give rise to the increased cornification and keratosis observed [Fig 5.2] (*Topley et al., 1999*); but excess expression in the upper layers may inhibit the latter stages of differentiation that results in the apparent lack of K1 expression (*Di Cunto et al., 1998*).

In terms of papilloma formation, p21 again aids p53 in the inhibition of tumours and appears quite potent even at this early stage. Indeed based on *HK1.ras/fos-K14creP.Δ5PTEN*$^{flx/flx}$ tumours this potent TSG effect remains as following p53 loss, p21 expression persists in wdSCC and limits further progression possibly via maintaining this inhibitory differentiation profile in basal layers, along side the increased adherence junctions, until lost quite late in carcinogenesis when membranous β-catenin was also diminished [chapter 3 Fig 3.3] and becomes nuclear alongside uniform AKT expression [not shown; paper in prep] giving progression to highly invasive pdSCC.

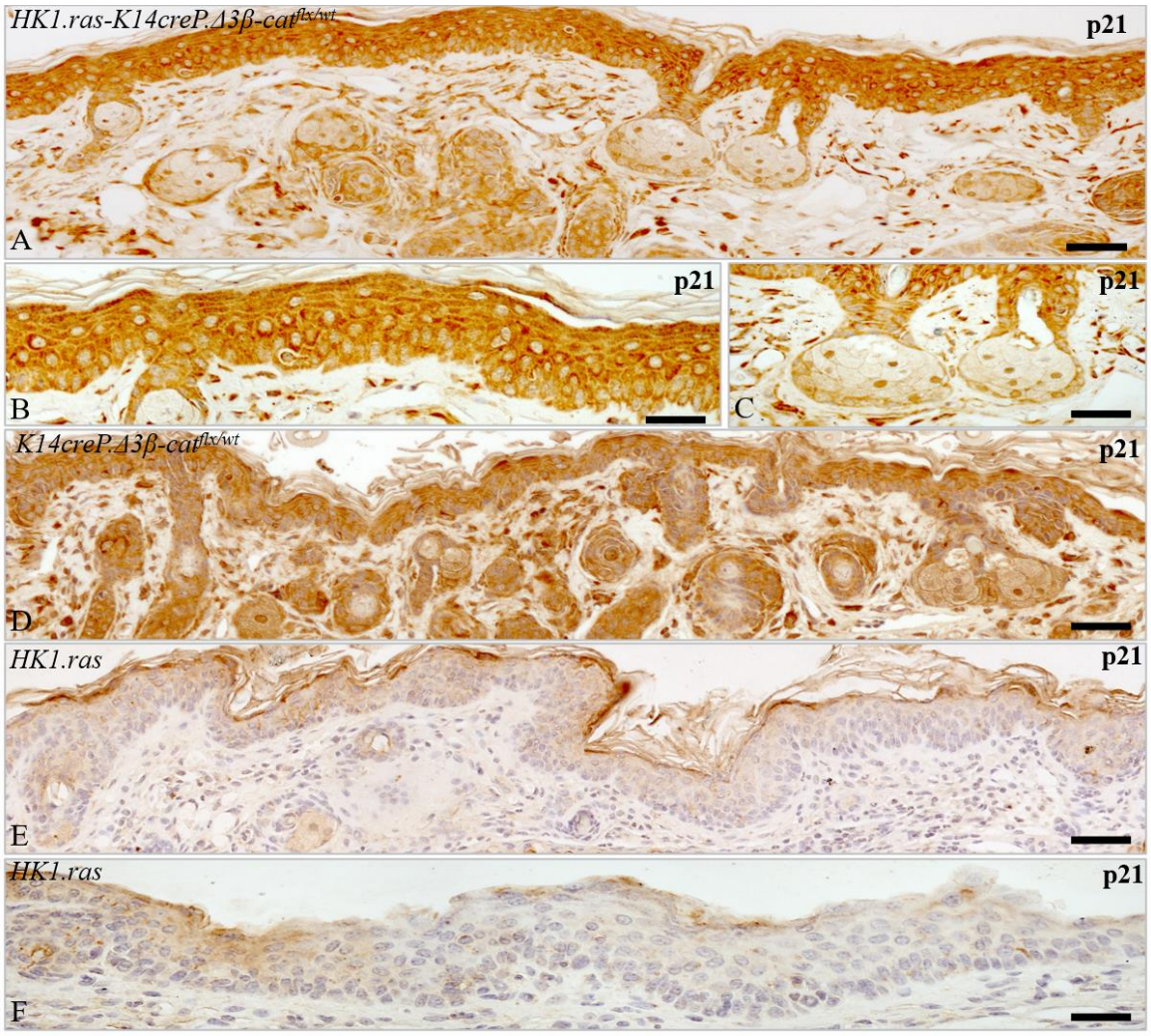

Figure 5. 12: p21 expression in *HK1.ras-K14creP.Δ3β-cat*$^{flx/wt}$ skin.

[A-C] At low and higher magnification, p21 expression mirrors that of p53 with strong nuclear expression in basal layer and suprabasal layers together with the hair follicle while [D] *K14creP.Δ3β-cat*$^{flx/wt}$ skin also shows slightly less intense expression of p21. [E & F] *HK1.ras hyperplasia* expresses low p21 levels until at the later papilloma stage. Scale bars: A, D & E: 100 µm; B & F: 50µm; C: 30µm

Table 5. 1: Summary of *HK1.ras-K14creP.Δ3β-cat$^{flx/wt}$* phenotypes.

Genotype analysed	[N]	Analysed for expression of	Data summary
HK1.ras hyperplasia	90	β-catenin, E-cadherin, K1, K6α, p53 and p21 expressions	-Control hyperplasia exhibiting suprabasal layer membranous β-catenin/E-cadherin expression -ordered terminal differentiation indicated by suprabasal layer K1 and expressing K6α in both supra and basal layer due to *HK1.ras* activation stress signals -weak basal layer p53/p21
K14creP.Δ3β-cat$^{flx/wt}$	74	β-catenin, E-cadherin, K1, K6α, p53 and p21 expressions	-No IFE tumours -HF tumours -minimal IFE hyperplasia -Increased cytoplasmic/nuclear basal layer β-catenin with increased membranous basal layer β-catenin/E-cadherin due to Δ3β-catenin -Altered terminal differentiation indicated by K1 expression but with normal K6α expression - Nuclear basal layer expression of p53/p21 halting Δ3β-catenin induced proliferation
HK1.ras-K14creP.Δ3β-cat$^{flx/wt}$ [No papillomas]	58	β-catenin, E-cadherin, K1, K6α, p53 and p21 expressions	-No IFE tumours -More HF tumours vs. *K14creP.Δ3β-cat$^{flx/wt}$* -Mild hyperplasia due to *HK1.ras* -Increased cytoplasmic/nuclear basal layer β-catenin with increased membranous basal layer β-catenin/E-cadherin due to Δ3β-catenin expression -More Aberrant confused terminal differentiation vs. *K14creP.Δ3β-cat$^{flx/wt}$* indicated by patchy K1 expression but still maintain fairly normal K6 expression - Nuclear basal layer expression of p53/p21 halting Δ3β-catenin-induced proliferation
Conclusion: constitutive β-catenin activation [*Δ3β-catenin*] with ras activation increases the severity of β-catenin associated HF abnormalities yet still blocks IFE tumour development due to compensatory early elevated levels of TSGs [p53/p21] which consequently resulted in the confused terminal differentiation whilst maintaining strengthened basal layer cell-cell adhesion [β-catenin/E-cadherin] aiding in the blockage of tumourigenesis.			

5.3 Analysis of the rare *HK1.ras-K14creP.Δ3β-cat$^{flx/wt}$* papillomas

On only two occasions over this study period did *HK1.ras-K14creP.Δ3β-cat$^{flx/wt}$* mice develop papillomas. In almost every case it appears that logically the p53 and p21 responses outline above blocked formation of both mild type 1 papillomas and the aggressive type 2. Thus, to address this point and compare the mechanism to HK1.ras alone, the backgrounds of these two individuals [Fig 5.1F&G; Fig 5.13A&B] were examined more closely to assess for clues to this papilloma aetiology. Firstly, it was noted that in each case [separated by 10 months] these two *HK1.ras-K14creP.Δ3β-cat$^{flx/wt}$* mice were almost full-sized when subjected to the tail biopsy and thus had been designated score 0. This indicated that in these mice the spontaneous cre did not leak early in the development. Furthermore, they still showed the typical Δ3β-catenin phenotypes post RU486 treatment [Fig 5.1F&G; insert Fig 5.13A & B].

However, with hindsight, a close examination of their records showed that RU486 treatment had commenced following PCR conformation, as these were likely originally assumed to be Δ3β-catenin or K14cre negative given their score 0 and full size. Thus, in the probable absence of major cre leakage and normal development, RU486 treatment to activate Δ3β-catenin likely occurred 10 -14 days post ear tagging, and it may be that the wound promotion of this period allowed for a commitment to a papilloma outcome. Thus, a later RU486 treatment when the p53 and p21 may have committed would also account for these papillomas formed in *HK1.ras-K14creP.Δ3β-cat$^{flx/wt}$* taking more than 10 weeks to appear and being much smaller [3-4 mm diameter]. In each case papillomas were about a third the size of their littermate papillomas in *HK1.ras* control that were larger [7-10 mm diameter] and began to appear as early as 6 weeks post tagging [Fig. 5.1F&G; Fig. 5.13A&B].

It thus appeared that these mice may have been the kind envisaged in the original aims and hypothesis [chapter 1]. Therefore, it was possible that despite their smaller size these RU486–treated *HK1.ras-K14creP.Δ3β-cat$^{flx/wt}$* papillomas may possess signs of further progression. However, histological analysis did not show any significant indication of invasiveness in theses *HK1.ras-K14creP.Δ3β-cat$^{flx/wt}$* papillomas aside from the size difference [Fig. 5.13], a result again consistent with a papilloma aetiology more typical of *HK1.ras* mice.

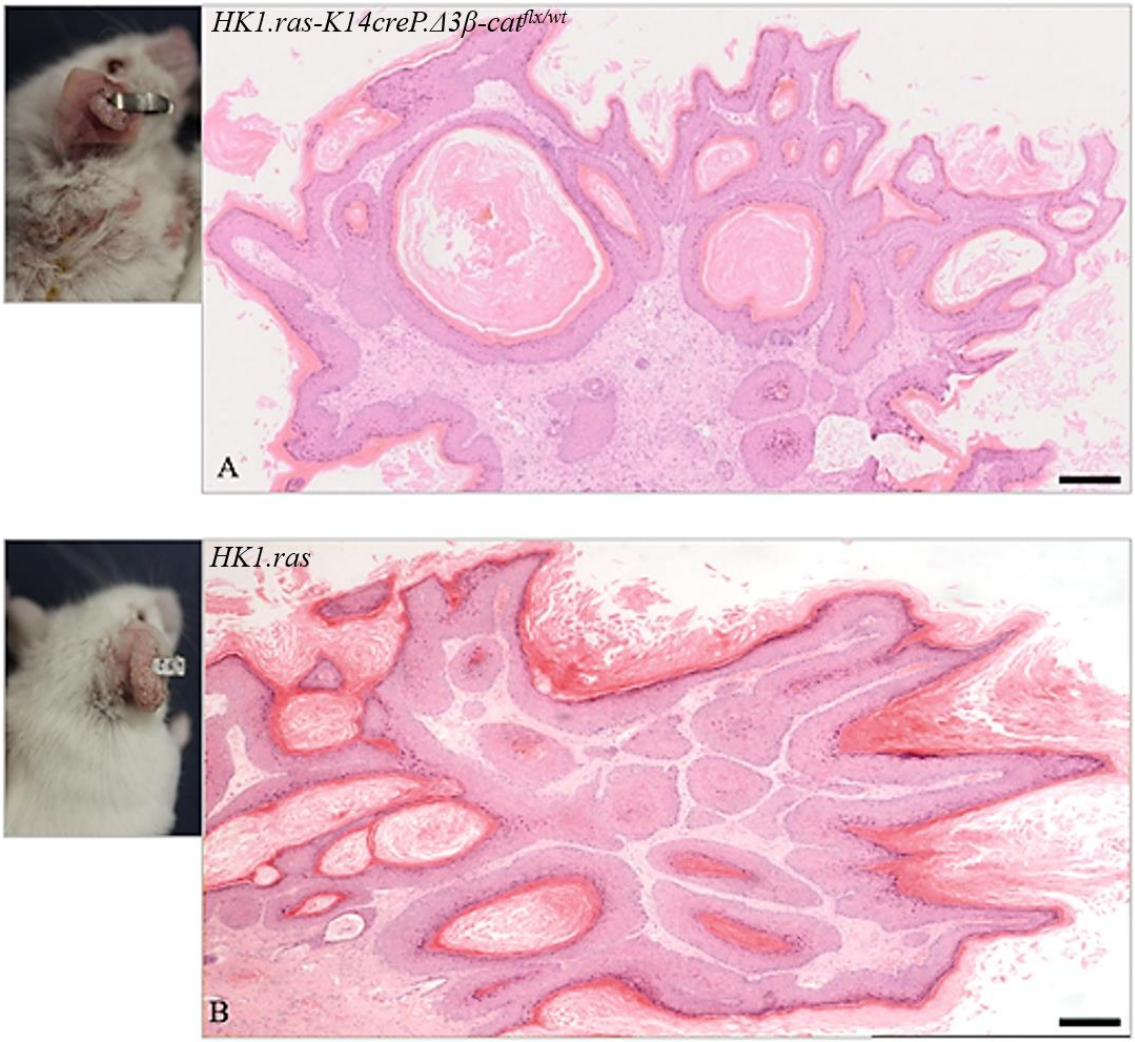

Figure 5. 13: Histological analysis of *HK1.ras-K14creP.Δ3β-cat*$^{flx/wt}$ papilloma against *HK1.ras* littermate papilloma.

[A] Insert shows overt smaller papilloma from *HK1.ras-K14creP.Δ3β-cat*$^{flx/wt}$ exhibits a typical benign papilloma histotype and lacking any sign of invasiveness despite Δ3β-catenin activation. Indeed this has a less aggressive papilloma histotype compared to [B] a *HK1.ras* benign papilloma which is approx. 3 fold larger in size but still lacks invasiveness. Scale bars A&B: 250µm

Consistent with the appearance of Δ3β-catenin phenotypes following RU486 treatment analysis of β-catenin expression in *HK1.ras-K14creP.Δ3β-cat*$^{flx/wt}$ papillomas again showed the typical strong membranous expression in both supra-basal and basal-layers with strong nuclear expression [Fig. 5.14A-D]. *HK1.ras* littermate controls showed typical membranous β-catenin expression mainly in the supra-basal layers with only sporadic expression [nuclear/membranous] in basal layer keratinocytes [Fig. 5.14E&F].

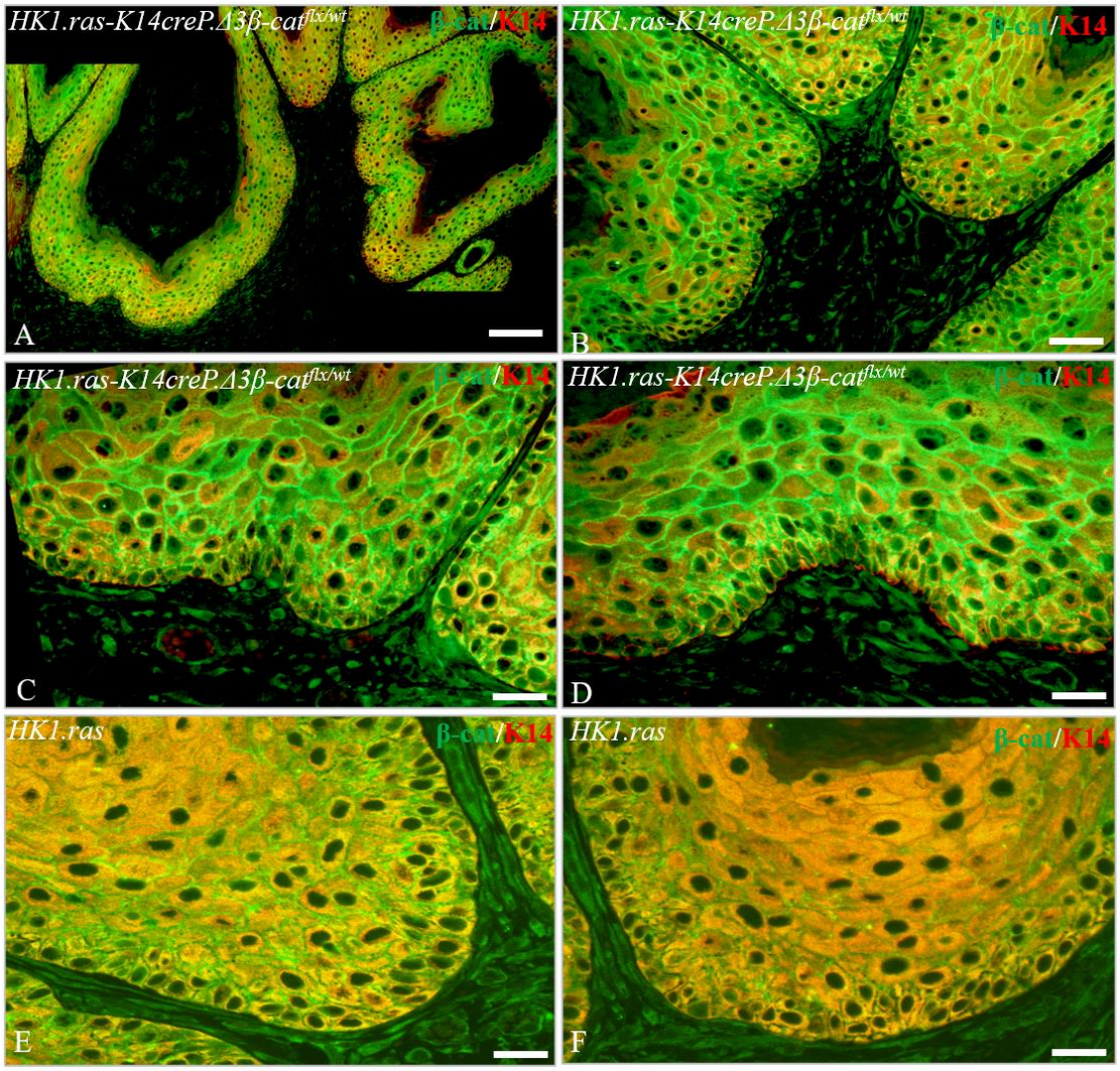

Figure 5. 14: Analysis of β-catenin expression in *HK1.ras-K14creP.Δ3β-cat*$^{flx/wt}$ and *HK1.ras* papillomas.

[A] Composite micrograph at low and [B] medium magnification shows strong uniform β-catenin expression in *HK1.ras-K14creP.Δ3β-cat*$^{flx/wt}$ papillomas. [C & D] At higher magnification *HK1.ras-K14creP.Δ3β-cat*$^{flx/wt}$ mice highlight strong nuclear and membranous β-catenin expression in papilloma basal layers. [E & F] *HK1.ras* papilloma shows mainly membranous expression in supra-basal layers and weak β-catenin in basal layers. Scale bars: A: approx.150µm; B:100µm C-F: 50µm

In addition, this result suggests that Δ3β-catenin activation and nuclear localization in *HK1.ras-K14creP.Δ3β-cat*$^{flx/wt}$ papillomas induced the responses that appeared in *K14.cre-Δ3β-catenin* mice and aided in limiting tumour progression, contrary to previous results seen in tri-genic *HK1.ras/fos-K14creP.Δ5PTEN*$^{flx/flx}$ where nuclear localization of endogenous β-catenin aided the progression of papilloma into carcinoma following p53 loss hence p53 /p21 analysis below. Similarly, whilst in the main E-cadherin expression in both these sets of

HK1.ras-K14creP.Δ3β-cat$^{flx/wt}$ papillomas generally paralleled that of β-catenin expression, it was noticed that in several instances strands of papilloma basal layers appeared to express less intense membranous E-cadherin [Fig. 5.15A&B; arrows]. This was not simply a squint cut of the tumour tissue as most of the remaining section did exhibit strong membranous basal layer E-cadherin. An example of squint cut appeared in *HK1.ras* controls [Fig. 5.15 C; arrows] *w*here an island of folded papilloma has been cut above the basal layers and shows apparent E-cadherin expression in all layers absent it the remaining section or the repeat experiments [Fig. 5.15D].

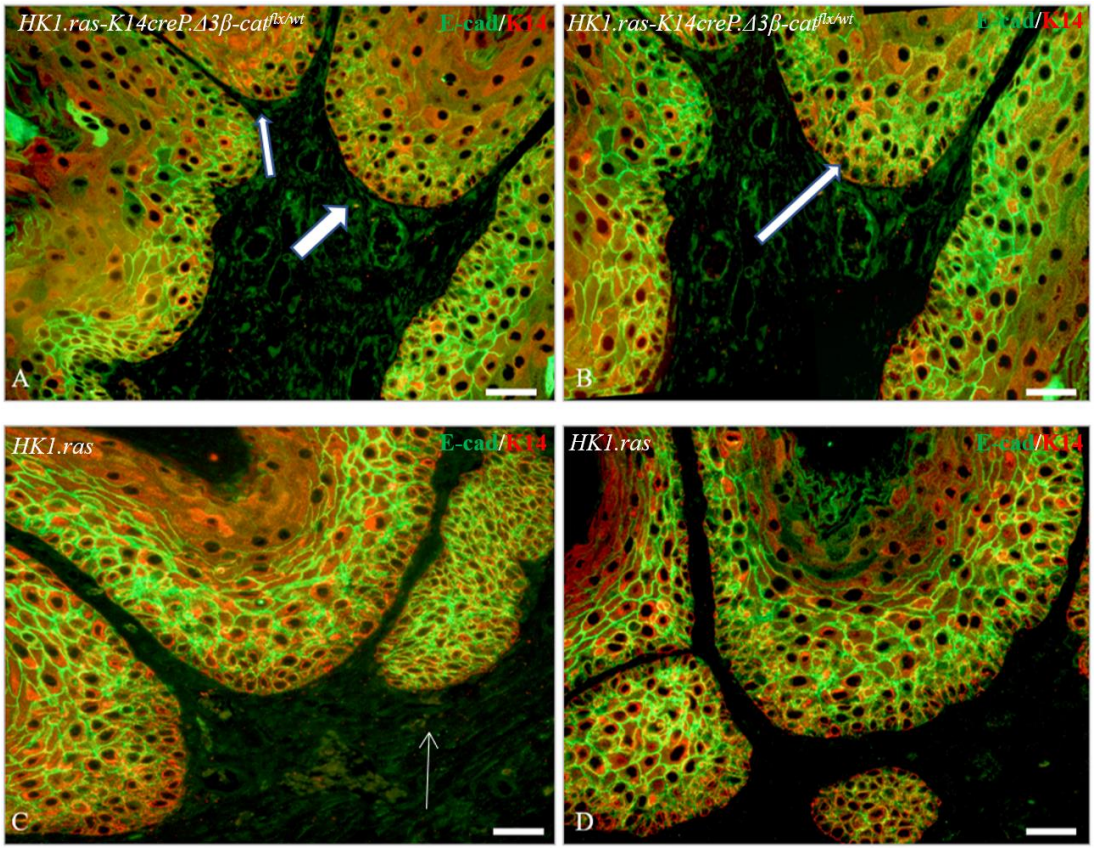

Figure 5. 15: Analysis of E-cadherin expression in *HK1.ras-K14creP.Δ3β-cat*$^{flx/wt}$ verses *HK1.ras* papilloma.

[A & B] Both sets of *HK1.ras-K14creP.Δ3β-cat*$^{flx/wt}$ papillomas mainly show strong membranous expression of E-cadherin in both supra-basal and basal layers with little nuclear expression. However, in each case strands of papilloma appear where E-cadherin appears confined to the suprabasal layers [arrows]. [C & D] *HK1.ras* papilloma shows only supra-basal layer E-cadherin expression, except for an island of squint cut [arrows C] where the folds of papilloma go into the image and the section was cut above the basal layer. Scale bars: A&C: 100µm; C&D: 75µm

These E-cadherin data suggest that there may have been a delay in the responses to β-catenin deregulation in these normal sized score 0 mice, this may have given less numbers of adherence junctions in the early basal layers of a wounded, tagged ear that allowed papillomas to start and this is reflected here by the remaining strands of supra-basal E-cadherin in some parts of the *HK1.ras-K14creP.Δ3β-cat*$^{flx/wt}$ papillomas.

Some of the clearest indications that the dominance of Δ3β-catenin expression was less in these two mice came from the analysis of differentiation markers K1 and K6α [Fig. 5.16 & Fig. 5.17]. In both individuals, K1 showed normal expression in *HK1.ras-K14creP.Δ3β-cat*$^{flx/wt}$ papilloma giving an intense, strong expression in the supra-basal layers similar to the typical expression in control *HK1.ras* papilloma [Fig. 5.16A&B vs. E&F]. However, it was noted that the transition from basal to suprabasal keratinocytes appeared disordered and ragged compared to the equivalent *HK1.ras* littermate papilloma [Fig. 5.16B vs. E&F]. This suggests that eventually Δ3β-catenin expression in the *HK1.ras-K14creP.Δ3β-cat*$^{flx/wt}$ papilloma epidermis again disrupts the ordered nature of keratinocyte differentiation, possibly due to the conflicting proliferative signals from β-catenin/Wnt deregulation vs. basal E-cadherin and excess p53 and/or the pro differentiation roles for deregulated p21 expression [outlined above] (*Di Cunto et al., 1998; Topley et al., 1999*).

Additionally, hyperproliferation marker K6α was now expressed strongly in *HK1.ras-K14creP.Δ3β-cat*$^{flx/wt}$ papillomas [Fig 5.17A & B] but again supporting a diminished yet increasing influence this K6 expression was patchy and these papillomas seem to be lacking the basal layer expression typically expressed in *HK1.ras* papilloma [Fig 5.17C & D]. Taken together, these results indicate that *HK1.ras-K14creP.Δ3β-cat*$^{flx/wt}$ papillomas were similar to typical *HK1.ras* papillomas possibly with some nuanced changes in the nature of the tumour due to Δ3β-catenin expression e.g. the patchy K6 expression could be due to excess p53/p21 reducing the overall proliferation leading to smaller tumour sizes or roles of alternate TSGs such as p63 or p73 [below chapter6]; whilst this lesser E-cadherin expression would suggest lesser adhesions and thus less cell-cell rigidity to facilitate tumour formation.

Returning to the theme that these papillomas appeared in full size mice, suggesting a lack of spontaneous cre leakage, coupled to a short delay in RU486 treatment it was speculated that p53 and p21 expression may have been delayed also and this aided the commitment to form papillomas. Unfortunately, this cannot be fully addressed as by the time of biopsy the

accompanying hyperplastic portion of these ears exhibit strong p53 /p21 expression similar to that expressed in *HK1.ras-K14creP.Δ3β-cat*$^{flx/wt}$ papillomas and also observed in *HK1.ras* control papillomas [Fig. 5.18 & 5.19], which adds another factor that confirms the benign nature of these tumours.

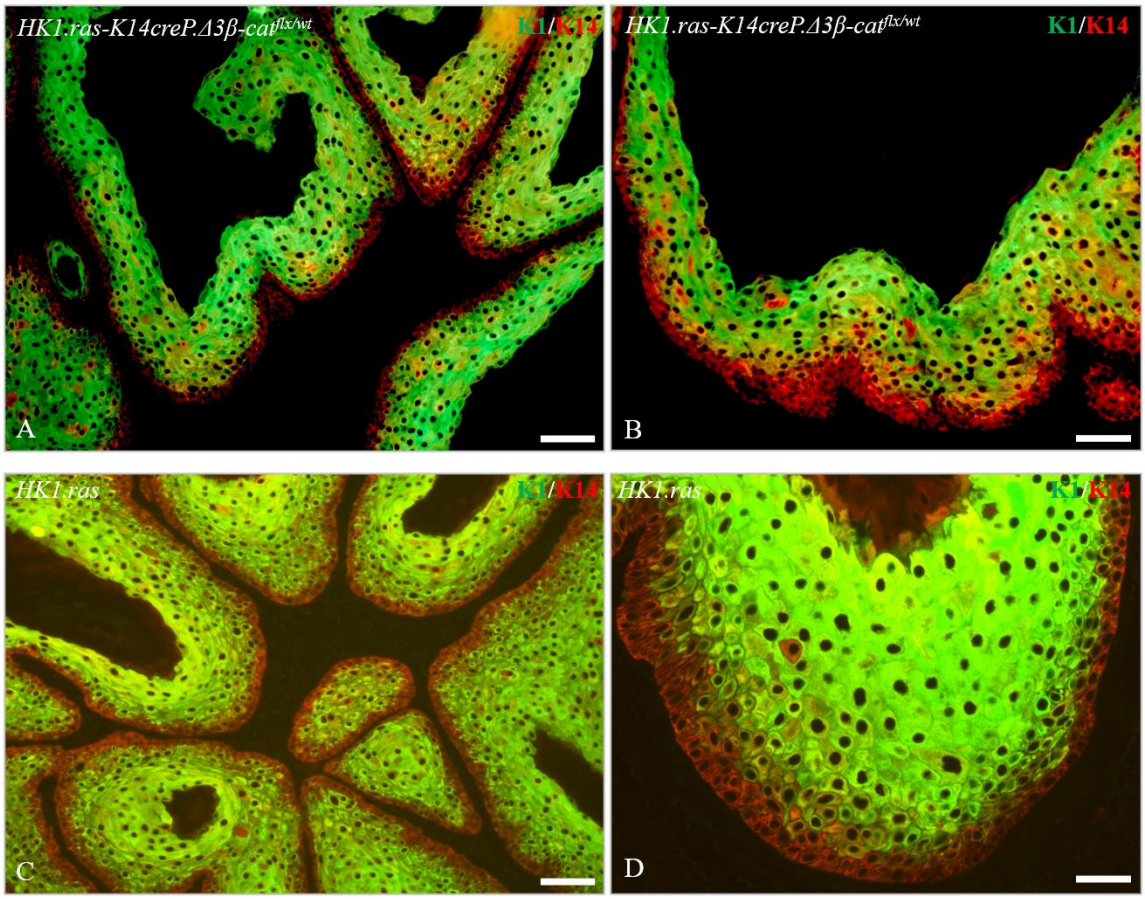

Figure 5. 16: Analysis of K1 expression in *HK1.ras-K14creP.Δ3β-cat*$^{flx/wt}$ and *HK1.ras* littermate papillomas.

[A & B] Again both *HK1.ras-K14creP.Δ3β-cat*$^{flx/wt}$ papillomas show strong and relatively normal K1 expression in supra-basal layers with a more expended basal layer in [B] and possibly a more ragged basal/supra-basal interaction compared to [C & D] the typical *HK1.ras* littermate papillomas with their ordered differentiation and smooth basal/supra-basal interactions. Scale bars: A&C:100µm; C&D: 50µm

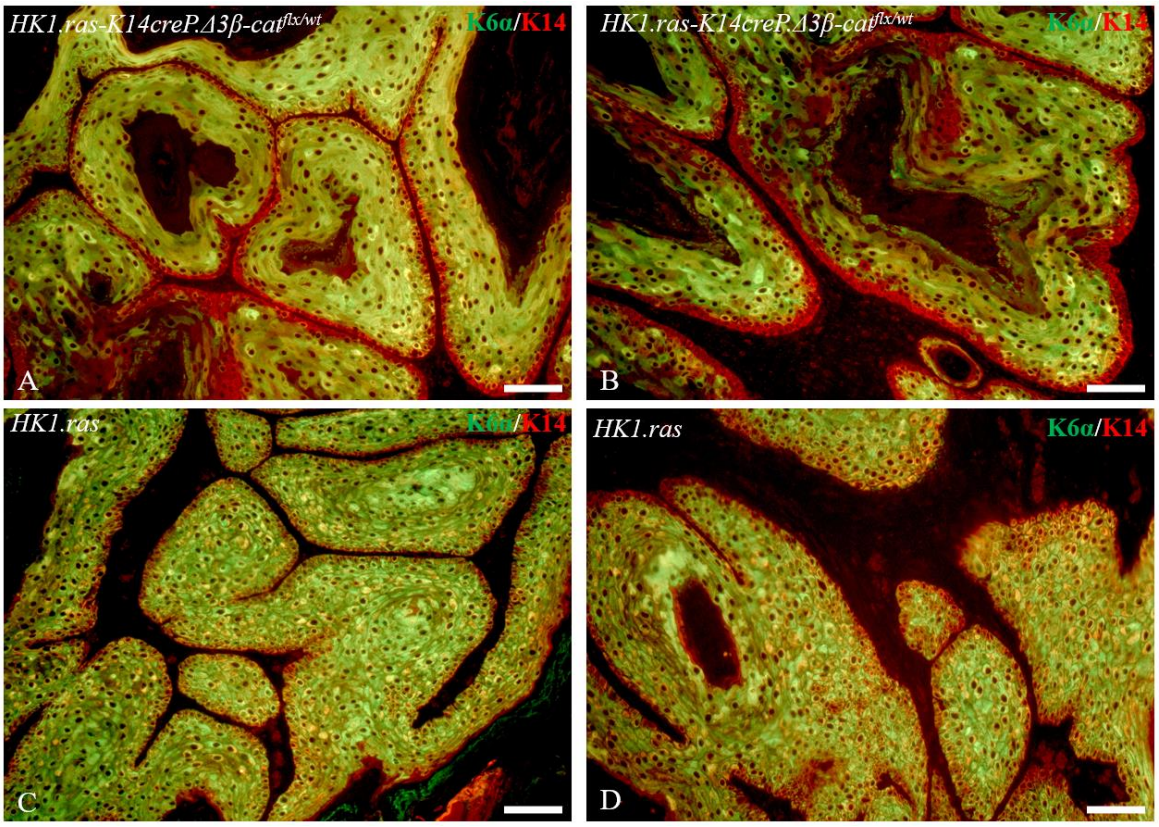

Figure 5. 17: Analysis of K6α expression in *HK1.ras-K14creP.Δ3β-cat*$^{flx/wt}$ and *HK1.ras* papillomas.

Both [A] and to a lesser extent [B] *HK1.ras-K14creP.Δ3β-cat*$^{flx/wt}$ papillomas show strong if patchy K6α expression in supra-basal layers but still oddly lacking in basal layers particularly in [B] with a more expanded basal layer. [C & D] Typical *HK1.ras* littermate papillomas shows strong expression in both supra-basal and basal layers; although D exhibits less basal layer K6α which can indicate a more aggressive papilloma consistent with the age and size of this specific littermate papilloma or occasional batch to batch differences in the polyclonal antibody. Scale bars: A&C: 100μm; C&D: 75μm

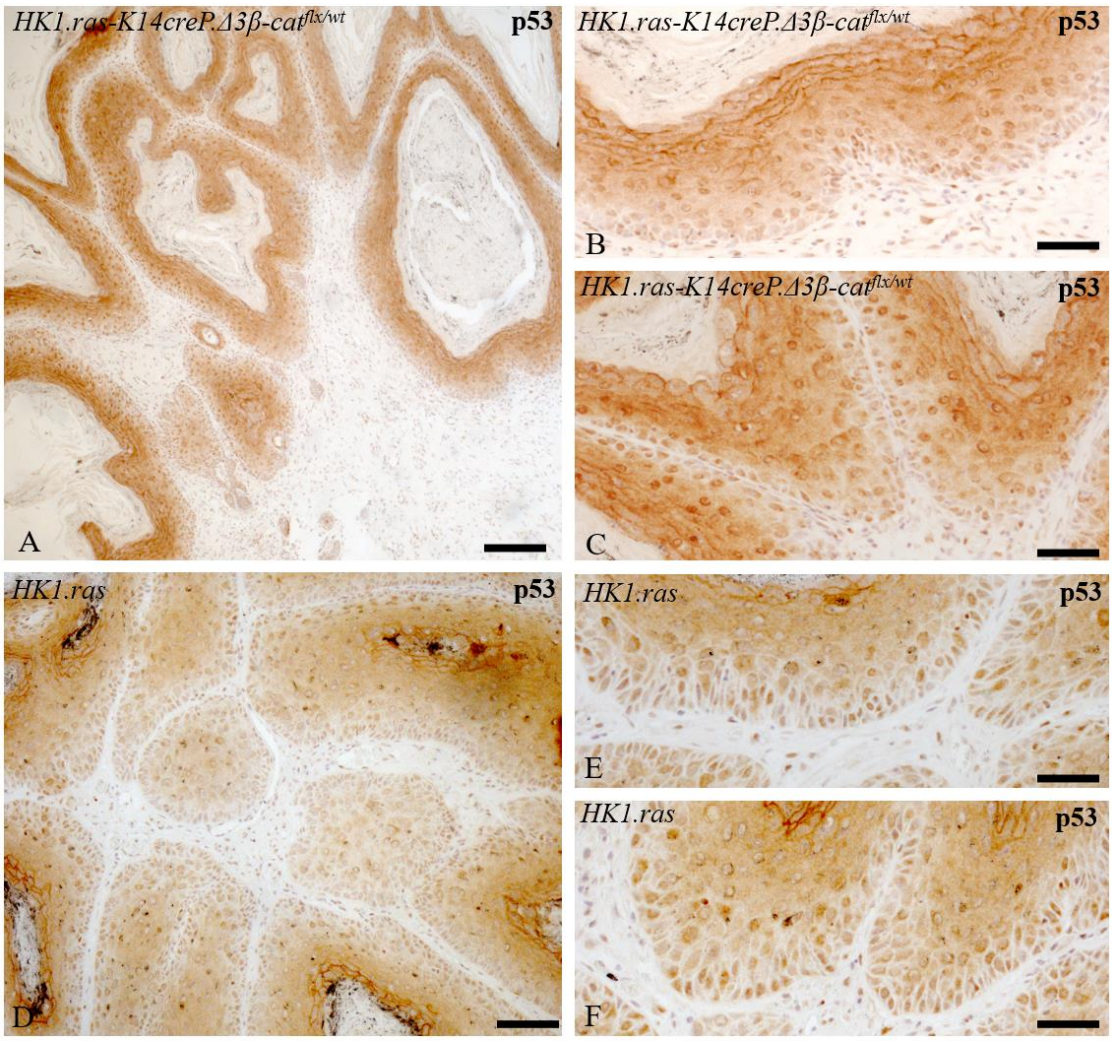

Figure 5. 18: Analysis of p53 expression in *HK1.ras-K14creP.Δ3β-cat*$^{flx/wt}$ and *HK1.ras* littermate papillomas.

[A] *HK1.ras-K14creP.Δ3β-cat*$^{flx/wt}$ papilloma exhibits the typical p53 expression observed in benign tumours with [B & C] an all over strong and nuclear expression of p53 in basal layer keratinocytes at higher magnification. [D-F] *HK1.ras* papillomas exhibit an identical p53 expression profile. Scale bars: A:200µm; D: 150µm B, C, E & F: 50µm.

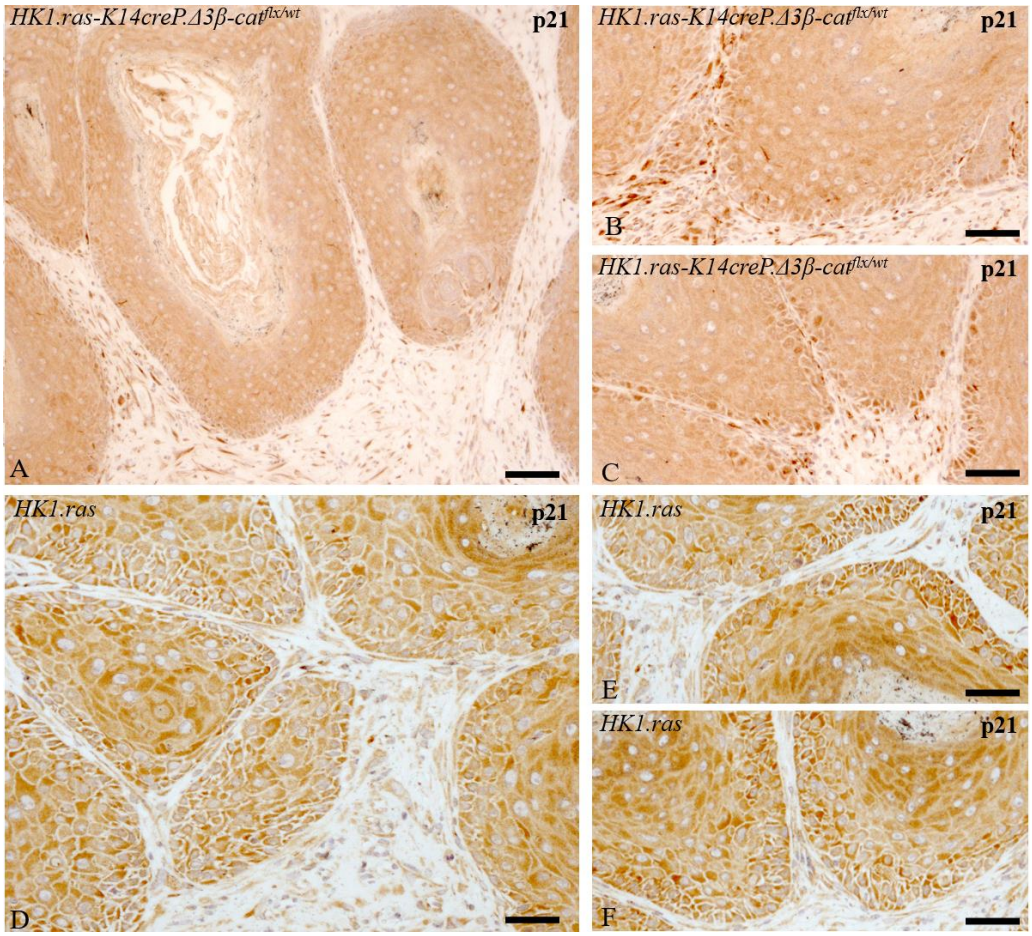

Figure 5. 19: Analysis of p21 expression in *HK1.ras-K14creP.Δ3β-cat*$^{flx/wt}$ and *HK1.ras* littermate papillomas.

[A] *HK1.ras-K14creP.Δ3β-cat*$^{flx/wt}$ papilloma exhibits p21 expression in all layers with [B & C] exhibiting a uniform cytoplasmic expression together with nuclear p21 expression in basal layer keratinocytes. [D-F] *HK1.ras* papillomas exhibit a similar p21 expression profile but with less numbers of nuclear positive basal keratinocytes, typical of these papillomas. Scale bars: A & D: 100 µm; B, C, E & F: 50µm.

Collectively, the results generated from the *HK1.ras-K14creP.Δ3β-cat*$^{flx/wt}$ cohort indicate that Δ3β-catenin activation in the epidermis induces protective responses against tumourigenesis highlighted by early expression of tumour suppresser genes [p53/p21] and confused differentiation with seemingly strengthened cell-cell adhesion. Additionally, the only two papillomas formed in *HK1.ras-K14creP.Δ3β-cat*$^{flx/wt}$ mice were benign and smaller than typical *HK1.ras* with no signs of invasiveness, indicating that *Δ3β-catenin* activation still resulted in protective responses against tumorigenesis at the benign tumour stage in these bi-genic mice compared to tri-genic *HK1.ras/fos-K14creP.Δ5PTEN*$^{flx/flx}$ mice; until p53 and later p21 were lost.

Thus, the findings of this cohort indicated that the most logical step to follow up the results of the *HK1.ras-K14creP.Δ3β-cat*$^{flx/wt}$ cohort was to induce conditional *p53* knockout followed by *p21* knockout in an attempt to provide a better understanding of the protective mechanism observed with Δ3β-catenin activation against tumourigenesis**.**

Table 5. 2: Summary of rare HK1.ras-K14creP.Δ3β-cat$^{flx/wt}$ papillomas phentypes

Genotype analysed	[N]	Analysed for expression of	Data summary
HK1.ras papilloma	90	β-catenin, E-cadherin, K1, K6α, p53 and p21 expressions	-Control papilloma size 7-10 mm diameter -Exhibiting membranous β-catenin/E-cadherin expression mainly in the supra-basal layers with only sporadic nuclear/cytoplasmic β-catenin expression in basal layers -ordered terminal differentiation indicated by suprabasal layer K1 and expression in K6α in both supra and basal layers due to HK1.ras activation stress signal -nuclear basal layer p53/p21 expression halts malignant conversion
HK1.ras-K14creP.Δ3β-cat$^{flx/wt}$ [papillomas]	2	β-catenin, E-cadherin, K1, K6α, p53 and p21 expressions	-papillomma size 3-4 mm diameter -Exhibiting Increased cytoplasmic/nuclear basal layer β-catenin with increased membranous basal layer β-catenin/E-cadherin due to Δ3β-catenin -Ordered terminal differentiation indicated by suprabasal layer K1 and expressing K6α mainly in suprabasal layer - Nuclear basal layer expression of p53/p21 halting malignant conversion
Conclusion: in the rare occasions when Δ3β-catenin activation was delayed [i.e. no cre leak], 2 individual *HK1.ras-K14creP.Δ3β-cat*$^{flx/wt}$ *mice* developed small papillomas vs. typical 100% of *HK1.ras* mice presumably due to delay in compensatory TSGs expression [p53/p21] to Δ3β-catenin that blocked papillomatogenesis in most cases; however here, that affect only began post RU486 treatment which restricted papilloma further development in terms of size via elevated TSGs expressions and strengthen adherence junctions in basal layers to prevent malignant conversion.			

5.3 SUMMARY

A literature search of previous studies showed the importance of β-catenin to the epidermis and specifically the regulation of hair follicle formation (*Gat et al., 1998; Chan et al., 1999 Van Mater et al., 2003 Grigoryan et al., 2008*). However, these transgenic mouse studies lack the understanding of β-catenin activation roles in SCCs. Despise its clear relevance observed in human SCC in conjunction with notch pathway deregulation (*Doglioni et al., 2003; Koch et al., 2007; Krishnamurthy et al., 2018*), to date it is odd that no mouse studies have been successfully established that employ these activated β-catenin transgenic mice to model β-catenin over expression in carcinogenesis. Perhaps the outcome of activating β-catenin in carcinogenesis was taken for granted as it would only facilitate tumour invasiveness and metastasis due the involvement of Wnt/β-catenin gain of function in the advancement of several types of carcinomas (*Morin, 1999; Grigoryan et al., 2008*). Indeed, only one study reports the essential roles for β-catenin as knockouts employed in classical two-stage DMBA/TPA chemical carcinogenesis experiments revealed a lack of tumours showing the integral requirement for β-catenin expression for tumorigenesis (*Malanchi et al., 2008*). Additionally, that result observed in *HK1.ras/fos-K14creP.Δ5PTEN*$^{flx/flx}$ mouse model clearly implicated endogenous β-catenin roles on tumorigenesis [See chapter 3].

As shown in the results section, in repeat experiments over 12-14 month period, almost all *HK1.ras-K14creP.Δ3β-cat*$^{flx/wt}$ mice lacked papilloma formation yet still exhibited the *K14creP.Δ3β-cat*$^{flx/wt}$ phenotypes, but with increased levels of severity in terms of increased scruffiness, enlarged extremities, effect on body size and increased hyperkeratosis in back skin. This was also consistent histologically as the hair follicle abnormalities such as formation of more cysts and hair follicle tumours were clearly more severe with increased interfollicular hyperplasia accompanied by abnormal and confused differentiation compared to both *K14creP.Δ3β-cat*$^{flx/wt}$ and *HK1.ras* alone.

The induced interfollicular hyperplasia in *HK1.ras-K14creP.Δ3β-cat*$^{flx/wt}$ could be attributed to *HK1.ras* activation as ras activation affects a plethora of other signalling pathways such as MAPK which consequently activate c-fos and PI3K which consequently activate p-AKT resulting in activating Wnt/β-catenin via de-activating GSK3- β. However, the IFE hyperplasia invoked in *HK1.ras-K14creP.Δ3β-cat*$^{flx/wt}$ was clearly less than the typical *HK1.ras*

hyperplasia due to the early elevated expressions of p53/p21, that is normally not induced in *HK1.ras* hyperplasia.

This affect was then prompted via *Δ3β-catenin,* which given its established role in carcinogenesis was expected to induce possibly accelerated papillomatogenesis as seen in *HK1.ras-K14creP.Δ5PTEN*$^{flx/flx}$ *(Yao et al., 2006*) or even SCCs as observed in *HK1.ras/fos-K14creP.Δ5PTEN*$^{flx/flx}$ (*Macdonald et al., 2014*). However, *HK1.ras-K14creP.Δ3β-cat*$^{flx/wt}$ showed only more aggressive phenotype of Δ3β-catenin with only a minimal affect in term of tumorigenesis, which indicates that Δ3β-catenin triggered an epidermal protective response against tumorigenesis. This is an unpreceded result as 100% of *HK1.ras* mice [n=80] produce benign papillomas within 6-8 weeks post ear tag (*Greenhalgh et al., 1993*); where as *HK1.ras-K14creP.Δ3β-cat*$^{flx/wt}$ remained tumour free for up to 16 weeks when the β-catenin phenotypes necessitated the animals to be culled.

This intriguing result does not fit the current dogma in the literature (*Morin, 1999; Grigoryan et al., 2008*) as conditionally knocking out β-catenin resulted in either blockage or regression of DMBA/TPA tumours, which again indicate that β-catenin expression was a necessity for the development of SCCs *(Malanchi et al., 2008; Grigoryan et al., 2008)*, and this is consistent with the result observed in *HK1.ras/fos.Δ5PTEN*, where nuclear localization of β-catenin facilitates tumorigenesis and invasiveness [see chapter 3] However, instead these data suggest that β-catenin overexpression in co-operation with ras activation induced early, protective responses against tumour formation possibly similar to the responses observed in *HK1.fos-K14creP.Δ5PTEN*$^{flx/flx}$ which resulted in the formation of benign KA (*Yao et al., 2008*) and a lack of malignant conversion in *HK1.ras.Δ5PTEN* mice (*Yao et al., 2006*).

To explore these possibilities, initially β-catenin and E-cadherin levels were assessed first to observe possible changes in cell-cell adhesions in *HK1.ras-K14creP.Δ3β-cat*$^{flx/wt}$ mice. β-catenin and E-cadherin showed identical expression with increased membranous expression and nuclear expression of β-catenin in basal layers as expected due to Δ3β-catenin activation. This suggests an increase in cell-cell adhesion signalling which possibly resulted in preventing formation of papillomas in a similar if later effect as seen in *HK1.fos-K14creP.Δ5PTEN*$^{flx/flx}$ KA (*Yao et al., 2008*) [see Chapter 3]. This also indicated that the cytoplasmic pool of β-catenin was not overtaken by Wnt signalling as seen in *HK1.ras/fos-K14creP.Δ5PTEN*$^{flx/flx}$ and rather showed increased expression in the basal layer with nuclear localization of β-catenin as

well. Here again in *HK1.ras-K14creP.Δ3β-cat*$^{flx/wt}$, cytoplasmic E-cadherin/β-catenin interaction was acting as a sponge and providing further regulation of β-catenin levels (*Huels et al., 2015*), that indeed seemed to be strengthened by Δ3β-catenin activation as observed in colon carcinogenesis (*Huels et al., 2015*) .

The early differentiation marker K1 showed a confused and patchy expression indicating that *HK1.ras-K14creP.Δ3β-cat*$^{flx/wt}$ co-operation disturbed the epidermal terminal differentiation. This patchy K1 expression could be attributed to excess expression of p21 in the upper IFE layers which may inhibit the latter stages of differentiation (*Di Cunto et al., 1998*), however basal layer expression of p21 with p53 accelerated epidermal terminal differentiation as seen in *HK1.fos-K14creP.Δ5PTEN*$^{flx/flx}$ KA (*Topley et al., 1999*; *Yao et al., 2008*)[see Chapter 3] and a recent study in ROCK-mediated β-catenin activation (*Masre et al., 2020*).

The disturbed epidermal differentiation could also be attributed to β-catenin roles in regulating epidermal pluripotent stem cells that are needed for epidermal terminal differentiation and hair follicle differentiation (*Watt and Collins, 2008*). As increased Wnt/β-catenin signalling affect the correct control of the stem cell niche, leading to continuously altering the differentiation programme fate resulting in possibly confused transit amplifying cells evident by the formation of K1 positive interfollicular proliferative dead end cysts which would also divert keratinocytes away from papilloma formation.

However, despite this aberrant expression of K1, the hyperproliferation marker K6α was completely absent from the epidermis, whereas usually it is strongly expressed in *HK1.ras* hyperplastic controls. One possible mechanism for this aberrant expression is a study that concluded the ability of constitutive activation of β-catenin to remodel the developed mouse dermis into a neonatal state (*Collins et al., 2011*). In neonates the epidermis is naturally hyperplastic but lacks k6 expression and remains confine to HF (*Rothnagel et al.,1999***),** similar to Δ3β-catenin activation phenotype.

Constitutive β-catenin activation [*Δ3β-catenin*] induces formation of new hair follicles observed in *K14creP.Δ3β-cat*$^{flx/wt}$ and *HK1.ras-K14creP.Δ3β-cat*$^{flx/wt}$, which normally only takes place in the embryonic and neonatal stage of life, (*Närhi et al., 2008; Grigoryan et al., 2008*) this affect leads to inducing new dermal proliferation similar to neonatal mice which deregulate the epidermal-dermis interaction needed to maintain interfollicular terminal differentiation (*Watt and Collins, 2008).* Although, Δ3β-*catenin* activation increased HF

placode formation, most of them fail to develop normal hair (*Närhi et al., et al.,2008*), hence why these mice suffer from alopecia. This perhaps could be attributed to elevated expression of p53/p21 in HFs which are normally involved in regulating HF differentiation (*Song and Lambert, 1999; Botchkarev et al., 2001*) as increased p53/p21 induces apoptosis to halt the excess HF proliferation leading to a general regression in HF development, which might be contributing to the lack of IFE tumours but not HF tumours.

Further these changes in K6α expression may also derive from the increase in adhesion junctions which in turn alters the hyperproliferation signals derived from cell-cell interactions that are typically disrupted in wounding. These are normally essential for cell division and keratinocyte migration and thus disruption of the filament network [intermediate and actinomycin] would affect movement that is carried out by the underlying cytoskeletal network that regulates mechanical tension through adhesion junctions and hemidesmosomes (*Masre et al., 2020; Samuel 2011*). Hence these data suggest that β-catenin overcomes the K6 responses typical of ras activation via increased E-cadherin, except in the possible aetiology of the two outlying papillomas where E-cadherin may have been less or delayed in their basal layers (*Takeichi, 1991; Young et al., 2003)*

This also brings the status of p53/p21 expression into question, because the increased cell-cell adhesions are also associated with elevated p53/p21 expression (*Wu et al., 1997*). The expression of p53/p21 confirmed this hypothesis showing strong expression was triggered via Δ3β-catenin as seen in *K14creP.Δ3β-cat*$^{flx/wt}$ mice thus overexpression would inhibit papilloma formation. Also, this result is constant with the elevation seen in KA due to endogenous β-catenin activation via inactivated GSK3-β/p-AKT activation. Again in *HK1.ras-K14creP.Δ3β-cat*$^{flx/wt}$ p53/p21 expression could possibly explain the absence of the hyperproliferation marker K6 from the IFE and the confused K1 expression seen in *HK1.ras-K14creP.Δ3β-cat*$^{flx/wt}$ mice, suggesting a disfunction in epidermal homeostasis due to ras and β-catenin cooperated activation. In contrast *HK1.ras* hyperplasia showed only weak p53/p21 expression until overt papilloma formation with normal K1 expression and strong K6 expression, in addition to β-catenin/E-cadherin showing similar membranous expression mainly in supra basal layer and to a lesser extent in basal layer. This indicates that the lack of basal layer p53/p21 in *HK1.ras* hyperplasia correlates with the reduced cell-cell adhesion [β-catenin/E-cadherin] which results in facilitating papilloma formation, unlike the early increased basal layer p53/p21 expression

in *HK1.ras-K14creP.Δ3β-cat*$^{flx/wt}$ corelating with increased cell-cell adhesion and halting tumour progression but also disturbing terminal differentiation as observed by K1 expression.

All of these data suggest that *K14creP.Δ3β-cat*$^{flx/wt}$ in co-operation with *HK1.ras* triggered early p53/p21 protective responses due to HK1.ras and Wnt signalling induced proliferation. This resulted in a confused and abnormal epidermal differentiation, as basal layer expression of p53/p21 halted the induced proliferation resulting in reduced IFE hyperplasia compared to HK1.ras, whilst the increased expression of p21 in the upper layers of the IFE distributed the terminal epidermal differentiation signalling evident by patchy expression of K1 but also resulted in strengthening cell-cell adhesion signalling due to β-catenin/E-cadherin elevated expression correlating with p53/p21 expression and preventing tumour development.

For the two outlier mice *HK1.ras-K14creP.Δ3β-cat*$^{flx/wt}$ that developed benign papillomas, these papillomas grossly and histologically looked smaller and less aggressive compared to typical *HK1.ras*^{1205} papillomas , which still contrary to the widely assumed notion that overexpression of β-catenin/Wnt signalling leads to more aggressive tumours and possibly malignant progression. This suggests that even in the rare event when the papilloma was formed in *HK1.ras-K14creP.Δ3β-cat*$^{flx/wt}$ strains, the papilloma could not progress to more aggressive tumour and possibly with more time would regress, which challenges the findings represented earlier in *HK1.ras/fos-K14creP.Δ5PTEN*$^{flx/flx}$ strains where nuclear localization of endogenous β-catenin seemed to be facilitating malignant progression. The mice also looked bigger and less phenotypic than the majority of *HK1.ras-K14creP.Δ3β-cat*$^{flx/wt}$ that did not develop the tumours. This indicates that probably the cre switch did not leak early [neonatal or juvenile] and only was activated post Ru-486 treatment, which gave *HK1.ras 1205* enough time to develop the distant papilloma before *Δ3β-catenin* activation.

The analysis of these *HK1.ras-K14creP.Δ3β-cat*$^{flx/wt}$ tumours, although showed increased nuclear β-catenin localization, it still maintained a strong membranous expression in the basal layer. This expression was also mainly mimicked by E-cadherin, which indicate that cell-cell adhesion was still intact despite β-catenin nuclear localization, similar to the expression profile in *HK1.ras/fos-K14creP.Δ5PTEN*$^{flx/flx}$ [see Chapter 3] and this would help prevent malignant progression. This suggests that even with delayed activation of *Δ3β-catenin* after initiation of

papillomatogenesis, unlike tri-genic *HK1.ras/fos.Δ5PTEN*, here nuclear localization of β-catenin did not facilitate invasion but as outlined above it could be argued in these two examples that it might hindered the tumourigenesis progression. However, its delay due to lack of cre leakage and in RU486 treatment, may have facilitated the commitment to papilloma formation as indicated by the differentiation marker K1 and K6 expression data being similar to *HK1.ras* expression and the speculation that p53 and p21 would be delayed and if expressed would be suprabasal also resulting in data similar to typical ras papillomatogenesis.

Lending further support to this idea it was noted that some strands of papilloma basal layers appeared to possess less membranous E-cadherin. This E-cadherin expression, therefore again suggest that a delay in the responses to β-catenin deregulation in these normal sized score 0 mice may have given less numbers of adherence junctions in the early basal layers of a wounded tagged ear, which allowed papillomas to start and is reflected here in the remaining strands of supra-basal E-cadherin in the *HK1.ras-K14creP.Δ3β-cat*$^{flx/wt}$ papillomas. This idea will be tested in future studies involving recently imported E-cadherin floxed mice.

The early differentiation marker K1 showed normal expression confined to the suprabasal layer as is always observed in *HK1.ras 1205* benign papillomas. However, the hyperproliferation marker K6 showed strong expression as well but interestingly was lacking in the basal layer, A finding that seems to be exclusive to *HK1.ras-K14creP.Δ3β-cat*$^{flx/wt}$ papilloma and is not seen in *HK1.ras* controls. This indicates that these tumours are benign but could Not be the same type of papilloma in *HK1.ras*^{1205} control as eventually *Δ3β-catenin* expression induces the responses to inhibit papilloma growth [indicated by patchy K6 expression]. This is also similar to *HK1.fos-K14creP.Δ5PTEN*$^{flx/flx}$ co-operation where papilloma were expected to be formed as observed previously in *HK1.ras/fos-K14creP.Δ5PTEN*$^{flx/flx}$ co-operation, however endogenous localization of β-catenin was delayed as it was a consequence of activating AKT resulting in diverting papillomatogenesis into KA aetiology.

The tumour suppresser genes[TSG] p53/p21 were both strongly expressed confirming the benign nature of these tumours and also correlating with strong cell-cell adhesion observed in the basal layer. This correlation between TSGs expression and cell-cell adhesion seems to be the key to the protective responses induced in response to β-catenin nuclear localization. Thus

in the next chapter a cohort of conditional knockout of p53 in *HK1.ras-K14creP.Δ3β-cat*$^{flx/wt}$ would be analysed to provide a better understanding of these results.

Chapter 6: Conditional loss of p53 in β-catenin transgenic mouse skin carcinogenesis

6.1 Introduction

The intriguing finding that in *HK1.ras-K14creP.Δ3β-cat*$^{flx/wt}$ cohorts responses to β-catenin activation appeared to block papilloma formation required further investigation to provide a better understanding in this genotype. The tumour suppresser genes p53 and p21 seemed to play a major role in these findings, highlighted by their immediate and strong expression triggered via *Δ3β-catenin* activation in both *HK1.ras-K14creP.Δ3β-cat*$^{flx/wt}$ and *K14creP.Δ3β-cat*$^{flx/wt}$ mice. This induction of p53 and p21expression appeared to only affect the IFE phenotypes produced by *ras*^{Ha} activation, as the follicular component remained unaffected; and indeed a sub-population of *HK1.ras-K14creP.Δ3β-cat*$^{flx/wt}$ mice [those designated score 2] possessed a significant increase in the degree of follicular abnormalities, yet their IFE possessed only mild hyperplasia.

That this inhibition of papilloma formation was not due to a technical feature such as inhibition of the HK1 promoter via *Δ3β-catenin* expression was excluded given that the neonatal *HK1.ras-K14creP.Δ3β-cat*$^{flx/wt}$ pups exhibited the standard wrinkled skin; juveniles exhibited an increased keratosis; and in adults, this increased keratosis compared to *K14creP.Δ3β-cat*$^{flx/wt}$ cohorts was induced by *HK1.ras*-specific expression in the IFE hyperplasia.

That this inhibition appeared to centre on p53 and p21 expression was also supported by previous findings at each stage of carcinogenesis in the HK1 model. Firstly in *HK1.ras/ROCK* co-operation (*Masre et al., 2020*), endogenous β-catenin expression also appeared in the basal layers, mediated by ROCK2-induced AKT inactivation of GSK3β, to induced p53 and p21 resulting in a block on papilloma formation. Secondly at the benign stages, the potency of this p53/p21 response to the dangers of anomalous β-catenin expression was clearly displayed in *HK1.fos-K14creP.Δ5PTEN*$^{flx/flx}$ mice, where this time PTEN-mediated AKT expression initially co-operated with *HK1.fos* to elicit early papillomas but again the build-up of p-GSK3β inactivation and an increasing degree of nuclear β-catenin [Chapter 3; Fig. 3.3] triggered a massive p53/p21 expression response diverting papilloma progression into massive differentiation, tumour keratosis and a KA outcome (*Yao et al., 2008*). Of note, this result is consistent with the significant differentiation and keratosis observed in the direct investigations of *HK1.fos/K14.Δ3β-cat*^{het}*.Δ5PTEN*$^{flx/flx}$ in Chapter 7. This differentiation may prevent tumour formation driven by β-catenin (*Clevers and Nussse, 2012*), given that the

regression phase of human KA aetiology was associated with β-catenin/Wnt down regulation (*Zito et al., 2014*).

At the malignant conversion stage, these links between ras/β-catenin and p53/p21 are again observed as here the addition of activated ras to *HK1.fos-K14creP.Δ5PTEN*$^{flx/flx}$ tumourigenesis resulted in the immediate expression of p53/p21 in *HK1.ras/fos-K14creP.Δ5PTEN*$^{flx/flx}$ hyperplasia (*Macdonald et al., 2014*), but as p53 became lost in papillomas this was paralleled by increased basal layer β-catenin leading to malignant conversion [Chapter 3; Fig. 3.3]. Moreover, later following p21 loss, nuclear β-catenin expression increased but became less membranous and this potential loss of cell-cell adherence coupled to increased Wnt deregulation via nuclear β-catenin expression probably contributes to the malignant progression of *HK1.ras/fos-K14creP.Δ5PTEN*$^{flx/flx}$ wdSCCs to pdSCCs (*Alyamani et al.,* manuscript in preparation).

Thus, all these data suggest that as p53 and p21 are common features of cutaneous SCC inhibition (*Brash et al., 1991; Topley et al., 1999; Macdonald et al., 2014*), their expression maybe targeted to specific responses mediated by Ras and/or β-catenin signalling deregulation. Similar p53/p21 responses to pGSK3β/β-catenin expression have been documented in K-Ras colon carcinogenesis; where following APC loss and failure of the pGSK3β complex to ubiquitinate and remove β-catenin (*Behrens et al., 1996; 1998; Ikeda et al., 1998*), coupled to potential failures of E-cadherin to act as a sink (*Huels et al., 2015*) the increased nuclear β-catenin again induced transcriptionally active p53 (*Damalas et al., 2001; Ghosh and Altieri, 2005; Clevers and Nussse, 2012*). Thus, it appears that in both models an elevated p53 attempts to provide protection against additional mutations, and an increased p21-associated differentiation response [below (*Topley et al.,1999*)] avoids excessive p53-induced apoptosis to maintain the paramount barrier function of skin (*Calautti et al., 2005; Yao et al., 2008; Macdonald et al., 2014*) also important in the function of colon epithelia.

Therefore, introducing p53 conditional knockout into *HK1.ras-K14creP.Δ3β-cat*$^{flx/wt}$ mice to generate the *HK1.ras-K14creP.Δ3β-cat*$^{flx/wt}$*.p53*$^{flx/flx}$ genotype was the most sensible approach to understand p53 roles in this mechanism to both confirm the protective response and assess if p53 loss influenced papilloma formation and then co-operated with Δ3β-catenin to induce malignant conversion, as seen in *HK1.ras/fos-K14creP.Δ5PTEN*$^{flx/flx\ flx}$ mice. This was a logical step, as previously classic DMBA/TPA chemical carcinogenesis studies employing

generic p53 knockout mice showed a significant increase in SCCs derived from DMBA-induced ras activation and TPA-mediated fos promotion (*Kemp et al., 1993*); whilst in reverse β-catenin KO inhibited two-stage DMBA/TPA carcinogenesis (*Malanchi, et al., 2008; Grigoryan et al., 2008*).

It should be pointed out that another less logical and to date a completely paradoxical result was seen via employment of generic p53 knockout mice in this HK1 model (*Donehower et al., 1992*). Here in *HK1.ras*; *HK1.fos* and *HK1.TGFα* mice loss of p53 function e.g. *HK1.gene.p53*$^{fl/flxx}$ co-operation, resulted in a lack of tumours similar to that observed in *HK1.ras-K14creP.Δ3β-cat*$^{flx/wt}$ mice; despite the loss of p53 protection. Whereas all wild type and heterozygous p53 progeny exhibited the standard papillomatogenesis of their parents (*Greenhalgh et al., 1996*). These data demonstrate the complexity of these signalling systems and here in this current study, generation of the control/breeder *HK1.ras-K14.p53*$^{flx/flx}$ genotypes showed that constitutive inducible p53 loss again provided the reverse paradoxical outcome expected of p53 roles; namely the inhibition of papilloma formation similar to the reverse outcome and lack of papillomas expected of ras^{Ha}/β-catenin co-operation in *HK1.ras-K14creP.Δ3β-cat*$^{flx/wt}$ mice.

Thus, development of *HK1.ras-K14creP.Δ3β-cat*$^{flx/wt}$*.p53*$^{flx/flx}$ cohorts served to answer these paradoxical results observed in this study and in earlier *HK1.ras/fos* mouse models. One of which was to understand the lack of papillomas in *HK1.ras-K14creP.Δ3β-cat*$^{flx/wt}$ mice and how conditional loss of p53 [and/or p21] could change these results. The other purpose was to understand β-catenin roles in the paradoxical result reported previously in *HK1.ras-K14.p53*$^{flx/flx}$ co-operation and assess whether introduction of *Δ3β-catenin* activation in *HK1.ras-K14creP.Δ3β-cat*$^{flx/wt}$ *.p53*$^{flx/flx}$ cohorts would overcome the paradoxical block of *HK1.ras/p53*^{flx} tumour formation? For instance, was *β-catenin* signalling the key to the block of ras^{Ha} tumours in these early *HK1.ras-K14.p53*$^{flx/flx}$ co-operation studies e.g., via increased p21. Hence was compensatory p53 [or p21] the key to blocking *HK1.ras-K14creP.Δ3β-cat*$^{flx/wt}$ papillomas? Once again, the results raised more questions than answers but demonstrated the close links between β-catenin and p53 expression in terms of the final phenotypes produced.

6.2 Conditional loss of p53 paradoxically *reduces* the severity of *Δ3β-catenin* phenotypes without IFE tumour development.

The same *K14.creP/loxP* gene switch system was used to induce conditional p53 knockout [Fig. 6.1A] via deletion of *p53* exons 2 to exon 10 [*K14creP.p53*$^{flx/flx}$] (*Jonkers et al., 2001*). Topical application of RU486 thus gives the non-functional *Δp53* allele [Fig. 6.1B&C]. These mice have been established in house for several years for studies on the paradoxical inhibition of *HK1.ras* papillomas by complete generic p53 knockout (*Greenhalgh et al., 1996*); but without any obvious phenotype. Indeed, consistent with this observation, typically little cre leakage activity was observed in untreated *K14cre.p53*$^{flx/flx}$ skin [Fig. 6.1C; lane 3] and no read through was observed in *K14creP*-negative *Δ3β-cat/p53*$^{flx/flx}$ skin [lane 6]; a result that was considered another possibility for the production of untreated phenotypes in this model but unlikely since no phenotypes were ever observed in [cre negative] *Δ3β-cat*$^{flx/flx}$ or new *Δ3β-cat*$^{flx/flx}$*/p53*$^{flx/flx}$ breeders. However, in both RU486-treated and untreated *K14creP.Δ3β-cat*$^{flx/wt}$*.p53*$^{flx/flx}$ skin, the *Δp53*^{flx} band at 612bp was typically strong in RU486-treated skin [lanes 1 & 2] but also now appeared in untreated *K14creP.Δ3β-cat*$^{flx/wt}$*.p53*$^{flx/flx}$ skin [score 0; lanes 4 & 5] with intriguing consequences.

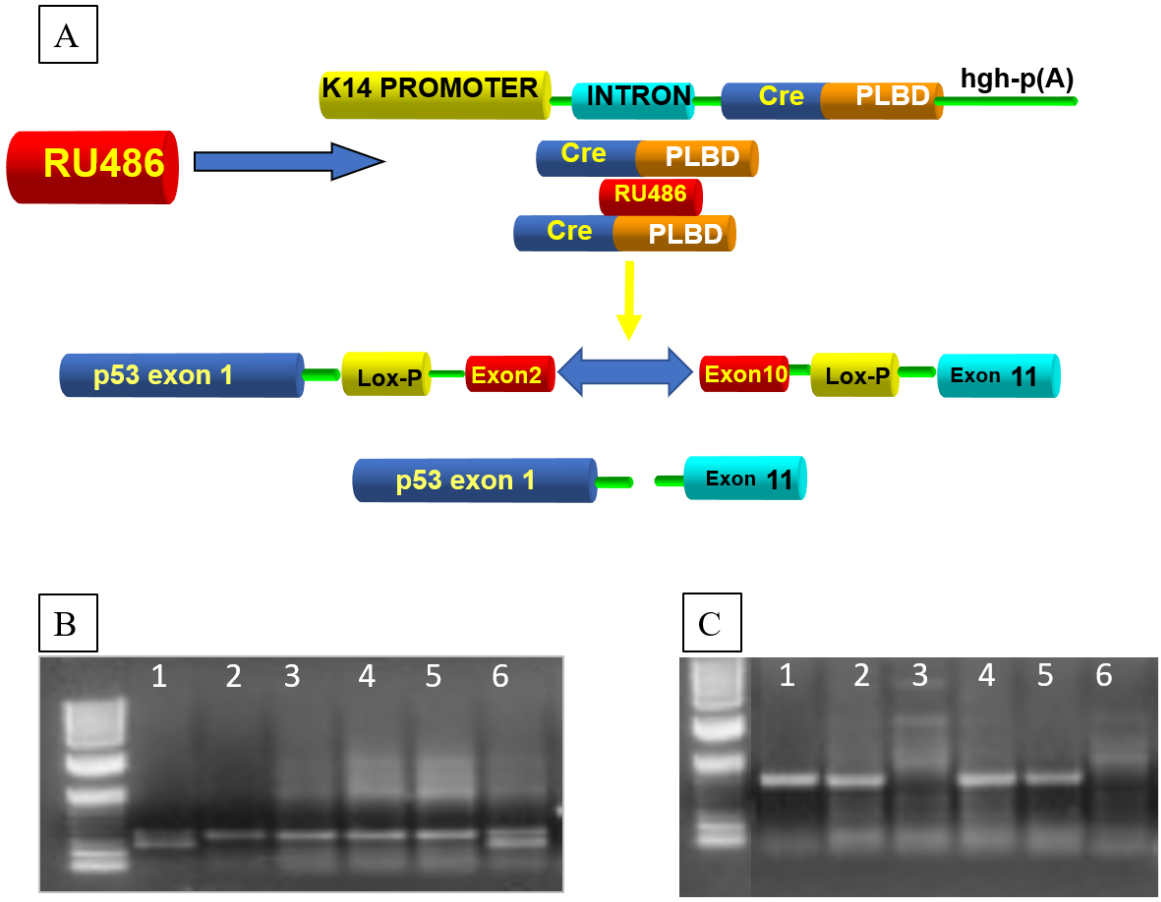

Figure 6. 1: Confirmation of p53 knockout.

[A] Schematic diagram of the RU468-inducible cre/loxP system employs the same keratin K14 promoter-driven cre regulator to achieve ablation of *p53* exons 2-10 in epidermis and hair follicles. [B] PCR analysis employing primers specific for the loxP modified intron 1 of the *Δp53*^{flx} allele shows the *p53*^{wt} band at 431bp [lane 1]; the *p53*$^{flx/flx}$ allele band at 584bp [lanes 2-5] and a doublet indicates *p53*$^{flx/wt}$ heterozygosity [lane 6]. [C] To confirm *K14cre*P activity employing an intron 1 forward and intron 10 reverse primer identifies a *Δp53*^{flx}-specific band at 612bp in RU486-treated *K14creP.Δ3β-cat*$^{flx/wt}$*.p53*$^{flx/flx}$ mice [lanes1-2; 4-5] which is absent in untreated *K14creP.p53*$^{flx/flx}$ RU486 control skin [lane 3] and *K14creP*-negative *Δ3β-cat*$^{flx/wt}$*/p53*^{flx} skin [lane 6].

The first interesting observation was immediately seen in the litters that generated *K14creP.Δ3β-cat*$^{flx/wt}$*.p53*$^{flx/flx}$ mice [Fig.6.2]. The appearance of overt phenotypes typically appeared in *K14creP.Δ3β-cat*$^{flx/wt}$ mice between 16-24d due to cre leakage [above Chapter 4]. Whilst the breeding to create these compound transgenic mice had given typical score 1 phenotypes at the juvenile stage of *K14creP.Δ3β-cat*$^{flx/wt}$ and *K14creP.Δ3β-cat*$^{flx/wt}$*.p53*$^{flx/wt}$ mice, in the first litters to give potential *K14creP.Δ3β-cat*$^{flx/wt}$*.p53*$^{flx/flx}$ it was noticed that there were more score 0 mice than previously observed which lacked the typical *Δ3β-catenin* skin phenotypes. In addition, whilst their size still varied there was a trend towards larger, more normal individuals [Fig. 6.2].

A comparison of typical 23/24day old littermates at the time of tail biopsy clearly shows this delay in the appearance of *Δ3β-catenin* phenotypes [Fig. 6.2A]. A comparison of phenotypes in *K14creP.Δ3β-cat*$^{flx/wt}$*.p53*$^{flx/flx}$ vs. *K14creP.Δ3β-cat*$^{flx/wt}$*.p53*$^{flx/wt}$ siblings showed a generally noticeable reduction in hyperkeratosis of back skin and dishevelled fur, as well as the overall severity of typical *K14creP.Δ3β-cat*$^{flx/wt}$ phenotypes [larger size, smaller feet, normal tails etc]. This inhibition of *Δ3β-catenin* phenotypes persisted in older adults even following treatment with RU486 [Fig. 6.2B], where *K14creP.Δ3β-cat*$^{flx/wt}$*.p53*$^{flx/flx}$ individuals maintained this score 0 phenotype compared to the Score 1 phenotype of a *K14creP.Δ3β-cat*$^{flx/wt}$*.p53*$^{flx/wt}$ heterozygotes. In some instances, this score 0 skin phenotype and larger size was maintained for over 8-10 weeks with only very minor patchy hyperkeratosis compared to increased levels of increasing hyperkeratosis in RU486-treated [score 1] *K14creP.Δ3β-cat*$^{flx/wt}$*.p53*$^{flx/wt}$ siblings [Fig. 6.2C vs. D].

This indicated that a p53-mediated response appears critical to the induction of the typical *Δ3β-catenin* phenotypes seen in *K14creP.Δ3β-cat*$^{flx/wt}$ genotypes, yet control *K14cre.p53*$^{flx/flx}$ mice appeared completely normal in terms of their development and hair cycles; a result consistent with the relative lack of p53 in a normal epidermis until hyperplasia approaches the papilloma development stage [above; Chapter 3].

In the *K14creP.Δ3β-cat*$^{flx/wt}$*.p53*$^{flx/flx}$ cohorts it may be that conditional loss of p53 reduced the severity of *Δ3β-catenin* phenotypes due to the lack of major apoptotic responses mediated by p53 that likely led to the internal problems and embryonic lethality observed in other models of β-catenin deregulation (*Järvinen et al.,2006; Grigoryan et al., 2008*). However, this lack of p53 function and despite β-catenin overexpression, failed to elicit IFE tumours. Furthermore,

in another interesting development p53 expression appears integral to the production of the HF anomalies as this histological analysis also showed that p53 loss blocks HF tumour formation.

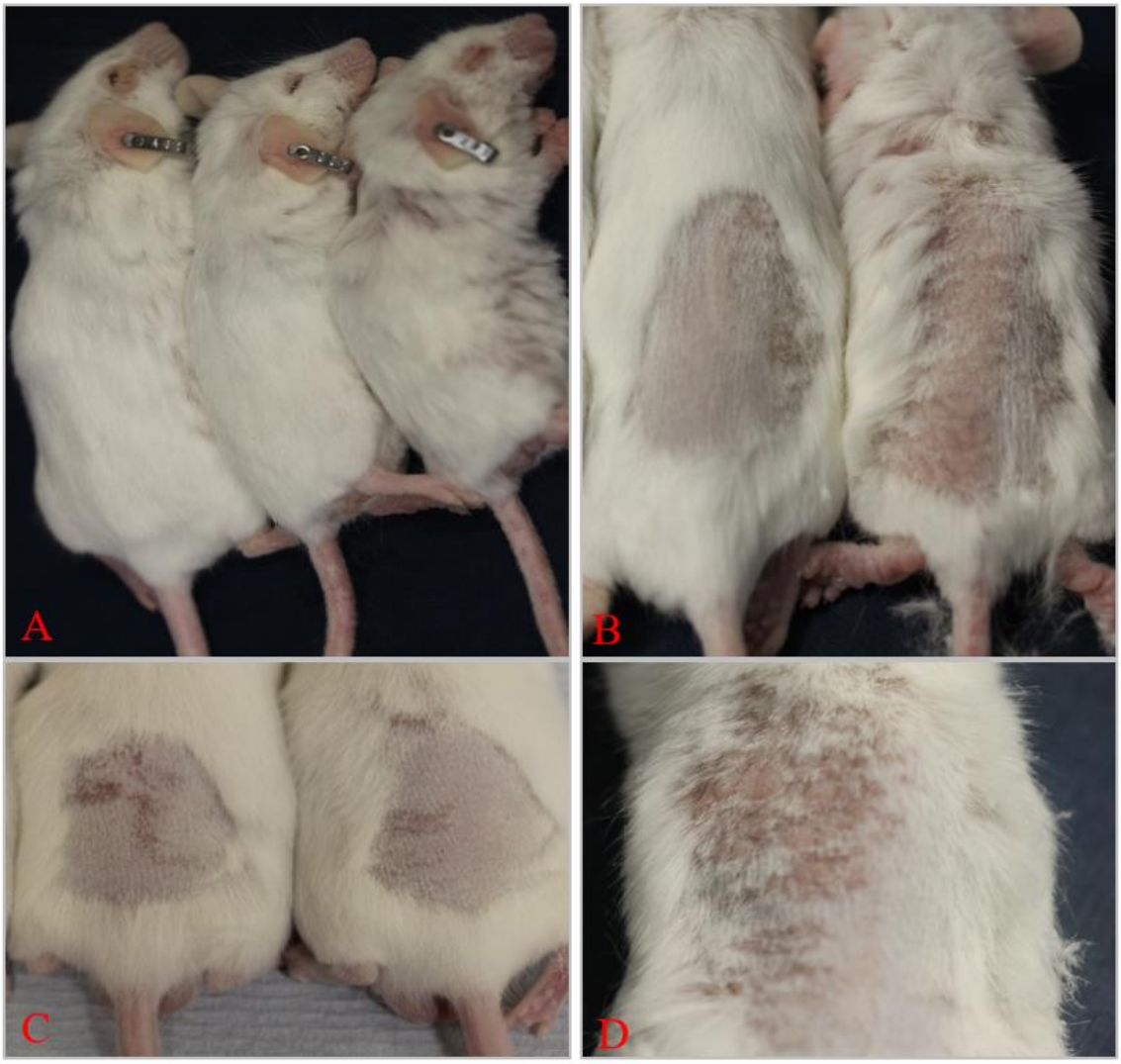

Figure 6. 2: Comparison of *K14creP.Δ3β-cat$^{flx/wt}$.p53$^{flx/flx}$* and *K14creP.Δ3β-cat$^{flx/wt}$.p53$^{flx/wt}$* phenotypes.

[A] Left to right: Typical lack of overt phenotypes in two 24d old juvenile *K14creP.Δ3β-cat$^{flx/wt}$.p53$^{flx/flx}$* mice compared to a *K14creP.Δ3β-cat$^{flx/wt}$.p53$^{flx/wt}$* sibling. Note *K14creP.Δ3β-cat$^{flx/wt}$.p53$^{flx/flx}$* mice appear slightly larger and lack the scruffy dishevelled fur or peri-orbital keratosis and large feet seen in the heterozygous *p53 K14creP.Δ3β-cat$^{flx/wt}$.p53$^{flx/wt}$* mouse. [B-D] A comparison of RU486-treated adults highlights the difference in hyperkeratosis between the two genotypes over time, where [B] at 4-5 weeks *K14creP.Δ3β-cat$^{flx/wt}$.p53$^{flx/flx}$* littermates still possess a mild score 0 phenotype with little keratosis compared to the uniform keratosis and wrinkled skin of the *K14creP.Δ3β-cat$^{flx/wt}$.p53$^{flx/wt}$* mouse. [C] At 8-10 weeks two separate *K14creP.Δ3β-cat$^{flx/wt}$.p53$^{flx/flx}$* mice exhibit minor hyperkeratosis compared to [D] the increased level of keratosis and wrinkled skin of their heterozygous *p53 K14creP.Δ3β-cat$^{flx/wt}$.p53$^{flx/wt}$* sibling.

Histological analysis confirmed these gross observations in *K14creP.Δ3β-cat$^{flx/wt}$.p53$^{flx/flx}$* mice compared to heterozygous *K14creP.Δ3β-cat$^{flx/wt}$.p53$^{flx/wt}$* littermates [Fig. 6.3 & Fig. 6.4]. At 3 weeks of age, both the ear and back histology of *K14creP.Δ3β-cat$^{flx/wt}$.p53$^{flx/flx}$* mice exhibited very weak histotypes associated with *Δ3β-catenin* overexpression [Fig. 6.3A&B]. Little IFE effects, other than a minimal hyperplasia were observable in the ear epidermis; example shown was one of the few to exhibit sporadic HF abnormalities [Fig. 6.3A]. In the 3-week old back skin at the end of the first anagen, few hair follicle abnormalities were present as all follicles appeared to be normal and there was a complete absence of cysts associated with *Δ3β-catenin* [Fig. 6.3B]. In comparison, the p53 heterozygous *K14creP.Δ3β-cat$^{flx/wt}$.p53$^{flx/wt}$* littermates already possessed typical Δ3β-catenin-associated abnormalities such as formation of multiple *de novo* hair follicle and cysts with minimal IFE hyperplasia [Fig. 6.3C&D].

These juvenile mice data clearly suggest that p53 was required to elicit the responses to deregulated β-catenin signalling in both IFE and more importantly the development not repression of HF anomalies and the analysis of RU486-treated *K14creP.Δ3β-cat$^{flx/wt}$.p53$^{flx/flx}$* adults at 8 weeks of age also strengthen this idea. As shown in Fig. 6.4, over time RU486 treatment of adult *K14creP.Δ3β-cat$^{flx/wt}$.p53$^{flx/flx}$* skin began to exhibit more *Δ3β-catenin* associated abnormalities [Fig. 6.4A&B], yet these were still very mild phenotypes compared to the increasing severity of phenotypes observed in heterozygous *K14.Δ3β-cat^{het}.p53^{het}*skin [Fig. 6.4C&D]. Again, this histological analysis emphasised the roles of p53 in affecting the level of severity of *Δ3β-catenin,* as even when these histotypes appeared they were mild and moreover in back skin *K14creP.Δ3β-cat$^{flx/wt}$.p53$^{flx/flx}$* mice lacked cysts and HF abnormalities were limited to follicular hyperplasia rather than progression to overt folliculoma as observed in the heterozygous littermate skin [Fig. 6.4B vs. D].

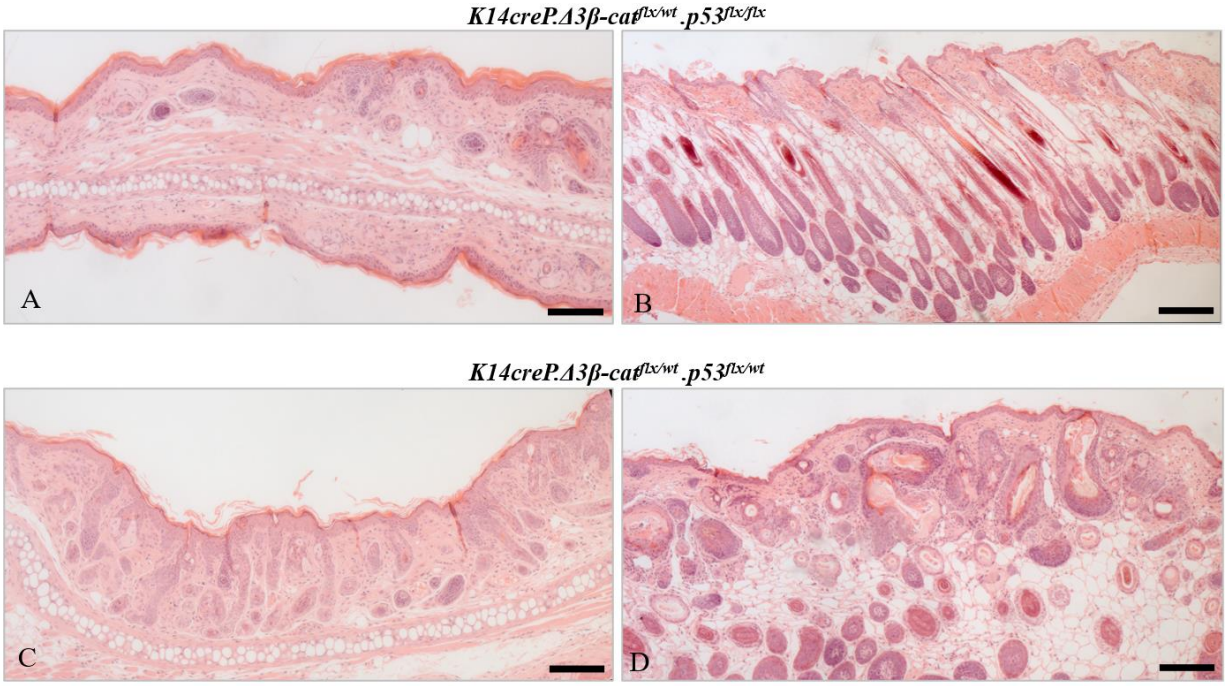

Figure 6. 3: Histological analysis of 3-week-old juvenile *K14creP.Δ3β-cat*$^{flx/wt}$ *.p53*$^{flx/flx}$ skin compared to a Δp53 heterozygous *K14creP.Δ3β-cat*$^{flx/wt}$ *.p53*$^{flx/wt}$ littermate.

[A & B] *K14creP.Δ3β-cat*$^{flx/wt}$ *.p53*$^{flx/flx}$ skin appears relatively normal. [A] Ear skin displays minimal IFE in this example with only sporadic HF abnormalities. [B] Back skin displays the final stages of the first anagen with many anagen 7 follicles yet each appears fairly normal and the skin lacks formation of multiple hair follicle abnormalities, folliculomas or cysts and the IFE displays only sporadic hyperplasia. [C & D] Δp53 heterozygous *K14creP.Δ3β-cat*$^{flx/wt}$ *.p53*$^{flx/wt}$ littermates already exhibits the typical *Δ3β-catenin* phenotypes multiple hair follicle abnormalities and cysts in both [C] ear and [D] back and mild IFE hyperplasia. Scale bars: A, & C: 150 µm; C & D: 100 µm

The reasons for this effect are unclear, but these results show that p53 was necessary to develop the phenotypes associated with *Δ3β-catenin* deregulation. It may be that p53 functions were required downstream to effect these changes or more logically as this is such a fundamental molecule that regulates many processes of proliferation, differentiation and apoptosis, it is likely that additional compensatory systems respond to this lack of p53. Indeed, this may be why few effects of p53 loss are observed in RU486-treated *K14creP.p53*$^{flx/flx}$ mice [Fig. 6.4E&F] and this observation remains even after 9 months.

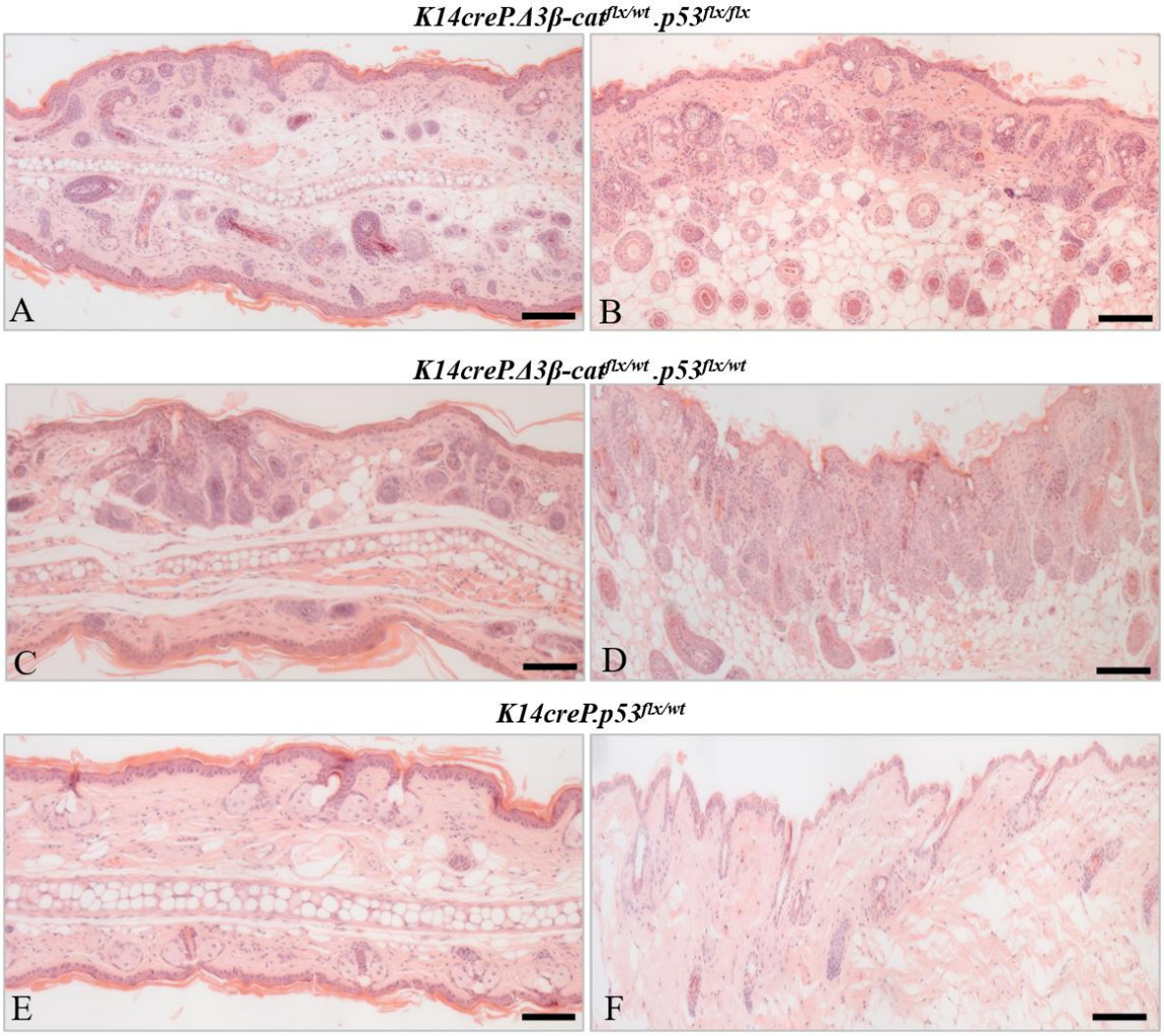

Figure 6. 4: Histological analysis of 8-week-old RU486-treated *K14creP.Δ3β-cat$^{flx/wt}$.p53$^{flx/flx}$* and heterozygous *K14creP.Δ3β-cat$^{flx/wt}$.p53$^{flx/wt}$* littermate skin compared to *K14creP.p53$^{flx/flx}$* controls.

[A & B] With time and RU486 treatment by 8 weeks a *K14creP.Δ3β-cat$^{flx/wt}$.p53$^{flx/flx}$* skin now displays mild *Δ3β-catenin* histotypes typical of a mouse with a score 0 designation. [A] Ear skin displays mild IFE hyperplasia and the sporadic HF abnormalities increased [B] Back skin also displays mild hyperplasia with increased numbers of hair follicle abnormalities but less progression to folliculoma nor any cyst production. [C & D] Δp53 heterozygous *K14creP.Δ3β-cat$^{flx/wt}$.p53$^{flx/wt}$* littermate exhibits a much more increased set of *Δ3β-catenin* phenotypes with multiple hair follicle abnormalities and cysts in both [C] ear and [D] back and increasing IFE hyperplasia consistent with the increased appearance of keratosis and thickened skin [*Fig. 6.2B & D*]. [E & F] RU486-treated *K14creP.p53$^{flx/flx}$* controls appear normal with only occasional displays of subtle epidermal hyperplasia in [E] the tagged ear. Scale bars: A-F: 100µm

This appears to be an important finding and identifies p53 status as a direct effector of β-catenin. Indeed, this appears to be a novel finding, given few other approaches have employed this strategy to investigate the consequences of β-catenin overexpression. In addition, the context of p53 loss appears to be important also, as whatever compensates for p53 loss to block effects of β-catenin activation in *K14creP.Δ3β-cat*$^{flx/wt}$*.p53*$^{flx/flx}$ genotypes fails to act in *HK1.ras/fos-K14creP.Δ5PTEN*$^{flx/flx}$ papillomas following p53 loss, which convert to malignancy given the increased signalling deregulation, loss of p53 guardian functions and in this context, nuclear β-catenin helps drive progression. Equally, in reverse where β-catenin loss inhibited chemical carcinogenesis *(Malanchi, et al., 2008)*, at some stage p53 was also lost and again any putative backup TSG effects were quickly circumvented due to the numerous other DMBA/TPA-induced mutations leading to SCC (*Malanchi, et al., 2008*). Thus, these ideas will be tested next via creation of *HK1.ras-K14creP.Δ3β-cat*$^{flx/wt}$*.p53*$^{flx/flx}$ genotypes to further assess the effect of this interaction between *Δ3β-catenin* and *p53*^{flx} on tumorigenesis.

6.3 Conditional loss of *p53* does not affect the lack of papillomatogenesis in most *HK1.ras-K14creP.Δ3β-cat*$^{flx/wt}$*.p53*$^{flx/flx}$ genotypes.

Following the interesting novel and reverse effects of p53 loss on reduction not expansion of the early *Δ3β-catenin* phenotypes, *HK1.ras-K14creP.Δ3β-cat*$^{flx/wt}$*.p53*$^{flx/flx}$ genotypes were generated. These mice were assessed for their ability to form papillomas and if so, would these tumours convert to carcinomas due to the loss of p53 protection, which was suspected to be the main cause in halting papilloma formation in *HK1.ras-K14creP.Δ3β-cat*$^{flx/wt}$ cohorts [above Chapter 4] and co-operated with β-catenin overexpression in the malignant conversion of *HK1.ras/fos-K14creP.Δ5PTEN*$^{flx/flx}$ papillomas.

As cited above, *K14cre.p53*$^{flx/flx}$ mice have been established in house for several years for studies of a similar paradoxical inhibition of *HK1.ras* papillomas induced by *p53* loss (*Greenhalgh et al., 1996*). Thus, these experiments assessed whether the responses that reduced β-catenin overexpression phenotypes following p53 loss were also able to inhibit papillomas observed in *HK1.ras-K14.p53*$^{flx/flx}$ mice and *HK1.ras-K14creP.Δ3β-cat*$^{flx/wt}$ cohorts;

or did the reverse happen, was β-catenin overexpression in *HK1.ras-K14creP.Δ3β-cat*$^{flx/wt}$*.p53*$^{flx/flx}$ cohorts able to overcome the paradoxical mechanism of tumour inhibition observed in *HK1.ras-K14.p53*$^{flx/flx}$ mice following p53 loss?

These are difficult questions that highlight the complexity of these signalling systems and that in different contexts result may differ – however it was the former idea that proved to be the case and led to investigations of alternate p53 family members, p63 and p73 together with assessment of p21 knockout [see below].

As shown in Fig.6.5, except for two instances [see section 6.4 below], most *HK1.ras-K14creP.Δ3β-cat*$^{flx/wt}$*.p53*$^{flx/flx}$ mice [N=22] again exhibited a complete lack of papillomas despite the loss of p53, similar to *HK1.ras-K14creP.Δ3β-cat*$^{flx/wt}$ [Fig. 6.5A-C]. Once again, their size varied but tended to be larger and *HK1.ras-K14creP.Δ3β-cat*$^{flx/wt}$*.p53*$^{flx/flx}$ mice grossly showed a noticeable reduction in severity of *Δ3β-catenin skin* phenotypes, similar to observations illustrated in *K14creP.Δ3β-cat*$^{flx/wt}$*.p53*$^{flx/flx}$ mice [above]. Whilst neonatal *HK1.ras-K14creP.Δ3β-cat*$^{flx/wt}$*.p53*$^{flx/flx}$ mice exhibited the wrinkled *HK1.ras*-associated skin phenotype [not shown], juvenile and early adults exhibited only mild spontaneous *Δ3β-catenin* associated phenotypes typically seen in *HK1.ras-K14creP.Δ3β-cat*$^{flx/wt}$ cohorts [Fig.6.5 D vs. E, F vs G].

Histological analysis was conducted on RU486-treated 4-week and 10-week old *HK1.ras-K14creP.Δ3β-cat*$^{flx/wt}$*.p53*$^{flx/flx}$ skin biopsies to observe changes in *Δ3β-catenin*-associated IFE hyperplasia compared to *HK1.ras-K14creP.Δ3β-cat*$^{flx/wt}$ skin [above Chapter 5]. At 4 weeks, following a single application of RU486, the histology of a juvenile *HK1.ras-K14creP.Δ3β-cat*$^{flx/wt}$*.p53*$^{flx/flx}$ skin showed only very mild *Δ3β-catenin* phenotypes with minimal IFE hyperplasia in both ear [Fig. 6.6A&B] and back specimens [Fig. 6.6E&F] together with significantly reduced problems with HF anomalies. In comparison, equivalent heterozygous *HK1.ras-K14.Δ3β-cat*^{het}*/p53*^{het} littermates exhibited the identical histotypes of *HK1.ras-K14creP.Δ3β-cat*$^{flx/wt}$ skin [not shown]; designated with a score 1 [above, chapter 5].

It was also noted that at higher magnification there was an increased disorder to the basal layer, yet there appeared to be few cysts [Fig. 6.6B, D&F]. This example also shows less hyperplasia than expected [see below Fig. 6.7A&B] consistent with the lack of keratosis [insert] and there is a distinct degree of disordered differentiation in upper epidermal layers [Fig. 6.6B, F&G]. This again suggests that supra-basal keratinocyte differentiation is disrupted

possibly due to increased supra-basal p21 [below Fig.6.12] affecting the final stages of differentiation as observed in *HK1.ras-K14creP.Δ3β-cat*$^{flx/wt}$ [above chapter 5 Fig. 5.9C] and K1 analysis in *HK1.ras-K14creP.Δ3β-cat*$^{flx/wt}$*.p53*$^{flx/flx}$ skin [below Fig.6.10B&C].

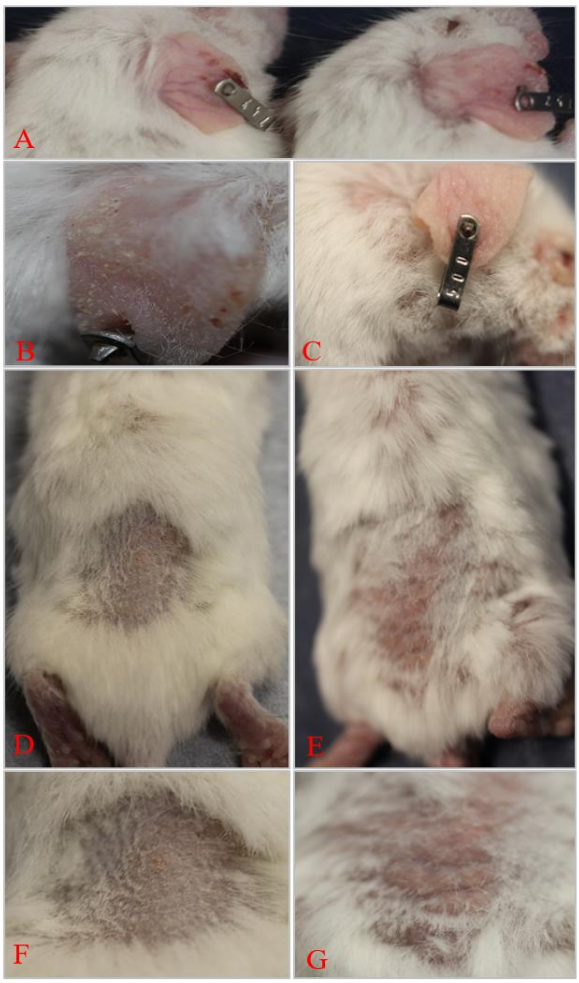

Figure 6. 5: *HK1.ras-K14creP.Δ3β-cat*$^{flx/wt}$*.p53*$^{flx/flx}$ genotypes lack papilloma formation.

[A & B] At 8 weeks post ear-tag wounding, RU486-treated *HK1.ras-K14creP.Δ3β-cat*$^{flx/wt}$*.p53*$^{flx/flx}$ tagged ears show a lack of papillomas similar to [C] RU486-treated *HK1.ras-K14creP.Δ3β-cat*$^{flx/wt}$ and each exhibits only a mild keratosis. [D] *HK1.ras-K14creP.Δ3β-cat*$^{flx/wt}$*.p53*$^{flx/flx}$ again show a reduced keratosis with less scruffiness to the fur compared to [E] treated *HK1.ras-K14creP.Δ3β-cat*$^{flx/wt}$ and comparison of [F] *HK1.ras-K14creP.Δ3β-cat*$^{flx/wt}$*.p53*$^{flx/flx}$ [G] with age-matched *HK1.ras-K14creP.Δ3β-cat*$^{flx/wt}$ control at 8 weeks again highlights the contrasting keratosis and wrinkled skin between these genotypes.

With time and further RU486 treatments, by 10 weeks *HK1.ras-K14creP.Δ3β-cat*$^{flx/wt}$*.p53*$^{flx/flx}$ skins exhibited phenotypes more typically associated with Δ3β-catenin expression as they showed more hair follicle abnormalities with a slightly increased *HK1.ras*-associated IFE, although again few cysts appeared. [Fig. 6.6C&D; G&H]. Indeed, consistent with a repression of Δ3β-catenin-associated phenotypes by *p53* inactivation, HF abnormalities appeared less compared to *HK1.ras-K14creP.Δ3β-cat*$^{flx/wt}$ skins, with little cyst formation [Fig. 6.7A vs. C]. However, again a disordered differentiation was noted in basal layer *HK1.ras-K14creP.Δ3β-cat*$^{flx/wt}$*.p53*$^{flx/flx}$ keratinocytes similar to the disordered differentiation of *HK1.ras-K14creP.Δ3β-cat*$^{flx/wt}$ expressing a wt *p53* [Fig. 6.7B vs. D] or heterozygous p53 *HK1.ras-K14creP.Δ3β-cat*$^{flx/wt}$ *.p53*$^{flx/wt}$ siblings.

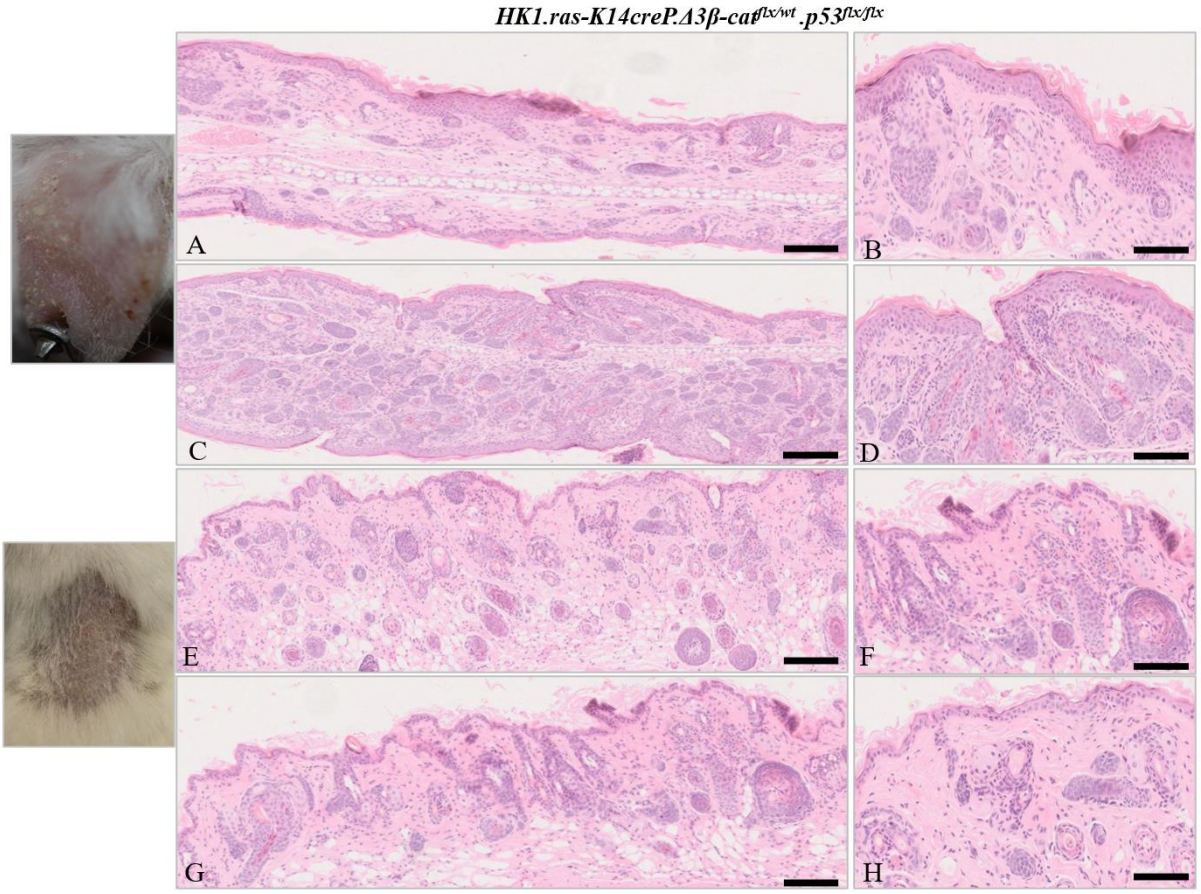

Figure 6. 6: Histological analysis of *HK1.ras-K14creP.Δ3β-cat$^{flx/wt}$.p53$^{flx/flx}$* skin biopsies at 4 and 10 weeks.

[A & B] At 4 weeks *HK1.ras-K14creP.Δ3β-cat$^{flx/wt}$.p53$^{flx/flx}$* ear skin [insert] shows minimal IFE hyperplasia and only minor effects of *Δ3β-catenin* on HF morphology. [C & D] At 10 weeks, RU486-treated *HK1.ras-K14creP.Δ3β-cat$^{flx/wt}$.p53$^{flx/flx}$* skin now shows a more typical *Δ3β-catenin* phenotype highlighted in [D] at higher magnification by multiple hair follicle abnormalities and again an increased disorder to the basal layer with hyper-chromatic nuclear keratinocytes. [E & F] A 4 week old *HK1.ras-K14creP.Δ3β-cat$^{flx/wt}$.p53$^{flx/flx}$* back skin also shows minimal IFE hyperplasia and minor HF effects. [G] By 10 weeks, *HK1.ras-K14creP.Δ3β-cat$^{flx/wt}$.p53$^{flx/flx}$* back skin shows the typical *Δ3β-catenin* effects of multiple hair follicle abnormalities, but with little cyst formation. [H] This example also shows less hyperplasia than expected [see Fig.6.7 A & B] consistent with the lack of keratosis [insert] and exhibits a distinct degree of disordered differentiation in upper epidermal layers. Scale bars: A,C,E&G: 100µm; B,D,F&H: 50µm

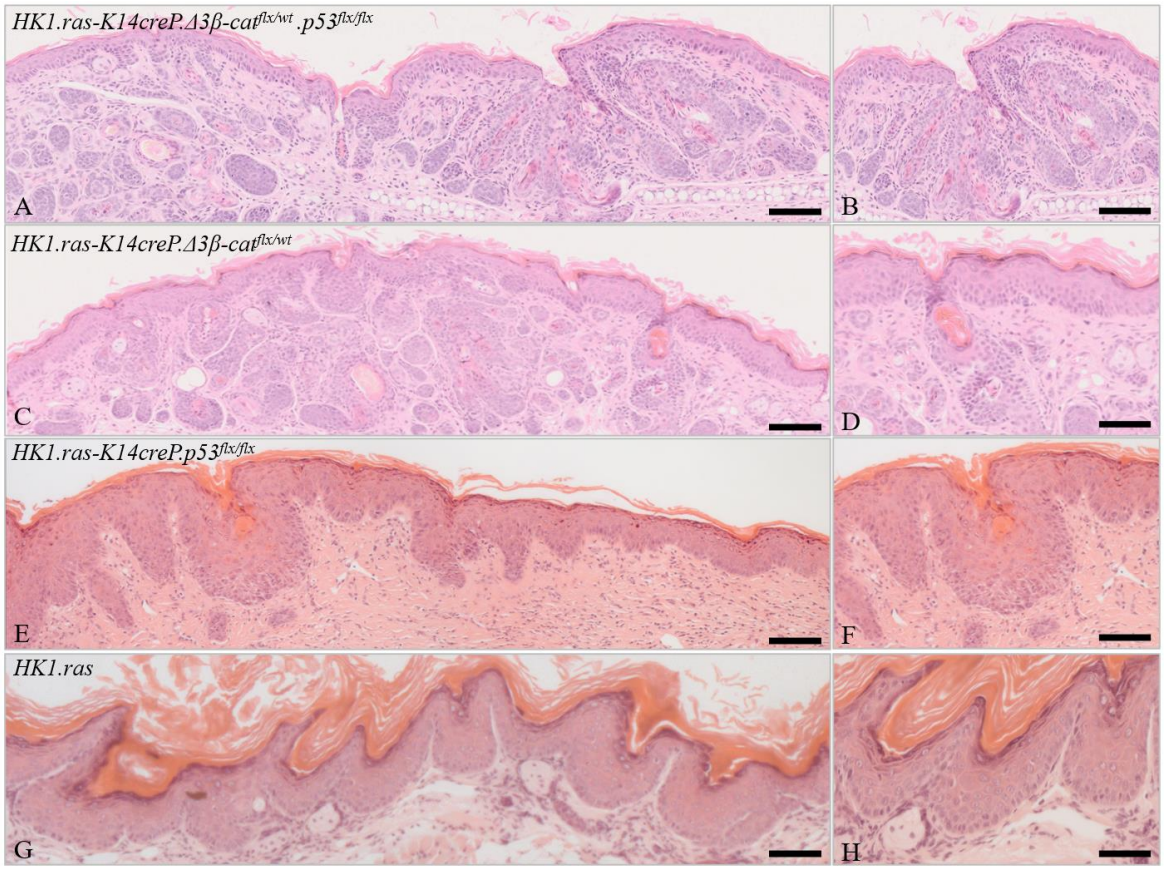

Figure 6. 7: Histological comparison of RU486-treated *HK1.ras-K14creP.Δ3β-cat$^{flx/wt}$ .p53$^{flx/flx}$* skin to *HK1.ras-K14creP.Δ3β-cat$^{flx/wt}$* , *HK1.ras-K14creP.p53$^{flx/flx}$* and *HK1.ras* epidermis.

[A & B] At 10 weeks and RU486 treatment *HK1.ras-K14creP.Δ3β-cat$^{flx/wt}$.p53$^{flx/flx}$* exhibits multiple hair follicle abnormalities but few cysts with a more IFE hyperplasia [compared to Fig.6.3 #2 G & H] and again this disordered differentiation of prominent nuclei in basal layer keratinocytes. [C & D] *HK1.ras-K14creP.Δ3β-cat$^{flx/wt}$* displays increased IFE hyperplasia and more hair follicle abnormalities including formation of multiple cysts, whilst [D] displays a disordered differentiation but lacks the prominent nuclei. [E & F] RU486-treated *HK1.ras-K14creP.p53$^{flx/flx}$* skin shows increased hyperplasia with an ordered differentiation; but [F] occasional patches of disturbed basal layer keratinocytes suggested attempts to undergo apoptosis due to p53 loss. [G & H] *HK1.ras* epidermis exhibits a more papillomatous hyperplasia with ordered differentiation. Scale bars: A,C,E&G:100µm; B,D,F&H: 50µm

In comparison to this *HK1.ras-K14creP.Δ3β-cat$^{flx/wt}$ .p53$^{flx/flx}$* histotype both RU486-treated *HK1.ras-K14creP.p53$^{flx/flx}$* and *HK1.ras* controls possessed a larger degree of IFE hyperplasia with increased papillomatogenesis and a smooth ordered differentiation [Fig.6.7 E-F]; although occasional patches of disturbed basal layer keratinocytes appeared in RU486-treated *HK1.ras.p53$^{fxl/flx}$* epidermis compared to *HK1.ras* alone [Fig.6.7F vs. H]; suggesting an anomalous premature differentiation or attempts to undergo apoptosis in response to loss of *p53* functions in screening DNA for repair. Indeed, it was speculated that the normal supra-

basal expression of AKT maybe geared to block p53-mediated apoptosis giving time for terminal differentiation (*Calautti et al., 2005; Macdonald et al., 2014*); thus, the loss of p53 in this context may allow for premature AKT expression in basal layers adding to the proliferation and the beginnings of a disordered differentiation or p53 independent apoptosis to counter basal AKT.

This analysis clearly illustrated an effect of p53 loss on the time of appearance and severity of *Δ3β-catenin* phenotypes, as little to no effect was observed on *HK1.ras-K14creP.Δ3β-cat*$^{flx/wt}$*.p53*$^{flx/flx}$ tumorigenesis, as seen in *HK1.ras-K14creP.Δ3β-cat*$^{flx/wt}$ [above] and the paradoxical block of papillomas in *HK1.ras-K14creP.p53*$^{flx/flx}$ mice. Therefore, to confirm this histological analysis and show that the mechanism remained the same, these biopsies were assessed by the standard analysis of β-catenin/E-cadherin status; assessment of keratinocyte differentiation via K1/K6 marker expression and analysis of p21 expression to determine whether this remained or increased in basal layers due to p53 loss and thus helped inhibit papilloma formation.

Analysis of β-catenin levels in 4-week-old *HK1.ras-K14creP.Δ3β-cat*$^{flx/wt}$*.p53*$^{flx/flx}$ mice showed the expected increased expression in basal layers, again with both membranous and elevated nuclear β-catenin [Fig. 6.8A&B] that was virtually identical to β-catenin levels and a greater degree of hyperplasia observed in *HK1.ras-K14creP.Δ3β-cat*$^{flx/wt}$ controls [Fig. 6.8C&D]. In comparison both *HK1.ras-K14creP.p53*$^{flx/flx}$ and *HK1.ras* control hyperplasia exhibited mainly suprabasal layer expression [Fig.6.8 E & F; G&H]. Thus, p53 loss did not appear to affect the epidermal location or levels of *Δ3β-catenin* expression in *HK1.ras-K14creP.Δ3β-cat*$^{flx/wt}$*.p53*$^{flx/flx}$ mice. Moreover this *HK1.ras-K14creP.p53*$^{flx/flx}$ result maybe important as it also suggests that the responses to p53 loss in *HK1.ras-K14creP.p53*$^{flx/flx}$ mice are independent of β-catenin expression at this stage and this inhibitory compensatory mechanism to p53 loss maybe generic, hence a lack of early papillomas in both contexts. Analysis of E-cadherin also showed an increase in basal layer expression in *HK1.ras-K14creP.Δ3β-cat*$^{flx/wt}$*.p53*$^{flx/flx}$ mice again mimicking that of *β-catenin* and also similar to *HK1.ras-K14creP.Δ3β-cat*$^{flx/wt}$ expression of E-cadherin, whilst both *HK1.ras-K14creP.p53*$^{flx/flx}$ and HK1.ras control hyperplasia exhibited a mainly suprabasal layer expression profile [Fig. 6.9].

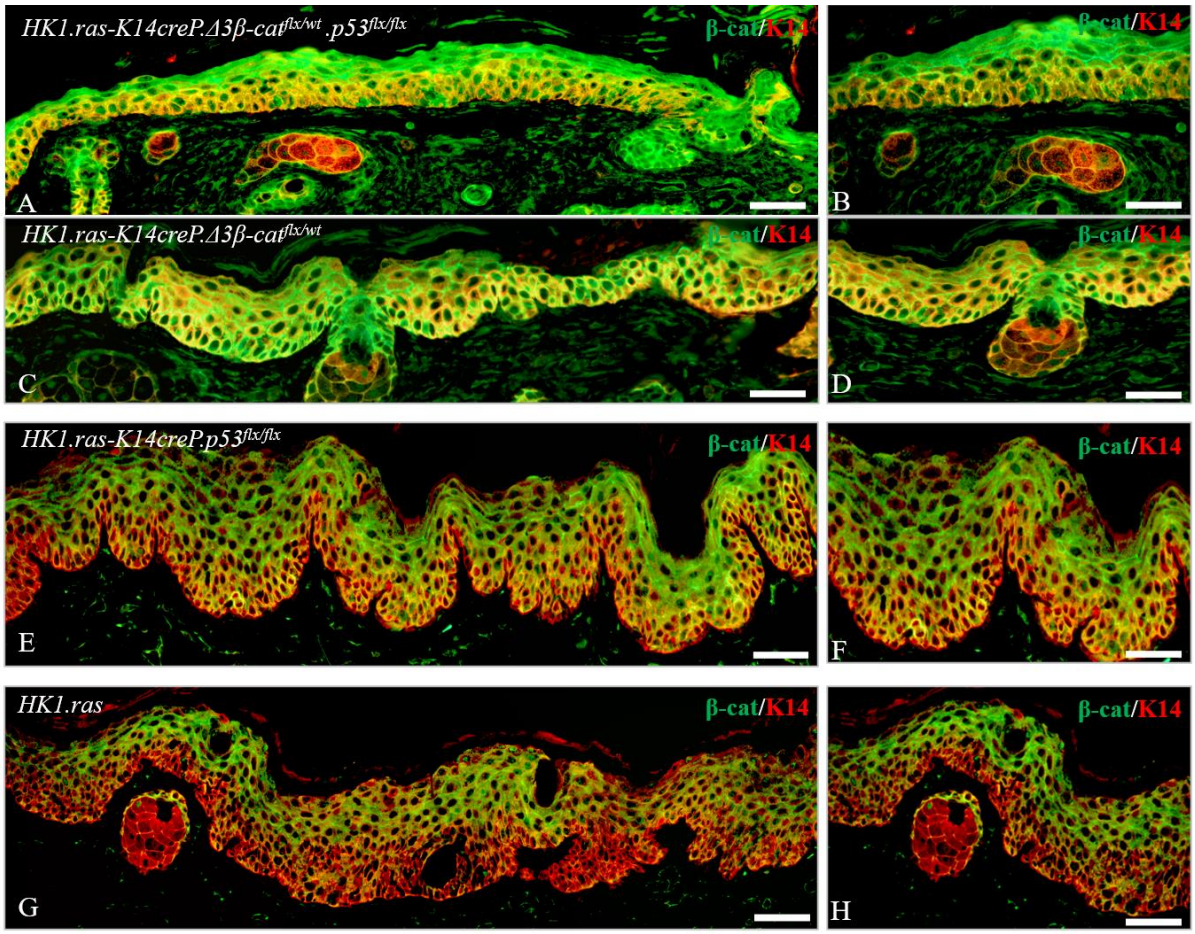

Figure 6. 8: Analysis of β-catenin expression in RU486-treated *HK1.ras-K14creP.Δ3β-cat$^{flx/wt}$.p53$^{flx/flx}$* compared to *HK1.ras-K14creP.Δ3β-cat$^{flx/wt}$* controls.

[A & B] *HK1.ras-K14creP.Δ3β-cat$^{flx/wt}$.p53$^{flx/flx}$* epidermis displays an overall strong uniform expression of β-catenin in IFE and hair follicles; where at higher magnification [B] shows nuclear localization of β-catenin with strong membranous and nuclear expression in basal-layer keratinocytes. [C & D] *HK1.ras-K14creP.Δ3β-cat$^{flx/wt}$* displays an identical β-catenin expression profile where [D] at higher magnification again shows nuclear localization of β-catenin with strong membranous basal-layer expression in IFE and hair follicles. [E & F] *HK1.ras.p53*$^{flx/fx}$ exhibits increased papillomatous hyperplasia and mainly suprabasal-layer expression of β-catenin similar to [G & H] supra-basal expression of β-catenin in *HK1.ras* hyperplasia. Scale bars: A,C,E&G: 75µm; B,D,F&H: 50µm

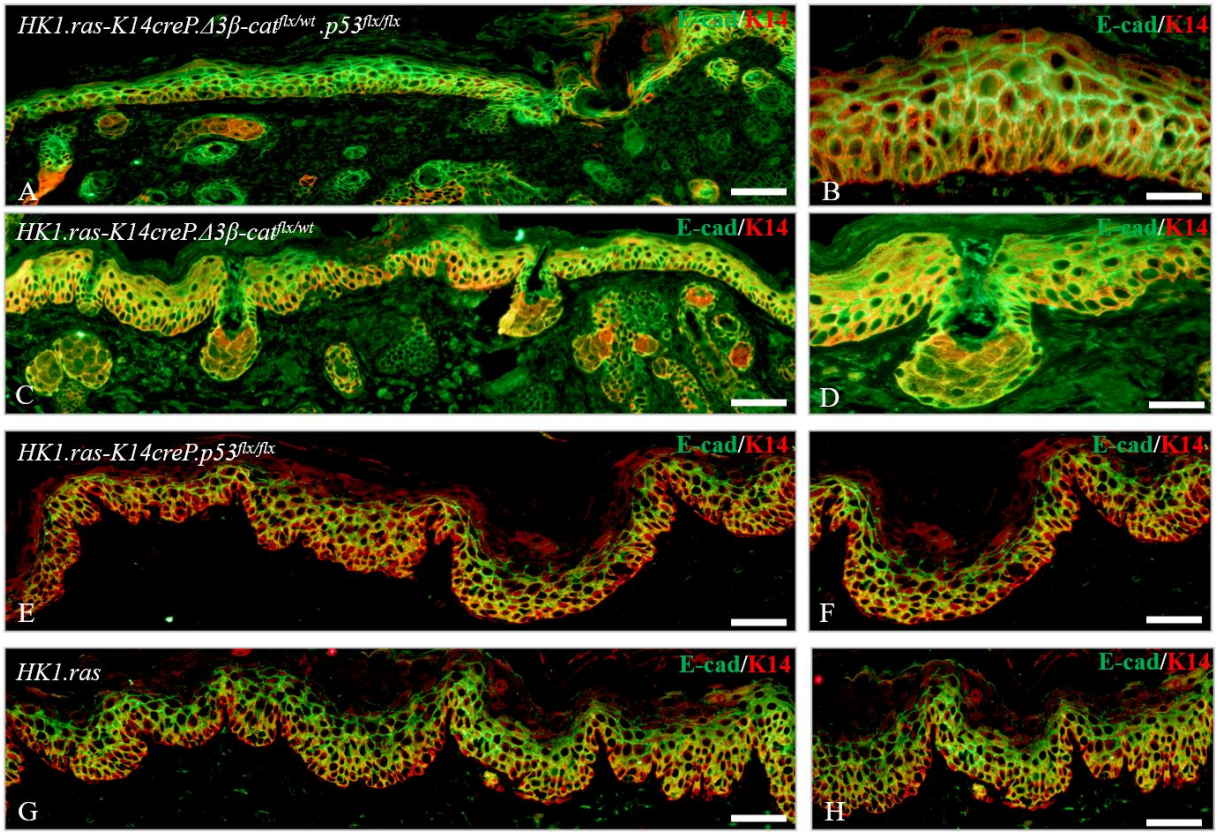

Figure 6. 9: Analysis of E-cadherin expression in RU486-treated *HK1.ras-K14creP.Δ3β-cat$^{flx/wt}$.p53$^{flx/flx}$* and *HK1.ras-K14creP.Δ3β-cat$^{flx/wt}$* epidermis.

[A & B] *HK1.ras-K14creP.Δ3β-cat$^{flx/wt}$.p53$^{flx/flx}$* epidermis displays strong uniform E-cadherin expression in the IFE and hair follicles that parallels β-catenin. [B] Higher magnification shows strong membranous E-cadherin expression in both supra-basal and basal layers with little detectable nuclear localization. [C & D] *HK1.ras-K14creP.Δ3β-cat$^{flx/wt}$*displays an identical profile. [E & F] *HK1.ras-K14creP.p53$^{flx/flx}$* exhibits only supra-basal E-cadherin expression identical to [G & H] supra basal expression in *HK1.ras* hyperplasia. Scale bars: A,C,E&G: 75µm; B,D,F&H: 50µm

These data indicate that despite the loss of p53 expression in *HK1.ras-K14creP.Δ3β-cat$^{flx/wt}$.p53$^{flx/flx}$*, an increased cell-cell adhesion was still maintained in basal layers by E-cadherin expression [Fig. 6.9A&B] and identical to that observed in *HK1.ras-K14creP.Δ3β-cat$^{flx/wt}$* epidermis [Fig. 6.9C&D]. In contrast, *HK1.ras-K14creP.p53$^{flx/flx}$* and *HK1.ras* control hyperplasia lacked this early expression which suggests the possibility of a mechanism of cell adhesion responses aiding tumour inhibition alongside altered differentiation or elevated p21. Furthermore E-cadherin expression appeared mainly membranous and cytoplasmic but not nuclear [Fig. 6.9A&B]. Thus, the proposed function to act as a sponge and provide additional regulation of β-catenin (*Huels et al., 2015*) remained intact in the cytoplasm [Fig. 6.9C&D; as seen previously for *HK1.ras-K14creP.Δ3β-cat$^{flx/wt}$* epidermis [see Chapter 5 Fig.5.8] but was

not present in the nucleus. Hence retention of nuclear β-catenin levels in basal keratinocytes also means that nuclear translocation of β-catenin was not affected by p53 loss, thus ruling out another possibility for the inhibition of Δ3*β-catenin* phenotypes.

In respect to differentiation, to explore the possibility of an increased differentiation response, the early differentiation marker keratin K1 and the hyperproliferation/disease-associated keratin K6α were investigated to assess whether a similar novel lack of K1 and K6α also appeared in *HK1.ras-K14creP.Δ3β-cat*$^{flx/wt}$*.p53*$^{flx/flx}$ mice [Fig. 6.10 & Fig. 6.11]. The disordered *HK1.ras-K14creP.Δ3β-cat*$^{flx/wt}$*.p53*$^{flx/flx}$ histotype was very similar to *HK1.ras-K14creP.Δ3β-cat*$^{flx/wt}$ hyperplasia and consistent with this observation K1 showed a very weak expression profile in *HK1.ras-K14creP.Δ3β-cat*$^{flx/wt}$*.p53*$^{flx/flx}$ skin [Fig. 6.10A-C]. Indeed, this was much more pronounced as K1 expression almost disappeared from the epidermis, whilst *HK1.ras-K14creP.Δ3β-cat*$^{flx/wt}$ showed patchy, confused expression [Fig. 6.10 D]. As observed previously in *HK1.ras-K14creP.Δ3β-cat*$^{flx/wt}$ mice, this patchy K1 expression disappeared quite abruptly in some parts of the epidermis suggesting all daughter cells form a specific epidermal stem cell unit underwent this changed differentiation pattern. If so then the loss of p53 compounded this result in *HK1.ras-K14creP.Δ3β-cat*$^{flx/wt}$*.p53*$^{flx/flx}$ histotypes [Fig. 6.10A-C vs. D] as not only was K1 virtually absent but also when actually present K1 expression appeared to be confined to the upper layers of the hyperplastic epidermis [Fig.6.10 B & C]. In contrast, RU486-treated *HK1.ras-K14creP.p53*$^{flx/flx}$ and *HK1.ras* control hyperplasia again exhibited a normal expression of K1 confined to the suprabasal layer with a smooth transition of basal keratinocytes to the supra basal layer [Fig. 6.10E&F] possibly due to the indifference of *HK1.ras* epidermis to a lack of p53 expression responses and the normal low expression of epidermal p21 [Chapter 3].

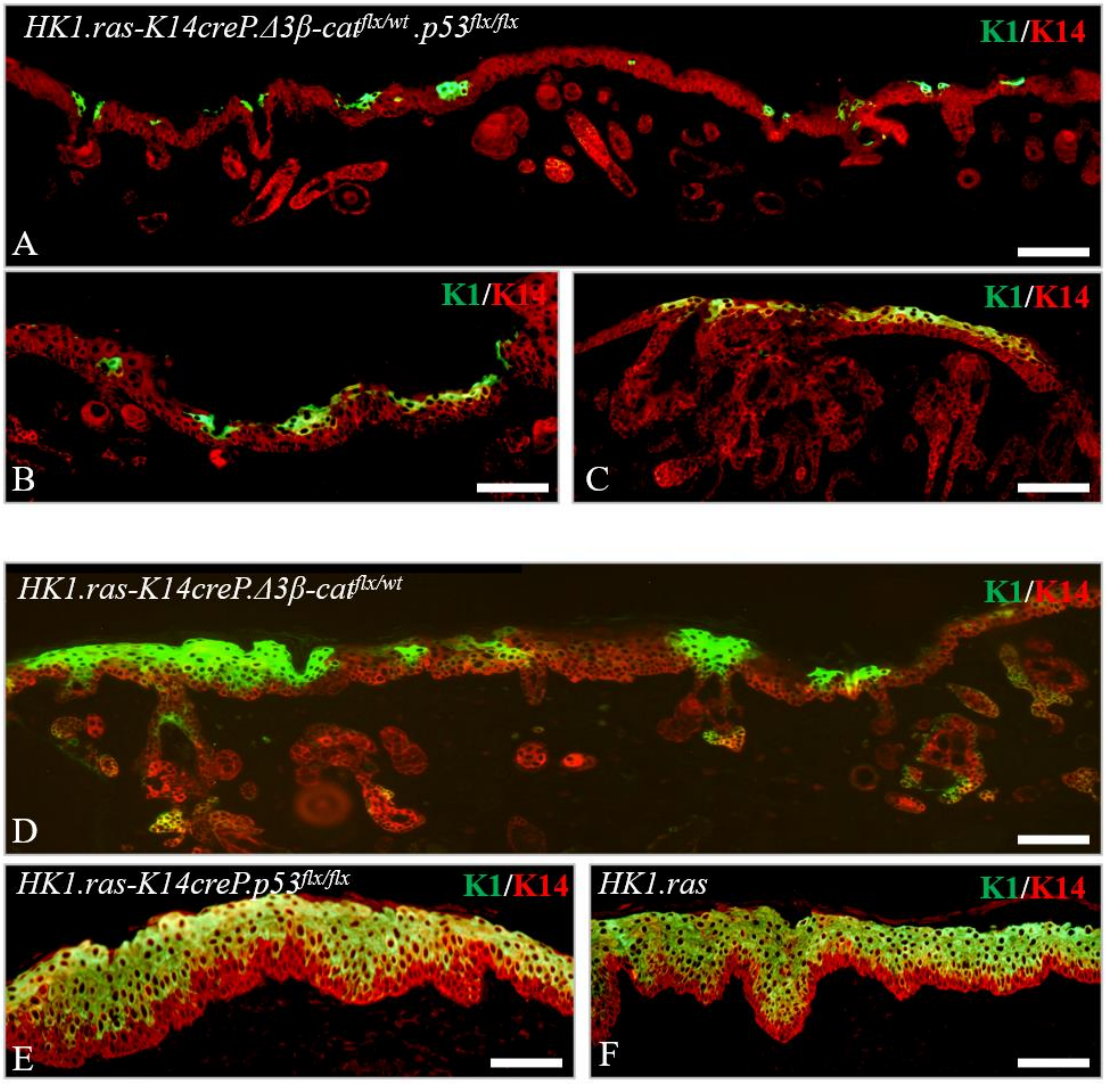

Figure 6. 10: Analysis of differentiation marker keratin K1 in *HK1.ras-K14creP.Δ3β-cat$^{flx/wt}$.p53$^{flx/flx}$* epidermis.

[A-C] K1 expression in *HK1.ras-K14creP.Δ3β-cat$^{flx/wt}$.p53$^{flx/flx}$* is very weak sporadic and absent in many areas. [B & C] K1 appears confined to the upper layers consistent with a delay in expression. [D] *HK1.ras-K14creP.Δ3β-cat$^{flx/wt}$* skin displays expression of K1 in specific patches. [E] Treated *HK1.ras-K14creP.p53$^{flx/flx}$* epidermis displays an ordered K1 profile despite the occasional disturbed differentiation observed in their histology. [F] *HK1.ras* shows smooth, ordered expression of K1 confined to the suprabasal layer. Scale bars: A&D: 100µm; B,C,E&F: 50µm

This expression of K1 in *HK1.ras-K14creP.Δ3β-cat$^{flx/wt}$.p53$^{flx/flx}$* epidermis clearly indicated that the terminal differentiation programme was highly disturbed following the loss of p53 and more so than previously observed in *HK1.ras-K14creP.Δ3β-cat$^{flx/wt}$* skin. Thus, this feature of K1 expression appears to be a significant marker of the altered differentiation caused by deregulated β-catenin expression and exacerbated by p53 loss-although exactly why is unclear

but may relate to the increased numbers of adherence junctions due to excess E-cadherin and the resultant increase in rigidity feeds back to alter the commitment to begin K1 expression in the early stages of differentiation as keratinocyte migrate from the different epidermal stem cell niches (*Watt and Collins, 2008*). Alternately, this effect on K1 maybe due to compensatory p21 expression [below] that appeared particularly strong in the upper layers of the epidermis following p53 loss.

Furthermore, it may be that these effects of β-catenin involve decisions by individual stem cells in the given niches as speculated above for *HK1.ras-K14creP.Δ3β-cat*$^{flx/wt}$ IFE (*Watt and Collins, 2008*). These are further altered following p53 loss in the IFE epidermis, and p53 loss also affected the typical HF anomalies *HK1.ras-K14creP.Δ3β-cat*$^{flx/wt}$*.p53*$^{flx/flx}$ HFs. Here overall, the response to p53 loss was potent enough to diminish the intensity of the HF anomalies including a lack of K1^{+ve} abnormal follicles [Fig. 6.10A-C vs. D] and their apparent ability to de –differentiate into a cyst appears to be absent also, suggesting that this too is mediated by p53 in attempts to avoid potential tumour progression in p53wt cells.

It may be that the resultant danger and potential proliferation of keratinocytes with increased susceptibility to genetic mutations due to loss of the p53 repair surveillance, subsequently affects the pluripotent HF stem cell niche. For instance, as this induced a more potent response to p53 loss one feature may result in causing specific stem cell populations to exit that niche in order to prevent production of proliferating cells gaining the mutations leading to follicular tumours. This protection thus manifests as a lesser degree of HF abnormalities and may also account for the reduced expression of the K15 stem cell marker in the IFE [see below]. Consequently, this idea possibly indicates that a loss of K15^{+ve} IFE stem cell targets for *HK1.ras* activation would thus account for the lack of papillomas and was investigated below.

If so, then this kind of inhibition of such potential mutant keratinocyte populations as a backup to p53 loss may also help account for the general total lack of hyperproliferation marker keratin K6α expression observed once again in *HK1.ras-K14creP.Δ3β-cat*$^{flx/wt}$*.p53*$^{flx/flx}$ mice [Fig.6.11]. Analysis of a variety of *HK1.ras-K14creP.Δ3β-cat*$^{flx/wt}$*.p53*$^{flx/flx}$ samples showed K6α expression was confined to the hair follicles [Fig.6.11A-C] as seen in *HK1.ras-K14creP.Δ3β-cat*$^{flx/wt}$ mice [Fig. 6.11D & E]. In contrast *HK1.ras-K14creP.p53*$^{flx/flx}$ and *HK1.ras* control hyperplasia both exhibited strong K6α expression in the IFE constant with

increased proliferation and a lack of p53 [*HK1.ras.p53*$^{flx/flx}$] or lack p53 induction [*HK1.ras*] [Fig. 6.11 F & G].

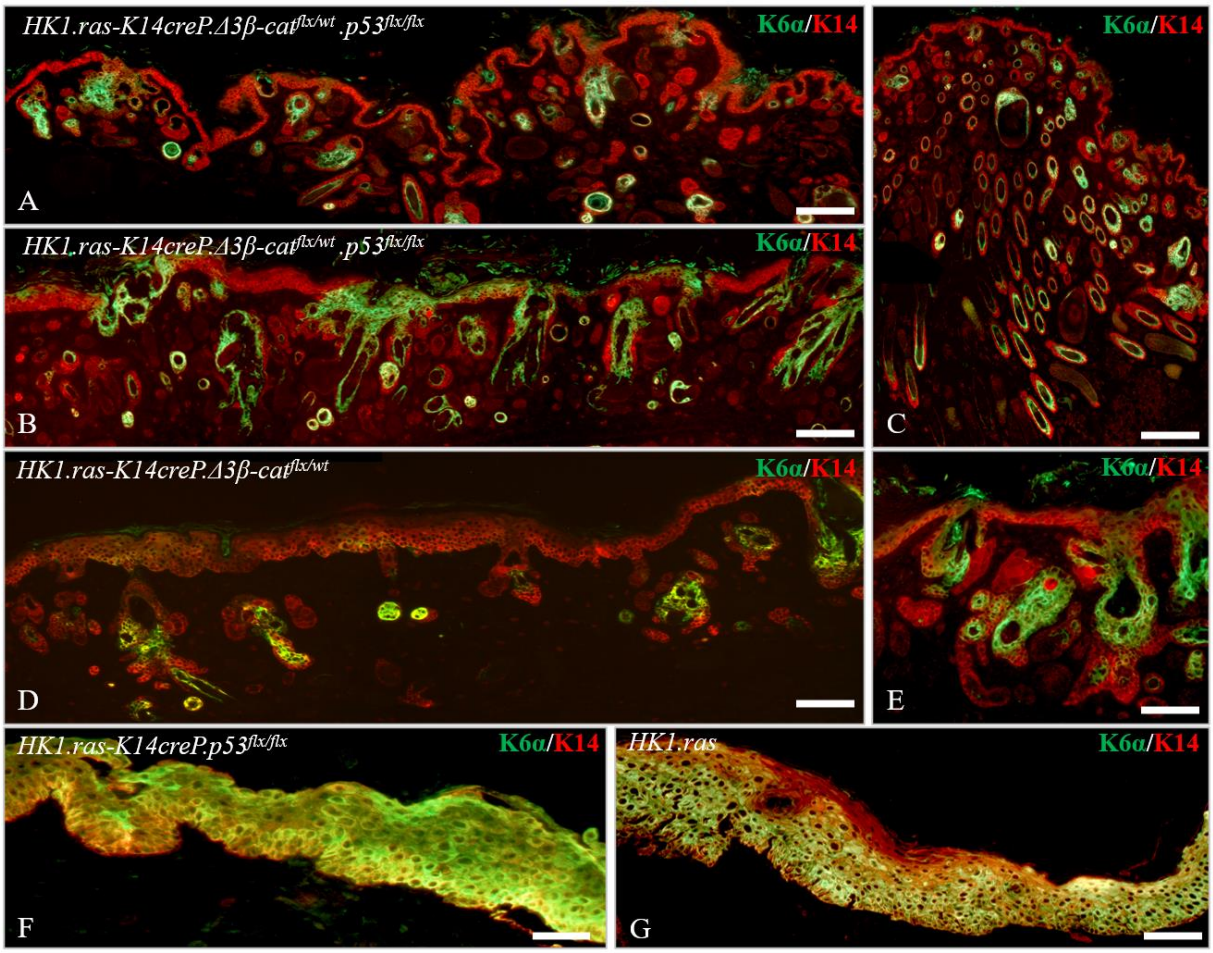

Figure 6. 11: Analysis of hyperproliferation marker K6α expression in HK1.ras-*K14creP.Δ3β-cat*$^{flx/wt}$*.p53*$^{flx/flx}$ epidermis.

[A-C] Separate examples of *HK1.ras-K14creP.Δ3β-cat*$^{flx/wt}$*.p53*$^{flx/flx}$ show K6α expression is absent in most epidermal areas with [B] expression in occasional patches of IFE otherwise K6 α is confined to the HFs and [C] some appear quite normal. Similarly, [D & E] *HK1.ras-K14creP.Δ3β-cat*$^{flx/wt}$ shows even less K6α expression in both IFE and only few HFs. [F] *HK1.ras-K14creP.p53*$^{flx/flx}$ and [G] *HK1.ras* both show strong K6α expression in IFE. Scale bars: A-F 150μm; G: 100μm

To-date this novel K6α observation remains unique to the *Δ3β-catenin* model and as speculated for K1 above, this change in K6α expression may reflect the alterations in adherence junction physiology that are normally essential for cell division and keratinocyte migration. These keratin data suggest that from a barrier viewpoint the keratins associated

with maintaining a supra-basal layer or in response to wounding are consistently reduced. In both cases this may be possibly due to p21 expression; as in some contexts excess p21 displays an inhibitory role in differentiation and affects a commitment to differentiate (*Di Cunto et al., 1998;Topley et al., 1999*) consistent with this delayed and patchy K1 finding; whilst p21 roles in cell cycle regulation would be consistent with reductions in K6α expression and a diminished level of hyperplasia in *HK1.ras-K14creP.Δ3β-cat*$^{flx/wt}$*.p53*$^{flx/flx}$ IFE and the hair follicle's reduced *Δ3βcatenin* phenotypes.

Therefore p21 levels were assessed which again showed strong nuclear expression in all IFE layers together with hair follicles in RU486-treated *HK1.ras-K14creP.Δ3β-cat*$^{flx/wt}$*.p53*$^{flx/flx}$ epidermis [Fig. 6.12 A]. The example shown at 8 weeks represents one of the most phenotypic examples and is included as this also clearly demonstrated the very strong levels of p21 in the upper layers of the hyperplastic *HK1.ras-K14creP.Δ3β-cat*$^{flx/wt}$*.p53*$^{flx/flx}$ IFE compared to an age matched *HK1.ras-K14creP.Δ3β-cat*$^{flx/wt}$ mouse also displaying a designated score 1 phenotype Fig. 6.12 A vs B]. In contrast *HK1.ras-K14creP.p53*$^{flx/flx}$ and *HK1.ras* control hyperplasia both lack such a compensatory p21 expression response consistent with their increased hyperplasia [Fig. 6.12D&E] and a general observation that p21 expression trailed that of p53 expression in papillomatogenesis [above; chapter 1: Fig.6]; becoming more effective at later stages in the inhibition of malignant progression as an antagonist to AKT and nuclear β-catenin (*Macdonald et al., 2014*). Thus, p21 expression in *HK1.ras* mice remained low unless the cell was committing to differentiate [Fig. 6.12 E].

Thus, as previously speculated for *HK1.ras-Δ3βcatenin* mice, increased compensatory basal layer p21 may inhibit the latter stages of differentiation and result in an apparent lack of K1 expression in *HK1.ras-K14creP.Δ3β-cat*$^{flx/wt}$*.p53*$^{flx/flx}$ (*Di Cunto et al., 1998*), with its roles in cell cycle reducing the proliferation hence reduced hyperplasia reflected by K6α, and in terms of papilloma formation, increased p21 would again inhibit tumours. Given that this effect of p21 expression appears immediately following p53 loss it appears quite a potent event at this early stage context alongside the apparent increase in adherence junctions mediated by elevated E-cadherin. This p21 expression and the lack of papillomas forming in *HK1.ras-K14creP.Δ3β-cat*$^{flx/wt}$*.p53*$^{flx/flx}$ mice indicated that elevated p21 levels maybe a key mechanism in halting early-stage tumorigenesis. However preliminary data suggests that p21ko may not be the key to tumour inhibition, as newly established *HK1.ras-K14creP.Δ3β-cat*$^{flx/wt}$*.p21KO* [n=5] were also devoid of tumour development [below Fig. 6.29]. Furthermore, all these data

highlight the complexity of these signalling systems and that in different contexts results may differ; and this was exemplified by the appearance of tumours in two *HK1.ras-K14creP.Δ3β-cat*$^{flx/wt}$*.p53*$^{flx/flx}$ mice.

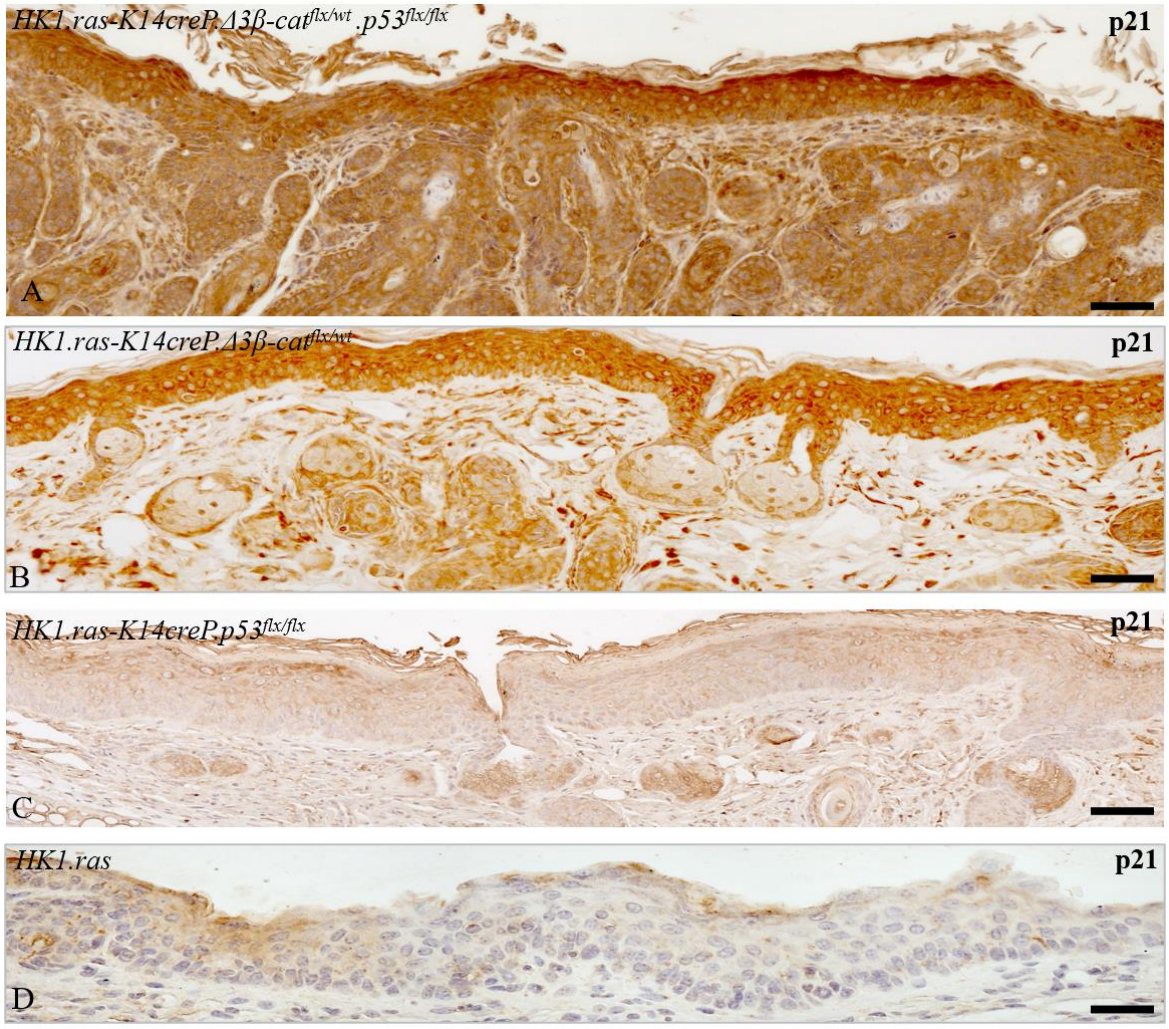

Figure 6. 12: Analysis of p21 expression in *HK1.ras-K14creP.Δ3β-cat*$^{flx/wt}$*.p53*$^{flx/flx}$ epidermis compared to *HK1.ras-K14creP.Δ3β-cat*$^{flx/wt}$ epidermis and treated *HK1.ras-K14creP.p53*$^{flx/flx}$ skin.

[A] Typically treated *HK1.ras-K14creP.Δ3β-cat*$^{flx/wt}$*.p53*$^{flx/flx}$ epidermis shows strong expression of p21 in all layers and HFs with a particular increase observable in the suprabasal layers. [B] *HK1.ras-K14creP.Δ3β-cat*$^{flx/wt}$ also shows strong expression in all layers and hair follicles but with less supra-basal expression. [C] Typical *HK1.ras-K14creP.p53*$^{flx/flx}$ epidermis lacks p21 compensatory expression to p53 loss similar to [D] weak expression almost absent from the *HK1.ras* IFE. Scale bars: A-C: 75µm; D: 50um.

Table 6. 1: Summary of *HK1.ras-K14creP.Δ3β-cat$^{flx/wt}$.p53$^{flx/flx}$* phenotypes and paradoxical lack of papillomatogenesis

Genotype analysed	[N]	Analysed for expression of	Data summary
HK1.ras hyperplasia	90	β-catenin, E-cadherin, K1, K6α, p53 and p21 expressions	-Control hyperplasia exhibiting membranous β-catenin/E-cadherin expression in supra-basal layers -ordered terminal differentiation indicated by supra-basal layer K1 and K6 expression in both supra- and basal layers due to HK1.ras activation -weak, sporadic basal layer p53/p21 expression
HK1.ras-K14creP.p53$^{flx/flx}$ hyperplasia	22	β-catenin, E-cadherin, K1, K6α, and p21 expressions	-Control hyperplasia exhibiting suprabasal layer membranous β-catenin/E-cadherin -ordered terminal differentiation indicated by suprabasal layer K1 and K6α expression in both supra and basal layers due to *HK1.ras* activation -weak basal layer p21
HK1.ras-K14creP.Δ3β-cat$^{flx/wt}$ [No papillomas]	58	β-catenin, E-cadherin, K1, K6α, p53 and p21 expressions	-No IFE tumours -More HF tumours and more cyts vs. *K14creP.Δ3β-cat$^{flx/wt}$* -Mild hyperplasia due to *HK1.ras* -Increased cytoplasmic/nuclear basal layer β-catenin with increased membranous basal layer β-catenin/E-cadherin due to Δ3β-catenin -More Aberrant confused terminal differentiation vs *K14creP.Δ3β-cat$^{flx/wt}$* indicated by patchy K1 expression but still maintain fairly normal K6α expression - Nuclear basal layer expression of p53/p21 halting Δ3β-catenin induced proliferation
HK1.ras-K14creP.Δ3β-cat$^{flx/wt}$.p53Flx [No papliommas]	15	β-catenin, E-cadherin, K1, K6α, and p21 expressions	-No IFE tumours -less HF tumours, less cysts and more normal looking HFs vs. *HK1.ras-K14creP.Δ3β-cat$^{flx/wt}$* genotyopes -Mild hyperplasia due to HK1.ras -Increased cytoplasmic/nuclear basal layer β-catenin with increased membranous basal layer β-catenin/E-cadherin due to Δ3β-catenin - Very disturbed terminal differentiation indicated by the almost complete absence of K1/ K6α expression exhibit for the normal expression of K6 in HF

			- Nuclear basal layer expression of p21 halting Δ3β-catenin induced proliferation
Conclusion: inducible loss of p53 with constitutive β-catenin activation [Δ3β-catenin] in conjunction with ras activation paradoxically block IFE tumours; a result similar to *HK1.ras-K14creP.Δ3β-cat*$^{flx/wt}$ yet with notable reduction in appearance and severity of Δ3β-catenin associated phenotypes. These data indicate that p53 expression played an integral role in inducing Δ3β-catenin phenotypes but not terms of blocking papillomatogenesis at this stage in juveniles following β-catenin activation			

6.4 Conditional loss of *p53* elicits rare *HK1.ras-K14creP.Δ3β-cat*$^{flx/wt}$*.p53*$^{flx/flx}$ papillomas and co-operated with β-catenin to produce SCC

Previous studies have shown another completely paradoxical inhibition of *HK1.ras* tumours occurred following generic *p53* knockout (*Donehower et al., 1992; Greenhalgh et al., 1996*) and hints at the potent responses available to the epidermis that help prevent tumours forming and are logical in a tissue most exposed to environmental carcinogens such as UV-B. Thus, employing the same *cre/loxP* system to target p53 loss to the epidermis, it was originally envisaged that constitutive inducible *HK1.ras-K14creP.p53*$^{flx/flx}$ would co-operate with Δ3β-catenin whereby β-catenin activation elicited papillomas that were prone to conversion due to p53 loss, as suggested in *HK1ras/fos.Δ5PTEN* experiments [Chapter 3]. However, to date only two *HK1.ras-K14creP.Δ3β-cat*$^{flx/wt}$*.p53*$^{flx/flx}$ individuals developed papillomas [Fig. 6.13A-C] and despite a similar timeline in their appearance, unlike the two papillomas formed in *HK1.ras-K14creP.Δ3β-cat*$^{flx/wt}$ mice which remained small and benign [Fig.6.13: D & E]; by 8 weeks post tag, the *HK1.ras-K14creP.Δ3β-cat*$^{flx/wt}$*.p53*$^{flx/flx}$ tumours had change their appearance to one more typical of conversion to wdSCC. Despite their relatively small size, both tumours adopted a redder colouring and an oval shape with a depressed centre [Fig.6.13: B & C]. These are all characteristics of SCC in this model [Chapters 1 & 3].

Again, of note, these two *HK1.ras-K14creP.Δ3β-cat*$^{flx/wt}$*.p53*$^{flx/flx}$ individuals were of a full size at the time of tail tip biopsy, with little evidence of the internal β-catenin phenotypes, and they remained relatively phenotype free even following treatment with RU486 [Fig. 6.13 F]. Their

skin also showed very weak hyperkeratosis consistent with the continued *Δp53*-mediated inhibition of *Δ3β-catenin* phenotypes compared to that of wt p53 *HK1.ras-K14creP.Δ3β-cat*$^{flx/wt}$ parents [Fig. 6.13F vs. G] or older p53 heterozygous *HK1.ras-K14.Δ3β-cat*^{het}*/p53*$^{flx/wt}$ littermates [above]. These data indicated that the tumour inhibitory responses to *Δ3β-catenin* activation appeared during development, in response to the time and degree of the cre leakage levels and the overall phenotypes in skin appear to depend upon the functions of p53; or responses to p53 loss.

The observation that papillomas appeared in full sized mice was identical to that observed in *HK1.ras-K14creP.Δ3β-cat*$^{flx/wt}$ [above] where full sized, score 0 mice were the only mice to go on to develop papilloma, as illustrated earlier in Chapter 5; although these exhibited a greater degree of keratosis when treated with RU486 [Fig. 6.13G]. In these instances of papilloma formation, the normal size of these mice, which appears independent of p53, appears to be required in both *HK1.ras-K14creP.Δ3β-cat*$^{flx/wt}$ and *HK1.ras-K14creP.Δ3β-cat*$^{flx/wt}$*.p53*$^{flx/flx}$ mice, otherwise the early responses to *Δ3β-catenin* activation inhibit papilloma, and now these results suggest that effects appear to be either independent of p53 too; or responses to loss of p53 give a similar effect to *Δ3β-catenin* overexpression [see below; p73 and 63 analysis]. However, a significant effect of p53 loss appeared later, as once allowed, the papillomas that formed in *HK1.ras-K14creP.Δ3β-cat*$^{flx/wt}$*.p53*$^{flx/flx}$ mice converted to malignant SCC [Figs 6.14 & 6.15].

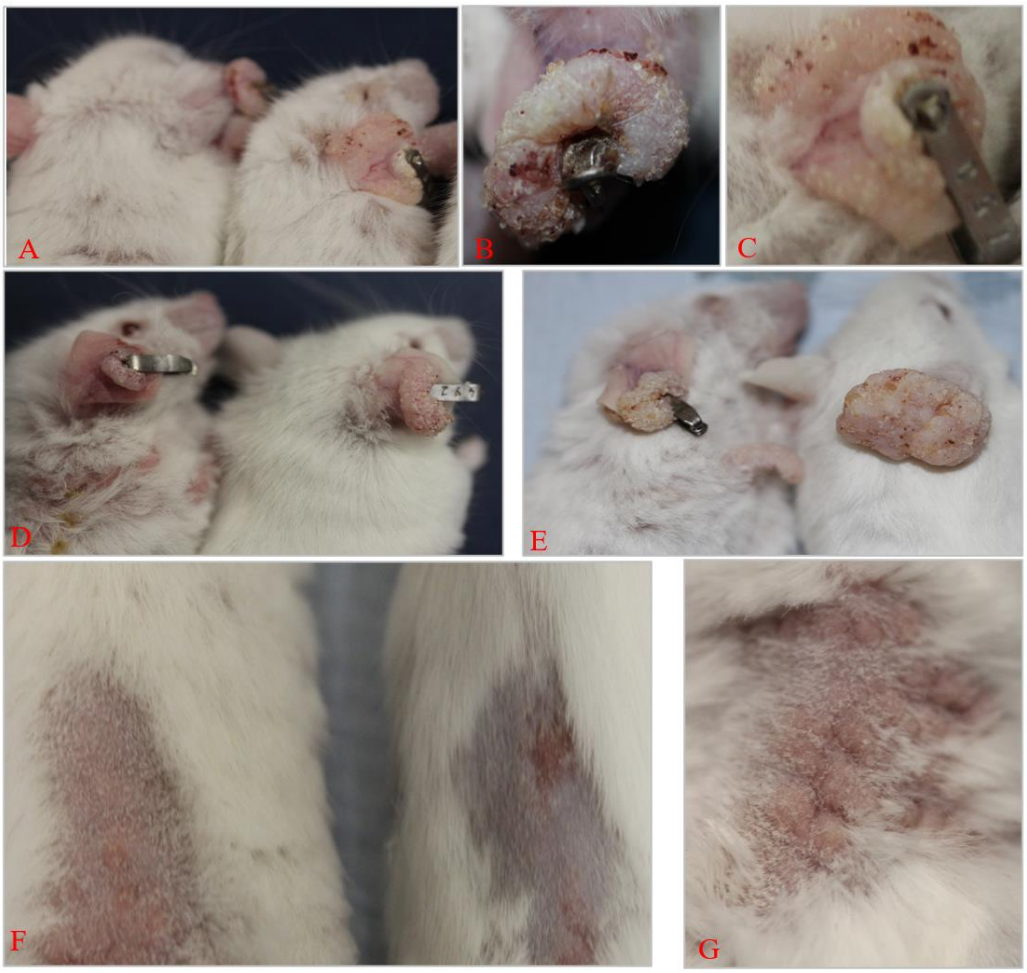

Figure 6. 13: Comparison of papillomas in *HK1.ras-K14creP.Δ3β-cat*$^{flx/wt}$*.p53*$^{flx/flx}$ to *HK1.ras-K14creP.Δ3β-cat*$^{flx/wt}$ and *HK1.ras* papillomas suggests malignant conversion.

[A-C] shows the only two examples of *HK1.ras-K14creP.Δ3β-cat*$^{flx/wt}$*.p53*$^{flx/flx}$ mice that developed tumours where at higher magnification [B] shows an aggressive, ovoid tumour a shape which suggests papilloma conversion and [C] smaller doughnut-shaped tumour with a depressed centre again typical of a papilloma converting to wdSCC. [D & E] For comparison [left] rare *HK1.ras-K14creP.Δ3β-cat*$^{flx/wt}$ papillomas remain small and [right] *HK1.ras* littermates exhibit bigger but still benign papillomas. [F] Shows that both *HK1.ras-K14creP.Δ3β-cat*$^{flx/wt}$*.p53*$^{flx/flx}$ mice that developed tumours were full sized and lack the hyperkeratosis seen in [G] their age-matched *HK1.ras-K14creP.Δ3β-cat*$^{flx/wt}$ equivalents.

In a change to the papilloma formation observed in *HK1.ras-K14creP.Δ3β-cat*$^{flx/wt}$ mice, the histological analysis of the larger *HK1.ras-K14creP.Δ3β-cat*$^{flx/wt}$*.p53*$^{flx/flx}$ tumour confirmed that this papilloma had become malignant [Fig. 6.14 & Fig. 6.15]. That this malignant conversion relied on acquisition of additional mutations due to loss of the p53 genomic guardian roles was suggested by the fact that this tumour possessed benign papilloma histotypes [Fig. 6.14A&B] together with a rapid progression to more aggressive SCC [Fig.

6.15 C & D] and also to areas of highly invasive pdSCC [Fig. 6.15E; confirmed by K1 expression].

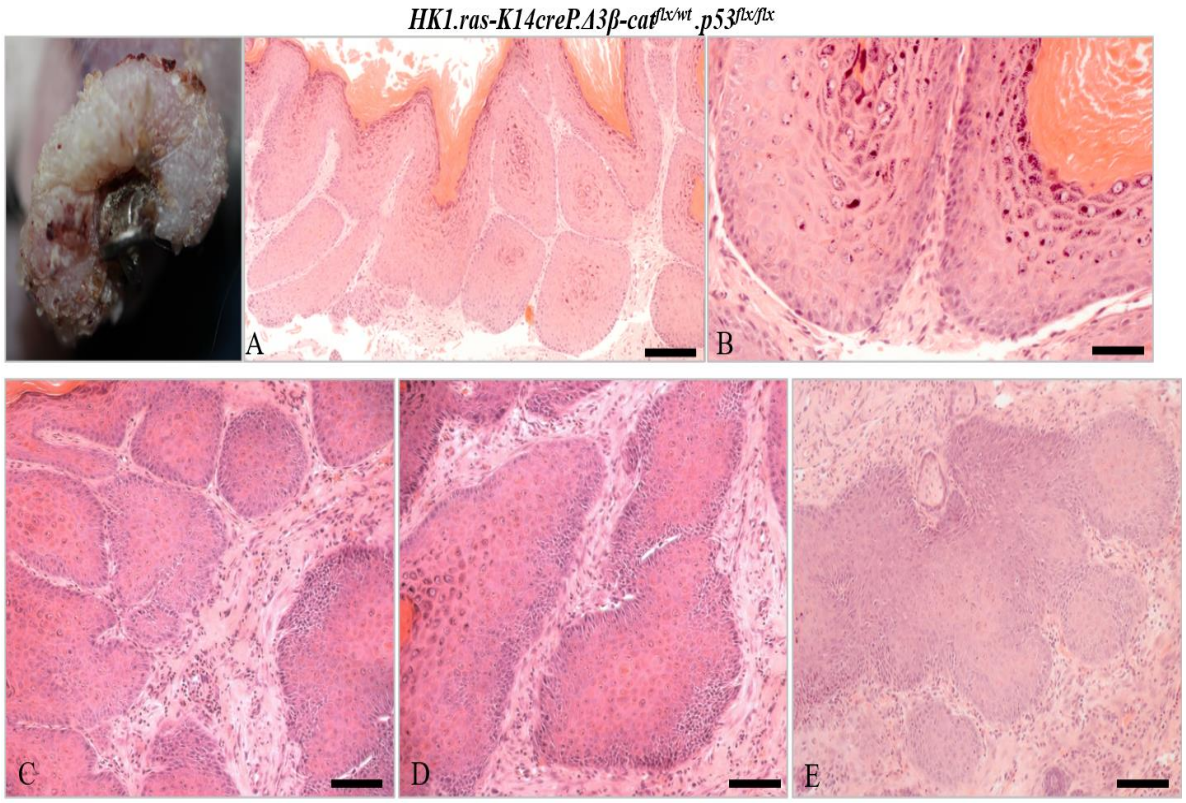

Figure 6. 14: Histological analysis of *HK1.ras-K14creP.Δ3β-cat$^{flx/wt}$.p53$^{flx/flx}$* tumours confirms papilloma conversion to aggressive SCC.

[A & B] *HK1.ras-K14creP.Δ3β-cat$^{flx/wt}$.p53$^{flx/flx}$* tumour [insert] shows a component of benign papilloma tissue evidenced by [B] at higher magnification, the ordered differentiation, lack of a disrupted basal layer and appearance of keratin pearls. [C-E] Alternate sections show malignant conversion to give [C] a mix of wdSCC and SCC; [D] more uniform aggressive SCC and progression to [E] poorly differentiated SCC as evidenced by the presence of highly invasive cells from a very disordered basal layer basal layer and the failure to differentiate correctly. scale bars: A C & D:100µ; B: 75µm; E: 150µm.

A comparison of histotypes between *HK1.ras-K14creP.Δ3β-cat$^{flx/wt}$.p53$^{flx/flx}$* tumours and the small papillomas in *HK1.ras-K14creP.Δ3β-cat$^{flx/wt}$* and typical larger *HK1.ras* papillomas [Fig. 6.15] showed that in these age matched tumours, already p53 loss in *HK1.ras-K14creP.Δ3β-cat$^{flx/wt}$.p53$^{flx/flx}$* tumours possessed many areas of malignancy and the papilloma appeared more aggressive compared to the small size or invasiveness of *HK1.ras-K14creP.Δ3β-cat$^{flx/wt}$* or even larger *HK1.ras* papillomas due the presence of normal p53 function.

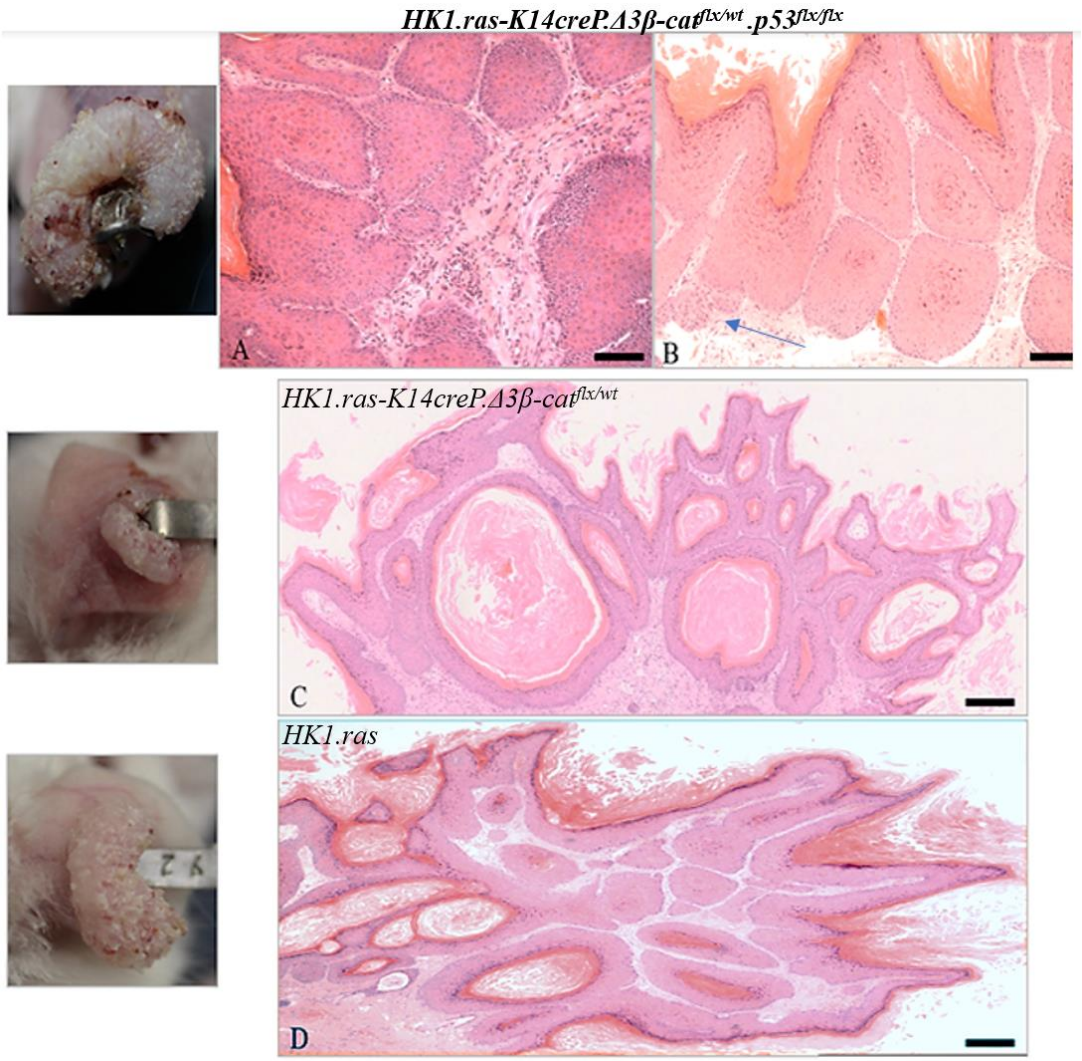

Figure 6. 15: Histological analysis of *HK1.ras-K14creP.Δ3β-cat*$^{flx/wt}$*.p53*$^{flx/flx}$ tumour against *HK1.ras-K14creP.Δ3β-cat*$^{flx/wt}$ and *HK1.ras* benign papillomas.

[A] *HK1.ras-K14creP.Δ3β-cat*$^{flx/wt}$*.p53*$^{flx/flx}$ displays a mix of wdSCC [left] and invasive SCC [right] and [B] shows benign papilloma with an ordered basal layer except in one part that looks like the beginnings of carcinoma *in situ* [arrow]. [C] The smaller [insert] *HK1.ras-K14creP.Δ3β-cat*$^{flx/wt}$ tumour shows uniform benign papilloma with many keratin pearls similarly [D] a typically larger [insert] *HK1.ras* papilloma also shows a uniform benign papilloma. Scale bars: A & B:100µm; C & D: 150µm

Analysis of β-catenin expression in *HK1.ras-K14creP.Δ3β-cat*$^{flx/wt}$*.p53*$^{flx/flx}$ tumours also suggested that the earlier benign papilloma histotypes were more aggressive, as papilloma histotypes already showed strong nuclear β-catenin expression but with reduced membranous expression in basal layers [Fig. 6.16A&B] consistent with a greater degree of papilloma progression due to p53 loss as indicated by their histotype [above Fig. 6.15B]. This pattern of expression was even present in parts of the ear hyperplasia prior to tumour formation, as it was already showing nuclear localization of β-catenin in all basal layer cells but with very weak

membranous expression [Fig. 6.16B]. Indeed, this effect was clearly demonstrated in areas of malignant progression [Fig. 6.16C-G] as wdSCC progressed through to SCC and further to pdSCC, as at each stage even stronger nuclear expression appeared with a complete loss of membranous β-catenin expression by the time the aggressive SCC and pdSCC stage was reached [Fig. 6.16D-G].

In contrast the rare *HK1.ras-K14creP.Δ3β-cat*$^{flx/wt}$ papillomas exhibited strong nuclear expression as well, but still maintained strong membranous β-catenin expression in basal layers [Fig. 6.16H], whilst *HK1.ras* papillomas exhibited membranous expression in mainly supra-basal layers with only sporadic nuclear expression [Fig. 6.16H]. This result therefore is in agreement with the original hypothesis, where endogenous β-catenin expression in *HK1.ras/fos-K14creP.Δ5PTEN*$^{flx/flx}$ SCC was theorised to facilitate conversion and tumour progression after the loss of p53 expression [See chapter 3].

With respect to E-cadherin, as outlined above, in general its expression had mirrored that of β-catenin [above section 6.3, Fig. 6.17A B] and despite p53 loss in *HK1.ras-K14creP.Δ3β-cat*$^{flx/wt}$*.p53*$^{flx/flx}$ mice, an increased cell-cell adhesion was still maintained in basal layers by E-cadherin expression [Fig. 6.17A&B] similar to *HK1.ras-K14creP.Δ3β-cat*$^{flx/wt}$ epidermis and the resultant papilloma inhibition. However, in *HK1.ras-K14creP.Δ3β-cat*$^{flx/wt}$*.p53*$^{flx/flx}$ papillomas, E-cadherin expression appeared more like that of a typical *HK1.ras* hyperplasia, in being mainly expressed in the supra-basal layers [Fig. 6.17A vs. G]. This again repeated a similar observation for *HK1.ras-K14creP.Δ3β-cat*$^{flx/wt}$ papillomas [Fig. 6.17A vs. H; above chapter 5]. This lack of basal layer expression appeared for both β-catenin and E-cadherin in *HK1.ras-K14creP.Δ3β-cat*$^{flx/wt}$*.p53*$^{flx/flx}$ mice destined to produce papillomas [a direct comparison is shown in Fig. 6.18A vs. B]. Thus, this suggests that if there was an absence of the responses to β-catenin deregulation in these normal sized mice due to p53 loss, the reduced numbers of adherence junctions may have allowed papillomas to form; and this is reflected by the supra-basal E-cadherin expression in most *HK1.ras-K14creP.Δ3β-cat*$^{flx/wt}$*.p53*$^{flx/flx}$ papillomas and some strands of *HK1.ras-K14creP.Δ3β-cat*$^{flx/wt}$ papilloma basal layers [Fig. 6.17A&H].

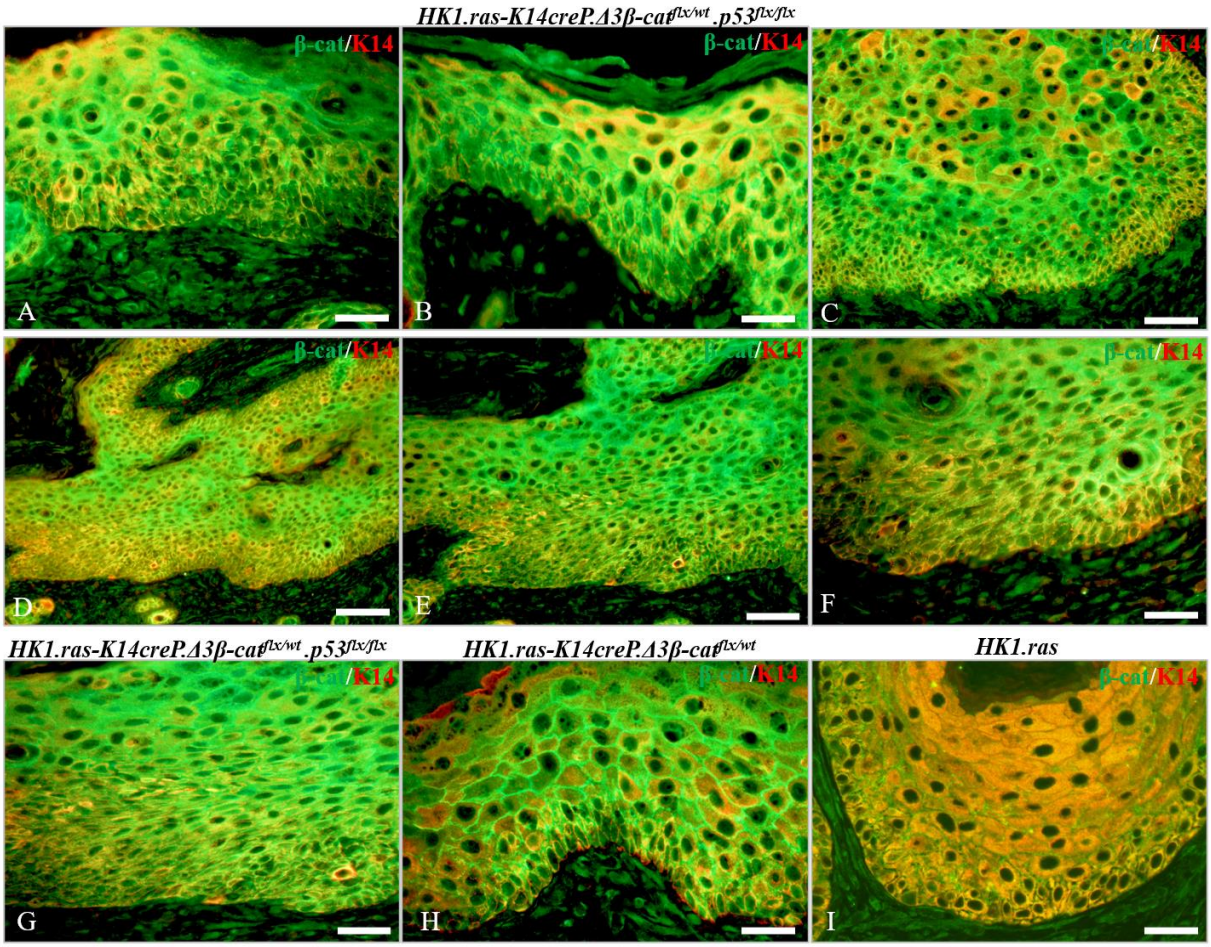

Figure 6. 16: Analysis of β-catenin expression in *HK1.ras-K14creP.Δ3β-cat*$^{flx/wt}$*.p53*$^{flx/flx}$ papilloma.

[A & B] Early *HK1.ras-K14creP.Δ3β-cat*$^{flx/wt}$*.p53*$^{flx/flx}$ ear hyperplasia displays elevated nuclear β-catenin expression in basal layer keratinocytes there is a clear reduction in membranous expression. [C-F] β-catenin expression increases as *HK1.ras-K14creP.Δ3β-cat*$^{flx/wt}$*.p53*$^{flx/flx}$ tumours convert to malignancy and undergo further malignant progression [C] wdSCC/SCC shows mostly nuclear but some membranous expression in the invasive basal layers which becomes progressively less in [D] SCC and [E] pdSCC at low and [F & G] higher magnification shows weak to no membranous β-catenin expression. [H] *HK1.ras-K14creP.Δ3β-cat*$^{flx/wt}$ papilloma exhibits both nuclear and membranous expression; whilst [I] *HK1.ras* papillomas exhibit only membranous, supra-basal expression. Scale bars: A, C, F, G & I : 75 µm; B & H: 50 µm; E: 100µm; D: 150 µm.

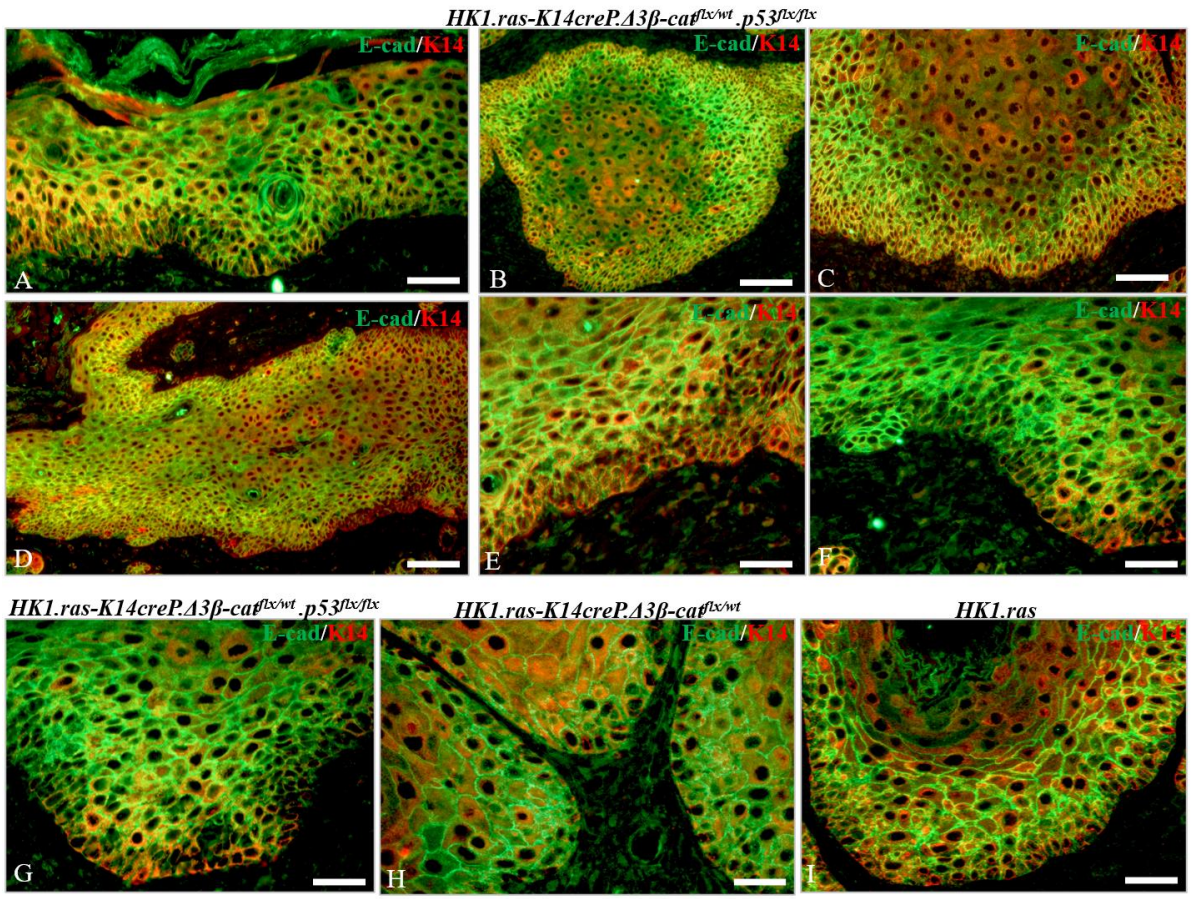

Figure 6. 17: Analysis of E-cadherin expression in *HK1.ras-K14creP.Δ3β-cat$^{flx/wt}$.p53$^{flx/flx}$* papilloma and malignant histotypes.

[A] *HK1.ras-K14creP.Δ3β-cat$^{flx/wt}$.p53$^{flx/flx}$* tumours with an early pre-papilloma histotype shows an ear skin where membranous E-cadherin expression in the basal layers is weak to none. [B-F] Expression of E-cadherin in progression of *HK1.ras-K14creP.Δ3β-cat$^{flx/wt}$ .p53$^{flx/flx}$* tumours from wdSCC through SCC and on pdSCC. [B] Initially wdSCC/SCCs exhibit strong E-cadherin expression in a halo of immediate supra-basal membranous expression, but with less membranous expression in the invasive cells of the basal layer. [C] Similarly, aggressive SCC exhibits an increase set of invasive basal layer cells that express little membranous E-cadherin. [D] Low magnification specimen of SCC and pdSCC shows a clear loss of membranous E-cadherin expression in the pdSCC [right; red of invasive basal layers]; highlighted at higher magnification in [E] SCC and [F] the edge of SCC and pdSCC. [G] E-cadherin expression in benign *HK1.ras-K14creP.Δ3β-cat$^{flx/wt}$.p53$^{flx/flx}$* papilloma exhibits little to no membranous expression in basal layers compared to [H] *HK1.ras-K14creP.Δ3β-cat$^{flx/wt}$* papilloma that mainly exhibits membranous suprabasal expression but possesses strands of E-cadherin negative basal layers. [I] *HK1.ras* papilloma exhibits membranous supra-basal expression. Scale bars: A, F, G & I: 75 µm; H: 50 µm; C: 100µm; B & D: 150 µm.

Moreover, with respect to tumour progression following p53 loss, there appears to be a very clear correlation between strong nuclear β-catenin expression and an increasing reduction of E-cadherin in the invasive basal layers that supports the collective model of tumour invasion (*Hesse et al., 2016*) via a loss of cell-cell adhesion mediated by adherence junctions [Fig. 6.17 and Fig. 6.18]. Analysis of E-cadherin as *HK1.ras-K14creP.Δ3β-cat*$^{flx/wt}$*.p53*$^{flx/flx}$ progressed from wdSCC through SCC and on to become pdSCC showed that initial membranous expression in basal layers correlated with that of nuclear β-catenin and resulted in a halo effect [Fig. 6.17B]. With time this strong membranous E-cadherin continued in supra-basal cells with less membranous expression in the invasive cells of the basal layers [Fig. 6.17C; Fig. 6.18C vs. D; E vs. F]. On malignant progression to a more uniform SCC histology, the increasing numbers of aggressive invasive basal layer cells gradually expressed less membranous E-cadherin, but the supra-basal expression remained [Fig. 6.17C&E]. On further progression to pdSCC [Fig. 6.17D&F] almost complete loss of E-cadherin expression was observed in the pdSCC component [Fig. 6.17D right hand side].

In contrast, as reported in Chapter 5 [Fig. 5.15] whilst the earlier *HK1.ras-K14creP.Δ3β-cat*$^{flx/wt}$ hyperplasia possessed strands of weaker basal layer E-cadherin expression, in its papilloma mainly membranous basal layer E-cadherin expression was observed, hence the lack of tumour progression [Fig. 6.17H]. *HK1.ras* control papillomas exhibited typical supa-basal and membranous E-cadherin expression [Fig. 6.17I] and a lack of progression in this case was due to the suprabasal expression of β-catenin [Fig. 6.16I] coupled to compensatory p53 and p21 expression. Additionally, a direct comparison of the expression of β-catenin/E-cadherin in *HK1.ras-K14creP.Δ3β-cat*$^{flx/wt}$*.p53*$^{flx/flx}$ papillomas showed the correlation between increased nuclear β-catenin localization with this reduced membranous expression of E-cadherin in basal layers but the retention in suprabasal cells as tumours became invasive.

In pre-papilloma ear skin [Fig. 6.18A vs. B], the beginnings of elevated nuclear β-catenin in basal layer keratinocytes appeared less membranous, and thus less E-cadherin expression appeared in the basal layers resulting in less cell-cell adhesion to form adherence junctions giving the susceptibility to form papillomas. Further, the appearance of the halo effect [Fig. 6.18C&D] at higher magnification shows the intensity of nuclear β-catenin expression directly correlates with the weakened E-cadherin expression in the invasive cells and a band of strong E-cadherin immediately behind this invasive front. These data are constant with *HK1.ras/fos-K14creP.Δ5PTEN*$^{flx/flx}$ β-catenin/E-cadherin interactions [see Chapter 3] and the literature

concerning expression of β-catenin/E-cadherin in the invasive modes driving SCC carcinoma (*Grigoryan et al., 2008; Clevers and Nussse, 2012; Hesse et al., 2016*).

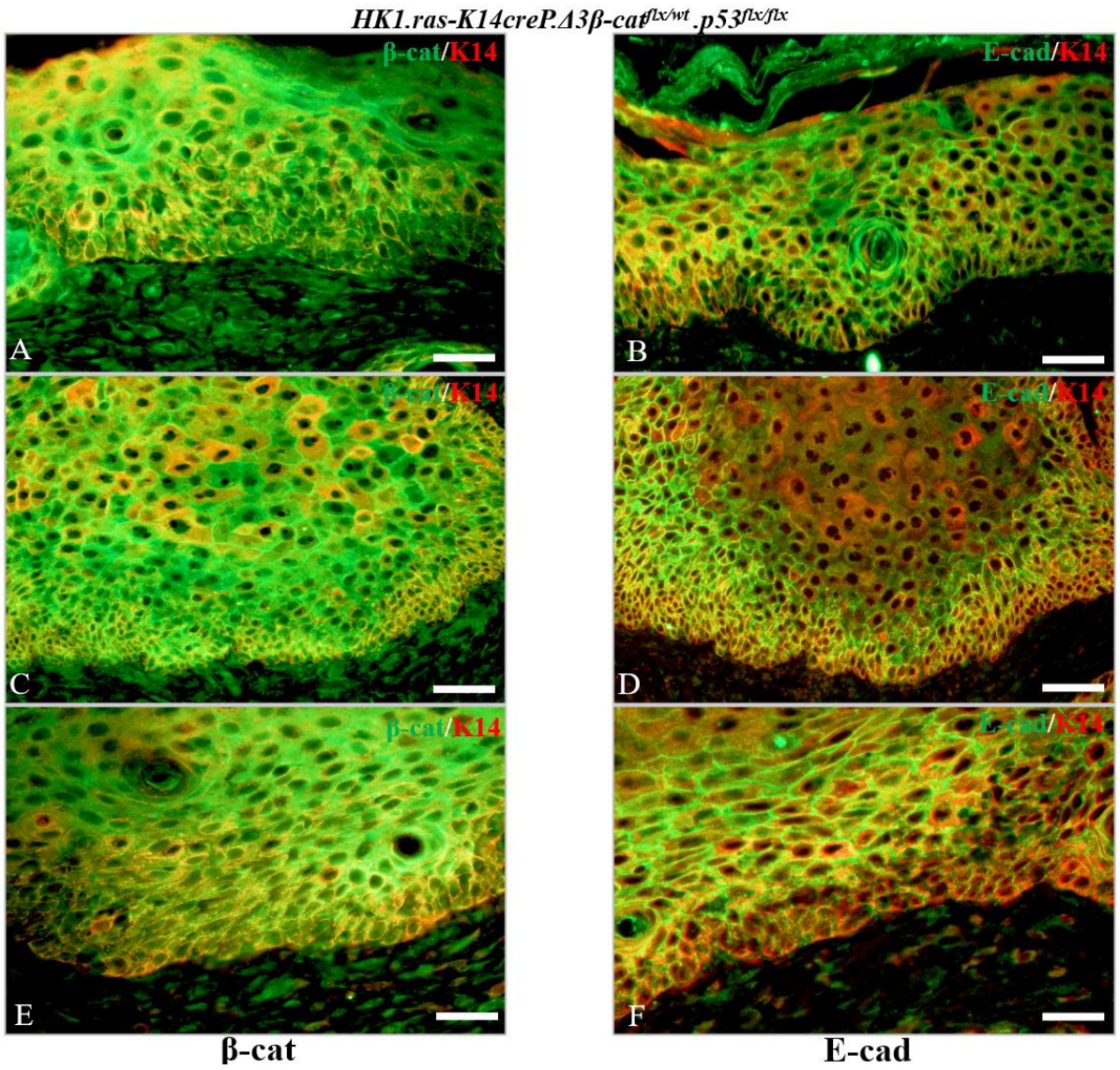

Figure 6. 18: Comparison of β-catenin and E-cadherin expression in *HK1.ras-K14creP.Δ3β-cat$^{flx/wt}$.p53$^{flx/flx}$* papilloma and malignant histotypes.

[A] β-catenin and [B] E-cadherin expression in early pre-papilloma histotype shows ear skin where elevated nuclear β-catenin expression appears in basal layer keratinocytes with reduced membranous expression, whereas membranous E-cadherin expression in the basal layers is weak to none. [C] β-catenin and [D] E-cadherin expression in [C] malignant wdSCC/SCC shows strong nuclear β-catenin expression with some residual membranous expression in the wdSCC component that disappears in the SCC part. [D] The serial section of E-cadherin expression parallels this result with an increasing level of low E-cadherin expression as the invasive layers increase. At higher magnification [E] β-catenin and [F] E-cadherin expression demonstrate that clear nuclear localization of β-catenin correlates with loss of membranous E-cadherin expression. Scale bars: A, B, E & F 50 µm; C & D: 75 µm.

Analysis of the early differentiation marker K1 showed a gradually disappearing expression profile as *HK1.ras-K14creP.Δ3β-cat*$^{flx/wt}$*.p53*$^{flx/flx}$ papillomas progressed from wdSCC through to SCC [Fig. 6.19A&B]. The example shown is the serial section from Fig. 6.16D and Fig. 6.17 D that also possessed areas of hyperplasia. Thus, unlike a typical *HK1.ras-K14creP.Δ3β-cat*$^{flx/wt}$*.p53*$^{flx/flx}$ epidermis [above], in this individual the hyperplasia was K1^{+ve}; although expression was more reduced following p53 loss [i.e., yellow/red not green/red] compared to K1 expression in the earlier *HK1.ras-K14creP.Δ3β-cat*$^{flx/wt}$ individuals that also went on to develop papillomas [Fig. 6.19C & D]. This result suggests as with their histology [Fig. 6.15B-arrow] the hyperplasia in *HK1.ras-K14creP.Δ3β-cat*$^{flx/wt}$*.p53*$^{flx/flx}$ -specific epidermis was more transformed hence production of larger papillomas once treated with RU486 to eliminate p53 and activate Δ3β-catenin expression consistent with the susceptibility to become malignant and the potential to progress to aggressive K1^{-ve} SCC.

On the other hand, the hyperproliferation marker K6α again showed an overall patchy expression profile in serial sections that was similar to expression in *HK1.ras-K14creP.Δ3β-cat*$^{flx/wt}$*.p53*$^{flx/flx}$ skin that lacked papilloma and in this p53 null context, K6α expression did not appear until overt papilloma/wdSCC formed [Fig. 6.20A]. Indeed although SCC/pdSCC exhibited strong levels of K6α tumours, the actual invasive layers were K6α negative [Fig. 6.20B] similar to the *HK1.ras-K14creP.Δ3β-cat*$^{flx/wt}$ individuals but not *HK1.ras* papillomas [Fig. 6.20C vs. D]. This again links to their β-catenin/E-cadherin profiles [above] where abnormal presence of adherence junctions in the basal layers send incorrect signals for the ordered differentiation and lead to a lack of K6α expression. Here, in this example the reduced responses to either β-catenin or p53 loss allowed a certain level of K6α expression [Fig. 6.20 A] consistent with a more aggressive hyperplasia [Fig. 6.15B] and this suggested this combination of p53 loss and β-catenin/E-cadherin profiles created a more aggressive papilloma [with weaker K1 expression; [Fig. 6.19A&B] prone to become malignant given the uniform levels of K6α observed in the SCC [Fig. 6.20B]. If so, these data also suggest that the aetiology of this carcinoma prone *HK1.ras-K14creP.Δ3β-cat*$^{flx/wt}$*.p53*$^{flx/flx}$ papilloma was already different at the earliest stage in this p53 null contact compared to earlier *HK1.ras-K14creP.Δ3β-cat*$^{flx/wt}$ individuals that developed papillomas. This idea and conclusion was also suggested by the keratin K15 analysis which again found a lack of this stem cell marker in *HK1.ras-K14creP.Δ3β-cat*$^{flx/wt}$*.p53*$^{flx/flx}$ vs. *HK1.ras-K14creP.Δ3β-cat*$^{flx/wt}$ papillomas [see section 6.5 Fig. 6.26 and Fig. 6.27].

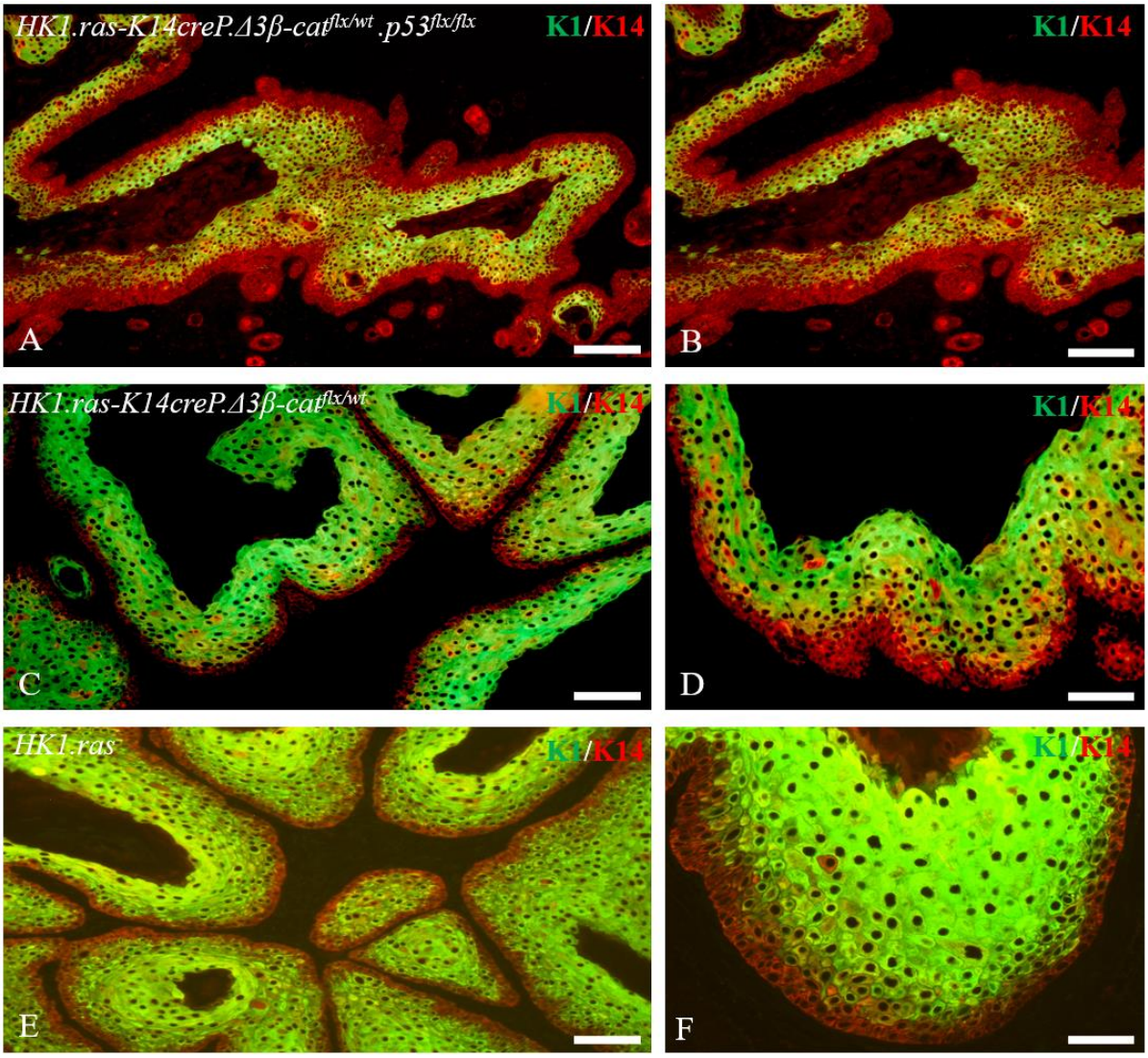

Figure 6. 19: Analysis of K1 expression in converting *HK1.ras-K14creP.Δ3β-cat$^{flx/wt}$.p53$^{flx/flx}$* papilloma.

[A & B] K1 expression in a *HK1.ras-K14creP.Δ3β-cat$^{flx/wt}$.p53$^{flx/flx}$* papilloma with areas converting to wdSCC shows a fairly uniform not patchy expression but levels overall are reduced expression in the K1 positive hyperplasia [i.e., yellow/red not green/red]. In the progression to wdSCC/SCC areas K1 expression is reduced further and becomes lost in aggressive SCC. [C & D] Low and high magnification of *HK1.ras-K14creP.Δ3β-cat$^{flx/wt}$* papilloma shows a relatively normal [green/red] K1 expression profile in supra-basal layers; whilst [E & F] exhibit the ordered differentiation and smooth basal/supra-basal interactions of typical *HK1.ras* papillomas. Scale bars: A & B: approx. 150 µm; C & E: 75 µm. D & F: 50 µm.

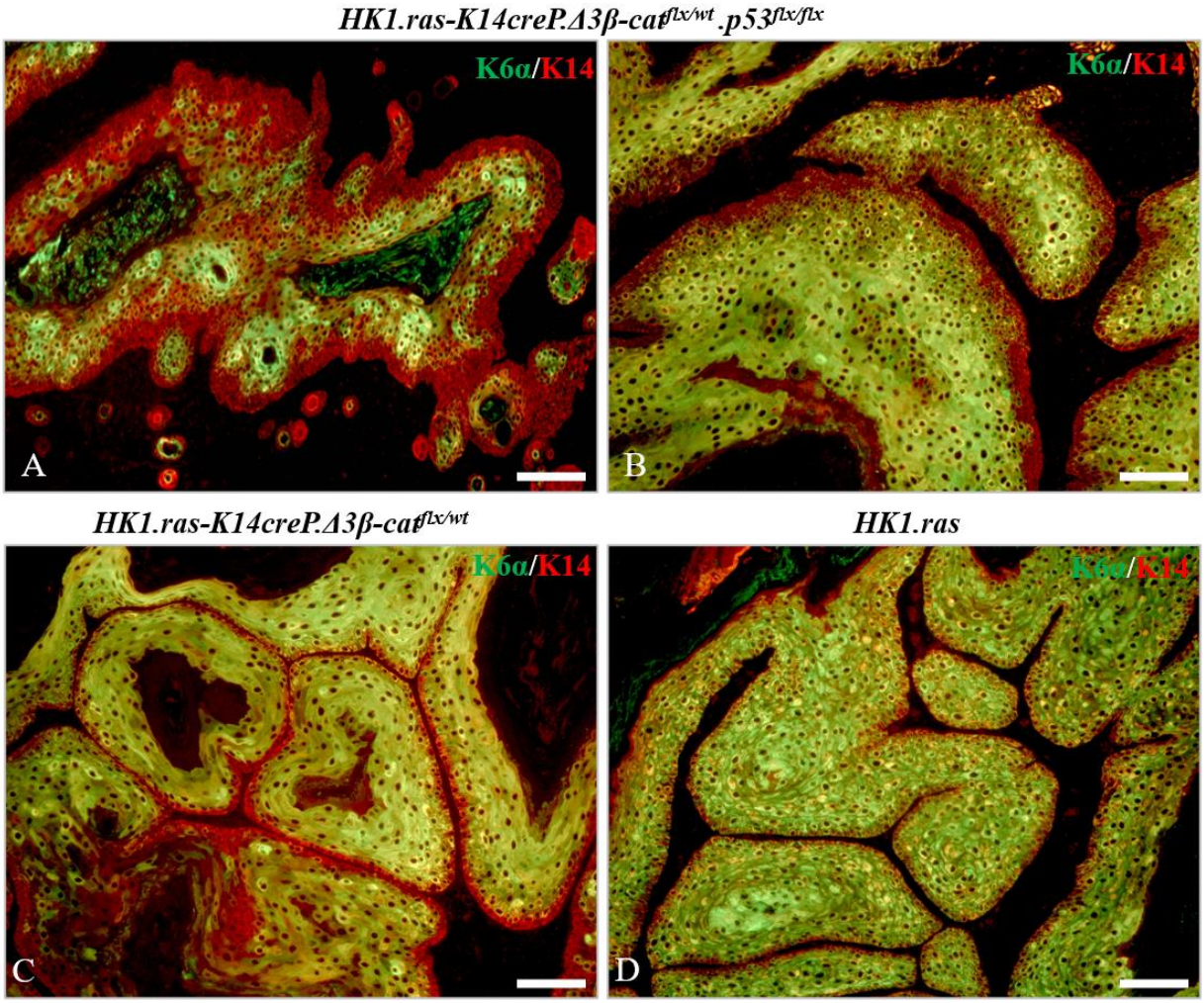

Figure 6. 20: Analysis of K6α expression in *HK1.ras-K14creP.Δ3β-cat*$^{flx/wt}$*.p53*$^{flx/flx}$ papilloma and carcinoma.

[A] K6α expression in *HK1.ras-K14creP.Δ3β-cat*$^{flx/wt}$*.p53*$^{flx/flx}$ hyperplasia/papilloma now shows patchy expression in areas converting to wdSCC/SCC that become uniform in [B] SCC/pdSCC tumours; although the invasive layers are K6α negative alongside that of nuclear β-catenin and the halo of suprabasal E-cadherin. [C] *HK1.ras-K14creP.Δ3β-cat*$^{flx/wt}$ papillomas exhibit strong K6α expression in suprabasal layer but again lacking in basal layers similar to [B]; whilst [D] shows *HK1.ras* papillomas express K6α in both supra-basal and basal layers Scale bars: A- D: 150μm

Thus, expression of both K1 and K6α in *HK1.ras-K14creP.Δ3β-cat*$^{flx/wt}$*.p53*$^{flx/flx}$ hyperplasia suggest that this papilloma-prone p53 null epidermis was closer to the phenotype of a typical *HK1.ras* skin. This was also suggested by the two papilloma forming *HK1.ras-K14creP.Δ3β-cat*$^{flx/wt}$ individuals, where a similar normalised expression of K1 and K6α was observed due to late expression of Δ3β-catenin. These data also suggest that if the inhibitory responses to β-catenin and/or p53 loss are similarly overcome, circumvented or simply not deployed [as

suspected] for *HK1.ras* epidermis [Chapter 1; Fig. 1.7]; once a papilloma formed in these *HK1.ras-K14creP.Δ3β-cat*$^{flx/wt}$*.p53*$^{flx/flx}$ mice it quickly converted to malignancy due to p53 loss and lack of p21 contributed to progression.

Furthermore, based on the odd patchy K6α expression and the K15 expression [below] it suggests that there is a separate type of papilloma forming from *HK1.ras-K14creP.Δ3β-cat*$^{flx/wt}$*.p53*$^{flx/flx}$ hyperplasias with a greater propensity to convert to malignancy e.g., a type 2 vs type 1 papilloma (*Hennings et al., 1993; Greenhalgh et al., 1989*). If so, unlike *HK1.ras-K14creP.Δ3β-cat*$^{flx/wt}$ papillomas or *HK1.ras/fos- Δ5PTEN*$^{flx/flx}$ genotypes, the resultant wdSCCs rapidly progressed to SCC and pdSCC histotypes within the same tumour. This not only highlights the instability of the genome following p53 loss, but also suggest a failure in other genes such as p21 that were present in *HK1.ras/fos- Δ5PTEN*$^{flx/flx}$ skin to offset expression of nuclear β-catenin [Chapter 1 Fig. 8; Chapter 3: Figs. 3.3] and activated AKT (*Macdonald et al., 2014*) and inhibit further malignant progression.

This proved to be the case as analysis of p21expression levels in these two individual *HK1.ras-K14creP.Δ3β-cat*$^{flx/wt}$*.p53*$^{flx/flx}$ found that tumour suppresser gene p21 expression was already absent at the papilloma stage [Fig. 6.21 A & B]. This was also indicative of the rapid conversion to malignancy and the lack of protection so that WDCSS rapidly progressed to SCC and pdSCC [Fig. 6.21C&D]. Again in contrast, *HK1.ras-K14creP.Δ3β-cat*$^{flx/wt}$ and *HK1.ras* benign papillomas strongly expressed p21 indicative of the benign nature of the tumour [Fig. 6.21 E & F].

Thus, at these early stages, as in *HK1.ras* epidermal hyperplasia, p21 was not significantly deployed [Chapter 1 Fig. 7], a lack of p21 in these papilloma prone *HK1.ras-K14creP.Δ3β-cat*$^{flx/wt}$*.p53*$^{flx/flx}$ individuals thus now allowed papilloma formation as in *HK1.ras-K14creP.Δ3β-cat*$^{flx/wt}$ and *HK1.ras* skin. However, these roles for p21 did not fully account for the inhibition of the β-catenin phenotypes observed in the majority of *HK1.ras-K14creP.Δ3β-cat*$^{flx/wt}$*.p53*$^{flx/flx}$ mice and again observed in these two papillomas prone individuals. Therefore, experiment proceeded to investigate the p53 family members p63 and p73, together with an analysis of potential stem cell marker K15.

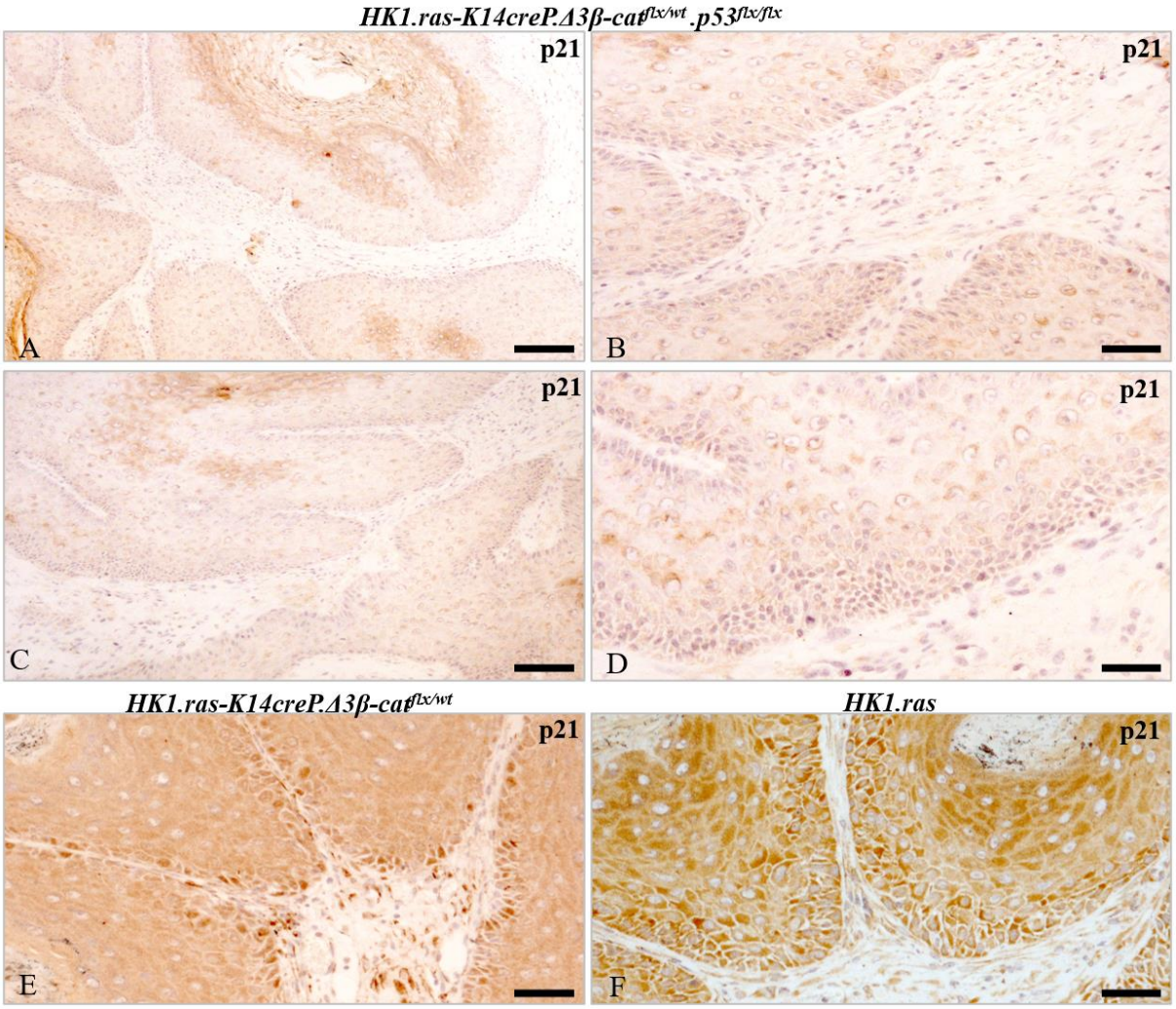

Figure 6. 21: Analysis of p21 expression in *HK1.ras-K14creP.Δ3β-cat$^{flx/wt}$.p53$^{flx/flx}$* papilloma and carcinoma.

[A] At low and [B] higher magnification an area of *HK1.ras-K14creP.Δ3β-cat$^{flx/wt}$.p53$^{flx/flx}$* hyperplasia/papilloma shows little to no p21 expression. Similarly [C & D] *HK1.ras-K14creP.Δ3β-cat$^{flx/wt}$.p53$^{flx/flx}$* wdSCC/SCC have no detectable p21 expression in any layers compared to strong expression in [E] *HK1.ras-K14creP.Δ3β-cat$^{flx/wt}$* and [F] *HK1.ras* papillomas confirming their benign nature. Scale bars: A & C: 100 µm; B, D, E & F: 75µm

Table 6. 2: Summary of rare *HK1.ras-K14creP.Δ3β-cat$^{flx/wt}$.p53$^{flx/flx}$* papillomas phenotypes and conversion to SCCs

Genotype analysed	[N]	Analysed for expression of	Data summary
HK1.ras papilloma	90	β-catenin, E-cadherin, K1, K6α, p53 and p21 expressions	-Control papilloma size 7-10 mm diameter -Exhibiting membranous β-catenin/E-cadherin expression mainly in the supra-basal layers with only sporadic nuclear/cytoplasmic β-catenin expression in basal layers -ordered terminal differentiation indicated by suprabasal layer K1 and expressing K6α in both supra and basal layers due to HK1.ras activation stress signal -nuclear basal layer p53/p21 expression halting malignant conversion
HK1.ras-K14creP.Δ3β-cat$^{flx/wt}$ [papilloma]	2	β-catenin, E-cadherin, K1, K6α, p53 and p21 expressions	-papilloma size 3-4 mm diameter -Exhibiting increased cytoplasmic/nuclear β-catenin in basal layers with increased membranous basal layer β-catenin/E-cadherin due to Δ3β-catenin -Ordered terminal differentiation indicated by suprabasal layer K1 and expressing K6α mainly in supra basal layer - Nuclear basal layer expression of p53/p21 halting malignant conversion
HK1.ras-K14creP.Δ3β-cat$^{flx/wt}$.p53 [SCCs]	2	β-catenin, E-cadherin, K1, K6α, p53 and p21 expressions	-SCCs 10mm diameter -Exhibit loss of membranous basal layer β-catenin/E-cadherin expression with increased cytoplasmic/nuclear basal layer β-catenin -Reduced levels of K1 indicating conversion to carcinoma and strong expressing of K6α - loss of basal layer p21 expression as another indicator of conversion to malignancy
Conclusion: Delayed phenotypes from β-catenin activation due to inducible loss of p53 in *HK1.ras-K14creP.Δ3β-cat$^{flx/wt}$.p53$^{flx/flx}$* resulted in accelerated papillomatogenesis and conversion to SCC. Malignant conversion correlated with reduced basal layer focal adhesion [β-catenin/E-cadherin] and cytoplasmic/nuclear β-catenin driving malignant progression following additional loss of p21. These data indicate that p53 loss at a later stages of papilloma development facilitate conversion to SCC, unlike *HK1.ras-K14creP.Δ3β-cat$^{flx/wt}$* [papilloma] where p53 expression restricted tumour development.			

6.5 Analysis of p63 and p73 status in *HK1.ras-K14creP.Δ3β-cat$^{flx/wt}$* and *HK1.ras-K14creP.Δ3β-cat$^{flx/wt}$.p53$^{flx/flx}$* mouse skin and tumours

The *HK1.ras-K14creP.Δ3β-cat$^{flx/wt}$* and *HK1.ras-K14creP.Δ3β-cat$^{flx/wt}$.p53$^{flx/flx}$* cohorts both resulted in a lack of papillomas forming in the vast majority of mice except for four outliers. One set developed papillomas in *HK1.ras-K14creP.Δ3β-cat$^{flx/wt}$* mice, but in *HK1.ras-K14creP.Δ3β-cat$^{flx/wt}$.p53$^{flx/flx}$* papillomas rapidly converted to wdSCC and progressed to pdSCC in the same tumour consistent with their genomic instability following p53 loss. Thus, these few mice produced results more consistent with the literature and as originally theorised co-operation between ras and β-catenin activation and loss of p53 TSG function would result in malignant SCCs as observed in *HK1.ras/fos-K14creP.Δ5PTEN$^{flx/flx}$* mice.

For the majority of mice however initially the results had suggested that this paradoxical lack of tumours in *HK1.ras-K14creP.Δ3β-cat$^{flx/wt}$* mice was attributed to early, increased levels of p53 and p21, triggered via RU486-independent *Δ3β-catenin* expression. This maybe true in that context, but subsequently the p53 knockout data suggested that p53 loss in itself was not the cause of this tumour inhibition, but with the background knowledge that p53 loss in *HK1.ras* mice also inhibit papillomas, the possibility remains that the same inhibitory factors play roles in papilloma inhibition in both models. Indeed for *HK1.ras-K14creP.Δ3β-cat$^{flx/wt}$.p53$^{flx/flx}$* cohorts results suggests that papilloma inhibition was attributed in part to increased levels of p21 expression.

These findings highlighted two necessities, one of which would involve investigating p21 knockout in *HK1.ras-K14creP.Δ3β-cat$^{flx/wt}$.p53$^{flx/flx}$* and *HK1.ras-K14creP.Δ3β-cat$^{flx/wt}$* to understand the roles of p21 in these results, and experiments are on-going. However, very preliminary data suggests that *p21* loss alone may not be the key to tumour inhibition either, as newly established *HK1.ras-K14creP.Δ3β-cat$^{flx/wt}$.p21KO* adults were also devoid of tumours at 12 weeks [see below; Fig. 6.29]. Moreover, all juvenile *K14creP.Δ3β-cat$^{flx/wt}$.p21KO* or *HK1.ras-K14creP.Δ3β-cat$^{flx/wt}$.p21KO* mice became score 1 [or 2] by day 20; and none exhibited the delay in of *Δβ-catenin* phenotypes that appeared in all *K14creP.Δ3β-cat$^{flx/wt}$.p53$^{flx/flx}$* and *HK1.ras-K14creP.Δ3β-cat$^{flx/wt}$.p53$^{flx/flx}$* mice, including those individuals that exhibited tumours.

This suggests that this intriguing phenotype was specific to p53 hence, it was fortuitous that the second investigation of alternate p53 family members, p63 and p73, had begun to try to decipher the intriguing observation that in terms of differentiation, p53 loss induced responses that blocked these *Δ3β-catenin* phenotypes, and which possibly could also account [or not] for the inhibition of papilloma formation by these p53 family members.

A brief review of their extensive literature shows that both *p63* and *p73* have important, highly complex functions in epidermal physiology (*Koster and Roop, 2007; Crum and McKeon, 2010; Su et al. 2013; Botchkarev and Flores, 2014*). Unlike *p53* itself which does not appear to be closely involved in development given *p53* null mice develop properly (*Donehower et al., 1992; Greenhalgh et al., 1996*), both *p63* and *p73* have important roles in development and maintenance of the epidermis (*Koster and Roop, 2007; Crum and McKeon, 2010; Botchkarev and Flores, 2014*). Here for both *p63* and *p73* genes there are two distinct isoform families that have separate roles of transcription repression [ΔN] or transcription activation [TA]. One form lacks an amino terminus transactivating domain *ΔNp63/ΔNp73* and represses target genes whilst the other isoforms *TAp63/TAp73* activate target gene expression and the sets of genes regulated do not overlap to a great extent (*Koster and Roop, 2007; Crum and McKeon, 2010; Su et al. 2013; Botchkarev and Flores, 2014*).

Thus, both *p63* and *p73* play important roles in maintaining homeostasis of epidermal proliferation and differentiation and most is known regarding p63 function. In the epidermis the dominant isoform is ΔNp63 which plays a vital role in development of the epidermis as shown in knockout mice. Here loss of *p63* resulted in the failure of the epidermis to stratify and disrupted the formation of hair follicles and the development of limbs (*Mills et al., 1999; Koster et al., 2004; Koster and Roop, 2007*). These studies suggest that a role for the ΔNp63 isoform is to maintain the basal layer proliferation, and a major role for ΔNp63 in the developing embryonic epidermis is geared to inhibit premature differentiation via repression of genes associated with differentiation including p21 and PTEN (*Westfall et al. 2003; Moll and Slade, 2004; Nguyen et al., 2006; Leonard et al., 2011*; *Botchkarev and Flores, 2014*), hence any compensatory expression of p53 backup may account for the lack of an apparent effect of *p21KO* in juvenile *K14creP.Δ3β-cat$^{flx/wt}$.p21KO* or *HK1.ras-K14creP.Δ3β-cat$^{flx/wt}$.p21KO* mice [below].

Of more significance to this Δ3β-catenin model, ΔNp63 inhibits stratification via repression of Notch and the induction of keratin K1 as cells commit to leave the basal layer (*Koster and Roop, 2007; Botchkarev and Flores, 2014*). This has implications for the patchy K1 observed in these mice and given that Notch repression results in elevated β-catenin (*Powell et al., 2006; Leigh et al., 2014; 2016*), these studies begin to link the results and observations in this *HK1.ras-K14creP.Δ3β-cat*$^{flx/wt}$*.p53*$^{flx/flx}$ model to the responses mediated by p53 to Δ3β-catenin overexpression and now to the functions of p63 and p73 family members.

In respect to carcinogenesis, roles for p63 and p73 are also unclear, indeed this is such a complex network that much controversy exists to determine whether these genes function as classic TSG or possess oncogenic functions in their own right (*Liefer et al., 2000; Moll and Slade, 2004; Mills, 2006*; *Koster and Roop, 2007*; *Koster et al., 2007*; *Botchkarev and Flores, 2014*). In human SCC the ΔNp63 isoform is highly expressed indicating that by this stage it may act as an oncogene. Consistent with this idea and its roles in maintaining proliferation and inhibiting differentiation [above], the ΔNp63 isoform was down-regulated in response to UV-B, thus allowing for expression of p53 to repair mutations (*Liefer et al., 2000*). However, in transgenic mice, one study suggested a lack of a TSG role for ΔNp63 as their p63$^{+/-}$ mice did not develop spontaneous tumours even following chemical carcinogenesis (*Keyes et al., 2006; Mills, 2006*); whilst a separate study showed that p63$^{+/-}$ mice did develop tumours suggesting TSG role (*Flores et al., 2005*). Adding further complexity to this system transgenic mice that overexpress the alternate TAp63 isoform did increase the numbers of DMBA/TPA SCCs, indicating that some p63 isoforms function as oncogenes in the appropriate context (*Koster et al., 2006*). Further specific TAp63 knockout mice develop highly metastatic SCCs similar to high grade metastatic human SCC that loose expression of TAp63 suggesting that that TAp63 is a suppressor of metastasis and again highlighting that the context of the tumour is important to suppression or progression (*Su et al., 2010*).

For p73 few studies have actually been reported, but again given the different functions assigned to different isoforms it is likely that the repressive ΔNp73 and transcriptionally active TAp73 isoforms exert completely differing functions. For instance, some studies suggest that the TAp73 isoform exhibits pro-apoptotic activity giving suppressor properties (*Rocco et al.,*

2006) and is activated to induce apoptosis following DNA damage (*Irwin et al., 2003*). It may be that ΔNp63 acts in an oncogenic role to inhibit TAp73-mediated apoptosis and show the complex interactions within this p53 family (*DeYoung and Ellisen, 2007*). Furthermore, whilst p73 is silenced in a number of tumour types through methylation, and transgenic mice heterozygous for p53 and p73 develop cutaneous SCC indicating TSG roles for p73 (*Flores et al., 2005*), in human cutaneous SCCs p73 remains strongly expressed indicating an oncogenic function (*Moll and Slade, 2004*). However, a major problem for these and this current study, is that the available p63 and 73 antibodies do not distinguish between the ΔN- or TA- isoforms. Therefore, against this highly complex background of close interactions between the p63 and p73 isoforms in both p53-dependent and p53-independent contexts the skins and papillomas/SCCs from *HK1.ras-K14creP.Δ3β-cat*$^{flx/wt}$ *and HK1.ras-K14creP.Δ3β-cat*$^{flx/wt}$*.p53*$^{flx/flx}$ were analysed for p63 and p73 status.

Analysis of p63 expression [Fig.6.22] in typical RU486-treated *HK1.ras-K14creP.Δ3β-cat*$^{flx/wt}$ skin found that strong expression was exhibited by all the anomalous hair follicles [Fig. 6.22A&B]; suggesting that its normal roles in HF here may have been subverted by Δ3β-catenin, given that *p63* knockout results in disruption of hair follicles (*Mills et al., 1999; Koster et al., 2004; Koster and Roop 2007*). Further in the hyperplastic IFE, p63 expression was not only sporadic but also any nuclear expression appeared in strands of basal layer keratinocytes and these were clumped together and separated by larger strands of negative keratinocytes [Fig.6.22A]. This suggests that these positive strands represent a niche of p63-regulated stem cells or perhaps a better term is the one coined by *Botchkarev and Flores, 2014*, namely Keratinocyte Precursor Cells [KPCs] as these could be the precursors of transit amplifying keratinocytes or the precursor's of cells about to commit to differentiate.

This result would be consistent with a major role for ΔNp63 in the developing epidermis that inhibits premature differentiation via repression of genes associated with differentiation such as Notch (*Koster and Roop, 2007; Crum and McKeon, 2010; Leonard et al., 2011; Botchkarev and Flores, 2014*), and the resulting inhibition of Notch would in turn lead to increased β-catenin expression (*Proweller et al 2006*). This idea thus indirectly links p63 to β-catenin whilst the expression of p63 in specific strands may account for the patchy K1 expression observed [see below]. Alternately the TAp63 isoform keeps KPC/stem cells in a quiescent state to avoid depletion and this provides the cells for wounding and helps suppress

tumorigenesis from mutated stem cells (*Su et al. 2009; 2013; Romano et al. 2012*). This idea may help account for the inhibition of papillomas as Δ3β-catenin is expressed in stem cells from the K14 promoter [chapter 1: Fig. 8] which also shows strands of [blue] KPC cells in the basal layer.

In *HK1.ras-K14creP.Δ3β-cat*$^{flx/wt}$*.p53*$^{flx/flx}$ epidermis the loss of p53 appears to increase the expression of p63 which is now elevated in hair follicles and increased in IFE [Fig. 6.22C&D]. Thus, again consistent with roles for p63 in normal HF development this increased expression of p63 may contribute to the overall lesser degree of HF anomalies observed in *HK1.ras-K14creP.Δ3β-cat*$^{flx/wt}$*.p53*$^{flx/flx}$ *skin.* Further, the increased p63 expression in the IFE not only appears in more strands of basal layer keratinocyte nuclei but also here p63 appears in the upper layers of the reduced ras associated hyperplasia and also appears in strands/block of expression.

These results again support the idea that p63 is induced in response to p53 loss, and in this context given its roles in inhibiting differentiation into the suprabasal layers it may account for the lesser degree of hyperplasia and keratosis observed in these mice [Fig.6.22 C & D]. Moreover, the appearance of p63 in blocks of IFE epidermis [Fig. 6.22 D] could now account for both the lack of K1 expression and its abrupt disappearance in blocks of *HK1.ras-K14creP.Δ3β-cat*$^{flx/wt}$*.p53*$^{flx/flx}$ IFE. This result also suggests that p63 may influence K6α expression in attempts to maintain order following disruption by Δ3β-catenin expression, as p63 mice are highly susceptible to spontaneous wounds from blistering (*Mills et al., 1999; Westfall et al. 2003*).

Interestingly, neither *HK1.ras* nor *HK1.ras-K14creP.p53*$^{flx/flx}$ hyperplasia exhibited p63 expression [Fig. 6.22E&F]. This indicates this p63 response appears specific to Δ3β-catenin expression and that ras activation appears to actually repress p63-hence the relatively normal differentiation observed and the general degree of increased hyperplasia. This result [as with p73 below] suggests that the inhibitory responses to p53 loss that inhibit *HK.ras.p53*$^{flx/flx}$ papilloma formation are separate to those observed in these *Δ3β-catenin* models, and further strengthen links of β-catenin to *p63* [and *p73*] roles in epidermal regulation.

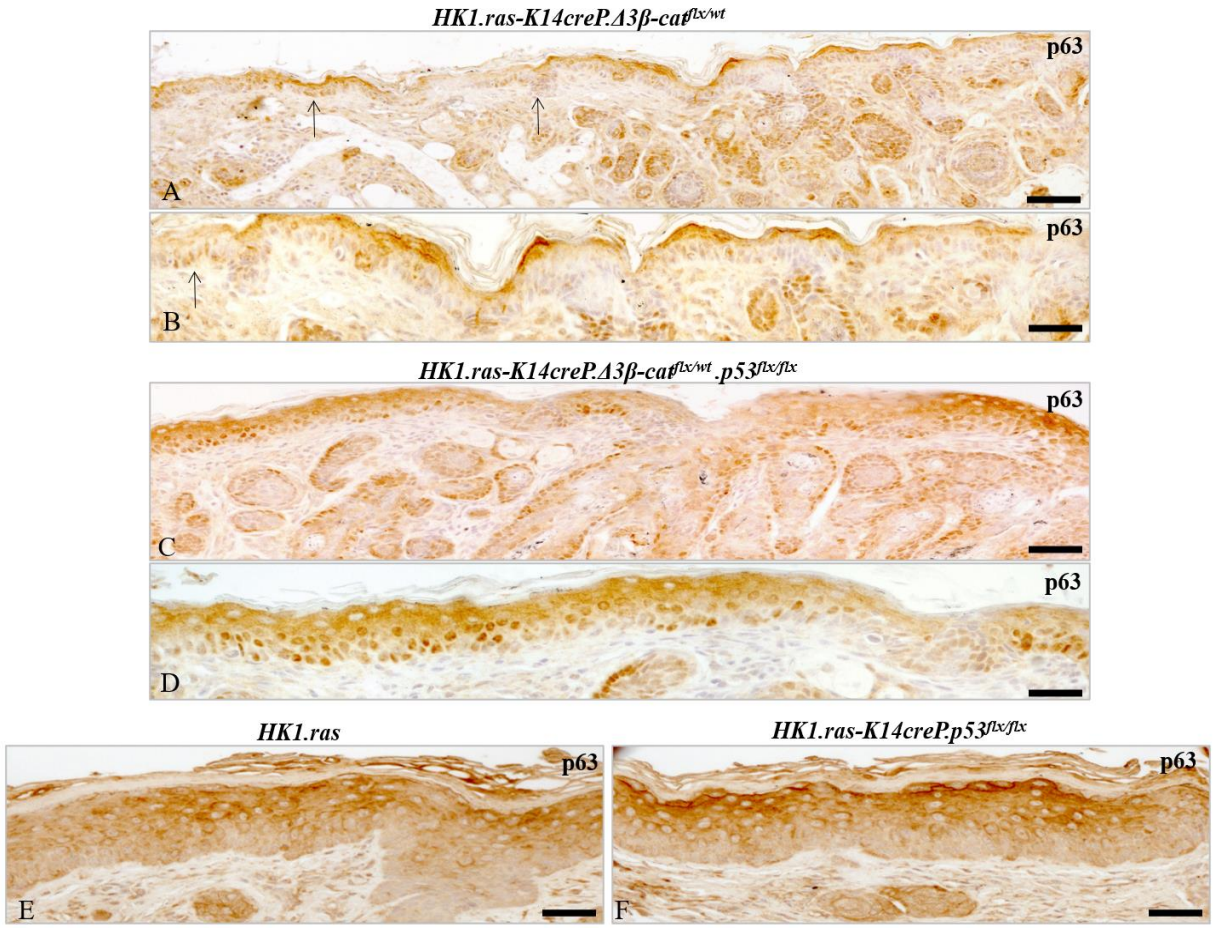

Figure 6. 22: Analysis of p63 expression in *HK1.ras-K14creP.Δ3β-cat*$^{flx/wt}$ and *HK1.ras-K14creP.Δ3β-cat*$^{flx/wt}$*.p53*$^{flx/flx}$ epidermis.

[A] Low and [B] higher magnification of composite images shows that a typical RU486-treated *HK1.ras-K14creP.Δ3β-cat*$^{flx/wt}$ exhibits strong follicular expression of p63 in the anomalous HFs. In the hyperplastic IFE p63 expression appears only sporadic, with nuclear expression appearing in strands of basal layer nuclei but clumped together [arrows] more prominent at higher magnification. [C & D] *HK1.ras-K14creP.Δ3β-cat*$^{flx/wt}$*.p53*$^{flx/flx}$ exhibits increased p63 expression in most basal layer keratinocytes and in the lesser transformed HFs at higher magnification. In addition, p63 appears in the upper layers of the reduced ras associated hyperplasia and also appears in strands/block of expression. [E] *HK1.ras* and [F] *HK1.ras-K14creP.Δp53*$^{flx/flx}$ hyperplasia both exhibit weak, if any expression of p63 in the IFE and little expression in the quiescent [telogen] HFs. Scale bars: A, & C: 150 µm; B & D: 75 µm; E & F: 50µm.

Analysis of p73 suggested that it plays an even greater role to both help combat co-expression of *HK1.ras* and *Δ3βcatenin* and moreover compensate for p53 loss particularly in the inhibition of the early *Δ3β-catenin* phenotypes of juvenile *HK1.ras-K14creP.Δ3β-cat$^{flx/wt}$.p53$^{flx/flx}$* mice [Fig. 6.23]. In comparison to *HK1.ras-K14creP.Δ3β-cat$^{flx/wt}$* skin, p73 expression was similar and strongly expressed in the transformed HFs yet in the hyperplastic IFE, p73 expression appeared more closely associated with keratinocytes emerging from the HFs [Fig.6.23 A & B; arrows]. This again is consistent with p73 roles in general epidermal development and the localisation to keratinocytes emerging from HFs is very interesting as it may reflect roles for the TAp73 isoform in regulating HF bulge stem cell decisions to enter anagen as its ablation stops follicle formation (*Rufini et al.,* 2012). Thus, here it would help combat the deregulated Δ3β-catenin expression in juvenile epidermis as the first hair cycle begins. Also, this TAp73 depletion accelerates cellular aging and this links to a return to the theme that *Δ3β-catenin* expression may return an epidermis to an earlier neonatal/juvenile state (*Collins et al., 2011*) as explored further *in vitro* [see Chapter 8].

However, the most striking increase in p73 expression appeared in *HK1.ras-K14creP.Δ3β-cat$^{flx/wt}$.p53$^{flx/flx}$* skin [Fig.6.23 C & D]. Here significant levels of increased p73 expression appeared in most basal layer keratinocyte nuclei and now p73 was very strongly expressed in the HFs. Closer examination of the IFE shows that again p73 also appears in the suprabasal layers and few strands/block of negative expression are observed [Fig.6.23 D]. In contrast *HK1.ras* and *HK1.ras-K14creP.p53$^{flx/flx}$* hyperplasia lacked such compensatory p73 expression [Fig. 6.23E&F]. It also again supports the idea that inhibitory responses to p53 loss that inhibit *HK.ras-K14creP.p53$^{flx/flx}$* papilloma formation are separate to those observed in these Δ3β-catenin models.

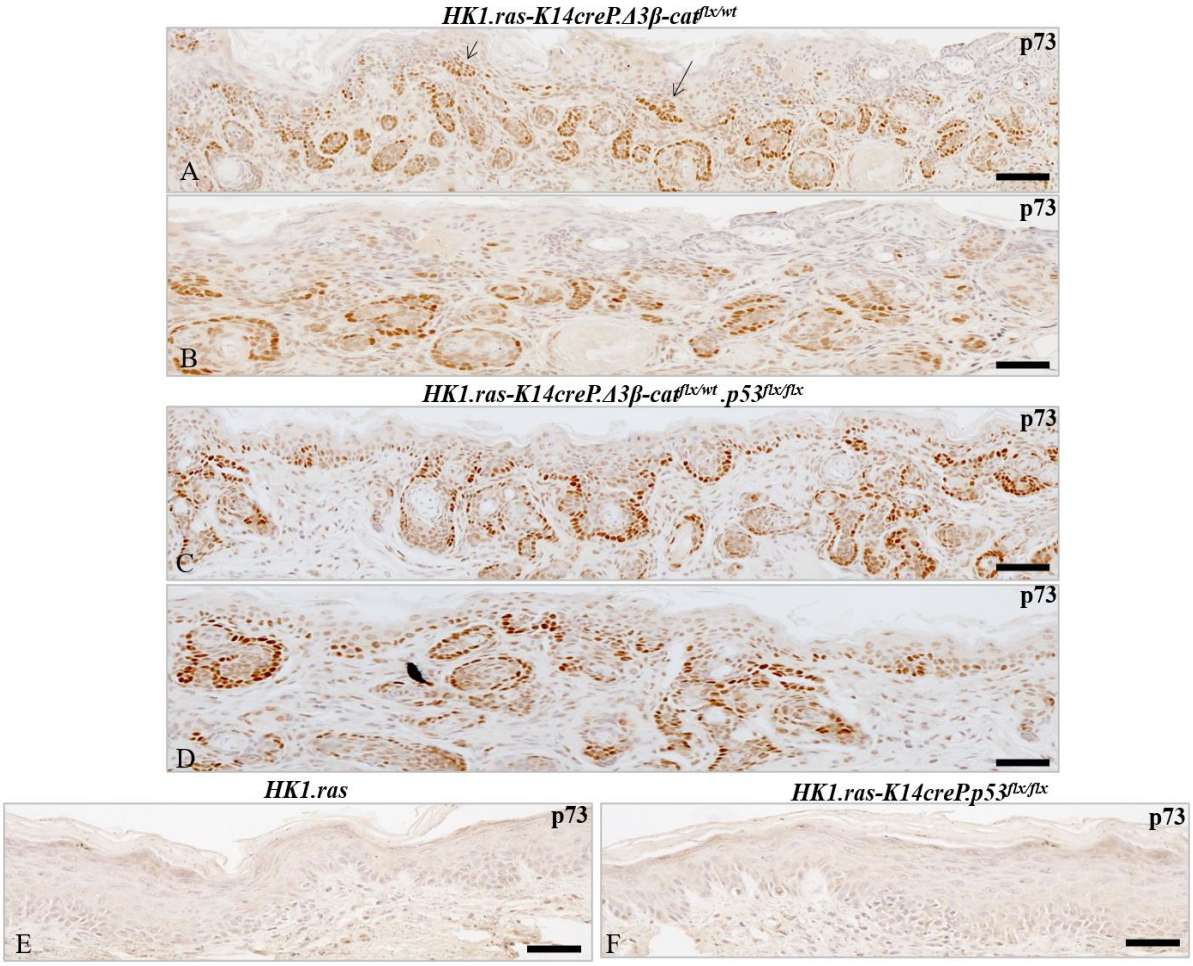

Figure 6. 23: Analysis of p73 expression in *HK1.ras-K14creP.Δ3β-cat*$^{flx/wt}$ and *HK1.ras-K14creP.Δ3β-cat*$^{flx/wt}$*.p53*$^{flx/flx}$ epidermis.

[A] Low and [B] higher magnification of RU486-treated *HK1.ras-K14creP.Δ3β-cat*$^{flx/wt}$ skin shows strong p73 expression transformed HFs and also appears in the hyperplastic IFE but in occasional strands close to the HFs [arrows]. [C & D] *HK1.ras-K14creP.Δ3β-cat*$^{flx/wt}$*.p53*$^{flx/flx}$ exhibits greater levels of p73 expression in most basal layer keratinocytes and also in the lesser transformed HFs. p73 expression appear in the suprabasal layers and also appears in most keratinocytes with few strands/blocks of negative expression. [E] *HK1.ras* and [F] *HK1.ras-K14creP.p53*$^{flx/flx}$ hyperplasia both exhibit weak, if any expression of p73 in the IFE or normal HFs. Scale bars: A, & C:100 µm; B & D-F: 75 µm.

These results show that p73 isoform expression was far more effective in blocking *Δ3β-catenin* phenotypes in juvenile skin following p53 loss than p63 isoforms. This is consistent with the roles often assigned to p73 in terms of pro-apoptotic TSG functions alongside those of p53 (*Rocco et al., 2006; DeYoung and Ellisen, 2007*). It is also consistent with the idea that β-catenin expression had to become basal before the p53 family members reacted to its anomalous expression; i.e. this p73 response was again β-catenin specific and the absence of basal layer β-catenin in *HK1.ras* or *HK1.ras-K14creP.p53*$^{flx/flx}$ hyperplasia resulted in a lack of compensatory p73 [and p63] expression. If so, this has significant implications for papillomatogenesis inhibition and may account for p73 appearance in human SCCs (*Moll and Slade, 2004*; *DeYoung and Ellisen, 2007*) following Notch repression by ΔNp63 (*Koster and Roop, 2007; Botchkarev and Flores, 2014*) thus resulting in β-catenin overexpression and invasive E-cadherin negative keratinocytes as observed in this current model [below].

This may be the case, given the results in the rare *HK1.ras-K14creP.Δ3β-cat*$^{flx/wt}$ papillomas and the progression to SCC in *HK1.ras-K14creP.Δ3β-cat*$^{flx/wt}$*.p53*$^{flx/flx}$ mice for p63 and p73 expression as shown in Fig.6.24 and Fig.6.25. Analysis of p63 in *HK1.ras-K14creP.Δ3β-cat*$^{flx/wt}$ papillomas showed weak basal layer expression [Fig. 6.24A&B]. Given that this was also paralleled by both p53 and p21 [above Chapter 5] hence any potential oncogenic properties of say the ΔNp63 isoform in conjunction with β-catenin[above] were successfully combatted by compensatory p53 and p21 expression [Chapter 5]. However, following p53 loss in *HK1.ras-K14creP.Δ3β-cat*$^{flx/wt}$*.p53*$^{flx/flx}$ tumours, p63 expression appeared to become stronger and more uniform [Fig. 6.24C&D] as tumour progressed and this does indeed suggest an oncogenic property of the ΔNp63 isoform in that it is known to down regulate p21 (*Koster and Roop, 2007; Botchkarev and Flores, 2014*) and this maybe the reason that *HK1.ras-K14creP.Δ3β-cat*$^{flx/wt}$*.p53*$^{flx/flx}$ tumours were devoid of p21 expression and this contributed to their rapid progression to SCC. This idea would also be supported by the findings that *HK1.ras* papillomas now showed similar but weaker p63 expression [Fig. 6.24E&F] than both sets of *Δ3β-catenin* papillomas, suggesting that p53 and p21 reacted to ras activation, but in the absence of basal β-catenin maintained low levels of p63 and a benign phenotype.

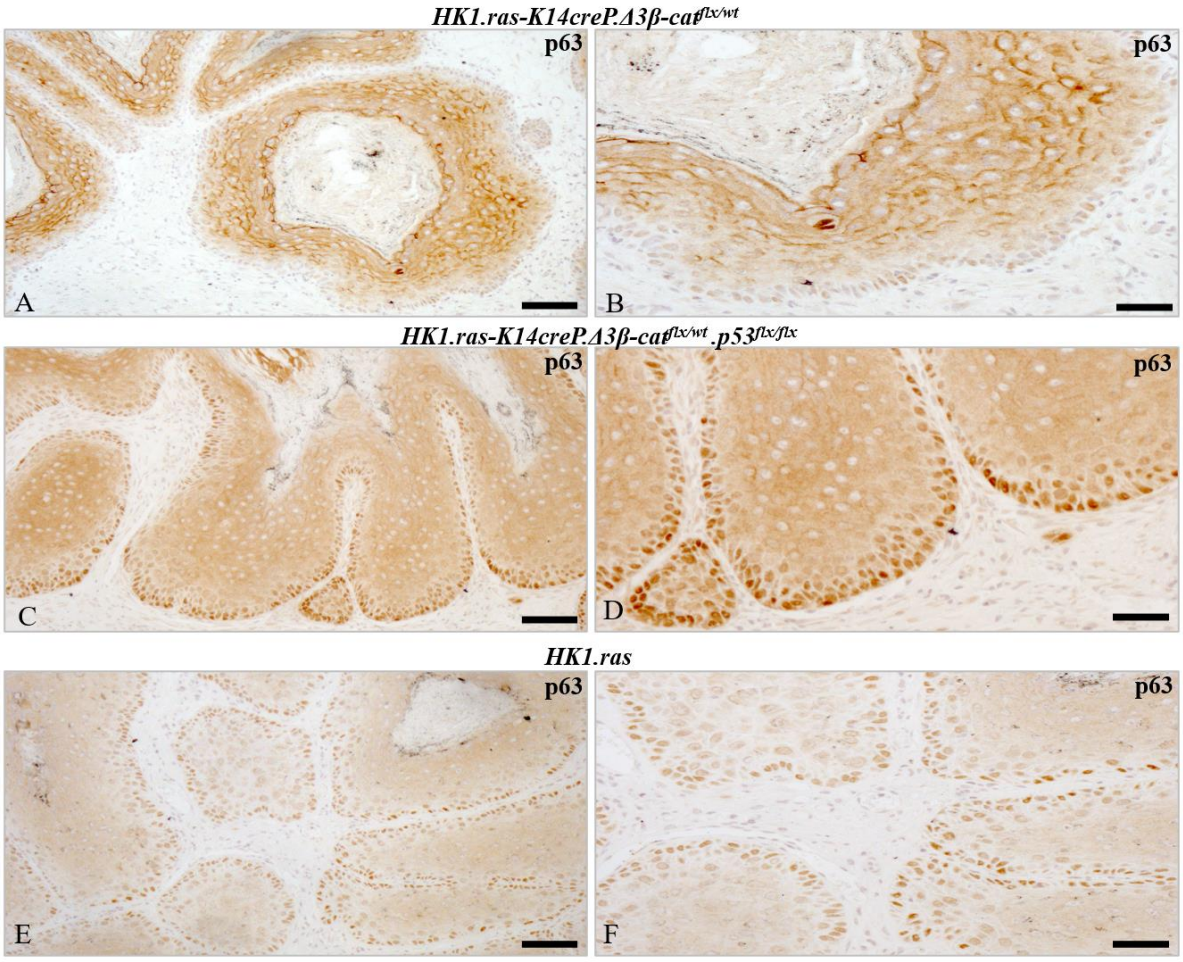

Figure 6. 24: Analysis of p63 expression in *HK1.ras-K14creP.Δ3β-cat*$^{flx/wt}$ and *HK1.ras-K14creP.Δ3β-cat*$^{flx/wt}$*.p53*$^{flx/flx}$ tumours.

[A & B] *HK1.ras-K14creP.Δ3β-cat*$^{flx/wt}$ papillomas show weak expression of p63 in basal layers. [C & D] *HK1.ras-K14creP.Δ3β-cat*$^{flx/wt}$*.p53*$^{flx/flx}$ *tumours a mix of* papilloma and wdSCC now show stronger expression of p63 than A or B consistent with their malignant progression and potential oncogenic roles of any *ΔNp63* isoform expression. [E & F] *HK1.ras* papilloma now also shows elevated expression of p63. Scale bars: A, C & E: approx. 100 µm; B: 50µm; D&F: 75µm

Analysis of p73 in *HK1.ras-K14creP.Δ3β-cat*$^{flx/wt}$ papillomas displayed strong expression in the proliferative basal layers [Fig. 6.25A&B] supporting its anti-tumour roles alongside that of p53, which may also inhibit ΔNp63 functions to prevent conversion as seen in Fig.6.24. However, whilst *HK1.ras-K14creP.Δ3β-cat*$^{flx/wt}$*.p53*$^{flx/flx}$ tumours showed a more intense p73 expression profile in the papilloma/wdSCC tumour in response to p53 loss [Fig. 6.25C&D] it may be that the TSG functions are now uncoupled by ΔNp63 functions and p21 loss. As outlined above this observation may reflect p73 appearance in human SCCs (*Moll and Slade, 2004*; *DeYoung and Ellisen, 2007*) following Notch and p21 repression by ΔNp63 (*Nguyen et*

al., 2006; *Koster and Roop, 2007; Botchkarev and Flores, 2014*) and results in fully deregulated β-catenin overexpression. Thus, despite p73 expression, the resulting lack of p21 [and possibly PTEN] (*Botchkarev and Flores, 2014*), coupled to nuclear βcatenin and the E-cadherin profile of halos of negative keratinocytes all combine to facilitate invasion as observed in this *HK1.ras-K14creP.Δ3β-cat*$^{flx/wt}$*.p53*$^{flx/flx}$ tumours context. For *HK1.ras* papillomas the relatively small and sporadic increase in p73 [Fig. 6.25E&F] again probably reflects the fact that *HK1.ras* papillomas carry little basal layer β-catenin even following *p53* loss, unlike the equivalent *HK1.ras/fos-K14creP.Δ5PTEN*$^{flx/flx}$ tumours [Chapter 3].

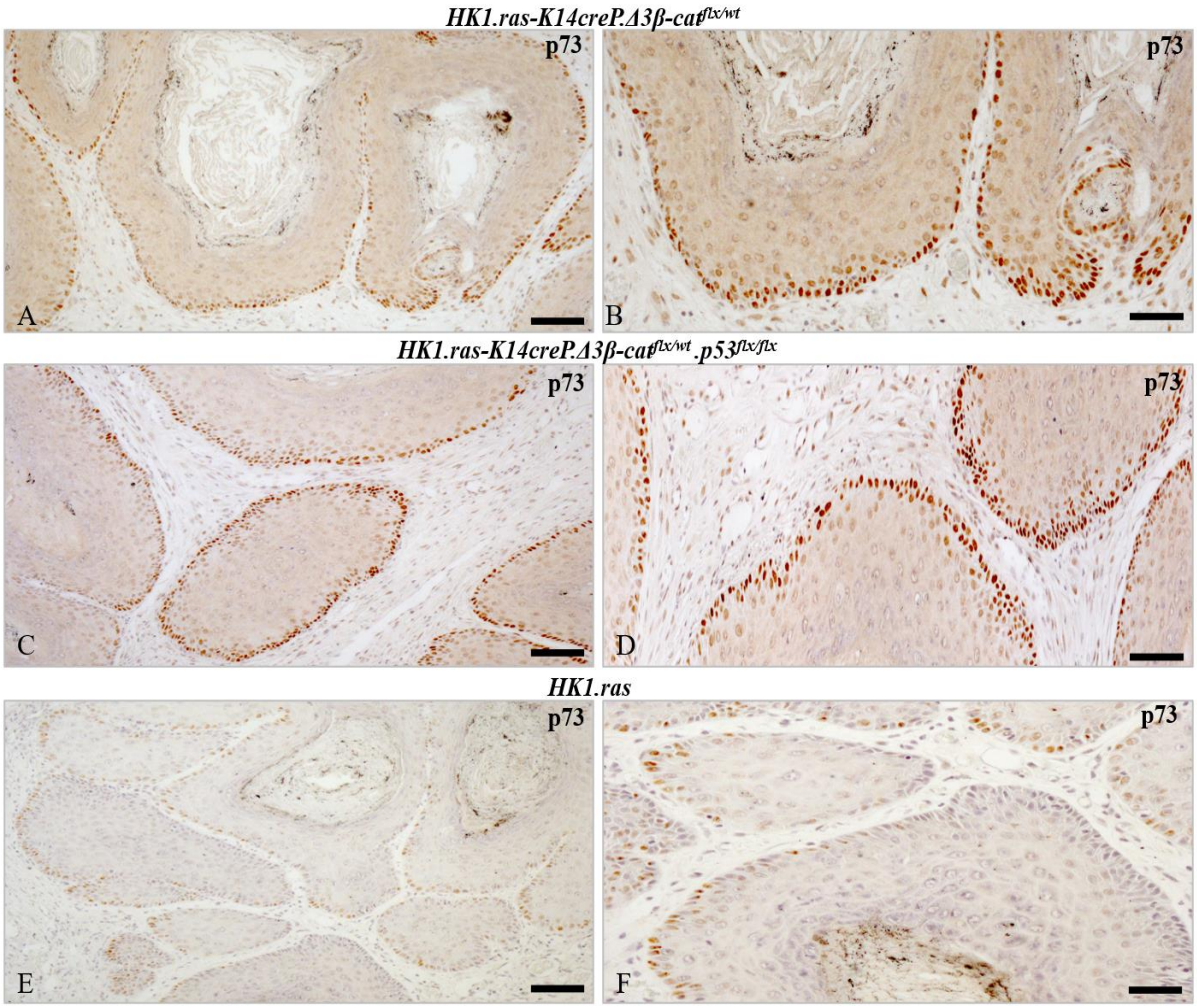

Figure 6. 25: Analysis of p73 expression in *HK1.ras-K14creP.Δ3β-cat*$^{flx/wt}$ and *HK1.ras-K14creP.Δ3β-cat*$^{flx/wt}$*.p53*$^{flx/flx}$ tumours.

[A & B] *HK1.ras-K14creP.Δ3β-cat*$^{flx/wt}$ papillomas show strong uniform p73 expression in all basal layers. [C & D] In *HK1.ras-K14creP.Δ3β-cat*$^{flx/wt}$*.p53*$^{flx/flx}$ tumors both papilloma and wdSCC show even stronger p73 expression consistent with responses attempting to compensate for both p53 and p21 loss. [E & F] *HK1.ras* papilloma shows only sporadic expression of p73 in strands of basal layer keratinocytes. Scale bars: A, & C: 100 µm; B, D & F: 75 µm.

6.6 Analysis of keratin K15 in *HK1.ras-K14creP.Δ3β-cat$^{flx/wt}$* and *HK1.ras-K14creP.Δ3β-cat$^{flx/wt}$.p53$^{flx/flx}$* skin show stem cell changes and an alternate tumour aetiology.

Taken collectively the above observations clearly link Δ3β-catenin overexpression in the *HK1.ras-K14creP.Δ3β-cat$^{flx/wt}$.p53$^{flx/flx}$* model to the responses mediated by *p53/p21* and now to the functions of p63 and p73 family members. Studies also show that major roles for p63 and p73 focus on regulation of stem cell activities, and the interesting findings that p63 and p73 were expressed in strands or blocks of basal cell keratinocytes suggested that these positive strands represent a niche of p63/73 regualted IFE stem cells. Indeed, supporting this idea, the putative non-oncogenic TAp63 isoform keeps KPC/stem cells in a quiescent state to both avoid their depletion and suppress tumorigenesis from a continual supply of mutated cells (*Su et al. 2009b; 2013; Romano et al., 2012*); whilst the TAp73 isoform appears to control HF bulge stem cells (*Rufini et al. 2012*) and these are clearly affected by anomalous changes in β-catenin and E-cadherin expression (*Gregorian, et al., 2008; Jeanes et al., 2008*). Given the emerging complexity of numerous stem cell niches within the epidermis (*Watt and Collins, 2008*) perhaps a better definition of these cells is keratinocyte precursor cells [KPC], as defined in the review by *Botchkarev and Flores, 2014*, as this broader definition can include the precursors of transit amplifying keratinocytes about to commit to differentiate.

The idea that anomalous β-catenin may alter specific KPC populations in the epidermal stem cell unit also came from the K1 data, which showed not only weaker and patchy expression [now consistent with p63 expression] but also the blocks of p63 would be consistent with the abrupt lateral edges to both K1 and on occasion K6 expression made by specific stem cell units in the IFE. This feature of K1 expression appears to be a significant marker of the altered differentiation caused by deregulated β-catenin expression and the increased numbers of adherence junctions due to excess E-cadherin. As suggested above [Chapters 4 and 5], the resultant increase in rigidity may feedback to alter the commitment to the early stages of differentiation as keratinocyte migrate from the different epidermal stem cell niches (*Watt and Collins, 2008*). In addition, effects from compensatory p21 expression that appeared

particularly strong in the upper layers of the epidermis particularly following p53 loss [Fig. 6.12] are also known to help regulate stem cell decisions to proliferate and differentiate (*Topley et al., 1999*).

Hence one possibility to explain the differences in papilloma formation in *HK1.ras-K14creP.Δ3β-cat*$^{flx/wt}$*.p53*$^{flx/flx}$ and *HK1.ras-K14creP.Δ3β-cat*$^{flx/wt}$ vs. *HK1.ras* may centre on the lack of p53/p63/p73 and p21 responses in *HK1.ras* hyperplasia given its lack of expression in HF bulge region keratinocytes [Chapter 1: Fig.3B]. Here, this provides the KPC population targets for papilloma formation (*Li et al., 2013*); whilst in reverse the responses to *Δ3β-catenin* activation in p53^{wt} or p53^{flx} possibly protect the KPC populations via maintaining their quiescence [see mitotic index analysis below] and at this very early stage there is a lack of potential papilloma forming cells due to protection form combinations of p53 and p21 backed up when necessary, by p63 and p73 and resultant anomalous differentiation.

To begin to address this idea, expression of keratin K15 was assessed in *HK1.ras-K14creP.Δ3β-cat*$^{flx/wt}$ and *HK1.ras-K14creP.Δ3β-cat*$^{flx/wt}$*.p53*$^{flx/flx}$ genotypes [Fig. 6.26 and Fig. 6.27] as it has been regarded as a stem cell marker (*Bose et al., 2013*); and its promoter is regularly employed to target gene expression/KO to bulge region stem cells (*Liu et al., 2003*) to model the effect of HF stem cell mutation in development of SCCs (*Chen et al., 2020*). Keratin K15 is also normally expressed in the basal layer of IFE (*Bose et al., 2013*), thus, this role as a stem cell marker appears inconsistent with its expression in the proliferative basal layers. However, much evidence supports K15 as a marker of stem/KPC cells at some point, as K15 is strongly expressed in bulge region keratinocytes (*Lyle et al., 1998*) and bulge cells that express a K15-promoter driven reporter gene reconstituted the entire epidermis with positive cells (*Liu et al 2003; Morris et al., 2004*). Also, K15 positive cells are also positive for the Lgr5 epithelial stem cell marker (*Jaks et al., 2008*); but unfortunately, in this Δ3β-catenin study, preliminary experiments that assessed Lgr5 [and Lgr6] gave very unclear results as the antibodies employed are suspected to cross react with alternate proteins in the epidermis.

It may be that the basal layer K15 expression observed in human tumours may reflect the KPCs with their proliferative potential within the transit amplifying cells given that in human skin cancer, K15 expression actually increases in BCCs (*Jih et al., 1999; Abbas and Bhawan, 2011*) in a role thought to echo its stem cell role that helps maintain an epithelial lineage and

not progress to undergo metastasis or EMT[epithelial-mesenchymal transition] (*Bose et al., 2013*). In SCCs, K15 expression appears and is then lost (*Abbas and Bhawann, 2011*) consistent with their de-differentiation and loss of K1 (*Porter et al., 2000*) and regulator control [p21/p53p63/p73 above].

Of interest to this study and consistent with β-catenin deregulation, was the fact that K15 was strongly expressed in human HF tumours (*Jih et al., 1999*). Also, in DMBA/TPA chemical carcinogenesis studies an initial burst of K15 expression would be consistent with amplification of a mutant stem cell population [that escape the p63/p73 control] and was later lost on progression to overt papilloma (*Troy et al., 2011*). However, Morris and co-workers showed that in labelling studies using the same RU486 gene switch and the K15 promoter crossed to the *Rosa 26 β-gal reporter gene* [*Krt1-15CrePR1;R26R*] the continued presence of keratinocytes derived from K15 positive stem cells persisted for many months (*Li et al., 2013*). This was again consistent with initiating DMBA mutations of K15 positive HF stem cells that gradually loose this marker as they distance themselves from the stem cell niche; but perhaps gain a cancer stem cell phenotype in the K15/β-gal positive papilloma cells destined to become SCC. Intriguingly, the fact that not all papilloma cells expressed this reporter shows their heterogenicity (*Li et al., 2013*), a result consistent with one of the ideas from above, that rare papillomas in *HK1.ras-K14creP.Δ3β-cat*$^{flx/wt}$ and *HK1.ras-K14creP.Δ3β-cat*$^{flx/wt}$*.p53*$^{flx/flx}$ genotypes derive from different cells than that of typical *HK1.ras* papillomas.

In both *HK1.ras-K14creP.Δ3β-cat*$^{flx/wt}$ and *HK1.ras-K14creP.Δ3β-cat*$^{flx/wt}$*.p53*$^{flx/flx}$ mouse skin, K15 analysis showed strong expression, mainly confined to the anomalous hair follicles [Fig. 6.26]. Closer inspection also showed that K15 was more strongly and more uniformly expressed in the more transformed HFs of *HK1.ras-K14creP.Δ3β-cat*$^{flx/wt}$ skin [Fig. 6.26A] vs. the lesser *Δ3β-catenin* HF phenotypes of *HK1.ras-K14creP.Δ3β-cat*$^{flx/wt}$*.p53*$^{flx/flx}$ [Fig. 6.26B]. This result would be consistent with the high K15 levels observed in human folliculoma (*Jih et al., 1999*) and also differences in K15 expression may reflect the expression of higher follicle levels of p21, p63 and especially p73 recorded following p53 loss [above].

The lack of K15 expression in IFE of *HK1.ras-K14creP.Δ3β-cat*$^{flx/wt}$ and *HK1.ras-K14creP.Δ3β-cat*$^{flx/wt}$*.p53*$^{flx/flx}$ was somewhat unexpected, given the roles of β-catenin in maintaining hair follicle stem cell proliferations and their differentiation which are essentials for epidermal homeostasis (*Watt and Collins, 2008; Närhi et al., 2008; Grigoryan et al.,*

2008). Therefore, overexpression of β-catenin was assumed to exhibit a more positive influence on the migration of K15-positive stem cells out of the HF and into the IFE basal layer- as suggested by the p73 expression profile which was associated with follicles in *HK1.ras-K14creP.Δ3β-cat*$^{flx/wt}$ hyperplasia [above Fig. 6.23A&B]. However, instead *Δ3β-catenin* expression has clearly had the opposite effect and interfered with the normal stem cell niches in a different manor. This too would reflect roles of p21, p63 and p73 in regulating these niche populations and attempts by p63 and p73 to keep the stem cells quiet and thus this K15 expression profile reflects these responses.

Further this lack of IFE K15 expression may show a lack of appropriate stem/KPC target cells for *HK1.ras* activation hence the lack of papillomas as the greater *HK1.ras* hyperplasia showed strong expression in IFE basal keratinocytes [Fig. 6.26C], as did the *HK1.ras/p53*$^{flx/flx}$ epidermis again suggesting the blockage of papillomas was different in these two models [Fig. 6.26A&B vs. C&D] and combined that the eventual papilloma aetiology may derive from different keratinocyte populations, as observed in DMBA/TPA papillomas (*Li et al., 2013*).

In respect to carcinogenesis, K15 expression showed a basal layer expression in both *HK1.ras-K14creP.Δ3β-cat*$^{flx/wt}$ papillomas and in the papilloma histotypes of *HK1.ras-K14creP.Δ3β-cat*$^{flx/wt}$*.p53*$^{flx/flx}$ tumours [Fig. 6.27A,B&D], whilst the SCC lacked K15 expression as did typical *HK1.ras* papillomas [Fig. 6.27C,E&F]. A closer inspection shows that the strong K15 expression was strictly confined to specific strands of basal layer *HK1.ras-K14creP.Δ3β-cat*$^{flx/wt}$ papilloma keratinocytes, but the benign papilloma histotype in *HK1.ras-K14creP.Δ3β-cat*$^{flx/wt}$*.p53*$^{flx/flx}$ mice exhibited strong basal layer expression in some areas but it was beginning to fade in others. Also, expression appeared multi-layered as in *HK1.ras* hyperplasias [Fig. 6.26C] and not confined to the basal layer keratinocytes suggesting the beginnings of conversion [Fig.6.27A, B vs. D]. In the serial sections that comprised hyperplasia papilloma and SCC histotypes K15 was already lost and was also not present in the hyperplasia suggesting it may never have been induced and any residual minimal K15 expression was erratic and appeared in several layers [Fig.6.27C]. At this stage, [12wks] *HK1.ras* papillomas were much larger and completely lacked the K15 expression seen earlier.

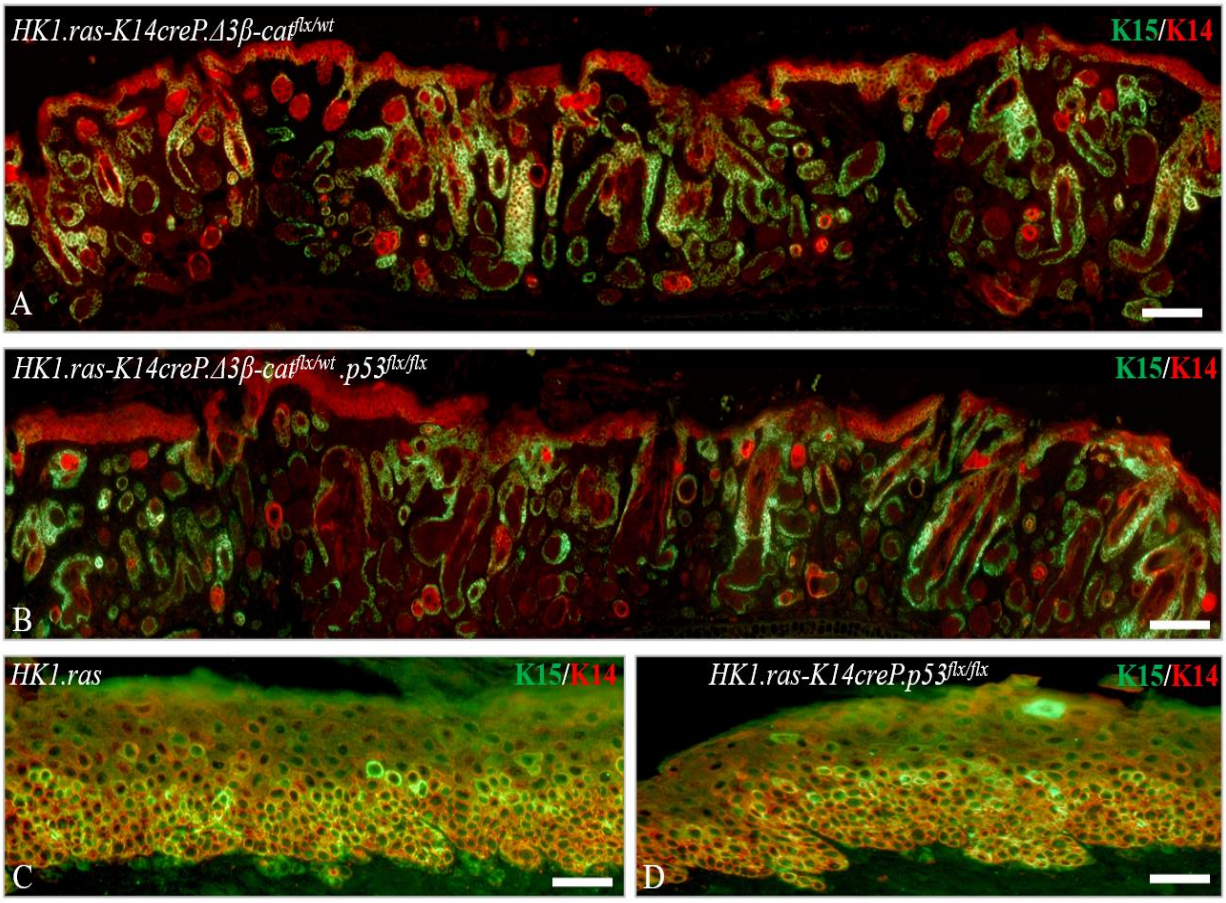

Figure 6. 26: Analysis of keratin K15 expression in *HK1.ras-K14creP.Δ3β-cat*$^{flx/wt}$ and *HK1.ras-K14creP.Δ3β-cat*$^{flx/wt}$*.p53*$^{flx/flx}$ skin.

[A & B] K15 expression in [A] *HK1.ras-K14creP.Δ3β-cat*$^{flx/wt}$ and [B] an older patch of RU486-treated keratotic *HK1.ras-K14creP.Δ3β-cat*$^{flx/wt}$*.p53*$^{flx/flx}$ skin is strong but confined to the hair follicle. [C] *HK1.ras* and [D] *HK1.ras-K14creP.p53*$^{flx/flx}$ hyperplasia show strong expression in the expanded proliferative IFE keratinocytes. Scale bars: A, & B: 150 µm; C & D: 75 µm.

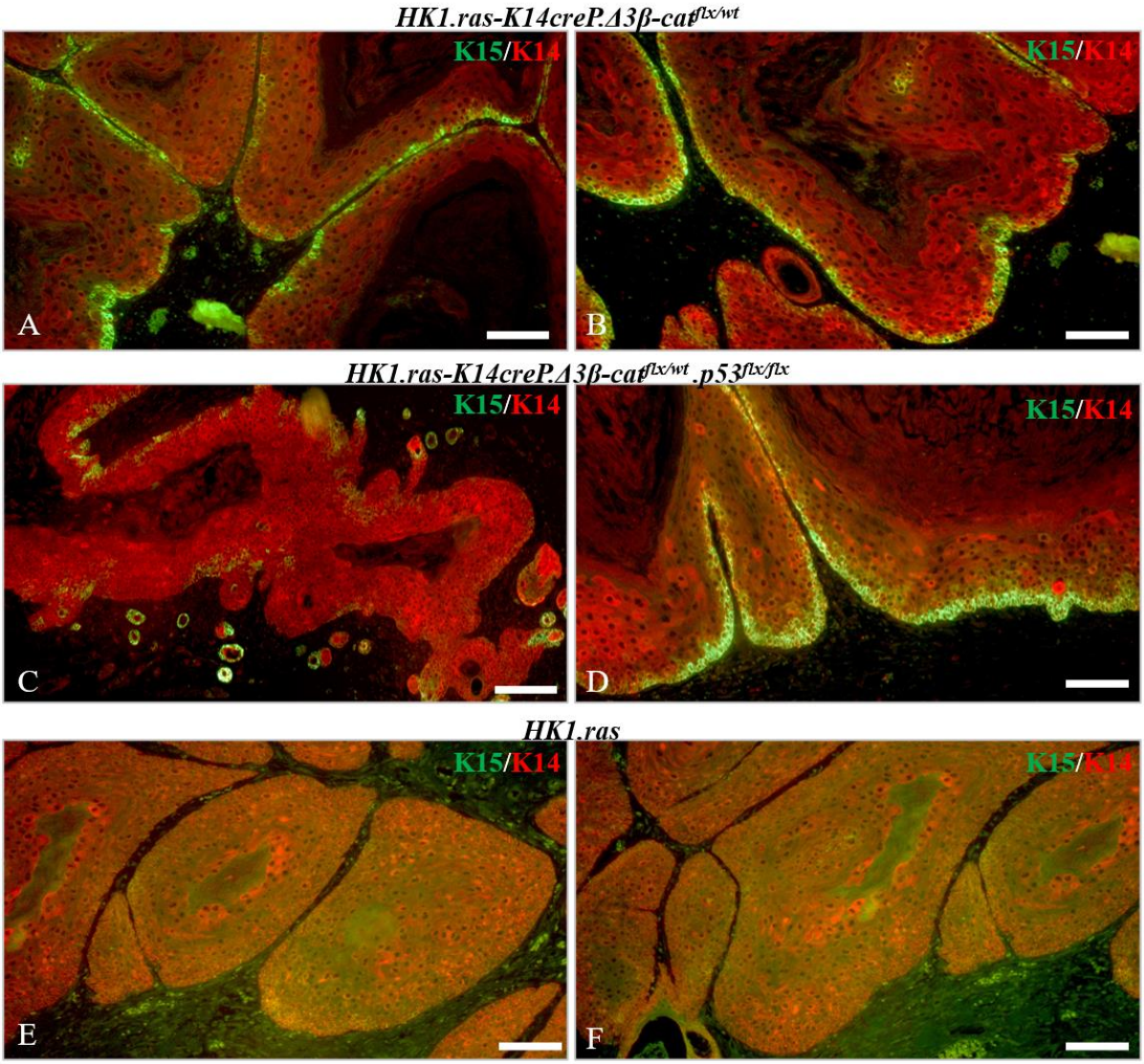

Figure 6. 27: Analysis of keratin K15 expression in rare *HK1.ras-K14creP.Δ3β-cat*$^{flx/wt}$ and *HK1.ras-K14creP.Δ3β-cat*$^{flx/wt}$*.p53*$^{flx/flx}$ tumours.

[A & B] The two RU486-treated *HK1.ras-K14creP.Δ3β-cat*$^{flx/wt}$ papillomas show strong K15 expression in specific strands of basal layer keratinocytes where K15 is also confined to basal layers. [C] The *HK1.ras-K14creP.Δ3β-cat*$^{flx/wt}$*.p53*$^{flx/flx}$ lacks K15 expression in the mix of hyperplastic, papilloma and SCC histotypes; and this minimal expression appears erratic and supra-basal. [D] At higher magnification, benign papilloma histotype of the *HK1.ras-K14creP.Δ3β-cat*$^{flx/wt}$*.p53*$^{flx/flx}$ tumour exhibits strong basal layer expression similar to [A & B]; but this is beginning to fade and of note the expression is wider and not confined to the basal layer keratinocytes. [E & F] By this time [12wks] *HK1.ras* papillomas are larger and completely lack the K15 expression observed in earlier hyperplasia. Scale bars: A, & B: 150 µm; C & D: 75 µm.

These K15 expression data again suggest that the reduced leakage and later *Δ3β-catenin* expression again allowed for K15 to be expressed in the *HK1.ras-K14creP.Δ3β-cat*$^{flx/wt}$ papilloma keratinocytes as observed in chemical carcinogenesis and a general lack of the early

inhibitory p63/p73 or p21 responses as observed in *HK1.ras* alone hyperplasia given that β-catenin expression remained supra-basal. However, following p53 loss in *HK1.ras-K14creP.Δ3β-cat$^{flx/wt}$.p53$^{flx/flx}$* mice this leads to unstable areas when coupled to nuclear and membranous β-catenin expression [above], where either K15 is missing or in the papilloma stage, the sporadic low K15 expression is multi-layered as seen in *HK1.ras* hyperplasia. Thus, as seen in human SCC (*Abbas and Bhawan, 2011*) and late-stage chemical papillomas (*Troy et al., 2011*), K15 expression becomes reduced and lost.

Furthermore, the different K15 expression profiles between papillomas developed with *Δ3β-catenin* activation compared to typical *HK1.ras* papillomas, again indicate that in *HK1.ras-K14creP.Δ3β-cat$^{flx/wt}$* and *HK1.ras-K14creP.Δ3β-cat$^{flx/wt}$.p53$^{flx/flx}$* mice their papillomas carry different characteristics and thus may derived from different KPC/stem cell niches particularly since the *HK1.ras* transgene is not expressed in HFs. These results are therefore consistent with the findings by Morris and co-workers who showed that in cell labelling studies using the *K15*-promoter crossed to the *Rosa 26 β-gal* reporter mouse (*Li et al.,* 2013) whilst many papilloma cells derived from K15-positive precursors, many papilloma keratinocytes were β-gal negative, a result consistent with multiple mutations in many KPC types derived from DMBA initiation indicating the overall potential heterogeneity of papillomas as observed here [Fig. 6.27A,B vs. D] and their different progression potential [Fig. 6.27C].

Finally, following these findings of compensatory p53 family responses and the excess expression of p21 coupled to these changes in the K15 KPC/stem cell marker, the effect of early *Δ3β-catenin*, βcatenin was also assessed in keratinocyte proliferation employing the standard BrdU labelling analysis [Fig.6.28]. This was used to assess whether reduced proliferation in the tumour free *HK1.ras-K14creP.Δ3β-cat$^{flx/wt}$* and *HK1.ras-K14creP.Δ3β-cat$^{flx/wt}$.p53$^{flx/flx}$* mice reflected the p63/p73 and p21 responses and this contributed to and was the possible reason for the reduced hyperplasia observed or even the overall lack of tumours.

This proved to be the case as in early untreated and RU486-treated *HK1.ras-K14creP.Δ3β-cat$^{flx/wt}$.p53$^{flx/flx}$* mice [n1] [Fig. 6.28A&B], the result showed a lower mitotic index of 10.20 [$^{+}$/- 2.5] compared to *HK1.ras-K14creP.Δ3β-cat$^{flx/wt}$* mice [n1] [Fig. 6.29C] at 19.6 [$^{+}$/- 1.1] or *HK1.ras* [n1] mice [Fig. 6.28D] with an index of 20.2 [$^{+}$/- 5.5] comparable to previous studies (*Yao et al., 2006; 2008; Macdonald et al., 2014*). Although this experiment was conducted qualitatively due to technical error in mice BrdU injection, these proliferation results were consistent with the reduced hyperplasia observed in *HK1.ras-K14creP.Δ3β-cat$^{flx/wt}$.p53$^{flx/flx}$* following p53 loss when compared to *HK1.ras-K14creP.Δ3β-cat$^{flx/wt}$* or *HK1.ras* IFE

hyperplasia. For *HK1.ras-K14creP.Δ3β-cat*$^{flx/wt}$*.p53*$^{flx/flx}$ epidermis this result probably reflects the increased expression of *p21*, *p63* and *p73* in the context of *Δ3β-catenin* overexpression and all targeted to protect the epidermis following the additional loss of p53 mediated cell cycle control.

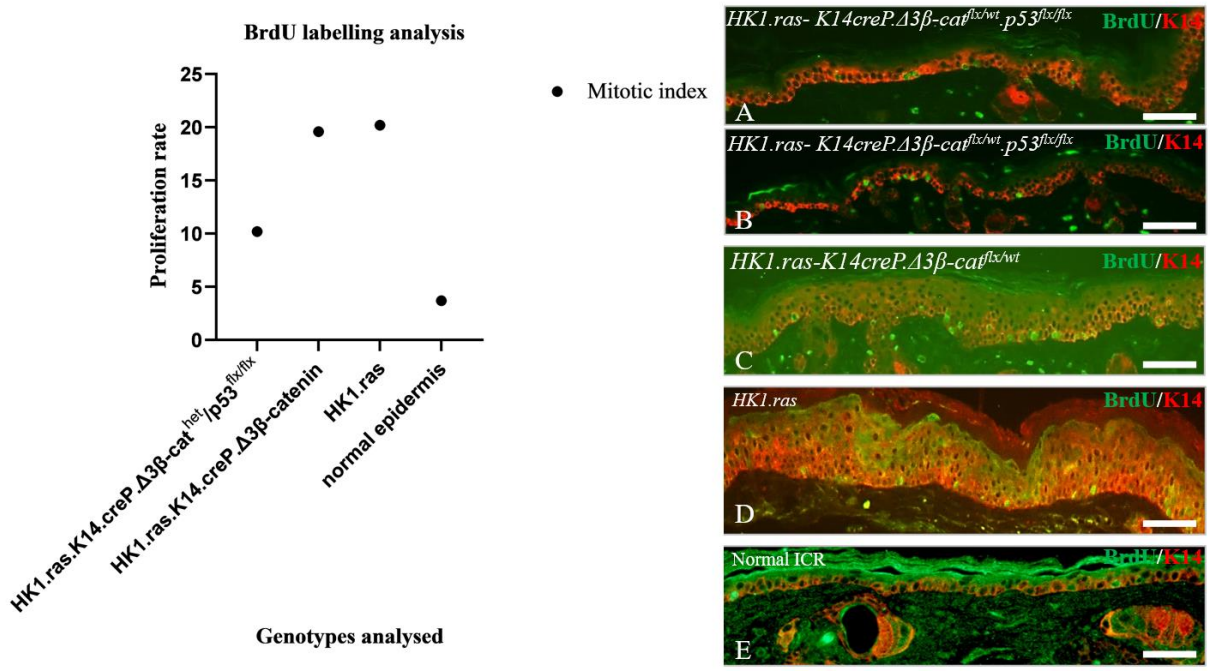

Figure 6. 28: BrdU labelling analysis of *HK1.ras-K14creP.Δ3β-cat*$^{flx/wt}$*.p53*$^{flx/flx}$ skin indicates a lower mitotic index compared to *HK1.ras-K14creP.Δ3β-cat*$^{flx/wt}$ skin.

Quantitation of BrdU labelling from the four genotypes is based on counts averaged from 8 fields to give a mitotic index of: [A & B] *HK1.ras-K14creP.Δ3β-cat*$^{flx/wt}$*.p53*$^{flx/flx}$ (n1): 10.20 [$^{+}$/$_{-}$ 2.5] cell per mm basement membrane. [B] *HK1.ras-K14creP.Δ3β-cat*$^{flx/wt}$ (n1): 19.6 [$^{+}$/$_{-}$ 1.1] cell per mm basement membrane; [D] *HK1.ras* (n1): 20.2 [$^{+}$/$_{-}$ 5.5] cell per mm basement membrane and [E] normal epidermis (n1): 3.70 cell per mm basement membrane. Scale bars: A-D: 75 µm; E: 50 µm.

When coupled to the K15 data, it also suggests that *Δ3β-catenin* alters the stem cell niches such that there may be reduced numbers of KPC targets for papilloma formation; an idea supported by the lack of these responses in all four mice that to date develop papillomas and those two that were prone to convert. This also applies to the similar lack of p53/p63/p73 and p21 responses observed in *HK1.ras* hyperplasia given its lack of expression in HF bulge region keratinocytes [Chapter 1: Fig.3B]. Hence, this change in potential KPC population targets for papilloma formation (*Li et al., 2013)* highlights that papillomas formed come from different cell types including those arising in *Δ3β-catenin* activation in p53^{wt} or p53^{flx} contexts as these have to overcome the p21/p53 and/or p63/p73 responses that normally protect theses

KPC populations that do not appear at this stage in *HK1.ras* mice but appear later to prevent their progression to SCC.

6.7 Preliminary analysis of p21 knockout in *HK1.ras-K14creP.Δ3β-cat$^{flx/wt}$* mice

The data from *HK1.ras-K14creP.Δ3β-cat$^{flx/wt}$* and *HK1.ras-K14creP.Δ3β-cat$^{flx/wt}$.p53$^{flx/flx}$* cohorts analysis clearly implicated p21 roles in multiple aspects such as inducing commitment to differentiation, halting tumor development and possibly maintaining KPC. Thus to directly assess these roles on-going experiments directly induced p21 loss via embryonic knockout (*Martín-Caballero et al., 2001*) to create the *K14creP.Δ3β-cat$^{flx/wt}$.p21KO* and *HK1.ras-K14creP.Δ3β-cat$^{flx/wt}$.p21KO* genotypes.

The preliminary data again demonstrated a lack of tumour formation in all *HK1.ras-K14creP.Δ3β-cat$^{flx/wt}$.p21KO* mice at 12 weeks of age [Fig.6.29: A & B] similar to that observed in *HK1.ras-K14creP.Δ3β-cat$^{flx/wt}$.p53$^{flx/flx}$* and *HK1.ras-K14creP.Δ3β-cat$^{flx/wt}$* mice [Fig. 6.29C&D]. However, all litters of *K14creP.Δ3β-cat$^{flx/wt}$.p21KO* or *HK1.ras-K14creP.Δ3β-cat$^{flx/wt}$.p21KO* mice became score 1 [or 2] and by day 20, showed the typical Δβ-catenin phenotypes in all adult mice [Fig.6.29: E & H] including the associated keratosis and scruffiness observed in *HK1.ras-K14creP.Δ3β-cat$^{flx/wt}$* littermates [Fig. 6.29G&J]. To date none of these *K14creP.Δ3β-cat$^{flx/wt}$.p21KO* or *HK1.ras-K14creP.Δ3β-cat$^{flx/wt}$.p21KO* individuals exhibited a delay in the onset of Δβ-catenin phenotypes that appeared in all *K14creP.Δ3β-cat$^{flx/wt}$.p53$^{flx/flx}$* and *HK1.ras-K14creP.Δ3β-cat$^{flx/wt}$.p53$^{flx/flx}$* mice [Fig. 6.29F&I].

These preliminary data clearly indicate that blocking tumour development was not dependent on p21 protection in at least the early stages of tumour development. Instead possibly the importance of p21 expression comes in once a tumour is formed, or even once it has converted to early malignancy, as losing p21 expression at that stage was associated with rapid progression to more invasive carcinomas as seen above in *HK1.ras-K14creP.Δ3β-cat$^{flx/wt}$.p53$^{flx/flx}$* SCC and *HK1.ras/fos-K14creP.Δ5PTEN$^{flx/flx}$ SCC* (*Macdonald et al., 2014*).

These data also indicate that delay in the onset of Δβ-catenin phenotypes depended upon p53 responses as *HK1.ras-K14creP.Δ3β-cat$^{flx/wt}$.p21KO* and *HK1.ras-K14creP.Δ3β-cat$^{flx/wt}$* phenotypically look indistinguishable from each other. However, these are initial observations and more analysis needs to be conducted on these mice to establish the similarly and

differences in protein expression to the loss of p21 in *HK1.ras-K14creP.Δ3β-cat*$^{flx/wt}$*.p21KO* ,*HK1.ras-K14creP.Δ3β-cat*$^{flx/wt}$ and *HK1.ras-K14creP.Δ3β-cat*$^{flx/wt}$*.p53*$^{flx/flx}$.

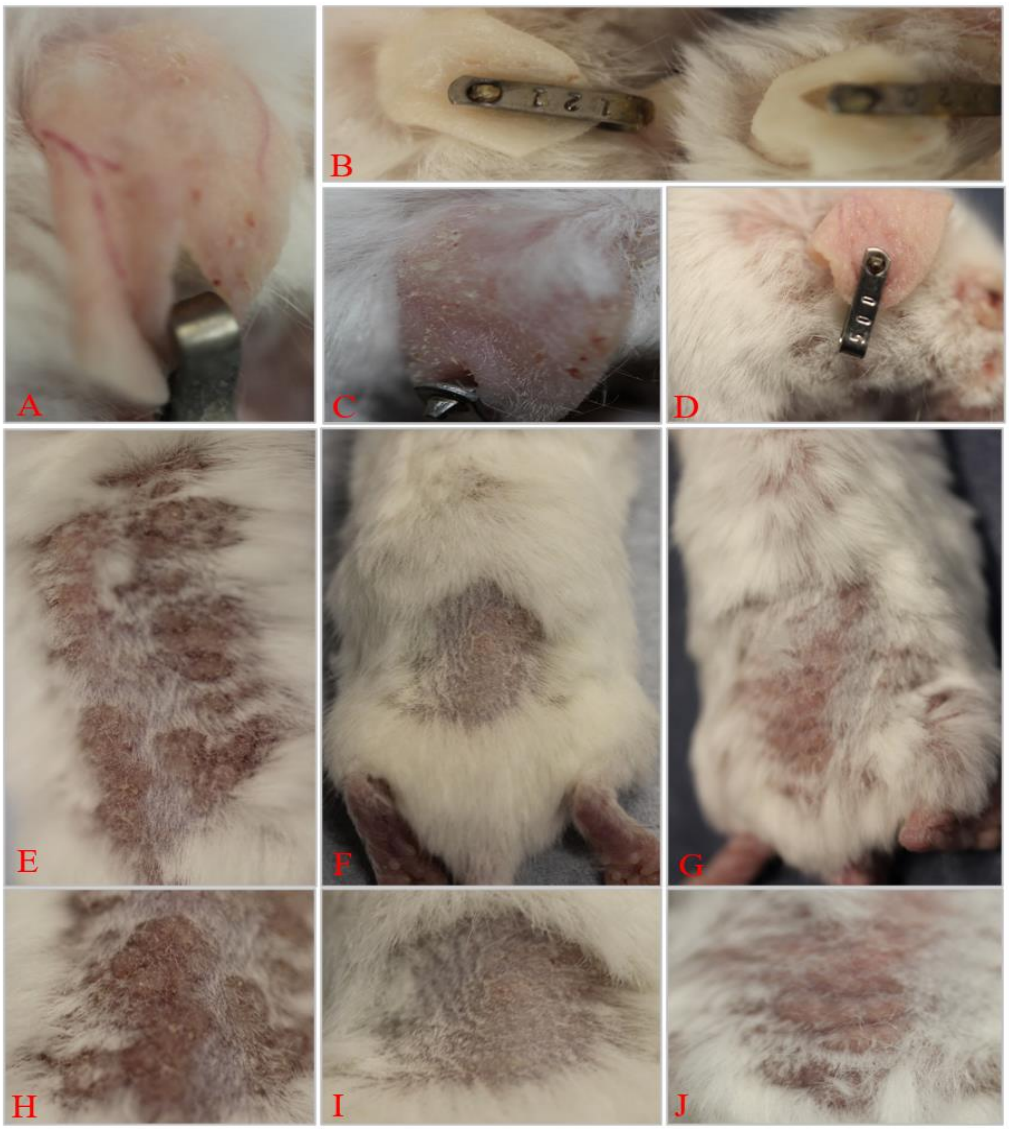

Figure 6. 29: *HK1.ras-K14creP.Δ3β-cat*$^{flx/wt}$*.p21KO* genotypes lack papilloma formation.

[A & B] At 8 weeks post ear-tag wounding shows RU486-treated tagged *HK1.ras-K14creP.Δ3β-cat*$^{flx/wt}$*.p21KO* lack any sign of tumour development as observed in [C] RU486-treated *HK1.ras-K14creP.Δ3β-cat*$^{flx/wt}$*.p53*$^{flx/flx}$. [D] *HK1.ras-K14creP.Δ3β-cat*$^{flx/wt}$ tagged ear at 8 weeks post ear-tag wounding also lacks tumour development. [E-G] shows typical keratosis of *Δ3β-catenin* in [G] *HK1.ras-K14creP.Δ3β-cat*$^{flx/wt}$*.p21KO* compared to greatly reduced keratosis in [F] *HK1.ras-K14creP.Δ3β-cat*$^{flx/wt}$ *.p53*$^{flx/flx}$, and the typical Δ3β-catenin keratosis in [G] *HK1.ras-K14creP.Δ3β-cat*$^{flx/wt}$. [H-J] A contrast between the differences in keratosis in [H] *HK1.ras-K14creP.Δ3β-cat*$^{flx/wt}$ *.p21KO* , [I] *HK1.ras-K14creP.Δ3β-cat*$^{flx/wt}$ *.p53*$^{flx/flx}$ and [J] *HK1.ras-K14creP.Δ3β-cat*$^{flx/wt}$ genotypes.

Table 6. 3: Summary of p63, p73 and keratin K15 status in *HK1.ras-K14creP.Δ3β-cat$^{flx/wt}$* and *HK1.ras-K14creP.Δ3β-cat$^{flx/wt}$.p53$^{flx/flx}$* mouse phenotypes

Genotype analysed	[N]	Analysed for expression of	Data summary
HK1.ras hyperplasia	90	p63,p73,K15, BRDU labeling	-No basal layer p63/p73 expression -Expressing K15 in both basal and supra-basal layers -Mitotic index: 20.2 [$^{+}$/- 5.5] cell per mm basement membrane
HK1.ras-K14creP.p53$^{flx/flx}$ hyperplasia	22	p63, p73,K15	-No basal layer p63/p73 expression -Expressing K15 in both basal and supra-basal layers
HK1.ras-K14creP.Δ3β-cat$^{flx/wt}$ [No papillomas]	58	p63,p73,K15, BRDU labeling	-Sporadic p63/p73 expression in basal layer with HF expression -K15 expression confined to HF - Mitotic index: 19.6 [$^{+}$/- 1.1] cell per mm basement membrane
HK1.ras-K14creP.Δ3β-cat$^{flx/wt}$.p53$^{flx/flx}$ [No papillomas]	15	p63,p73,K15, BRDU labeling	-Increased basal layer expression of p63/p73 with HF expression -K15 expression confined to HF - Mitotic index: 10.20 [$^{+}$/- 2.5] cell per mm basement membrane
Conclusion: β-catenin activation triggered compensatory p63/p73 TSG expression in efforts to possibly regulate incorrect control of the stem cell niche and consequently the IFE terminal differentiation especially with p53 loss, as stem cell marker K15 was not present in the IFE, contrary to the control hyperplasia due to elevated p63/p73. This elevation coupled to p53/p21 or p21 consequently resulted in the low mitotic index observed in Δ3β-catenin associated genotypes.			

Table 6. 4: Summary of p63 and p73 status in *HK1.ras-K14creP.Δ3β-cat$^{flx/wt}$* and *HK1.ras-K14creP.Δ3β-cat$^{flx/wt}$.p53$^{flx/flx}$* tumours.

Genotype analysed	[N]	Analysed for expression of	Data summary
HK1.ras papilloma	90	p63, p73, K15	-Basal layer expression of p63 and sporadic, basal layer expression of 73 -Lack of K15 expression
HK1.ras-K14creP.Δ3β-cat$^{flx/wt}$ papilloma	2	p63, p73, K15	-Weak basal p63 expression and increased p73 basal layer expression -Basal layer K15 expression
HK1.ras-K14creP.Δ3β-cat$^{flx/wt}$.p53$^{flx/flx}$ SCCs	2	p63, p73, K15	-Increased basal layer expression of both p63/p73 -Basal layer K15 expression
Conclusion: elevated expression of p63/p73 in *HK1.ras-K14creP.Δ3β-cat$^{flx/wt}$ p53$^{flx/flx}$* SCCs is consistent with reported expression in carcinomas following loss of p53 and p21.			

6.8. SUMMARY

The previous chapters illustrated the impact of constitutive β-catenin activation [*K14creP.Δ3β-cat*$^{flx/wt}$] on epidermal homeostasis and regulation of hair follicle formation as well as different body organs such as extremities [feet and tail]. All the *K14creP.Δ3β-cat*$^{flx/wt}$ data were generally in agreement with the literature (*Närhi et al., 2008; Grigoryan et al., 2008*) in terms of HF anomalies, yet even in score 2 skin there was a relatively weak degree of hyperplasia as also seen previously (*Gat et al., 1998; Celso et al., 2003*) and in that context this was now shown to be due to early elevated levels of p53/p21 TSGs expression that inhibited Δ3β-catenin induced proliferation and altered the keratinocyte differentiation programme [Chapter 4].

In Chapter 5, *HK1.ras-K14creP.Δ3β-cat*$^{flx/wt}$ mice demonstrated a paradoxical block of papillomatogenesis except in two cases of full-sized mice where papillomas appeared and maintained a benign histotype when biopsied. Thus, indicating that in a model more consistent with what was expected for β-catenin and ras co-operation, here again expression of p53/p21 was so strongly present in *HK1.ras-K14creP.Δ3β-cat*$^{flx/wt}$ papillomas, that Δ3-βcatenin was unable to induce conversion; a result consistent with findings in *HK1.ras/fos* papillomas where β-catenin expression remained supra-basal. This expression of p53 and p21 was also assumed to result in the blockage of tumour forming in vast majority of mice, as in these cohorts the leakage of Δ3β-catenin resulted in pronounced p53 and p21 expression in the IFE thus preventing papillomas forming.

The influence of Δ3β-catenin-mediated compensatory p53/p21 expression on the fate of papillomas forming was clearly apparent when IFE hyperplasia invoked high levels of p53/p21 that were not observed in *HK1.ras* controls, which eventually develop benign papillomas in 100% of mice. This indicted that in this context of *HK1.ras-K14creP.Δ3β-cat*$^{flx/wt}$ mice, such compensatory p53/p21 expression halted the proliferation needed for papilloma development and whilst the disordered differentiation indicated by aberrant K1/K6α expression also suggested a contribution to tumour inhibition in this context of wtp53/p21.

Thus, to validate this theory, a logical approach induced conditional p53 knockout first in *K14creP.Δ3β-cat*$^{flx/wt}$ genotypes and then in *HK1.ras-K14creP.Δ3β-cat*$^{flx/wt}$ to understand p53

roles in these contexts. However, the results indicated that in this new context *HK1.ras-K14creP.Δ3β-cat*$^{flx/wt}$*.p53*$^{flx/flx}$ genotype not only was p53 loss unable to induce papillomas [except on two occasions discussed below], but also the juvenile skin data of *K14creP.Δ3β-cat*$^{flx/wt}$*.p53*$^{flx/flx}$ mice demonstrated that the Δ3β-catenin phenotypes were directly dependent upon wild type p53 function. Both *K14creP.Δ3β-cat*$^{flx/wt}$*.p53*$^{flx/flx}$ and *HK1.ras-K14creP.Δ3β-cat*$^{flx/wt}$*.p53*$^{flx/flx}$ mice grossly lacked typical *Δ3β-catenin* hyperkeratosis and with minimal effect on body size and extremities. Histologically *K14creP.Δ3β-cat*$^{flx/wt}$*.p53*$^{flx/flx}$, at 3 weeks [~24d], mice appeared fairly normal and exhibited few to none Δ3β-catenin phenotypes*;* whilst at 8 weeks showed a mild level of Δ3β-catenin phenotype with a lack of hair follicle tumours such as folliculoma frequently seen in *K14creP.Δ3β-cat*$^{flx/wt}$ mice (*Gat et al., 1998; Celso et al., 2003*). This clearly implicated p53 roles in both the appearance and the intensity of *Δ3β-catenin* phenotypes as well as in the follicular tumours associated with *Δ3β-catenin* overexpression and prevented the internal problems that have dogged this project in terms of animal viability.

The reasons for this unique and potent block of Δ3β-catenin phenotypes by p53 loss are again very unclear but this does appear to be a very important finding and as discussed below the p63 and p73 data suggest that it may be expression responses to p53 loss that also altered keratinocyte proliferation/differentiation that possibly had major effects on the stem cell /KPC populations that reduced or countered the effects of deregulated β-catenin to some extent and thus the numbers of pluripotent targets for ras activation and β-catenin overexpression.

There are strong links between p53 and β-catenin and during embryonic development p53 has been found to normally regulate embryonic stem cell proliferation via the β-catenin dependent canonical Wnt signalling among other pathways (*Lee et al., 2010*). This canonical Wnt signalling also regulates embryonic epidermal stem cell proliferation required for hair follicle morphogenesis and epidermal differentiation (*Grigoryan et al., 2008*). Thus it may be that deregulated overexpression of Δ3β-catenin during juvenile development which results in *de novo* hair follicle placodes and hair follicle tumours as well as effects on general body size and limbs, requires a competent p53 system to sense the problems caused, as observed in *K14creP.Δ3β-cat*$^{flx/wt}$ cohorts (*Gat et al., 1998; Van Mater et al., 2003;Grigoryan et al., 2008*) [see Chapter4] and these responses in *K14creP.Δ3β-cat*$^{flx/wt}$*.p53*$^{flx/flx}$ and *HK1.ras-K14creP.Δ3β-cat*$^{flx/wt}$*.p53*$^{flx/flx}$ are lacking.

Indeed, from this it can be speculated, that in developing juvenile *K14creP.Δ3β-cat*$^{flx/wt}$ genotypes [and the internal problems], it is the overexpression of p53 in response to Δ3β-catenin that plays an unavoidable role in the induction of phenotypes. Here, in this context, a feedback loop maybe established where elevated p53 activates the canonical Wnt signalling receptors to alter the stem cell niches which induce anomalous proliferation/differentiation/cysts/and HF anomalies via adding heterozygous endogenous β-catenin expression to that of *Δ3β-catenin* activation resulting in typical *Δ3β-catenin* phenotypes (*Gat et al., 1998; Niemann et al., 2002Van Mater et al., 2003; Grigoryan et al., 2008; Lee et al., 2010; Kretzschmar et al., 2015*). Thus, it appears that p53 was necessary for Δ3β-catenin by activating Wnt receptors to proliferate embryonic stem cells,

If this scenario of elevated p53 expression in *K14creP.Δ3β-cat*$^{flx/wt}$ induced the excess HF proliferation (*Song and Lambert, 1999; Botchkarev et al., 2001)* and *p53* loss led to general regression in HF development, it would explain to some extent why these mice had more alopecia and scruffiness, whilst *K14creP.Δ3β-cat*$^{flx/wt}$*.p53*$^{flx/flx}$ had less p53-mediated responses available resulting in a more normal looking hair follicle and bigger body size as seen in histology and gross phenotype analysis. The other aspect of this scenario may be more logical, on considering the actual general responses mounted by the epidermis to loss of potent protection which could be the cause for the striking reduction in the appearance and the intensity of *Δ3β-catenin* phenotype following p53 loss in *K14creP.Δ3β-cat*$^{flx/wt}$*.p53*$^{flx/flx}$ that might be influenced by roles of p63/p73 and the changes in the KPC indicated by K15 expression. As discussed below in terms of the continued lack of tumours following p53 loss, the induction of p63 and p73 expression responses would alter overall IFE and HF keratinocyte proliferation/differentiation with major effects on the stem cell /KPC populations as indicated by K15 expression.

The p63 and p73 gene share many similarities in epidermal function, perhaps more so than p53 which is simply involved with maintaining cell cycle and inducing apoptosis or responding to anomalous situations as outlined above. p63 and p73 have important generic roles that maintain correct epidermal stem cell/PCK niches ready for proliferation or later for the commitment or inhibition of the commitment to terminal differentiation; and also hair follicle morphogenesis *(Moll and Slade 2004; Koster et al., 2007; Botchkarev et al., 2014*).

For instance, p63 loss induces a failure of the epidermis to stratify and also disrupted the formation of hair follicles and the development of limbs *(Mills et al., 1999; Koster et al., 2004; Koster and Roop 2007*) which echoes the phenotypes induced by β-catenin deregulation. The ΔNp63 isoform is essential in maintaining basal layer proliferation and inhibiting premature differentiation via repression of genes such as p21 and PTEN (*Westfall et al. 2003; Moll and Slade 2004; Nguyen et al., 2006; Leonard et al., 2011*; *Botchkarev and Flores, 2014*) thus again linking to the normal suprabasal expression of β-catenin. For p73, pro-apoptotic roles inducing apoptosis following DNA damage (*Irwin et al., 2003; Rocco et al., 2006)* also associate with elevated expression in human SCC (*Moll and Slade, 2004),* and has also been detected in preliminary analysis of *HK1.ras/fos-K14creP.Δ5PTEN$^{flx/flx}$ SCC* [not shown].

Thus, in wild type p53 contexts the generally strong p63/p73 expression in hair follicles appearing in *K14creP.Δ3β-cat$^{flx/wt}$.p53$^{flx/flx}$* and *HK1.ras-K14creP.Δ3β-cat$^{flx/wt}$.p53$^{flx/flx}$* mice may attempt to antagonise Δ3β-catenin, constant with p63/p73 roles in maintaining hair follicle stem cells and differentiation *(Moll and Slade 2004; Koster et al., 2007; Botchkarev et al., 2014)*. However, with conditional loss of p53 in *HK1.ras-K14creP.Δ3β-cat$^{flx/wt}$.p53$^{flx/flx}$* mice an increase in basal layer expression of p63/p73 was noted in comparison to sporadic basal layer expression in *HK1.ras-K14creP.Δ3β-cat$^{flx/wt}$* with wild type p53. This indicated that p63/p73 elevated expression in *HK1.ras-K14creP.Δ3β-cat$^{flx/wt}$.p53$^{flx/flx}$* skin was possibly compensating for the lack of p53 expression to regulate epidermal homeostasis. The intense increase of p73 in basal layer clearly compensated for lack of p53 as this basal expression was not seen in p53 positive basal layers of *HK1.ras-K14creP.Δ3β-cat$^{flx/wt}$* mice which is constant with pro-apoptotic roles of p73 alongside those of p53 (*Rocco et al., 2006; DeYoung and Ellisen, 2007*).

This directly links to the idea that anomalous β-catenin alter specific KPCs populations in the epidermal stem cell unit, as the weaker and patchy K1 expression would be consistent with blocks of p63 expression that repress differentiation and also the abrupt lateral edges to both K1 and on occasion K6 expression made by specific stem cell units in the IFE (*Porter et al., 2000*). This feature of K1 expression appears to be a significant marker of the altered differentiation caused by deregulated β-catenin expression and the increased numbers of adherence junctions due to excess E-cadherin –which too may play a role in the reduced

response to β-catenin now mediated by p63 and p73 compensatory roles in HF and IFE physiology.

Therefore, following the analysis of p63/p73 and given the intense expression they exhibit in hair follicles of Δ3β-catenin activated genotypes and the role they might play in regulating the stem cell niche, keratin K15 was analysed as a stem cell marker. K15 is normally expressed in the bulge region of hair follicles and is considered to be a stem cell marker, which is also normally expressed in basal layer of IFE (*Bose et al., 2013*). Given the stem cell proliferation presumably induced via Δ3β-catenin activation, it was expected that K15 would exhibit strong expression in the IFE epidermis. However, K15 exhibited mainly strong expression confined to the hair follicle and was absent from the epidermis in *K14creP.Δ3β-cat*$^{flx/wt}$*.p53*$^{flx/flx}$ and *HK1.ras-K14creP.Δ3β-cat*$^{flx/wt}$*.p53*$^{flx/flx}$.

These results suggest that possibly the danger from excess stem cell/PCK cell proliferation induced via Δ3β-catenin triggered p63/p73 expression which resulted in the lack of K15 expression in the IFE. This too is consistent with the responses to *Δ3β-catenin* activation in p53^{wt} or p53^{flx} backgrounds, which are possibly geared to protect the KPC populations via maintaining their quiescence yet allowing for their availability e.g., upon wounding that involve communication between the β-catenin/wnt and the p53/63/p73 signalling cascades to mobilise the correct cells and is clearly deregulated in terms of K6α expression.

This scenario is also paralleled by the actual additional responses to p53 that are of greater significance to the continued lack of tumours in *HK1.ras-K14creP.Δ3β-cat*$^{flx/wt}$*.p53*$^{flx/flx}$, which also led to a similar effect on the otherwise well-known anti-tumorigenic roles of p53 giving the paradoxical block of papillomatogenesis in *HK1.ras-K14.p53*$^{flx/flx}$ observed over the past 25 years [discussed below; (*Greenhalgh et al., 1996*)]. Following the interesting observation *in K14creP.Δ3β-cat*$^{flx/wt}$*.p53*$^{flx/flx}$, ras activation was added to *K14creP.Δ3β-cat*$^{flx/wt}$*.p53*$^{flx/flx}$ to answer two questions. One of which is to understand p53 protective roles in *HK1.ras-K14creP.Δ3β-cat*$^{flx/wt}$*.p53*$^{flx/flx}$ by directly knocking-out the gene [p53^{flx}]. The other purpose of this cohort was to investigate Δ3β-catenin in *HK1.ras-K14creP.p53*$^{flx/flx}$ co-operation which paradoxically resulted in lack of tumours in a previous study and was also repeated in this cohort as control genotype showing identical result. Therefore, *HK1.ras-K14creP.Δ3β-cat*$^{flx/wt}$*.p53*$^{flx/flx}$ cohort potentially served as an important tool to understand β-catenin/p53 interaction in relation to tumour development with *HK1.ras* activation and the *HK1-ras-*

K14creP.Δ3β-cat$^{flx/wt}$*.p53*$^{flx/flx}$ cohorts showed another striking result as the majority of mice were tumour free, except for two mice that developed accelerated aggressive SCC within 8 weeks. Thus, compensatory mechanisms are elicited.

This result thus challenges the current dogma in the literature where β-catenin nuclear localization and p53 loss facilitate tumour invasion and metastasis (*Polakis 2000; Gunther et al., 2003; Yao et al., 2008).* This also shows that the context and timing of these co-operating mutations is important given that in *HK1.ras/fos-K14creP.Δ5PTEN*$^{flx/flx}$ [see Chapter 3], the overt papillomas expressed little membranous or nuclear β-catenin in basal layers until p53 was lost when endogenous β-catenin nuclear localization and p53 loss facilitated the progression of papillomas into SCCs.

The other interpretation of these data in *HK1.ras-K14creP.Δ3β-cat*$^{flx/wt}$*.p53*$^{flx/flx}$ cohort, taking into account the reported findings of *HK1.ras-K14creP.p53*$^{flx/flx}$ mice was that possibly the tumorigenesis paradoxically required the expression of p53, due to the lack of papilloma development in both genotypes. This echoes the theory outline above that p53 created a feed back loop to elicit β-catenin phenotypes. This suggestion can be supported by the observation in *HK1.ras-K14creP.p53*$^{flx/flx}$ cohorts that if RU486 treatment was delayed by 2 or 3 weeks by 10-12 weeks papillomas would result and by 16 -20 weeks could progress to aggressive SCC in some cases, however this approach could not be achieved in *HK1.ras-K14creP.Δ3β-cat*$^{flx/wt}$ *.p53*$^{flx/flx}$ cohorts due to uncontrollable early cre leakage with *Δ3β-catenin* but may have happened on two occasions [see below].

Collectively, both indications bring up the old discussion regarding p53 fundamental roles in carcinogenesis, as in *HK1.ras-K14creP.Δ3β-cat*$^{flx/wt}$ and similarly *HK1.fos-K14creP.Δ5PTEN*$^{flx/flx}$ co-operation, p53 expression was essential in halting tumour development, which is constant with p53 role as tumour suppresser gene. However, in *HK1.ras-K14creP.Δ3β-cat*$^{flx/wt}$*.p53*$^{flx/flx}$ and similarly in *HK1.ras-K14creP.p53*$^{flx/flx}$ mice the responses to p53 loss maybe equally or more potent in the inhibition of tumour development. This indicates that despite the wide spectrum of studies conducted on p53 roles, it is not yet entirely understood how *HK1.ras-K14creP.Δ3β-cat*$^{flx/wt}$*.p53*$^{flx/flx}$ and *HK1.ras-K14creP.p53*$^{flx/flx}$ cohorts could lack tumour development and thus further analysis was conducted on possible contributors to this paradoxical result via investigations of p63, p73,p21 and K15 [below].

As with *K14creP.Δ3β-cat$^{flx/wt}$.p53$^{flx/flx}$* mice, investigation of *HK1.ras-K14creP.Δ3β-cat$^{flx/wt}$.p53$^{flx/flx}$* phenotypes showed clear reduction in the severity of phenotypes compared to *HK1.ras-K14creP.Δ3β-cat$^{flx/wt}$* . The histological analysis of *HK1.ras-K14creP.Δ3β-cat$^{flx/wt}$.p53$^{flx/flx}$* showed a minimal effect of *Δ3β-catenin* in terms of de novo hair follicle and formation of cysts, which seems to be gradually increasing with age until it reaches typical degree of phenotype in some cases e.g., post 10 weeks of age. Another observation was that in *HK1.ras-K14creP.Δ3β-cat$^{flx/wt}$.p53$^{flx/flx}$* unlike *K14creP.Δ3β-cat$^{flx/wt}$.p53$^{flx/flx}$*, hair follicle tumours such as trichofolliculoma which appeared only in some cases and after a significant delay of more than 8 weeks compared to *HK1.ras-K14creP.Δ3β-cat$^{flx/wt}$* or *K14creP.Δ3β-cat$^{flx/wt}$* , where they developed hair follicle tumours sooner. The IFE hyperplasia was also slightly less than that of *HK1.ras-K14creP.Δ3β-cat$^{flx/wt}$* but it still had the similar disordered differentiation, and both were clearly less than *HK1.ras-K14creP.p53$^{flx/flx}$* or *HK1.ras* typical ordered differentiation.

Here analysis of β-catenin/E-cadherin expression in tumour free *HK1.ras-K14creP.Δ3β-cat$^{flx/wt}$.p53$^{flx/flx}$*, showed increased membranous expression in both supra and basal layer with nuclear localization of β-catenin. This indicated that an increase in cell-cell adhesion signalling helped prevent papillomas similar to *HK1.ras-K14creP.Δ3β-cat$^{flx/wt}$* findings. This also indicated that increased cell-cell adhesion in *HK1.ras-K14creP.Δ3β-cat$^{flx/wt}$ .p53$^{flx/flx}$* was not dependent on p53 expression, as suggested by *HK1.ras-K14creP.Δ3β-cat$^{flx/wt}$* data; yet in the context of *HK1.fos-K14creP.Δ5PTEN$^{flx/flx}$* KA aetiology compensatory p53 and p21 appeared to be associated with increased cell-cell adhesions [β-catenin/E-cadherin expression], thus this may depend upon p21, hence following p21 loss in *HK1.ras/fos-K14creP.Δ5PTEN$^{flx/flx}$* SCCs E-cadherin is reduced at the invasive front.

However, despite the loss of p53 which is essential in maintaining the homeostasis of cellular adhesion *(Wu et al., 1997)*, in the *HK1.ras-K14creP.Δ3β-cat$^{flx/wt}$.p53$^{flx/flx}$* context, the cytoplasmic pool of β-catenin/E-cadherin interactions to maintain cell-cell adhesion seems unaffected. Thus, the proposed function of E-cadherin to act as a sponge to provide additional regulation of β-catenin (*Huels et al., 2015*) remained intact similar to the observations in *HK1.ras-K14creP.Δ3β-cat$^{flx/wt}$* [Chapter 5].

By default, these data also show that the responses to p53 loss which inhibited papillomatogenesis in *HK1.ras-K14creP.p53$^{flx/flx}$* mice were also independent of β-catenin

expression; as Δ3β-catenin was unable to overcome the paradoxical inhibition of papillomas. Thus, this suggests that the inhibitory compensatory mechanism to p53 loss maybe generic, hence a lack of early papillomas in both contexts. Thus, future experiments such as genomic and proteomic profiling of these different contexts that are designed to identify the component pathways could be of significant value for future therapeutics.

The early differentiation marker K1 showed weak expression almost disappearing from the epidermis in *HK1.ras-K14creP.Δ3β-cat*$^{flx/wt}$*.p53*$^{flx/flx}$ as seen in *HK1.ras-K14creP.Δ3β-cat*$^{flx/wt}$ and the odd confused patchy expression was amplified by the loss of p53 in *HK1.ras-Δ3β-cat*^{het}*/p53*$^{flx/flx}$. This was odd given that p53 loss greatly disturbed terminal differentiation in *HK1.ras-K14creP.Δ3β-cat*$^{flx/wt}$*.p53*$^{flx/flx}$ but papillomas did not develop and the hyperproliferation marker K6α was also not expressed in the epidermis. It may be that this further reduction in K1 expression in *HK1.ras-K14creP.Δ3β-cat*$^{flx/wt}$*.p53*$^{flx/flx}$ epidermis could be due to basal layer p63 expression that inhibits the commitment to terminally differentiate and maintain a population of proliferative keratinocytes. As above, blocks of p63 would give the abrupt lateral edges to both K1 made by specific stem cell units in the IFE (*Porter et al., 2000*). This feature of K1 expression also appears to be a significant marker of the altered differentiation caused by deregulated β-catenin expression and the increased numbers of adherence junctions due to excess E-cadherin.

This latter point would also contribute to the inhibition of tumours in these mice. Here it might be that basal layer p53 in *HK1.ras-K14creP.Δ3β-cat*$^{flx/wt}$ were attempting to regulate the Δ3β-catenin effect on epidermal differentiation by promoting differentiation signals with p21 as seen with the accelerated differentiation in *HK1.ras/fos-K14creP.Δ5PTEN*$^{flx/flx}$ KA due to endogenous β-catenin overexpression. Alongside p63 and p73 the lack of basal p53 in *HK1.ras-K14creP.Δ3β-cat*$^{flx/wt}$*.p53*$^{flx/flx}$ and lack of K1 expression despite the increased basal layer p21 which maybe promoting epidermal differentiation in response to loss of stress signal p53-mediated responses and the suggestion above that p21 may be more important to E-cadherin and adherence junction formation in KAs.

The lack of K1 yet elevated p21 was also constant with the proposed function of p21 in the upper layers of the IFE epidermis (*Topley et al., 1999; Devagn et al., 2006*) as increased expression here could induce inhibitory differentiation signals as seen in both *HK1.ras-K14creP.Δ3β-cat*$^{flx/wt}$*.p53*$^{flx/flx}$ and *HK1.ras-K14creP.Δ3β-cat*$^{flx/wt}$. Similarly, the lack of K6α

expression could be attributed to high levels of basal layer p21 expression similar to *HK1.ras-K14creP.Δ3β-cat*$^{flx/wt}$. Another hypothesised mechanism for the lack of tumour was that p53 loss might have led to a lack in regulating stem cell proliferation due to Δ3β-catenin activation, which in return invoked compensatory responses of other TSGs to halt this oncogenic proliferation, hence analysis of p63/p73 together with assessing K15 as stem cell marker and the mitotic index in both *HK1.ras-K14creP.Δ3β-cat*$^{flx/wt}$*.p53*$^{flx/flx}$ and *HK1.ras-K14creP.Δ3β-cat*$^{flx/wt}$.

Conditional loss of p53 in *HK1.ras-K14creP.Δ3β-cat*$^{flx/wt}$*.p53*$^{flx/flx}$ gave an increase in basal layer expression of p63/p73 indicating again that they may have been expressed to compensate for p53 loss in the inhibition of tumours. The intense increase of p73 in basal layers clearly supports this idea as this basal expression was not seen in p53 positive basal layers of *HK1.ras-K14creP.Δ3β-cat*$^{flx/wt}$ and is constant with TSG roles of p73 (*Rocco et al., 2006; DeYoung and Ellisen, 2007*). This also might indicate that p73 response was more effective in *HK1.ras-K14creP.Δ3β-cat*$^{flx/wt}$*.p53*$^{flx/flx}$ to block typical Δ3β-catenin where alternatively p53 failed to reduce Δ3β-catenin effectively in *HK1.ras-K14creP.Δ3β-cat*$^{flx/wt}$.

This suggest that possibly the excess stem cell proliferation induced via Δ3β-catenin triggered early compensatory TSGs [p53/p21/p63/p73] expression resulted in the lack of K15 expression in the IFE. This also might explain the aberrant K1/K6 expression seen in *HK1.ras-K14creP.Δ3β-cat*$^{flx/wt}$ and *HK1.ras-K14creP.Δ3β-cat*$^{flx/wt}$*.p53*$^{flx/flx}$ as TSGs expression halted the tumour development but at the same time possibly depleted the stem cell niche required for normal terminal differentiation.

This is consistent with the responses to *Δ3β-catenin* activation in p53^{wt} or p53^{flx} possibly to protect the KPC populations via maintaining their quiescence and at this very early stage there is a lack of potential papilloma forming cells due to protection form combinations of p53 and p21 backed up when necessary by p63 and p73 and resultant anomalous differentiation. This was also reflected in BrdU-labelling analysis, where a low mitotic index suggested possibly a loss of stem cell targets as the cause for the lack of tumours forming in both tumour free *HK1.ras-K14creP.Δ3β-cat*$^{flx/wt}$*.p53*$^{flx/flx}$ and *HK1.ras-K14creP.Δ3β-cat*$^{flx/wt}$ as evident by the lack of K15 in the IFE due to the KPC populations being protected by TSGs.

With respect to the two tumours that developed in *HK1.ras-K14creP.Δ3β-cat*$^{flx/wt}$*.p53*$^{flx/flx}$ these now began to make more logical sense for the outcome of p52 loss and β-catenin co-operation

with activated ras^{Ha}. Firstly, they appeared, suggesting that again full sized mice which lacked developmental phenotypes would produce papillomas as observed in *HK1.ras-K14creP.Δ3β-cat*$^{flx/wt}$ mice if the skin was allowed to develop normally. Moreover, consistent with p53 loss in these *HK1.ras- K14creP.Δ3β-cat*$^{flx/wt}$*.p53*$^{flx/flx}$ mice both tumours converted to carcinoma the histological analysis confirmed progression to aggressive SCC. This histotype was confirmed by early differentiation marker K1 expression disappearing, consistent with progression of the papilloma to carcinoma. The hyperproliferation marker K6α also showed weak expression in the converted pdSCC and also strong expression in the benign part; but both lacked basal layer expression This suggested that perhaps early progression to *HK1.ras-K14creP.Δ3β-cat*$^{flx/wt}$*.p53*$^{flx/flx}$ carcinoma was not the same as that in *HK1.ras/fos-K14creP.Δ5PTEN*$^{flx/flx}$ SCC due to *Δ3β-catenin* effects.

However, *HK1.ras-K14creP.Δ3β-cat*$^{flx/wt}$*.p53*$^{flx/flx}$ showed p53 loss correlated with reduced membranous expression of β-catenin /E-cadherin and increased nuclear localization of β-catenin. This was becoming more constant with endogenous β-catenin expression analysis in *HK1.ras/fos-K14creP.Δ5PTEN*$^{flx/flx}$ [see Chapter 3] that showed similar correlation and both examples were also constant with the literature dogma (*Polakis 2000; Gunther et al., 2003; Yao et al., 2008; Jeanes et al., 2008)*. Thus as *HK1.ras-K14creP.Δ3β-cat*$^{flx/wt}$*.p53*$^{flx/flx}$ tumours progressed from wdSCC through SCC and finally pdSCC. this correlated with increasing nuclear localization of β-catenin and loss of membranous β-catenin/E-cadherin expression at the invasive front.

This mechanism appeared distinct from papillomatogenesis in *HK1.ras-K14creP.Δ3β-cat*$^{flx/wt}$ mice, which showed increased nuclear β-catenin but with stable strong membranous β-catenin/E-cadherin expression similar to the expression profile of endogenous β-catenin in *HK1.fos-K14creP.Δ5PTEN*$^{flx/flx}$ KA [Chapter3]. Thus, indicating that as long as the cytoplasmic pool of β-catenin/E-cadherin is functioning correctly, nuclear localization of β-catenin can not induce conversion to carcinoma without p53 loss; whilst invasive progression requires p21 loss and loss of E-cadherin at the invasive front.

Furthermore, in *HK1.ras-K14creP.Δ3β-cat*$^{flx/wt}$*.p53*$^{flx/flx}$ and similarly in *HK1.ras/fos-K14creP.Δ5PTEN*$^{flx/flx}$ SCCs both lost p21 expression, unlike benign papillomas in *HK1.ras-K14creP.Δ3β-cat*$^{flx/wt}$ or the tumour free *HK1.ras-K14creP.Δ3β-cat*$^{flx/wt}$ and *HK1.ras-K14creP.Δ3β-cat*$^{flx/wt}$*.p53*$^{flx/flx}$ where high levels of p21 appeared in their hyperplasia. This

indicates that p21 protective responses might be as effective to counter AKT/β-catenin in later stages of tumour progression as well as earlier; given loss of p21 appears in both *HK1.ras-K14creP.Δ3β-cat*$^{flx/wt}$*.p53*$^{flx/flx}$ progression and following conversion in *HK1.ras/fos-K14creP.Δ5PTEN*$^{flx/flx}$ mice (*Macdonald et al., 2014*).

Moreover, additional anti-tumour assistance and possibly progression may have come from high levels of p63/p73 in *HK1.ras-K14creP.Δ3β-cat*$^{flx/wt}$*.p53*$^{flx/flx}$ SCCs consistent with previous reports *(Moll and Slade 2004; Koster et al., 2007; Botchkarev et al., 2014*) as seen in analysis of *HK1.ras/fos-K14creP.Δ5PTEN*$^{flx/flx}$ SCC [not shown]. On one hand the release of p63 [i.e. ΔNp63] in the context of aggressive p53-null papillomas, may exert an oncogenic property that successfully countered p21-mediated responses and which also circumvented elevated p73 TSG responses. Whereas, in rare *HK1.ras-K14creP.Δ3β-cat*$^{flx/wt}$ benign papillomas the weaker p63 [ΔNp63] expression was probably suppressed by p53/p21 expression and elevated p73 to maintaining the benign nature of this papilloma. This again indicated that once tumour development escaped the early protective responses to Δ3β-catenin/p53 loss where cre did not leak, the progression and conversion to carcinoma of these tumours was highly dependent on p53 response.

Additionally, K15 expression was analysed in papillomas developed in *HK1.ras-K14creP.Δ3β-cat*$^{flx/wt}$ and the SCCs developed in *HK1.ras-K14creP.Δ3β-cat*$^{flx/wt}$*.p53*$^{flx/flx}$ where in both cases basal layer expression was observed in tumours, which was not seen in HK1.ras^{1205} control papillomas. This expression of K15 therefore seems to be exclusive to tumours developed in genotypes carrying *Δ3β-catenin* which could be a key marker in understanding the development of tumours in these genotypes. This idea is supported by reports that K15-positive cells derived from hair follicle stem cells contribute to papilloma development (*Li et al., 2013*). Thus, tumours developed in *HK1.ras-K14creP.Δ3β-cat*$^{flx/wt}$ and *HK1.ras-K14creP.Δ3β-cat*$^{flx/wt}$*.p53*$^{flx/flx}$ mice may derive from such excess stem cell proliferation initially mediated by ΔNp63 expression that escaped the early p73 TSGs responses due to cre leakage of *Δ3β-catenin.*

Given the implications of p21 roles in halting tumour development and the observation that it loss in *HK1.ras-K14creP.Δ3β-cat*$^{flx/wt}$*.p53*$^{flx/flx}$ SCC facilitated conversion, on-going experiments investigated p21 knockout (*Martín-Caballero et al., 2001*) in *HK1.ras-K14creP.Δ3β-cat*$^{flx/wt}$*.p21KO* genotypes. The preliminary data indicate that p21 loss does not

facilitate tumour formation in conjunction with Δ3β-catenin and *HK1.ras* as these mice remained tumour free 12 weeks. This again indicated that p21 roles on in antagonising tumour development appear at later stages rather than early prevention of tumorigenesis. The other major finding demonstrated that *K14creP.Δ3β-cat*$^{flx/wt}$*.p21KO* and *HK1.ras-K14creP.Δ3β-cat*$^{flx/wt}$*.p21KO* and look indistinguishable from *HK1.ras-K14creP.Δ3β-cat*$^{flx/wt}$ in terms of juvenile Δ3β-catenin phenotypes. This result indicating that the delayed onset of Δ3β-catenin was directly associated with p53 loss.

Collectively, these data suggest that *Δ3β-catenin* activation invoked several epidermal protective responses and halting tumour development and was not exclusively dependent on p53 expression, however p53 seems to play two major roles in these cohorts. One of which was influencing the severity of Δ3β-catenin phenotype, as Δ3β-catenin/p53^{flx} co-operation which results in reducing the severity of the presented phenotype. The other role of p53 was controlling the fate of tumours converting to carcinomas, as seen in the rare examples when they developed in *HK1.ras-K14creP.Δ3β-cat*$^{flx/wt}$*.p53*$^{flx/flx}$ SCCs or *HK1.ras-K14creP.Δ3β-cat*$^{flx/wt}$ benign papillomas. However, these are only the preliminary findings and much work remains to identify and validate whether p63 and p73 are indeed the key facets that block papillomatogenesis in both *HK1.ras-K14creP.Δ3β-cat*$^{flx/wt}$*.p53*$^{flx/flx}$ and possibly *HK1.ras-K14creP.Δ3β-cat*$^{flx/wt}$. Although, this finding clearly suggests p21 as an easy answer for blocking of tumours, early data of *HK1.ras-K14creP.Δ3β-cat*$^{flx/wt}$*.p21KO* suggest that p21 is not responsible for either blocking of tumour or repression of *Δ3β-catenin* phenotypes which appears p53-specific.

These data also suggest that early activation of *Δ3β-catenin* elicits multiple protective responses with or without p53; resulting in blocking of tumorigenesis. However, in the rare cases where Δ3β-catenin was not prematurely activated by a leaking cre within 20-24d of age it appeared that *HK1.ras* associated papillomas were given enough time to develop. Thus, producing a very different tumour outcome in the context of *HK1.ras-K14creP.Δ3β-cat*$^{flx/wt}$ where wt p53 maintained a papilloma vs. Δ3β-catenin/ras^{Ha} in *HK1.ras-K14creP.Δ3β-cat*$^{flx/wt}$*.p53*$^{flx/flx}$ where loss of p53 expression more logically governed the fate of papilloma conversion and indicates the temporal effects of mutation in different contexts elicit different outcomes.

Chapter 7: β-catenin overexpression in *HK1.fos-K14creP.Δ5PTEN*$^{flx/flx}$ transgenic mouse skin

7.1 Introduction

As investigated above, analysis of *HK1.ras* or *HK1.ras/fos* papillomas showed that β-catenin expression was supra-basal and membranous, similar to normal β-catenin expression. In *HK1.fos-K14creP.Δ5PTEN$^{flx/flx}$* KA formation, loss of PTEN regulation and a specific level of AKT-mediated GSK3β inactivation allowed β-catenin expression to become strongly basal and also strongly nuclear and this triggered compensatory p53/p21 expression. This compensatory p53/p21 expression diverted the papillomatogenesis expected from *HK1.fos-K14creP.Δ5PTEN$^{flx/flx}$* co-operation into one of massive differentiation, which gave the keratoacanthoma aetiology [see chapter 3 (*Yao et al., 2008*)]. Endogenous β-catenin levels in *HK1.fos-K14creP.Δ5PTEN$^{flx/flx}$* KA showed increased expression in basal layers, with nuclear localization correlating with the trigger of p53/p21. Meanwhile, together with E-cadherin expression, this strong membranous β-catenin expression would aid in cell-cell adhesion which led to a KA outcome rather than invasive SCC [above Chapter 3; (*Yao et al., 2008*)]. This analysis confirmed β-catenin involvement in the formation of *HK1.fos-K14creP.Δ5PTEN$^{flx/flx}$* KA as a consequence of *Δ5PTEN loss/*AKT activation and associated GSK3-β inactivation (*Alyamani et al., manuscript in preparation*).

In *HK1.ras/fos-K14creP.Δ5PTEN$^{flx/flx}$* mice, basal layer β-catenin expression was already detectable in hyperplasia and papillomas that also exhibited p53 and p21 expression. However, as the tumours converted to malignancy following p53 loss (*Macdonald et al., 2014*), nuclear β-catenin expression increased in basal keratinocytes that expressed less membranous β-catenin [above; Chapter 3 Fig. 3.3]. This was paralleled by initial increases in E-cadherin, but again following p53 loss, as the profile of excess nuclear/reduced membranous β-catenin expression became widespread, E-cadherin was progressively lost at the invasive front and thus cell-cell adhesion was reduced and this aided tumour invasion [Chapter 3 Fig. 3.3].

Therefore, as hypothesised in the aims, it was expected that crossing *K14creP.Δ3β-cat$^{flx/wt}$* mice with *HK1.fos* mice would lead to more rapid papilloma formation, with β-catenin acting as an initiator and fos as a promoter; since the fos transcription factor in AP1 is a target of Wnt signalling (*Toualbi et al., 2007; Saadeddin et al., 2009*). It was also thought that as Δ3β-catenin expression was now independent of deregulated PTEN/AKT/GSK3β signalling, it may circumvent the protective p53 responses observed in *HK1.fos-K14creP.Δ5PTEN$^{flx/flx}$* mice and

thus in *HK1.fos-K14creP.Δ5PTEN$^{flx/flx}$.Δ3β-cat$^{flx/wt}$* mice this could result in SCC not KA formation.

Instead, an unexpected block of either KA or papilloma was observed in *HK1.fos-K14creP.Δ5PTEN$^{flx/flx}$.Δ3β-cat$^{flx/wt}$* mice, and in this case it appears that increased differentiation was a major inhibitory event. Indeed, the levels of differentiation not only resulted in a significant keratosis but the folding observed in *Δ3β-catenin* skin now became not just folds but the accelerated keratinocyte differentiation which led to an almost scale –like appearance that overtly resembled a pangolin skin – the only scaled mammal; hence the reference to a pangolin phenotype thorough this chapter. However, there was clear co-operation between Δ5PTEN mutation and Δ3β-catenin overexpression in the development of follicular tumours in both these and *K14.Δ5PTEN.Δ3β-catenin* mice. Further, in preliminary experiments, again an effect of *p53* loss was observed in the IFE of these mice that protected against the effects of *Δ3β-catenin*.

7.2 HK1.fos-K14creP.Δ5PTEN$^{flx/flx}$.Δ3β-cat$^{flx/wt}$ co-operation resulted in massive keratinocyte differentiation and formation of a unique folded skin phenotype.

These experiments were originally designed to assess β-catenin activation in the *HK1.ras/fos* model based on the co-operative effects of *PTEN/p-AKT/p-GSK3β* signalling observed in previous studies that confirmed β-catenin's role in Chapter 3 and also investigate the effects of p53 loss given the malignant conversion of rare p53 null tumours in *HK1.ras-K14creP.Δ3β-cat$^{flx/wt}$.p53$^{flx/flx}$* vs. *HK1.ras-K14creP.Δ3β-cat$^{flx/wt}$* mice with wild type p53. Thus, to directly test whether activated *Δ3β-catenin* will facilitate tumorigenesis or induce similar protective responses as seen in *HK1.ras-K14creP.Δ3β-cat$^{flx/wt}$* and *HK1.ras-K14creP.Δ3β-cat$^{flx/wt}$.p53$^{flx/flx}$* [See chapters 4 & 5] cohorts of *HK1.fos-K14creP.Δ5PTEN$^{flx/flx}$.Δ3β-cat$^{flx/wt}$* were established.

This approach also investigated *Δ3β-catenin* co-operation with *HK1.fos* alone and *HK1.ras^{1276} /fos* to mimic previous studies outlined in chapter 3 (*Yao et al., 2008; Macdonald et al., 2014*) using *Δ3β-catenin* activation instated of *Δ5PTEN/AKT.* Here the use of *HK1.ras^{1276}* mice was necessary given that the sensitivity of *HK1.ras^{1205}* mice to *HK1.fos* promotion would result in

phenotypes too severe for UK experimentation and *HK1.ras*^{1276} are used in PTEN experiments also.

The first notable results in *HK1.fos-K14creP.Δ5PTEN*$^{flx/flx}$*.Δ3β-cat*$^{flx/wt}$ mice and also observed in *HK1.fos-K14creP.Δ3β-cat*$^{wt/flx}$ and *HK1.ras/fos-K14creP.Δ3β-cat*$^{flx/wt}$ was the complete lack of tumour development [Fig. 7.1]. This was again consistent with protection protective responses induced via *Δ3β-catenin* activation as seen previously in *HK1.ras-K14creP.Δ3β-cat*$^{flx/wt}$ and *HK1.ras-K14creP.Δ3β-cat*$^{flx/wt}$*.p53*$^{flx/flx}$. Indeed, in all the mice produced for these genotypes and regardless of size none of the mice produced any tumours to date unlike the non β-catenin controls which repeated their previous KA or SCC aetiology [Fig. 7.1A-C vs. D&E]. However, all these genotypes shared a novel phenotype resulting in the formation of an overlapping scaly skin, resembling the scales of a pangolin. The most severe from appeared in *HK1.fos-K14creP.Δ5PTEN*$^{flx/flx}$*.Δ3β-cat*$^{flx/wt}$ mice [Fig. 7.1F-H] and this was not observed in any previous genotypes even those of the score 2 [see Chapter 5] in *HK1.ras-K14creP.Δ3β-cat*$^{flx/wt}$ or *K14creP.Δ3β-cat*$^{flx/wt}$ mice [Fig. 7.1I&J].

Thus the appearance of this skin phenotype in all genotypes associated with *HK1.fos-K14creP.Δ5PTEN*$^{flx/flx}$ co-operation suggest that these epidermal responses were a result of the combine roles for fos (*Fisher et al., 1991; Greenhalgh et al., 1993b; Basset-Seguin et al., 1994; Angel et al., 2001*) expression in normal keratinocyte differentiation and that of β-catenin (*Karim et al., 2004*), consistent with fos being a downstream transcription factor target of Wnt signalling (*Toualbi et al., 2007; Saadeddin et al., 2009*) and the fos roles in the decisions of HF stem cells to become HF or IFE (*Gerdes et al., 2006*).

Figure 7. 1: Analysis of skin phenotypes in *HK1.fos-K14creP.Δ5PTEN$^{flx/flx}$.Δ3β-cat$^{flx/wt}$* , *HK1.ras/fos-K14creP.Δ3β-cat$^{flx/wt}$* and *HK1.fos-K14creP.Δ3β-cat$^{flx/wt}$*.

[A-C] RU486-treated mice lack any tumor development 10-12 weeks post ear tag in: [A] *HK1.fos-K14creP.Δ5PTEN$^{flx/flx}$.Δ3β-cat$^{flx/wt}$*; [B] *HK1.ras/fos-K14creP.Δ3β-cat$^{flx/wt}$* and [C]*HK1.fos-K14creP.Δ3β-cat$^{flx/wt}$* mice; compared to [D] benign KA in *HK1.fos-K14creP.Δ5PTEN$^{flx/flx}$* and [E] SCC in *HK1.ras/fos-K14creP.Δ5PTEN$^{flx/flx}$* cohorts. [F] Adult *HK1.fos-K14creP.Δ5PTEN$^{flx/flx}$.Δ3β-cat$^{flx/wt}$* mouse exhibits a significant increase in Δ3β-catenin skin where the disheveled scruffy appearance has been replaced by a thickened folded skin devoid of hair. The folds overlap giving a unique phenotype resembling the shape of scales on a pangolin skin. [G & H] At higher magnification this overlapping fold is clearly visible when compared to [I] the typical hyperkeratosis in *HK1.ras-K14creP.Δ3β-cat$^{flx/wt}$* and [J] mild hyperkeratosis in *K14creP.Δ3β-cat$^{flx/wt}$* mice.

The histological analysis of *HK1.fos-K14creP.Δ5PTEN$^{flx/flx}$.Δ3β-cat$^{flx/wt}$* is shown in Fig. 7.2 and the variations in the histotypes are contrasted to those of *HK1.fos-K14creP.Δ3β-catwt/flx* and *HK1.ras/fos-K14creP.Δ3β-cat$^{flx/wt}$* in Fig. 7.3 and Fig. 7.4. Analysis of *HK1.fos-K14creP.Δ5PTEN$^{flx/flx}$.Δ3β-cat$^{flx/wt}$* adult ear skin [Fig 7.2] at 10 weeks post tagging showed a very different, unique histotype of more disturbed and abnormal IFE differentiation, with a severe case of increased hair follicle tumours again with a very different histology [Fig. 7.2 A-C]. Here, in *HK1.fos-K14creP.Δ5PTEN$^{flx/flx}$.Δ3β-cat$^{flx/wt}$* RU486 treatment induced a novel *Δ3β-catenin/Δ5PTEN*-associated histotype of excess keratosis with areas missing an IFE or strands of mild hyperplasia with a massive degree of acanthosis associated with a dominance of spinus layer keratinocytes weakly stained in the epidermis [Fig. 7.2 B&C]. In addition the numbers and severity of HF anomalies and cysts increased, moreover these HF tumours no longer possessed a *trichofolliculomas* appearance but now the HF tumour histotype produced a separate tumour type that closely resembles HF trichilemmomas produced in Cowden's disease (*Liaw et al 1997; Fistarol et al., 2002; Suzuki et al., 2003*) suggesting a direct co-operation between β-catenin overexpression and PTEN mutation in their aetiology consistent with the fact that both induced HF anomalies in transgenic mice (*Grigoryan et al., 2008; Suzuki et al., 2003*); an idea currently being pursued in separate studies.

RU486-treated adult *HK1.fos-K14creP.Δ5PTEN$^{flx/flx}$.Δ3β-cat$^{flx/wt}$* skin also exhibited the same disturbed IFE and now with an even more pronounced cyst formation that merged into the IFE to contribute to the folded keratosis effect and areas devoid of an IFE [Fig. 7.2 E-G]. Again, the very different HF trichilemmomas -like tumour histotype is quite clear whilst the histology of their upper regions suggests a derivation from the HF outer root sheath. In the IFE of *K14.Δ5PTEN$^{flx/flx}$* mice a similar effect of blooms of keratosis was observed (*Yao et al., 2006;2008*) consistent with a role for PTEN in the latter stages of epidermal differentiation that lead to the characteristic mild keratosis of Cowden patients (*Liaw et al 1997; Fistarol et al., 2002*) and which led to keratinisation and a KA aetiology (*Yao et al., 2006; 2008*). These too are again consistent with interactions with fos (*Fisher et al., 1991; Greenhalgh et al., 1993b; Basset-Seguin et al., 1994; Angel et al.,* 2001) and may underlie the degree of acanthosis observed with additional *Δ3β-catenin* and the reappearance of K1 [below]; which together suggests that an accelerated differentiation is another compensatory element to inhibit *Δ3β-catenin* in this model (*Candi et al., 2005; Mehic et al., 2005; Gerdes et al., 2006*).

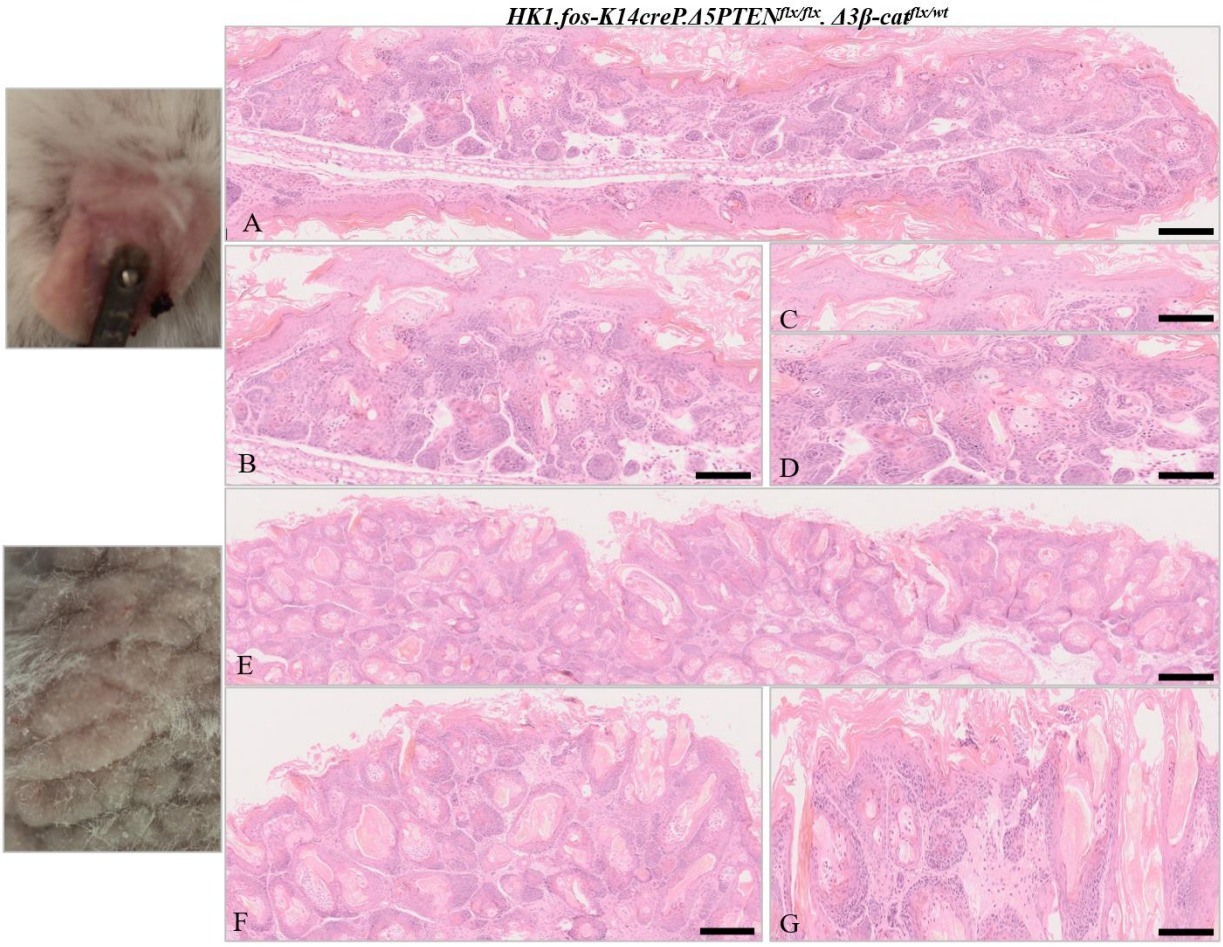

Figure 7. 2: Histological analysis of *HK1.fos-K14creP.Δ5PTEN$^{flx/flx}$.Δ3β-cat$^{flx/wt}$* skin and HF tumours.

[A-C] RU486-treated *HK1.fos-K14creP.Δ5PTEN$^{flx/flx}$.Δ3β-cat$^{flx/wt}$* tagged ear [insert] exhibits a severe Δ3β-catenin/Δ5PTEN-associated increase in phenotype on the RU486 treated dorsal surface with both excess keratosis; strands of mild vs. increased hyperplasia and quite different HF anomalies and increased numbers of cysts. [B] At higher magnification the IFE exhibits a highly disturbed epidermal differentiation, with [C] a massive degree of acanthosis also unique to this cohort. In addition, the numbers of hair follicle tumours and cysts formation are increased and [D] shows a separate HF tumour histotype that resembles HF trichilemmomas produced in Cowden's disease. [E-G] RU486-treated adult *HK1.fos-K14creP.Δ5PTEN$^{flx/flx}$.Δ3β-cat$^{flx/wt}$* skin [insert] also exhibits a highly disturbed epidermis accompanied by [E] a more pronounced predominance of cyst formation that [F] appear to break through into the IFE and contribute to the folded keratosis effects. At low and [G] higher magnification again the different HF trichilemmomas tumour histotype is clear and their upper regions suggest a derivation from the HF outer root sheath. Scale bars: A & E:150µm; B,C & F:100µm; D & G: 75 µm

The ear and back histology of this increased pangolin-like skin phenotype was examined across the three genotypes *HK1.fos-K14creP.Δ5PTEN$^{flx/flx}$.Δ3β-cat$^{flx/wt}$* , *HK1.ras/fos-K14creP.Δ3β-cat$^{flx/wt}$* and *HK1.fos-K14creP.Δ3β-cat$^{wt/flx}$* to investigate the degree of severity in regards to genotype and the formation of trichilemmomas vs. folliculaomas [Fig. 7.3 and Fig. 7.4]. A comparison of the ear histology of *HK1.fos-K14creP.Δ5PTEN$^{flx/flx}$.Δ3β-cat$^{flx/wt}$* [Fig. 7.3A&B] to that of *HK1.ras/fos-K14creP.Δ3β-cat$^{flx/wt}$* [Fig. 7.3C&D] and *HK1.fos-K14. Δ3β-catenin* [Fig. 7.3E&F] showed that while these genotypes exhibited a similar degree of IFE severity, with slightly decreased hyperplasia in *HK1.fos Δ3β-catenin* genotypes; the IFE was essentially complete and lacked the acanthosis observed in *HK1.fos-K14creP.Δ5PTEN$^{flx/flx}$.Δ3β-cat$^{flx/wt}$* histotypes [Fig. 7.3B]. In these examples, an important observation was that whilst the pangolin-like state remained fairly constant in the IFE, the HF histotypes in *HK1.ras/fos-K14creP.Δ5PTEN$^{flx/flx}$* and *HK1.fos-K14creP.Δ5PTEN$^{flx/flx}$* skins were essentially similar to that of the earlier *HK1.ras-K14creP.Δ3β-cat$^{flx/wt}$* and *K14creP.Δ3β-cat$^{flx/wt}$* ears [Fig. 7.3G&H], although by this time at 10 weeks post tagging they were quite aggressive yet the HF anomalies, remained of a folliculoma nature, consistent with the lack of both deregulated PTEN and β-catenin [Fig. 7.3C-F] (*Gat et al., 1998**;** Rankin et al., 1992Niemann et al., 2002; Kretzschmar et al., 2015; Suzuki et al., 2003*).

Another important observation was again recorded on comparison of the IFE in the various histopathologies of *HK1.fos-K14creP.Δ5PTEN$^{flx/flx}$.Δ3β-cat$^{flx/wt}$* , *HK1.ras/fos-K14creP.Δ3β-cat$^{flx/wt}$* and *HK1.fos-K14creP.Δ3β-catwt/flx* back skin [Fig.7.4]. In the more severe histology of *HK1.fos-K14creP.Δ5PTEN$^{flx/flx}$.Δ3β-cat$^{flx/wt}$* skin, in many areas the IFE was absent or completely acanthotic; i.e. the epidermis was comprised of differentiated spinus keratinocytes giving a pale staining to the epidermis termed acanthiosis [Fig. 7.4A; Fig. 7.4B arrows] (*Candi et al., 2005; Mehic et al., 2005; Gerdes et al., 2006*). This was also accompanied by many of the cysts breaking through giving areas lacking a complete IFE; and particularly prominent in *HK1.fos-K14creP.Δ5PTEN$^{flx/flx}$.Δ3β-cat$^{flx/wt}$* skin. This acanthosis, associated with a dominance of spinus layer keratinocytes, also appeared in the more hyperplastic *HK1.ras/fos-K14creP.Δ3β-cat$^{flx/wt}$ IFE* [Fig. 7.4C; Fig. 7.4D arrow] and more rarely in *HK1.fos-K14creP.Δ3β-catwt/flx*skin where the IFE was less hyperplasia and exhibited folliculoma, but the banding leading to scale-like formation can still be seen with a trough between the ridges [Fig. 7.4E&F]. In comparison, the score 0 examples of *HK1.ras-K14creP.Δ3β-cat$^{flx/wt}$* and *K14creP.Δ3β-cat$^{flx/wt}$* back skin phenotypes exhibited the typical Δ3β-catenin phenotypes but

with few cysts and fewer hair follicle tumours and more hyperplasia *HK1.ras-K14creP.Δ3β-cat*$^{flx/wt}$ IFE [Fig. 7.4G&H].

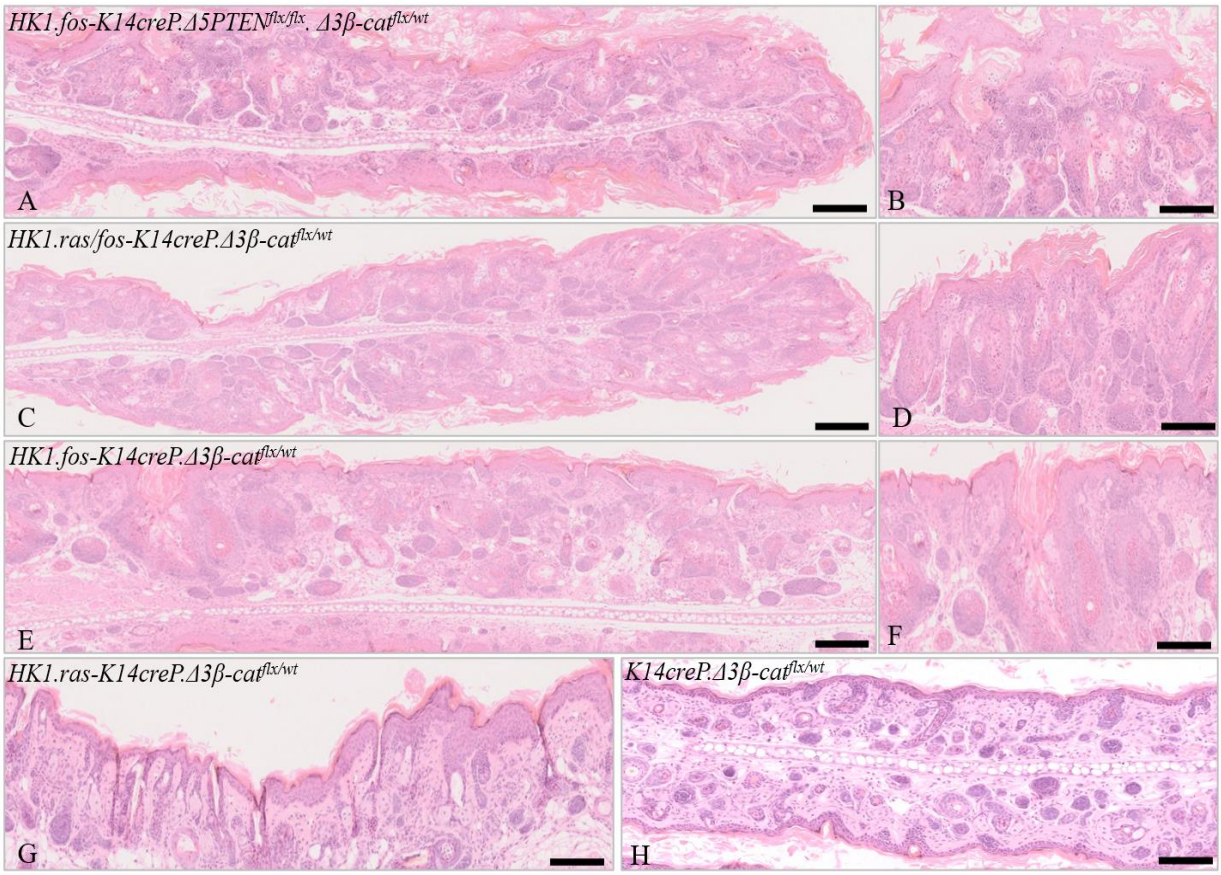

Figure 7. 3: Comparison of *HK1.fos-K14creP.Δ5PTEN*$^{flx/flx}$*.Δ3β-cat*$^{flx/wt}$ ear histotypes to *HK1.ras/fos-K14creP.Δ3β-cat*$^{flx/wt}$ and *HK1.fos-K14creP.Δ3β-cat*$^{flx/wt}$ mice.

[A & B] Severe Δ3β-catenin phenotypes appear in *HK1.fos-K14creP.Δ5PTEN*$^{flx/flx}$*.Δ3β-cat*$^{flx/wt}$ at 10 weeks with the highly disturbed IFE and trichilemmomas that mimic HF tumours of Cowden disease.[C & D] At the same 12week time point, *HK1.ras/fos-K14creP.Δ3β-cat*$^{flx/wt}$ mice display the increased IFE hyperplasia of ras and fos co-operation but the IFE lacks the acanthosis, is complete and there are less cysts. Also, all the follicle tumours are again folliculomas and present a completely different histotype. [E & F] At this time point, HK1.fos-*K14creP.Δ3β-cat*$^{flx/wt}$ are the least phenotypic but still exhibit highly disturbed epidermal differentiation, with hair follicle tumours and cyst formation appearing similar to [G] HK1.ras-*K14creP.Δ3β-cat*$^{flx/wt}$ exhibiting moderate (used in Fig. 5.4A) and [H] *K14creP.Δ3β-cat*$^{flx/wt}$ tagged ears exhibiting only mild levels of Δ3β-catenin phenotypes in this score 0 mouse (used in Fig. 5.4D). Scale bars: A C & E: 150µm; B D-H:100µm.

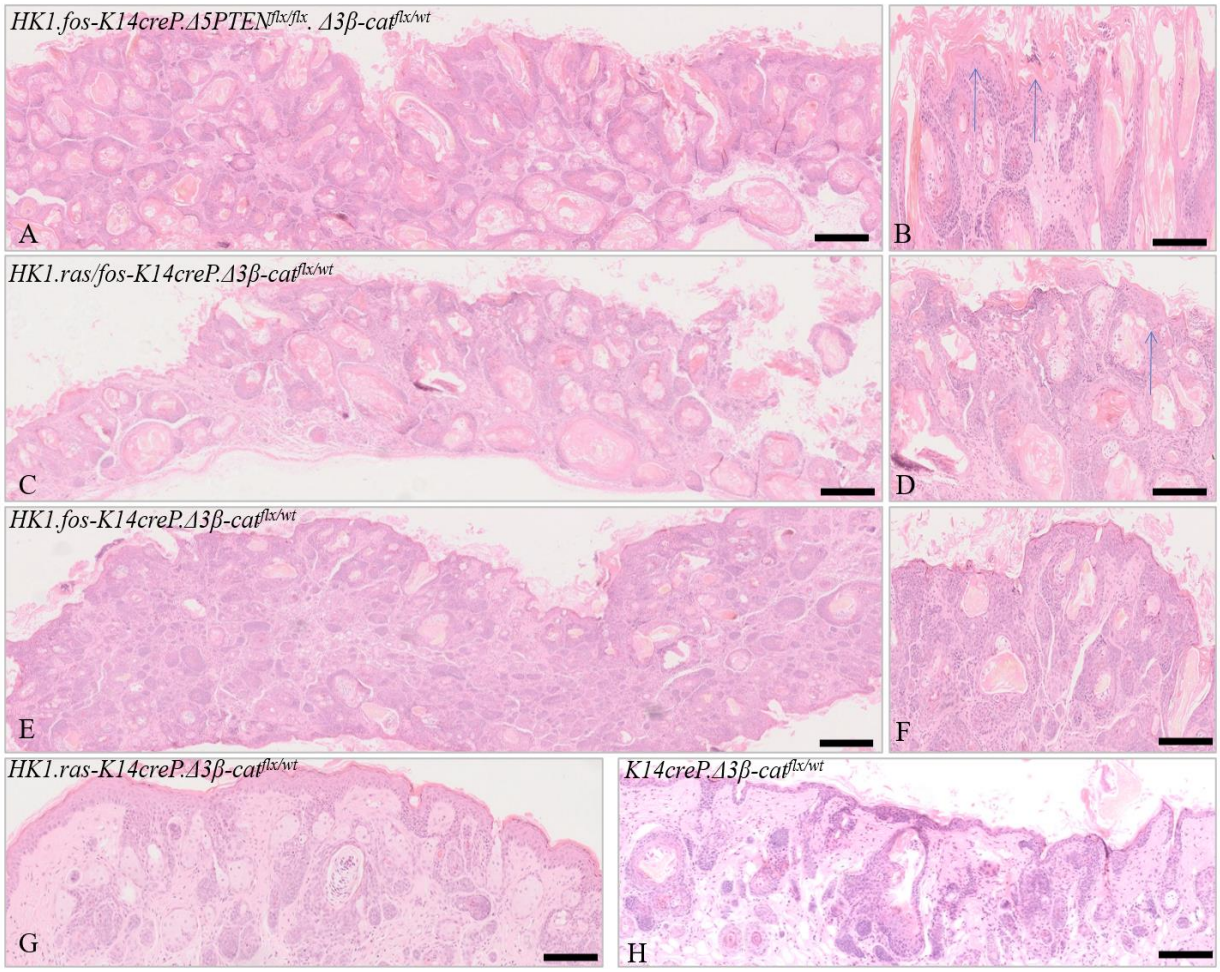

Figure 7. 4: Histological variation of the "pangolin" phenotype in back skin demonstrates areas of IFE acanthosis.

[A & B] *HK1.fos-K14creP.Δ5PTEN$^{flx/flx}$.Δ3β-cat$^{flx/wt}$* shows histology typical of the most sever phenotype associated with a highly disturbed epidermis accompanied by predominance of cyst formation that [B] seem to be overtaking the IFE in many areas; giving rise to a lack of IFE or acanthosis [arrows].[C & D] *HK1.ras/fos-K14creP.Δ3β-cat$^{flx/wt}$* show a similar feature but with HF folliculomas and more IFE hyperplasia, here again the cysts break through to give strands of acanthosis associated with a dominance of spinus layer keratinocytes [arrow]. [E & F] *HK1.fos-K14creP.Δ3β-cat$^{flx/wt}$* IFE has less hyperplasia, folliculomas and at low magnification the banding leading to scale-like formation is shown with a trough between. [G] *HK1.ras-K14creP.Δ3β-cat$^{flx/wt}$* (used in Fig. 5.3F) and [H] *K14creP.Δ3β-cat$^{flx/wt}$* back skin (used in Fig. 4.3C) exhibits only moderate and mild levels of phenotype with more IFE hyperplasia in [G] *HK1.ras-K14creP.Δ3β-cat$^{flx/wt}$* compared to [H] *K14creP.Δ3β-cat$^{flx/wt}$* back skin. Scale bars: A, C, E, G & H:150µm; D & F:100µm; B: 75µm.

Although not shown, as they are part of a separate study, the formation of *trichilemmomas* vs. *folliculomas* was also observed in the HFs of *K14creP.Δ5PTEN.Δ3β-cat* histotypes. Thus, the

histological analysis suggests that *Δ3β-catenin* and *HK1.fos* co-operation amplified the *Δ3β-catenin* phenotypes, giving a highly disturb IFE differentiation with many areas of acanthosis. This indicated that a significant degree of differentiation was associated with overexpression of both *Δ3β-catenin* (*Gat et al., 1998**;** Niemann et al., 2002; Kretzschmar et al., 2015 ; Rankin et al., 1992; Yao et al., 2008; Macdonald et al., 2014*) and *fos* activation (*Fisher et al., 1991;Basset-Seguin et al., 1994; Angel et al., 2001*) as observed in previous studies (*Greenhalgh et al., 1993b Yao et al., 2008; Macdonald et al., 2014*) that associate fos with the decisions of keratinocytes to commit to terminal differentiation (*Candi et al., 2005; Mehic et al., 2005; Gerdes et al., 2006*).

In addition, increased formation of cysts and trichilemmomas vs folliculomas is a novel tumour phenotype associated with overexpression of both *Δ3β-catenin* and *Δ5PTEN.* This would again be consistent with roles for β-catenin in HF development (*Gat et al., 1998; Huelsken et al., 2001; Niemann et al., 2002*) in co-operation with PTEN mutation and AKT activation (*Suzuki et al., 2003*) and possibly with the high levels of E-cadherin associated with the development of these specific HF tumours [below (*Young et al., 2003*)]. It may be that the lipo-phosphatase PTEN scaffolding functions at the membrane independent of phosphatase/AKT regulation (*Kotelevets et al., 2001; Tamura et al., 1998; Subauste et al., 2005*) that aid in cell-cell adhesion (*Kotelevets et al., 2001; Young et al., 2003*) remain intact and these help with resistance to tumour formation. Indeed, these lipo-phosphatase roles may even increase as part of efforts to increase the Δ5PTEN phosphatase function that feeds back to its promoter from increased AKT; although this idea will require further investigation in new *K14.Δ5PTEN.Δ3β-catenin* studies.

As expected for the model, analysis of β-catenin in *HK1.fos-K14creP.Δ5PTEN*$^{flx/flx}$*.Δ3β-cat*$^{flx/wt}$ showed increased expression in both suprabasal and basal layers, with both membranous and nuclear β-catenin appearing in basal layer cells [Fig. 7.5A-D]. However, it was noted that in certain areas, the proliferative keratin K14 was absent [Fig. 7.5B; arrow]; and it is interesting to speculate whether K14 was replace by K15 (*Bose et al., 2013*), given that these areas expressed strong levels of membranous β-catenin and E-cadherin [below]. Thus, this strong cell-cell binding [also consistent with PTEN scaffolding roles above] and the increased differentiation, suggested by K1 expression [below] would all contribute to the tumour inhibition observed.

β-catenin expression in *HK1.ras/fos-K14creP.Δ3β-cat*$^{flx/wt}$ and *HK1.fos-K14creP.Δ3β-cat*$^{wt/flx}$ skin [not shown] was identical to the expression observed in *HK1.ras-K14creP.Δ3β-cat*$^{flx/wt}$ and *K14creP.Δ3β-cat*$^{flx/wt}$ [Fig. 7.5E&F]. Furthermore, this early β-catenin expression in *HK1.fos-K14creP.Δ5PTEN*$^{flx/flx}$*.Δ3β-cat*$^{flx/wt}$ skin was also similar to nuclear and membranous expression of β-catenin in *HK1.fos-K14creP.Δ5PTEN*$^{flx/flx}$ KA [Chapter 3], whilst *HK1.fos* hyperplasia showed only supra-basal membranous expression similar to that of *HK1.ras*. This suggests that early activation of *Δ3β-catenin* in *HK1.fos-K14creP.Δ5PTEN*$^{flx/flx}$*.Δ3β-cat*$^{flx/wt}$ genotypes or the triggered activation in *HK1.fos-K14creP.Δ5PTEN*$^{flx/flx}$ KA aetiology led to an identical response of massive differentiation and keratosis to inhibit tumour formation or progression.

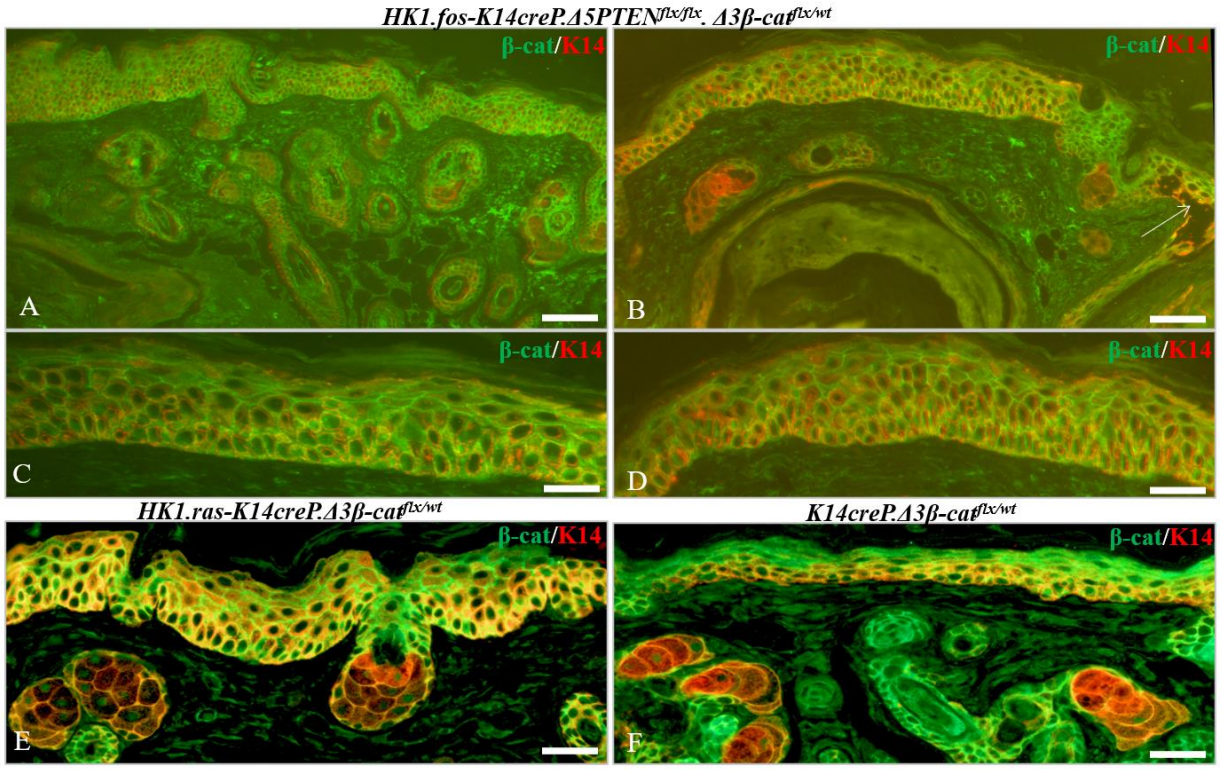

Figure 7. 5: Analysis of β-catenin expression in *HK1.fos-K14creP.Δ5PTEN*$^{flx/flx}$*.Δ3β-cat*$^{flx/wt}$ IFE.

[A] IFE shows strong β-catenin expression in all layers and the trichilemmomas-like HF tumours. [B] At higher magnification IFE shows an area of β-catenin positivity accompanied by a lack of K14 expression [arrow]. [C & D] Other sections higher magnification show strong membranous expression in both suprabasal and basal layers with nuclear expression in most basal layers cells. For comparison [E] *HK1.ras-K14creP.Δ3β-cat*$^{flx/wt}$ (used in Fig. 5.6E) and [F] *K14creP.Δ3β-cat*$^{flx/wt}$ (used in Fig. 5.6F) display an all over strong expression of Δ3β-catenin. Scale bars: A: 100µm; B: 75µm; C & D: 30-40µm; E & F: 50µm.

The analysis of E-cadherin levels in *HK1.fos-K14creP.Δ5PTEN$^{flx/flx}$.Δ3β-cat$^{flx/wt}$* also demonstrated an increase in IFE basal layer expression [Fig. 7.6A&B] and it was noticed that E-cadherin expression was particularly strongly in the trichilemmomas -like HF tumours; and also in the surrounding cysts [Fig. 7.6C&D]. In several IFE strands that mimicked β-catenin expression [above], areas again lacked K14 expression, being green only; whilst the areas that lacked hyperplasia or were acanthotic were strongly positive for E-cadherin. Again, this intense E-cadherin expression profile was exclusive to these animals as *HK1.ras/fos-K14creP.Δ3β-cat$^{flx/wt}$* and *HK1.fos-K14creP.Δ3β-cat$^{wt/flx}$* skin [not shown] exhibited a HF expression similar to *HK1.ras-K14creP.Δ3β-cat$^{flx/wt}$* and *K14creP.Δ3β-cat$^{flx/wt}$* [Fig. 7.6E&F] and an IFE of similar intensity also.

These E-cadherin results exhibited by *HK1.fos-K14creP.Δ5PTEN$^{flx/flx}$.Δ3β-cat$^{flx/wt}$* trichilemmomas and cysts is another novel tumour feature suggesting a significant degree of co-operation between *Δ3β-catenin* and *Δ5PTEN* in HF development (*Gat et al., 1998; Huelsken et al., 2001; Niemann et al.,2002*)and the resulting HF tumour type (*Suzuki et al., 2003*). Further, the excess numbers of HF-derived cysts suggests a response to this HF progression was a diversion of anomalous HF formation into cysts (*Young et al., 2003*) as observed in *HK1.ras/fos-K14cre.Δ5PTEN* mice (*Macdonald et al ., 2014*). In the IFE of all three *fos/Δ3β-catenin* genotypes, this increased E-cadherin might also contribute to the inhibition of papillomas as suggested in previous studies (*Kotelevets et al., 2001*) alongside the differentiation responses elicited by *HK1.fos* [below; (*Candi et al., 2005; Mehic et al., 2005*) that also diverted progression to KA (*Macdonald et al., 2014*).

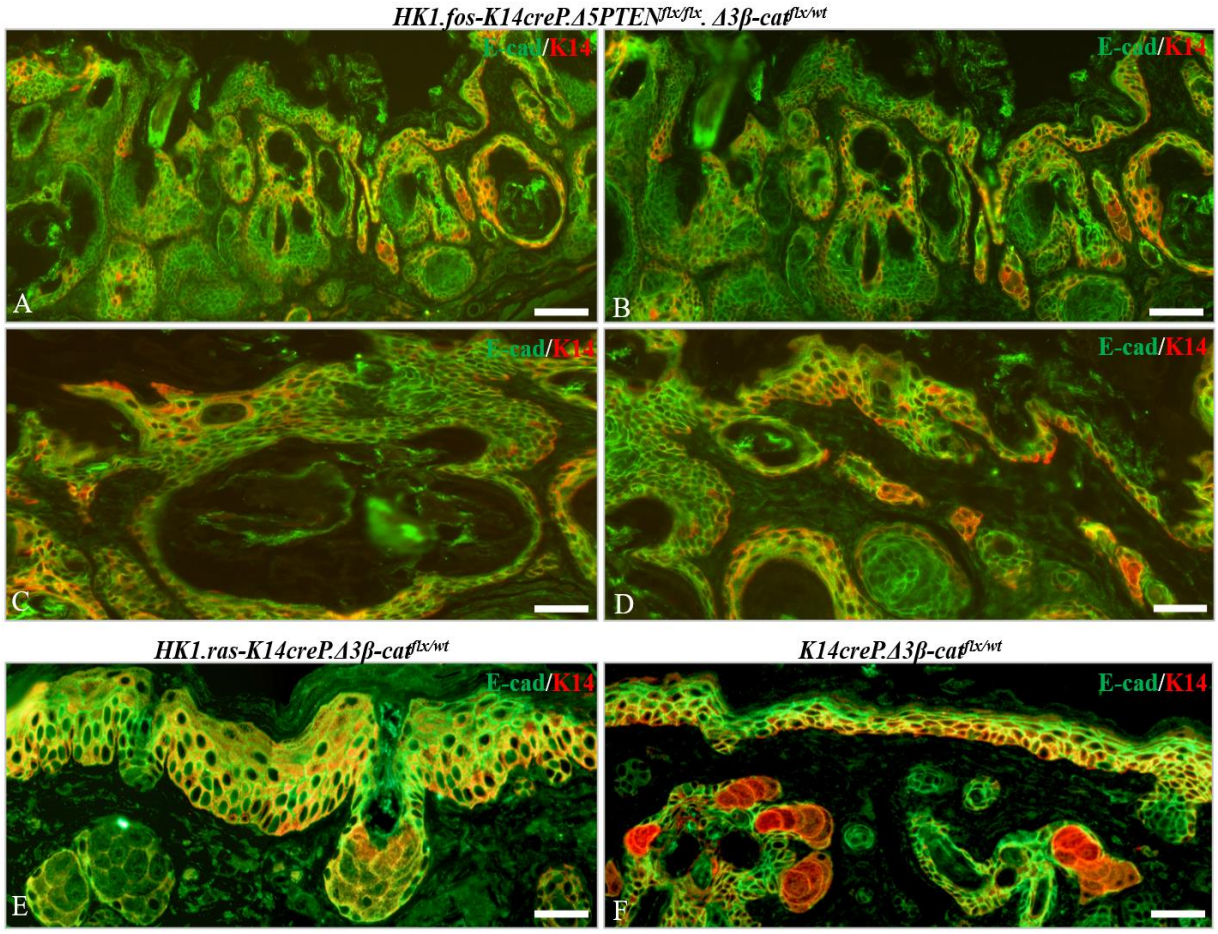

Figure 7. 6: Analysis of E-cadherin expression in *HK1.fos-K14creP.Δ5PTEN*$^{flx/flx}$*.Δ3β-cat*$^{flx/wt}$ IFE and tumours.

[A & B] *HK1.fos-K14creP.Δ5PTEN*$^{flx/flx}$*.Δ3β-cat*$^{flx/wt}$ exhibits very strong expression in supra and basal layers of the IFE together with even stronger expression in the trichilemmomas - like HF tumours; [C] At higher magnification E-cadherin also appears around the cysts whilst [D] shows areas of minimal hyperplasia still expressing basal layer E-cadherin; yet some areas lack K14 expression [green]. [E] *HK1.ras-K14creP.Δ3β-cat*$^{flx/wt}$ (used in Fig. 5.8B) and [F] *K14creP.Δ3β-cat*$^{flx/wt}$ (used in Fig. 5.8C) exhibit elevated supra and basal layers E-cadherin expression together with hair follicles, but the absence of K14 and the IFE remains hyperplastic. Scale bars: A: 100µm; B-D: 75µm; E & F: 50µm.

The analysis of early differentiation marker K1 expression also supported the idea that an accelerated or premature differentiation response was occurring in the pangolin-like skins of *HK1.fos-K14creP.Δ5PTEN*$^{flx/flx}$*.Δ3β-cat*$^{flx/wt}$ mice. Unlike the non-*fos/PTEN* models [above] wherever strands of hyperplastic IFE were actually present, in this instance K1 was also expressed [Fig. 7.7A-C]. However, as seen in Fig. 7.7 B and C, not only was K1 expressed but the expression was ragged, suggesting confusion to the progression of basal into *spinous*

keratinocytes; which indicated an accelerated differentiation, consistent with the degree of novel acanthosis observed in their histopathology [above; Fig. 7.2B&C; Fig. 7.4].

Supporting this idea, strands of K1 expression appeared in basal layer keratinocytes, suggesting a premature commitment of basal layer keratinocytes to terminal differentiation, a result also suggested in KA aetiology (*Macdonald et al., 2014*) and possibly amplified by increased early HK1.fos expression due to the premature basal K1 expression (*Fisher at al.,1991; Greenhalgh et al., 1993b; Basset-Seguin et al., 1994*). Meanwhile closer examination of the IFE shows that K1 expression was not uniform with weaker areas appearing [Fig. 7.2C], a result confirming the disturbed differentiation and consistent with the degree of acanthosis observed or possibly premature fos-mediated cornification (*Candi et al., 2005*). Furthermore, in addition to the highly disturbed IFE hyperplasia and K1 expression was also noted in the cysts [Fig. 7.7A], suggesting that a response to help inhibit progression to trichilemmomas in the aberrant HFs which expressed K1 in their upper regions may pave the way for cyst formation (*Kotelevets et al.,2001; Niemann et al.,2002; Suzuki et al., 2003*) in addition to that mediated by excess E-cadherin expression [above].

This K1 expression in *HK1.fos-K14creP.Δ5PTEN*$^{flx/flx}$*.Δ3β-cat*$^{flx/wt}$ was quite different to the aberrant, laterally confined patchy expression of K1 in *HK1.ras-K14creP.Δ3β-cat*$^{flx/wt}$ or the less altered expression in *K14creP.Δ3β-cat*$^{flx/wt}$ where strands of positive K1 expression appear but again with many patches where K1 is thin or lost [Fig. 7.7D&E]. In contrast K1 expression in *HK1.fos* hyperplasia exhibits the relatively normal supra-basal K1 profile [Fig. 7.7F] whilst *HK1.fos-K14creP.Δ5PTEN*$^{flx/flx}$ KA shows the very strong K1 expression masking the K14 counterstain [Fig. 7.7G] with a very thin basal layer, which again indicates a far more accelerated and premature differentiation pattern due to elevated p53/p21 expression responding to endogenous β-catenin nuclear localization [above Chapter 3; (*Macdonald et al., 2014*)].

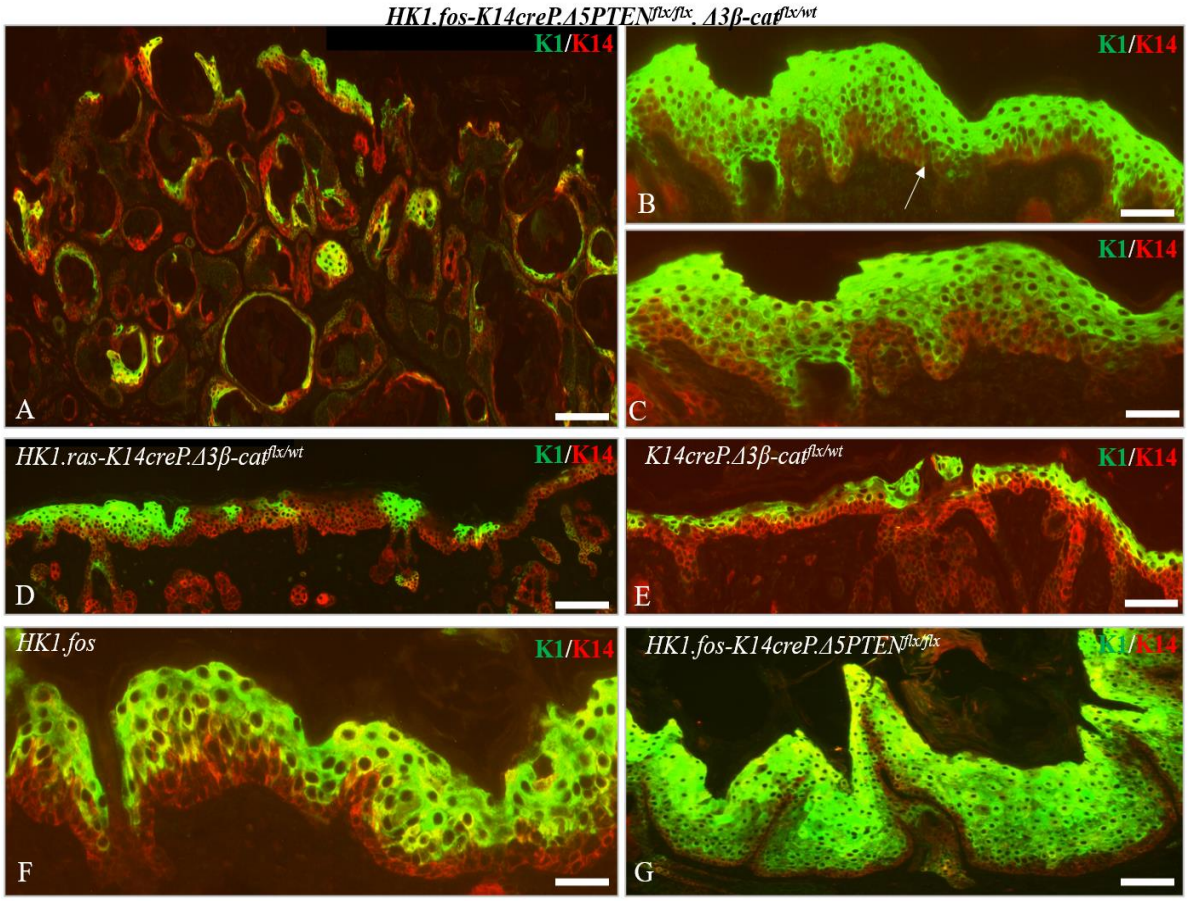

Figure 7. 7: Analysis of keratin K1 in *HK1.fos-K14creP.Δ5PTEN$^{flx/flx}$.Δ3β-cat$^{flx/wt}$* IFE and HF tumours.

[A] Low magnification of a typical skin shows aberrant K1 expression in areas of highly disturbed IFE hyperplasia and K1 expression was also noted in the cysts, suggesting that the aberrant HFs which also expressed K1 in the upper regions, paved the way for cyst formation. [B] At higher magnification strands of IFE hyperplasia show a ragged K1 expression at the junction between basal and supra-basal layers. Also strands of basal layer keratinocytes are positive for K1 expression [arrow]. [C] Closer examination of this site shows K1 expression is not uniform with weaker areas appearing, a result possibly consistent with the degree of acanthosis observed or possibly early fos-mediated cornification. [D] For comparison a typical *HK1.ras-K14creP.Δ3β-cat$^{flx/wt}$* (used in Fig. 5.9A) epidermis shows patchy expression of K1 with only occasional HFs being weakly positive for K1; whilst [E] this *K14creP.Δ3β-cat$^{flx/wt}$* (used in Fig. 5.9D) example shows a strand of positive K1 expression but again with many patches where K1 is thin or lost. [F] *HK1.fos* hyperplasia exhibits a relatively normal K1 profile with expression confined to supra-basal layers; whilst [G] shows very strong K1 expression in *HK1.fos-K14creP.Δ5PTEN$^{flx/flx}$* KA (used in Fig. 3.2K) that masks the K14 counterstain; whilst the very thin basal layer in this example indicates an accelerated or premature differentiation. Scale bars: A,D & G: 100µm; E: 75µm; B: 60µm; C: 50µm; F: 30µm.

Analysis of the hyperproliferation marker K6α in *HK1.fos-K14creP.Δ5PTEN$^{flx/flx}$.Δ3β-cat$^{flx/wt}$* showed that in strands of IFE hyperplasia expression was barely detectable and when present

it was only patchy. [Fig. 7.8A]. K6α was mainly expressed in hair follicles, trichilemmomas and also around the edges of the cysts, which may indicate that these cysts maybe those of a proliferative histotype as seen in the epidermis of younger *HK1.ras/fos.K14.Δ5PTEN* mice (*Macdonald et al., 2014*). Overall, K6α expression seemed diminished compared to the follicular expression seen in *HK1.ras-K14creP.Δ3β-cat*$^{flx/wt}$ and *K14creP.Δ3β-cat*$^{flx/wt}$ or the strong IFE expression in *HK1.fos* hyperplasia Fig. 7.8A-D], similar to that of HK1.ras [above] and previously observed in the aetiology *HK1.fos-K14creP.Δ5PTEN*$^{flx/flx}$ KAs (*Yao at al., 2008*). This lesser expression may also indicate an effect of an accelerated differentiation and possibly diversion of proliferation into cysts formation appearing to be a major anti-tumorigenic mechanism in this *HK1.fos-K14creP.Δ5PTEN*$^{flx/flx}$*.Δ3β-cat*$^{flx/wt}$ genotype.

To-date in the *HK1* model this observation is only the second instance where K6α expression was weak and again suggests that this result is unique to *Δ3βcatenin* expression. As speculated for K1 above [and in earlier chapters], this change in K6α expression may also reflect the increased E-cadherin expression, which in turn alters the hyperproliferation signals derived from cell-cell interactions that are typically disrupted in wounding. Hence, these and other responses to *HK1.fos* activation that induce K6 expression (*Rothnagel et al., 1999*) are overcome by those elicited in both *HK1.fos-K14creP.Δ5PTEN*$^{flx/flx}$*.Δ3β-cat*$^{flx/wt}$ and *HK1.ras-K14creP.Δ3β-cat*$^{flx/wt}$ skin models. i.e. p53 and p21 [below] and others e.g. p63 and p73 [above] that have yet to be analysed.

Another possible mechanism returns to the idea that constitutive activation of β-catenin returns the adult mouse skin to one resembling a neonatal state (*Collins et al., 2011*). Here the epidermis is naturally hyperplastic but lacks K6α expression, which remains confined to the developing HFs. Thus in *HK1.fos-K14creP.Δ5PTEN*$^{flx/flx}$*.Δ3β-cat*$^{flx/wt}$ skin, so many new HFs are being created due to the effects of *Δ3β-catenin* expression that are then further compromised by *K14.Δ5PTEN* expression and fail to differentiate properly; hence reduced K6α and degeneration into increased numbers of cysts.

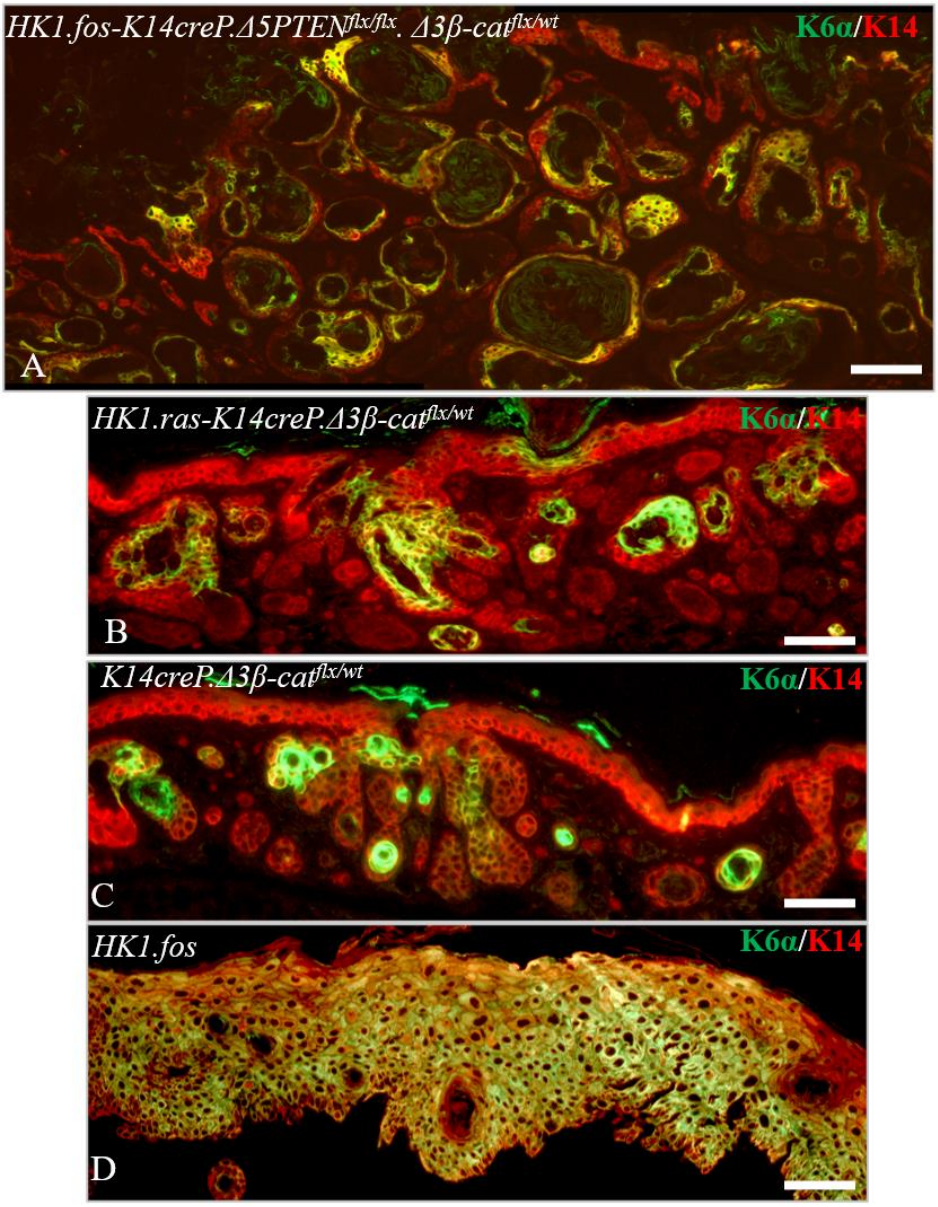

Figure 7. 8: Analysis of keratin K6α in *HK1.fos-K14creP.Δ5PTEN*$^{flx/flx}$*.Δ3β-cat*$^{flx/wt}$ IFE and HF tumours.

[A] Typical *HK1.fos-K14creP.Δ5PTEN*$^{flx/flx}$*.Δ3β-cat*$^{flx/wt}$ skin shows little K6α expression in the IFE and also weaker expression in the trichilemmomas and abnormal HFs. In addition, K6α expression was also noted in outer regions of the cysts, suggesting that cyst formation results in proliferative cysts; hence the generally larger size in *HK1.fos-K14creP.Δ5PTEN*$^{flx/flx}$*.Δ3β-cat*$^{flx/wt}$ skin and their propensity to emerge into the IFE. For comparison [B] *HK1.ras-K14creP.Δ3β-cat*$^{flx/wt}$ (used in Fig. 5.10C) and [C] *K14creP.Δ3β-cat*$^{flx/wt}$ (used in Fig. 5.10D) IFE also lack K6α expression, except in a few strands but strongly express K6α in the folliculoma of [B]. [D] Strong K6α in expression appears in all layers of older *HK1.fos* hyperplasia as in typical younger *HK1.ras* hyperplasia. Scale bars: A:100μm; B: 75μm; C & D: 60μm.

The K1/K6 observations suggested that accelerated differentiation in *HK1.fos-K14creP.Δ5PTEN$^{flx/flx}$.Δ3β-cat$^{flx/wt}$* mice played a role in the formation of the pangolin-like skin phenotype. Therefore, as outlined above in previous chapters, this may involve roles for p53 to halt proliferation and p21 expression to instigate differentiation in co-operation with roles for fos. This is an attractive idea given that fos-mediated photo-carcinogenesis associates with both AKT activation and GSK3β inactivation, hence another direct link to β-catenin activity (*Gonzales and Bowden, 2002*). Further linking fos and β-catenin, UV-B-mediated p53 mutation and subsequent PTEN inhibition [and thus increased p-AKT/p-GSK3β/nuclear β-catenin], induces AP-1 expression and an initial protective differentiation response (*Wang et al., 2005*).

In addition, p21 expression would add to the commitment to differentiation (*Di cunto et al., 1998*; *Topley et al., 1999*) whilst the increased AKT expression may also contribute to differentiation given its normal supra-basal roles in antagonising p53 to prevent apoptosis giving time to committee to differentiation (*Calautti et al., 2005; Macdonald et al., 2014*). Both these findings being consistent with the return of K1 in the patchy IFE; whilst p21 roles in cell-cycle regulation would be consistent with reductions in K6α expression.

This proved to be the case when p53/p21 status was assessed *HK1.fos-K14creP.Δ5PTEN$^{flx/flx}$.Δ3β-cat$^{flx/wt}$* IFE [Fig. 7.9 and Fig. 7.10]. For both p53 and p21, strong expression appeared in *HK1.fos-K14creP.Δ5PTEN$^{flx/flx}$.Δ3β-cat$^{flx/wt}$* skin particularly in the anomalous hair follicles, overt trichilemmomas and cysts; and of note also appeared in the strands of sporadic IFE hyperplasia [p53: Fig. 7.9A arrows; p21: Fig. 7.10A]. Indeed, both p53 and p21 expression appeared more intense in *HK1.fos-K14creP.Δ5PTEN$^{flx/flx}$.Δ3β-cat$^{flx/wt}$* skin compared to that of *HK1.ras-K14creP.Δ3β-cat$^{flx/wt}$* or *K14creP.Δ3β-cat$^{flx/wt}$* [Fig. 7.9B&C; Fig. 7.10B&C]; whilst *HK1.fos-K14creP.Δ5PTEN$^{flx/flx}$* bi-genic mice expressed p53/p21 in all IFE layers and follicles [not shown], but similar to *HK1.ras-K14creP.Δ3β-cat$^{flx/wt}$* ; and *HK1.fos* hyperplasia displayed only supra-basal and mainly cytoplasmic p53/p21 expression until overt papillomas formed [Fig. 7.9D; Fig. 7.10D].

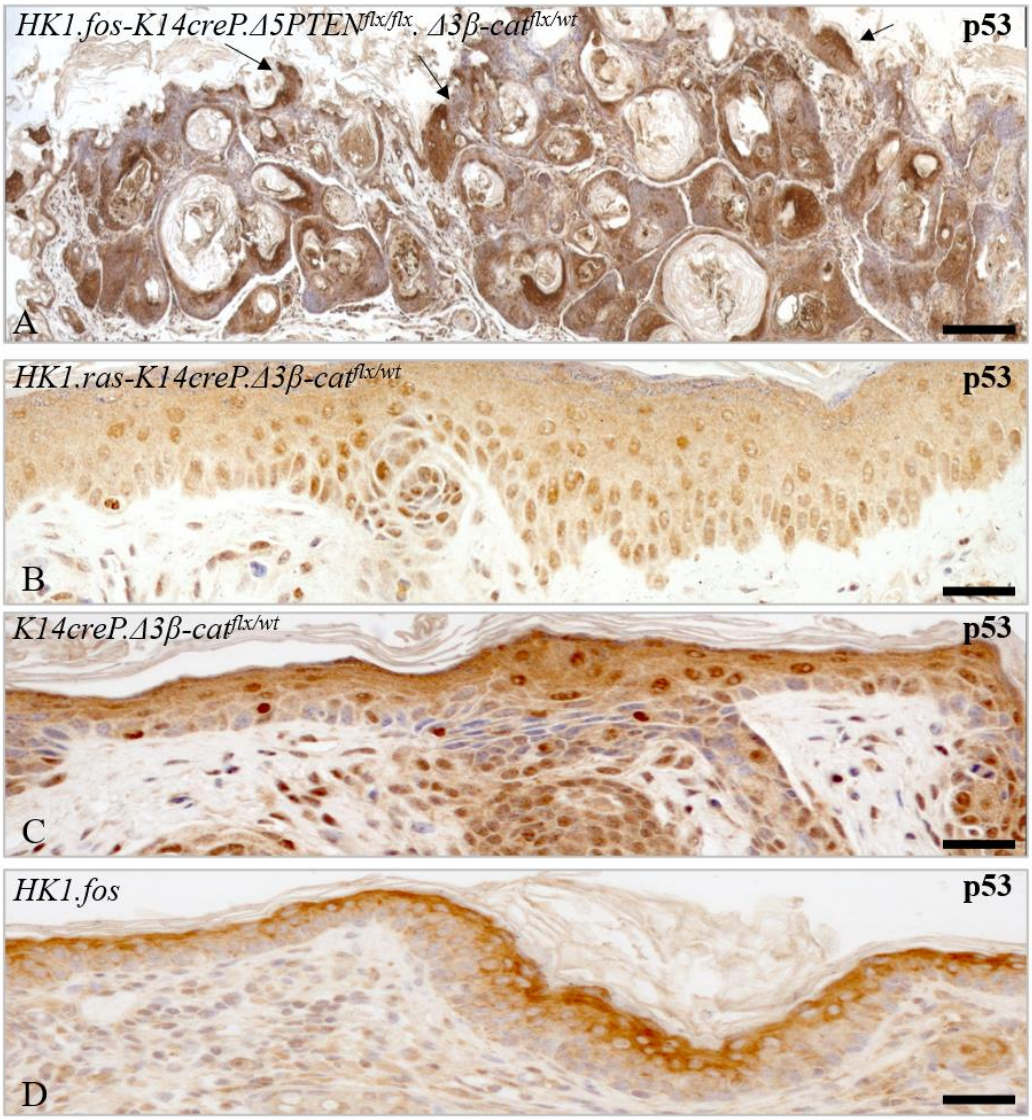

Figure 7. 9: Analysis of p53 expression in *HK1.fos-K14creP.Δ5PTEN$^{flx/flx}$.Δ3β-cat$^{flx/wt}$* IFE and HF tumours.

[A] Strong expression of p53 appears in *HK1.fos-K14creP.Δ5PTEN$^{flx/flx}$.Δ3β-cat$^{flx/wt}$* skin mainly in hair follicles, the trichilemmomas, and cysts and also in many strands of sporadic IFE hyperplasia [arrows]. [B] *HK1.ras-K14creP.Δ3β-cat$^{flx/wt}$* (used in Fig. 5.11B) and [C] *K14creP.Δ3β-cat$^{flx/wt}$* (used in Fig. 5.11D) also express p53 in all IFE layers and follicles, whilst [D] HK1.fos hyperplasia shows only supra-basal cytoplasmic expression until an overt papilloma forms. Scale bars: A:150μm; B & D: 60μm; C: 50μm.

Thus, these results confirm p53/p21 involvement in the formation of the pangolin-like phenotype, again protecting against tumour/KA formation in the IFE due to anomalous β-catenin expression at this early, initiating stage. Indeed, as above in *HK1.ras-K14creP.Δ3β-cat$^{flx/wt}$* skin this excess p53/p21 expression possibly explains the confused manor of the

returned K1 expression seen in the sporadic IFE and the continued the absence of hyperproliferation marker K6 from the IFE Fig. 7.7B&C; Fig. 7.8A] suggesting a dysfunction in epidermal homeostasis due to combinations of fos, PTEN and β-catenin co-operation.

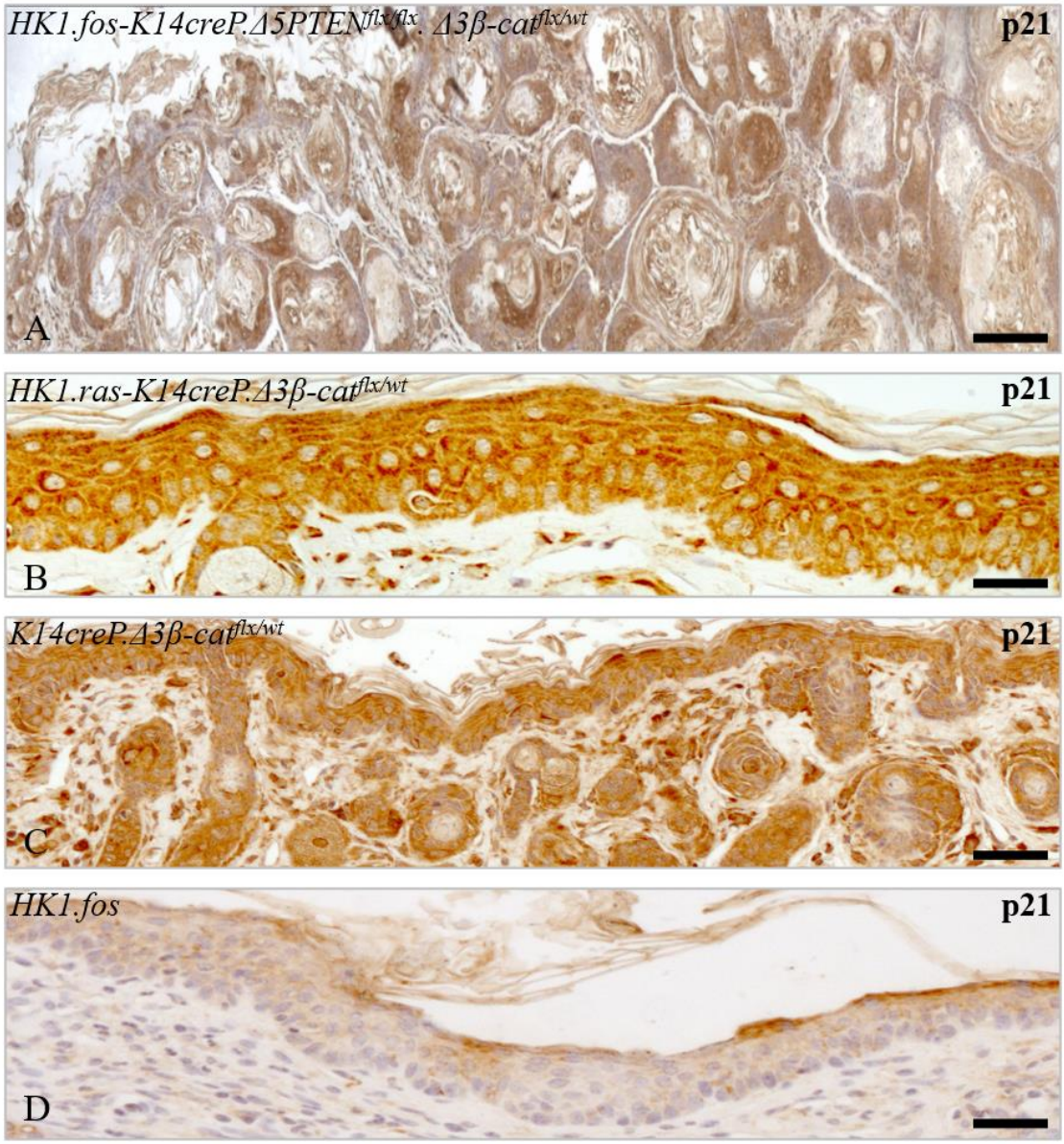

Figure 7. 10: Analysis of p21 expression in *HK1.fos-K14creP.Δ5PTEN$^{flx/flx}$.Δ3β-cat$^{flx/wt}$* IFE and HF tumours.

[A] *HK1.fos-K14creP.Δ5PTEN$^{flx/flx}$.Δ3β-cat$^{flx/wt}$* skin displays strong p21 expression appears mainly in the trichilemmomas and cysts; but some expression appears in IFE hyperplasia. For comparison [B] *HK1.ras-K14creP.Δ3β-cat$^{flx/wt}$* (used in Fig. 5.12B) and [C] *K14creP.Δ3β-cat$^{flx/wt}$* (used in Fig. 5.12D) express p21 in all IFE layers and follicles, whereas [D] *HK1.fos* hyperplasia shows only weak supra-basal expression. Scale bars: A:150µm; B: 50µm; C & D: 60µm.

These data also suggest that the β-catenin trigger of p53 and p21 which resulted in the keratosis observed in earlier *HK1.fos-K14creP.Δ5PTEN*$^{flx/flx}$ mice and their resultant KA outcome (*Macdonald et al., 2014*) again gave the massive differentiation programme observed here. However, in this new *HK1.fos-K14creP.Δ5PTEN*$^{flx/flx}$*.Δ3β-cat*$^{flx/wt}$ model, this defence was deployed at the immediate stage of leakage as Δ3β-catenin was now constitutive and independent of deregulated PTEN/AKT/GSK3β, to prevent tumour forming rather than KAs converting to SCC. In this juvenile IFE, Δ3β-catenin then co-operated with the differentiation signals regulated by fos expression in the epidermis, particularly in the decisions to commit to differentiation that account for the return of keratin K1 expression (*Fisher et al., 1991; Greenhalgh et al., 1993b; Basset-Seguin et al., 1994; Angel et al., 2003; Candi et al., 2005; Mehic et al., 2005; Gerdes et al., 2006; Yao et al., 2008; Macdonald et al., 2014*). Thus, elevated K1 expression appears to be a marker of the altered differentiation caused by deregulated β-catenin expression and the increased adherence junctions due to excess E-cadherin in combination with fos activation.

That a stronger p53/p21 expression appeared in *HK1.fos-K14creP.Δ5PTEN*$^{flx/flx}$*.Δ3β-cat*$^{flx/wt}$ skin [p53: Fig. 7.9A; p21: Fig. 7.10A] compared to *HK1.ras-K14creP.Δ3β-cat*$^{flx/wt}$ expression [p53: Fig. 7.9B; p21: Fig. 7.10B] also supports the idea that the novel co-operation between anomalous β-catenin and mutant PTEN expression gave rise to the trichilemmomas and that p53/p21 expression may have contributed to the increased numbers of cysts in an attempt to minimise anomalous HF progression into these trichilemmomas. This would be consistent with a model of constitutive *Δ3β-catenin* activation inducing formation of new [if anomalous hair follicles] in *K14creP.Δ3β-cat*$^{flx/wt}$ and *HK1.ras-K14creP.Δ3β-cat*$^{flx/wt}$ mice coupled to PTEN mutation in *HK1.fos-K14creP.Δ5PTEN*$^{flx/flx}$*.Δ3β-cat*$^{flx/wt}$ diverting the tumour outcome to trichilemmomas not folliculoma, as HF hyperplasia was also observed in previous constitutive [not inducible] *Δ5PTEN* studies (*Suzuki et al., 2003*).

Overall, these experiments again found an inhibited tumour formation where the IFE expression analysis data suggest that in this case it was the increased differentiation that appears a major inhibitory event. This idea of Δ3β-catenin enhanced fos-mediated differentiation responses is consistent with the differentiation signals regulated by fos expression in the epidermis particularly those in the decisions to commit to differentiation (*Fisher et al., 1991; Greenhalgh et al 1993b; Basset-Seguin et al., 1994; Angel et al., 2001; Mehic et al., 2005; Gerdes et al., 2006*); whilst the roles for fos in cornification (*Candi et al.,*

2005) may contribute to the early accelerated differentiation that gave rise to the IFE acanthosis and the significant keratosis so that each epidermal fold became the overt scales of the pangolin-like skin. It remained to be seen whether this response to the combinations of fos/PTEN and β-catenin co-operation were dependent on p53, p21 or both.

7.3 Loss of p53 in *HK1.fos-K14creP.Δ3β-cat$^{flx/wt}$* mice blocks Δ3β-catenin phenotypes

As outlined above, the responses *to Δ3β-catenin* activation in *HK1.fos-K14creP.Δ3β-cat$^{wt/flx}$* mice appeared to completely block tumour formation, as previously observed in *HK1.ras-K14creP.Δ3β-cat$^{flx/wt}$* cohorts, even with up to three potent mutations as in *HK1.fos-K14creP.Δ5PTEN$^{flx/flx}$.Δ3β-cat$^{flx/wt}$* cohorts. Further, here there was a distinct and novel increase in the differentiation responses that led to a pangolin-like skin. Alongside roles for excessive E-cadherin co-operation with *Δ3β-catenin* that led to the return of [a confused] K1 expression profile in basal layers was the increased expression of p53 and p21 in the resultant sporadic IFE and their strong expression in the HFs. Previous studies showed compensatory p53/p21 was also observed in *HK1.fos-K14creP.Δ5PTEN$^{flx/flx}$* KA aetiology (*Yao et al., 2008*) and this suggests that again in juvenile mice with a leaky K14cre gene switch, elevated p53/p21 [amongst others eg p63/p73/K15] were quickly deployed to counter anomalous β-catenin expression.

Consistent with *Δ3β-catenin* enhancement of *HK1.fos* interference with normal *c-fos* functions in proliferation, stem cell decisions and differentiation (*Angel et al., 2001; Mehic et al., 2005; Gerdes et al., 2006*) logically, increased p53 inhibits proliferation and provides protection against additional mutations; whilst increased p21-associated differentiation responses (*Topley et al.,1999*) avoids potential p53-induced apoptosis to maintain the paramount barrier function of skin (*Calautti et al.,2005; Yao et al., 2008; Macdonald et al., 2014*) and also aids in proliferation control to inhibit tumourigenesis.

However, it remained to be seen whether the combinations of fos/PTEN and β-catenin co-operation would now give rise to tumours if p53 was lost and whether this resulted in KA or malignancy. Generating the *HK1.fos-K14creP.Δ3β-cat$^{flx/wt}$.p53$^{flx/flx}$* genotype not only tested whether this could elicit tumours, but also addressed whether these excess differentiation responses to fos [PTEN] and β-catenin co-operation were dependent on specific p53-mediated

responses to β-catenin activation, as observed in *HK1.ras-K14creP.Δ3β-cat*$^{flx/wt}$*.p53*$^{flx/flx}$ models.

Yet several questions remained, i.e. if the strong differentiation responses observed in *HK1.fos-K14creP.Δ3β-catwt/flx*mice were again blocked by p53 loss, it may indicate that this was a general response to β-catenin deregulation and not just specific to *HK1.ras-K14creP.Δ3β-cat*$^{flx/wt}$*.p53*$^{flx/flx}$ models. This block may depend upon wild type p53 expression functions or alternately may depend upon specific responses e.g. whether p63/73 expression in response to p53 loss again altered specific KPC populations [via K15 expression/Lgr 5 & 6] that also successfully nullified anomalous *β-catenin/HK1.fos* co-operation.

Therefore, to begin to examine the role of p53 in tumour inhibition and the appearance of the pangolin-like skin phenotype, a conditional *p53* knockout was bred in *HK1.fos-K14creP.Δ5PTEN*$^{flx/flx}$ and the preliminary data from initial *HK1.fos-K14creP.Δ3β-cat*$^{flx/wt}$ - *p53*$^{flx/flx}$ cohorts are shown in [Fig. 7.11]. These experiments showed both a continued lack of tumours and again a block of the pangolin-like skin presented in *HK1.fos.K14.Δ5PTEN*. Indeed, even by 10 weeks all [n=7] *HK1.fos-K14creP.Δ3β-cat*$^{flx/wt}$*.p53*$^{flx/flx}$ mice showed only mild hyper keratosis, if any; and a relatively normal fur [Fig. 7.11 A-C]. By this stage, the tagged ears also had little keratosis [Fig. 7.11 B] with a phenotype similar to *HK1.fos* and earlier *HK1.fos-K14creP.p53*$^{flx/flx}$ studies, which often possessed very minimal hyperkeratosis at only 10 weeks post tagging (*Greenhalgh et al., 1993b;1996*).

Close inspection of *HK1.fos-K14creP.Δ3β-cat*$^{flx/wt}$*.p53*$^{flx/flx}$ back skin displayed less keratosis than RU486-treated *HK1.ras-K14creP.Δ3β-cat*$^{flx/wt}$*.p53*$^{flx/flx}$ mice which usually exhibited patches of keratosis after 4-5 weeks RU486 treatment [above; Chapter 5]; although not the pangolin like skin that emerged again in repeat parallel experiments giving typical *HK1.fos-K14creP.Δ5PTEN*$^{flx/flx}$*.Δ3β-cat*$^{flx/wt}$ mice [Fig. 7.11D-F]. This suggests that similar to previously illustrated *HK1.ras-K14creP.Δ3β-cat*$^{flx/wt}$*.p53*$^{flx/flx}$ mice, p53 loss in *HK1.fos-K14creP.Δ3β-cat*$^{flx/wt}$*.p53*$^{flx/flx}$ was more potent and completely blocked the severity of *Δ3β-catenin* without facilitating tumorigenesis.

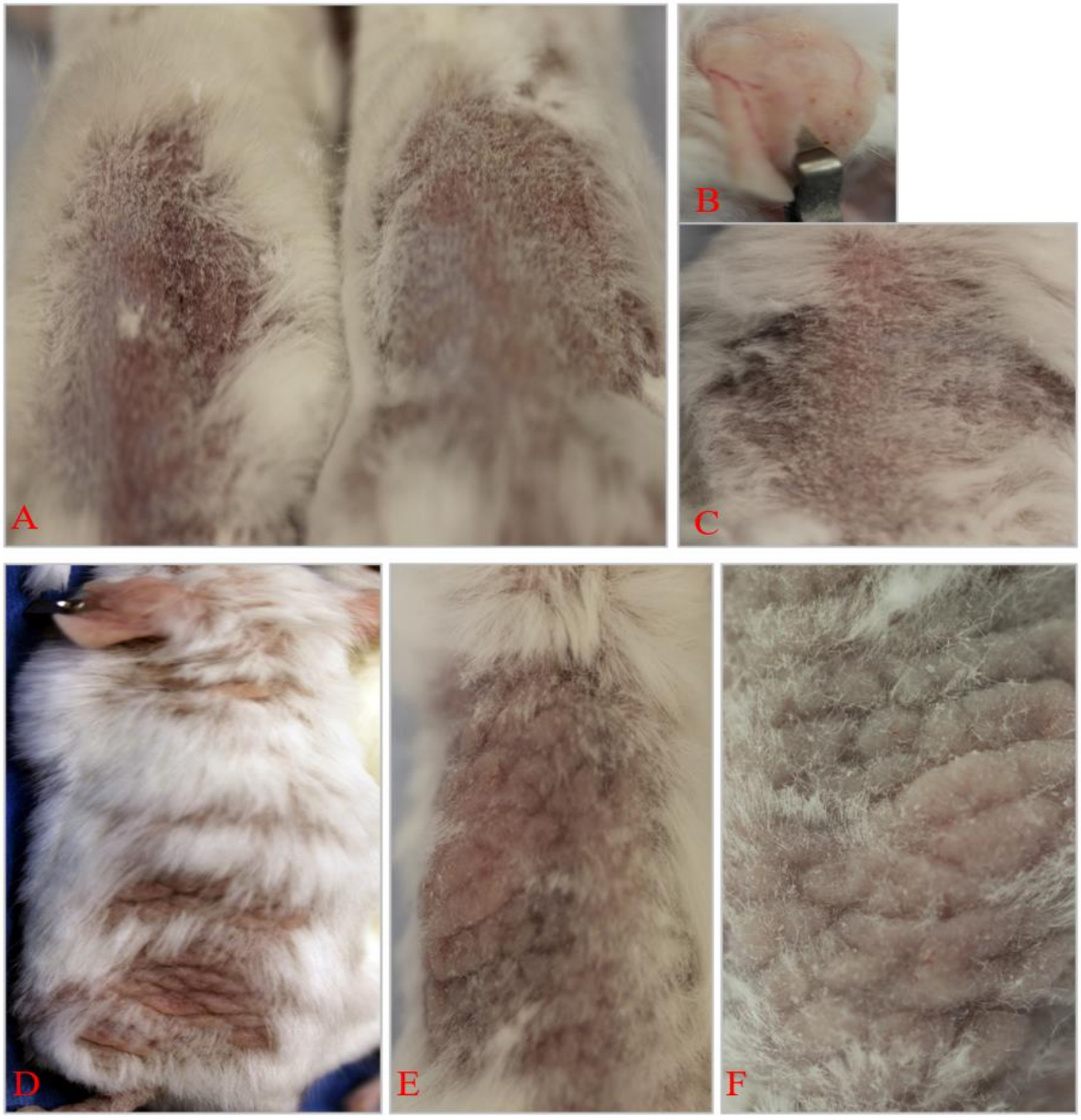

Figure 7. 11: Comparison of skin phenotypes in *HK1.fos-K14creP.Δ3β-cat$^{flx/wt}$-p53$^{flx/flx}$* and *HK1.fos-K14creP.Δ5PTEN$^{flx/flx}$.Δ3β-cat$^{flx/wt}$* mice.

[A] Two typical examples of RU486-treated *HK1.fos-K14creP.Δ3β-cat$^{flx/wt}$.p53$^{flx/flx}$* at 10 weeks show only mild hyper keratosis, if any; and little in the way of a scruffy fur. [B] At this stage the tagged ear also has little keratosis which was similar to *HK1.fos-K14creP.p53$^{flx/flx}$* or *HK1.fos* controls with no tumour development at this time. [C] Another *HK1.fos-K14creP.Δ3β-cat$^{flx/wt}$.p53$^{flx/flx}$* back skin at higher magnification again lacks any keratosis; even less than a typical *HK1.ras-K14creP.Δ3β-cat$^{flx/wt}$.p53$^{flx/flx}$* and certainly far less than the pangolin-like phenotype seen in [D-F] typical *HK1.fos-K14creP.Δ5PTEN$^{flx/flx}$.Δ3β-cat$^{flx/wt}$* mice.

The observation from *HK1.fos-K14creP.Δ5PTEN*$^{flx/flx}$ and *HK1.fos-K14creP.Δ5PTEN*$^{flx/flx}$*.Δ3β-cat*$^{flx/wt}$ mice demonstrated that early activation of *Δ3β-catenin* in juvenile skin had a more severe effect on differentiation to prevent tumourigenesis compared to similar *HK1.ras* models and this again appeared to rely on compensatory p53 and p21 expression. However, it appears that a major discovery again centres on these *HK1.fos-K14creP.Δ3β-cat*$^{flx/wt}$*.p53*$^{flx/flx}$ data, which demonstrate that these inhibitory responses appear to be directly dependent upon the presence of p53 and its loss which again completely blocked even the hyper-response mediated by the *Δ3β-catenin* enhanced *HK1.fos*-mediated differentiation. Moreover, unlike *HK1.ras-K14creP.Δ3β-cat*$^{flx/wt}$*.p53*$^{flx/flx}$ models where some degree of keratosis was observed, p53 loss in *HK1.fos-K14creP.Δ5PTEN*$^{flx/flx}$ completely reduced the appearance of *Δ3β-catenin* phenotypes over a longer period of time; yet without facilitating tumourigenesis as to date no KAs have been observed let alone SCC.

The reasons are very unclear. In *HK1.fos* models this appears to be a potent response, affecting migration from the stem cell niches and reducing the numbers of KPC cells that potentially give rise to tumours, and that affect overall IFE and HF differentiation. Although yet to be analysed, it may be that strong compensatory p63 and p73 expression moved the proliferative keratinocytes out of their stem cell niche and quickly through the KPC niches and transit amplifying stages and this rapid transit somehow avoided the differentiation responses. Alternatively, the lack of p53 failed to trigger the alarms in this context thus allowing for normal proliferation. However, further experimentation will be required to increase animal numbers to assess if any individual can bi-pass this tumour inhibition, assess histopathology and differentiation markers and determine whether p63/p73/K15 observations also appear in *HK1.fos.K14.Δ5PTEN.p53*$^{flx/flx}$ models and if this is specific to p53 via creation of *HK1.fos.K14.Δ5PTEN.p21KO* mice. It will be important to discover what is causing inhibition and assess what can be exploited in new treatments.

Table 7. 1: Summary of *HK1.fos-K14creP.Δ5PTEN$^{flx/flx}$.Δ3β-cat$^{flx/wt}$* lack of tumours and unique skin phenotype

Genotype analysed	[N]	Analysed for expression of	Data summary
HK1.fos hyperplasia	23	β-catenin, E-cadherin, K1, K6α, p53 and p21 expressions	-Control hyperplasia exhibiting suprabasal expression of β-catenin/E-cadherin -ordered terminal differentiation indicated by suprabasal layer K1 but expressing K6α in both supra and basal layers due to HK1.fos activation -weak basal layer p53/p21
HK1.fos-K14creP.Δ5PTEN$^{flx/flx}$.Δ3β-cat$^{flx/wt}$	8	β-catenin, E-cadherin, K1, K6α, p53 and p21 expressions	-No IFE tumours -Sever increase in HF tumours and greater cyst formation vs *HK1.ras-K14creP.Δ3β-cat$^{flx/wt}$* results in a pangolin like-skin phenotype -Predominance of IFE cysts formation -Highly disorganized epidermis -Increased cytoplasmic/nuclear basal layer β-catenin with increased membranous basal layer β-catenin/E-cadherin due to Δ3β-catenin -Accelerated terminal differentiation of IFE keratinocytes indicated by premature basal layer K1 also appearing in IFE cysts indicating confused keratinocytes that express K6α as well indicating completely disrupted terminal differentiation - Nuclear expression of p53/p21in basal layers and in IFE cysts possibly halting Δ3β-catenin/fos-induced proliferation and inducing the differentiation phenotype
HK1.ras/fos.K14creP.Δ3β-cat$^{flx/wt}$	8		
HK1.fos.K14creP.Δ3β-cat$^{flx/wt}$	15		
HK1.fos.K14creP.Δ3β-cat$^{flx/wt}$ -p53$^{flx/flx}$	6	ND	-Complete blockage of IFE tumours and pangolin skin phenotype of *HK1.fos-K14creP.Δ3β-cat$^{flx/wt}$*

Conclusion: β-catenin activation co-operation with *HK1.fos* results in increased differentiation responses that block IFE tumour formation accompanied by a severe skin phenotype amplified by PTEN loss or HK1.ras co-operation. However, this skin phenotype was absent in *HK1.fos-K14creP.Δ3β-cat*$^{flx/wt}$*p53*$^{flx/flx}$ with inducible p53 loss, thus emphasising p53 roles or responses to p53 loss in generating even this severe skin phenotype.

7.4 SUMMARY

The observation from *HK1.fos-K14creP.Δ5PTEN$^{flx/flx}$.Δ3β-cat$^{flx/wt}$* mice suggest that early activation of Δ3β-catenin in these juveniles had a more severe effect on differentiation to prevent tumorigenesis. Overall, these experiments found an inhibited tumor formation again involving p53 and p21 expression, but the K1 and K6 expression analysis in the IFE suggest it was the increased differentiation that appears to be the most significant event. These data showed that Δ3β-catenin interference of normal roles in differentiation (*Gat et al., 1998**;** Niemann et al., 2002; Grigoryan et al., 2008; Kretzschmar et al., 2015*) enhanced the *HK1.fos*-mediated interference of differentiation normally regulated by sporadic c-fos expression in basal layers (*Fisher et al., 1991; Greenhalgh et al., 1993b; Basset-Seguin et al., 1994; Angel et al., 2001)* and the HF stem cell decisions to form IFE, sebocytes or HF cells (Gerdes *et al., 2006*) coupled to major roles in regulation of keratinocyte cornification in supra-basal layers (*Candi et al., 2006*). This role in cornification may be quite important given the supra-basal roles for both fos and β-catenin and that fos/β-catenin-mediated co-operation enhance not only an accelerated differentiation but also the significant premature cornification that led to early keratosis, so that each proliferative fold gave rise to a scale-like structure hence the reference to a pangolin-like skin.

Thus, for the first time these *HK1.fos-K14creP.Δ5PTEN$^{flx/flx}$.Δ3β-cat$^{flx/wt}$* mice identified a direct link between fos and β-catenin activation in regulation of keratinocyte differentiation, consistent with photo-carcinogenesis studies that associates both instant and delayed c-fos responses to UV-B exposure in the epidermis with AKT activation and GSK3β inactivation (*Gonzales and Bowden, 2002*). This too strengthens links to co-operation between failure of PTEN-mediated AKT regulation and the axis of GSK3β/β-catenin and fos. Indeed, the often-neglected lipo-phosphatase functions of PTEN at the cell membrane that act as a scaffolding protein in the assembly of adherence junctions and cell-matrix interactions (*Tamura et al., 1998; Subauste et al., 2005*), could also contribute to the increased levels of E-cadherin observed that would also add to the degree of keratosis.

Another important discovery in these experiments was the finding that mutant PTEN co-operation with Δ3-βcatenin deregulation gave a novel HF histotype that closely resembles the trichilemmomas, a hair follicle tumour histotype produced in Cowden's disease, a familial (*Liaw et al 1997; Fistarol et al., 2002; Suzuki et al., 2003*) cancer predisposition syndrome

(*Liaw et al., 1997*) associated with cutaneous hyperkeratosis (*Fistarol et al., 2002*). This again is a logical finding consistent with the fact that deregulation of both these proteins induces HF anomalies in transgenic mice (*Gat et al., 1998**;** Niemann et al., 2002; Grigoryan et al., 2008; Kretzschmar et al., 2015; Suzuki et al., 2003*); and this discovery is currently being actively pursued in separate studies.

It appears that another major finding centres on the role of p53 in this complex model as its loss fails to elicit tumours yet appears necessary for either the appearance of or the inhibition of this intense differentiation response. These *HK1.fos-K14creP.Δ3β-cat*$^{flx/wt}$*.p53*$^{flx/flx}$ data again demonstrated that these inhibitory responses appear to be directly dependent upon the presence of p53 as its loss completely blocked the *Δ3β-catenin* enhanced *HK1.fos*-mediated differentiation; unlike the *HK1.ras-K14creP.Δ3β-cat*$^{flx/wt}$*.p53*$^{flx/flx}$ model where some degree of keratosis was eventually observed. However, the fact that this occurred in two separate models suggests that these strong differentiation responses that depend upon p53 one way or another are a general response to β-catenin deregulation, and not just specific to *HK1.ras- or HK1.fos-K14creP.Δ3β-cat*$^{flx/wt}$*.p53*$^{flx/flx}$ models; an idea consistent with the finding of a similar response to endogenous β-catenin deregulation following inducible activation of ROCK2 signalling to the AKT/GSK3β/β-catenin axis in this *K14.creP* model that also altered the differentiation response (*Masre et al., 2020*).

This differentiation response was also observed previously in the synergy between *HK1.fos-K14creP.Δ5PTEN*$^{flx/flx}$ that resulted in KA instead of SCC. Here again, Δ5PTEN-derived increases in p-AKT activation inactivated GSK3-β triggering compensatory p53/p21(*Yao et al., 2008*), which has now been confirmed to be also associated with elevated membranous/nuclear β-catenin and the corresponding increased E-cadherin [see chapter 3 Fig. 3.3C&G; *Alyamani et al.,* manuscript in preparation]. This KAs analysis demonstrated that the protective responses to endogenous β-catenin activation played a major role in KA aetiology, but only once a threshold level of GSK3 β-catenin inactivation was achieved (*Yao et al., 2008*) to deliver the necessary levels of nuclear β-catenin [Fig. 3.3C&G]. The fact that this was dependent upon p53 was revealed by progression to SCC in *HK1.ras/fos-K14creP.Δ5PTEN*$^{flx/flx}$ mice following p53 loss [Fig. 3.3D&H] where now the membranous β-catenin component was lost, leaving the nuclear component to drive invasion alongside loss of E-cadherin at the invasive front. Whereas in the *HK1.fos-K14creP.Δ5PTEN*$^{flx/flx}$*.Δ3β-cat*$^{flx/wt}$ mice, strong membranous expression of β-catenin was maintained together with strong levels

of E-cadherin, as observed in KA [Fig.3.3 vs Fig. 7.5 & Fig. 7.6] and again suggesting that the differentiation response to deregulated β-catenin involves a general differentiation response mediated by p53.

The analysis of endogenous β-catenin expression in both *HK1.fos-K14creP.Δ5PTEN$^{flx/flx}$* KA and *HK1.ras/fos-K14creP.Δ5PTEN$^{flx/flx}$* SCC showed that depending on the context of different oncogene expression together with specific TSGs responses and the time when nuclear β-catenin localization was induced governed the fate of tumour progression and conversion. It was these latter observations on tumour inhibition and the KA vs. SCC outcome in different contexts that led to questioning whether direct, earlier *Δ3β-catenin* activation in co-operation with *HK1.fos-K14creP.Δ5PTEN$^{flx/flx}$* [and similarly *HK1.ras/fos*] would lead to malignant progression, or still give protective responses in the shape of a KA outcome and now in the light of the tumour inhibitory data seen in *HK1.ras-K14creP.Δ3β-cat$^{flx/wt}$* mice, would there be a similar out come in *HK1.fos-K14creP.Δ5PTEN$^{flx/flx}$.Δ3β-cat$^{flx/wt}$* mice? In the final analysis in terms of IFE tumourigenesis co-operation in *HK1.fos-K14creP.Δ5PTEN$^{flx/flx}$.Δ3β-cat$^{flx/wt}$* , *HK1.ras/fos.Δ3β-catenin* and *HK1.fos-K14creP.Δ5PTEN$^{flx/flx}$* all resulted in a lack of tumours which reinforce the fact that early Δ3β-catenin activation resulted in triggering epidermal protective responses even in the presence of several potent oncogenes: fos, Δ3β-catenin or loss of PTEN-mediated AKT inhibition.

However, in this case, the hallmark of each *HK1.fos-K14creP.Δ5PTEN$^{flx/flx}$.Δ3β-cat$^{flx/wt}$* , *HK1.ras/fos.Δ3β-catenin and HK1.fos-K14creP.Δ5PTEN$^{flx/flx}$* co-operation was the appearance of a novel skin phenotype of overlapping and highly keratotic bands or scales with a concentric geometric harlequin pattern. This pattern supposes that the proliferation induced resulted in a folded skin which then differentiated into hardened scales resembling a pangolin skin [the only scaled mammal]. As this gross phenotype was observed in all three genotypes, it suggests that the underlying mechanism for the development of this novel pangolin like-skin phenotype was specifically associated with epidermal responses to β-catenin and fos dysfunctional interactions on normal skin homeostasis. This would be consistent with disruption of β-catenin roles in regulating epidermal pluripotent stem cells that are needed for epidermal terminal differentiation and hair follicle differentiation (*Gat et al., 1998**;** Niemann et al., 2002; Grigoryan et al., 2008; Kretzschmar et al., 2015*) coupled to those of c-fos that also plays roles in the commitment to terminal differentiation (*Fisher et al., 1991; Greenhalgh*

et al., 1993b; Basset-Seguin et al., 1994; Angel et al., 2001; Candi et al., 2006) and the HF stem cell decisions to form IFE, sebocytes or HF cells (*Gerdes et al., 2006*).

Further, the histology of the *HK1.fos-K14creP.Δ5PTEN$^{flx/flx}$.Δ3β-cat$^{flx/wt}$* mice in particular demonstrate a very abnormal epidermis dominated by the formation of numerous novel HF tumours and cysts. This epidermal response is indicative of the potency of these genotypes to generate this type of protective response from the epidermis, in this case diversion of excessive proliferation into either differentiation and massive keratosis or formation of dead-end cysts. Either mechanism would prevent further tumour formation. This novel skin phenotype becomes more severe with additional *Δ5PTEN* mutation due to AKT-associated activation that promotes cellular proliferation and tumourigenesis (*Downward, 2004; Segrelles et al., 2006; Yao et al., 2008; Macdonald et al., 2014),* which also disturbs epidermal terminal differentiation (*Callutti et al., 2005*). Indeed, it was speculated above that given in normal epidermis AKT expression is supra-basal (*Masre et al., 2020*), it may be geared to block p53-mediated apoptosis giving time for terminal differentiation (*Callutti et al., 2005; Yao et al., 2008; Macdonald et al.,2014*). Thus, the loss of PTEN may allow for premature AKT expression in basal layers adding to the proliferation and the beginnings of a disordered differentiation and induction of p53/p21 apoptosis to counter p-AKT activation.

However, hair follicles tumours previously associated with *Δ3β-catenin* such as folliculoma and pilomatricoma (*Gat et al., 1998**;** Niemann et al., 2002; Kretzschmar et al., 2015*) have now significantly changed in *HK1.fos-K14creP.Δ5PTEN$^{flx/flx}$.Δ3β-cat$^{flx/wt}$* mice when compared to those produced in *HK1.fos-K14creP.Δ3β-cat$^{wt/flx}$* which were similar to *HK1.ras-K14creP.Δ3β-cat$^{flx/wt}$* mice previously analysed. Thus in *HK1.fos-K14creP.Δ5PTEN$^{flx/flx}$.Δ3β-cat$^{flx/wt}$* mice, mutant PTEN co-operation with Δ3-βcatenin deregulation gave a novel increased numbers of HF and with a tumour histotype that appears to be trichilemmoma, a hair follicle tumour histotype also produced in Cowden's disease, (*Liaw et al., 1997; Fistarol et al., 2002; Suzuki et al., 2003*). This again is a logical finding consistent with the fact that deregulation of both these proteins induces HF anomalies in transgenic mice (*Gat et al., 1998**;** Niemann et al., 2002; Kretzschmar et al., 2015; Suzuki et al., 2003*); whilst the increased cyst formation [also in *HK1.fos-K14creP.Δ5PTEN$^{flx/flx}$* co-operation] maybe another underlying reason for the protective response against tumourigenesis. Previously excessive cyst formation was also prompted by the activation of other oncogenes such as ras and fos in conjunction with

Δ5PTEN (*Macdonald et al., 2014*). Thus, as formation of cysts has been reported previously in separate studies in association with over expression of β-catenin (*Gat et al., 1998; Niemann et al., 2002; Kretzschmar et al., 2015*) and also fos (*Yao et al., 2008; Macdonald et al., 2014*) this indicates that cyst formation is a common intertwined phenotype as a result of β-catenin/fos and PTEN co-operation.

E-cadherin levels also increased in *HK1.fos-K14creP.Δ5PTEN*$^{flx/flx}$*.Δ3β-cat*$^{flx/wt}$ IFE basal layers and it was noticed that E-cadherin expression was particularly strongly in the trichilemmoma-like HF tumours. This mimicked β-catenin expression, and this intense E-cadherin expression profile was exclusive to these *HK1.fos-K14creP.Δ5PTEN*$^{flx/flx}$*.Δ3β-cat*$^{flx/wt}$ animals as neither *HK1.fos-K14creP.Δ3β-catwt/flx*skin nor *HK1.ras-K14creP.Δ3β-cat*$^{flx/wt}$ possessed this intense E-cadherin profile. Thus, increased E-cadherin exhibited by *HK1.fos-K14creP.Δ5PTEN*$^{flx/flx}$*.Δ3β-cat*$^{flx/wt}$ trichilemmomas and cysts is another novel tumour feature and suggests co-operation between *β-catenin* and *PTEN* in HF development (*Gat et al., 1998; Huelsken et al., 2001; Niemann et al.,2002*) and the resulting HF tumour type (*Suzuki et al., 2003*).

Moreover, the excess numbers of HF-derived cysts again suggest this is a common response to divert anomalous HF formation away from tumour formation and into the dead end of cyst formation (*Young et al., 2003*) as observed in *HK1.ras/fosΔ5PTEN* mice (*Macdonald et al., 2014*). Nonetheless in the IFE of all three *fos/Δ3β-catenin* genotypes, increased E-cadherin would contribute to the inhibition of papillomas as suggested in previous studies (*Kotelevets et al., 2001*) alongside the differentiation responses elicited by *HK1.fos* [below; (*Candi et al., 2005; Mehic et al., 2005*) that also diverted progression to KA (*Macdonald et al., 2014*). Thus, whilst β-catenin expression was strongly nuclear and membranous in the basal layer which was also confirmed via E-cadherin analysis indicative of strengthened cell-cell adhesions. This also correlated with strong p53/p21 expression, similar to that seen previously in *HK1.fos-K14creP.Δ5PTEN*$^{flx/flx}$ KA (*Macdonald et al., 2014*); and in analysis of *HK1.ras-K14creP.Δ3β-cat*$^{flx/wt}$ or *K14creP.Δ3β-cat*$^{flx/wt}$ skin [see Chapters 3 & 5]
Thus, in all of these genotypes, the membranous β-catenin component, and increased E-cadherin strengthened cell-cell adhesion and with the increased p53/p21 to divert excess KPC proliferation into differentiation, which together combined to block tumour formation. In support of this idea histological analysis of the early differentiation marker K1 showed patches

of accelerated differentiation marked by basal layer K1 expression which also appeared around the cysts; whilst the hyperproliferation marker K6 showed only patchy IFE expression at best. As K1 possessed the AP1 binding sites that allow for fos regulation as keratinocytes commit to differentiate [and that are missing in the *HK1* vector, hence its basal layer expression [Chapter 1] it now explains why K1 expression appeared in the IFE basal layers and accelerate differentiation. Indeed, K1 expression in the sporadic *HK1.fos-K14creP.Δ5PTEN*$^{flx/flx}$*.Δ3β-cat*$^{flx/wt}$ IFE was quite different to the aberrant, laterally confined patchy expression in *HK1.ras-K14creP.Δ3β-cat*$^{flx/wt}$ which was often fairly thin. This again indicates a far more accelerated and premature differentiation pattern due to elevated p53/p21 expression responding to excess β-catenin/E-cadherin, and the odd ragged nature to K1 expression in the many patches of acanthosis possibly reflects the role of fos [and PTEN] in cornification (*Candi et al., 2006*) that are now subverted by *HK1.fos/Δ3β-catenin* expression.

Another possible mechanism returns to the idea that constitutive activation of β-catenin returns the adult mouse skin to one resembling more of a neonatal state (*Collins et al., 2011*) a theme explored further in the *in vitro* experimentation Scatter Assay [below]. In neonatal skin for the first 5-6 days the epidermis is naturally hyperplastic but e.g., lacks K6α expression and p-AKT is uniformly expressed in the suprabasal layer (*Masre et al., 2020*). Also, at day 4-6 HK development begins, thus in leaky *HK1.fos-K14creP.Δ5PTEN*$^{flx/flx}$*.Δ3β-cat*$^{flx/wt}$ skin so many new HFs are being created in juveniles due to the effects of *Δ3β-catenin* expression that are then further compromised by *K14.Δ5PTEN* expression and fail to differentiate properly; hence reduced K6α and rapid degeneration into increased numbers of cysts by adulthood.

Analysis of the hyperproliferation marker K6α supports this return to a juvenile state (*Collins et al., 2011*) as in strands of IFE *HK1.fos-K14creP.Δ5PTEN*$^{flx/flx}$*.Δ3β-cat*$^{flx/wt}$ hyperplasia K6α expression was barely detectable; and whilst K6α was expressed in hair follicles and trichilemmomas, overall K6α expression seemed diminished compared to the follicular expression seen in *HK1.ras-K14creP.Δ3β-cat*$^{flx/wt}$ folliculomas suggesting a less developed, primitive less differentiated HF. This reduced expression may again induce the response to divert odd anomalous HF cell proliferation into cyst formation, and not just in the KHFs but also in the IFE as K1 was also noted to be expressed in some cysts. This K1/K6α analysis indicated that these cysts originated from both IFE and HFs and that expression had fallen off

possibly due to the greatly disturbed terminal differentiation by *HK1.fos-K14creP.Δ5PTEN$^{flx/flx}$.Δ3β-cat$^{flx/wt}$* co-operation.

To-date in the *HK1* model this lack of K6α expression is only the second instance where it was weak even in HFs and suggests that this is unique to *Δ3βcatenin* expression and may also reflect the excess increased E-cadherin expression observed in *HK1.fos-K14creP.Δ5PTEN$^{flx/flx}$.Δ3β-cat$^{flx/wt}$* skin, which in turn alters the hyperproliferation signals derived from cell-cell interactions which are overcome by i.e. p53 and p21 [below] and possibly others e.g. p63 and p73 [above] that have yet to be analysed.

Collectively, despite the difference in phenotype between *HK1.fos-K14creP.Δ5PTEN$^{flx/flx}$.Δ3β-cat$^{flx/wt}$* and earlier *HK1.ras-K14creP.Δ3β-cat$^{flx/wt}$* mice, the essence of the defensive mechanism seems to carry similar pattern to that observed in previous *HK1.fos-K14creP.Δ5PTEN$^{flx/flx}$* KA aetiology but appearing earlier, during epidermal development; hence the more severe epidermal response in *HK1.fos-K14creP.Δ5PTEN$^{flx/flx}$.Δ3β-cat$^{flx/wt}$* . In *HK1.fos-K14creP.Δ5PTEN$^{flx/flx}$* KA aetiology, β-catenin activation led to a triggering of p53/p21 responses resulting in accelerated differentiation halting any possible malignant progression. Whereas in *HK1.fos-K14creP.Δ5PTEN$^{flx/flx}$.Δ3β-cat$^{flx/wt}$* or *HK1.fos-K14creP.Δ5PTEN$^{flx/flx}$* epidermis the timing of β-catenin activation seems to be the key condition that governed the appearance of massive keratosis. Here, in this context the data suggested that p53-mediated proliferation and increased p21-mediated differentiation aided the developing pangolin like-skin preventing further progression via cyst production. This was similar to the conclusions made in *HK1.ras-K14creP.Δ3β-cat$^{flx/wt}$* analysis, where p53/p21 responses to *Δ3β-catenin* appeared to be the main reasons for blocking tumours formation [outlined above; chapters 4 & 5], although perhaps not via the massive differentiation responses observed here and those from KA aetiology (*Macdonald et al., 2014*).

However, the situation became more complicated when conditional p53 loss was introduced to create the *HK1.ras-K14creP.Δ3β-cat$^{flx/wt}$.p53$^{flx/flx}$* genotype and began to confirm this theory in terms of p53 protection at least. This resulted in an inhibition of these leaky *Δ3β-catenin* phenotypes and whilst full sized non leaky mice failed to display the initial phenotypes and thus this unique paradoxical result was missed, despite p53 loss and ras and β-catenin activation, only two mice gave tumours; but these did convert to malignancy consistent with the original hypothesis as

observed in *HK1.ras/fos-Δ4PTEN* mice. It remained to be seen whether this response to the combinations of fos/PTEN and β-catenin co-operation were dependent on p53 or p21 or both given their clear implication in developing the pangolin like-skin phenotype as anti-tumorigenesis response.

HK1.fos-K14creP.Δ3β-cat$^{flx/wt}$-p53$^{flx/flx}$ again confirmed the essential requirement for p53 to elicit these *Δ3β-catenin* phenotypes and highlighted the fact that this co-operation completely blocked the appearance of a pangolin like-skin phenotype. Indeed unlike *HK1.ras-K14creP.Δ3β-cat$^{flx/wt}$.p53$^{flx/flx}$* where some degree of keratosis was observed, p53 loss in *HK1.fos-K14creP.Δ3β-cat$^{flx/wt}$-p53$^{flx/flx}$* mice completely blocked *Δ3β-catenin* phenotypes over longer periods of time; yet without facilitating tumorigenesis, as to date no KAs have been observed, even in full sized mice.

The reasons for this intriguing result are unclear. It may be that p53 functions are essential to trigger this overall response as observed in KA aetiology and were lacking in SCC, or alternatively compensatory p63 and p73 expression observed above, may alter the KPC niches to maintain a proliferative cell barrier that in this case negates the fos and p21 induction of an excessive commitment to terminal differentiation. However, further experimentation will be required to increase animal numbers to assess if any individual can bi-pass this tumour inhibition, assess histopathology and differentiation markers and determine whether p63/p73/K15 observations also appear in *HK1.fos.K14.Δ5PTEN.p53$^{flx/flx}$* models.

The total disappearance of these phenotypes suggest that it is a p53-mediated response to *HK1.fos-K14creP.Δ5PTEN$^{flx/flx}$* that plays a major role in generating the pangolin like skin, but possibly not necessary for the blockage of tumours. This again returns to the central p53 paradox: that p53 loss blocks *HK1.ras* or *HK1.fos* papilloma formation (*Greenhalgh et al., 1996*) and this cannot be overcome by β-catenin activation in *ras* or *fos* models. In one context this appears to be due to inhibitory responses to β-catenin deregulation that depended on the presence of wt p53 [but possibly not p21]; another involves responses to p53 loss, possibly mediated by p63 and 73 that alter the stem cell niche to prevent tumour development and possibly return differentiation to that of a *HK1.fos.K14.Δ5PTEN.p53$^{flx/flx}$* skin.

These potent responses to p53 loss may be quite general appearing in ras/β-catenin/p53; fos β-catenin/p53; ras/p53 and fos/p53 models to inhibit early benign tumour [papilloma/KA] aetiology and it remains to be seen if this response to p53 loss can inhibit PTEN/β-catenin co-

operation in development of HF tumours also. Thus, an epidermis in being most exposed to environmental carcinogens has many options to prevent benign tumour formation; which may become lost in aggressive papillomas leading to conversion as observed in Chapter 3. This latter point and these results above show the importance of both context and temporal expression of oncogenic tumour promotion events vs. endogenous TSGs responses will govern the final outcome in this very complex mechanism. In the final analysis it will be important to exploit these findings to discover exactly what is achieving this tumour inhibition and find new targets for new treatments.

Chapter 8: In vitro analysis of primary transgenic keratinocytes and cell lines derived from β-catenin activation

8.1 Establishment of keratinocyte lines and resistance to calcium-induced terminal differentiation

As outlined above, the co-operation between *Δ3β-catenin, HK1.ras, HK1.fos* and *K14.Δ5 PTEN* expression *in vivo* resulted in a novel lack of carcinogenesis either with or without p53; and a novel co-operation between *K14creP.Δ3β-cat*$^{flx/wt}$ and *K14.Δ5 PTEN* expression resulting in tumours that mimicked human trichilemmomas produced in Cowden's disease patients. These results were novel, unexpected and demonstrated the power of the epidermis to resist early-stage tumour formation by a variety of responses and show the importance of regulated β-catenin to epidermal homeostasis in adults and developing juvenile epidermis. Further, these data show that only the analysis of β-catenin in the original *HK1.fos-K14creP.Δ5PTEN*$^{flx/flx}$ KA and *HK1.ras/fos-K14.Δ5 PTEN* SCC models [plus four instances in *Δ3β-catenin* mice] appear to be consistent with the original hypothesis: that β-catenin would co-operate with ras and fos to either convert papillomas to malignancy and/or increase invasiveness following p53 [and p21] loss and reduced E-cadherin.

Therefore, to begin to explore these discoveries further and to directly manipulate cells *in vitro* in normal and transgenic keratinocytes, classic keratinocyte culture assays were performed employing cell lines derived from primary neonatal keratinocytes cultured *in vitro* (*Hennings et al., 1980*) with modifications that prevent spontaneous transformation (*Greenhalgh et al., 1989*). These experiments assessed effects of transgene expression on differentiation signals and assessed: the ability of early passage cell lines [<10] to grow clonally as an indication of transformation; to compare cell motility as an indication of invasive potential; and seeding ability to test the idea that *Δ3β-catenin* expression had somehow returned an adult epidermis to a more juvenile state, as reported in previous studies (*Collins et al., 2011*).

In total culturing and maintaining primary keratinocytes from mouse epidermis for 3-4 months successfully established seventeen cell lines of low passage (SC3-10) keratinocytes [Table. 8.1] for assessment of calcium-induced differentiation in response to a staggered increased in calcium [0.05- 0.075-0.15 Ca^{2+} mM] and a test of transformation via standard carcinogenicity assays involving abilities to grow from single cells in low calcium media [immortalised/benign] or High calcium media [transformed and malignant]. It was envisaged that these lines would also be assessed by westerns that explored differentiation marker

expression [K1, K6α, K10, K14, K15] and repeat the same analysis on cells grown on coverslips in Low KGM low cal or Hi cal via IF and IHC. Similarly p53,p21 p63 p73 and Lgr5 & 6 were also planned to be investigated, together with PTEN/AKT1/β-catenin and E-cadherin to investigate cell migration in classic scratch assays. However, these experiments remain to be completed.

Table 8. 1: Cell lines created and summary of in vitro properties.

Primary keratinocyte genotype	Number of lines created	Phenotype
Normal ICR [wt 1 ; ICR1] *Δ3β-catenin* [B1, B2 B3]	2 3	Normal phenotype: no resistance to Ca^{2+}-mediated terminal differentiation; no clonal growth
K14creP.Δ3β-cat$^{flx/wt}$ KB 1 & 2	2	Immortalized cell line; some resistance to Ca^{2+}-induced terminal differentiation sporadic clonal growth only in Low Ca^{2+} KGM
HK1.ras-K14creP.Δ3β-cat$^{flx/wt}$ KRB 1 & 2	2	Transformed cell line; resistance to Ca^{2+}-induced terminal differentiation with clonal growth in Low & High Ca^{2+}
HK1.ras/fos.K14creP.Δ3β-cat$^{flx/wt}$ KRFB1 and KRFB2	2	Transformed cell lines; rapid growth and resistance to Ca^{2+}- induced terminal differentiation; Clonal growth in Low & High Ca^{2+}media
HK1.fos.K14creP.Δ3β-cat$^{flx/wt}$ KFB 1 & 2	2	Immortalized cell line; differentiated squames in Low Ca^{2+}; some resistance to terminal differentiation. Clonal growth in Low Ca^{2+} & slow High Ca^{2+}
HK1.fos-K14creP.Δ5PTEN$^{flx/flx}$.Δ3β-cat$^{flx/wt}$ KFPB1; KFPB2; KFPB3	3	Transformed cell lines; rapid growth and resistance to Ca^{2+}- induced terminal differentiation; Clonal growth in Low & High Ca^{2+}media
K14creP.Δ5PTEN$^{flx/flx}$.Δ3β-cat$^{flx/wt}$ KPB 1 & 2	2	Immortalized cell line; some resistance to calcium induced terminal differentiation Clonal growth in Low & High Ca^{2+}
ras.fos [transformed control] T52	2	Transformed cell line and resistance to calcium induced terminal differentiation with Clonal growth in Low & High Ca^{2+}

Primary keratinocytes from all possible combinations of *K14creP.Δ3β-cat*$^{flx/wt}$ with *HK1.ras/fos-K14creP.Δ5PTEN*$^{flx/flx}$ were established (*Greenhalgh et al., 1989*), including normal ICR controls, and lines were established for each genotype and their phenotype assessed as summarised in Table. 8.1. All cells were initially established in low 0.05mM Ca^{2+} media supplemented with 10% [chelated] FCS and 20% KGM and 20% fibroblast conditioned media, designed to prevent spontaneous keratinocyte transformation which is revealed by a sudden ability to easily sub-culture and maintain (*Greenhalgh et al., 1989*). Subsequently for transformed transgenic lines, most were cultured in 0.05mM Ca^{2+} media supplemented with 10% chelexed FCS and 10% KGM. All cell lines were induced to differentiate by increasing the calcium concentration to 0.075mM for the first 24h to instigate a supra-basal morphology and then high calcium concentration of 0.125mM Ca^{2+} for a further 24hrs to complete differentiation resulting in morphology of squamous and cross-linked keratinocytes, which is the case in normal cell lines [Fig. 8.1] (*Hennings et al., 1980*; *Greenhalgh et al., 1989*).

In Low Cal [0.05mM Ca^{2+}] media, *HK1.ras-K14creP.Δ3β-cat*$^{flx/wt}$ *line*s rapidly achieved a packed monolayer within 4-5 days of plating in 60mm dishes, indicative of a lack of contact inhibition as the cells appear much smaller [Fig. 8.1A]. This suggests a fully transformed cell line, however in echoes of the *in vivo* observation that certain responses inhibited tumours in *HK1.ras-K14creP.Δ3β-cat*$^{flx/wt}$ mice, after 24hrs in 0.075mM Ca^{2+} media surprisingly these cells adopted a morphology typical of spinus keratinocytes; thus mimicking transition to the supra basal layer as *in vivo*. However, these keratinocytes continued to grow in Hi calcium, unlike benign papilloma lines such as SP1 or 308 keratinocytes (*Strickland et al., 1988; Greenhalgh and Yuspa, 1988*). *HK1.ras-K14creP.Δ3β-cat*$^{flx/wt}$ keratinocytes also became more tightly packed
after 24 hours in 0.125mM Ca^{2+} media and showed no further signs of differentiation such as stratification or cornification into squamous cell [Fig. 8.1A]; a phenotype also exhibited by the T52 SSC line positive control [not shown (*Greenhalgh and Yuspa, 1988*)].

Similarly, *HK1.fos-K14creP.Δ5PTEN*$^{flx/flx}$*.Δ3β-cat*$^{flx/wt}$ lines also exhibit a transformed morphology at confluence; but now with numerous squames and other indications of anomalous early differentiation in proliferative Low Cal media, such as larger spinus and granular cells. Thus, this was consistent with the *in vivo* observations that differentiation was accelerated in this genotype [Fig. 8.1B]. However, indicating a greater degree of

transformation, after 24hr in 0.075mM Ca^{2+} media these keratinocytes appeared indifferent to terminal differentiation and still retain a degree of the proliferative cobblestone morphology in Low Cal. Nonetheless, in Hi Cal 0.125mM Ca^{2+} media, *HK1.fos-K14creP.Δ5PTEN$^{flx/flx}$.Δ3β-cat$^{flx/wt}$* keratinocytes showed an increased degree of terminal differentiation compared to *HK1.ras-K14creP.Δ3β-cat$^{flx/wt}$* cells; such as attempted stratification and formation of granular cells [Fig. 8.1B], again consistent with the increased differentiation observed *in vivo*.

In contrast, *K14creP.Δ3β-cat$^{flx/wt}$* lines showed a near normal basal layer morphology in Low Cal 0.05mM Ca^{2+} media, with normal sized cells that committed to differentiate in 0.075mM Ca^{2+} media but got no further and exhibit a similar spinus layer morphology in Hi Cal media rather than stratification and cornification [Fig. 8.1C]; a result again consistent with the lack of hyperplasia observed *in vivo* and only sporadic K1 expression. For comparison, normal keratinocytes showed the typical cobblestone morphology in proliferative 0.05mM Ca^{2+} media and almost complete stratification and cell loss in response to calcium induced terminal differentiation in both 0.075mM Ca^{2+} and 0.125mM Ca^{2+} media; thus showing their sensitivity to media conditions and the continued use of media supplemented with 20% fibroblast conditioned media to maintain their growth (*Greenhalgh et al., 1989*).

Collectively, these data suggests that *in vitro*, β-catenin activation induced cellular transformation and proliferation in a manner more consistent with accepted dogma (*Morin, 1999; Polakis, 1999; Doglioni et al., 2003; Grigoryan et al., 2008; Krishnamurthy and Kurzrock, 2018*)*;* and also demonstrate the differences in phenotypes *in vitro* compared to *in vivo* even in early passage lines due to the disruption of tissue homeostasis.

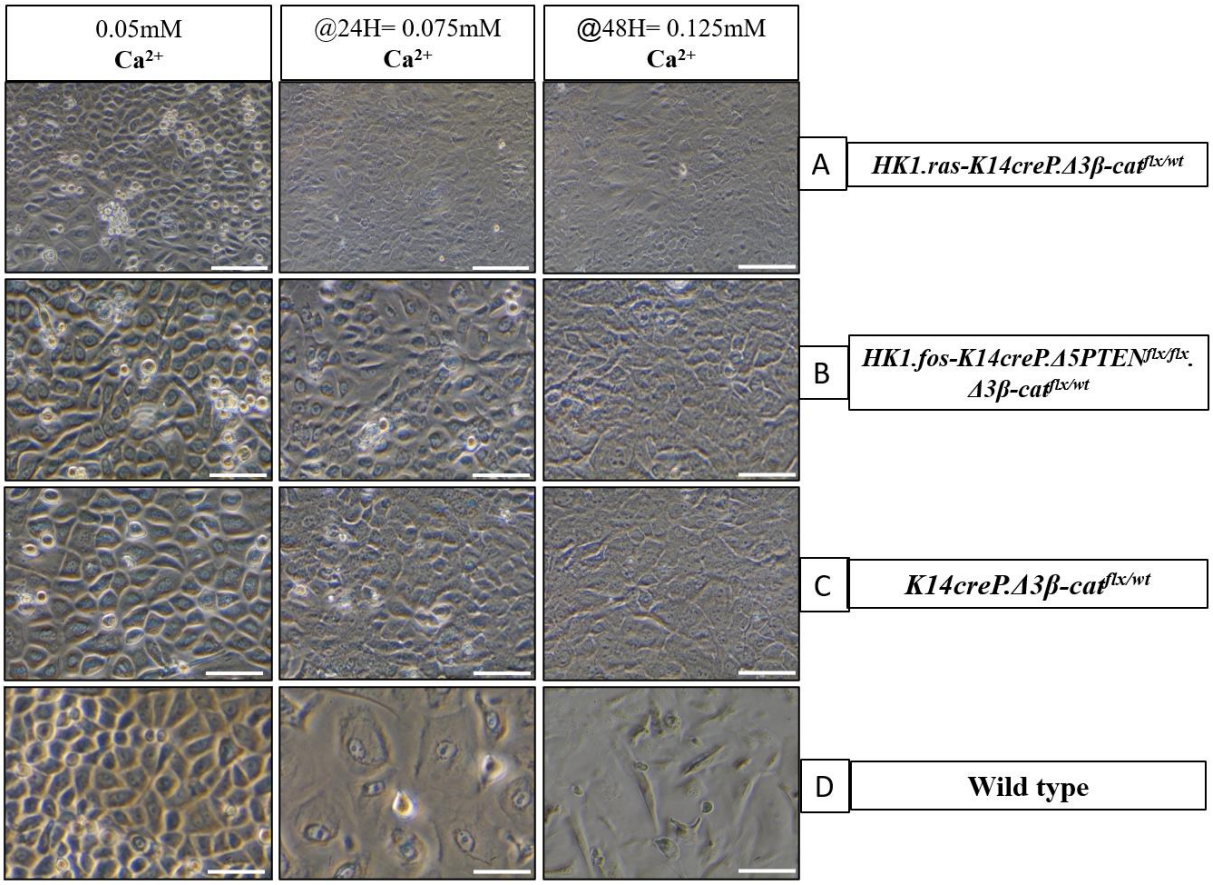

Figure 8. 1: Assessment of cell line growth in Low calcium media and response to calcium-induced terminal differentiation.

Cells were seeded at 5x 10^6 cells per dish in 0.05mM Ca^{2+} and three days later cells were switched to 0.075mM Ca^{2+} for 24hours to initiate differentiation and then to 0.125mM Ca^{2+} for a further 24 hours to complete the latter stages of differentiation and formation of cornified squames.

[A] In low Cal media *HK1.ras-K14creP.Δ3β-cat*$^{flx/wt}$ line KRB1 exhibits a packed monolayer indicative of a lack of contact inhibition as the cells appear much smaller with many floating cells. At 24hr in 0.075mM Ca^{2+} media surprisingly these cells adopted a morphology typical of spinus keratinocytes; thus mimicking transition to the supra basal layer; but cells continue to grow and became packed tighter after 24 hours in 0.125mM Ca^{2+} media and show no further signs of differentiation such as stratification or cornification into squamous cells

[B] *HK1.fos-K14creP.Δ5PTEN*$^{flx/flx}$*.Δ3β-cat*$^{flx/wt}$ line KFPB1 exhibits a transformed morphology at confluence; with numerous squames and other indications of anomalous differentiation in proliferative Low Cal media. At 24hr in 0.075mM Ca^{2+} media these keratinocytes still retain a degree of Low Cal morphology consistent with their transformed nature. In 0.125mM Ca^{2+} media, these cells show a degree of terminal differentiation such as attempted stratification and formation of granular cells. [C] *K14creP.Δ3β-cat*$^{flx/wt}$ line KB1 shows a near normal basal layer morphology in Low Cal 0.05mM Ca^{2+} media with normal sized cells that commit to differentiate in 0.075mM Ca^{2+} media but go no further and exhibit this spinus layer morphology in Hi Cal 0.125mM Ca^{2+}media rather than stratification and cornification.

[D] Normal ICR1 keratinocytes show the typical cobblestone morphology in 0.05mM Ca^{2+} and almost complete stratification and cell loss in response calcium induced terminal differentiation in both 0.075mM Ca^{2+} and 0.125mM Ca^{2+} media; thus showing their sensitivity to media conditions. Scale Bar: 20μm.

8.2 Analysis of cell lines growth from clonal density and correlation with a transformed or immortalised phenotype

Clonal growth assays were conducted on all cell lines to assess their ability to grow from single cells which for primaries cultured in Low Cal 0.05mm Ca^{2+} KGM media represents immortalisation and early-stage transformation no longer requiring communication with other cells; whilst culture and growth in Hi cal 0.125mm Ca^{2+} media is a stringent test of their transformation status. In repeat experiments, 12 dishes per cohort of low passage [Sc 3-5] cell lines were plated at approx. 250 cells per 60mm dish in 0.05mm Low Ca*2+* [6 Dishes] and 24 hours later a cohort was switched to Hi Cal media 0.125mm Ca2+ [6 Dishes]. Cells were maintained for 30 days and then formalin fixed and stained with Rhodamine B, a keratinocyte specific stain. Although all cell lines were assessed, the salient results from representative lines are given in [Fig. 8.2].

Both *HK1.ras-K14creP.Δ3β-cat*$^{flx/wt}$ and *HK1.fos-K14creP.Δ5PTEN*$^{flx/flx}$*.Δ3β-cat*$^{flx/wt}$ grew well at-clonal density in both Low and Hi Cal media indicating a highly transformed state. Indeed by 28 days even in Hi Cal media cohorts of *HK1.fos-K14creP.Δ5PTEN*$^{flx/flx}$*.Δ3β-cat*$^{flx/wt}$ lines KFPB1 [shown], KFPB2 and KFPB3 were fully confluent; whilst *HK1.ras-K14creP.Δ3β-cat*$^{flx/wt}$ lines KRB1 [shown] and KRB2 were still growing from colonies; although the Low Cal cohorts were fully confluent by this time [Fig. 8.2A vs. B]. *HK1.ras.fos.K14creP.Δ3β-cat*$^{flx/wt}$ lines KRFB1 and KRFB2 also exhibited this more fully transformed growth producing confluent dishes in both Hi and Low Cal media, as did the ras/fos T52 SCC line (*Greenhalgh and Yuspa, 1988*); whereas *HK1.fos-K14creP.Δ3β-cat*$^{wt/flx}$ lines KFB1 and KFB2 were more similar to *HK1.ras-K14creP.Δ3β-cat*$^{flx/wt}$ line KRB1 with confluence reached by day 28, but only producing colonies in Hi Cal media [not shown].

K14creP.Δ3β-cat$^{flx/wt}$ lines KB1 [and KB2 not shown] grew from clonal density only in Low Cal [0.05mM Ca2+] media [Fig. 8.2C], which suggests that this line is immortalized but not fully transformed to malignancy; although grafting or sub-cutaneous injection would be needed to confirm this and to confirm their benign nature based on previous studies would produce either a hyperplastic skin or benign papilloma when grafted onto nude mice, but no sub-cutaneous tumours (*Greenhalgh and Yuspa, 1988; Greenhalgh et al., 1989*). In contrast all lines without *K14.creP* or *HK1.ras and fos* showed no growth at all even from clonal density e.g. *Δ3β-catenin* [Fig. 8.2D B1; B2 & B3 not shown].

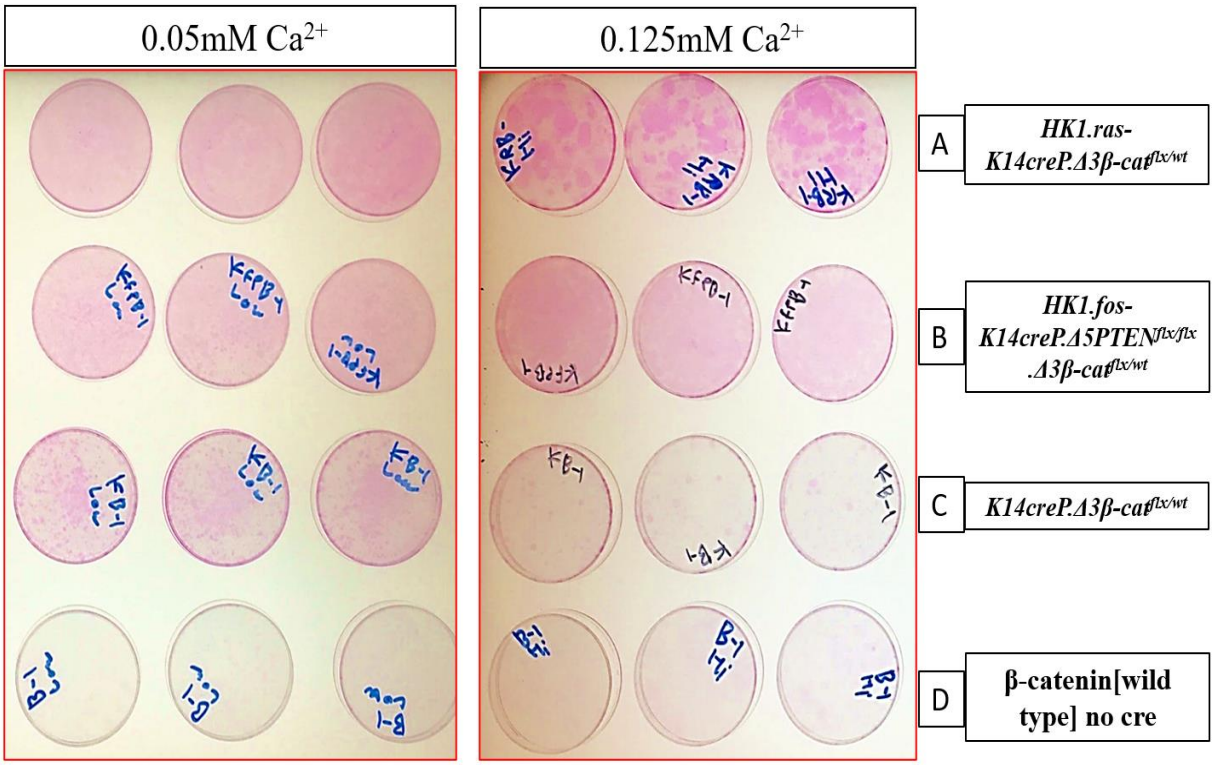

Rpt expts: n = 12 dishes/line; plated @ ~500 cells/dish low Ca^{2+}; switched Hi Ca^{2+} @48hrs; maintained 4-5 wks; MC 3x/wk DMEM 10% chelexed serum/20% KGM

Figure 8. 2: Assessment of cell line clonal growth in Low calcium [proliferative] or Hi calcium [differentiation] media.

[A] *HK1.ras-K14creP.Δ3β-cat*$^{flx/wt}$ line KRB [passage 4] and [B] *HK1.fos-K14creP.Δ5PTEN*$^{flx/flx}$*.Δ3β-cat*$^{flx/wt}$ [passage 5] showed growth from clonal density in both low calcium (0.05mM Ca2+) and high calcium (0.12mM Ca2+) concentrations, which indicates these lines are fully transformed and malignant. [C] *K14creP.Δ3β-cat*$^{flx/wt}$ line KB1 [passage 3] grows in low calcium concentration (0.05mM Ca2+) only, which suggest this line is transformed but benign. [D] *Δ3β-catenin* line B1 [passage 3] without *K14creP* displays normal growth behavior identical to wild type controls [not sown] with no growth at all in either calcium concentrations.

8.3 Analysis of cell line ability to seed from a confluent monolayer indicative of a juvenile phenotype

The above experiments assessed effects of transgene expression on differentiation and clonal growth as an indication of transformation. In a third series of experiments, transgenic cell lines were assessed not just for their motility as an indication of invasive potential; i.e. the rate cells grow past a specific point after they reached confluence as in standard scratch assays; but also to assess their ability to seed from a confluent monolayer. This simple experiment was primarily designed to test whether the fully transformed cell lines exhibited a loss of adhesion by being able to seed and scatter to form outlying colonies and thus mimic individual rather than collective modes of tumour invasion (*Hesse et al., 2016*) and experiments were planned to assess expression of β-catenin and E-cadherin at the monolayer edge but remain to be performed. This experiment also tested the idea that *Δ3β-catenin* expression returns adult keratinocytes to a more juvenile state, as reported in previous studies (*Collins et al., 2011*) and as suggested by K6α and p63/K15 expression *in vivo*.

Typically, non-transformed but immortalised keratinocyte lines established by this method (*Greenhalgh et al., 1989*) cease to be able to seed such satellite colonies by passage 3-5; unlike their normal primary counterparts where satellite colonies are common- as an indication of the presence of numerous stem–like/PCK cells in keratinocyte monolayers derived from new born vs. adult mouse skin, which are far more complicated to culture (*Morris et al.,2004*; and references therein).

A Scatter Assay involved simply initial culturing of lines in T25s flasks plated at 30^0 angle, and grown to confluence. Three/Four days later these T25s were laid flat and carefully treated with appropriate calcium concentrations [Low and High] to observe their ability to migrate past a determined growth line and also seed the free areas and then produce colonies [Fig. 8.3]. For each cell line six T25s were prepared and after reaching confluence three flasks were kept in low calcium concentrations and three challenged with high calcium to induce differentiation. Two weeks later, cells were fixed stained and their ability to form colonies assessed blind by 3 individual and the average number of colonies per flask from repeat experiments was recorded and expressed as a scatter factor (SF) score between 1 and 5.

The most transformed *HK1.fos-K14creP.Δ5PTEN$^{flx/flx}$.Δ3β-cat$^{flx/wt}$* line showed the highest SF scores in both low (5/5) and high (4/5) calcium media, suggesting that this line was quite malignant with a high probability of invasive capabilities [Fig. 8.3A]. This result was consistent with the loss of E-cadherin at the invasive front of *HK1.ras/fos-K14creP.Δ5PTEN$^{flx/flx}$* SCCs together with nuclear β-catenin but was inconsistent with the strong E-cadherin observed *in vivo* in these cohorts. Similarly transformed *HK1.ras-K14creP.Δ3β-cat$^{flx/wt}$* line KRB1 showed a high scatter factor score in low (4/5) calcium concentration; but less so in Hi Cal with a lower score (2/5) in high calcium concentration [Fig. 8.3B] indicating that this line may be malignant but still possessed sufficient focal adhesions to invade collectively rather than individually during malignant progression. Ideally growth on coverslips and assessment of E-cadherin and β-catenin via IF /IHC would help answer this question.

K14creP.Δ3β-cat$^{flx/wt}$ line KB1 also had a SF score of 2/5 in Low Cal but no seeding was observed in high calcium medium [Fig. 8.3C]. This indicates Δ3β-catenin activation alone may achieve a return to the juvenile phenotype ability to seed colonies but the line may remain benign given the lack of seeding in Hi Cal media, with possibly minimal reduction of focal adhesion. The normal appearing *Δ3β-catenin* line B-1 [Fig. 8.3D], along with wild type line ICR1 [not shown], scored a scatter factor of 0/5 in both calcium concentrations, confirming that typically immortalised normal mouse lines lose the capacity to seed, unlike primary keratinocytes; unless spontaneously transformed (*Greenhalgh et al., 1989*).

These data therefore suggest that all *Δ3β-catenin* lines are able to seed/scatter in a manner similar to neonatal primary keratinocytes and support the idea that β-catenin overexpression may return the epidermis to a more juvenile state as suggested in previous studies (*Watt and Collins, 2008*; *Collins et al., 2011*) an idea also suggested by epidermal lineage studies (*Kretzschmar et al., 2015*). This ability was especially pronounced in *HK1.fos-K14creP.Δ5PTEN$^{flx/flx}$.Δ3β-cat$^{flx/wt}$* and *HK1.ras-K14creP.Δ3β-cat$^{flx/wt}$* lines and may indicate a reduction in cell-cell adhesion signalling causing these to mimic invasion consistent with a malignant phenotype. This observation is also constant with endogenous β-catenin activation *in vivo* where loss of focal adhesion with E-cadherin facilitated malignant progression in tri-genic *HK1.ras/fos-K14creP.Δ5PTEN$^{flx/flx}$* mice [see Chapter 3]. These data also highlight that *in vitro* β-catenin activation [*Δ3β-catenin*] apparently results in a decrease in cell-cell adhesion in certain combinations which facilitate cell invasion, unlike *in vivo* were the epidermis is able

to respond to Δ3β-catenin activation via an increase in cell-cell adhesion as demonstrated by E-cadherin analysis [see Chapters 4, 5 & 7].

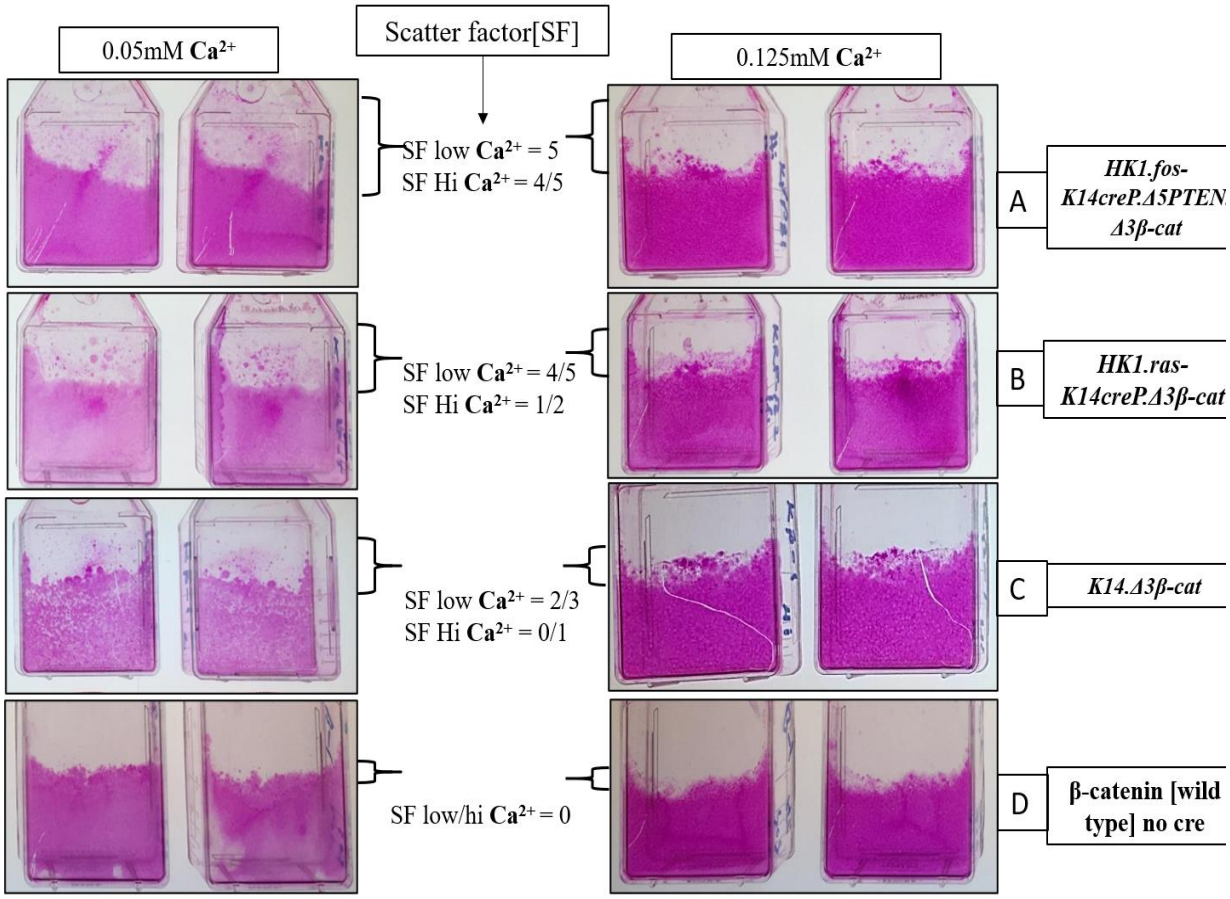

Figure 8. 3: Scatter Assay: assessment of cell line ability to migrate and seed colonies.

Cells were seeded at 5x10^6 cells per 25cm flask in 0.05mM Ca^{2+} and flasks grown at an angle of 30^0 for three days until confluent. Flasks were carefully re-fed and cultured horizontally with one set switched to 0.075mM Ca^{2+} for 24hours to initiate differentiation and then to 0.125mM Ca^{2+} for 10 days. Cells were fixed in formalin and stained with Rhodamine B. The ability to seed was given a scatter factor of 1-5; independently scored blind by 3 individuals and averaged from counts of 3 flasks per cohort in repeat experiments.
[A] Transformed *HK1.fos-K14creP.Δ5PTEN*$^{flx/flx}$*.Δ3β-cat*$^{flx/wt}$ line KFPB1 showed the highest SF score in both low (5/5) and high (4/5) calcium media and scattered the farthest [brackets] also the main bulk of these cells migrated the farthest. [B] Transformed *HK1.ras-K14creP.Δ3β-cat*$^{flx/wt}$ line KRB1 also showed a high scatter factor score in low (4/5) calcium concentration; but less so in Hi Cal with a lower score (2/5). [C] *K14creP.Δ3β-cat*$^{flx/wt}$ line KB1 showed a scatter score of 2/5 in Low Cal with no seeding observed in high calcium medium. Also, the colonies were close to the confluent migrating front. [D] Normal appearing transgenic line B-1 [non-creP*Δ3β-catenin*] scored a scatter factor of 0/5 in both calcium concentrations, [as did ICR1 and wt-1] confirming that typically immortalised normal mouse lines lose the capacity to seed unlike primary keratinocytes; unless spontaneously transformed.

8.4 SUMMARY

Classic keratinocyte culture assays were performed employing cell lines derived from primary neonatal keratinocytes cultured *in vitro* to assess effects of transgene expression on differentiation and transformation and provide cells for western/IF/IHC analysis. The first series of experiments assessed differentiation responses to calcium-induced terminal differentiation via a challenge with 0.125mM Ca^{2+} [High calcium] medium. The second tested the ability to grow clonally again as an indication of immortalisation and partial transformation. Finally, a third series of experiments tested the seeding ability and cell motility, not only as an indication of invasive potential but also to test the idea that *Δ3β-catenin* expression maintains a neonatal/juvenile phenotype, as suggested in previous studies that investigated β-catenin expression in keratinocytes and the ECM (*Collins et al., 2011*) and also β-catenin effects on the emerging variety of KPC/stem cell niches (*Watt and Collins, 2008; Kretzschmar et al 2015).*

In classic calcium induced terminal differentiation assays (*Hennings et al., 1980; Greenhalgh et al., 1989; Morgan et al., 1992*) all compound lines such as *HK1.fos-K14creP.Δ5PTEN$^{flx/flx}$.Δ3β-cat$^{flx/wt}$* and *HK1.ras-K14creP.Δ3β-cat$^{flx/wt}$* displayed resistance to Calcium-induced differentiation, as expected given their rapid growth and carrying multiple oncogenes activation in addition to *Δ3β-catenin.* These data are more consistent with what was originally hypothesised as these cells exhibited classic patterns of transformed keratinocytes, which indicate that *Δ3β-catenin* activation *in vitro* induced transformation via overexpression of the canonical Wnt signalling pathway resulting in increased proliferation and a delay or resistance to normal epidermal differentiation which was also constant with the literature dogma that β-catenin gain of function would facilitate tumorigenesis (*Morin, 1999; Polakis, 1999; Doglioni et al., 2003; Grigoryan et al., 2008; Krishnamurthy and Kurzrock, 2018).*

Nonetheless, whilst these results contrasted with the *in vivo* observations most likely due to disruption of tissue homeostasis and thus monolayers *in vitro* lack the responses available *in vivo* to counter β-catenin deregulation there were subtle differences between these lines that echo *in vivo* results. For instance, *HK1.ras-K14creP.Δ3β-cat$^{flx/wt}$* lines adopted a morphology typical of spinus keratinocytes in 0.075mM Ca^{2+}; thus mimicking an accelerated transition to the supra basal layer as suggested *in vivo.* However consistent with a lack of correct K1

expression in vivo these cells continued to grow in Hi calcium consistent with a fully transformed malignant line, as finally observed in the rare SCC tumours of *HK1.ras-K14creP.Δ3β-cat*$^{flx/wt}$*.p53*$^{flx/flx}$ mice. Often *in vitro* p53 is also lost/mutated as cells become immortalised and transformed e.g. the spontaneous human HaCaT keratinocyte cell line (*Boelsma et al., 1999*), and the transformed SP1 benign papilloma cell line being derived from DMBA/TPA papillomas with activated ras^{Ha} which are transformed but not malignant in nude mouse graft assays and T52 malignant keratinocyte cell line where SP1 cells were transfected with FBJ v-fos to become malignant (*Strickland et al., 1988; Greenhalgh and Yuspa, 1988*). Hence, p53 has been found to normally regulate embryonic stem cell proliferation by activating β-catenin dependent, canonical Wnt signalling amongst other pathways (*Lee et al., 2010*).

HK1.fos-K14creP.Δ5PTEN$^{flx/flx}$*.Δ3β-cat*$^{flx/wt}$ lines also exhibit a transformed morphology at confluence, but possessed numerous squames and many floating cells suggesting attempts to differentiate in low Cal. However, these keratinocytes resisted forming spinus cells in 0.075mM Ca^{2+} and required full Hi Cal to commence differentiation; but then these did differentiate to some extent consistent with the excess keratosis observed *in vivo* and the return of K1. These lines thus echo the odd differentiation evoked by fos/PTEN/βcatenin co-operation and it may be that the excess of floating cells continually observed in low Cal media and the granular/squames in Hi Cal reflect attempts to de-differentiated into cysts and die.

Furthermore, whist *K14creP.Δ3β-cat*$^{flx/wt}$ exhibited a normal cobblestone basal layer morphology in Low Cal 0.05mM Ca^{2+} media and committed to differentiate in 0.075mM Ca^{2+} media this differentiation appeared to stall at this spinus morphology stage and exhibit a similar spinus layer morphology in Hi Cal media rather than stratification and cornification. This result echoes the sporadic K1 expression and may reflect the minimal interfollicular hyperplasia compared to a *HK1.ras* as the supra-basal roles of β-catenin in regulating terminal differentiation are altered by *Δ3β-catenin* (*Grigoryan et al., 2008*). Thus, in planned western/IF and IHC analysis, early differentiation marker K1 maybe abnormally expressed in Low Cal whilst expression of the hyperproliferation marker K6α maybe reduced again as in previous studies that showed altered K6 expression with a gain-of-function β-catenin (*Van Mater et al., 2003*).

The second series of experiments conducted on these cells tested their ability to grow from clonal density in both low and high calcium concentrations, which is a classic carcinogenicity assay (*Hennings et al., 1980; Greenhalgh et al., 1989; Morgan et al., 1992*). Clonal growth assays for cells cultured in Low Cal 0.05mm Ca^{2+} KGM media represents immortalisation and early-stage transformation, with cells being somewhat self sufficient no longer requiring communication with other cells; whilst culture and growth in Hi Cal 0.125mm Ca^{2+} media is a stringent test of their transformation status. In addition, this assay also tests for stem-like or KPC phenotypes that have been maintained or reactivated by β-catenin overexpression as suggested in previous studies (*Watt and Collins, 2008*) and epidermal lineage studies (*Kretzschmar et al., 2015*).

Most of the β-catenin overexpressing cell lines were able to grow from clonal density in Low Cal media but only *HK1.ras-K14creP.Δ3β-cat*$^{flx/wt}$ and *HK1.fos-K14creP.Δ5PTEN*$^{flx/flx}$*.Δ3β-cat*$^{flx/wt}$ lines were able to grow from clonal density in Hi Cal media which indicated their fully transformed nature. Cells able to grow in low calcium such as *K14creP.Δ3β-cat*$^{flx/wt}$ alone are usually benign in nature when grafted onto nude mice and those able to grow in high calcium are often malignant in this assay (*Strickland et al., 1998; Greenhalgh and Yuspa, 1998; Greenhalgh et al., 1989; 1990; Morgan et al., 1992*). Since these data now show growth in high calcium concentrations in cell lines carrying *Δ3β-catenin* in co-operation with *ras/fos/Δ5PTEN*, suggesting that *K14creP.Δ3β-cat*$^{flx/wt}$ alone achieves a benign hit and in co-operation with other oncogenes, deregulated β-catenin results in a malignant phenotype that fits the current dogma of β-catenin oncogenicity (*Morin, 1999; Polakis, 1999; Doglioni et al., 2003; Grigoryan et al., 2008; Krishnamurthy and Kurzrock, 2018*) but miss the nuances of the *in vivo* findings.

Some of the most fascinating *in vitro* data came from the simple scatter assays that were originally envisaged to test whether the fully transformed cell lines mimicked an individual or collective mode of tumour invasion via migrating as an invasive front or via seeding. These experiments also tested the idea that *Δ3β-catenin* expression returned adult keratinocytes to a more juvenile state, as reported in previous studies (*Collins et al., 2011*) as suggested by K6α and p63/K15 expression data *in vivo*. Typically, normal immortalised keratinocyte lines established by this method (*Greenhalgh et al., 1989*) cease to be able to seed such satellite colonies by passage 3-5; unlike their normal primary counterparts where

satellite colonies are common given the presence of more numerous stem–like/KPC populations derived from newborn vs. adult mice, (*Morris et al., 2004*).

These experiments showed that all Δ3β-catenin lines were able to seed/scatter especially in *HK1.fos-K14creP.Δ5PTEN*$^{flx/flx}$*.Δ3β-cat*$^{flx/wt}$ and *HK1.ras-K14creP.Δ3β-cat*$^{flx/wt}$ cohorts. This indicated a reduction in cell-cell adhesion signalling giving the cells this ability to invade as a series of individuals consistent with a malignant phenotype and progression to aggressive possibly metastatic nature. Although yet to be analysed these observations would be consistent with endogenous β-catenin activation becoming less membranous, as observed *in vivo*, together with reduced E-cadherin at the invasive front, which would result in a loss of focal adhesions to facilitate the invasion observed in *HK1.ras/fos-K14creP.Δ5PTEN*$^{flx/flx}$ tri-genic mice. This also brings in the necessity of future analysis for these cell lines via western blot for expression of different proteins [p53, p21, K1,AKT,etc] as initial western analysis to date has only confirmed the cre-mediated expression of *Δ3β-catenin*.

Nonetheless, the ability of these lines to seed coupled to the seeding displayed by *K14creP.Δ3β-cat*$^{flx/wt}$ cells but not normal non-cre *Δ3β-catenin* β-1 cells nor ICR-1 or Wt-1 lines does indeed suggest that here deregulated β-catenin expression may return *K14creP.Δ3β-cat*$^{flx/wt}$ cells to a more juvenile/neonatal state now able to seed distant colonies as observed in all primary keratinocyte cell cultures. This result was consistent with the lack of K6 expression observed in this model and previous studies that concluded that gain-of-function β-catenin affects the dermal extra cellular matrix and appeared to return the skin to neonatal state (*Collins et al., 2011*). This idea was also suggested by epidermal lineage studies (*Kretzschmar et al., 2015*) and this ability was especially pronounced in *HK1.fos-K14creP.Δ5PTEN*$^{flx/flx}$*.Δ3β-cat*$^{flx/wt}$ and *HK1.ras-K14creP.Δ3β-cat*$^{flx/wt}$ lines which would also be consistent with a de differentiation into a highly proliferative state as observed in neonatal epidermis-an idea supported by hyperproliferation marker K6α being barely detectable as in neonatal mice (*Rothnagel et al., 1999; Masre et al., 2020*).

Collectively these data suggest that all *Δ3β-catenin* lines are able to seed/scatter in a manner similar to neonatal primary keratinocytes to support the idea that β-catenin overexpression returns the epidermis to a more juvenile state (Watt and Collins 2008; *Collins et al., 2011 Kretzschmar et al., 2015*) They also show the major differences between *in vitro* and *in vivo*

findings that indicate the *in vitro* analysis lacks the biological spectrum needed to generate results observed *in vivo*. However, clonal growth and seeding in Low Cal would be consistent with Δ3β-catenin mediated influences on stem cells or a return to a more stem-like PCK phenotype; whilst growth in Hi Cal demonstrate that at least in vitro these combinations with β-catenin definitely fulfilled all criteria requited for a malignant phenotype in these classic transformation assays; consistent with the *HK1.ras/fos/PTEN* model of Chapter 3 and the current dogma associated with β-catenin oncogenicity in SCC.

Chapter 9: Discussion & future directions

Discussion

The β-catenin protein is known to have two main functions. In the cytoplasm, β-catenin bind to E-cadherin to form the cell-cell adhesion complex that is needed for calcium dependent adhesion between the cells that aids roles in morphogenesis and tissue homeostasis (*Takeichi, 1991; Young et al., 2003*), thus impairment of this function has been associated with facilitating tumourigenesis most likely in terms of cell invasion (*Jeanes et al., 2008*). The other major function of β-catenin is in the nucleus as a transcriptional activator of canonical Wnt/β-catenin signalling nuclear targets [LEF/TCF] and again increased nuclear expression of β-catenin has been associated with facilitating cancer invasion and metastasis (*Morin, 1999; Grigoryan et al., 2008*). Given that β-catenin controls these two critical cellular functions, gain-of-function mutations in β-catenin i.e., particularly those in exon 3 that prevent down regulation, have been associated with diverse types of cancers such as colon, prostate, ovarian, melanoma and non-melanoma skin cancers (*Morin, 1999; Gerdes and Yuspa, 2005; Grigoryan et al., 2008*).

In this study these roles for β-catenin overexpression were investigated in a transgenic mouse model of multistage skin carcinogenesis to assess the causal roles and determine when β-catenin became active. These models were envisaged to mimic the development of non-melanoma skin cancers specifically SCC given the more clinically aggressive nature and potential for metastasis, as BCC were mostly associated with de-regulation of Wnt signalling at earlier stages e.g., sonic hedgehog [SHH] (*Clifford and DiGiovanni, 2010; Huang and Balmain, 2014*). The implication of β-catenin in developing SCC in human is driven from the fact that Wnt/β-catenin nuclear overexpression was a known phenomena in humans SCC aetiology (*Malanchi, et al., 2008*) and that mutations often resulted in constitutive overexpression via either direct β-catenin gene mutation in exon 3 or in genes that regulate β-catenin levels such as APC and GSK3β (*Grigoryan et al., 2008*). Further in reverse, the importance of β-catenin in carcinogenesis was supported by findings in two-stage chemical carcinogenesis studies, where similar endogenous β-catenin gain of function was reported in DMBA/TPA induced SCCs (*Malanchi, et al., 2008; Grigoryan et al., 2008*) whilst functional inactivation resulted in tumour inhibition (*Malanchi, et al., 2008; Grigoryan et al., 2008*).

These studies indicated that β-catenin was a necessity for developing SCC and additional studies also suggested that β-catenin overexpression contributes directly to the development of cancer stem cells to incorrectly control of β-catenin regulation in the HF bulge region; a logical conclusion given this is the location of a major stem cell niche in the skin (*Malanchi, et al., 2008*). However, despite the clear relevance of β-catenin in the development of SCC, surprisingly to date, it appears that no study has directly explored constitutive activation of β-catenin in the classic multi-stage carcinogenesis model to unravel the exact mechanism of the roles of β-catenin in SCC. This maybe due to the fact that most studies of β-catenin [both overexpression and functional knockout] in mouse skin were associated with the HF anomalies and HF tumours derived from the Wnt/β-catenin roles in regulating HF differentiation and morphogenesis via activation of LEF/TCF; but it may also be due to unreported findings such as those in this current study that effect viability (*Järvinen et al., 2006*).

To begin to address this, inducible constitutive β-catenin overexpression was targeted to the skin employing a Cre/loxP system and co-operation assessed with activated *ras* and *fos* oncogenes and loss of TGS *PTEN, p53* and *p21*. This approach derived from previous studies which showed that the HK1 mouse model of carcinogenesis in this model, loss of PTEN, and overexpression of AKT-mediated GSK3-β inactivation was found to trigger compensatory p53/p21 expression in KA formation in *HK1.fos-K14creP.Δ5PTEN*$^{flx/flx}$ mice; whilst in *HK1.ras/fos-K14creP.Δ5PTEN*$^{flx/flx}$ mice, p53 loss resulted in malignant at conversion and p21 loss resulted in malignant progression, all associated with AKT/GSK3 and thus implicating β-catenin. As shown in Chapter 3 this proved to be the case as now formal investigation of endogenous β-catenin demonstrated that overexpression in the proliferative basal layers appeared in papillomas and KAs whilst invasive SCCs demonstrated strong nuclear β-catenin expression associated with a lack of membranous expression that supported a role alongside loss of E-cadherin in tumour invasion. This result was consistent with the literature, as was the initial series of experiments reported in Chapter 4 that targeted constitutive β-catenin expression to the epidermis, as *K14creP.Δ3β-cat*$^{flx/wt}$ mice showed all the hallmarks of HF anomalies, altered bone development, and general keratosis observed in the classic earlier studies- but with a lack of IFE tumours showing the necessity of additional initiating and promoting events.

However, these logical results appeared to be highly context dependant and dependent upon the cell type [stem/KPC/transit amplifying] or timing of β-catenin deregulation. This was clearly seen in Chapter 5 and the intriguing results of inducible β-catenin[Δ3β-catenin] in co-operation with *HK1.ras*, where the vast majority of mice lacked tumours development probably due to compensatory p53/p21 expression in this context. Moreover, and adding further complexity, this lack of tumour development was also repeated in *HK1.ras-K14creP.Δ3β-cat*$^{flx/wt}$ co-operation experiments with inducible conditional loss of *p53*, where most mice still resulted in a lack of tumorigenesis [see Chapter 6]. Another important finding was that the epidermal responses to β-catenin deregulation appeared to be dependent upon p53 expression [but apparently not p21]. Yet in the rare instances of papilloma formation which overcame this paradoxical tumour block in *HK1.ras-K14creP.Δ3β-cat*$^{flx/wt}$ genotypes the tumours remained papilloma whereas in *HK1.ras-K14creP.Δ3β-cat*$^{flx/wt}$ *.p53*$^{flx/flx}$ mice once started the papillomas rapidly converted to tumours with histotypes of papilloma, wdSCC, SCC and pdSCC within the same tumour; consistent with loss of the *p53* guardian roles and increasing mutations and again nuclear β-catenin with loss of E-cadherin at the invasive front. All findings more consistent with the literature on progression and invasion.

The induction of *HK1.fos* and *Δ5PTEN* with Δ3β-catenin also resulted in a lack of tumours but with more aggressive skin keratosis due to mainly differentiation responses to the activation of these oncogenic hits [See Chapter 7]. These experiments demonstrated direct co-operation between fos and β-catenin deregulation, and the excess differentiation observed is consistent with their roles in the commitment to differentiate and their roles in the decision-making of stem cells in their various niches. Another important finding was observed in *K14.Δ5PTEN.Δ3β-catenin* mice which demonstrated a change in HF tumours from folliculoma to trichilemmomas observed in Cowden's Disease; also consistent with their roles in HF development and this model may be useful to explore further this HF tumour type.

In vitro, activation of Δ3β-catenin with ras/fos/and PTEN loss again showed classic signs of immortalisation and transformation to a malignant phenotype, similar to known β-catenin roles in carcinogenesis reported in the literature but cultured cell cannot deploy the same responses as intact tissue. This chapter discusses the most possible reasoning for the intriguing and unique findings of this study and possible future directions.

9.1 Endogenous β-catenin overexpression in multistage *HK1.ras/fos-K14creP.Δ5PTEN$^{flx/flx}$* carcinogenesis fits current dogma.

The HK1model of carcinogenesis was ideal to study possible β-catenin roles at each stage of tumour formation (*Greenhalgh et al., 1993a-c*; *Yao et al., 2006; 2008; Macdonald et al., 2014*) given the stage-specific stability of the induced phenotypes where benign papillomas do not spontaneously convert (*Greenhalgh et al., 1993c*) without an additional oncogenic activity such as activation of AKT via inducible PTEN loss or TPA promotion *(Yao et al., 2006; 2008; Macdonald et al., 2014).* β-catenin was implicated in this model following results that highlighted inactivated GSK3-β via AKT mediated by PTEN loss triggered elevated levels of p53 and p21 diverting papilloma formation into massive accelerated differentiation giving the classic benign KA aetiology (*Yao et al., 2008*). These compensatory responses deployed by the epidermis to maintain its homeostasis and inhibit tumour progression are a theme running through all the findings in these experiments.

The assumed overexpression of β-catenin was then confirmed in this study (*Alyamani et al.*, in prep) and the β-catenin expression profile showed that KAs maintained elevated levels of nuclear β-catenin whilst still maintaining membranous β-catenin/E-cadherin expression correlated with elevated levels of basal p53/p21 that accelerated commitment to differentiation evident by basal K1 expression (*Yao et al., 2008*). Thus, indicating that in this context responses to β-catenin overexpression can have inhibitory roles on tumorigenesis via invoking compensatory TSGs [p53/p21] expression. This highlights the sensitivity of the epidermis to alterations in β-catenin levels as a similar observation was repeated in ROCK2 mice where again such β-catenin -mediated p53 expression inhibited papilloma formation (*Masre et al., 2020*).

However, in *HK1.ras/fos-K14creP.Δ5PTEN$^{flx/flx}$* co-operation SCCs were formed, and again β-catenin overexpression was hypothesised due to AKT associated GSK3-β inactivation. Here with added HK1.ras activation, the expression profile was different than that of KA, where β-catenin exhibited mostly an increase in nuclear localization with greatly reduced membranous β-catenin/E-cadherin expressions [cell-cell adhesion] following the loss of p53/p21 expression in these SCCs. Thus, in this context, this expression profile reinforced β-catenin involvement in aiding malignant progression as it suggests that the loss of p53 and nuclear localization of β-catenin in SCCs greatly reduce E-cadherin ability to form focal adhesion junctions in the

invasive front; an observation consistent with the collective invasion profiles observed in human SCC (*Hesse et al., 2016*).

This analysis of endogenous β-catenin suggested that overexpression of β-catenin in different contexts or at different times may yield different outcomes as in early stages of tumour development as in *HK1.fos-K14creP.Δ5PTEN*$^{flx/flx}$ KA, the response to β-catenin nuclear localization elicit protective responses by TGSs[p53/p21],that halt tumour progression, However when these TSGs response fails to halt tumour progression as in *HK1.ras/fos-K14creP.Δ5PTEN*$^{flx/flx}$ SCCs at later stages of tumour progression, β-catenin seems to drive and facilitate malignant progression. These findings made it clear that β-catenin roles in SCC required a better understanding which was tested by inducing constitutive activation of β-catenin using a an inducible K14.creP/loxP gene switch [*K14.creΔ3β-catenin*] similar to the induction of PTEN loss in this model.

9.2 Constitutive activation of β-catenin in mouse skin which paradoxically blocks *HK1.ras* mediated IFE tumour development but not HF tumours.

The constitutive activation of β-catenin over expression was achieved using an inducible *K14.creP/loxP* gene switch [*K14.creΔ3β-catenin*], where RU486 treatment would result in deleting exon 3 sequence flanked by loxP site; preventing formation of the β-catenin destruction complex [GSK3-β/APC/Axin] and sustained activation of β-catenin. This approach thus mimics the mutation hotspots in exon3 observed in human carcinomas, which are also frequently reported in two-stage DMBA/TPA carcinogenesis (*Malanchi, et al., 2008; Grigoryan et al., 2008*).

Unfortunately, due to cre expression independent of RU486 treatment, which to date is a phenomenon seen in *K14creP.Δ3β-cat*$^{flx/wt}$ mice and rarely appeared previously in this model, due to the potency of *Δ3β-catenin* expression in epithelial cells this resulted in the gross appearance of *Δ3β-catenin* phenotypes around 16 to 24 days of age post the first anagen and also appears to promote internal problems leading to smaller mice (*Huels et al., 2015*). However, of note, if these mice were driven by a non-inducible keratin promoter, such as K5.cre available in the lab, β-catenin overexpression proved to be lethal in this study and in others (*Järvinen et al., 2006*).

Thus, it may be that this lack of viability may underlie the lack of these mice in development of a transgenic skin carcinogenesis models; rather each focussed on effects on hair follicle development and later to effects on stem cells but oddly, none exploit these mice in the development of classic skin carcinogenesis models only constitutive knockouts have been investigated (*Malanchi, et al., 2008; Grigoryan et al., 2008*). Aside from these unavoidable features *K14creP.Δ3β-cat*$^{flx/wt}$ mice displayed identical phenotypes to previous studies that targeted β-catenin overexpression to the skin or follicles in terms of alopecia, scruffiness, bigger ears, abnormal feet and tail as well as a variation in body sizes compared to a normal ICR mouse (*Gat et al., 1998*).

The increased numbers of de novo hair follicles and formation of benign hair follicle tumours [trichofolliculoma and pilomatricoma] (*Gat et al., 1998; Huelsken et al., 2001; Grigoryan et al., 2008*) are consistent with β-catenin mediated over expression of Wnt signalling transcriptional targets LEF1 and TCF and disruption of their normal roles in hair follicle formation. Further, the alopecia that *K14creP.Δ3β-cat*$^{flx/wt}$ mice usually exhibit can be explained by the finding that, despite the increased formation of hair placode due Δ3β-catenin activation, most of the initiated HFs fail to produce normal hair due to incorrect control of Wnt/β-catenin signalling (*Närhi, et al., 2008*). Thus, HF tumors arise such as trichofolliculoma and again observed here following *K14creP.Δ3β-cat*$^{flx/wt}$ overexpression (*Gat et al., 1998; Chan et al., 1999 Grigoryan et al., 2008*), which have also been reported also reported in human SCC as result of similar gain of function mutations the β-catenin gene that lead to its overexpression (*Grigoryan et al., 2008; Chan et al., 1999*).

The effects on body size and limb abnormalities can be attributed to the major roles that canonical Wnt/β-catenin signalling plays in embryonic and juvenile stages of development. Embryonically Wnt/β-catenin signalling is highly involved in the formation of the body anterior and posterior axis, hence why null mutation of β-catenin induced embryonic lethality as it resulted in a failure in forming body axis in mouse studies (*Närhi et al 2008; Grigoryan et al., 2008*). For instance, Wnt/β-catenin activation up regulates Bone Morphogenic Protein [BMP] thus the leaked *K14creP.Δ3β-cat*$^{flx/wt}$ would alter epithelial signalling needed for correct bone, cartilage and muscle formation (*Närhi, et al., 2008),* hence the enlarged extremities.

Aside from these constitutive activations of β-catenin phenotypes, effects of *K14creP.Δ3β-cat*$^{flx/wt}$ on the IFE manifest as minimal hyperplasia and a alteration to epidermal terminal differentiation evidenced by anomalous and to date a unique profile of K1 & K6α differentiation marker expression. This altered epidermal differentiation was attributed to elevated levels of basal layer p53/p21 expression which halted proliferation and induce differentiation whilst exhibiting strengthened cell-cell adhesion evident by elevated membranous β-catenin/E-cadherin together with nuclear localization of β-catenin that alter regulation of pluripotent stem epidermal cells that are needed for terminal differentiation or hair follicle differentiation (*Watt and Collins, 2008; Grigoryan et al., 2008*).

Indeed, later in this study this p53 response was found to be a major contributor to the epidermal responses to β-catenin, as conditional knockout of p53 in *K14creP.Δ3β-cat*$^{flx/wt}$*.p53*$^{flx/flx}$ resulted in a significant reduction in the severity of *Δ3β-catenin* associated phenotypes. This too indicated that p53 response was not exclusive to halting IFE tumorigenesis and these data may also suggest that p53 status plays a major role in regulating Δ3β-catenin anomalies, which appeared necessary for the HF anomalies observed in previous studies of constitutive β-catenin activation.

One of the major findings in this study was that when *K14creP.Δ3β-cat*$^{flx/wt}$ mice were crossed with *HK1.ras* mice the vast majority of *HK1.ras-K14creP.Δ3β-cat*$^{flx/wt}$ lacked papilloma development, whereas *HK1.ras* controls developed papillomma within 6-8 weeks of ear tag wounding. This intriguing result does not fit the current dogma reported in the literature (*Morin, 1999; Grigoryan et al., 2008*) as in reverse, conditional knockout of β-catenin resulted in the inhibition of DMBA/TPA tumours that possessed similar ras ^{Ha} activation, indicating that β-catenin expression was necessary for SCC development *(Malanchi et al., 2008; Grigoryan et al., 2008)* consistent with *HK1.ras/fos-K14creP.Δ5PTEN*$^{flx/flx}$ where in both cases p53 loss was also implicated.

However, this paradoxical lack of tumours in *HK1.ras-K14creP.Δ3β-cat*$^{flx/wt}$, was not due to a loss of HK1.ras expression as the pups exhibited typical HK1.ras phenotypes and there was increased levels of severity of *Δ3β-catenin* in terms of increased scruffiness and increased hyperkeratosis in back skin. This was also consistent histologically as the hair follicle abnormalities such as formation of more cysts and hair follicle tumours was clearly more

severe with increased interfollicular hyperplasia accompanied by abnormal and confused differentiation.

Thus, it may be that adding *HK1.ras* activation to these Δ3β-catenin phenotypes invoked increased elevated levels of p53/p21 resulting in more confused and disturbed IFE and a block of the events that initiated papillomatogenesis, given that *HK1.ras, HK1.fos* and *HK1.ras/fos* mice all exhibited suprabasal levels of β-catenin and only minimal p53 p21 expression until an overt papilloma had formed. Thus, they collectively inhibited conversion until p53 was lost in *HK1.ras/fos-K14creP.Δ5PTEN*$^{flx/flx}$ and β-catenin became nuclear to drive further progression alongside E-cadherin. In addition, another factor helping to inhibit papillomatogenesis in *HK1.ras-K14creP.Δ3β-cat*$^{flx/wt}$, may centre on cytoplasmic E-cadherin/β-catenin interactions as E-cadherin can act as a sponge providing further regulation of β-catenin levels (*Huels et al., 2015*). Thus, the elevated expression observed in *HK1.ras-K14creP.Δ3β-cat*$^{flx/wt}$ that seemed to be strengthened by Δ3β-catenin activation [as observed in colon carcinogenesis (*Huels et al., 2015*), would help inhibit papilloma formation. This would be coupled to the excess membranous expression of β-catenin/ E-cadherin that together increased the cell-cell adhesion in the hyperplastic basal layers that would also inhibit the early formation of papillomas.

This inhibition of papilloma formation was also supported by the fact that the epidermal differentiation was highly disturbed indicated by K1 confused and patchy expression which could attributed to excess expression of p21 (*Di Cunto et al., 1998*) and this coupled to basal layer expression of p53 helped accelerated epidermal terminal differentiation, as seen in *HK1.fos-K14creP.Δ5PTEN*$^{flx/flx}$ KA (*Topley et al., 1999*; *Yao et al., 2008*) and again in a recent study in ROCK-mediated β-catenin activation (*Masre et al., 2020*). However, the hyperproliferation marker K6α was completely absent from the epidermis, whereas usually it is strongly expressed in *HK1.ras* hyperplastic controls, thus again indicating that possibly the anti-proliferative roles of p53 and the pro differentiation roles for p21 contributed to papillomatogenesis inhibition.

Here of note, another possible mechanism for this aberrant K6α expression is a study that concluded the ability of constitutive activation of β-catenin to remodel the developed mouse dermis into a neonatal state (*Collins et al., 2011*). In neonates the epidermis is naturally hyperplastic but lack K6 expression which remains confine to developing HFs (*Rothnagel et al., 1999*). Thus, as increased Wnt/β-catenin signalling affects the correct control of stem cell

niche, it alters the keratin expression profiles leading to a continuously altered differentiation programme fate resulting in confused transit amplifying cells as evidenced by formation of K1 positive cysts which would also divert keratinocytes away from papilloma formation.

Furthermore, the analysis of the only two mice that developed papillomas in *HK1.ras-K14creP.Δ3β-cat*$^{flx/wt}$ may confirm that many of the epidermal responses and paradoxical tumour inhibition derived from altered developmental responses to β-catenin overexpression. ie this was an anomalous deregulation of the natural hyperplasia/hyperkeratosis state and HF formation that normally appears during development. Thus, these mice also looked bigger and were less phenotypic than the majority of *HK1.ras-K14creP.Δ3β-cat*$^{flx/wt}$ mice that did not develop the tumours. This indicate that probably the cre switch did not leak early whether in neonatal or juvenile development and only became activated post RU486 treatment, which gave *HK1.ras* effects enough time to develop the foundations of papilloma formation before the responses to Δ3β-catenin activation [p53/p21/excess E-cadherin] were deployed in an adult epidermis.

Once formed in an adult skin more closely resembling that of *HK1.ras* controls, the eventual papillomas grossly and histologically looked smaller and less aggressive compared to a typical *HK1.ras* papillomas. This was still contrary to the widely assumed notion that overexpression of β-catenin/Wnt signalling leads to more aggressive tumours and possibly malignant progression but again these mice did exhibit the Δ3β-catenin activated response following RU486 treatment p53/p21/excess E-cadherin suggesting that even in the rare event where papillomas avoided the paradoxical block in *HK1.ras-K14creP.Δ3β-cat*$^{flx/wt}$ mice, they could not progress to more aggressive tumours and possibly with more time could even be regressing. Hence whilst *HK1.ras-K14creP.Δ3β-cat*$^{flx/wt}$, papillomas showed increased nuclear localization the increased membranous β-catenin/E-cadherin expression and strong p53/p21 aided in halting malignant progression similar to that observed in *HK1.fos-K14creP.Δ5PTEN*$^{flx/flx}$ KA (*Yao et al., 2008*).

Another piece of evidence suggesting that an adult epidermis needed to form correctly prior to β-catenin deregulation was supported by a normal K1 expression confined to the suprabasal layer appeared in *HK1.ras-K14creP.Δ3β-cat*$^{flx/wt}$ papillomas as always observed in *HK1.ras* papillomas. However, the hyperproliferation marker K6α showed strong expression as well but interestingly was lacking in basal layers, a finding exclusive to *HK1.ras-K14creP.Δ3β-*

cat$^{flx/wt}$ papillomas and not seen in *HK1.ras* controls that echoes K6α expression in the non-tumour baring mice. Thus, whilst K1 expression confirms their benign nature, K6α expression may indicates that these tumours are not the same type of papilloma as seen in *HK1.ras* controls. These maybe the beginnings of the more aggressive type 2 papillomas hence their ability to overcome the paradoxical tumour block. Nonetheless this correlation between TSGs expression and cell-cell adhesion seemed to be the key to the protective responses induced in response to β-catenin nuclear localization. Thus, conditional knockout of p53 was tested in *HK1.ras-K14creP.Δ3β-cat*$^{flx/wt}$ co-operation.

9.3 p53 is essential to develop *K14creP.Δ3β-cat*$^{flx/wt}$ phenotypes and loss cannot overcome the paradoxical lack of *HK1.ras-K14creP.Δ3β-cat*$^{flx/wt}$ tumours.

To validate the roles of p53 as suggested by the lack of tumours in *Δ3β-catenin* phenotypes, conditional knockout of p53 was introduced first in *K14creP.Δ3β-cat*$^{flx/wt}$ then in *HK1.ras-K14creP.Δ3β-cat*$^{flx/wt}$. Here another major unexpected finding showed that p53 loss resulted in a significant reduction in the severity of *K14creP.Δ3β-cat*$^{flx/wt}$*.p53*$^{fl/flx}$ phenotypes. This centred on skin phenotypes, as p53 loss had minimal effect on body size and extremities. At 3 weeks old [~24d] all mice exhibited little effects of *Δ3β-catenin;* whilst at 8 weeks following RU486 treatment, only mild levels of Δ3β-catenin phenotype appeared and histologically *K14creP.Δ3β-cat*$^{flx/wt}$ *.p53*$^{flx/flx}$ skin reflected this milder phenotype, which was also paralleled by a reduction in hair follicle abnormalities and thus tumours such as Trichofolliculoma that were seen in heterozygous or wild type p53 *K14creP.Δ3β-cat*$^{flx/wt}$ mice (*Gat et al., 1998; Celso et al., 2003*).

These data clearly implicated p53 roles in both the appearance and the intensity of Δ3β-catenin phenotypes as well as in the reduced degree of follicular tumours associated with Δ3β-catenin overexpression. The reasons for this unique and potent block of Δ3β-catenin phenotypes by p53 loss are again very unclear but this does appear to be a very important finding. Given that p53 normally regulates embryonic stem cell proliferation via activating canonical Wnt signalling [β-catenin dependent] among other pathways (*Lee et al., 2010*), it now appears that during juvenile development, similar responses require a competent p53

system and are lacking in both *K14creP.Δ3β-cat*$^{flx/wt}$*.p53*$^{flx/flx}$ and *HK1.ras-K14creP.Δ3β-cat*$^{flx/wt}$*.p53*$^{flx/flx}$ genotypes. Thus, the epidermis cannot mount the differentiation responses to deregulated overexpression of *Δ3β-catenin* at this juvenile stage (*Gat et al., 1998; Van Mater et al., 2003; Grigoryan et al., 2008*).

These data suggest that expression responses to p53 loss which altered keratinocyte proliferation/differentiation derived from effects of deregulated β-catenin on the stem cell/KPC populations (*Lee et al., 2010*) and these normal roles which are subverted by deregulated Δ3β-catenin overexpression requires a competent p53 system to sense the problems caused. Hence in developing juvenile *K14creP.Δ3β-cat*$^{flx/wt}$ genotypes it is the overexpression of p53, in response to Δ3β-catenin, that plays an unavoidable but essential role in the induction of these phenotypes. As outlined above [Chapter 6], a feedback loop maybe established whereby elevated levels of p53 activate Wnt signalling receptors which results in anomalous proliferation/differentiation, cysts and HF anomalies via adding heterozygous endogenous β-catenin expression to that of *Δ3β-catenin* activation; which in turn induced more p53 (*Gat et al., 1998; Niemann et al., 2002Van Mater et al., 2003; Grigoryan et al., 2008; Lee et al., 2010; Kretzschmar et al., 2015*). Thus, the lack of this elevated p53 expression in *K14creP.Δ3β-cat*$^{flx/wt}$*.p53*$^{flx/flx}$ and *HK1.ras-K14creP.Δ3β-cat*$^{flx/wt}$*.p53*$^{flx/flx}$ genotypes led to a less dramatic, potent response with less alopecia and scruffiness, resulting in a more normal looking hair follicles and bigger body size.

This too may involve the increased levels of E-cadherin observed and this may not only increase cell adhesion but the proposed function of E-cadherin to act as a sponge to provide additional regulation of β-catenin (*Huels et al., 2015*) may act as a sink to help remove excess β catenin and further minimised phenotype [see below]. In addition, the induction of p63 and p73 expression responses would again alter overall IFE and HF keratinocyte proliferation/differentiation profiles in response to p53 loss, with major effects on the stem cell /KPC populations as indicated by K15 expression. Further this inhibition of *Δ3β-catenin* activation centres exclusively on p53 as this was not observed in p21 nor PTEN co-operation experiments, but did appear to be very potent as it also prevented the excessive differentiation observed in *HK1.fos-K14creP.Δ3β-cat*$^{wt/flx}$ experiments [below].

This unexpected result following p53 loss was also observed in *HK1.ras-K14creP.Δ3β-cat*$^{flx/wt}$*.p53*$^{flx/flx}$ mice with an identical reduction in juvenile *Δ3β-catenin* phenotypes, but the

most striking finding was the continued lack of tumour development in the vast majority of mice, except for the two mice that developed accelerated aggressive SCC [discussed below]. This result challenges the current dogma in the literature where β-catenin nuclear localization and p53 loss facilitate tumour invasion and metastasis (*Polakis 2000; Gunther et al., 2003*) as seen also in *HK1.ras/fos-K14creP.Δ5PTEN*$^{flx/flx}$ SCCs (*Macdonald et al., 2014*). Indeed, a paradoxical lack of benign papillomas following p53 loss has been present in this model for many years (*Greenhalgh et al., 1996*) without resolution and it was hoped that given the links between β-catenin and p53 signalling, this approach employing β-catenin overexpression may have been the key to unlocking this paradox, but not so. Nonetheless, given these links it suggests that a common block of early stage papillomatogenesis is deployed in both cases, which may be similar involving changes to the feedback loops as discussed above; or a separate more generic response to p53 loss as it appears in *HK1.ras*, *HK1 fos* and *HK1.TGFα* models (*Greenhalgh et al., 1996*) and most recently manifest again in separate models of *14-3-3σ/ras* co-operation [*McMenemy and Greenhalgh*, manuscript in preparation.].

However, the data indicated two possibilities: one of which is that responses to the loss of p53 protection co-operated with those deployed against constitutive activation β-catenin in *HK1.ras-K14creP.Δ3β-cat*$^{flx/wt}$*.p53*$^{flx/flx}$ such as p63/p73 and increased E-cadherin [below] acted to prevent the onset of benign tumour development in most cases. Alternatively, in this epidermal context possibly tumorigenesis paradoxically required the expression of p53, as papillomatogenesis were lacking in both genotype an idea supported by the requirement for p53 to engender the epidermal responses to β-catenin in *HK1.ras-K14creP.Δ3β-cat*$^{flx/wt}$ cohorts.

This latter, dogma challenging suggestion (*Wahl, 2006*) is also supported to some extent by the observation that in *HK1.ras-K14creP.p53*$^{flx/flx}$ controls, if RU486 treatment was delayed by 10 -14 days small papillomas did eventually appear and moreover once established these were prone to convert to aggressive SCC; as seen in the rare examples of *HK1.ras-K14creP.Δ3β-cat*$^{flx/wt}$*.p53*$^{flx/flx}$ carcinogenesis [below]. This again echoes the theory outlined above that p53 creates a feedback loop necessary to elicit β-catenin phenotypes and the fact that a relatively normal epidermis appeared to be required to begin the rare instances of papillomatogenesis in both *HK1.ras-K14creP.Δ3β-cat*$^{flx/wt}$*.p53*$^{flx/flx}$ and *HK1.ras-K14creP.Δ3β-cat*$^{flx/wt}$ cohorts coupled to the fact that hyperplastic *HK1.ras* skin expresses low levels of p53 yet papillomas

have very high levels. Thus, this inhibitory compensatory mechanism to p53 loss maybe generic, hence a lack of early papillomas in both contexts and that β-catenin overexpression cannot overcome the paradoxical inhibition of papillomas following p53 loss in *HK1.ras-K14creP.p53$^{flx/flx}$* mice (*Greenhalgh et al., 1996*).

Overall, in the majority of cases, the β-catenin expression profile in *HK1.ras-K14creP.Δ3β-cat$^{flx/wt}$.p53$^{flx/flx}$* again demonstrated increased nuclear localization with increased cell-cell adhesion signalling [β-catenin/E-cadherin expression] that probably helped prevent papillomas similar to *HK1.ras-K14creP.Δ3β-cat$^{flx/wt}$* findings. This indicated that increased cell-cell adhesions in *HK1.ras-K14creP.Δ3β-cat$^{flx/wt}$.p53$^{flx/flx}$* were not dependent on p53 expression, unlike the conclusions from *HK1.ras-K14creP.Δ3β-cat$^{flx/wt}$* data; yet if both were present, such as in *HK1.fos-K14creP.Δ5PTEN$^{flx/flx}$ KA* aetiology, this β-catenin/E-cadherin mediated increased in cell-cell adhesion, coupled to strong expression of p53, was quite potent in preventing further progression, consistent with the results observed for *HK1.ras/fos-K14creP.Δ5PTEN$^{flx/flx}$* SSC where p53 loss, nuclear β-catenin and the lack of membranous E-cadherin contributed to malignant progression and invasion. However, despite the loss of p53, β-catenin/E-cadherin interactions appeared to maintain cell-cell adhesion in *HK1.ras-K14creP.Δ3β-cat$^{flx/wt}$.p53$^{flx/flx}$* epidermis and E-cadherin may actually increase to aid in the inhibition of papilloma formation. In addition, the proposed function of E-cadherin to act as a sponge to provide additional regulation of β-catenin (*Huels et al., 2015*) remained intact such that together with increased β-catenin/E-cadherin mediated cell-cell adhesion in basal layers, it helped prevented the permissive epidermal context that gave rise to papillomatogenesis.

Another potent response following p53 loss centred on attempts to regulate Δ3β-catenin effects via elevated p21 expression in its cell cycle regulatory roles as *HK1.ras-K14creP.Δ3β-cat$^{flx/wt}$.p53$^{flx/flx}$* IFE hyperplasia was less than that of *HK1.ras-K14creP.Δ3β-cat$^{flx/wt}$*, as determine by BrdU labelling. This increased p21 expression in response to p53 loss also appears to have led to more complex responses such as the increased numbers of dead-end cysts rather than increased differentiation. This idea was suggested by reduced K1 expression despite the increased basal layer p21 which usually promotes keratinocyte commitment to epidermal differentiation- but this may reflect increased levels of p63 [below] and its role in maintaining a basal layer rather than commit to differentiate. Similarly, lack of K6α

expression could be attributed to reduced proliferation given high levels of basal layer p21 expression, similar to that observed in *HK1.ras-K14creP.Δ3β-cat*$^{flx/wt}$ mice.

This lack of aberrant differentiation and papilloma formation may also involve potential responses that changed the regulation of stem cell niches and Keratinocyte Precursor Cells [KPCs] populations via compensatory responses mediated by *p63/p73* and indicated by K15 expression. *p63* and *p73* share many functional similarities to p53 in terms of maintaining the cell cycle, inducing roles that maintain epidermal proliferation, terminal differentiation and hair follicles morphogenesis *(Moll and Slade 2004; Koster et al., 2007; Botchkarev et al., 2014)* rather than p53 responses to stress.

Already links to βcatenin are suggested by the fact that p63 loss causes the epidermis to fail to stratify, disrupts HF formation and effects limb development which echoes the phenotypes induced by β-catenin deregulation *(Mills et al., 1999; Koster et al., 2004; Koster and Roop 2007*). In particular the ΔNp63 isoform is essential to maintaining basal layer proliferation and geared to inhibit premature differentiation via repression of genes such as p21 and PTEN (*Westfall et al. 2003; Moll and Slade 2004; Nguyen et al., 2006; Leonard et al., 2011*; *Botchkarev and Flores, 2014*), hence the disruption to K1 expression mediated by p63 responses to p53 loss that involved p21 [above]. The p63 roles in HF development may also account for the general reduction in HF abnormalities and tumours in *HK1.ras-K14creP.Δ3β-cat*$^{flx/wt}$*.p53*$^{flx/flx}$ and elevated expression *p63* [and *p73*] in HFs maybe a key inhibitor of Δ3β-catenin phenotypes as opposed to a requirement for p53 functions.

The intense p63/p73 expression also suggest changes to stem cell populations maintenance, as for p63 an interesting expression profile appeared in both in *HK1.ras-K14creP.Δ3β-cat*$^{flx/wt}$ and *HK1.ras-K14creP.Δ3β-cat*$^{flx/wt}$ *.p53*$^{flx/flx}$ suggesting a direct effects on regulation of KPC. Here, strands of p63-postive keratinocytes appeared similar to the patchy K1 expression pattern, suggesting K1 inhibition in these specific epidermal stem cell units. In agreement *HK1.ras-K14creP.Δ3β-cat*$^{flx/wt}$*.p53*$^{flx/flx}$ IFE possessed more strands of positive p63 basal cells with even less K1 expression and this could be attributed to p63 in repressing epidermal differentiation that may also counterbalance elevated levels of p21 in *HK1.ras-K14creP.Δ3β-*

cat$^{flx/wt}$*.p53*$^{flx/flx}$ in attempts to provide sufficient cells to maintain the barrier given weaker hyperplasia.

Further, these blocks of p63 positive keratinocytes may demark specific subpopulations of KPC cells, as also suggested by β-catenin lineage experiments (*Watt and Collins, 2008*) that would be also consistent with the abrupt lateral edges to both K1 and K6 expression made by specific stem cell units in the IFE (*Porter et al., 2000*). Although the isoform is not known this result would be consistent ΔNp63 inhibition of premature differentiation via repression of Notch (*Koster and Roop, 2007; Crum and McKeon, 2010; Leonard et al., 2011; Botchkarev and Flores, 2014*), and the resulting Notch inhibition leads to increased β-catenin expression (*Proweller et al 2006*); thus another feed back loop becomes, established which links p63 to β-catenin but this cannot overcome the requirement for p53. Alternately the TAp63 isoform keeps KPC/stem cells in a quiescent state to avoid their depletion and provide cells for wounding and thus suppress tumourigenesis from mutated stem cells (*Su et al. 2009b; 2013; Romano et al. 2012*). This isoform helps account for papillomas inhibition as Δ3β-catenin is expressed in stem cells from the K14 promoter [chapter 1: Fig. 8]. Interestingly, neither *HK1.ras* nor *HK1.ras-K14creP.p53*$^{flx/flx}$ hyperplasia exhibited this p63 expression, indicating that this p63 response is specific to Δ3β-catenin expression. Therefore, this result [as with p73 below] suggests that the inhibitory responses to p53 loss that inhibit *HK.ras.p53*$^{flx/flx}$ papilloma formation are more generic; and perhaps even separate to those observed in the context of *Δ3β-catenin* models.

For p73 few studies have actually been reported, but it is likely that the repressive ΔNp73 and transcriptionally active TAp73 isoforms exert completely differing functions. The TAp73 isoform exhibits pro-apoptotic functions following DNA damage (*Irwin et al., 2003*) and suppressor properties (*Rocco et al., 2006)* are supported as p73 expression is often lost through methylation, and transgenic mice heterozygous for p53 and p73 develop cutaneous SCC (*Flores et al., 2005*); yet in human cutaneous SCCs p73 remains strongly expressed indicating an oncogenic function (*Moll and Slade, 2004*), or a failed attempt at inhibition given p53 was lost also. Thus, the intense increase of p73 in *HK1.ras-K14creP.Δ3β-cat*$^{flx/wt}$*.p53*$^{flx/flx}$ basal layer IFE clearly supports the idea that this p53 family member was closely allied to the presence of p53 hence it may be that the p73 response was perhaps more effective in blocking Δ3β-catenin phenotypes in *HK1.ras-K14creP.Δ3β-cat*$^{flx/wt}$*.p53*$^{flx/flx}$ in response to p53 loss.

This maybe so, as a comparison to *HK1.ras-K14creP.Δ3β-cat*$^{flx/wt}$ skin, whilst p73 expression was similar and strongly expressed in the transformed HFs yet in the hyperplastic IFE, p73 expression appeared more closely associated with keratinocytes emerging from the HFs. This result would be consistent with p73 roles in general epidermal development and the localisation to keratinocytes emerging from HFs is very interesting as it may reflect roles for the TAp73 isoform in regulating HF bulge stem cell decisions to enter anagen as its ablation results stops follicle formation (*Rufini et al.,* 2012). Thus, here it would help combat the deregulated Δ3β-catenin expression in juvenile epidermis as the first hair cycle begins. Also, this TAp73 depletion accelerates cellular aging and this links to a return to the theme that *Δ3β-catenin* expression may return an epidermis to an earlier neonatal/juvenile state (*Collins et al., 2011*) as explored further *in vitro.*

However, the striking p73 expression increase in *HK1.ras-K14creP.Δ3β-cat*$^{flx/wt}$*.p53*$^{flx/flx}$ basal layers, and which was not seen in *HK1.ras-K14creP.Δ3β-cat*$^{flx/wt}$ and is constant with the TSG roles mainly attributed to p73 (*Rocco et al., 2006; DeYoung and Ellisen, 2007*). Significant levels of p73 expression appeared in most keratinocyte nuclei and p73 was very strongly expressed in the HFs. In contrast, *HK1.ras* and also *HK1.ras-K14creP.p53*$^{flx/flx}$ hyperplasia lacked such compensatory p73 expression again supporting the idea that inhibitory responses to p53 loss which inhibited *HK.ras.p53*$^{flx/flx}$ papilloma formation are separate to those observed in these Δ3β-catenin models. These data are also consistent with the idea that β-catenin expression had to become basal before the p53 family members reacted to its anomalous expression, i.e. this p73 response was specific to β-catenin and lack of basal layer β-catenin in *HK1.ras* or *HK1.ras-K14creP.p53*$^{flx/flx}$ hyperplasia resulted in a lack of compensatory p73 [and p63] expression. If so, this may account for p73 appearance in human SCCs (*Moll and Slade, 2004*; *DeYoung and Ellisen, 2007*) as following Notch repression by ΔNp63 (*Koster and Roop, 2007; Botchkarev and Flores, 2014*) the resulting β-catenin overexpression may have elicited a p73 response.

This proposed alteration to KPCs populations by TSGs response led to investigating K15 as a stem cell marker and interestingly K15 was not expressed in the IFE in either *HK1.ras-K14creP.Δ3β-cat*$^{flx/wt}$ or *HK1.ras-K14creP.Δ3β-cat*$^{flx/wt}$*.p53*$^{flx/flx}$ mice. This suggests that *Δ3β-catenin* alters the stem cell niches such that the cells migrate out of this niche to reduce the numbers of KPC targets for papilloma formation. This lack of IFE K15 expression was also constant with the reduced hyperplasia and low mitotic index of *HK1.ras-K14creP.Δ3β-*

cat$^{flx/wt}$*.p53*$^{flx/flx}$ cells and together with the *HK1.ras-K14creP.Δ3β-cat*$^{flx/wt}$ data it suggests that in early-stage hyperplasia Δ3β-catenin activation invokes TSGs responses involving p21/p53 and/or p63/p73 following p53 loss to protect theses KPC populations. This does not appear in early stages in *HK1.ras* hyperplasia as β-catenin remains suprabasal and the HK1 vector is not expressed in HFs, so that these HF niches remain unaffected and K15 expression remains relatively normal; however, the precursor cells for papilloma formation are beginning to form hence the gradual increase in p53 which becomes uniform in overt papilloma appearing later to prevent progression to SCC.

Hence K15 expression developed in the rare papillomas exhibited by both *HK1.ras-K14creP.Δ3β-cat*$^{flx/wt}$ and the SCCs developed in *HK1.ras-K14creP.Δ3β-cat*$^{flx/wt}$*.p53*$^{flx/flx}$ unlike *HK1.ras* papillomas. This expression of K15 therefore seems to be exclusive to tumours developed in genotype carrying *Δ3β-catenin* which could be a key marker in understanding the development of tumours in these genotypes and again suggests a disruption to stem/PCK physiology. This idea is also supported by reports that K15-positive cells derived from hair follicle stem cells contribute to papilloma devolvement (*Li et al., 2013*). Thus, tumours that developed in *HK1.ras-K14creP.Δ3β-cat*$^{flx/wt}$ and *HK1.ras-K14creP.Δ3β-cat*$^{flx/wt}$*.p53*$^{flx/flx}$ mice may derive from such excess stem cell proliferation initially mediated by ΔNp63 expression that escaped the early p73 TSGs responses due to cre leakage of *Δ3β-catenin*.

Moreover, the rare papillomas that developed in *HK1.ras-K14creP.Δ3β-cat*$^{flx/wt}$ and *HK1.ras-K14creP.Δ3β-cat*$^{flx/wt}$*.p53*$^{flx/flx}$ mice had a more logical and distinctly different outcome as p53 null papillomas converted to SCCs. Also, these SCCs displayed a reduced membranous β-catenin/E-cadherin more consistent with loss of cell-cell adhesion in basal layers that aided in tumour invasion; whilst nuclear localization of β-catenin in almost all cells of basal layers, coupled to p53 loss, showed a similar β-catenin/E-cadherin expression profile to that of malignant conversion/progression in *HK1.ras/fos-K14creP.Δ5PTEN*$^{flx/flx}$ mice (*Macdonald et al., 2014*). A result finally consistent with the literature dogma (*Polakis 2000; Gunther et al., 2003; Yao et al., 2008; Jeanes et al., 2008).*

Thus, *HK1.ras-K14creP.Δ3β-cat*$^{flx/wt}$*.p53*$^{flx/flx}$ and similarly *HK1.ras/fos-K14creP.Δ5PTEN*$^{flx/flx}$ SCC both lost p21 expression, unlike papilloma of *HK1.ras-K14creP.Δ3β-cat*$^{flx/wt}$ or tumour free *HK1.ras-K14creP.Δ3β-cat*$^{flx/wt}$ and *HK1.ras-K14creP.Δ3β-cat*$^{flx/wt}$*.p53*$^{flx/flx}$ epidermis with high levels of p21. This again indicates that p21 exerts a protective response even at later

stages of tumour progression and losing p21 would facilitate malignant progression rather than conversion *(Macdonald et al., 2014).* The SCCs developed in *HK1.ras-K14creP.Δ3β-cat*$^{flx/wt}$*.p53*$^{flx/flx}$ also exhibited high levels of p63/p73 and this was gain consistent with the potential oncogenic roles assigned to p63 and the failed TSG roles for p73 discussed above. Thus, as this was also reported in human cutaneous SCCs *(Moll and Slade 2004; Koster et al., 2007; Botchkarev et al., 2014*) this model may be a close relevant mimic.

These implications of p21 roles in halting tumour development and loss being associated with SCC development as seen *HK1.ras-K14creP.Δ3β-cat*$^{flx/wt}$*.p53*$^{flx/flx}$ and in *HK1.ras/fos-K14creP.Δ5PTEN*$^{flx/flx}$ SCCs, an on-going experiment investigated p21 knockout (*Martı et al., 2001*). Preliminary *HK1.ras-K14creP.Δ3β-cat*$^{flx/wt}$*.p21KO* data indicated that p21 loss also failed to facilitate papillomatogenesis as these mice remained tumour free 12 weeks consistent with later p21 roles in tumourigenesis. However, the other major finding was that p21 knockout in *K14creP.Δ3β-cat*$^{flx/wt}$*.p21ko* and *HK1.ras-K14creP.Δ3β-cat*$^{flx/wt}$ *.p21KO* did not show any delay or reduction in the onset of juvenile *Δ3β-catenin* phenotypes. Thus, the responses to *Δ3β-catenin* overexpression were specifically associated with *p53* loss and experiments are on going to assess the roles of p63/73 and also explore AKT status in the p21 knockout genotypes, given the apparent AKT1/p21 antagonism in *HK1.ras/fos-K14creP.Δ5PTEN*$^{flx/flx}$ malignant progression (*Macdonald et al., 2014*) and the axis of AKT/GSK3β/β-catenin.

9.4 *HK1.fos-K14creP.Δ5PTEN*$^{flx/flx}$*.Δ3β-cat*$^{flx/wt}$ co-operation blocks tumour development via keratinocyte differentiation giving a novel skin phenotype.

Analysis of *HK1.fos–Δ5PTEN*^{flx} KA formation demonstrated that loss of PTEN-mediated AKT regulation led to AKT-mediated GSK3β inactivation which triggered compensatory p53/p21 expression to divert excess keratinocyte proliferation to the massive differentiation that gives the keratosis of classic KA (*Yao et al., 2008*). Indeed, it was this set of experiments that prompted analysis of β-catenin overexpression in this project, as it was assumed that β-catenin played a significant role in this mechanism. This proved to be correct as endogenous β-catenin levels in *HK1.fos-K14creP.Δ5PTEN*$^{flx/flx}$ KA increased with strong membranous β-catenin/E-cadherin expression and nuclear localization that correlated with induction of compensatory p53/p21, as seen in the *Δ3β-catenin* models. Together with E-cadherin

expression, strong membranous β-catenin expression leading in cell-cell adhesion which led to a KA outcome rather than invasive SCC (*Yao et al., 2008*) and confirmed direct β-catenin involvement in KA aetiology as a consequence of *Δ5PTEN-medaited* AKT activation and associated GSK3-β inactivation Further, in *HK1.ras /fos–Δ5PTEN^{flx}* mice, basal layer β-catenin expression became increasingly nuclear and keratinocytes expressed less membranous β-catenin paralleled loss of E-cadherin at the invasive front and reduced cell-cell adhesion(*Alyamani et al., manuscript in preparation*). Therefore, it was expected that *K14creP.Δ3β-cat$^{flx/wt}$* in *HK1.fos* mice would lead to a similar KA outcome as Δ3β-catenin expression was now independent of deregulated PTEN/AKT/GSK3β signalling; and since the fos transcription factor AP1 is also a target of Wnt signalling (*Toualbi et al., 2007; Saadeddin et al., 2009*) another feedback loop may become established that leads to SCC if p53 or p21 became compromised or were experimentally introduced in this model.

Once again, establishment of *HK1.fos-K14creP.Δ3β-cat$^{flx/wt}$, HK1.ras/fos-K14creP.Δ3β-cat$^{flx/wt}$* and *HK1.fos-K14creP.Δ5PTEN$^{flx/flx}$.Δ3β-cat$^{flx/wt}$* genotypes resulted in a lack of benign tumours of any kind, neither papilloma nor KA. This reinforced the idea that early Δ3β-catenin activation triggers a general protective response in the epidermis, even in the presence of several potent oncogenes: fos, Δ3β-catenin or loss of PTEN-mediated AKT inhibition. In terms of HF tumourigenesis a major finding identified novel co-operation between PTEN mutation and β-catenin in the aetiology of trichochleomas, one of the many tumour types affecting Cowden's Disease patients that are already heterozygous for familial mutations in PTEN.

Another hallmark of these genotypes was the novel epidermal response giving a skin phenotype of an overlapping and highly keratotic bands or scales with a concentric geometric harlequin pattern. This pattern results from the keratinocyte proliferation that gives a papillomatous hyperplasia, i.e., a folded epidermis, where the keratinocytes subsequently differentiated giving rise to overlapping keratosis and hardened scales resembling a pangolin skin [the only scaled mammal]. This suggests that the keratotic responses observed in KA aetiology appeared here at an earlier stage of juvenile development. This then provided an underlying mechanism for the development of this novel pangolin like-skin phenotype specifically associated with epidermal responses to dysfunctional *Δ3β-catenin* and *HK1.fos* interactions on normal skin homeostasis; eg those β-catenin roles in regulating stem cells, terminal differentiation and hair follicle formation (*Gat et al., 1998**;** Niemann et al., 2002;*

Grigoryan et al., 2008; Kretzschmar et al., 2015) combined with those of c-fos that in the commitment to terminal differentiation (*Fisher et al., 1991; Greenhalgh et al., 1993b; Basset-Seguin et al., 1994; Angel et al., 2001; Candi et al., 2006*) and the HF stem cell decisions to form IFE, sebocytes or HF cells (*Gerdes et al., 2006*).

Astonishingly, experiments again found that this potent skin phenotype was effectively blocked by p53 loss in the IFE of these mice showing again the necessity for a functional p53 to elicit these specific effects of *Δ3β-catenin.* Nonetheless, the development of the pangolin-like skin response in all *HK1.fos-K14creP.Δ5PTEN*$^{flx/flx}$*.Δ3β-cat*$^{flx/wt}$ genotypes suggested that in these contexts tumourigenesis was inhibited via aggressive differentiation of the keratinocyte proliferation elicited by *fos/Δ5PTEN/Δ3β-catenin* interaction as juvenile skin developed i.e., this diversion into differentiation the prevented KA conversion here prevented overt tumour formation. Overall, experiments found that in each genotype tumor inhibition was again associated with p53 and p21 expression as seen with *HK1.ras-K14creP.Δ3β-cat*$^{flx/wt}$ *mice,* but here the histotype and K1 and K6 expression analysis demonstrated that a unique differentiation profile appears to be the most significant. These experiments also suggest that Δ3β-catenin enhanced the *HK1.fos*-mediated interference of normal differentiation giving a dominance of spinus layer keratinocytes that explained the general acanthosis observed in the IFE.

Furthermore, c-fos has major roles in the regulation of keratinocyte cornification in supra-basal layers (*Candi et al., 2006*) and this may be quite important when overlaid on fos/β-catenin-mediated co-operation in suprabasal layers that accelerated differentiation, but premature cornification would give rise to early keratosis, such that each fold became a scale-like structure. Supporting this idea, strands of K1 expression now appeared in basal layer keratinocytes, suggesting a premature commitment of basal layer keratinocytes to terminal differentiation, a result also found in KA aetiology (*Macdonald et al., 2014*) and possibly amplified by increased *HK1.fos* expression in parallel with premature basal K1 expression (*Fisher at al.,1991; Greenhalgh et al., 1993b; Basset-Seguin et al., 1994*). In contrast K6α expression remained diminished which may also indicate an effect of accelerated differentiation and possibly diversion of proliferation into cyst formation which appeared to be another anti-tumorigenic mechanism in this *HK1.fos-K14creP.Δ5PTEN*$^{flx/flx}$*.Δ3β-cat*$^{flx/wt}$ genotype [below].

Therefore, for the first time these *HK1.fos-K14creP.Δ5PTEN$^{flx/flx}$* and *HK1.fos-K14creP.Δ5PTEN$^{flx/flx}$.Δ3β-cat$^{flx/wt}$* mice identified a direct link between fos and β-catenin activation in regulation of keratinocyte differentiation, consistent with earlier photo-carcinogenesis studies that associated epidermal c-fos responses following UV-B exposure with AKT activation and GSK3β inactivation (*Gonzales and Bowden, 2002*) whilst UV-B-mediated p53 mutation and subsequent PTEN inhibition increased p-AKT/p-GSK3β/nuclear β-catenin to induce differentiation responses mediated by fos/jun/AP1 expression (*Wang et al., 2005*). This latter point strengthens co-operation given PTEN-mediated AKT regulation of downstream GSK3β/β-catenin signalling already co-operated with activated *HK1.fos* to induce KA; and K14.Δ5PTEN expression gives blooms of hyperkeratosis (*Macdonald et al., 2014*) [the classic sign of pre-tumours in Cowden's patients (*Liaw et al., 1997; Fistarol et al., 2002*)] which would also contribute to premature differentiation thus giving the most extreme examples of pangolin-like skin in *HK1.fos-K14creP.Δ5PTEN$^{flx/flx}$.Δ3β-cat$^{flx/wt}$* mice. Indeed, the lipo-phosphatase functions of PTEN that act as a scaffolding protein at the cell membrane aid assembly of adherence junctions and cell-matrix interactions (*Tamura et al., 1998; Subauste et al., 2005*) and this helped explained the increased E-cadherin observed in the IFE that would also add to the degree of keratosis and inhibit the onset of tumorigenesis.

This mechanism of co-operation in the IFE appears to be deployed in the aetiology of the novel trichilemmomas produced in Cowden's disease, (*Liaw et al 1997; Fistarol et al., 2002; Suzuki et al., 2003*). This again is a logical finding, consistent with the fact that deregulation of both these proteins induces HF anomalies in transgenic mice (*Gat et al., 1998**;** Niemann et al., 2002; Grigoryan et al., 2008; Kretzschmar et al., 2015; Suzuki et al., 2003*). Here again the deregulation of the AKT/GSK3β/β-cat axis mediated by PTEN loss would add to that from constitutive Δ3β-catenin to begin the HF anomalies; whilst the additional functions, such as the scaffolding roles in AJ formation, may explain increased E-cadherin observed in the HFs. Indeed, this may be of significance in the aetiology of trichilemmomas, a tumour of the ORS keratinocytes vs that of the more common folliculoma and the production of cysts another feature of Cowden disease skin. This idea is supported by K6α analysis given in *HK1.fos-K14creP.Δ5PTEN$^{flx/flx}$.Δ3β-cat$^{flx/wt}$* trichilemmomas expression was lower than expression seen in *HK1.fos-K14creP.Δ3β-cat$^{wt/flx}$* folliculomas. This suggests a less developed, less differentiated HF which may induce the response to divert odd anomalous HF cell proliferation into cyst formation, and not just in the HFs as K1 expression was identified

showing cyst formation is a general response to the greatly disturbed differentiation and originate from both IFE and HF sources. This is a logical conclusion as cyst formation is likely to be a common response to divert anomalous from tumour formation and into this dead end (*Young et al., 2003*) as observed in early *HK1.ras/fosΔ5PTEN* hyperplasia (*Macdonald et al., 2014*) and later in KA aetiology to prevent further progression (*Yao et al., 2008*).

Thus, in all of these genotypes, one way or another, the membranous β-catenin component, and increased E-cadherin that strengthened cell-cell adhesion helped divert excess PCK proliferation into differentiation. This was again paralleled by increased p53/p21, which together with accelerated differentiation combined to minimise IFE hyperplasia as exemplified by the return of sporadic K1 expression in the *HK1.fos-K14creP.Δ5PTEN*$^{flx/flx}$*.Δ3β-cat*$^{flx/wt}$ IFE which was often fairly thin. This correlated with elevated levels of p53/p21 expression, similar to that seen previously in *HK1.fos-K14creP.Δ5PTEN*$^{flx/flx}$ KA (*Macdonald et al., 2014*); and in analysis of *HK1.ras-K14creP.Δ3β-cat*$^{flx/wt}$ or *K14creP.Δ3β-cat*$^{flx/wt}$ skin. Thus, to block the beginnings of tumour formation, early elevated p53/p21 expression responding to excess β-catenin/E-cadherin initiated a far more accelerated and premature differentiation program in juvenile *HK1.fos-K14creP.Δ5PTEN*$^{flx/flx}$*.Δ3β-cat*$^{flx/wt}$ skin. This gave rise to an odd, ragged K1 expression in patches of acanthosis that reflects the role of fos [and PTEN] in cornification (*Candi et al., 2006*) that are now subverted by *HK1.fos-K14creP.Δ5PTEN*$^{flx/flx}$ expression.

In *HK1.fos-K14creP.Δ5PTEN*$^{flx/flx}$*.Δ3β-cat*$^{flx/wt}$ or *HK1.fos-K14creP.Δ5PTEN*$^{flx/flx}$ epidermis the timing of β-catenin activation seems to be the key element that governed this massive keratosis. In this context p53-mediated proliferation and increased p21-mediated differentiation aided the developing pangolin like-skin and preventing further progression via cyst production. This was similar to the conclusions made in *HK1.ras-K14creP.Δ3β-cat*$^{flx/wt}$ analysis, where p53/p21 responses to Δ3β-catenin appeared to be the main reasons for blocking tumours formation. Another possible mechanism centres on the idea that constitutive activation of β-catenin returns an adult skin to a neonatal/juvenile state (*Collins et al., 2011*)- as suggested in Scatter Assays [below]. In neonatal skin for the first 5-6 days the epidermis is naturally hyperplastic but e.g., lacks K6α expression and p-AKT is uniformly expressed in the suprabasal layer (*Masre et al., 2020*). By day 4-6 HK development begins, thus in leaky *HK1.fos-K14creP.Δ5PTEN*$^{flx/flx}$*.Δ3β-cat*$^{flx/wt}$ skin so many new HFs are being created in juveniles due to the effects of *Δ3β-catenin* expression that are then further compromised by

K14.Δ5PTEN expression such that p53 and p21 responses to AKT and βcatenin are deployed in to avoid rapid degeneration of the IFE hence the acanthosis and keratosis to protect the barrier function and divert failing HF into cysts collectively again inhibiting the onset of early tumorigenesis.

Again, the p53 roles in these findings were tested and, adding more complexity to these models, as in *HK1.ras-K14creP.Δ3β-cat*$^{flx/wt}$*.p53*$^{flx/flx}$ conditional p53 loss in the context of *HK1.fos-K14creP.Δ3β-cat*$^{flx/wt}$ *-p53*$^{flx/flx}$ mice completely blocked the *Δ3β-catenin* IFE responses. There was a total disappearance of pangolin-like phenotype and again the *HK1.fos-K14creP.Δ3β-cat*$^{flx/wt}$*.p53*$^{flx/flx}$ mice suggest that it is a general p53-mediated response to β-catenin deregulation in IFE. Indeed, despite repeated RU486 treatments *Δ3β-catenin* phenotypes were blocked over longer periods of time; yet without facilitating tumorigenesis, as to date no KAs have been observed, even in full sized mice.

The reasons remain quite unclear. It appears clear that p53 functions are essential to trigger this overall response as observed in *HK1.fos-K14creP.Δ5PTEN*$^{flx/flx}$ KA aetiology and this is lacking in p53 null *HK1.ras/fos.K14.Δ5PTEN* papillomas that convert to SCC. As discussed above, p63/p73 expression profiles may alter the PCK niches to return the epidermis to a more normalised state and negates *Δ3β-catenin* effects in the *HK1.fos* models as observed in *HK1.ras* and thus there is no reason for an epidermis to respond with induction of an excessive commitment to terminal differentiation. That this is targeted to differentiation reinforced by the complete block of differentiation in fos vs the partial block in ras that maybe due to the roles for fos in the commitment to differentiate. This again returns to the central p53 paradox: that p53 loss blocks *HK1.ras* or *HK1.fos* papilloma formation (*Greenhalgh et al., 1996*) and this cannot be overcome by β-catenin activation in *ras* or *fos* models as seen in *HK1.fos-K14creP.Δ3β-cat*$^{flx/wt}$ *-p53*$^{flx/flx}$ and most cases of *HK1.ras-K14creP.Δ3β-cat*$^{flx/wt}$ *.p53*$^{flx/flx}$. However, further experimentation will be required to increase animal numbers to assess if any individual can bi-pass this tumour inhibition, assess histopathology and differentiation markers and determine whether p63/p73/K15 observations also appear in *HK1.fos.K14.Δ5PTEN.p53*$^{flx/flx}$ models.

9.5 β-catenin activation *in vitro* induces keratinocyte transformation, resistance to calcium-induced differentiation and a neonatal phenotype.

The *in vivo* analysis of constitutive β-catenin activation in *HK1.ras*, *HK1.fos* and *Δp53/Δ5PTEN/p21KO* genotypes resulted in a paradoxical blockage of tumour development contrary to the original hypothesis that evolved from β-catenin analysis in *HK1.ras/fos-K14creP.Δ5PTEN*$^{flx/flx}$ mice and the literature dogma that predicted β-catenin overexpression would facilitate tumourigenesis (*Morin, 1999; Polakis, 1999; Doglioni et al., 2003; Grigoryan et al., 2008; Krishnamurthy and Kurzrock, 2018*). In contrast *in vitro* experiments that further explored *Δ3β-catenin* signalling and effect on keratinocyte transformation and differentiation gave results more consistent with this original hypothesis. The consequences of Δ3β-catenin activation were assessed in a variety of genotypes was tested in three different experiments. The first experiments assessed differentiation responses to calcium-induced terminal differentiation via a challenge with 0.125mM Ca2+ [High calcium] medium. The second tested the ability to grow clonally again as an indication of immortalisation and partial transformation. Finally, a third series of experiments tested the seeding ability and cell motility, not only as an indication of invasive potential but also to test the idea that *Δ3β-catenin* expression maintains neonatal/juvenile phenotype, as suggested in previous studies that investigated β-catenin expression on keratinocytes and the ECM (*Collins et al., 2011*) as well as β-catenin effects on the emerging variety of KPC/stem cell niches (*Watt and Collins 2008; Kretzschmar et al 2015*).

In the first experiment of classic calcium induced terminal differentiation assays (*Hennings et al., 1980; Greenhalgh et al., 1989; Morgan et al., 1992*), *Δ3β-catenin* co-operation with other oncogenes displayed resistance to calcium-induced differentiation in all compound lines consistent with their rapid growth and oncogenes activation in addition to *Δ3β-catenin.* These data indicated that *Δ3β-catenin* activation induced transformation via overexpressing the canonical Wnt signalling pathway resulting in increased proliferation and a delay or resistance to normal epidermal differentiation which was also constant with the literature dogma that β-catenin gain of function would facilitate tumorigenesis (*Morin, 1999; Polakis, 1999; Doglioni et al., 2003; Grigoryan et al., 2008; Krishnamurthy and Kurzrock, 2018).* Although, there were subtle differences, for instance *HK1.fos-K14creP.Δ5PTEN*$^{flx/flx}$*.Δ3β-cat*$^{flx/wt}$ lines

exhibited a transformed morphology at confluence but possessed numerous squames and many floating cells suggesting attempts to differentiate in Low Cal media that would be consistent with the excessive differentiation observed *in vivo*. In addition, whilst these keratinocytes resisted forming spinus cells in 0.075mM Ca^{2+} consistent with a highly transformed phenotype; in Hi Cal these cells did differentiate now producing the cornified cells and squamous of highly differentiated cells again consistent with the excess keratosis observed *in vivo* and the return of K1. Thus under proliferative conditions fos/PTEN/βcatenin co-operation inhibits differentiation but in Hi Cal these cells have a significant excess response to elevated calcium. This seemed to imitate the confused differentiation signals and aberrant differentiation evoked *in vivo* consistent with the excess of floating cells continually observed in low Cal media, and the granular/squames in Hi Cal which may reflect attempts to de-differentiated into cysts and die, which was a highlighted feature *in vivo HK1.fos-K14creP.Δ5PTEN$^{flx/flx}$.Δ3β-cat$^{flx/wt}$* mice.

Similarly, whilst *HK1.ras-K14creP.Δ3β-cat$^{flx/wt}$* lines adopted a typical spinus morphology in 0.075mM Ca^{2+}; in Hi Cal these cells continued to grow in Hi calcium consistent with a fully transformed malignant line and lack of K1 expression *in vivo*. This would be the equivalent of the rare SCC tumours of *HK1.ras-K14creP.Δ3β-cat$^{flx/wt}$.p53$^{flx/flx}$* p53 null mice. As often *in vitro* p53 could be lost/mutated as cells become immortalised and transformed e.g., in the immortalised human HaCaT keratinocyte cell line (*Boelsma et al., 1999*). Further compounding these results was the finding that whilst *K14creP.Δ3β-cat$^{flx/wt}$* lines exhibited a normal, cobblestone basal layer morphology in Low Cal 0.05mM Ca^{2+} media and committed to differentiate in 0.075mM Ca^{2+} media differentiation stalled at this spinus morphology stage and in Hi Cal media these cells failed to stratify and undergo cornification to produce squames. This result might be mimicking the sporadic differentiation suggested by K1 expression giving a relatively thin IFE as the supra-basal roles of β-catenin in regulating terminal differentiation are altered by *Δ3β-catenin* and this prevented the final stages of differentiation (*Grigoryan et al., 2008*). It would have been interesting to see the levels of p63 in this line to assess whether this result echoed the p63 roles in limiting terminal differentiation.

Another classic carcinogenicity assay tested cell line ability to grow from clonal density in both low and high calcium concentrations. This assessed the stem-like or KPC phenotypes that

may have been maintained or reactivated by β-catenin overexpression as suggested in previous studies (*Watt and Collins, 2008*) and epidermal lineage studies (*Kretzschmar et al., 2015*). Typically, the ability to clonally grow in Low calcium but not Hi calcium was previously associate with a benign phenotype producing papillomas when grafted onto nude mice; whilst growth in High calcium gave lines producing SCC and metastasis in this assay (*Strickland et al., 1998; Greenhalgh and Yuspa, 1998; Greenhalgh et al., 1989; 1990; Morgan et al., 1992*). Generally, Δ3β-catenin induced a transformed but benign phenotype as most cell line grew in Low Cal media, and only *HK1.ras-K14creP.Δ3β-cat*$^{flx/wt}$ and *HK1.fos-K14creP.Δ5PTEN*$^{flx/flx}$*.Δ3β-cat*$^{flx/wt}$ lines were able to grow from clonal density in Hi Cal media which indicated a probably malignant phenotype. These data suggested that deregulation of *K14creP.Δ3β-cat*$^{flx/wt}$ alone achieves a benign hit and at least *in vitro,* co-operation with other oncogenes [*HK1.ras-K14creP.Δ3β-cat*$^{flx/wt}$ and *HK1.fos-K14creP.Δ5PTEN*$^{flx/flx}$*.Δ3β-cat*$^{flx/wt}$] results in a malignant phenotype to fit the current dogma of β-catenin oncogenicity (*Morin, 1999; Polakis, 1999; Doglioni et al., 2003; Grigoryan et al., 2008; Krishnamurthy and Kurzrock, 2018*).

Given the roles for β-catenin and E-cadherin in cell-cell adhesion and the evidence that *in vivo* nuclear β-catenin expression and loss of E-cadherin at the invasive front, an experiment was designed to not only assess migration but also test cell line abilities to seed satellite colonies as a determinant of transformation and invasion (*Hesse et al., 2016*). In this experiment all *K14creP.Δ3β-cat*$^{flx/wt}$ lines were able to seed/scatter to some extent in proliferative Low Cal conditions but only the fully transformed potentially malignant lines *HK1.fos-K14creP.Δ5PTEN*$^{flx/flx}$*.Δ3β-cat*$^{flx/wt}$ and *HK1.ras-K14creP.Δ3β-cat*$^{flx/wt}$ were able to seed in Hi Cal media. In contrast, lines without Δ3β-catenin activation were unable to seed in this assay. This observation for lines in Low Cal would again be consistent with a stem cell –like or PCK phenotype would be consistent with endogenous β-catenin activation altering p63 and p73 *in vivo* and the expression of K15- although westerns and IF remain to be done in this Scatter assay to confirm. These seeding data are also in agreement with the rare *HK1.ras-K14creP.Δ3β-cat*$^{flx/wt}$*.p53*$^{flx/flx}$ SCCs and carcinomas in *HK1.ras/fos-K14cre.Δ5PTEN* that showed followingp53 loss, β-catenin became less membranous and together with reduced E-cadherin resulted in a loss of focal adhesions to facilitate the invasion. Again, IF experiments on the migrating and seeding colonies will be required to confirm this idea as a model of invasion/metastasis *in vitro*.

These experiments also tested the reported potential of *Δ3β-catenin* expression to return an adult epidermis to a more juvenile state which was also suggested by *in vivo* analysis of K6α and p63/K15 expression profiles. This approach was suggested by previous studies that concluded in vivo, constitutive β-catenin over expression affected the dermal extra cellular matrix and appeared to return the skin to neonatal state (*Collins et al., 2011*). In these seeding experiments typical immortalised keratinocyte cell lines by passage 3-5 do not efficiently seed (*Greenhalgh et al., 1989*) as seen in normal non-cre *Δ3β-catenin* β-1-3; ICR-1 or Wt-1 lines, unlike their normal primary counterparts were seeding satellite colonies is a common property given the presence of more numerous stem–like/PCK populations derived from newborn vs. adult mice (*Morris et al., 2004*). Therefore, the ability of all *K14creP.Δ3β-cat*$^{flx/wt}$ lines to seed distant colonies, even *K14creP.Δ3β-cat*$^{flx/wt}$ alone cells, as observed in all primary neonatal keratinocyte cultures would be consistent with β-catenin overexpression resulting in a return to juvenile/neonatal primary cell phenotypes. This conclusion would also be supported in this current model by the findings of β-catenin effects on the decisions of stem cells/ PCK cells that appear to centre on juvenile epidermal development rather than adults as exemplified by those mice that were full sized and had an epidermis which developed relatively normally eg following p53 loss and the roles for proteins such as p63 and 73 that directly regulate early epidermal and HF development.

Collectively, these data suggest that all Δ3β-catenin lines are transformed to some extent or even malignant and demonstrates the major differences between *in vivo* and *in vitro* experimentation which lacks the tissue homeostasis needed to elicit the biological spectrum of responses observed. However, clonal growth and seeding in Low Cal would be consistent with Δ3β-catenin mediated influences on stem cells or a return to a more stem-like PCK phenotype; whilst growth in Hi Cal demonstrate that these combinations can co-operate with β-catenin to fulfil the criteria required for a malignant phenotype in classic keratinocyte transformation assays and are thus more consistent with the endogenous β-catenin oncogenicity observed in the original *HK1.ras/fos/PTEN* SCC model and the literature associated with β-catenin in human SCC.

9.6 Conclusion and future directions

This study was conducted to help unravel the exact causal roles for constitutive β-catenin activation in development of SCCs employing a well characterised transgenic mouse model of multi-stage carcinogenesis. The findings of this study were intriguing and shed light on several aspects that can be pursued in the future to gain understanding and fill the void in the current literature concerning the causal roles for β-catenin overexpression in cutaneous carcinogenesis. Clearly if an epidermis was allowed to develop normally, endogenous β-catenin in conjunction with *HK1.ras, HK1.fos* and PTEN loss, plays a significant role in the conversion of papillomas to carcinomas as suggested by knockout in classic chemical carcinogenesis experiments and the cell line phenotypes derived in this study. In the rare instances of tumour formation these roles again appear and demonstrate that they directly contribute to SCCs due to incorrect control of β-catenin (*Malanchi, et al., 2008*) in a two fold manner; one involving β-catenin maintenance of the cell-cell adhesion by binding to E-cadherin, as impairment of this function facilitated malignant progression in *HK1.ras-K14creP.Δ3β-cat*$^{flx/wt}$*.p53*$^{flx/flx}$ SCCs and carcinomas in *HK1.ras/fos-K14cre.Δ5PTEN* (*Jeanes et al., 2008; Macdonald et al., 2014*); the second depending upon basal layer expression of nuclear β-catenin and thus deregulation of canonical Wnt signalling and disruption of the stem cell niches (*Watt and Collins, 2008*).

Given this integral role in regulation of the HF bulge stem cells niche and the KPC populations that reside in the IFE the premature activation of Δ3β-catenin in the juvenile skin of this HK1 study led to incorrect control of stem cell niche/KPC, which is integral component in maintaining epidermal haematosis and keratinocyte differentiation, thus compensatory TSGS [p53/p21/p73/p63] levels were elevated to suppress the susceptibility to IFE tumours and this depended upon a functional p53, as exemplified by the novel unique co-operation between fos and β-catenin deregulation which generated the pangolin-like skin of *HK1.fos-K14creP.Δ5PTEN*$^{flx/flx}$*.Δ3β-cat*$^{flx/wt}$ mice being completely blocked in *HK1.fos-K14creP.Δ3β-cat*$^{flx/wt}$*.p53*$^{flx/flx}$ mice.

These compensatory responses of TSGs led to aberrant alteration in epidermal terminal differentiation and these alteration were more potent in co-operation of Δ3β-catenin with other oncogenes resulting in aggressive skin phenotype in term of keratosis and HF abnormalities

but no IFE tumours as seen in *HK1.ras-K14creP.Δ3β-cat*$^{flx/wt}$ and *HK1.fos-K14creP.Δ5PTEN*$^{flx/flx}$*.Δ3β-cat*$^{flx/wt}$ cohorts even following p53 loss. Indeed, p53 mediated responses seemed to be the key in driving these juvenile skin phenotypes in response to Δ3β-catenin, as they were blocked by conditional loss of p53 Δ3β-catenin associated skin phenotypes in both *HK1.fos-K14creP.Δ3β-cat*$^{flx/wt}$ *-p53*$^{flx/flx}$ and *HK1.ras-K14creP.Δ3β-cat*$^{flx/wt}$*.p53*$^{flx/flx}$ models; and this was p53 specific not being observed with p21^{ko}. However, and more consistent with the original aims if the K14.cre regulator did not leak the delayed activation of Δ3β-catenin in a fully developed adult epidermis provided enough time to establish a context where papillomas could develop and which converted rapidly to SCC following loss of p53 as observed in *HK1.ras/fos-K14Δ5PTEN* mice. Thus again reinforcing the idea that Δ3β-catenin associated phenotypes derived from deregulation of β-catenin during epidermal development, and that losing p53 makes the adult skin more susceptibility to IFE tumours; whist in juvenile stages, Δ3β-catenin oncogenic activation can be overcome by possibly other TSGs [p21, p63,p73], however later stages of tumour development p53 loss in conjunction with Δ3β-catenin facilitate SCC development.

The *in vitro* activation of Δ3β-catenin was more in line with literature finding in term of inducing transformation and malignant phenotypes in co-operation with other oncogenes such as *HK1.fos-K14creP.Δ5PTEN*$^{flx/flx}$*.Δ3β-cat*$^{flx/wt}$ and *HK1.ras-K14creP.Δ3β-cat*$^{flx/wt}$ cell lines. However, another most interesting observation in the *in vitro* part of the study was the ability of β-catenin to re-programme the epidermis to a more neonatal/juvenile state. This indicated the affect *Δ3β-catenin* could be context dependent and many aspects could be investigated to understand these paradoxical results further.

Future Directions

To extrapolate these findings both *in vivo* and *in vitro* several actions can be taken in terms of protein analysis to determine the mechanism further via completion of the western analysis. Given the large amount of data complied, the induction of new transgenes that interact with these Δ3β-catenin effect on the epidermis would also answer several of the questions posed by these studies such as the following:

- Western blot protein analysis and immunocytochemistry analysis *in vitro* analysis is an essential future analysis to contrasts in vivo results in terms of protein expressions such as K1,K6,K15,p53,p21,p63,p73,E-cadherin, β-catenin and AKT
- Investigating an ongoing study to test induction of p53 conditional loss together with embryonic knockout of p21 in *HK1.ras.K14.Δ3β-cat-p53$^{flx/flx}$.p21KO* to assess their effect on papilloma development, epidermal differentiation and reduced/increased severity of Δ3β-catenin phenotype. This most likely would have to be performed with the now non leaky XJ5 creP regulator.
- Due to the early cre leak *K14creP.Δ3β-cat$^{flx/wt}$* , same cohorts will be repeated again using XJK5creP* gene switch which initially showed no early cre leak indicted by the lack of Δ3β-catenin phenotype in these mice; although to date these appear to require extensive, prolonged RU486 treatment and more time to produce phenotypes.
- Given the implications in the responses to p53 loss in terms of KPC proliferation and differentiation in this study, another interesting approach would be to investigate *K14creP.Δ3β-cat$^{flx/wt}$-p63KO and K14creP.Δ3β-cat$^{flx/wt}$-p73KO* to assess their effect on altering differentiation and again in conjunction with *HK1.ras* activation to assess their effect on papilloma formation. Similarly in conjunction with *K14creP.Δ3β-cat$^{flx/wt}$-ΔN63 and K14creP.Δ3β-cat$^{flx/wt}$-ΔN73*
- Investigating inducible E-cadherin knock out in co-operation with Δ3β-catenin is a experiment that will be performed in the near future, in conjunction also with HK1.ras and p53 loss, to assess how the epidermis will cope with E-cadherin loss and Δ3β-catenin activation in regard to cell-cell adhesion and whether it will facilitate tumorigenesis.
- Given the reported ability of β-catenin to reprogramme the epidermis to a more neonatal/juvenile state (*Collins et al., 2011),* which was an affect suggested in this study in both vivo and in vitro, assessing extra cellular matrix protein marker such as integrins and Tenascin-C (*Yoshida et al., 2015*) would give a further insight into how β-catenin effects the dermis-epidermis interaction.
- One of the main analysis to be conducted on the different genotypes of this study is assessing stem cell markers other than K15 such as CD34 and LGR5/6. Although an attempt was already made to test LGR5/6 the analysis was inconclusive due cross reactivity of the antibodies used.

- Another target to be analysed in this study is perhaps BCL-2 as several studies suggested that β-catenin overexpression could influence apoptosis via overexpressing BCL2 (*Ming et al., 2012*) which could be interesting to see given β-catenin effect on apoptosis associated TSGs p53/p73/p63.
- Given the implicated ability of *K14creP.Δ3β-cat*$^{flx/wt}$ cultured cells to return the epidermis to neonatal/juvenile state, it would be interesting to see if these cultured cells would have wound healing ability, for example as skin grafts by testing onto nude mice.

- Finally, a series of genomic and proteomic analysis of frozen skin biopsies may identify the targets responsible the paradoxical lack of tumours in p53 null genotypes

Concluding statement

An epidermis in being most exposed to environmental carcinogens has many options to prevent benign tumour formation; which may become lost in aggressive papillomas leading to conversion. This model shows the importance of both context and temporal expression of oncogenic tumour promotion events vs. endogenous TSGs responses that will determine the phenotypic outcome. These potent responses to β-catenin deregulation maybe be quite general given they appear in response to ras/β-catenin/p53; fos β-catenin/p53; ras/p53 and fos/p53 models and thus could be equally applicable to internal epithelia in the inhibition of early benign tumour [papilloma/KA] aetiology which are circumvented during malignant conversion /progression. In the final analysis it will be important to exploit these findings to discover exactly what is achieving this tumour inhibition and find new targets for new treatments.

References

Abbas, O. and Bhawan, J. 2011. Expression of stem cell markers nestin and cytokeratin 15 and 19 in cutaneous malignancies. *Journal of the European Academy of Dermatology and Venereology*, 25, 311-316.

Aberle, H., Butz, S., Stappert, J., Weissig, H., Kemler, R. and Hoschuetzky, H. 1994. Assembly of the cadherin-catenin complex in vitro with recombinant proteins. *Journal of Cell Science*, 107, 3655-3663.

Alonso, L. and Fuchs, E. 2003. Stem cells of the skin epithelium. *Proceedings of the National Academy of Sciences*, 100, 11830-11835.

Ambler, C.A. and Watt, F.M. 2007. Expression of Notch pathway genes in mammalian epidermis and modulation by β-Catenin. *Developmental dynamics: an official publication of the American Association of Anatomists*, 236, 1595-1601.

Angel, P., Szabowski, A. and Schorpp-Kistner, M. 2001. Function and regulation of AP-1 subunits in skin physiology and pathology. *Oncogene*, 20, 2413-2423.

Balmain, A. 1985. Transforming ras oncogenes and multistage carcinogenesis. *British Journal of Cancer*, 51, 1.

Balmain, A. and Yuspa, S.H. 2014. Milestones in skin carcinogenesis: the biology of multistage carcinogenesis. *J Invest Dermatol*, 134, E2-7.

Bailleul, B., Surani, M.A., White, S., Barton, S.C., Brown, K., Blessing, M., Jorcano, J. and Balmain, A. 1990. Skin hyperkeratosis and papilloma formation in transgenic mice expressing a ras oncogene from a suprabasal keratin promoter. *Cell*, 62, 697-708.

Barton, V., Armeson, K., Hampras, S., Ferris, L.K., Visvanathan, K., Rollison, D. and Alberg, A.J. 2017. Nonmelanoma skin cancer and risk of all-cause and cancer-related mortality: a systematic review. *Archives of Dermatological Research*, 309, 243-251.

Basset-Séguin, N., Escot, C., Blanchard, J.M., Kerai, C., Verrier, B., Mion, H. and Guilhou, J.J. 1990. High levels of c-fos proto-oncogene expression in normal human adult skin. *Journal of Investigative Dermatology*, 94.

Basset-Seguin, N., Demoly, P., Moles, J.P., Tesnieres, A., Gauthier-Rouviere, C., Richard, S., Blanchard, J.M. and Guilhou, J.J. 1994. Comparative analysis of cellular and tissular expression of c-fos in human keratinocytes: evidence of its role in cell differentiation. *Oncogene*, *9*, 765-771.

Behrens, J., von Kries, J.P., Kuhl, M. and Bruhn, L. 1996. Functional interaction of beta-catenin with the transcription factor LEF-1. *Nature*, 382, 638.

Behrens, J., Jerchow, B.A., Würtele, M., Grimm, J., Asbrand, C., Wirtz, R., Kühl, M., Wedlich, D. and Birchmeier, W. 1998. Functional interaction of an axin homolog, conductin, with β-catenin, APC, and GSK3β. *Science*, 280, 596-599.

Benavides, F., Rülicke, T., Prins, J.B., Bussell, J., Scavizzi, F., Cinelli, P., Herault, Y. and Wedekind, D. 2020. Genetic quality assurance and genetic monitoring of laboratory mice and rats: FELASA Working Group Report. *Laboratory Animals*, 54, 135-148.

Berton, T.R., Wang, X.J., Zhou, Z.J., Kellendonk, C., Schütz, G., Tsai, S. and Roop, D.R. 2000. Characterization of an inducible, epidermal-specific knockout system: differential expression of lacZ in different Cre reporter mouse strains. *Genesis*, 26, 160-161.

Boelsma, E., Verhoeven, M.C. and Ponec, M. 1999. Reconstruction of a human skin equivalent using a spontaneously transformed keratinocyte cell line (HaCaT). *Journal of Investigative Dermatology*, 112, 489-498.

Bose, A., Teh, M.T., Mackenzie, I.C. and Waseem, A. 2013. Keratin k15 as a biomarker of epidermal stem cells. *International Journal of Molecular Sciences*, 14, 19385-19398.

Botchkarev, V.A. and Flores, E.R. 2014. p53/p63/p73 in the epidermis in health and disease. *Cold Spring Harbor Perspectives in Medicine*, 4, p.a015248.

Botchkarev, V.A., Komarova, E.A., Siebenhaar, F., Botchkareva, N.V., Sharov, A.A., Komarov, P.G., Maurer, M., Gudkov, A.V. and Gilchrest, B.A. 2001. p53 Involvement in the control of murine hair follicle regression. *The American Journal of Pathology*, 158, 1913-1919.

Branda, C.S. and Dymecki, S.M., 2004. Talking about a revolution: The impact of site-specific recombinases on genetic analyses in mice. *Developmental cell*, 6, pp.7-28.

Brash, D.E., Rudolph, J.A., Simon, J.A., Lin, A., McKenna, G.J., Baden, H.P., Halperin, A.J. and Ponten, J. 1991. A role for sunlight in skin cancer: UV-induced p53 mutations in squamous cell carcinoma. *Proceedings of The National Academy of Sciences*, 88, 10124-10128.

Brennan, J.K., Mansky, J., Roberts, G. and Lichtman, M.A. 1975. Improved methods for reducing calcium and magnesium concentrations in tissue culture medium: application to studies of lymphoblast proliferation in vitro. *In vitro*, 11, 354-360.

Blanpain, C. and Fuchs, E. 2006. Epidermal stem cells of the skin. *Annu. Rev. Cell Dev. Biol.*, 22, 339-373.

Brown, K., Quintanilla, M., Ramsden, M., Kerr, I.B., Young, S. and Balmain, A. 1986. v-ras genes from Harvey and BALB murine sarcoma viruses can act as initiators of two-stage mouse skin carcinogenesis. *Cell*, 46, 447-456.

Brown, K., Strathdee, D., Bryson, S., Lambie, W. and Balmain, A. 1998. The malignant capacity of skin tumours induced by expression of a mutant H-ras transgene depends on the cell type targeted. *Current Biology*, 8, 516-524.

Calautti, E., Li, J., Saoncella, S., Brissette, J.L. and Goetinck, P.F. 2005. Phosphoinositide 3-kinase signaling to Akt promotes keratinocyte differentiation versus death. *Journal of Biological Chemistry*, 280, 32856-32865.

Candi, E., Schmidt, R. and Melino, G. 2005. The cornified envelope: a model of cell death in the skin. *Nature Reviews Molecular Cell Biology*, 6, 328-340.

Casola, S. 2010. Mouse models for miRNA expression: the ROSA26 locus. In *MicroRNAs and the Immune System*. Humana Press, Totowa, NJ, pp. 145-163.

Celso, C.L., Prowse, D.M. and Watt, F.M. 2004. Transient activation of β-catenin signalling in adult mouse epidermis is sufficient to induce new hair follicles but continuous activation is required to maintain hair follicle tumours. *Development*, 131, 1787-1799.

Chan, E., Gat, U., McNiff, J.M. and Fuchs, E. 1999. A common human skin tumour is caused by activating mutations in β-catenin. *Nature genetics*, 21, 410-413.

Chen, S.M., Li, B., Nicklawsky, A.G., Krinsky, A.L., Brunetti, T., Woolaver, R.A., Wang, X., Chen, Z., Young, C.D., Gao, D. and Wang, X.J. 2020. Deletion of p53 and Hyper-Activation of PIK3CA in Keratin-15+ Stem Cells Lead to the Development of Spontaneous Squamous Cell Carcinoma. *International Journal of Molecular Sciences*, 21, 6585.

Chiles, M.C., Ai, L., Zuo, C., Fan, C.Y. and Smoller, B.R. 2003. E-cadherin promoter hypermethylation in preneoplastic and neoplastic skin lesions. *Modern Pathology*, 16, 1014-1018.

Clevers, H. and Nusse, R. 2012. Wnt/β-catenin signaling and disease. *Cell*, 149, 1192-1205.

Clifford, J.L. and DiGiovanni, J. 2010. The promise of natural products for blocking early events in skin carcinogenesis. *Cancer Prevention Research*, 3, 132-135.

Collins, C.A., Kretzschmar, K. and Watt, F.M. 2011. Reprogramming adult dermis to a neonatal state through epidermal activation of β-catenin. *Development*, 138, 5189-5199.

Crum, C.P. and McKeon, F.D. 2010. p63 in epithelial survival, germ cell surveillance, and neoplasia. *Annual Review of Pathology: Mechanisms of Disease*, 5, 349-371.

Damalas, A., Kahan, S., Shtutman, M., Ben-Ze'ev, A. and Oren, M. 2001. Deregulated β-catenin induces a p53-and ARF-dependent growth arrest and cooperates with Ras in transformation. *The EMBO Journal*, 20, 4912-4922.

Deng, T. and Karin, M. 1994. c-Fos transcriptional activity stimulated by H-Ras-activated protein kinase distinct from JNK and ERK. *Nature*, 371, 171-175.

Deyoung, M.P. and Ellisen, L.W. 2007. p63 and p73 in human cancer: defining the network. *Oncogene*, 26, 5169-5183.

Di Cunto, F., Topley, G., Calautti, E., Hsiao, J., Ong, L., Seth, P.K. and Dotto, G.P. 1998. Inhibitory function of p21Cip1/WAF1 in differentiation of primary mouse keratinocytes independent of cell cycle control. *Science*, 280, 1069-1072.

Doglioni, C., Piccinin, S., Demontis, S., Cangi, M.G., Pecciarini, L., Chiarelli, C., Armellin, M., Vukosavljevic, T., Boiocchi, M. and Maestro, R. 2003. Alterations of β-catenin pathway in non-melanoma skin tumors: loss of α-ABC nuclear reactivity correlates with the presence of β-catenin gene mutation. *Am J Pathol* 163, 2277-2287.

Doma, E., Rupp, C. and Baccarini, M., 2013. EGFR-ras-raf signaling in epidermal stem cells: roles in hair follicle development, regeneration, tissue remodeling and epidermal cancers. *International Journal of Molecular Sciences*, 14, 19361-19384.

Donehower, L.A., Harvey, M., Slagle, B.L., McArthur, M.J., Montgomery, C.A., Butel, J.S. and Bradley, A. 1992. Mice deficient for p53 are developmentally normal but susceptible to spontaneous tumours. *Nature*, 356, 215-221.

Downward, J.2004. PI 3-kinase, Akt and cell survival. *In Seminars in Cell & Developmental Biology*, 177-182. Academic Press.

Eckert, R.L., Adhikary, G., Young, C.A., Jans, R., Crish, J.F., Xu, W. and Rorke, E.A. 2013. AP1 transcription factors in epidermal differentiation and skin cancer. *Journal of Skin Cancer*, 2013.

Fernández-Medarde, A. and Santos, E. 2011. Ras in cancer and developmental diseases. *Genes & Cancer*, 2, 344-358.

Flores, E.R., Sengupta, S., Miller, J.B., Newman, J.J., Bronson, R., Crowley, D., Yang, A., McKeon, F. and Jacks, T. 2005. Tumor predisposition in mice mutant for p63 and p73: evidence for broader tumor suppressor functions for the p53 family. *Cancer Cell*, 7,363-373.

Fisher, C.H.R.I.S., Byers, M.R., Iadarola, M.J. and Powers, E.A. 1991. Patterns of epithelial expression of Fos protein suggest important role in the transition from viable to cornified cell during keratinization. *Development*, 111, 253-258.

Fistarol, S.K. and Anliker, M.D. 2002. Cowden disease or multiple hamartoma syndrome-cutaneous clue to internal malignancy. *European Journal of Dermatology*, 12, 411-21.

Gao, C., Wang, Y., Broaddus, R., Sun, L., Xue, F. and Zhang, W. 2018. Exon 3 mutations of CTNNB1 drive tumorigenesis: a review. *Oncotarget*, 9, 5492.

Gat, U., DasGupta, R., Degenstein, L. and Fuchs, E. 1998. De novo hair follicle morphogenesis and hair tumors in mice expressing a truncated β-catenin in skin. *Cell*, 95, 605-614.

Gerdes, M.J. and Yuspa, S.H. 2005. The contribution of epidermal stem cells to skin cancer. *Stem Cell Reviews*, 1, 225-231.

Gerdes, M.J., Myakishev, M., Frost, N.A., Rishi, V., Moitra, J., Acharya, A., Levy, M.R., Park, S.W., Glick, A., Yuspa, S.H. and Vinson, C. 2006. Activator protein-1 activity regulates epithelial tumor cell identity. *Cancer Research*, 66, 7578-7588.

Ghosh, J.C. and Altieri, D.C. 2005. Activation of p53-dependent apoptosis by acute ablation of glycogen synthase kinase-3β in colorectal cancer cells. *Clinical Cancer Research*, 11, 4580-4588.

Gonzales, M. and Bowden, G.T. 2002. The role of PI 3-kinase in the UVB-induced expression of c-fos. *Oncogene*, 21, 2721-2728.

Gordon, J.W. and Ruddle, F.H. 1981. Integration and stable germ line transmission of genes injected into mouse pronuclei. *Science*, 214, pp.1244-1246.

Green, K.J. and Jones, J.C. 1996. Desmosomes and hemidesmosomes: structure and function of molecular components. *The FASEB Journal*, 10, pp.871-881.

Greenhalgh, D.A. and Yuspa, S.H. 1988. Malignant conversion of murine squamous papilloma cell lines by transfection with the fos oncogene. *Molecular Carcinogenesis*, 1, 134-143.

Greenhalgh, D.A. and Roop, D.R., 1994. Dissecting molecular carcinogenesis: development of transgenic mouse models by epidermal gene targeting. *Advances in Cancer Research*, 64, 247-296.

Greenhalgh, D.A., Welty, D.J., Strickland, J.E. and Yuspa, S.H. 1989. Spontaneous Ha-ras gene activation in cultured primary murine keratinocytes: Consequences of Ha-ras gene activation in malignant conversion and malignant progression. *Molecular Carcinogenesis*, 2, 199-207.

Greenhalgh, D.A., Welty, D.J., Player, A. and Yuspa, S.H. 1990. Two oncogenes, v-fos and v-ras, cooperate to convert normal keratinocytes to squamous cell carcinoma. *Proceedings of the National Academy of Sciences*, 87, 643-647.

Greenhalgh, D.A., Rothnagel, J.A., Quintanilla, M.I., Orengo, C.C., Gagne, T.A., Bundman, D.S., Longley, M.A. and Roop, D.R. 1993a. Induction of epidermal hyperplasia, hyperkeratosis, and papillomas in transgenic mice by a targeted v-Ha-ras oncogene. *Molecular Carcinogenesis*, 7, 99-110.

Greenhalgh, D.A., Rothnagel, J.A., Wang, X.J., Quintanilla, M.I., Orengo, C.C., Gagne, T.A., Bundman, D.S., Longley, M.A., Fisher, C. and Roop, D.R. 1993b. Hyperplasia, hyperkeratosis and benign tumour production in transgenic mice by a targeted v-fos oncogene suggest a role for fos in epidermal differentiation and neoplasia. *Oncogene*, 8, 2145-2157.

Greenhalgh, D.A., Quintanilla, M.I., Orengo, C.C., Barber, J.L., Eckhardt, J.N., Rothnagel, J.A. and Roop, D.R. 1993c. Cooperation between v-fos and v-rasHA induces autonomous papillomas in transgenic epidermis but not malignant conversion. *Cancer Research*, 53, 5071-5075.

Greenhalgh, D.A., Wang, X.J., Eckhardt, J.N. and Roop, D.R. 1995. 12-O-tetradecanoylphorbol-13-acetate promotion of transgenic mice expressing epidermal-targeted v-fos induces rasHA-activated papillomas and carcinomas without p53 mutation: association of v-fos expression with promotion and tumour autonomy. *Cell growth & Differentiation*, 6, 579-586.

Greenhalgh, D.A., Wang, X.J., Donehower, L.A. and Roop, D.R. 1996. Paradoxical tumor inhibitory effect of p53 loss in transgenic mice expressing epidermal-targeted v-rasHa, v-fos, or human transforming growth factor α. *Cancer Research*, 56, 4413-4423.

Grigoryan, T., Wend, P., Klaus, A. and Birchmeier, W. 2008. Deciphering the function of canonical Wnt signals in development and disease: conditional loss-and gain-of-function mutations of β-catenin in mice. *Genes & Development*, *22*, 2308-2341.

Gunther, E.J., Moody, S.E., Belka, G.K., Hahn, K.T., Innocent, N., Dugan, K.D., Cardiff, R.D. and Chodosh, L.A. 2003. Impact of p53 loss on reversal and recurrence of conditional Wnt-induced tumorigenesis. *Genes & Development*, *17*, 488-501.

Hanahan, D. and Weinberg, R.A. 2011. Hallmarks of cancer: the next generation. *cell*, 144, pp.646-674.

Harada, N., Tamai, Y., Ishikawa, T.O., Sauer, B., Takaku, K., Oshima, M. and Taketo, M.M. 1999. Intestinal polyposis in mice with a dominant stable mutation of the β-catenin gene. *The EMBO Journal*, 18, 5931-5942.

Hennings, H., Michael, D., Cheng, C., Steinert, P., Holbrook, K. and Yuspa, S.H. 1980. Calcium regulation of growth and differentiation of mouse epidermal cells in culture. *Cell*, 19, 245-254.

Hennings, H., Glick, A.B., Greenhalgh, D.A., Morgan, D.L., Strickland, J.E., Tennenbaum, T. and Yuspa, S.H., 1993. Critical aspects of initiation, promotion, and progression in multistage epidermal carcinogenesis. *Proceedings of the Society for Experimental Biology and Medicine*, 202, 1-8.

Hesse, K., Satzger, I., Schacht, V., Köther, B., Hillen, U., Klode, J., Schaper, K. and Gutzmer, R. 2016. Characterisation of prognosis and invasion of cutaneous squamous cell carcinoma by podoplanin and E-cadherin expression. *Dermatology*, 232, 558-565.

Hobbs, G.A., Der, C.J. and Rossman, K.L. 2016. RAS isoforms and mutations in cancer at a glance. *Journal of Cell Science*, 129, 1287-1292.

Hohenstein, P., Slight, J., Ozdemir, D.D., Burn, S.F., Berry, R. and Hastie, N.D. 2008. High-efficiency Rosa26 knock-in vector construction for Cre-regulated overexpression and RNAi. *Pathogenetics*, 1, pp.1-10.

Hopkins, B.D. and Parsons, R.E. 2014. Molecular pathways: intercellular PTEN and the potential of PTEN restoration therapy. *Clinical Cancer Research*, 20, 5379-5383.

Huang, P.Y. and Balmain, A. 2014. Modeling cutaneous squamous carcinoma development in the mouse. *Cold Spring Harbor Perspectives in Medicine*, 4, 013623.

Huels, D.J., Ridgway, R.A., Radulescu, S., Leushacke, M., Campbell, A.D., Biswas, S., Leedham, S., Serra, S., Chetty, R., Moreaux, G. and Parry, L., 2015. E-cadherin can limit the transforming properties of activating β-catenin mutations. *The EMBO Journal*, 34, 2321-2333.

Huelsken, J., Vogel, R., Erdmann, B., Cotsarelis, G. and Birchmeier, W. 2001. β-Catenin controls hair follicle morphogenesis and stem cell differentiation in the skin. *Cell*, 105, 533-545.

Hülsken, J., Birchmeier, W. and Behrens, J. 1994. E-cadherin and APC compete for the interaction with beta-catenin and the cytoskeleton. *The Journal of Cell Biology*, 127, 2061-2069.

Ikeda, S., Kishida, S., Yamamoto, H., Murai, H., Koyama, S. and Kikuchi, A. 1998. Axin, a negative regulator of the Wnt signaling pathway, forms a complex with GSK-3β and β-catenin and promotes GSK-3β-dependent phosphorylation of β-catenin. *The EMBO Journal*, 17, 1371-1384.

Irwin, M.S., Kondo, K., Marin, M.C., Cheng, L.S., Hahn, W.C. and Kaelin Jr, W.G. 2003. Chemosensitivity linked to p73 function. *Cancer Cell*, 3, 403-410.

Iwakuma, T. and Lozano, G. 2007. Crippling p53 activities via knock-in mutations in mouse models. *Oncogene*, 26, pp.2177-2184.

Jaks, V., Barker, N., Kasper, M., Van Es, J.H., Snippert, H.J., Clevers, H. and Toftgård, R. 2008. Lgr5 marks cycling, yet long-lived, hair follicle stem cells. *Nature Genetics*, 40, 1291.

Järvinen, E., Birchmeier, W., Taketo, M.M., Jernvall, J. and Thesleff, I., 2006. Continuous tooth generation in mouse is induced by activated epithelial Wnt/β-catenin signaling. *Proceedings of The National Academy of Sciences*, 103, 18627-18632.

Jeanes, A., Gottardi, C.J. and Yap, A.S. 2008. Cadherins and cancer: how does cadherin dysfunction promote tumour progression?. *Oncogene*, 27, 6920-6929.

Jih, D.M., Lyle, S., Elenitsas, R., Elder, D.E. and Cotsarelis, G. 1999. Cytokeratin 15 expression in trichoepitheliomas and a subset of basal cell carcinomas suggests they originate from hair follicle stem cells. *Journal of Cutaneous Pathology*, 26, 113-118.

Jones, J.C., Kam, C.Y., Harmon, R.M., Woychek, A.V., Hopkinson, S.B. and Green, K.J. 2017. Intermediate filaments and the plasma membrane. *Cold Spring Harbor perspectives in biology*, 9, p.a025866.

Jones, O.T., Ranmuthu, C.K., Hall, P.N., Funston, G. and Walter, F.M. 2020. Recognising skin cancer in primary care. *Advances in Therapy*, 37, 603-616.

Jonkers, J., Meuwissen, R., van der Gulden, H., Peterse, H., van der Valk, M. and Berns, A. 2001. Synergistic tumour suppressor activity of BRCA2 and p53 in a conditional mouse model for breast cancer. *Nature Genetics*, 29, 418-425.

Jou, T.S., Stewart, D.B., Stappert, J., Nelson, W.J. and Marrs, J.A. 1995. Genetic and biochemical dissection of protein linkages in the cadherin-catenin complex. *Proceedings of the National Academy of Sciences*, 92, 5067-5071.

Karim, R.Z., Tse, G.M., Putti, T.C., Scolyer, R.A. and Lee, C.S. 2004. The significance of the Wnt pathway in the pathology of human cancers. *Pathology*, 36, 120-128.

Kastenhuber, E.R. and Lowe, S.W. 2017. Putting p53 in context. *Cell*, 170, 1062-1078.

Kern, F., Niault, T. and Baccarini, M. 2011. Ras and Raf pathways in epidermis development and carcinogenesis. *British Journal of Cancer*, 104, 229-234.

Kellendonk, C., Tronche, F., Monaghan, A.P., Angrand, P.O., Stewart, F. and Schütz, G. 1996. Regulation of Cre recombinase activity by the synthetic steroid RU 486. *Nucleic Acids Research*, 24, pp.1404-1411.

Kellendonk, C., Tronche, F., Casanova, E., Anlag, K., Opherk, C. and Schütz, G. 1999. Inducible site-specific recombination in the brain. *Journal of molecular biology*, 285, pp.175-182.

Keyes, W.M., Vogel, H., Koster, M.I., Guo, X., Qi, Y., Petherbridge, K.M., Roop, D.R., Bradley, A. and Mills, A.A. 2006. p63 heterozygous mutant mice are not prone to spontaneous or chemically induced tumors. *Proceedings of the National Academy of Sciences*, 103, 8435-8440.

Kim, H., Kim, M., Im, S.K. and Fang, S. 2018. Mouse Cre-LoxP system: general principles to determine tissue-specific roles of target genes. *Laboratory Animal Research*, 34, pp.147-159.

Koch, U. and Radtke, F. 2007. Notch and cancer: a double-edged sword. *Cellular and Molecular Life Sciences*, 64, 2746-2762.

Konishi, H., Karakas, B., Abukhdeir, A.M., Lauring, J., Gustin, J.P., Garay, J.P., Konishi, Y., Gallmeier, E., Bachman, K.E. and Park, B.H. 2007. Knock-in of Mutant K-ras in Nontumorigenic Human Epithelial Cells as a New Model for Studying K-ras–Mediated Transformation. *Cancer research*, 67, pp.8460-8467.

Koster, M.I. and Roop, D.R. 2007. Mechanisms regulating epithelial stratification. *Annual Review of Cell and Developmental Biology*, 23.

Koster, M.I., Dai, D. and Roop, D.R. 2007. Conflicting roles for p63 in skin development and carcinogenesis. *Cell Cycle*, 6, 269-273.

Koster, M.I., Kim, S., Mills, A.A., DeMayo, F.J. and Roop, D.R. 2004. p63 is the molecular switch for initiation of an epithelial stratification program. *Genes & Development*, 18, 126-131.

Koster, M.I., Lu, S.L., White, L.D., Wang, X.J. and Roop, D.R. 2006. Reactivation of developmentally expressed p63 isoforms predisposes to tumor development and progression. *Cancer Research*, 66, 3981-3986.

Kotelevets, L., van Hengel, J., Bruyneel, E., Mareel, M., Van Roy, F. and Chastre, E. 2001. The lipid phosphatase activity of PTEN is critical for stabilizing intercellular junctions and reverting invasiveness. *The Journal of Cell Biology*, 155, 1129-1136.

Kretzschmar, K., Cottle, D.L., Schweiger, P.J. and Watt, F.M. 2015. The androgen receptor antagonizes Wnt/β-catenin signaling in epidermal stem cells. *Journal of Investigative Dermatology*, 135, 2753-2763.

Krishnamurthy, N. and Kurzrock, R. 2018. Targeting the Wnt/beta-catenin pathway in cancer: Update on effectors and inhibitors. *Cancer Treatment Reviews*, 62, 50-60.

Lee, S.E. and Lee, S.H. 2018. Skin barrier and calcium. *Annals of Dermatology*, 30, 265-275.

Lee, K.H., Li, M., Michalowski, A.M., Zhang, X., Liao, H., Chen, L., Xu, Y., Wu, X. and Huang, J. 2010. A genomewide study identifies the Wnt signaling pathway as a major target of p53 in murine embryonic stem cells. *Proceedings of the National Academy of Sciences*, 107, 69-74.

Leonard, M.K., Kommagani, R., Payal, V., Mayo, L.D., Shamma, H.N. and Kadakia, M.P. 2011. ΔNp63 α regulates keratinocyte proliferation by controlling PTEN expression and localization. *Cell Death & Differentiation*, 18, 1924-1933.

Li, S., Park, H., Trempus, C.S., Gordon, D., Liu, Y., Cotsarelis, G. and Morris, R.J. 2013. A keratin 15 containing stem cell population from the hair follicle contributes to squamous papilloma development in the mouse. *Molecular Carcinogenesis*, 52, 751-759.

Liaw, D., Marsh, D.J., Li, J., Dahia, P.L., Wang, S.I., Zheng, Z., Bose, S., Call, K.M., Tsou, H.C., Peacoke, M. and Eng, C. 1997. Germline mutations of the PTEN gene in Cowden disease, an inherited breast and thyroid cancer syndrome. *Nature Genetics*, 16, 64-67.

Liefer, K.M., Koster, M.I., Wang, X.J., Yang, A., McKeon, F. and Roop, D.R. 2000. Down-regulation of p63 is required for epidermal UV-B-induced apoptosis. *Cancer Research*, 60, 4016-4020.

Lim, X. and Nusse, R. 2013. Wnt signaling in skin development, homeostasis, and disease. *Cold Spring Harbor Perspectives in Biology*, 5, 008029.

Liu, Y., Lyle, S., Yang, Z. and Cotsarelis, G. 2003. Keratin 15 promoter targets putative epithelial stem cells in the hair follicle bulge. *Journal of Investigative Dermatology*, 121, 963-968.

Lyle, S., Christofidou-Solomidou, M., Liu, Y., Elder, D.E., Albelda, S. and Cotsarelis, G. 1998. The C8/144B monoclonal antibody recognizes cytokeratin 15 and defines the location of human hair follicle stem cells. *Journal of Cell Science*, *111*, 3179-3188.

Macdonald, F.H., Yao, D., Quinn, J.A. and Greenhalgh, D.A. 2014. PTEN ablation in Ras Ha/Fos skin carcinogenesis invokes p53-dependent p21 to delay conversion while p53-independent p21 limits progression via cyclin D1/E2 inhibition. *Oncogene*, 33, 4132-4143.

Malanchi, I., Peinado, H., Kassen, D., Hussenet, T., Metzger, D., Chambon, P., Huber, M., Hohl, D., Cano, A., Birchmeier, W. and Huelsken, J. 2008. Cutaneous cancer stem cell maintenance is dependent on β-catenin signalling. *Nature*, 452, 650-653.

Martín-Caballero, J., Flores, J.M., García-Palencia, P. and Serrano, M. 2001. Tumour susceptibility of p21Waf1/Cip1-deficient mice. *Cancer Research*, 61, 6234-6238.

Martincorena, I., Roshan, A., Gerstung, M., Ellis, P., Van Loo, P., McLaren, S., Wedge, D.C., Fullam, A., Alexandrov, L.B., Tubio, J.M. and Stebbings, L. 2015. High burden and pervasive positive selection of somatic mutations in normal human skin. *Science*, 348, 880-886.

Martini, M., De Santis, M.C., Braccini, L., Gulluni, F. and Hirsch, E. 2014. PI3K/AKT signaling pathway and cancer: an updated review. *Annals of Medicine*, 46, 372-383.

Masre, S.F., Rath, N., Olson, M.F. and Greenhalgh, D.A., 2017. ROCK2/ras Ha co-operation induces malignant conversion via p53 loss, elevated NF-κB and tenascin C-associated rigidity, but p21 inhibits ROCK2/NF-κB-mediated progression. *Oncogene*, 36, pp.2529-2542.

Masre, S.F., Rath, N., Olson, M.F. and Greenhalgh, D.A., 2020. Epidermal ROCK2 induces AKT1/GSK3β/β-catenin, NFκB and dermal tenascin C; but enhanced differentiation and p53/p21 inhibit papilloma. *Carcinogenesis*, 41, pp.1409-1420.

McCubrey, J.A., Rakus, D., Gizak, A., Steelman, L.S., Abrams, S.L., Lertpiriyapong, K., Fitzgerald, T.L., Yang, L.V., Montalto, G., Cervello, M. and Libra, M. 2016. Effects of mutations in Wnt/β-catenin, hedgehog, Notch and

PI3K pathways on GSK-3 activity—Diverse effects on cell growth, metabolism and cancer. *Biochimica et Biophysica Acta (BBA)-Molecular Cell Research*, 1863, 2942-2976.

Mehic, D., Bakiri, L., Ghannadan, M., Wagner, E.F. and Tschachler, E. 2005. Fos and jun proteins are specifically expressed during differentiation of human keratinocytes. *Journal of Investigative Dermatology*, 124, 212-220.

Mills, A.A. 2006. p63: oncogene or tumor suppressor?. *Current Opinion in Genetics & Development*, 16, 38-44.

Mills, A.A., Zheng, B., Wang, X.J., Vogel, H., Roop, D.R. and Bradley, A., 1999. p63 is a p53 homologue required for limb and epidermal morphogenesis. *Nature*, *398*(6729), pp.708-713.

Ming, M., Wang, S., Wu, W., Senyuk, V., Le Beau, M.M., Nucifora, G. and Qian, Z. 2012. Activation of Wnt/β-catenin protein signaling induces mitochondria-mediated apoptosis in hematopoietic progenitor cells. *Journal of Biological Chemistry*, 287, 22683-22690.

Misago, N., Toda, S. and Narisawa, Y. 2012. Folliculocentric squamous cell carcinoma with tricholemmal differentiation: a reappraisal of tricholemmal carcinoma. *Clinical and Experimental Dermatology: Clinical dermatology*, 37, 484-491.

Moll, U.M. and Slade, N. 2004. p63 and p73: Roles in Development and Tumor Formation National Cancer Institute. *Molecular Cancer Research*, 2, 371-386.

Mollereau, B. and Ma, D. 2014. The p53 control of apoptosis and proliferation: lessons from Drosophila. *Apoptosis*, 19, 1421-1429.

Morgan, D., Welty, D., Glick, A., Greenhalgh, D., Hennings, H. and Yuspa, S.H. 1992. Development of an in vitro model to study carcinogen-induced neoplastic progression of initiated mouse epidermal cells. *Cancer Research*, 52, 3145-3156.

Morin, P.J. 1999. β-catenin signaling and cancer. *Bioessays*, 21, 1021-1030.

Morris, R.J., Liu, Y., Marles, L., Yang, Z., Trempus, C., Li, S., Lin, J.S., Sawicki, J.A. and Cotsarelis, G. 2004. Capturing and profiling adult hair follicle stem cells. *Nature Biotechnology*, 22, 411-417.

Närhi, K., Järvinen, E., Birchmeier, W., Taketo, M.M., Mikkola, M.L. and Thesleff, I. 2008. Sustained epithelial β-catenin activity induces precocious hair development but disrupts hair follicle down-growth and hair shaft formation. *Development*, 135, 1019-1028.

Nguyen, B.C., Lefort, K., Mandinova, A., Antonini, D., Devgan, V., Della Gatta, G., Koster, M.I., Zhang, Z., Wang, J., Di Vignano, A.T. and Kitajewski, J. 2006. Cross-regulation between Notch and p63 in keratinocyte commitment to differentiation. *Genes & Development*, 20, 1028-1042.

Niemann, C., Owens, D.M., Hülsken, J., Birchmeier, W. and Watt, F.M. 2002. Expression of ΔNLef1 in mouse epidermis results in differentiation of hair follicles into squamous epidermal cysts and formation of skin tumours. *Development*, 129, 95-109.

Ogilvie, L.A., Kovachev, A., Wierling, C., Lange, B.M. and Lehrach, H. 2017. Models of models: a translational route for cancer treatment and drug development. *Frontiers in oncology*, 7, p.219.

Pai, L.M., Kirkpatrick, C., Blanton, J., Oda, H., Takeichi, M. and Peifer, M., 1996. Drosophila α-catenin and E-cadherin bind to distinct regions of Drosophila Armadillo. Journal of Biological Chemistry, 271, pp.32411-32420.

Parsons, R., 2004, April. Human cancer, PTEN and the PI-3 kinase pathway. In *Seminars in Cell & Developmental Biology*, 15, 171-176. Academic Press.

Polakis, P. 2000. Wnt signaling and cancer. *Genes & Development*, *14*, 1837-1851.

Porter, R.M., Lunny, D.P., Ogden, P.H., Morley, S.M., McLean, W.I., Evans, A., Harrison, D.L., Rugg, E.L. and Lane, E.B. 2000. K15 expression implies lateral differentiation within stratified epithelial basal cells. *Laboratory Investigation*, 80, 1701-1710.

Proweller, A., Tu, L., Lepore, J.J., Cheng, L., Lu, M.M., Seykora, J., Millar, S.E., Pear, W.S. and Parmacek, M.S. 2006. Impaired notch signaling promotes de novo squamous cell carcinoma formation. *Cancer Research*, 66, 7438-7444.

Rangel-Huerta, E. and Maldonado, E. 2017. Transit-amplifying cells in the fast lane from stem cells towards differentiation. *Stem Cells International*, *2017*.

Rankin, C.A., Grantham, J.J. and Calvet, J.P. 1992. C-fos expression is hypersensitive to serum-stimulation in cultured cystic kidney cells from the C57BL/6J-cpk mouse. *Journal of Cellular Physiology*, 152, 578-586.

Roberts, P.J. and Der, C.J., 2007. Targeting the Raf-MEK-ERK mitogen-activated protein kinase cascade for the treatment of cancer. *Oncogene*, 26, 3291-3310.

Rocco, J.W., Leong, C.O., Kuperwasser, N., DeYoung, M.P. and Ellisen, L.W. 2006. p63 mediates survival in squamous cell carcinoma by suppression of p73-dependent apoptosis. *Cancer cell*, 9, 45-56.

Rodilla, V., Villanueva, A., Obrador-Hevia, A., Robert-Moreno, À., Fernández-Majada, V., Grilli, A., López-Bigas, N., Bellora, N., Albà, M.M., Torres, F. and Duñach, M. 2009. Jagged1 is the pathological link between Wnt and Notch pathways in colorectal cancer. *Proceedings of the National Academy of Sciences*, 106, 6315-6320.

Romano, R.A., Smalley, K., Magraw, C., Serna, V.A., Kurita, T., Raghavan, S. and Sinha, S., 2012. ΔNp63 knockout mice reveal its indispensable role as a master regulator of epithelial development and differentiation. *Development*, 139, 772-782.

Roop, D.R., Lowy, D.R., Tambourin, P.E., Strickland, J., Harper, J.R., Balaschak, M., Spangler, E.F. and Yuspa, S.H. 1986. An activated Harvey ras oncogene produces benign tumours on mouse epidermal tissue. *Nature*, 323, 822-824.

Rosenthal, D.S., Steinert, P.M., Chung, S., Huff, C.A., Johnson, J., Yuspa, S.H. and Roop, D.R., 1991. A human epidermal differentiation-specific keratin gene is regulated by calcium but not negative modulators of differentiation in transgenic mouse keratinocytes. *Cell Growth Differ*, 2, 107-13.

Rothnagel, J.A., Greenhalgh, D.A., Wang, X.J., Sellheyer, K., Bickenbach, J.R., Dominey, A.M. and Roop, D.R. 1993. Transgenic models of skin diseases. *Archives of Dermatology*, 129, 1430-1436.

Rothnagel, J.A., Seki, T., Ogo, M., Longley, M.A., Wojcik, S.M., Bundman, D.S., Bickenbach, J.R. and Roop, D.R. 1999. The mouse keratin 6 isoforms are differentially expressed in the hair follicle, footpad, tongue and activated epidermis. *Differentiation*, 65, 119-130.

Rufini, A., Niklison-Chirou, M.V., Inoue, S., Tomasini, R., Harris, I.S., Marino, A., Federici, M., Dinsdale, D., Knight, R.A., Melino, G. and Mak, T.W. 2012. TAp73 depletion accelerates aging through metabolic dysregulation. *Genes & Development*, 26, 2009-2014.

Saadeddin, A., Babaei-Jadidi, R., Spencer-Dene, B. and Nateri, A.S. 2009. The links between transcription, β-catenin/JNK signaling, and carcinogenesis. *Molecular Cancer Research*, 7, 1189-1196.

Saez, E., Rutberg, S.E., Mueller, E., Oppenheim, H., Smoluk, J., Yuspa, S.H. and Spiegelman, B.M. 1995. c-Fos is required for malignant progression of skin tumours. *Cell*, 82, 721-732.

Saunders, T.L. 2015. New Transgenic Technologies. In *Movement Disorders*. Academic Press, pp. 45-57

Segrelles, C., Moral, M., Lara, M.F., Ruiz, S., Santos, M., Leis, H., Garcia-Escudero, R., Martinez-Cruz, A.B., Martinez-Palacio, J., Hernandez, P. and Ballestin, C. 2006. Molecular determinants of Akt-induced keratinocyte transformation. *Oncogene*, 25, 1174-1185.

Sherwood, V. and Leigh, I.M. 2016. WNT signaling in cutaneous squamous cell carcinoma: a future treatment strategy?. *Journal of Investigative Dermatology*, 136, 1760-1767.

Schlingemann, J., Hess, J., Wrobel, G., Breitenbach, U., Gebhardt, C., Steinlein, P., Kramer, H., Fürstenberger, G., Hahn, M., Angel, P. and Lichter, P. 2003. Profile of gene expression induced by the tumour promotor TPA in murine epithelial cells. *International Journal of Cancer*, 104, 699-708.

Simões, M.F., Sousa, J.S. and Pais, A.C. 2015. Skin cancer and new treatment perspectives: A review. *Cancer letters*, 357, 8-42.

Smeyne, R.J., Curran, T. and Morgan, J.I. 1992. Temporal and spatial expression of a fos-lacZ transgene in the developing nervous system. *Molecular Brain Research*, 16, 158-162.

Song, S. and Lambert, P.F. 1999. Different responses of epidermal and hair follicular cells to radiation correlate with distinct patterns of p53 and p21 induction. *The American Journal of Pathology*, 155, 1121-1127.

Song, M.S., Salmena, L. and Pandolfi, P.P. 2012. The functions and regulation of the PTEN tumour suppressor. *Nature Reviews Molecular Cell Biology*, 13, 283-296.

South, A.P., Purdie, K.J., Watt, S.A., Haldenby, S., Den Breems, N.Y., Dimon, M., Arron, S.T., Kluk, M.J., Aster, J.C., McHugh, A. and Xue, D.J. 2014. NOTCH1 mutations occur early during cutaneous squamous cell carcinogenesis. *Journal of Investigative Dermatology*, 134, 2630-2638.

Stewart, T.A., Pattengale, P.K. and Leder, P. 1984. Spontaneous mammary adenocarcinomas in transgenic mice that carry and express MTV/myc fusion genes. *Cell*, 38, 627-637.

Stiles, B., Groszer, M., Wang, S., Jiao, J. and Wu, H. 2004. PTENless means more. *Developmental Biology*, 273, 175-184.

Strickland, J.E., Greenhalgh, D.A., Koceva-Chyla, A., Hennings, H., Restrepo, C., Balaschak, M. and Yuspa, S.H. 1988. Development of murine epidermal cell lines which contain an activated rasHa oncogene and form papillomas in skin grafts on athymic nude mouse hosts. *Cancer Research*, 48, 165-169.

Su, X., Cho, M.S., Gi, Y.J., Ayanga, B.A., Sherr, C.J. and Flores, E.R. 2009. Rescue of key features of the p63-null epithelial phenotype by inactivation of Ink4a and Arf. *The EMBO Journal*, 28, 1904-1915.

Su, X., Chakravarti, D., Cho, M.S., Liu, L., Gi, Y.J., Lin, Y.L., Leung, M.L., El-Naggar, A., Creighton, C.J., Suraokar, M.B. and Wistuba, I. 2010. TAp63 suppresses metastasis through coordinate regulation of Dicer and miRNAs. *Nature*, 467, 986-990.

Su, X., Chakravarti, D. and Flores, E.R. 2013. p63 steps into the limelight: crucial roles in the suppression of tumorigenesis and metastasis. *Nature Reviews Cancer*, 13, 136-143.

Subauste, M.C., Nalbant, P., Adamson, E.D. and Hahn, K.M. 2005. Vinculin controls PTEN protein level by maintaining the interaction of the adherens junction protein β-catenin with the scaffolding protein MAGI-2. *Journal of Biological Chemistry*, 280, 5676-5681.

Sundberg, J.P. and King Jr, L.E. 1996. Mouse mutations as animal models and biomedical tools for dermatological research. *Journal of Investigative Dermatology*, 106, 368-376.

Sutter, C., Greenhalgh, D.A., Ueda, M., Abhyankar, S., Ngai, P., Hennings, H., Schweizer, J., Yuspa, S.H. and Strickland, J.E., 1994. SENCAR mouse skin tumors produced by promotion alone have A to G mutations in codon 61 of the c-rasHa gene. *Carcinogenesis*, 15, 1975-1978.

Suzuki, A., Itami, S., Ohishi, M., Hamada, K., Inoue, T., Komazawa, N., Senoo, H., Sasaki, T., Takeda, J., Manabe, M. and Mak, T.W. 2003. Keratinocyte-specific Pten deficiency results in epidermal hyperplasia, accelerated hair follicle morphogenesis and tumour formation. *Cancer Research*, 63, 674-681.

Suzuki, A., de la Pompa, J.L., Stambolic, V., Elia, A.J., Sasaki, T., del Barco Barrantes, I., Ho, A., Wakeham, A., Khoo, W., Fukumoto, M. and Mak, T.W. 1998. High cancer susceptibility and embryonic lethality associated with mutation of the PTEN tumour suppressor gene in mice. *Current Biology*, 8, 1169-1178.

Tan, M.H., Mester, J.L., Ngeow, J., Rybicki, L.A., Orloff, M.S. and Eng, C. 2012. Lifetime cancer risks in individuals with germline PTEN mutations. *Clinical Cancer Research*, 18, 400-407.

Takeichi, M. 1991. Cadherin cell adhesion receptors as a morphogenetic regulator. *Science*, 251, 1451.

Tamura, M., Gu, J., Matsumoto, K., Aota, S.I., Parsons, R. and Yamada, K.M. 1998. Inhibition of cell migration, spreading, and focal adhesions by tumor suppressor PTEN. *Science*, 280, 1614-1617.

Topley, G.I., Okuyama, R., Gonzales, J.G., Conti, C. and Dotto, G.P. 1999. p21WAF1/Cip1 functions as a suppressor of malignant skin tumor formation and a determinant of keratinocyte stem-cell potential. *Proceedings of The National Academy of Sciences*, 96, 9089-9094.

Toualbi, K., Güller, M.C., Mauriz, J.L., Labalette, C., Buendia, M.A., Mauviel, A. and Bernuau, D. 2007. Physical and functional cooperation between AP-1 and β-catenin for the regulation of TCF-dependent genes. *Oncogene*, 26, 3492-3502.

Troy, T.C., Arabzadeh, A. and Turksen, K. 2011. Re-assessing K15 as an epidermal stem cell marker. *Stem cell reviews and reports*, 7, 927-934.

Van Mater, D., Kolligs, F.T., Dlugosz, A.A. and Fearon, E.R. 2003. Transient activation of β-catenin signaling in cutaneous keratinocytes is sufficient to trigger the active growth phase of the hair cycle in mice. *Genes & Development*, 17, 1219-1224.

Wahl, G.M. 2006. Mouse bites dogma: how mouse models are changing our views of how P53 is regulated in vivo. *Cell Death & Differentiation*, 13, 973-983.

Wang, X.J., Greenhalgh, D.A., Lu, X.R., Bickenbach, J.R. and Roop, D.R. 1995. TGF alpha and v-fos cooperation in transgenic mouse epidermis induces aberrant keratinocyte differentiation and stable, autonomous papillomas. *Oncogene*, 10, 279-289.

Wang, X.J., Greenhalgh, D.A., Bickenbach, J.R., Jiang, A., Bundman, D.S., Krieg, T., Derynck, R. and Roop, D.R. 1997. Expression of a dominant-negative type II transforming growth factor β (TGF-β) receptor in the epidermis of transgenic mice blocks TGF-β-mediated growth inhibition. *Proceedings of the National Academy of Sciences*, 94, 2386-2391.

Wang, X.J., Greenhalgh, D.A., Jiang, A., He, D., Zhong, L., Medina, D., Brinkley, B.R. and Roop, D.R. 1998. Expression of a p53 mutant in the epidermis of transgenic mice accelerates chemical carcinogenesis. *Oncogene*, 17, 35-45.

Wang, N.J., Sanborn, Z., Arnett, K.L., Bayston, L.J., Liao, W., Proby, C.M., Leigh, I.M., Collisson, E.A., Gordon, P.B., Jakkula, L. and Pennypacker, S. 2011. Loss-of-function mutations in Notch receptors in cutaneous and lung squamous cell carcinoma. *Proceedings of the National Academy of Sciences*, 108, 17761-17766.

Watt, F.M. and Collins, C.A. 2008, January. Role of β-catenin in epidermal stem cell expansion, lineage selection, and cancer. In *Cold Spring Harbor Symposia on Quantitative Biology*, 73, 503-512. Cold Spring Harbor Laboratory Press.

Westfall, M.D., Mays, D.J., Sniezek, J.C. and Pietenpol, J.A., 2003. The ΔNp63α phosphoprotein binds the p21 and 14-3-3σ promoters in vivo and has transcriptional repressor activity that is reduced by Hay-Wells syndrome-derived mutations. *Molecular and Cellular Biology*, *23*, 2264-2276.

Wu, R.C. and Schönthal, A.H. 1997. Activation of p53-p21 waf1 pathway in response to disruption of cell-matrix interactions. *Journal of Biological Chemistry*, 272, 29091-29098.

Wu, H., Goel, V. and Haluska, F.G. 2003. PTEN signaling pathways in melanoma. *Oncogene*, 22, 3113-3122.

Yao, D., Alexander, C.L., Quinn, J.A., Porter, M.J., Wu, H. and Greenhalgh, D.A. 2006. PTEN loss promotes rasHa-mediated papillomatogenesis via dual up-regulation of AKT activity and cell cycle deregulation but malignant conversion proceeds via PTEN-associated pathways. *Cancer Research*, 66, 1302-1312.

Yao, D., Alexander, C.L., Quinn, J.A., Chan, W.C., Wu, H. and Greenhalgh, D.A. 2008. Fos cooperation with PTEN loss elicits keratoacanthoma not carcinoma, owing to p53/p21WAF-induced differentiation triggered by GSK3β inactivation and reduced AKT activity. *Journal of Cell Science*, 121, 1758-1769.

Yoshida, T., Akatsuka, T. and Imanaka-Yoshida, K. 2015. Tenascin-C and integrins in cancer. *Cell Adhesion & Migration*, 9, 96-104.

Young, P., Boussadia, O., Halfter, H., Grose, R., Berger, P., Leone, D.P., Robenek, H., Charnay, P., Kemler, R. and Suter, U. 2003. E-cadherin controls adherens junctions in the epidermis and the renewal of hair follicles. *The EMBO Journal*, 22, 5723-5733.

Young, M.R., Li, J.J., Rincón, M., Flavell, R.A., Sathyanarayana, S.B., Hunziker, R. and Colburn, N. 1999. Transgenic mice demonstrate AP-1 (activator protein-1) transactivation is required for tumour promotion. *Proceedings of The National Academy of Sciences*, 96, 9827-9832.

Yuspa, S.H. 1994. The pathogenesis of squamous cell cancer: lessons learned from studies of skin carcinogenesis—thirty-third GHA Clowes Memorial Award Lecture. *Cancer Research*, 54, 1178-1189.

Yuspa, S.H., Kilkenny, A.E., Steinert, P.M. and Roop, D.R. 1989. Expression of murine epidermal differentiation markers is tightly regulated by restricted extracellular calcium concentrations in vitro. *The Journal of Cell Biology*, 109, 1207-1217.

Waterston, R.H. and Pachter, L. 2002. Initial sequencing and comparative analysis of the mouse genome. *Nature*, 420, pp.520-562.

Whitfield, J., Littlewood, T., Evan, G.I. and Soucek, L. 2015. The estrogen receptor fusion system in mouse models: a reversible switch. *Cold Spring Harbor Protocols*, 2015,pp.pdb-top069815.

Zhou, Z., Wang, D., Wang, X.J. and Roop, D.R. 2002. In utero activation of K5.CrePR1 induces gene deletion. *Genesis*, 32, pp.191-192.

Ziegler, A., Jonason, A.S., Leffellt, D.J., Simon, J.A., Sharma, H.W., Kimmelman, J., Remington, L., Jacks, T. and Brash, D.E. 1994. Sunburn and p53 in the onset of skin cancer. *Nature*, 372, 773-776.

Zito, G., Saotome, I., Liu, Z., Ferro, E.G., Sun, T.Y., Nguyen, D.X., Bilguvar, K., Ko, C.J. and Greco, V. 2014. Spontaneous tumour regression in keratoacanthomas is driven by Wnt/retinoic acid signalling cross-talk. *Nature Communications*, 5, 1-13.